THE UNIVERSITY
of EDINBURGH

Alkyne Metathesis: A new tool for the self-assembly of complex molecular architectures

Ektoras Yiannakas

THE UNIVERSITY *of* EDINBURGH

A thesis submitted for the degree of
Doctor of Philosophy

The University of Edinburgh
2021

Declaration

This thesis is submitted in part fulfilment of the requirement for the degree of Doctor of Philosophy at the University of Edinburgh. Unless otherwise stated the work described in this thesis is original and has not been submitted previously in whole or in part for any degree or other qualification at this, or any other university. In accordance with the regulations this thesis does not exceed 100000 words in length.

Ektoras Yiannakas
September 2021

The work presented was created under the joined guidance of Prof. Alison N. Hulme and Prof. Alois Fürstner from September 2017 to September 2021 in the School of Chemistry at the University of Edinburgh, UK and the Max-Planck Institut für Kohlenforschung (MPI) in Mülheim an der Ruhr, Germany.

A major component of the work presented has already been published in the following journal articles:

[1] J. Hillenbrand, M. Leutzsch, E. Yiannakas, C. Gordon, C. Wille, N. Nöthling, C. Copéret, A. Fürstner, *J. Am. Chem. Soc.* **2020**, *142*, 11279 – 11294.

[2] E. Yiannakas, M. Grimes, J. Whitelegge, A. Fürstner, A. N. Hulme, *Angew. Chem. Int. Ed.* **2021**, *60*, 18504− 18508.

Acknowledgements

I would like to express my thanks to my supervisors. Firstly, to Alison Nicola Hulme, thank you for keeping up with my chemical insanity for the past four years, for always giving me the encouragement and freedom to pursue my own ideas and helping me tame the "chemical beast". Thank you to Alois Fürstner for your invaluable advice and wonderful opportunity to spend 15-months of my PhD at Max-Planck Institut für Kohlenforschung (MPI), Germany. It has been a great inspiration to work alongside two talented and inspirational individuals.

I thank the EPSRC/UKRI, Leverhulme Trust (LHT) and the A.G. Leventis Foundation for the funding which has allowed me to undertake this work. I am also grateful for the opportunity that the SAR studentship funded by the LHT, gave me to carry out a 15-month placement at the MPI.

Thank you to everyone at MPI for welcoming me, and to all who made my time in Germany so enjoyable. With such a diverse project, many people have helped me along the way. Firstly, I would like to thank all the technicians (Saskia Schulthoff, Karin Radkowski, Christian Wille, Christopher Rustemeier and Roswitha Leichtweiß) in the Fürstner group at the MPI for keeping up with my cypriot/ non-german chemical exuberance. Furthermore, I would like to thank Sandra Kestermann, Heike Hinrichs, Sophia Begoihn, Conny Wirtz, Dr. Markus Leutzsch, Andrea Hennig-Bosserhoff, Nils Nöthling, Dr. Richard Goddard and Jörg Rust from the analytical service and administrative departments at MPI for their amazing technical support and help. In addition, I would like to thank Julius Hillenbrand for his help and work during our collaborative project.

Special thanks go to my chemical family over in Germany [Saskia Schulthoff (aka "the big german sister"), Samira Speicher (aka "the lovely work wife"), Simon M. Spohr (aka "SPMS"), Lorenz E. Löffler (aka "King Löffler"), Van-Anh Tran, Dr. Romain Melot (aka "French Mafia"), Dr. Paola Caramenti (aka "Paolina"), Dr. Marc Heinrich (aka "Marc^{3}"), Karin Radkowski and Christian Wille (aka "Williee")] for the endless banter in the lab, the enlightening chemical and non-chemical discussions at the smoking area at the MPI, the amazing trips and nights out but above all for making my stay at the MPI an absolute pleasure.

Thanks also to members of the Thomas, Love and McKeown groups in the School of Chemistry at the University of Edinburgh for generously letting me use your equipment, without this I would not have been able to carry out some of my experiments. I would like to thank all members, past and present, of the Hulme group for being great lab mates for making the everyday life of my PhD so enjoyable. Thank you to Dr. Richard Brewster for all the long and interesting chemistry chats and advice. A big thank you to all my project students for their hard work and banter in the lab (Marina Economidou (aka "NMR in Marination"), Craig Steven, Jamie Whitelegge, Mark Grimes, Callum Savage, Chengming Guo). Special thanks go to Maria Eleni Kouridaki (aka "the little chemical sister"), Edith Sandström (aka "the Swedish warrior princess") and Craig Steven (aka "the Scottish Raman Prince") for your friendship and support.

My thanks go to all support staff in the at the School of Chemistry at the University of Edinburgh and beyond whose hard work has made everyday life run smoothly. Thank you to Stuart Johnstone for his truly amazing glassblowing skills, George Steedman for his magnificent mechanical works, Juraj Bella for his help with NMR and Dr. Logan McKay, Dr. Faye Cruickshank and Alan Taylor for MS.

A massive thanks goes to my family for all their support and encouragement during this time, and especially to my mum, who was the first person to introduce me to chemistry. Thanks to all my friends in Edinburgh and beyond who have made these four years so enjoyable.

Abstract

Macrocyclic scaffolds have attracted considerable attention over the past two decades because of their unique properties and promising potential in a wide range of applications in drug discovery, material science and supramolecular chemistry. Recent approaches to accessing complex macrocyclic architectures from simple precursors include metathesis-based cyclooligomerisations, which are described as one-pot alkyne/alkene cross-metathesis/ ring-closing metathesis reactions (CM/RCM or ACM/RCAM) in this thesis. The collection of vignettes presented in Chapter 1, clearly exemplifies that one-pot iterative metathesis reactions provide a powerful and versatile set of tools for the rapid construction of highly decorated architectures of variable ring sizes with a wide range of properties and applications.

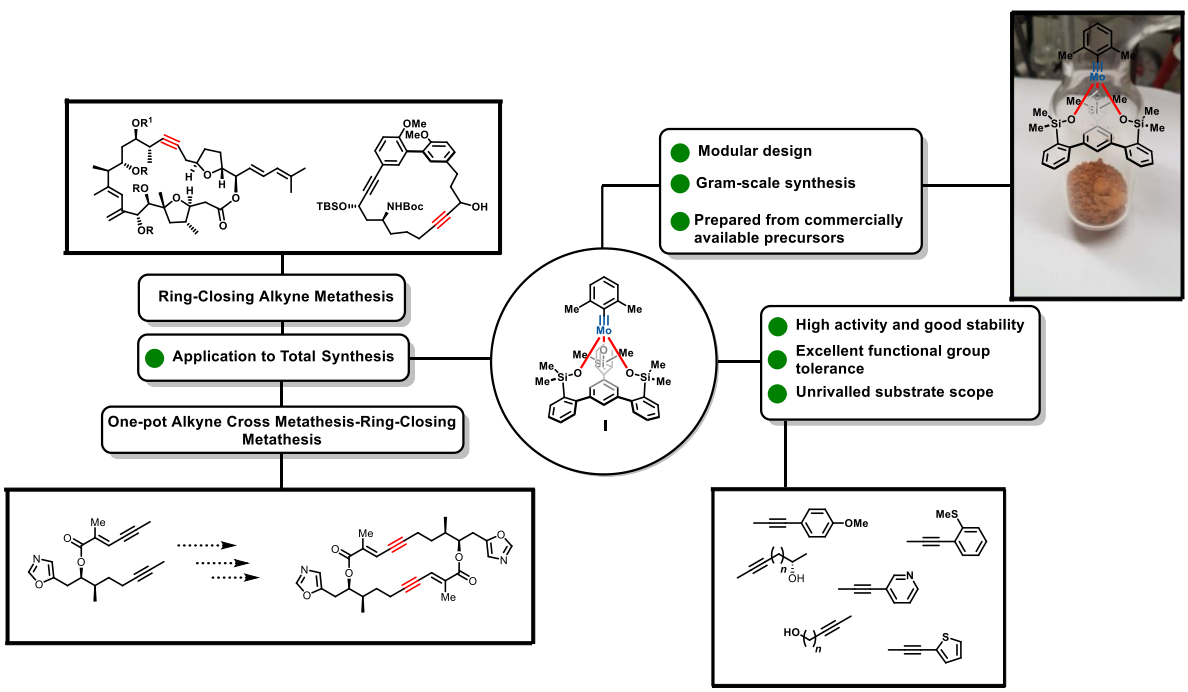

Since the utility of alkyne metathesis-based synthetic methodologies such as the one-pot ACM/RCAM reaction is limited by the availability of well-defined and user-friendly alkyne metathesis catalysts. In Chapter 2, the development of a new alkyne metathesis catalyst was investigated. The newly developed catalyst (**I**) also termed “canopy catalyst” is endowed with the privileged tripodal silanolate ligand framework. The unrivaled catalytic performance of this complex is illustrated by its broad functional group tolerance. The catalyst works well in the presence of unprotected primary alcohols and

even tolerates substrates having multiple donor sites, including basic nitrogen and heterocycles. Moreover, the ease of formation of key intermediates in the total synthesis of marine natural products including amphidinolide F and nor-cembranoid sinulariadiolide further highlights the unrivalled catalytic activity of this catalyst.

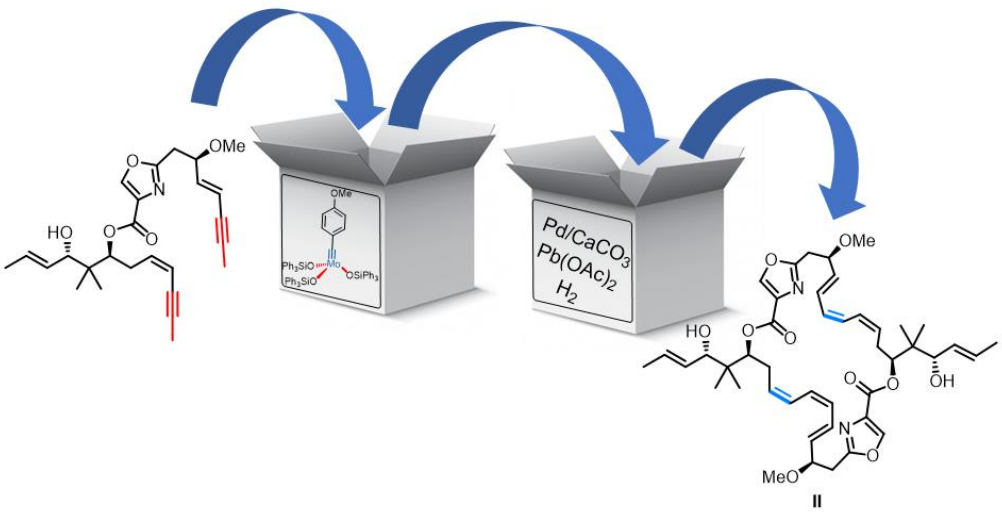

II

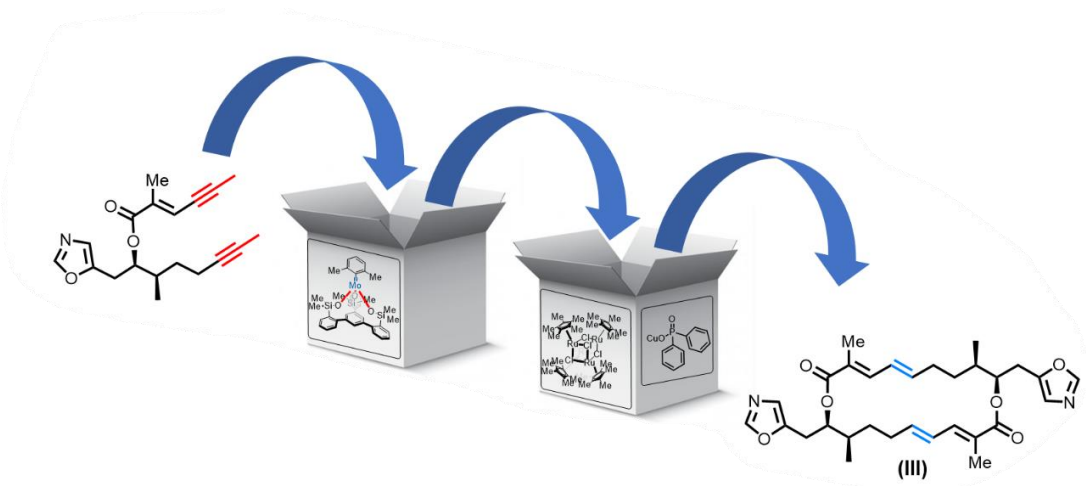

The total synthesis of cytotoxic marine-derived bis(lactone) disorazole C_1 (**II**), discussed in Chapter 1, reported by our group in 2015, features the first example of an alkyne-metathesis-based homodimerization approach applied to the synthesis of natural products. Capitalising on this synthetic methodology in Chapter 3, the first total synthesis of C_2-symmetric antimalarial samroiyotmycin A (**III**) is described (9 steps longest linear sequence with an overall 6%). The convergent synthetic strategy used,

involves a bisalkyne fragment-assembly via an unprecedented Schöllkopf-type condensation on a substituted β-lactone and a late-stage one-pot ACM–RCAM reaction. The demanding alkyne metathesis sequence was successfully achieved using the newly developed alkyne metathesis catalyst, discussed in Chapter 2. Contemporary ruthenium catalysed hydrometallation chemistry enabled the final elaboration into the required *E*-alkenes.

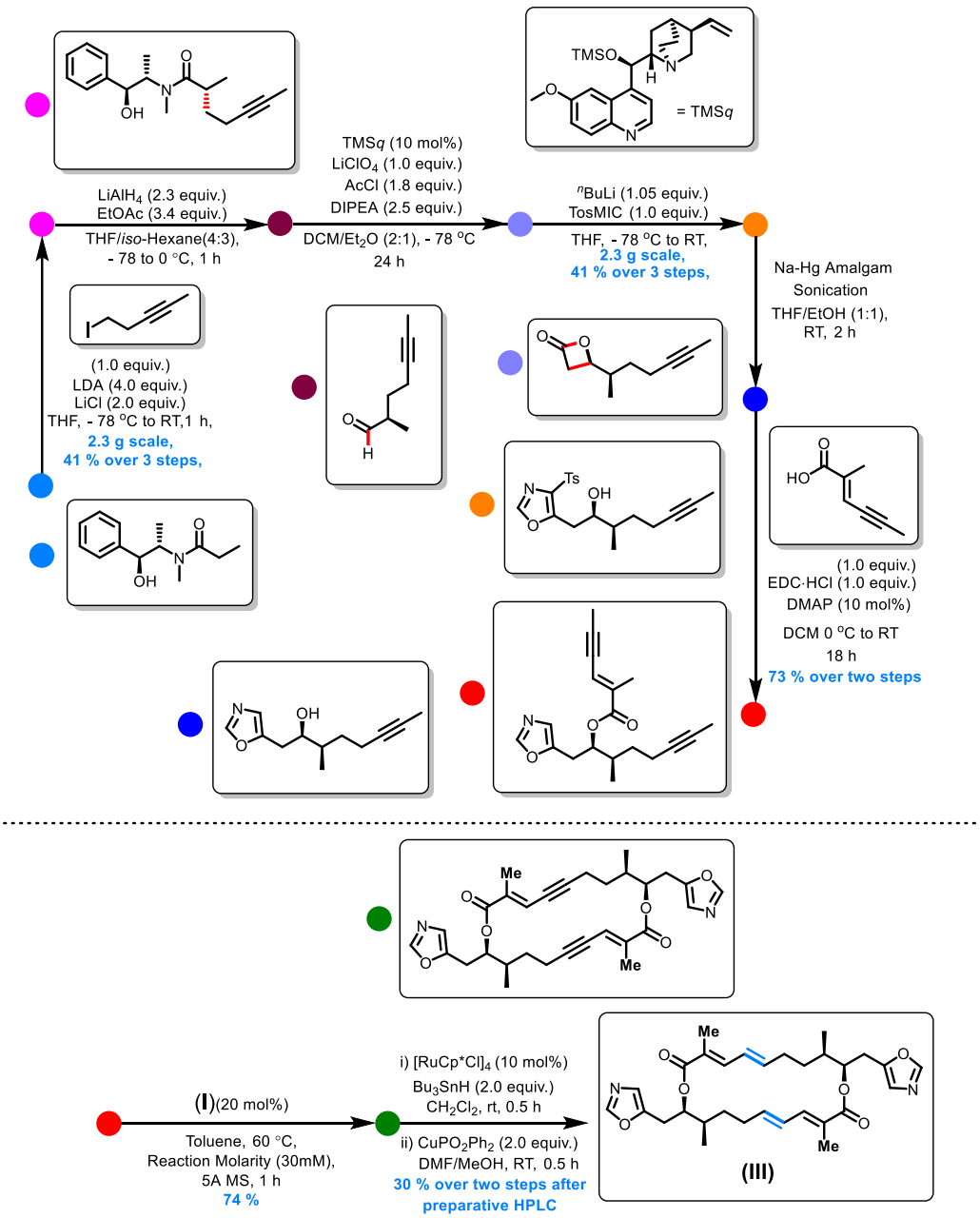

Lay Abstract

Macrocyclic natural products are a family of complex doughnut- shaped molecules found in nature. These exhibit unique biological properties, such as the selective disruption of protein-protein interactions (PPIs) in many diseased pathologies including cancer, bacterial infections, leukaemia and neurodegenerative diseases. PPIs are less druggable than most targets in drug discovery. Although macrocyclic natural products are produced only in minute quantities in nature, an effective method for assembling these molecular doughnuts in the lab is called alkyne metathesis. Unfortunately, its practical use is limited by the water and air sensitivity of catalysts that can promote this approach for constructing molecular doughnuts. In this study, a new highly efficient alkyne metathesis catalyst was developed. The robustness of the newly developed catalyst is highlighted by its successful use in the synthesis of a recently discovered macrocyclic natural product with promising anti-malarial properties.

Contents

Appendices:

Abbreviations

Ac	acetyl
ACM	alkyne cross metathesis
Anal.	analytically
aq.	aqueous
Bn	benzyl
br	broad
Bu	butyl
Bz	benzoyl
calc.	calculated
cat.	catalytic
CDI	1,1'-Carbonyldiimidazole
CI	chemical ionization
conc.	Concentrated
COSY	Correlation spectroscopy
Cp	Cyclopentadienyl
δ	*chemical shift*
d	doublet
diff.	difference
DMAP	4-Dimethylaminopyridine
DME	dimethoxyethane
DMF	*N*,*N*-dimethylformamide
DMSO	dimethyl sulfoxide
dr	Diastereomeric ratio
ee	Enantiomeric excess
EI	electron ionization
ESI	electronspray ionization
Et	ethyl
Equiv.	equivalents
GC	gas chromatography
h	hour

GCMS	Gas chromatography mass spectrometry
HMBC	Heteronuclear multiple bond correlation
HMDS	Bis(trimethylsilyl)amide
HPLC	High performance liquid chromatography
HRMS	High resolution mass spectrometry
HSQC	Heteronuclear single quantum coherence
I	*iso*
^{i}Pr	Isopropyl
IR	Infrared
J	*coupling constant*
L	Ligand
LDA	Lithium isopropyl amide
m	*meta*
m	multiplet
M	molar: mol L^{-1}
m/z	mass per charge
Me	methyl
Mes	Mesityl
MOM	methoxymethyl
Mp.	melting point
MS	mass spectrometry
MS	molecular sieves
MTBE	methyl *tert*-butyl ether
NBS	*N*-bromosuccinimide
n.d.	not detected
NMR	nuclear magnetic resonance
NOE	Nuclear Overhauser Effect
NR	no reaction
p	*para*
o	*ortho*
Ph	phenyl
phen	1,10-phenanthroline

PMB	*para*-methoxybenzyl
ppm	parts per million
PPTS	pyridinium *p*-toluenesulfonate
q	quartet
quant.	quantitative
quinuc	quinuclidine
R	organic substituent
rac	Racemic
RCAM	ring-closing alkyne metathesis
ROESY	Rotating frame Overhauser Effect SpectroscopY
RT	ambient temperature
s	singlet
sat.	saturated
sm	starting material
t	triplet
T	temperature
TBAF	Tetrabutylammonium fluoride
TBC	tert-Butylcatechol
TBS	*tert*-butyldimethylsilyl
TCB	trichlorobenzene
TCCA	Trichloroisocyanuric acid
tert	*tertiary*
TES	triethylsilyl
TFA	Trifluoroacetic acid
Theor.	theoretical
THF	tetrahydrofuran
TLC	thin layer chromatography
TMS	trimethylsilyl
Ts	tosyl
VT	variable temperature

Chapter 1: Introduction

1.1. Metathesis: Transforming elegant structural simplicity into marvelous molecular complexity.

A significant portion of drugs currently on the market are descended from macrocyclic natural products. These are more commonly encountered in cases, where protein-protein interactions (PPIs) are implicated in the underlying diseased pathologies. Therefore, macrocyclic structures are prevalent in anticancer, antifungal and antibiotic compounds.[1-5] In contrast to their acyclic counterparts, macrocyclic architectures possess an intrinsic conformational preorganization due to their restricted bond rotation. The preorientation induced by the reduced conformational freedom and shape, offers significant stability and reduced entropic penalties upon binding to the site of interest, while the flexibility of these scaffolds renders them adequately adaptive for optimal fit. Therefore, these molecules often exhibit high affinity and selectivity even for shallow pockets that are difficult to target otherwise. [6-8]

Construction of these macrocyclic frameworks usually proceeds via the macrocyclization of an acyclic precursor. Despite the entropic loss and potential ring strain accrued due to ring closure, nature has integrated several types of macrocyclization reactions into biosynthetic pathways to facilitate the assembly of these molecules with remarkable efficiency and ease. Although macrocyclization reactions through purely chemical means were previously deemed either impractical undertakings, substantial progress in the "classic" macrocyclisation strategies (macrolactonization and macrolactamization) over recent years demonstrates that formation of macrocycles is not seriously limiting.[9-12] The wide range of transition metal-catalyzed carbon−carbon (C−C) bond-forming reactions that has emerged over the two past decades has revolutionized the way synthetic chemists conceptualize and construct these molecules, providing a robust toolkit for constructing C−C bonds between molecules that previously seemed impossible to achieve. Arguably these reactions have led to the greatest leaps forward in removing the established notion of the "macrocyclic challenge".[13] One such organometallic mediated C−C bond forming methodology is metathesis. Metathesis refers to the redistribution of atoms or fragments between two molecules to afford two new hybrid molecular entities. Metathesis processes where the statistical rearrangement of unsaturated fragments is aided by a metal alkylidene or alkylidyne are categorized as diene, diyne or enyne metathesis based on the types of the participant π-systems. Even

though the combination of coupling partners involved in these metathesis reactions may vary, they all share the same elementary steps: [2+2] cycloaddition, to generate a metallacyclobutane (diene metathesis)/ metallacyclobutadiene (diyne metathesis)/ metallacyclobutene (enyne metathesis) intermediate, followed by cycloreversion. While the π-system exchange in the case of alkyne metathesis is facilitated by metal alkylidynes, both diene and enyne metathesis are promoted by metal alkylidenes (Figure 1.1).

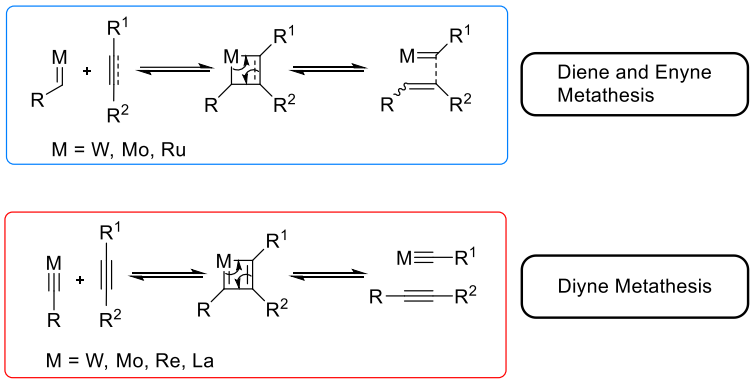

Figure 1.1. Elementary steps in metathesis processes.

These metathesis processes can be further classified into six closely related major categories (Figure 1.2): (i) cross-metathesis (CM/ ACM), an intermolecular metathesis between two alkenes or alkynes; (ii) ring-closing metathesis (RCM/RCAM), a process in which a 1,n-diene/yne cyclizes to generate an acyclic byproduct and a cycloalkene/yne product; (iii) ring-opening metathesis polymerization (ROPM/ROAMP), which refers to the ring-opening of strained cycloalkenes and cycloalkynes to afford polyenes or polyynes respectively and (iv) acyclic metathesis polymerization (ADMET/ADIMET), whereby polymeric compounds can be generated from the corresponding acyclic dienes or diynes. Enyne metathesis (v) is the transition metal-mediated intramolecular (RCEYM) or intermolecular re-organization reaction between an alkene and an alkyne to afford a 1,3-diene. In addition, metathesis cyclooligomerization (vi) also termed one-pot CM/RCM and one-pot ACM/RCAM are processes in which bis(alkenes) and bis(alkynes) undergo a double or multiple sequential metathesis reactions to furnish macrocyclic products.[14]

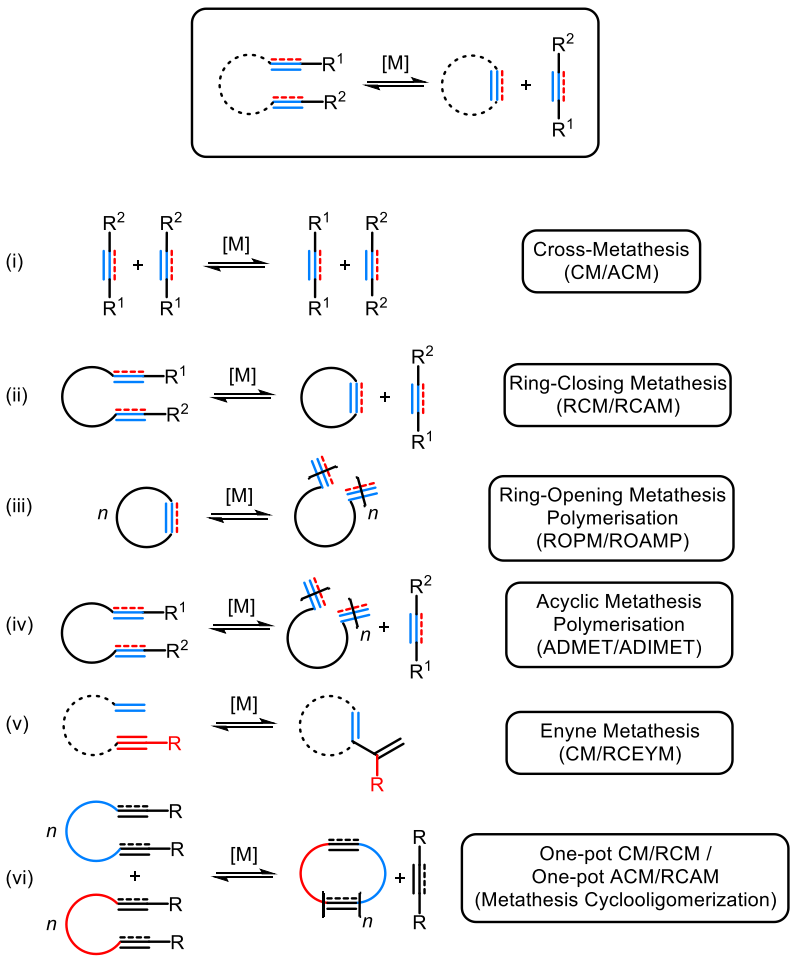

Figure 1.2. Repertoire of metathesis reactions.

The field of metathesis has seen tremendous progress over the past two decades, ranging from the discovery of bench-stable (**G1** & **G2**), *Z*-selective (**SHa** & **SHb**) and stereoselective (**ZG1** & **ZG2**, **ZH**) homogeneous alkene metathesis catalysts (Figure 1.3 (i)), to the development of catalytic systems that can effect the alkyne metathesis reactions of simple building blocks under open-air conditions.[15-18] Despite the close mechanistic relationship of these metathesis reactions, the scope of alkyne metathesis does not yet rival that of alkene metathesis. Since the seminal discovery of the first well-defined alkyne metathesis catalyst [W(CCMe3)(O^{t}Bu)3] (**W^{I}**) (Figure 1.3 (ii)) reported by Schrock and co-workers,[19-21] several different monodentate ligands were investigated to uncover the key elements to efficient alkyne metathesis catalyst design including sterically demanding fluorinated alkoxides (**Mo^{A}**, **W^{II}**) and silanols

(**Mo^{B}**). Yet, the advent of multidentate ligand-based molybdenum complexes (**Mo^{D}** & **Mo^{E}**) with enhanced catalytic activity and functional group tolerance over the recent years, clearly marks a big step forward in bridging the gap between these closely related metathesis reactions (Figure 1.3 (ii)).

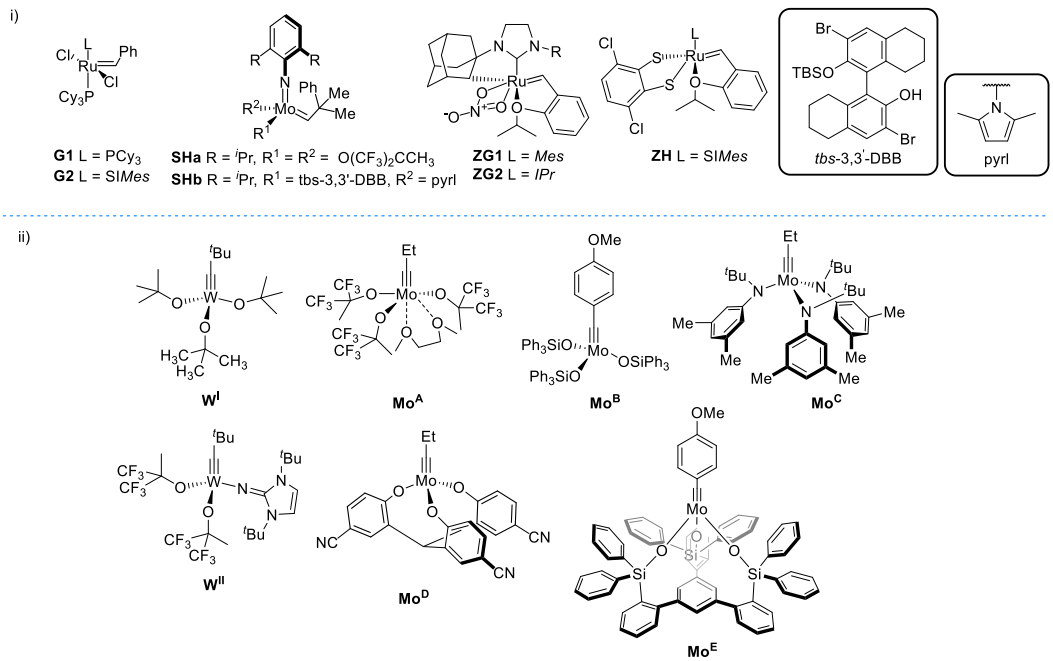

Figure 1.3. Commonly used (i) alkene and (ii) alkyne metathesis catalysts.

Among the numerous syntheses of macrocyclic natural products reported over the past few decades, the key ring-closing step is often achieved via a late-stage ring-closing alkene or alkyne metathesis. The broad array of metathesis catalysts developed for these metathesis transformations set them as textbook approaches. This in turn has earned metathesis a place in applications ranging from academic research to critical segments of the chemical industry, including bio-/agro-chemicals, advanced materials, pharmaceuticals, and cosmetics. Two recent metathesis-based strategies for the construction of macrocyclic scaffolds are the one-pot CM/RCM and the one-pot ACM/RCAM. In this introduction, a selection of examples employing these two metathesis-based macrocyclisation manifolds for the assembly of complex molecular architectures including natural products, cyclophanes, oligosaccharides, cyclic peptides, molecular electronic and artificial transporters will be discussed.

1.2. Cyclophanes

1.2.1 Synthesis of Cyclophanes via one-pot CM/RCM

Cyclophanes are a family of strained cyclic poly-arylated molecules interconnected by aliphatic units, which are widely used in supramolecular chemistry and materials science. Therefore, there is a continuous demand for the development of new and streamlined approaches for their synthesis. A broad range of protocols are available for the synthesis of these including metathesis reactions.[22]

Tae and Yang investigated the synthesis of [*n*]paracyclophanes via a one-pot CM/RCM-approach utilising a homologous series of *para*-substituted alkenyl derivatives **1a**-**g** (Scheme 1.1). The metathesis reactions of alkenyl derivatives under high dilution conditions in the presence of Ru-complexes **G1** and **G2** delivered [*n*] (**2**), [*n*,*n*] (**3**) and [*n*,*n*,*n*] (**4**) paracyclophanes (Scheme 1.1). Monomers bearing short alkenyl chains (**1a**-**c**, **1e** and **1g**) afforded [*n*,*n*] and [*n*,*n*,*n*]paracyclophanes (**3** & **4**) via dimerisation or trimerization, respectively. On the other hand, acyclic monomers (**1d** & **1f**) substituted with alkenyl chains of adequate length, were found to engage selectively in an intramolecular cyclisation furnishing the corresponding [*n*]paracyclophanes **2d** and **2f**.[23]

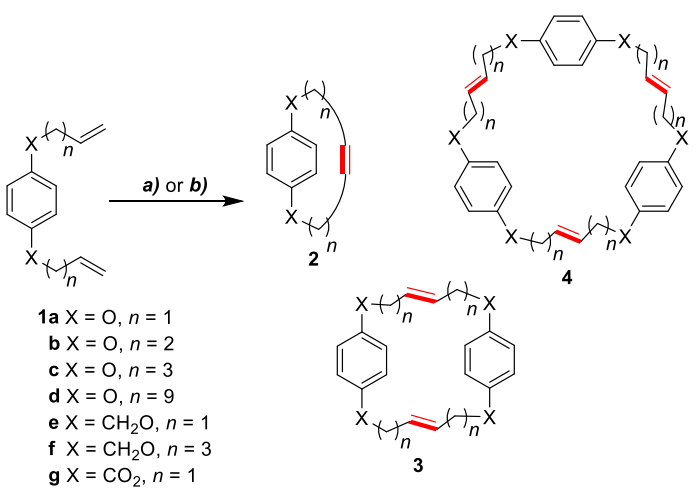

Scheme 1.1. Macrocyclic paracyclophane synthesis via one-pot CM/RCM.[23] *Reagents and Conditions: (a)* **G1** (10 mol%), CH_2Cl_2, 45 °C, (**3a**, 74 %; **3b**, 42 %; **4b**, 35 %; **3c**, 81 %; **2d**, 33 %; **3d**, 47 %; **3e**, 72 %; **4e**, 23 %; **2f**, 70 %); *(b)* **G2** (7 mol%), CH_2Cl_2, 45 °C, (**4g**, 60 %).

The synthesis of macrocyclic dienes **9a**/**b** disclosed by Kotha and co-workers is an excellent example where one-pot CM/RCM reactions can be employed in the construction of 1,3-indanedione cyclophane derivatives (Scheme 1.2). Double alkylation of commercial 1,3-indanedione **5** with *meta*-and *para*-bromobenzyl bromides using freshly prepared KF-celite, followed by a Pd-catalysed Suzuki coupling catalyzed in the presence an excess of commercial allyl boronic acid gave the desired diallyl compounds *m*-**6a** and *p*-**6b**. These were then subjected to one-pot CM/RCM reactions with metathesis catalyst **G1** (10 mol%) in the presence of Ti(O^iPr)$_4$ (20 mol%) to afford the desired dimeric macrocycles **8a** (54 %) and **8b** (45 %). Hydrogenation of these using Pd/C gave the corresponding 1,3-indanedione cyclophane derivatives **9a** and **9b** in 80 % yield.[24]

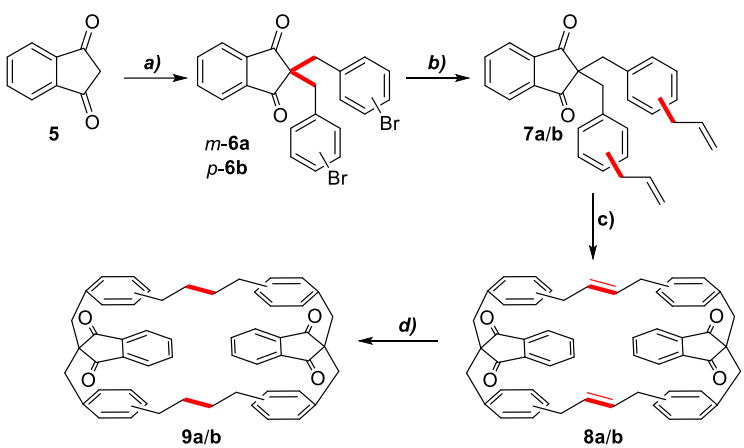

Scheme 1.2. Macrocyclic indanedione-derived cyclophane synthesis via one-pot CM/RCM.[24] *Reagents and Conditions*: *(a)* *m*-bromobenzylbromide/*p*-bromobenzylbromide, KF-Celite, MeCN, RT, (**6a**, 74 %, **6b**, 70 %); *(b)* allylboronic acid, CsF, Pd(PPh_3)$_4$, THF, reflux, (**7a**, 76 %, **7b**, 78 %); *(c)* **G1** (10 mol%), Ti(O^iPr)$_4$ (20 mol%), CH_2Cl_2, 40 °C, 6 mM, (**8a**, 54 %; **8b**, 45 %); *(d)* 5 % Pd/C (20 mol%), H_2 (1 atm), EtOAc, RT, (**9a**, 80 %; **9b**, 80 %).

Heterocyclophanes are a family of cyclophanes with a diverse range of properties and applications ranging from metal-binding scaffolds for catalysis to novel anti-cancer agents.[25] Access to normuscopyridine (**16**), an analogue of naturally occurring musk-derived muscopyridine, have been reported through a range of RCM-based strategies.[26-27] Taking advantage of the conformational effects imposed by stereo-directing sulfone groups proximal to the (hetero)aryl ring, Kotha and co-workers disclosed an RCM-based synthesis

of normuscopyridine (**16**) (Scheme 1.3).[27] Diastereomeric bisalkenes **12a**/**b** were prepared via a short two-step sequence from commercial bis(bromomethyl) pyridine **10**. Sulfonylation of lutidine dibromide **10** with sodium benzenesulfinate gave the corresponding bissulfone **11**, which was then alkylated using commercial bromoalkene **14** in the presence of NaH to deliver an inseparable mixture of *trans*- and *cis*-sulfones **12a**/**b**, which was subjected to metathesis reactions catalysed by **G1** (5 mol%).

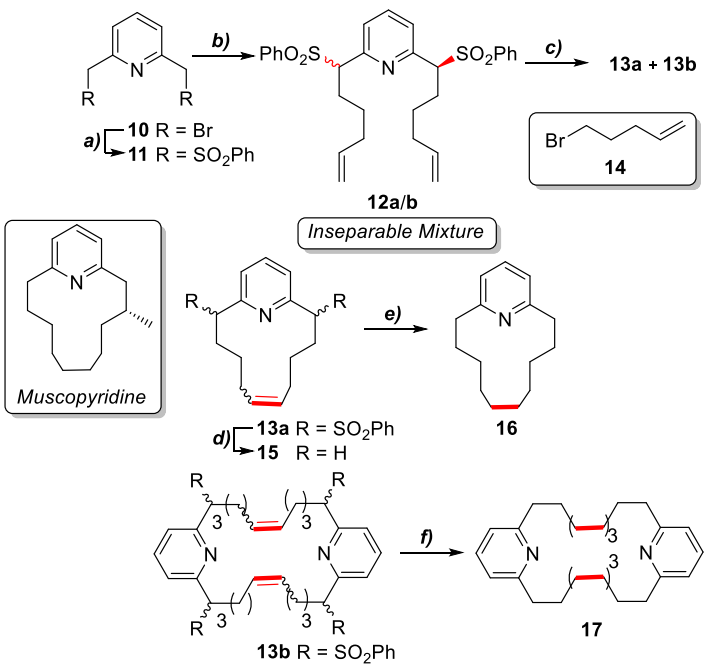

Scheme 1.3. Metacyclophane synthesis via alkene metathesis.[27] *Reagents and Conditions*: *(a)* $NaSO_2Ph$, TBAB, MeCN, Reflux, 24 h (**11**, quant.); *(b)* NaH, **14**, THF, RT, 24 h (**12a**/**b**, 65 %); *(c)* **G1** (5 mol%), CH_2Cl_2, 30 h (**13a**, 51 %, **13b**, 20 %); *(d)* Mg/TMSCl, 1,2-dibromoethane, ethanol, reflux, 12 h (**15**, 80 %); *(e)* H_2, 5% Pd/C, MeOH, RT, 10 h, (**16**, 84 %); *(f) (i)* Mg/TMSCl, 1,2-dibromoethane, ethanol, reflux, 12 h; *(ii)* H_2, 5% Pd/C, MeOH, RT, 10 h, (**17**, 64 %).

A mixture of monomeric (**13a** (51%) and dimeric (**13b** (20%)) cycloalkenes was obtained. Reductive desulfonylation of diastereomeric macrocycles **13a** and **b** using Mg/EtOH in the presence of TMSCl, followed by alkene reduction with Pd/C gave normuscopyridine **16** and heterocyclophane **17** in 64% and 74% yield respectively, over two steps. Adaptation of the above synthetic sequence also gave benzene-based bissulfones **20** and **21**, which were separable on silica (Scheme 1.4). Although *cis*-sulfone **20** only gave the monomeric cycloalkene **22**, *trans*-sulfone **21** gave exclusively macrocyclic dimer **23** during the

metathesis reaction. Reductive desulfonylation of cycloalkene **22** and subsequent reduction gave macrocycle **25**. Similarly, desulfonylation of cyclodiene **23** and alkene reduction furnished cyclophane **26.**

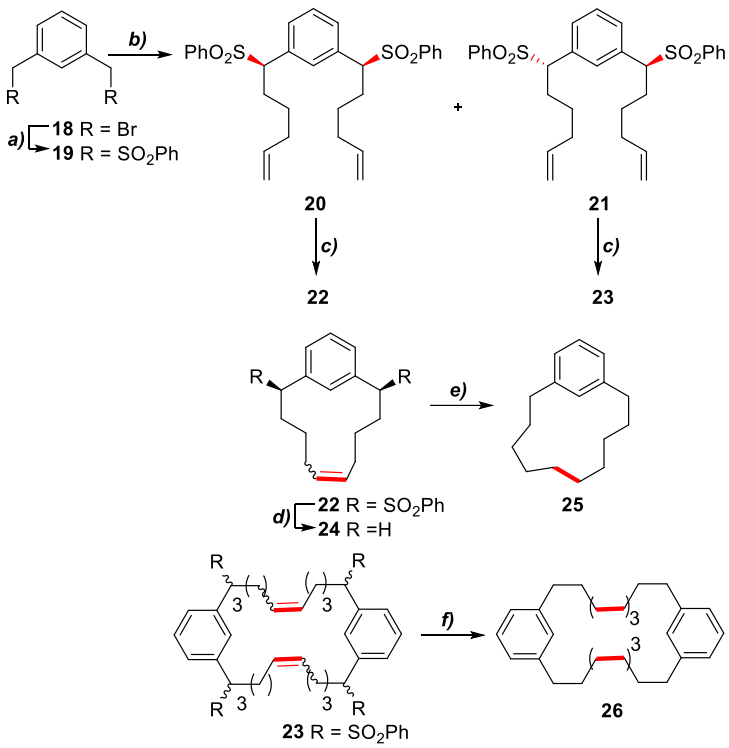

Scheme 1.4. Metacyclophane synthesis via alkene metathesis.[27] *Reagents and Conditions*: *(a)* $NaSO_2Ph$, TBAB, MeCN, Reflux, 24 h (**19**, 87 %); *(b)* NaH, **14**, THF, RT, 24 h (**20**, 29 %, **21**, 30 %); *(c)* **G1** (5 mol%), CH_2Cl_2, 30 h (**22**, 51 %, **23**, 42 %); *(d)* Mg/TMSCl, 1,2-dibromoethane, ethanol, reflux, 12 h (**24**, 81 %); *(e)* H_2, 5% Pd/C, MeOH, RT, 10 h, (**25**, 92 %); *(f) (i)* Mg/TMSCl, 1,2-dibromoethane, ethanol, reflux, 12 h; *(ii)* H_2, 5% Pd/C, MeOH, RT, 10 h, (**26**, 78 % over two steps).

1.2.2 Applications of one-pot CM/RCM in Natural Product Synthesis

Cylindrocyclophanes are a class of naturally occurring cyclophanes that possess unique structural and biological properties. Originally isolated from a blue-green algae of the species *Cylindrospermum licheniforme* Kützing (ATCC 29204) by Moore and co-workers in 1990, these macrocyclic molecules exhibit cytotoxic activity against KB and LoVo tumor cancer lines (IC_{50} = 2–10 μg/mL).[28] Synthetic endeavors towards cylindrocyclophane family members began in the early 2000s, with several syntheses of (–)-cylindrocyclophanes **A** and **F** and related analogues.[29-31] A diverse range of synthetic methodologies have been employed to forge the *[7,7]*-paracyclophane scaffold and introduce the various stereocentres.

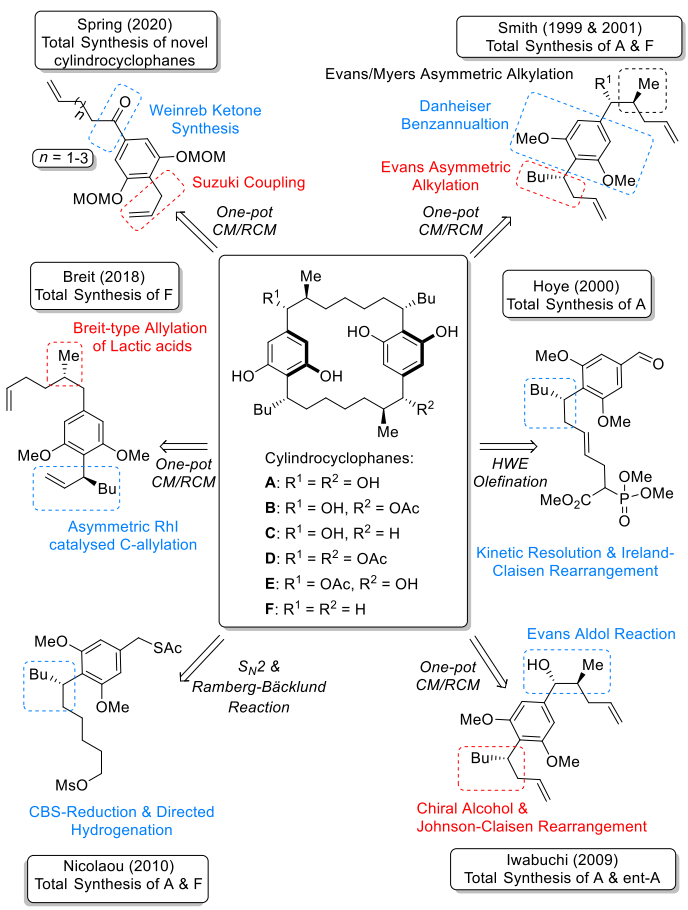

Figure 1.4. Synthetic approaches to natural and unnatural Cylindrocyclophanes.

Elegant contributions to the total syntheses of cylindrocyclophanes **A** and **F** were reported by the Hoye group (2000) and Nicolaou and co-workers (2010) (Figure 1.4); however these relied on the assembly of the macrocyclic frame through non-metathesis-based approaches and therefore will not be discussed in this section.[32-33]

In 2001, Smith and co-workers reported the first total syntheses of (–)-cylindrocyclophane **A** utilizing a late-stage one-pot CM/RCM approach, while construction of the aryl motif in the bis(alkene) monomer **27** was achieved via a Danheiser benzannulation (Figure 1.4).[34-35] One-pot CM/RCM reaction of TES-silyl ether **27** using Schrock's catalyst **SHa**, gave the macrocyclic bis(alkene) **28** with high *E,E*-selectivity in 77% yield (Scheme 1.5(i)). Desilylation of macrocycle **28**, alkene hydrogenation using Adam's catalyst and a final demethylation afforded (–)-cylindrocyclophane **A** in 60 % yield over three steps. In 2009, utilising a similar one-pot CM/RCM-based strategy, Iwabuchi and Shibata reported an enatiodivergent synthesis of (-)-cylindrocyclophane **A** and (+)-cyclindrocyclophane **A** (Figure 1.4).[36] Access to both enantiomers was possible using a key chiral platform **29** (Scheme 1.5(ii)), which could be converted directly to the two monomers (-)-**27** and (+)-**27**. Dimerisation of these monomers was best achieved via a one-pot CM/RCM in the presence of Grubb's catalyst **G2** in DCE. Desilylation of macrocycles **28** and **30**, alkene reduction and demethylation, delivered both enantiomers of cylindrocyclophane **A**. Rigorous biological testing indicated that the 2,5-dialkylresorcinol motif is the primary source of the inherent cytotoxicity in these compounds, while the *[7.7]*paracyclophane scaffold appears to have an enhancing effect on the potency of the resorcinol toxicophore. *In vitro* testing of synthetic (−)-cylindrocyclophane **A** and (+)-cyclindrocyclophane **A** revealed that both enantiomers exhibited the same levels of cell growth inhibition in both KB and LoVo tumor cell lines (GI_{50} = 2 μM). This demonstrates that the observed biological implications of (−)-cylindrocyclophane **A** elicit through a series of biochemical events where chirality does not seem to play a dominant role.

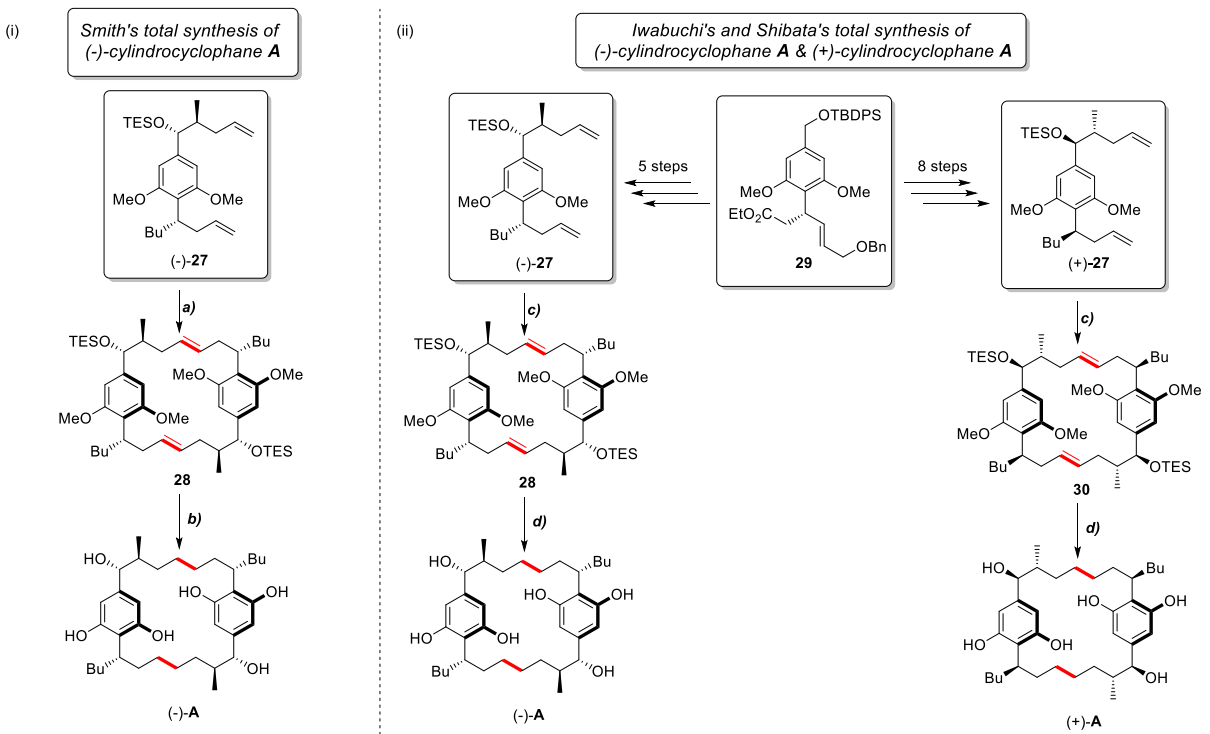

Scheme 1.5. Total syntheses of (–)-cylindrocyclophane **A**: *(i)* Smith's total synthesis of (–)-cylindrocyclophane **A**; *(ii)* Iwabuchi's and Shibata's total synthesis of (–)-cylindrocyclophane **A** & (+)-cylindrocyclophane **A**.[34-36] *Reagents and conditions*: *(a)* **SHa** (34 mol%), benzene, RT, 75 min, (**28**, 77 %); *(b)* TBAF, THF, 0 °C to RT, 2 h, 71 % then H_2 (1 atm), PtO_2 (cat.), EtOH, RT, 75 min, quant. then PhSH, K_2CO_3, NMP, 215 °C, 6 h, ((-)-**A**, 85%); *(c)* **G2** (34 mol%), DCE, 80 °C, h; *(d)* TBAF, THF, 0 °C to RT, 2 h, then H_2 (1 atm), PtO_2 (cat.), EtOH, RT, 75 min, quant. then PhSH, K_2CO_3, NMP, 215 °C, 6 h, ((−)-**A**, 85 % over two steps; (+)-**A**, 85 % over two steps).

The first total synthesis of (–)-cylindrocyclophane **F** was also reported by Smith and co-workers. Assembly of the resorcinol core in the desired dimerization precursor **32** was achieved in an overall 63 % yield via a three step-sequence also featuring an initial benzannulation reaction (Figure 1.4).[35] The one-pot CM/RCM reactions of monomer **31** were subsequently examined utilising a range of alkene metathesis catalysts (Scheme 1.6 (i)). The target molecule ((−)-**F**) was obtained through alkene hydrogenation and removal of the methyl ether groups in 60 % yield over three steps. In 2018, Breit and co-workers also reported the total synthesis of cylindrocyclophane **F** (Figure 1.4).[37] Forging of the C_2-symmetric [*7,7*]-paracyclophane core was achieved via a late-stage homodimerisation of allylic building block **33**, through a one-pot CM/RCM cascade utilising Grubb's second-generation catalyst **G2**, providing dimer **34** in 84% yield. Alkene reduction and aryl methyl ether deprotection gave cylindrocyclophane **F** in 79% yield over two steps (Scheme 1.6 (ii)).

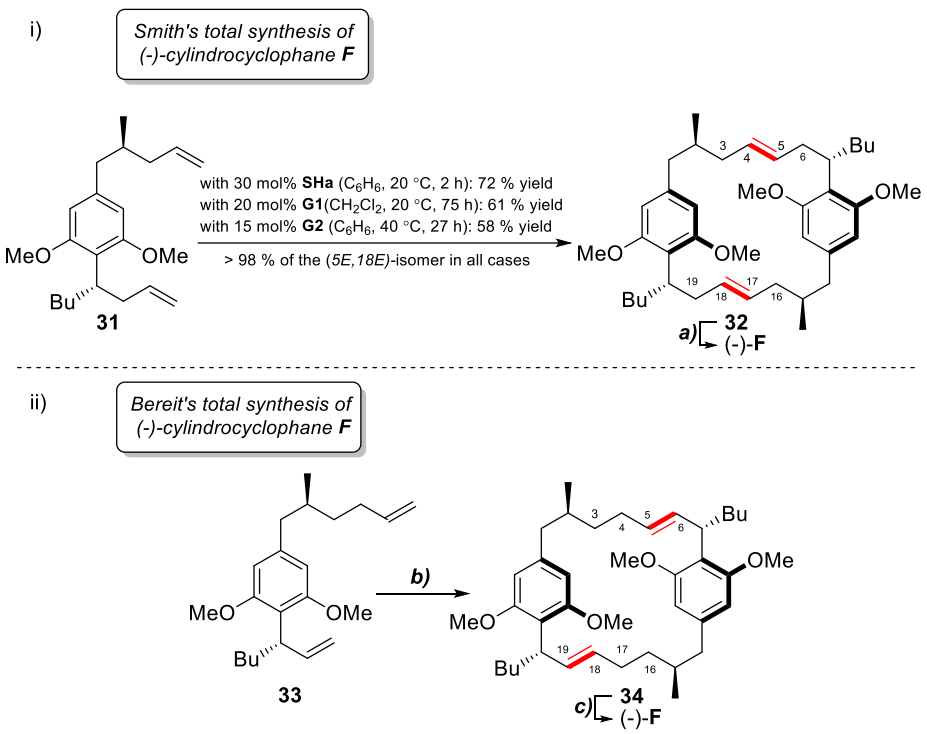

Scheme 1.6. Total syntheses of (–)-cylindrocyclophane **F**: *(i)* Smith's total synthesis of (–)-cylindrocyclophane **F**; *(ii)* Bereit's total synthesis of (–)-cylindrocyclophane **F**.[35,37] *Reagents and conditions*: *(a)* **32**, H_2 (1 atm), Pd/C (10 wt%, 1.61 mg/mmol), EtOAc, RT, 20 h; then BBr_3, CH_2Cl_2, RT, 2.5 h,(**F**, 84 %); %); *(b)* **G2** (15 mol%), CH_2Cl_2, 60 °C, 6 h, (**34**, 84%); *(c) (i)* Pd/C (10 wt%, 200 mg/mmol), H_2 (1 atm), EtOAc, RT, 12 h; *(ii)* BBr_3, CH_2Cl_2, 0 °C to RT, 5 h, (**F**, 79% over 2 steps).

Smith's total synthesis of cylindrophane **F**, features the first example of a synthetic study whereby chemical synthesis and *in silico* methods were used to uncover the sequence of metathesis events underlying one-pot CM/RCM reactions.[35] As commented by the authors, since both Mo and Ru based complexes delivered selectively macrocycle **32** (Scheme 1.6 (i)); the selectivity of these one-pot iterative alkene metathesis reactions must stem from a cascade of reversible metathesis steps, which drives these reactions towards the formation of the most energetically favoured isomer (**32**) via an initial CM reaction. To explore this hypothesis from a theoretical perspective, a series of Monte Carlo conformational searches were performed using the MM2 force field to determine the relative energies of all possible cyclic dimers of bisalkene **31**. These calculations indicated that the macrocycle **32** is the lowest energy isomer relative to all other possible dimers by 2.6−4.7 kcal mol^{-1}. To gain experimental evidence for their proposed cascade of reversible metathesis steps favouring the selective formation of head-to-tail (H-to-T) dimer **32**,

the RCM reactions of linear dimers **35** and **36** were investigated. Despite the expected predisposition of these acyclic dimers to form the *[8,6]*-macrocycle **37** via RCM reactions, trienes **35** and **36** afforded only the *[7,7]-E,E*-paracyclophane **32** in yields ranging from 75 to 81% for the Schrock alkylidene (**SHa**) and from 66 to 70% for the Grubbs second generation catalyst (**G2**) (Scheme 1.7).[35]

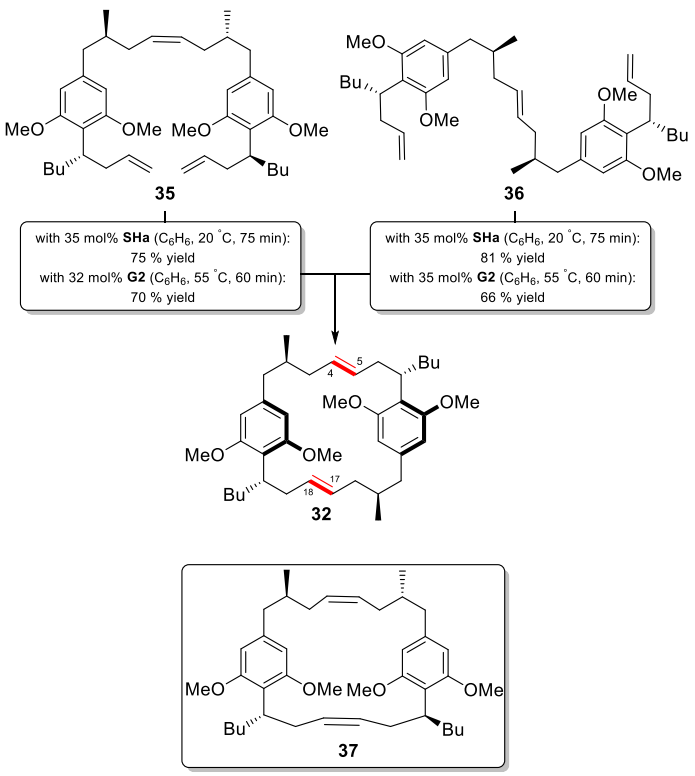

Scheme 1.7. RCM reactions of linear dimers **35** & **36** catalysed by alkene metathesis catalysts **SHa** and **G2**.[35]

The above results clearly demonstrate that the high selectivity favouring the H-to-T dimer **32** arises through the initial formation of a CM product that undergoes macrocyclisation. Conversely, any higher energy linear dimers formed, presumably undergo rapid molecular editing via a cascade of alkene metathesis reactions which eventually give rise to the thermodynamically favoured *[7,7]-E,E*-paracyclophane **32**.

More recently, Spring and co-workers reported a one-pot CM/RCM based divergent synthesis of unnatural novel cylindrocyclophanes of variable ring sizes, functionalisation and levels of oxidation around the macrocyclic framework.[38] Of these several novel inhibitors of *Staphylococcus aureus* and methicillin-resistant *S. aureus* were identified. The one-pot CM/RCM reactions of a homologous series of acyclic

monomers (**38a**-**c**) of variable alkenyl chain lengths were investigated (Scheme 1.8). H-to-T cyclodimersations of acyclic precursors catalysed by Grubb's catalysts **G2**, followed by basic hydrolysis furnished a collection of *[m.n]*paracyclophane scaffolds **40a**-**c** (87-89 %).

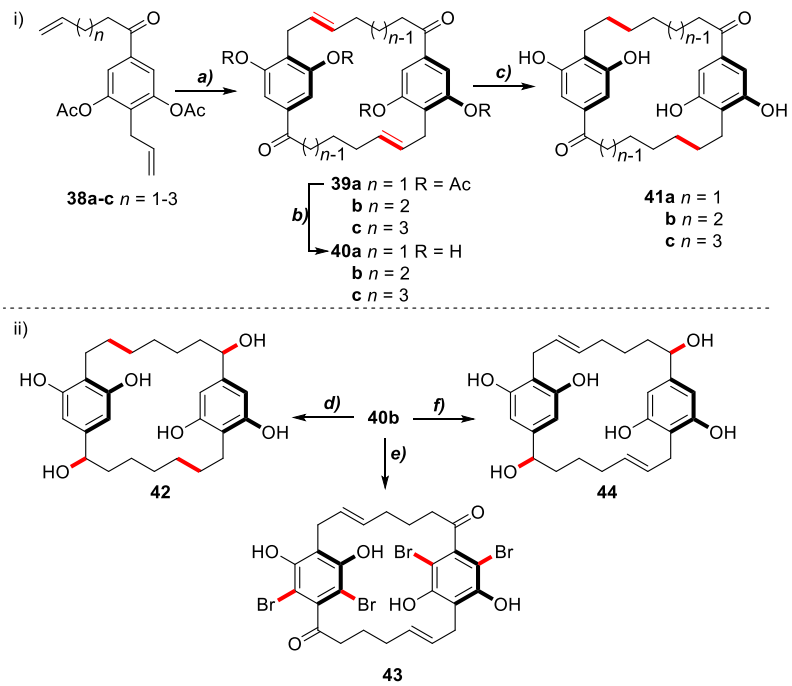

Scheme 1.8. Final steps in the Spring synthesis of novel cylindrocyclophane analogues and downstream functionalisation.[38] *Reagents and conditions*: *(a)* **G2** (5 mol %), CH_2Cl_2, reflux, 20 h, (**39a**, 16 %; **39b**, 61 %; **39c**, 6 %); *(b)* NaOH, MeOH/CH_2Cl_2/H_2O (4:1:1), RT, 1 h, (**40a**, 87 %; **40b**, 89 %; **40c**, 87 %); *(c)* H_2 (1 atm), Pd/$BaSO_4$ (10 wt %), acetone, RT, overnight, (**41a**, 60 %; **41b**, 35 %; **41c**, 47 %); *(d)* $NaBH_4$, MeOH, RT, 30 min, then Pd/$BaSO_4$ (10 wt %), acetone, RT, overnight, (**42**, 68 %); *(e)* pyridinium tribromide, EtOH, RT, overnight, (**43**, 23 %); *(f)* $NaBH_4$, MeOH, RT, 30 min, (**44**, 55 %).

The reduced isolated yields reported for macrocycles **39a** (16 %) and **39c** (6 %), were due to the formation of both symmetric and unsymmetric cyclic trimers. Alkene reduction using Rosenmund's catalyst afforded unnatural cylindrocyclophane analogues **41a**-**c** (35-60%). Downstream functionalization of *[7.7]*cylindrocyclophane **40b** also led to a small set of macrocyclic analogues (**42**-**44**) such as the tetrabrominated cylindrocyclophane **43**. In vitro testing of these macrocycles, indicated that both [*7.7*]cylindrocyclophanes (**40b** & **41b**) and [*8.8*]cylindrocyclophanes (**40c** & **41c**) were effective inhibitors of *S. aureus* and *EMRSA-15*. In light of the above results, the authors suggested that expansion of the 22-

membered macrocyclic ring might tolerated but not contraction. This was further corroborated by the fact that both [*6.6*] cylindrocyclophanes **40a** and **40a** exhibited little activity in all assays.[38] Furthermore, tetrabrominated analogue **43** (MIC 12.5 µM), unlike its unsubstituted congener **40b** (MIC > 200 µM) was remarkably more efficient at arresting bacterial growth for both *S. aureus* and *EMRSA-15*. In turn, this highlights the favourable impact of unnatural substitutions such as bromination in the development of novel antibiotics.

1.3. Applications of one-pot CM/RCM in the Synthesis of Biomolecules

1.3.1. Oligosaccharides via one-pot CM/RCM

Oligocationic macromolecules including polyamines play a crucial role in a range of key biological processes, including DNA replication and RNA synthesis. Their pharmacological activity stems from their ability to selectively bind to polynucleotides. Naturally occurring aminodeoxy sugars are usually present in glycoconjugates such as daunorubicin and neomycin.[39] Kirschning and co-workers investigated the alkene metathesis reactions of bisaminooligosaccharides **45** and **48a**/**b**.[40] Interestingly, the outcome of these reactions were highly dependent on the configuration of saccharide starting material. When a solution of arabinose-configured acyclic bisalkene **45** in benzene was treated with complex **G1** at 47 °C, monomeric cycloalkene **46** was obtained as a single product in 67 % yield (Scheme 1.9).

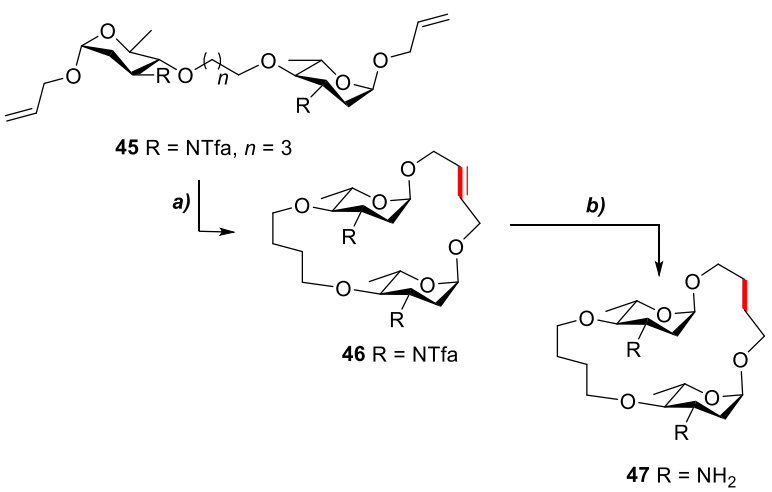

Scheme 1.9. Metathesis reaction of *arabino*-configured disaccharide and alkene reduction.[40] *Reagents and conditions*: *(a)* **G1** (20 mol%), C_6H_6, 47 °C, 24 h, (**46**, 67%; *(b)* (i) PtO_2, H_2, CH_2Cl_2/MeOH (10:1), RT, 16 h; (ii) aq. NaOH/THF (2:1), RT, 24 h, (**47**, 87 %).

Hydrogenation with Adam's catalyst, followed by hydrolysis gave the fully saturated macrocycle **47** in 87% yield. On the other hand, subjecting the ribose-configured monomer **48a** to the same reaction conditions, gave a mixture of two aminoglycosides: dimer **49a** (64%) and trimer **50a** (16%) (Scheme 1.10). As

commented by the authors, a subtle change in the configuration of substituents in aminodeoxyhexose fragments, such as the introduction of an axial amino group at C-3 might be hindering the intramolecular cyclization of acyclic monomer **48a** and therefore favouring the formation of cyclic dimer **49a** and trimer **50a**. Catalytic hydrogenation followed by basic hydrolysis of the dimer and trimer delivered the corresponding tetrasaccharide **51a** and hexasaccharide **52a** in quantitative yields. Preparation of the ^{15}N-labelled derivatives **51b** and **52b** was possible via the same route as macrocycles **51a** and **52a**.[41] NMR studies focused on unraveling the binding properties of macrocyclic derivatives **51b** and **52b** with RNA structures, revealed that these scaffolds preferentially bind to mRNA regions such as the interior loops and stem-loops.

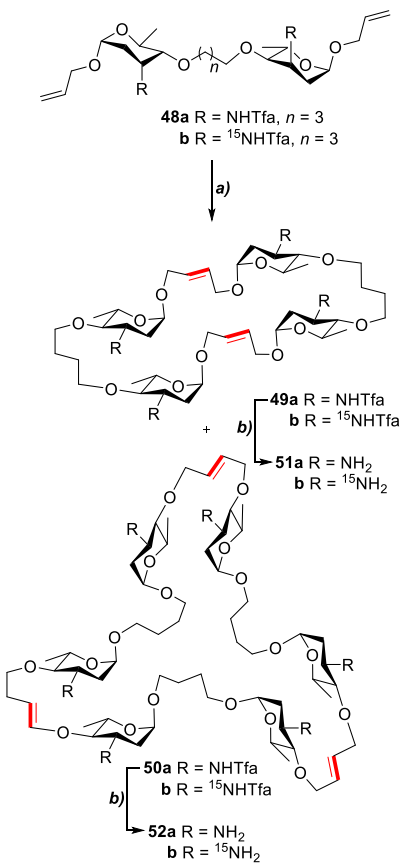

Scheme 1.10. Metathesis reaction of ribose-configured disaccharide and alkene reduction.[41] *Reagents and conditions*: *(a)* **G1** (20 mol %), benzene, 50 °C, 20 h (**49a**/**b**, 64%; **50a**/**b**, 16%); *(b)* (i) PtO_2, H_2, EtOAc, RT, 24 h; (ii) aq. NaOH/THF (2:1), RT, 24 h, (**51a**/**b**, quant.; **52a**/**b**, quant.).

1.3.2. Cyclic Peptides via one-pot CM/RCM.

Cyclic peptides are a special class of polypeptides, with a diverse range of biological and therapeutic activities, including anti-cancer, immunosuppressive as well as antibacterial activity. These are commonly found in several living organisms including bacteria and plants.[42]

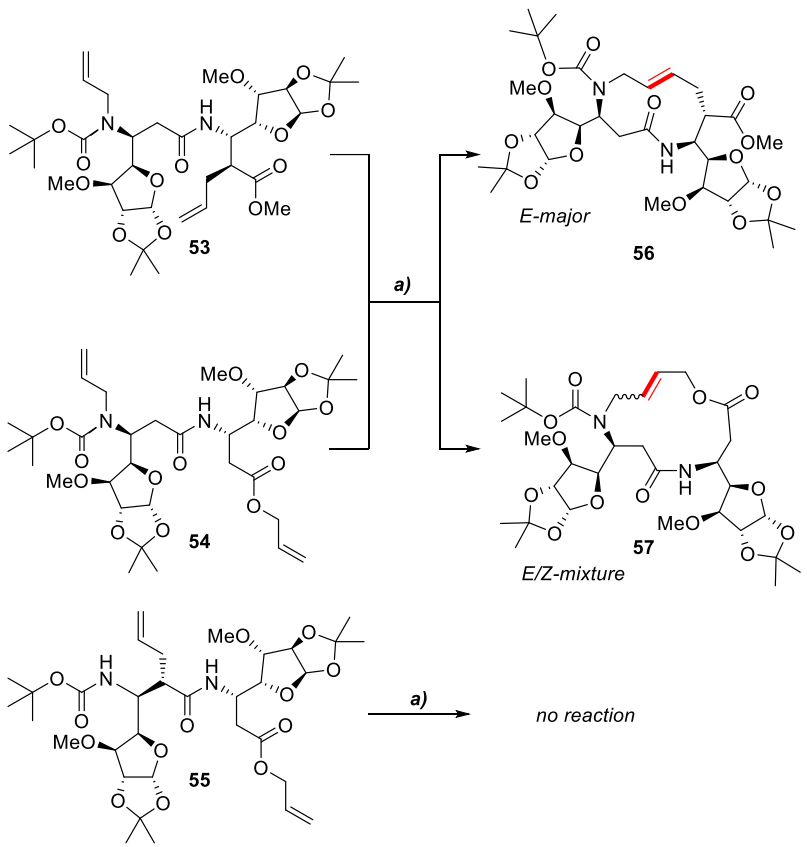

Scheme 1.11. Alkene Metathesis Reactions of β-Dipeptides **53**-**55**.[43] *Reagents and conditions*: *(a)* **G2** (5 mol%), toluene, 80 °C, 16 h, (**56**, 71 %; **57**, 84 %).

The alkene metathesis reactions of β-dipeptides synthesised from β-amino acids substituted with a pentose side chain at the Cβ position and armed with two allyl groups either at the Cα, O, or N positions, catalysed by complex **G2** were reported by Bruneau and co-workers.[43] Depending on the positions of the allyl arms along the dipeptide backbone and the availability of the reactive terminal olefin groups, no reaction, RCM (Scheme 1.11) and one-pot CM/RCM products (Scheme 1.12) were obtained. Cyclic

peptides were obtained in good yields with dipeptides substituted with BocN-allyl/C allyl groups (**53**) and BocN-allyl/O-allyl groups (**54**) (Scheme 1.11). Conversely, when the allyl groups branched off the alpha-carbon, the metathesis reaction was not possible. Dipeptides **58a**-**c** with C-allyl and O-allyl groups preferentially undergo one-pot CM/RCM to give the *E,E*-cyclic dimers **59a**/**b**/**c** as the major product in 74-78% yield (Scheme 1.12). Trace amounts of cyclic monomer **60c** were also observed upon treatment of diene **58c** with catalytic amounts of complex **G2** in toluene at 80 °C. The subtle difference in reactivity observed highlights the pronounced effects of both steric hindrance at the beta-carbon and hydrogen bonding in these peptides.

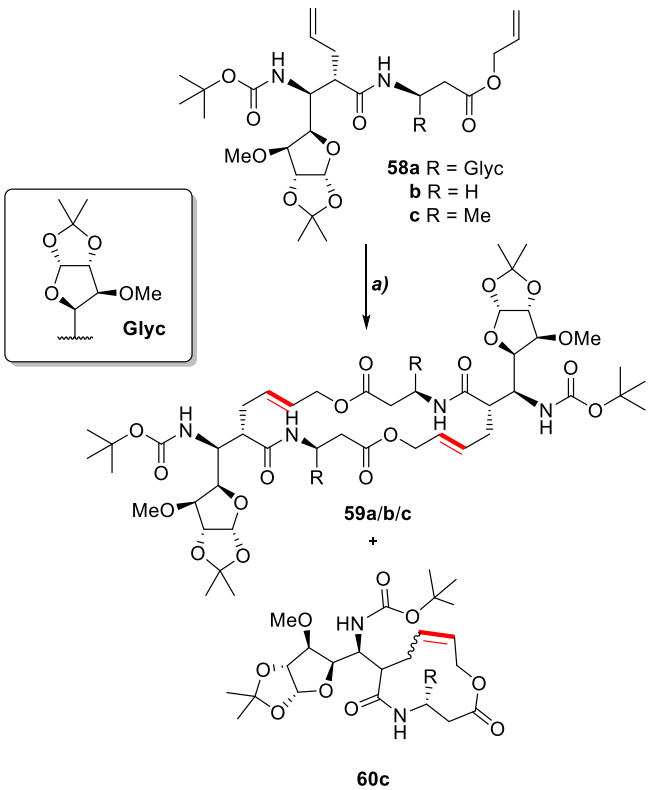

Scheme 1.12. One-pot CM/RCM Reactions of β-Dipeptides with C-allyl and O-allyl Groups.[43] *Reagents and conditions*: *(a)* **G2** (5 mol%), toluene, 80 °C, 16 h, (**59a**, 76 %; **59b**, 78 %; **59c**, 74 %).

1.4. Polyaromatics via one-pot CM/RCM

1.4.1. Synthesis of Artificial Transmembrane Channels via one-pot CM/RCM and ACM/RCAM

Phenylene vinylene macrocycles (PVMs) are a family of cyclophane molecules with a shape-persistent skeleton. The first successful example of a one-step synthesis of phenylene vinylene macrocycles (PVMs) through a one-pot CM/RCM reactions of diene building blocks **61** and **63** was reported by Jin *et al.* (2010).[44] Cyclooligomerisation of the divinyl substituted precursors **61** and **63** was catalysed by Ru-alkylidene **G2**, under a steady stream of nitrogen or vacuum to removal the released ethylene (Scheme 1.13). Separation of the desired thermodynamically stable macrocycles **62** and **64** from higher-order oligomers or polymers was possible via gel permeation chromatography (**62**, 64 %; **64**, 57%).

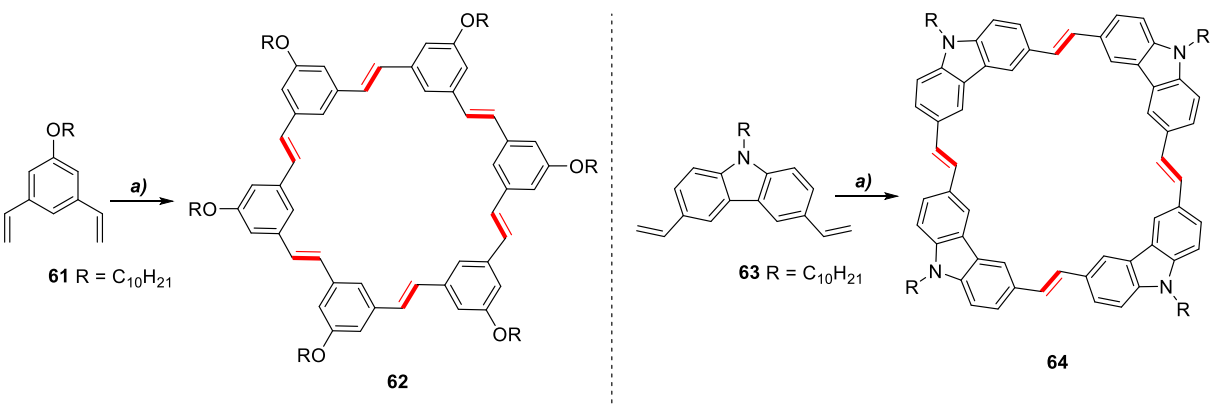

Scheme 1.13. Phenylene vinylene macrocycles (PVMs) via one-pot CM/RCM.[23] *Reagents and Conditions*: *(a)* **G2**, 1,2,4-TBC, 35 °C, 16 h (**62**, 64 %; **64**, 57 %).

Artificial membrane channels or pores have received considerable attention over the recent years due to the wide-ranging biological functions of natural transmembrane channels.[45] Flexible macrocyclic scaffolds such as crown ethers and cyclodextrins substituted with functional hydrophobic arms are among the most commonly used designs of artificial receptors, whilst more rigid shape-persistent variants are less explored.[46] A small library of PVMs was investigated by Zhang and co-workers as potential transmembrane ion channels (Scheme 1.14).[47] Hexameric PVMs were synthesised through the one-pot

metathesis reactions of *m*-divinylbenzenes (**65a**-**d**). Alkene metathesis reactions were carried out in the presence of catalyst **G2** at 40 °C under a stream of nitrogen to remove the released ethylene. Routine chromatography sufficed to obtain PVMs **66a**-**d** in fair to very good yields (45 – 85%).

The mass transport activity of these macrocycles was assessed by a fluorescence-based assay using unilamellar liposomes and 8-hydroxypyrene-1,3,6-trisulfonate (HPTS) as the fluorescent probe. In general, ion transport activity observed in PVMs **68a**-**d** could be attributed to the increased flexibility of the PVM-scaffold, which facilitates both their insertion into lipid bilayers and rearrangement for ion transportation. Furthermore, the fine balance between length and polarity of substituent decorating the periphery of PVMs plays a crucial role in their ion-transport ability.

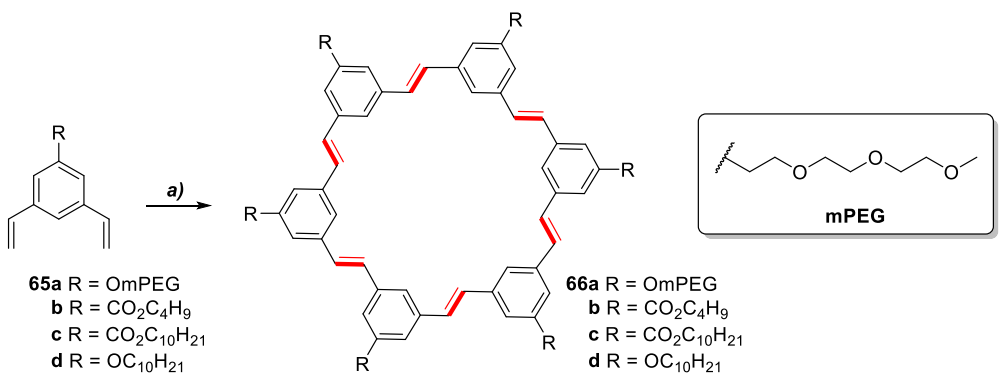

Scheme 1.14. Artificial receptor synthesis via one-pot metathesis reactions.[47] *Reagents and Conditions*: *(a)* **G2** (10 mol%), 1,2,4-TBC, 40 °C (**66a**, 85 %; **66b**, 74 %; **66c**, 45 %; **66d**, 64 %).

Although the exact nature of the PVM-assemblies incorporated in the lipid bilayer remains elusive, PVMs bearing hydrophilic substituents exhibit poor affinity for lipid membranes. More specifically, PEG-substituted macrocycle PVM **66a** was completely inactive in the HPTS assay. Conversely, truncated variants such as PVM **66b** tend to rapidly self-aggregate in solution, leading to slow incorporation therefore low activity in the fluorescence-based assay. On the other hand, long aliphatic sidechains generally have a higher affinity for membranes and a tendency to incorporate rapidly into the lipid layer (**66c** and **66d**). The highest activity was observed for decylether chain substituted PVM **66d**.

1.4.2. Molecular Electronics via One-pot CM/RCM

Hexa-*peri*-hexabenzocoronenes (HBCs) are polycyclic aromatic hydrocarbons that self-assemble in a face-to-face fashion to generate columnar architectures. These highly cohesive thermotropic columnar mesophases are even observed with monomeric HBCs decorated with flexible substituents and remain intact well above 400 °C. Moreover, these molecules can also readily form aggregates in common organic solvents that persist well below micromolar concentrations. Interestingly, single HBC disks were shown to exhibit diode-like behaviour in a circuit between highly ordered synthetic graphite and the tip of a scanning-tunnelling microscope (STM).[48]

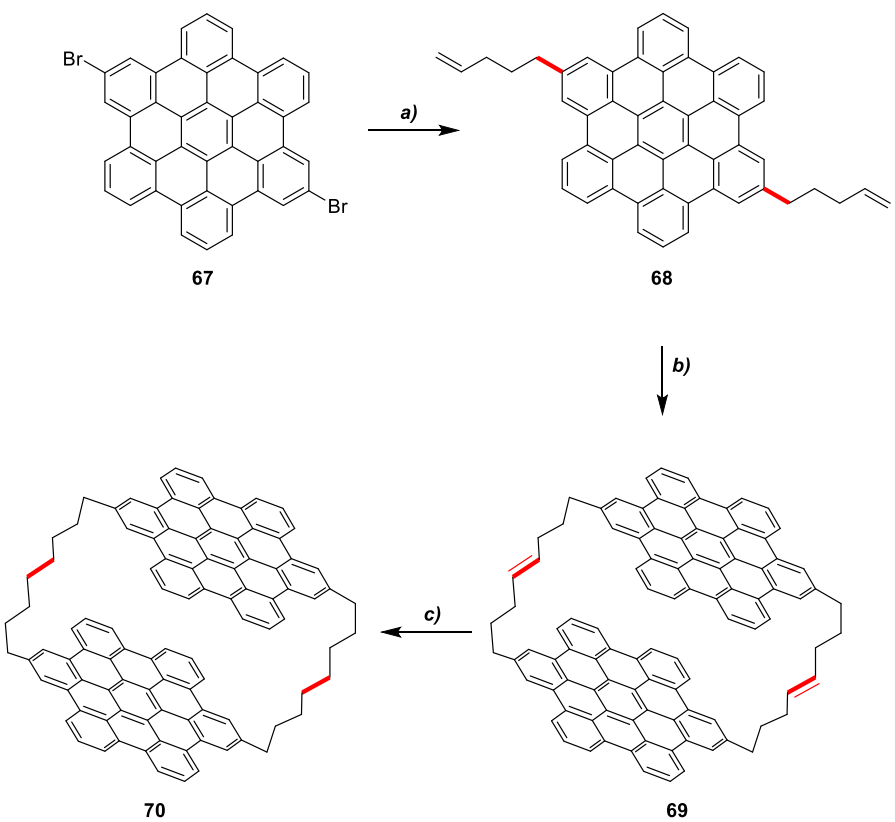

Scheme 1.15. Hexa-*peri*-hexabenzocoronene disks via one-pot CM/RCM.[49] *Reagents and Conditions: (a)* 4-pentenyl magnesium bromide, $Pd(dppf)Cl_2 \cdot CH_2Cl_2$, THF, 55 °C, (**68**, 94 %); *(b)* **G1** (5 mol%), toluene, RT, (**69**, 64%); *(c)* H_2, 10% Pd/C, THF, RT, 10 h, (**70**, quant.).

Capitalizing on the inherent ability of these polycyclic scaffolds to aggregate in solution even under moderate dilution, Müllen and co-workers reported the covalent trapping of HBC-based cyclophanes, utilising a one-pot CM/RCM-Pd-hydrogenation approach. Kumada coupling of dibromo HBC **67** in the presence of 4-pentenylmagnesium bromide afforded bisalkene **68** in almost quantitative yield (Scheme 1.15).[49] One-pot CM/RCM in toluene in presence of catalytic amounts of Grubbs' ruthenium benzylidene **G1** gave macrocycle **69** in 64 % yield.[49] Alkene reduction using Pd/C afforded HBC cyclophane **70** in quantitative yield. Assessment of the electrical properties of cyclophane **70** by STM revealed that this molecule also exhibits diode-like properties similar to those previously reported for HBC disks. The covalent linkages introduced did not appear to induce any measurable changes in the intra-or intermolecular stacking, or the packing of the columnar scaffolds.

1.5. Cyclophanes

1.5.1 Synthesis of Cyclophanes via one-pot ACM/RCAM

In contrast to the CM/RCM synthesis of cyclophanes, ACM/RCAM strategies require the use of metal alkylidynes as catalysts. Moreover, the resultant cyclophane scaffolds are characterised by a more rigid macrocyclic skeleton in comparison to their alkene equivalents.

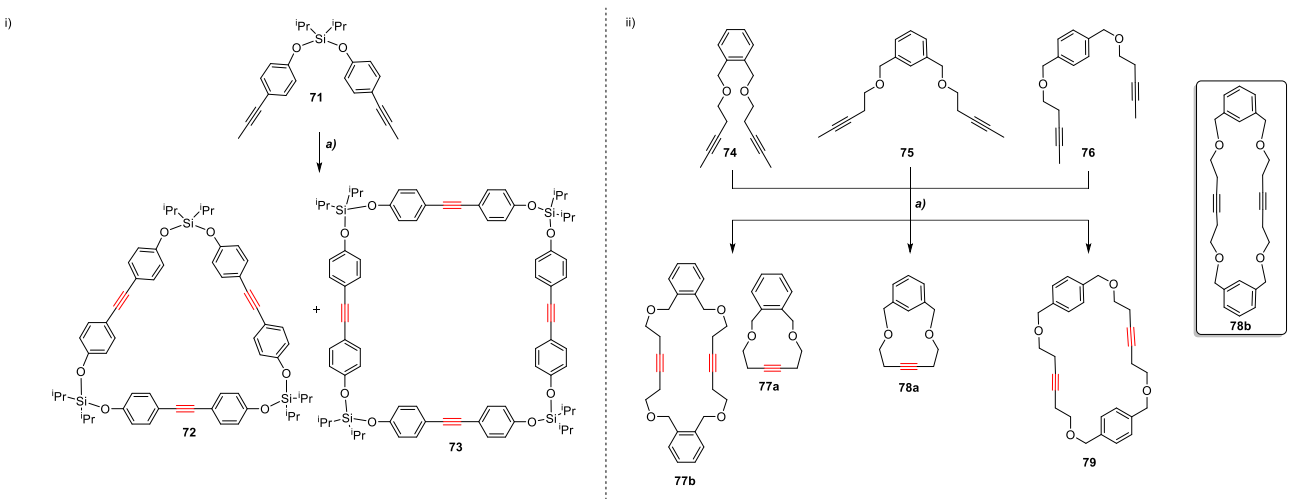

Scheme 1.16. Synthesis of Polysiloxane and *o*-/*m*-/*p*-Cyclophanes via one-pot ACM/RCAM.[50-51] *Reagents and conditions*: *(i) (a)* $Mo(CO)_6$ (*cat.*), Chlorophenol, 140 °C, (**72**, 14 %, **73**, 18 %); *(ii) (a)* **W^{II}** complex (2.0 mol%), *n*-hexane, RT, 350 mbar, 2 h, (**77a**, 18 %; **77b**, 65 %; **78a**, 93 %; **79**, 68 %).

In 2000, Pschirer *et. al.*, reported the synthesis of trimeric and tetrameric polysiyloxanes through the one-pot ACM/RCAM reaction of dipropynylsilylether **71**.[50] Reaction of commercial dichlorodiisopropylsilane with an excess of para-iodophenol, followed by Sonogashira coupling with propyne in the presence of catalytic amounts of $Pd(PPh_3)_2Cl_2$ and CuI gave methyl-capped bisalkyne precursor **71**. Alkyne metathesis of building block **71** in chlorophenol at 140 °C in the presence of $Mo(CO)_6$ gave the corresponding trimeric and tetrameric silyl ethers **72** and **73** in 14-18% yield (Scheme 1.16 (i)). An alkyne metathesis-based protocol for the synthesis of *para*-cyclophane **83** was also reported by Beer *et al.* [51] This strategy also extends to both the *ortho*-, *meta*- and *para*-derivatives (Scheme 1.16 (ii)). Treatment of 1,3-bis(3-pentynyl oxymethyl) benzene building blocks **75**-**76** at room temperature with catalytic amounts of imidazolin-2-

iminato tungsten alkylidyne **W^{II}** under reduced pressure to remove released 2-butyne led to the formation of the corresponding *[10]meta*cyclophane **78a** (93 %) or *[10.10]para*cyclophane **79** (68 %) respectively. Conversely, the one-pot ACM/RCAM reaction of *ortho*-substituted diyne **74** gave a mixture of the dimeric and monomeric cycloalkynes **77a** (18 %) and **77b** (65 %). DFT calculations carried out to rationalize these results, indicated that [*10.10*]*metacyclophane* **78b** is the highest energy dimer relative to [*10.10*]*ortho*cyclophane **78a** (ΔG°= − 2.78 kcal mol^{-1}) and [*10.10*]*para*cyclophane **79** (ΔG°= −9.66 kcal mol^{-1}) by ca. 6.78 – 13.66 kcal mol^{-1}.

1.5.2. Applications of one-pot ACM/RCAM in Natural Product Synthesis

Ring-closing alkyne metathesis (RCAM) in conjunction with stereoselective partial reduction of the cycloalkyne product, furnishes an elegant and reliable approach used extensively in natural product synthesis for generating large ring sizes from relatively simple precursors, whilst offering full control over the stereochemistry of the product alkene.[52-67] More recently, a one-pot ACM/RCAM-based total synthesis was reported featuring a late-stage Lindlar reduction step. The first example of an alkyne-metathesis-based homodimerization approach applied in the synthesis of natural products was reported by Hulme and co-workers. Assembly of the 30-membered macrocyclic core of disorazole C_1 (**80**), was achieved through a highly convergent, modular strategy featuring a late stage-cyclization through a one-pot ACM/RCAM self-assembly process of bisalkyne precursor **81**, followed by Lindar-reduction (Scheme 1.17).[68] Installation of the critical *anti*-steoreorelationship at C(14)-C(16) in the chiral diol fragment **82** was possible through a Sm^{II}-catalysed Evans–Tishchenko reaction of β-hydroxy ketone **83**, while access to the oxazole-containing acid **84** was readily achieved starting from cheap commercially available mannitol derivative **85**. Yamaguchi esterification, through the addition of activated ester derived from acid **84** to alcohol **82** gave the acyclic precursor **81** in 71 % yield. One-pot ACM/RCAM dimerisation of bisalkyne **81** was achieved under optimised conditions using triphenylsilanolate catalyst **Mo^{B}** to give the required head-to-tail (H-to-T) dimer **86a** in 51 % yield. Subsequent PMB deprotection, followed by Lindar reduction afforded macrodiolide **80** in 26 % yield over two steps.

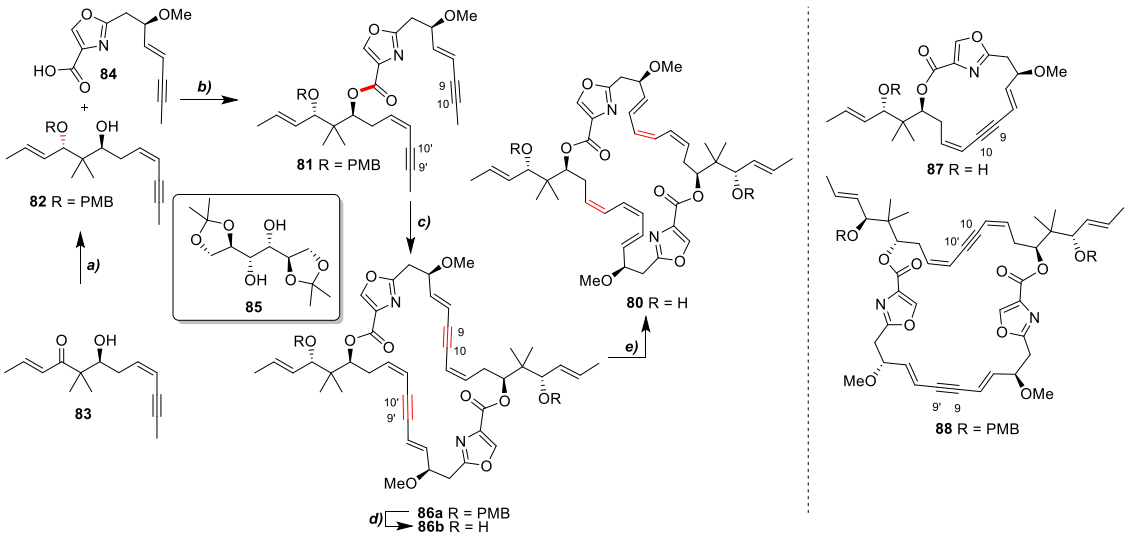

Scheme 1.17. Synthesis of Disorazole C_1 via one-pot ACM/RCAM self-assembly process.[68] *Reagents and conditions*: (a) *(i)* 3-NO_2PhCHO, SmI_2, THF, −20 °C, 4 h, 94 %; (*ii)* PMB-TCA, $Sc(OTf)_3$, toluene, 0 °C to RT, 1 h, 79 % (*iii*) LiOH, MeOH:H_2O (10:1), reflux, 18 h, (**82**, 91 %); *(b)* 2,4,6-trichlorobenzoyl chloride, Et_3N, toluene, DMAP, 40 °C, 18 h, (**81**, 71 %); *(c)* **Mo^B** (20 mol%), 4 Å/5 Å MS (1:1), RT, 16 h (**86a**, 51 %), (**88**, 11 %); *(d)* DDQ, CH_2Cl_2: phosphate buffer (1:1), RT, 30 min, (**86b**, 61%); *(e)* H_2, Lindlar catalyst, EtOAc, RT, 6 h, (**80**, 11%)

In 2006, Hoffmann *et al.* investigated the synthesis of tetrahydro-disorazole C_1 **86b** via a stepwise dimerization approach through initial intermolecular esterification, followed by lactonisation.[69] While an *in silico* analysis indicated the preferential formation of H-to-T dimer **86b** over the cyclic monomer **87** by 136 kJ mol^{-1}, [70] neither were observed under a range of experimental reaction conditions.[71] Conversely, DFT calculations carried out by the Hulme group indicated a predicted ratio of 3:1 with respect to H-to-T (**86a**) and head-to-head (H-to-H) dimers (**88**). Moreover, this predicted ratio (3:1) was in line with the experimental data also provided by the Hulme group; treatment of bis(enyne) **81** with triphenylsilanolate complex **Mo^B**, afforded a mixture of bis(lactones) **86a** and **88** in 62 % yield, while an experimental ratio of 5:1 was observed with respect to H-to-T (**86a**) and H-to-H (**88**) dimers.

1.6. Polyaromatics via one-pot ACM/RCAM

1.6.1. Applications of the one-pot ACM/RCAM in the Synthesis of PEMs.

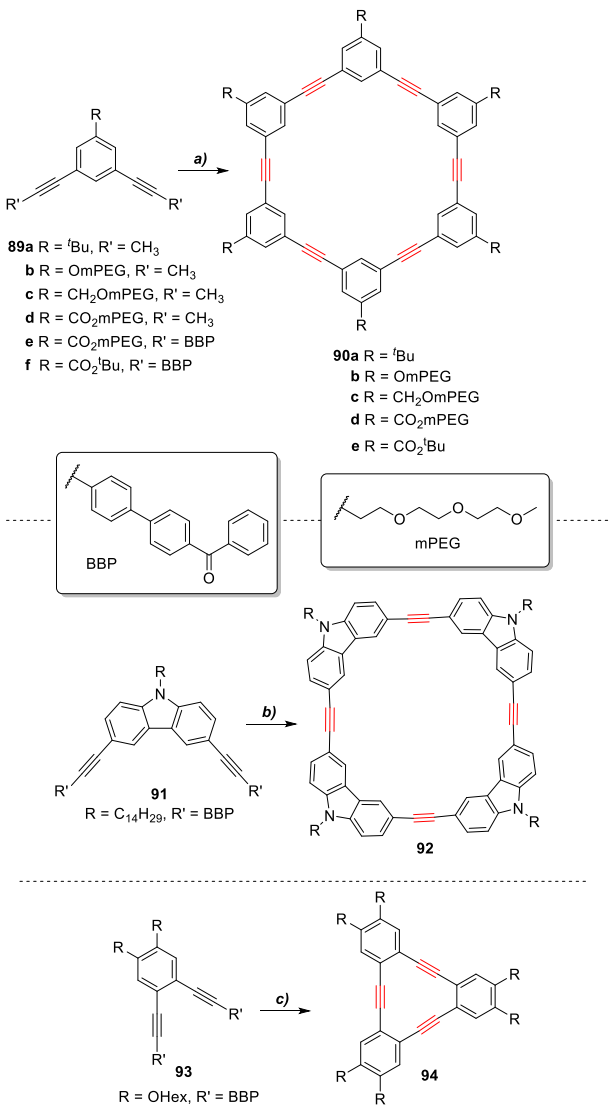

Scheme 1.18. Precipitation-Driven one-pot ACM/RCAM mediated synthesis of PEMs.[72,73] *Reagents and conditions*: *(a)* **Mo^C** complex (10 mol%), *p*-nitrophenol (30.0 mol%), CCl_4, 30 °C, 22 h (**90a**, 61 %; **90b**, 68 %; **90c**, 65 %; **90d**, 76 %, **90e**, 77-81 %, **90d**, 79 %); *(b)* **Mo^C** complex (10 mol%), *p*-nitrophenol (30 mol%), CCl_4, 30 °C, 22 h, (**92**, 84 %); *(c)* **Mo^C** complex (10 mol%), *p*-nitrophenol (30 mol%), CCl_4, 30 °C, 22 h, (**94**, 86 %).

Phenylene ethynylene macrocycles (PEMs) are another family of cyclophane molecules similar to PVMs, which also possess a shape-persistent skeleton. Due to their unique structural properties, these have attracted considerable attention over the past decade due to their promising potential in a wide range of applications including fullerene purification/separation, material science, guest-host chemistry, and chemical sensing. Traditionally, these were prepared through various inter-/intramolecular coupling reactions including Suzuki, Sonogashira, Ellington-Glaser and Stephens-Castro, in conjunction with either intramolecular ring-closure of bifunctional oligomeric building blocks or one-step cyclo-oligomerisation. Unfortunately, several of these strategies are not scalable and low-yielding, due to irreversible, undesired oligomerisation.[74-80] Moore and Zhang anticipated that a one-pot ACM/RCAM approach would be a more robust and efficient method to access PEMs. To test this, methyl-capped bisalkynes **89a**-**d** were subjected to metathesis reactions in TBC in the presence of trisamido alkylidyne **Mo^{C}** and *p*-nitrophenol under reduced pressure (1 mmHg) to remove released 2-butyne.[72] On small scale, the desired macrocycles **90a**-**d** were isolated in good yields (61-76%), while alkyne metatheses performed on gram-scale only led to low conversion and poor yields due to competing oligomerisation (Scheme 1.18). Confronted by this impasse, a precipitation-driven strategy was investigated to circumvent this problem.[72,73]

Benzoylbisphenyl-substituted bisalkynes **89e**-**f**, **91** and **93** were synthesised such that subsequent one-pot ACM/RCAM in TCC would lead to the formation of the desired cycloalkynes **90d**-**e** and **92** along with insoluble byproducts that could be readily removed by simple filtration (Scheme 1.18). This precursor design led to the successful synthesis of three types of PEMs **90**, **92** and **94**.[72] To prove the dynamic behaviour of this alkyne metathesis-based approach, scrambling experiments were performed. Treatment of an equimolar mixture of hexameric macrocycles **90a** and **90d** in TCC at 30 °C with alkylidyne **Mo^{C}** and *p*-nitrophenol, furnished a mixture of mixed hexamers (Scheme 1.19 (i)); demonstrating that macrocycle formation is reversible. Moreover, subjecting a 1:2 mixture of trimeric **94** and hexameric **95** cycloalkynes to the same reaction conditions gave the tetrameric PEM **96** as the only product (Scheme 1.19 (ii)).[73,81] These results indicated that the synthesis of PEM via this iterative alkyne metathesis-based approach is thermodynamically controlled.

Variable temperature studies on the one-pot ACM/RCAM reactions of monomer **89e** (30 °C to 95 °C), revealed a temperature-dependent decrease in the ratio of hexameric and pentameric PEMs **90d** and **97** formed (6.5:1 to 2.9:1) (Scheme 1.19 (iii)).[73,81] Assessment of the thermodynamic stabilities of the observed macrocycles by computational methods showed that hexamer **90d** is more stable than

pentameric PEM **97** at 30 °C, as it is enthalpically favoured due to its reduced ring strain. Yet, the decrease in the ratio of hexameric PEM **90d** to pentamer **97** at higher temperatures indicates that the formation of the smaller macrocycle (**97**) is entropically favoured.

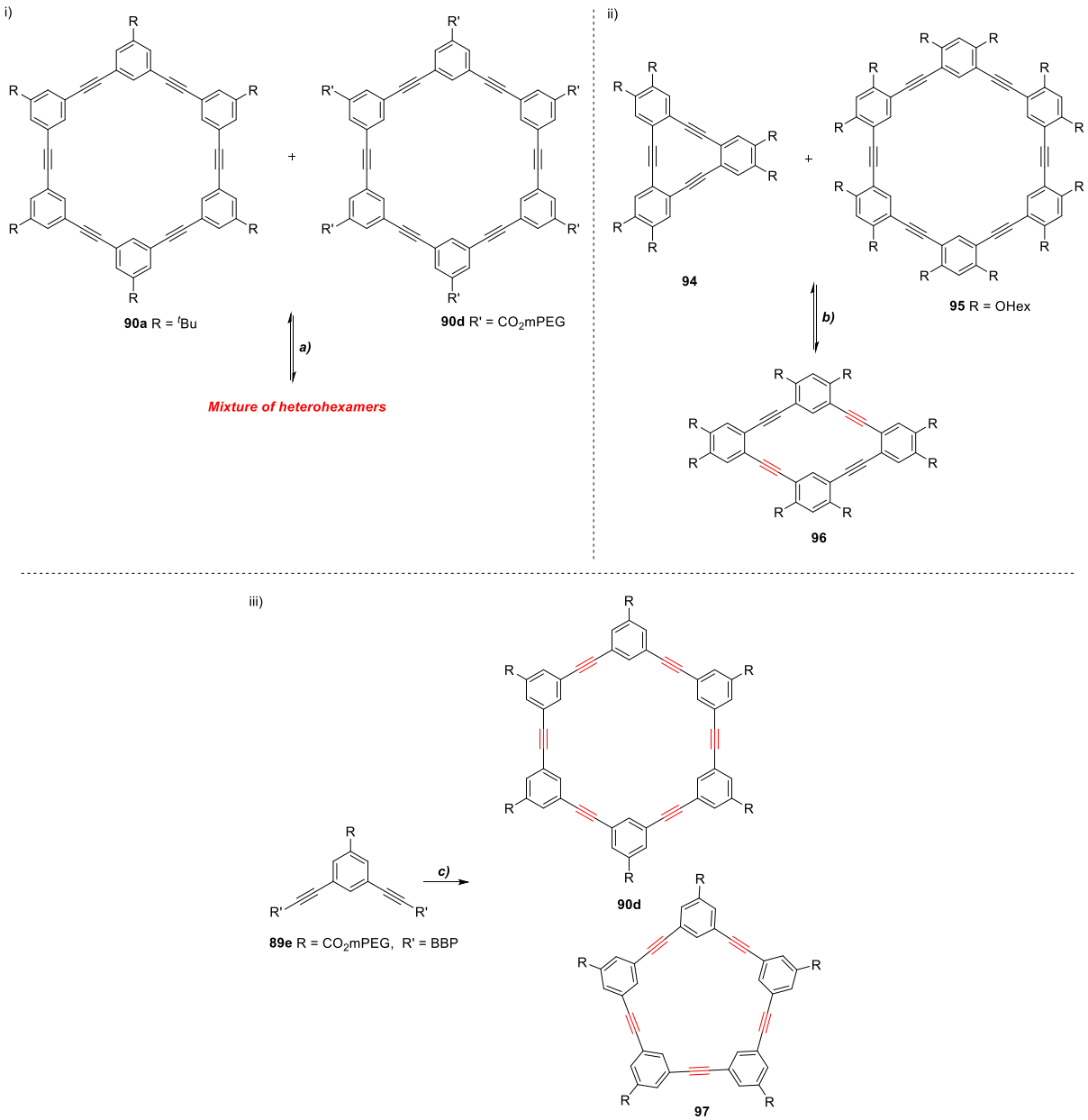

Scheme 1.19. Scrambling and Variable temperature Metathesis experiments of PEMs.[73,81] *Reagents and conditions*: *(a)* **Mo^{C}** complex (10.0 mol%), p-nitrophenol (30.0 mol%), CCl_4, 30 °C; *(b)* **Mo^{C}** complex (10.0 mol%), *p*-nitrophenol (30.0 mol%), CCl_4, 30 - 90 °C; *(c)* **Mo^{C}** complex (10.0 mol%), p-nitrophenol (30.0 mol%), CCl_4, 30 °C, 22 h.

The distribution of products observed in these variable temperature experiments suggests that the energy difference between the cyclic hexamer **90d** and cyclic pentamer **97** is not sufficiently large to afford an exclusive product at equilibrium, however this energy difference appears to be larger at lower temperatures.[82]

1.6.2. Assembly of PEM-derived Fullerene Complexation Agents empowered by one-pot ACM/RCAM reactions.

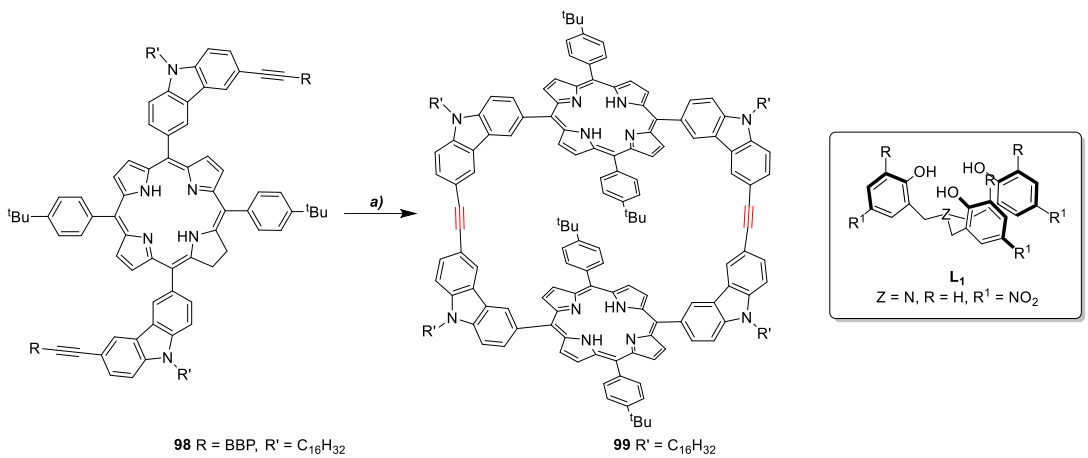

Scheme 1.20. Synthesis of Porphyrin-based via one-pot ACM/RCAM reactions.[83] *Reagents and conditions*: *(a)* **Mo^C** (13 mol%), **L$_1$** (13 mol%), CCl_4, 45 °C, 16 h, (**99**, 60 %).

Fullerenes are fascinating supramolecular scaffolds with a broad range of applications in the pharmaceutical, photovoltaic, and microelectronic industry, primarily due to their unique physical properties. Unfortunately, their practical applications are limited due to their costly preparation, poor processibility and energy-demanding purification.[83a] The synthesis of polycyclic non-covalent binders that exhibit high binding affinity and selectivity for fullerenes is an active research area that aims to develop complexation agents, which not only improve their solubility but also facilitate their purification. Zhang and co-workers reported the one-pot ACM/RCAM based synthesis of PEM-type agents, through a precipitation-driven macrocyclisation protocol, effected by catalytic amounts of trisamido pre-catalyst **Mo^C** and polyphenolic ligand **L$_1$** (Scheme 1.20).[83b] Bisporphyrin macrocycle **99** was prepared in a single step from porphyrin containing diyne **98** (60 %). A small collection of trimeric porphyrin-based macrocycles **101a**-**b** were also synthesised in a similar manner from diynes **100a**-**b** in good yield (82-83%,

Scheme 1.21).[84] Interestingly, porphyrin macrocycle **99** exhibits preferential binding to C_{84} over C_{70}, while the Zn-adduct of macrocycle **101a** shows a high binding affinity for terpyridine guest molecules. This in turn highlights the synthetic ease and efficiency that the one-pot ACM/RCAM methodology has to offer in assembling molecular scaffolds that engage in such complex molecular recognition events.

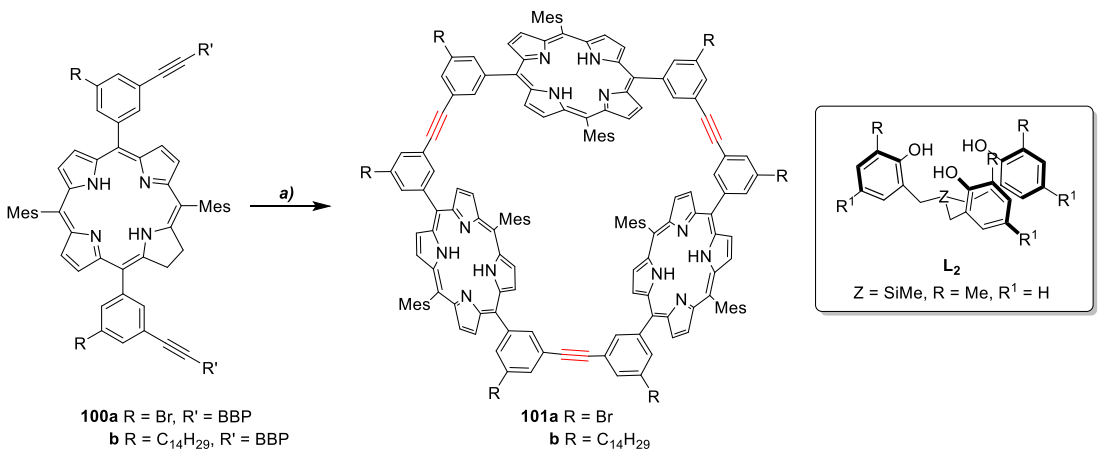

Scheme 1.21. Synthesis of Porphyrin-based via one-pot ACM/RCAM reactions.[84] *Reagents and conditions*: *(a)* **Mo^C** (17 mol%), **L$_2$** (17 mol%), CCl_4, 45 °C, 16 h, (**101a**, 83 %; **101b**, 82 %).

1.7. Maximizing the Performance of one-pot ACM/RCAM protocols

1.7.1. Improving the Yields of one-pot ACM/RCAM Reactions through the Removal of Volatile Byproducts

Despite its extensive utility in synthesis of PEMs, a precipitation-drive alkyne metathesis-based strategy suffers from low atom-economy. In addition, the low solubility of metathesis precursors in reaction media often leads to the formation insoluble oligomers. Recently a potential alternative approach was reported by Zhang and co-workers; PEM **108** was synthesised through an open-air one-pot ACM/RCAM reaction of methyl-capped monomer **107** catalysed by multidentate-polyphenolate ligand-based alkylidyne **Mo^D**. Open flask evaporation of the released 2-butyne during the reaction gave cyclic trimer **108** in almost

quantitative yield (Scheme 1.22 (i)).[85] An elegant atom-economic alternative was also reported by Fürstner and co-workers. Efficient one-pot ACM/RCAM mediated oligomerisation /cyclization to access PEM **96** was achieved on gram-scale from methyl-capped bisalkyne **109** using catalytic amounts of monodentate silanolate ligand-based complex **Mo^{B}** in the presence of 5 Å molecular sieves to trap released 2-butyne. This gave macrocycle **96** in 83 % yield (Scheme 1.22 (ii)).[86]

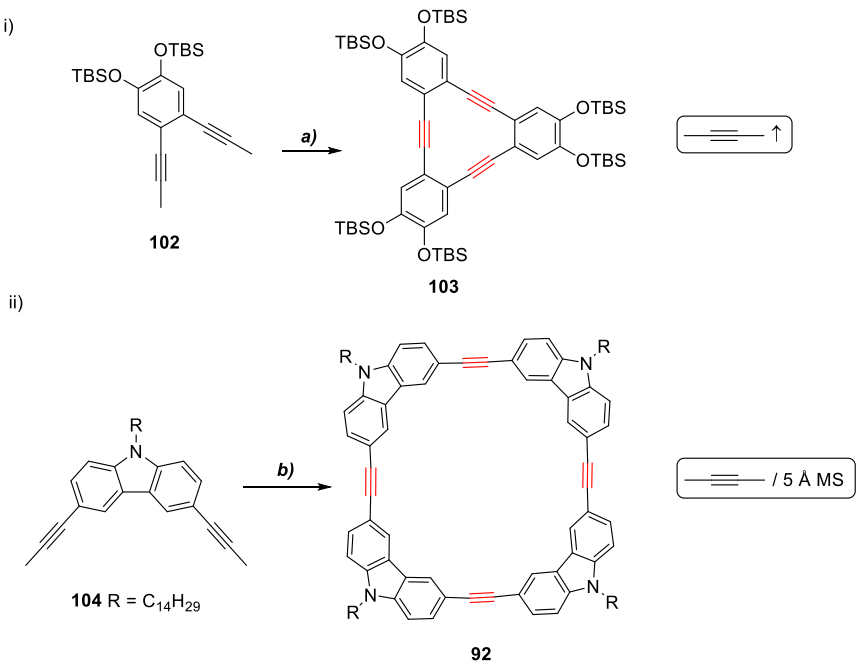

Scheme 1.22. Non-precipitation driven One-pot ACM/RCAM mediated synthesis of PEMs **103** & **92**.[85-86] *Reagents and conditions*: (i) *(a)* **Mo^{D}** (2 mol%), CCl_4, 70 °C, 10 min, (**103**, 95 %); (ii) *(b)* **Mo^{B}** (5 mol%), 5 Å MS, toluene, RT, 1 h, (**92**, 83 %).

As previously mentioned, in these thermodynamically controlled metathesis processes, the structural features of the monomer such as geometry and bond angles play a determining role in the product macrocycles formed. In certain instances, however, the steric effects of monomers can give rise to kinetic effects that change the activation energy barriers of reaction intermediates and thus the product structures observed. Employing the same strategy reported previously by Fürstner and co-workers to scavenge released 2-butyne and *in situ* generated triphenylsilanolate catalyst **Mo^{B}**, Moore and co-workers disclosed the synthesis of a twisted Möbius cyclic architecture **106** through the one-pot ACM/RCAM reaction of sterically encumbered helicene bisalkyne monomer **105** (Scheme 1.23 (i)).[87] Single crystal X-

ray data confirmed that this strained framework consisted of an enantiomeric pair of AAB/BBA (A - right-handed helix, B - left-handed helix).

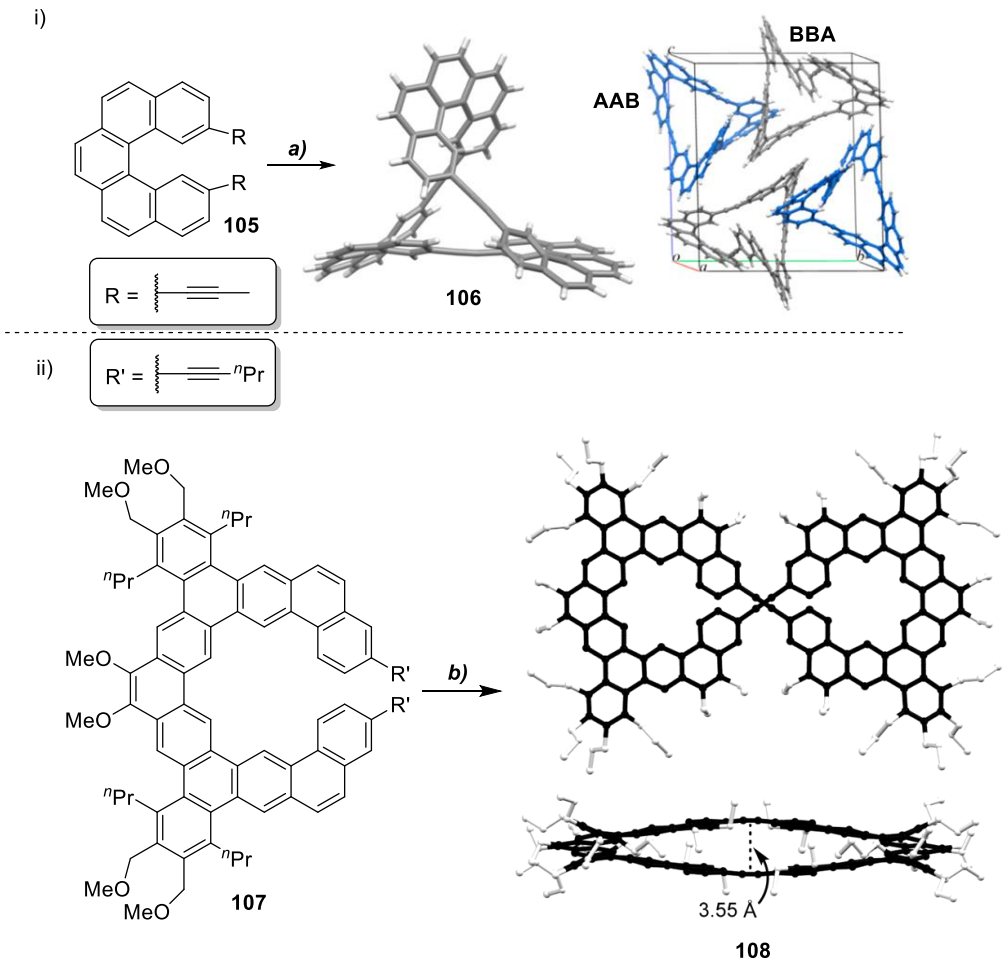

Scheme 1.23. Synthesis of supramolecular helices via one-pot ACM/RCAM reactions.[87-88] *Reagents and conditions*: *(a)* **Mo^{C}** (10 mol%), Ph_3SiOH (60 mol%), 5 Å MS, $CHCl_3$, 60 °C, 18 h, (**106**, 71 %); *(b)* **Mo^{A}** (10 mol%), 5 Å MS, toluene, 80 °C, 16 h, (**108**, 77 %). (Adapted with permission from refs. 87-88 @ copyright 2021 American Chemical Society).

Although based on energy calculations the AAA/BBB enantiomeric pair appears to be the thermodynamically stable product, in practice the AAB/BBA enantiomeric pair was predominately formed.[88] Furthermore, DFT calculations indicated an energy difference of 15.4 kcal/mol^{-1} between the activation energy barriers of the rate-limiting steps leading to formation of these two enantiomeric pairs (AAB/BBA vs. AAA/BBB). As commented by the authors, the observed behaviour can be attributed to the

high energy barriers of the metallacyclobutene intermediates associated with the formation of AAA/BBB, which rendered it kinetically prohibited.

Later, Tilley and co-workers reported the synthesis of helicene based dimeric macrocycle **108** via the one-pot ACM/RCAM reaction of dipropyl-capped helicene monomer **107**, catalysed by complex **Mo^{A}** endowed with monodentate fluorinated alkoxide ligands (Scheme 1.23(ii)).[88] The released byproduct 4-octyne in this case was also scavenged using 5Å molecular sieves. X-ray diffraction data obtained from solution-phase grown crystals indicated that the dimeric macrocycle crystallises also in supramolecular helices with a *non*-centrosymmetric space group *P*6422, where all constituent molecules are homochiral (AA/BB helicity). In the crystal packing, each macrocycle engages in π-stacking interactions with another eight neighboring molecules, while the with a shortest π-stacking distance in the enormous π-surface in the crystal is 3.55 Å.[88]

1.7.2. An Atom Economic Alternative to Conventional Domino Alkyne Metathesis Reactions: One-pot Depolymerisation – ACM/RCAM reactions

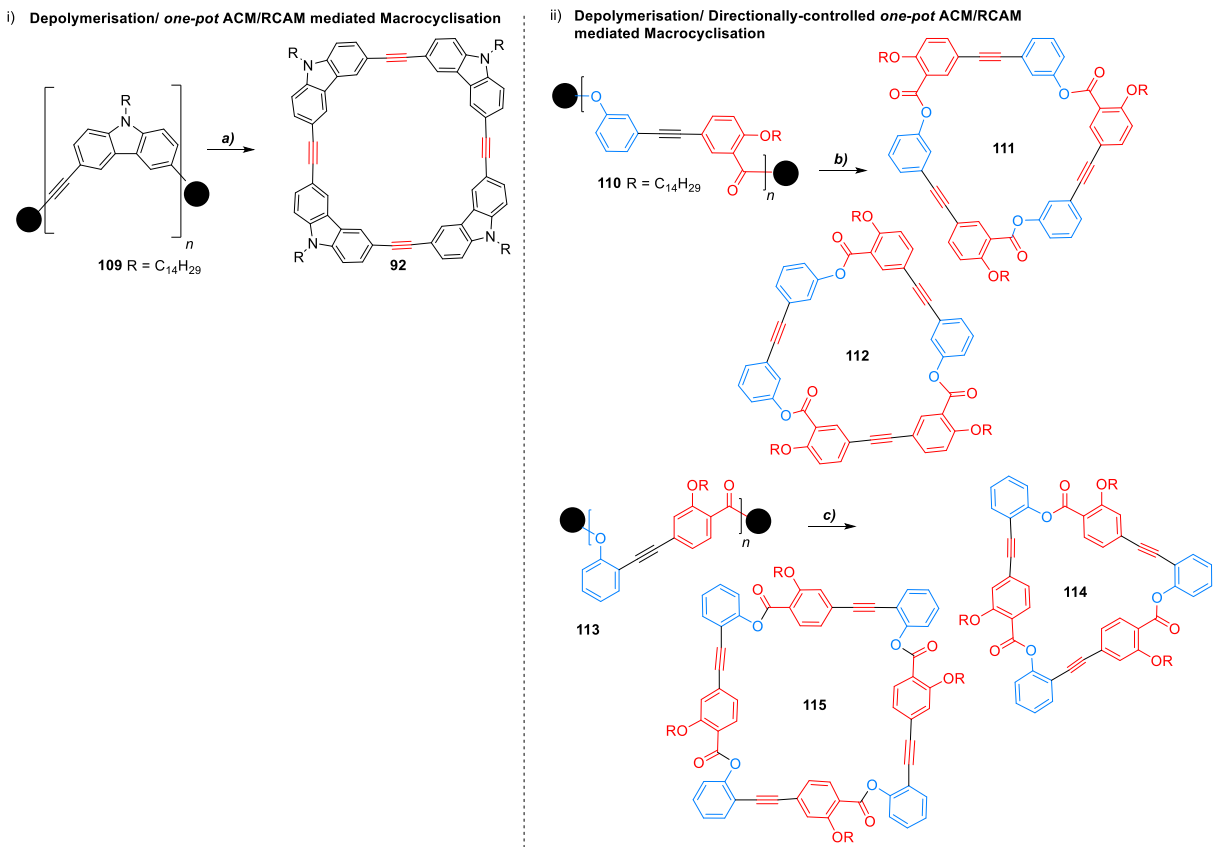

Scheme 1.24. Macrocyclisation through depolymerisation/ non-directional and directionality-controlled one-pot-ACM/RCAM reactions of homopolymers.[89-91] *Reagents and conditions*: *(i) (a)* **Mo^{C}** (10 wt%), Ph_3SiOH (20 wt%), TCB, 50 °C, 24 h, (**92**, 70%); *(ii) (b)* **Mo^{C}** (10 wt%), Ph_3SiOH (15 wt%), TCB, RT, 24 h, (**111**/**112**, (3:1), 17 %); *(c)* **Mo^{C}** (10 wt%), Ph_3SiOH (15 wt%), TCB, RT, 24 h, (**114**, 35 %, **115**, 19 %).

In their quest for a more atom-economic alternative to precipitate-driven one-pot ACM/RCAM-based construction of complex macrocyclic scaffolds, Moore and co-workers investigated an alkyne metathesis mediated depolymerization-macrocyclization approach. When homopolymer **109** was subjected to alkyne metathesis catalysed by *in situ* generated triphenylsilanolate catalyst **Mo^{B}**, the tetrameric macrocycle **92** was obtained in 70 % yield in the absence of any byproduct formation (Scheme 1.24 (i)).[89-90] Encouraged by these results, the bias towards controlled macrocyclisation via a one-pot ACM/RCAM reaction using

information-specific polymeric precursors was investigated (Scheme 1.24 (ii)). Evaluation of the thermodynamic preference of directional polymer precursors to afford directionally uniform macrocycles, was possible using polyynes **110** and **113**.[91] The difference in directionality in these arises due to the configuration of their ester units. Depolymerisation-macrocyclisation effected by *in situ* generated triphenylsilanolate complex **Mo^{B}**, gave a statistical mixture (1:3) of trimeric products **111** and **112**. These were isolated in 17 % yield. Conversely, in the case of polymer **113**, while utilising the same reaction conditions, a separable mixture of directionally uniform macrocyclic trimer **114** (35 %) and tetramer **115** (19 %) was obtained.[91]

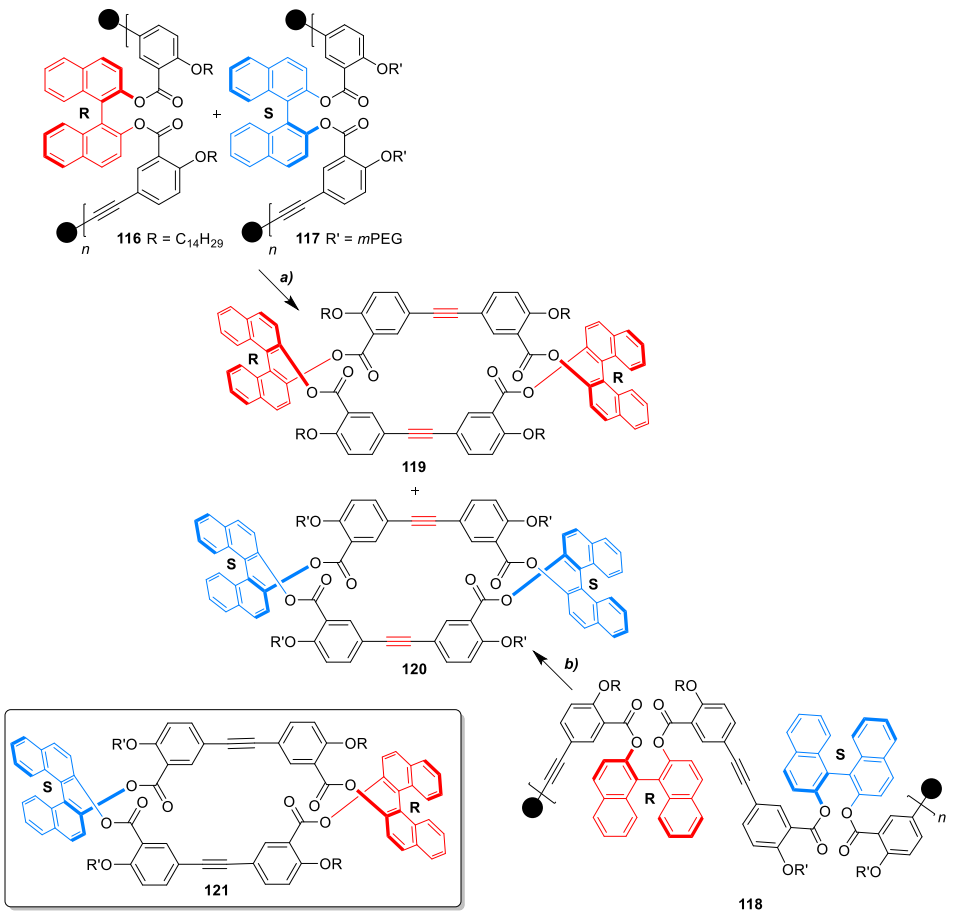

Scheme 1.25. Macrocyclisation through the one-pot-ACM/RCAM reactions of homochiral polymers.[92] *Reagents and conditions*: *(a)* **Mo^{C}** (10 wt%), Ph_3SiOH (15 wt%), TCB, RT, 24 h; *(b)* **Mo^{C}** (10 wt%), Ph_3SiOH (15 wt%), toluene, 5 °C, 24 h.

Chirality-induced self-sorting was also examined using homochiral polymers **116** and **117** and heterochiral polymer **118**. Enantiopure polymers **116** and **117** when subjected separately to metathesis conditions gave C_2 -symmetrical homochiral macrocycles **119** (*R,R*, 51%) and **120** (*S,S*, 55%).[92] Depolymerisation-macrocyclisation of an equimolar mixture of the two enantiopure polymers also furnished homochiral macrocycles **119** (*R,R*) and **120** (*S,S*). Depolymerisation and subsequent one-pot ACM/RCAM reaction of heterochiral polymer **118**, only afforded homochiral dimers **119** and **120** (Scheme 1.25). Despite the close structural similarly of the three macrocyclic dimers (**119**, **120**, **121**), computational modeling at the HF/3-21G* level revealed that the observed selectivity arises due a ΔG of ca. −2.05 kcal mol^{-1} caused by the increased symmetry of the homochiral dimers over their heterochiral counterpart.[92]

1.8. One-pot ACM/RCAM Reactions: Post-Functionalistion

As discussed in Section 1.2.2, combining one-pot CM/RCM reactions with alkene hydrogeneration furnishes an elegant approach to highly decorated scaffold such as cylindrocyclophanes **A** and **F**. In addition to the elaborate structures directly obtained through one-pot iterative alkyne metathesis reactions, various complementary downstream functionalisation strategies are used, which harness the alkyne reactivity in the newly formed macrocyclic polyne product(s) to access highly decorated and structurally diverse architectures.

Moore and co-workers first demonstrated that novel ethynylene-linked molecular belts including cycloparaphenylene-acetylene (CPPA) **124** can be readily accessed through the one-pot ACM/RCAM reactions of cyclohexadienyl-containing diyne precursors such as bisalkyne **122**, followed by reductive aromatisation using sodium naphthalenide.[93] Subjecting monomer **122** to alkyne metathesis with *in situ* generated complex **Mo^{B}** in TCB, gave macrocycle **123** in almost quantitative yield. Despite the ease of formation of cyclohexadienyl-containing triyne **123**, the resulting molecular belt **124** ([3]CPP^{3}A) formed by reductive aromatisation was found to be unstable to air and moisture (Scheme 1.26 (i)). Surprisingly, its stability could be readily enhanced upon complexation to C_{70}. While the resulting adduct is bench-stable for months, single-crystal X-ray diffraction data confirmed the strained molecular structure of CPPA **129** and indicated that alkyne bond angles in this molecular belt are significantly smaller than the normal 180° angle. As a result of the accrued strain in trimer CPPA **124**, this readily engages in strain-promoted azide-alkyne cycloaddition (SPAAC), to form macrocycle **125**. Later in 2019, Lee and co-workers disclosed a follow-up work on the synthesis of CPPAs utilizing a similar strategy.[94] Synthesis of trimeric molecular

belts of variable sizes such as [3]CPPA[4] **127**, was achieved via the late-stage one-pot ACM/RCAM reactions of polyarylated diynes in the presence of complex **Mo^C**, Ph_3SiOH and 5 Å molecular sieves (Scheme 25 (ii)). Reductive aromatisation using sodium naphthalenide once again furnished molecular belts including CPPA **128** in good overall yields (85 – 88%). This two-step strategy evidently provides an efficient pathway for converting planar scaffolds to molecular belts, with potential applications in the assembly of other fascinating supramolecular constructs such as nanotubes.

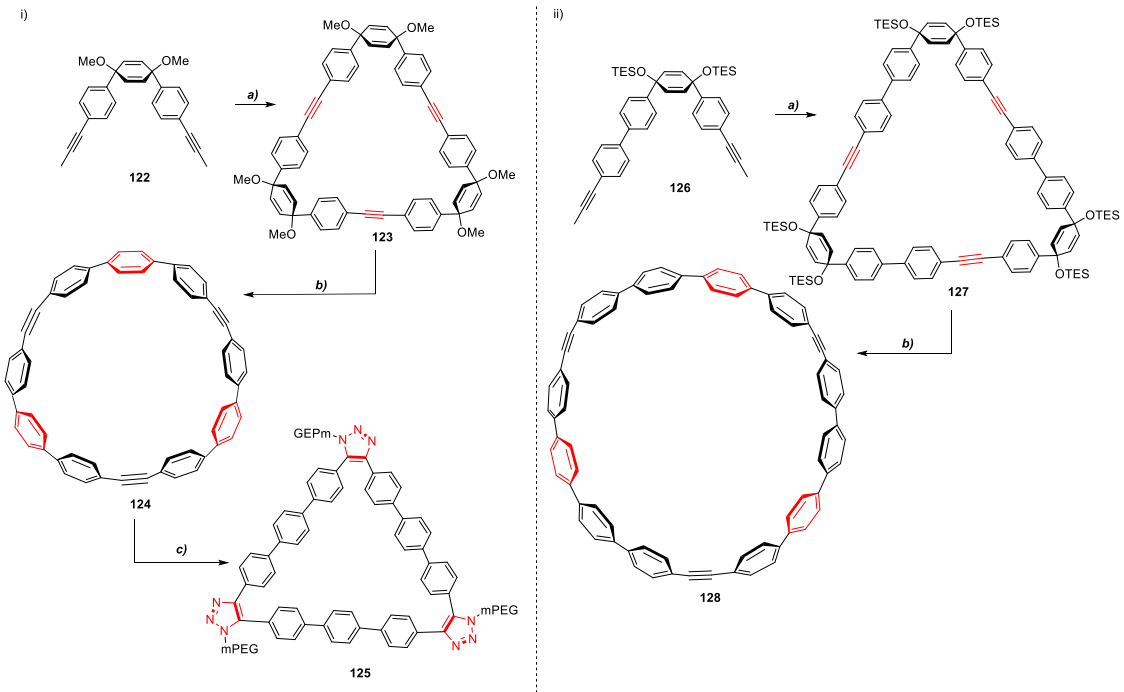

Scheme 1.26. Synthesis of Molecular Belts via one-pot ACM/RCAM-Reductive Aromatisation.[93-94] *Reagents and conditions*: *(i) (a)* **Mo^C** (2 mol%), Ph_3SiOH (12 mol%), 5 Å MS, toluene, 70 °C, 18 h, (**123**, quant.); *(b)* NaNaphth, THF, -78 °C, 1 h, (**124**, 70 %); *(c)* N_3*mPEG*, toluene, 50 °C, 2 h, (**125**, 82 %); *(ii) (a)* **Mo^C** (5 mol%), Ph_3SiOH (15 mol%), 5 Å MS, toluene, 60 °C, 18 h, (**127**, 82 %); *(b)* NaNaphth, THF, -78 °C, 10 mins, (**128**, 88 %).

1.9. Conclusion

This collection of vignettes described, clearly exemplifies that one-pot iterative metathesis reactions particularly as CM/RCM and ACM/RCAM methods can provide a powerful and versatile set of tools for the rapid construction of highly decorated macrocyclic architectures of variable ring sizes with a wide range of properties and applications. The diverse range of applications of one-pot CM/RCM reactions is illustrated through the synthesis natural products, cyclic peptides macrocyclic oligosaccharides as well as the construction of molecular electronics and artificial membrane channels.

The use of one-pot CM/RCM reactions by Smith and coworkers to secure the macrocyclic core of cylindrocyclophanes **A** and **F** (Section 1.2.2) efficiently and stereoselectively, feature the first and most influential examples of an alkene metathesis-based homodimerization approach applied in the synthesis of natural products (Figure 1.4). Forging of the *[7,7]-E*,*E*-paracyclophane core via a metathesis-based cyclisation of diene building blocks was one of the earliest indications that highly decorated macrocyclic scaffolds can be constructed both efficiently and reliably through one-pot iterative metathesis reactions (Scheme 1.5 (i)). The reversible (thermodynamic control) nature of this metathesis-based methodology is demonstrated through Smith's total synthesis of cylindrocyclophane **F**. Irrespective of the catalyst used, the tandem CM/RCM reactions of bisalkene precursor **31** delivered selectively the H-to-T dimer **32** (Scheme 1.6 (i)). *In silico* analysis revealed that *[7,7]-E*,*E*-paracyclophane **32** is the lowest energy structure relative to all other possible dimers and assembles through the macrocyclisation of a H-to-T linear dimer. Moreover, the self-correcting character of the one-pot CM/RCM reactions is highlighted through the RCM reactions of H-to-H (**35**) and T-to-T (**36**) linear dimers (Scheme 1.7). Treatment of trienes **35** and **36** with **SHa** or **G2** afforded exclusively macrocyclic diene **32**.

Modification of biomolecules (Section 1.3) or assembly of artificial membrane channels (Section 1.4.1) through cyclisation via one-pot iterative metathesis reactions enables a facile approach to more rigid and conformationally restricted constructs relative to their acyclic congeners with unprecedented structural and biological properties. The latter could provide an elegant collection of useful molecular tools for biology and medicine. Owing to the intense power consumption and expensive production methods needed for miniaturising conventional silicon devices, assembly of electronic circuits using molecules as working components offers a more promising alternative for size reduction in electronic devices.

Combining one-pot CM/RCM reactions with alkene hydrogenation furnishes a robust strategy for the rapid construction of such circuit components including molecular diodes (Section 1.4.2).

Although the scope of applications of one-pot ACM/RCAM reaction does not rival that of tandem CM/RCM reactions, the future of this synthetic manifold holds great promise. Over the past two decades, alkyne metathesis catalysts have evolved from poorly defined *in situ* generated mixtures (Scheme 1.16 (i)) to well-defined and highly active multidentate catalysts (Figure 1.3 (ii)). In addition to the wide range of macrocyclic structures directly obtained through one-pot iterative alkyne metathesis reactions, various downstream functionalization approaches are employed to introduce further structural diversity by utilising the inherent alkyne reactivity in the tandem ACM/RCAM products (Section 1.5.2). Conversely, most of the alkene-metathesis based examples discussed earlier regarding the assembly of macrocyclic architectures are either limited to hydrogenation or no post-metathetic elaboration of the one-pot CM/RCM product(s).

In contrast to conventional cross-coupling reactions, iterative alkyne metathesis-based synthetic approaches can provide the desired product(s) in a single step in high yields, which can significantly shorten synthetic routes to macrocyclic scaffolds. An elegant demonstration of this concept is the synthesis novel PEM-derived fullerene complexation agents via a precipitation-driven one-pot ACM/RCAM reactions of porphyrin containing diynes (Section 1.6.2).

Moreover, copious efforts have been dedicated to improving the synthetic performance of iterative alkyne metathesis-based methods, by optimising the end groups of bisalkyne building blocks or the removal of byproducts through the use of scavengers (5 Å MS) or evaporation. For instance, the 1-pentynyl and methyl groups shows great potential in serving as optimal end groups due to their solubility, ease of installation and byproduct sequestration; a series of novel macrocycles have been synthesized, including Möbius rings and CPPA structures (Section 1.7.1).

The construction of directionally uniform macrocycles via an atom economic depolymerisation–domino alkyne metathesis reactions of polyesters demonstrates that an appropriately designed bisalkyne monomer unit can lead to a narrower macrocyclic product distribution (Section 1.7.2). The influence of the monomer shape on the reactivity observed in depolymerization–one-pot ACM/RCAM reactions highlights the necessity for a better understanding of the implications of different degrees of freedom,

shapes, and geometries on the macrocyclization energy landscape (Scheme 1.24 (ii)). Additionally, the synthesis of chiral PEMs through a depolymerisation–one-pot iterative alkyne metathesis reaction enabled the discovery of an unprecedented entropy-driven macrocyclisation as result of the increased symmetry of homochiral products over their heterochiral counterparts (Scheme 1.25). Potential applications of this thermodynamic and symmetry-driven macrocyclisation protocol include dynamic chiral resolution and asymmetric catalyst design.

In conclusion, the profound implications of building block structure on the kinetic factors and energy landscape of these thermodynamically controlled metathesis-based processes, highlight the importance of careful monomer design. *In silico* analysis on potential intermediates could be instructive for fine-tuning of monomer structure and the reaction conditions which would enable the assembly of a specific target scaffold. Ring strain and entropy play a crucial role in determining the ring size of the product(s) generated by such domino metathesis-based synthetic protocols. Furthermore, the conformational rigidity and structure of the monomer dictates whether a given macrocyclic product is strain-free or strained. The energy difference between the desired macrocyclic product and other possible macrocyclic or oligomeric products, would determine whether the target macrocycle will be formed as the major product at equilibrium.

1.10. Thesis Overview and Research Aims

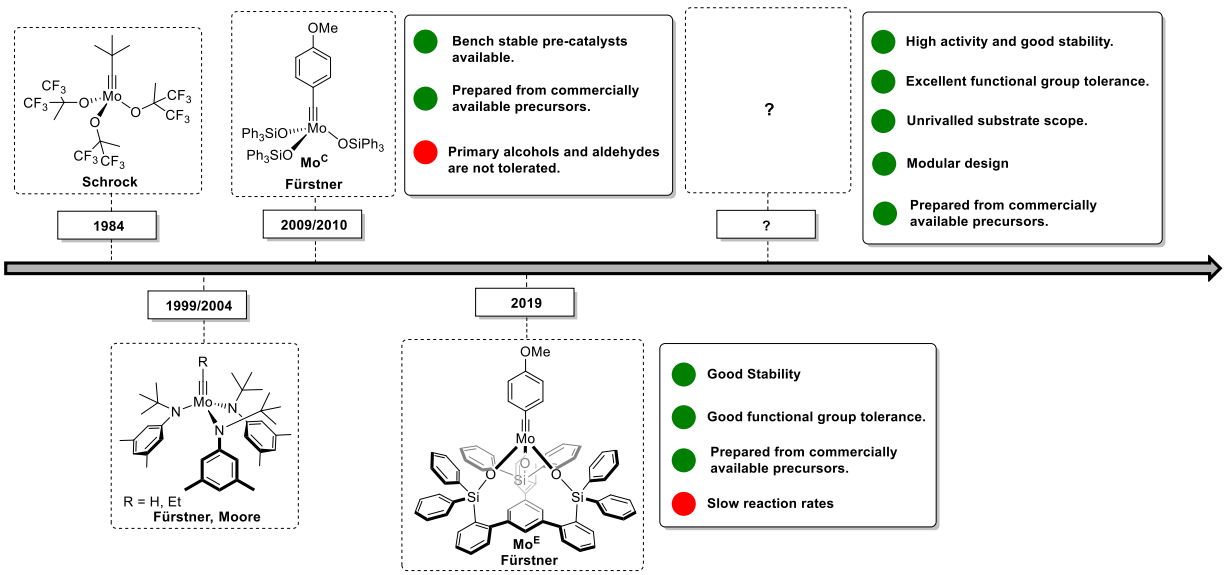

Figure 1.5. Milestones in Molybdenum-Catalysed Alkyne Metathesis: Well-defined Alkyne Metathesis Catalysts.

The previous work discussed in this chapter has highlighted how one-pot metathesis cascade reactions can be an effective and flexible synthetic tool for the rapid assembly of complex molecular architectures with a diverse range of properties and applications. Unfortunately, the utility of alkyne metathesis-based synthetic methodologies such as the one-pot ACM/RCAM reactions is limited by availability of well-defined and user-friendly alkyne metathesis catalysts due to their sensitivity to moisture and air. Therefore, it was deemed necessary to initially explore the development of a new alkyne metathesis catalyst. Alkyne metathesis catalyst **Mo^{E}** bears the privileged tripodal silanolate ligand scaffold. This exhibits the same catalytic activity and selectivity as seen in the parent molybdenum alkylidyne **Mo^{B}** but shows better functional group tolerance (Figure 1.5).[95-98]

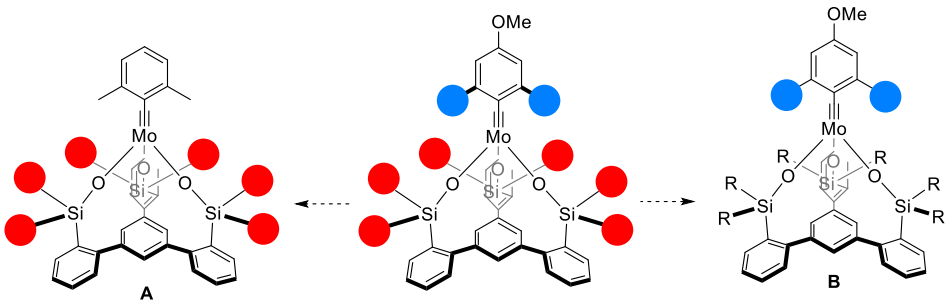

Figure 1.6. Two strategies for circumventing the issues associated with catalyst **Mo^{E}**: Novel designs for developing a canopy type metathesis catalyst; A = Replacement of the *ortho*-benzylidyne protons with alkyl substituents, **B** = Substitution of the phenyl groups in the periphery of the tripodal silanolate ligand framework.

Although tripodal catalyst **Mo^{E}** exists as a dimer in the solid state, it works well in the presence of unprotected primary alcohols, β-ketoesters, potentially chelating groups such as Weinreb amides as well as substrates having multiple donor sites, including secondary and tertiary amines and heterocycles. Although aggregation did not prove limiting for metathesis, the slow reaction rates and need for heating to generate the monomeric species to attain efficient turnover, are rather limiting and not ideal for catalysis.[95] Replacement of the *ortho*-benzylidyne protons with more sterically demanding substituents or substituting the phenyl groups in the tripodal silanolate ligand framework, furnish an elegant set of strategies for circumventing the issues associated with the tripodal silanolate catalyst **Mo^{E}** (Figure 1.6). This could potentially foster the development of a new well-defined monomeric "canopy complex" with superior functional group tolerance and catalytic activity.

Earlier work reported by the Hulme group showed that a one-pot alkyne metathesis homodimersation followed by stereoselective partial alkyne reduction, furnished an elegant synthetic strategy to access C_2-symmetric natural products such as the cytotoxic marine-derived bislactone Disorazole C_1 (**84**) (Scheme 1.16).[68] To further illustrate this point, the aim of this current work is to demonstrate that one-pot ACM/RCAM reactions when combined with stereoselective partial reduction, provide a robust method for constructing large ring sizes from relatively simple precursors, whilst offering full control over the stereochemistry of the diene products. Since Lindlar reduction was investigated as a post-metathetic transformation in the total synthesis of Disorazole C_1, this work will focus on *trans*-reduction via ruthenium-catalysed *trans*-hydrometallation.

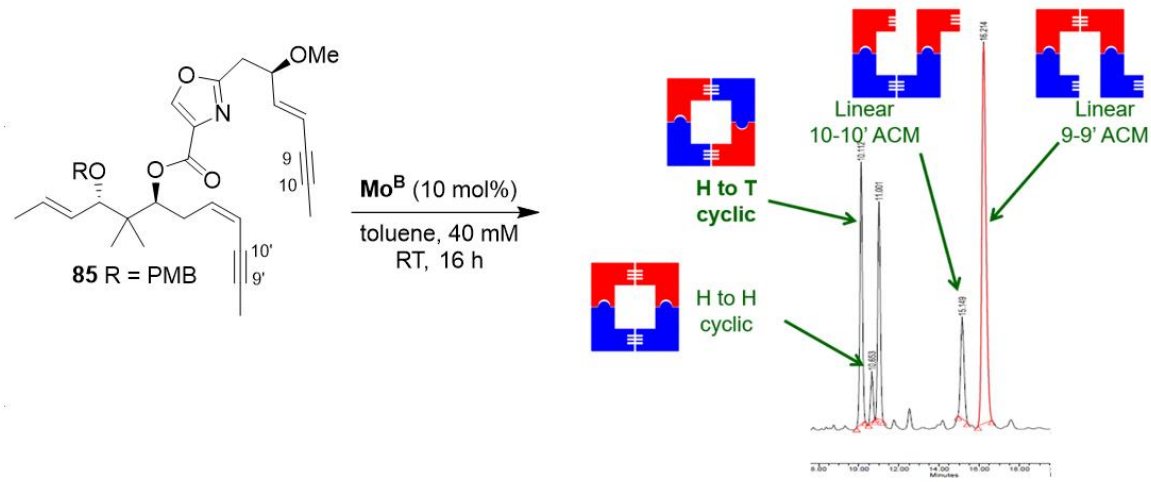

Figure 1.7. Crude aliquot of one-pot ACM/RCAM reaction of bis(enyne) **84** after 16 h at rt, 10 mol% cat. loading **Mo^{B}**, Reaction Molarity: 40 mM (Reaction followed by UPLC @ 254 nm, unoptimised reaction conditions).[68]

Previously, the one-pot ACM/RCAM reactions of bis(enyne) building block **85** were examined en route to the total synthesis of Disorazole C_1. Although, a complex mixture of head-to-head (H-to-H), head-to-tail (H-to-T) and tail-to-tail (T-to-T) dimers was initially obtained (Figure 1.7), carefully optimisation of the reaction conditions delivered the desired H-to-T cyclic dimer **91** in 61 % yield over two steps (Scheme 1.28, Figure 1.7).[68] For this new alkyne metathesis-based study, however, the one-pot ACM/RCAM reactions of bisalkyne monomers **134** and **135** will be examined (Chapter 3), as part of a total synthesis campaign towards anti-malarial macrodiolide samroiyotmycin A (**136**). Capitalising on the propensity of electron-poor enynes and ynoates for cross-coupling over homodimerisation in presence of a second electron-rich alkyne, [86,96-98] it is anticipated that the one-pot ACM/RCAM reactions of these bifunctional building blocks **134** and **135**, catalysed by the newly developed catalyst (Chapter 2) would give the best selectivity for the desired H-to-T cyclic dimers **136** and **137** (Figure 1.8).

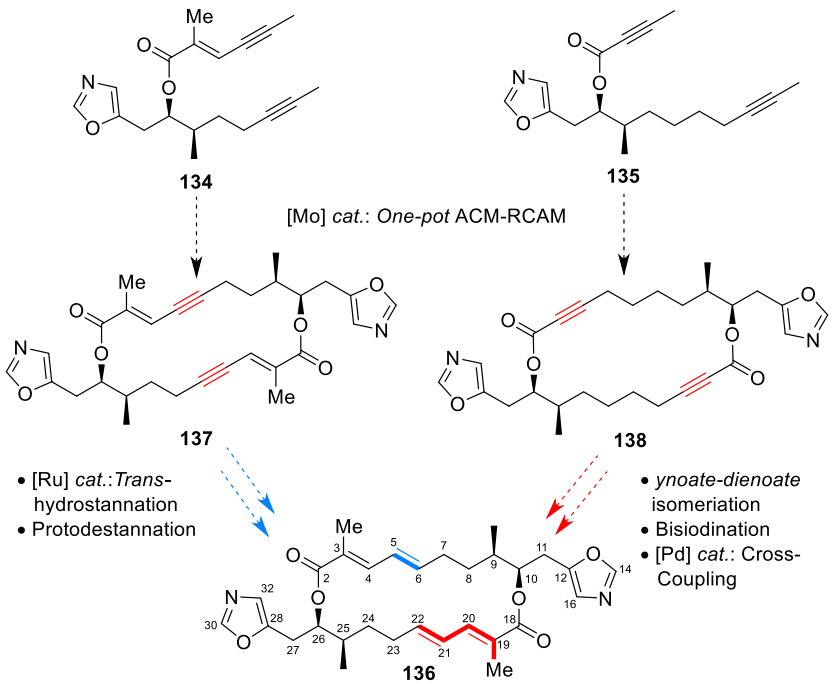

Figure 1.8. Two conceivable convergent approaches to Samroiyotmycin A based on one-pot ACM/RCAM reactions: Ring assembly via routes based on C(5)-C(6)/C(21)-C(22) or C(3)-C(4)/C(19)-C(20) disconnections.

As discussed in Chapter 3, for the final elaboration of the two H-to-T cyclic dimers **137** and **138** to macrodiolide **136**, two conceivable convergent approaches will be investigated (Figure 1.6). In the first, it was envisaged that conversion of bis(enyne) **137** to the required *E*-configured alkenes would be possible via a late-stage bis*(trans*-hydrostannation-protodestannation) sequence. While a second back-up strategy commencing from macrocycle **138**, will introduce the two *E*,*E*-diene units through a three-step sequence consisting of an ynoate-dienoate isomerisation, [99-106] bisiodination [107] and a final double Stille/ Negishi coupling.[108,109]

1.11. References

[1] E. M. Driggers, S. P. Hale, J. Lee, N. K. Terrett, *Nat. Rev. Drug. Discov.* **2008**, *7*, 608–624.

[2] D. J. Newman,G. M. Cragg, Bioactive Macrocycles from Nature. in *Macrocycles in Drug Discovery*; Royal Society of Chemistry, **2015**; p. 1– 36.

[3] J. Mallinson, I. Collins, *Future Med. Chem*. **2012**, *4*, 1409–1438.

[4] E. Marsault, M. L. Peterson*, J. Med. Chem.* **2011**, *54*, 1961–2004.

[5] P. Ermert, *Chimia (Aarau)* **2017**, *71*, 678– 702

[6] A. K. Yudin, *Chem. Sci.* **2015**, *6*, 30–49.

[7] V. Martí-Centelles, M. D. Pandey, M. I. Burguete, S. V. Luis, *Chem. Rev.* **2015**, *115*, 8736–8834.

[8] J. Blankenstein, J. Zhu, *Eur. J. Org. Chem.* **2005**, *2005*, 1949–1964.

[9] C. X. Zhuo, A. Fürstner, *J. Am. Chem. Soc.* **2018**, *140*, 10514–10523.

[10] G. O'Neil, J. Ceccon, S. Benson, M.-P. Collin, B. Fasching, A. Fürstner, *Angew. Chem. Int. Ed.* **2009**, *48*, 9940–9945.

[11] S. Benson, M.P. Collin, G. W. O'Neil, J. Ceccon, B. Fasching, M. D. B. Fenster, C. Godbout, K. Radkowski, R. Goddard, A. Fürstner, *Angew. Chem. Int. Ed.* **2009**, *121*, 10130–10134.

[12] Z. Meng, A. Fürstner, *J. Am. Chem. Soc.* **2019**, *141*, 805–809.

[13] A. Fürstner, *Acc. Chem. Res.* **2021**, *54*, 861–874.

[14] R. H. Grubbs, Ed., Handbook of Metathesis, Wiley-VCH, Weinheim, Germany, **2003**, p. 445-501

[15] Y. Ge, S. Huang, Y. Hu, L. Zhang, L. He, S. Krajewski, M. Ortiz, Y. Jin, W. Zhang, *Nat. Commun.* **2021**, *12*, 1136.

[16] *(a)* A. H. Hoveyda, *J. Org. Chem.* **2014**, *79*, 4763–4792; *(b)* J. Li, T. S. Ahmed, C. Xu, B. M. Stoltz, R. H. Grubbs, *J. Am. Chem. Soc.* **2019**, *141*, 154–158; *(c)* B. K. Keitz, K. Endo, P. R. Patel, M. B. Herbert, R. H. Grubbs, *J. Am. Chem. Soc.* **2012**, *134*, 693–699.

[17] K. Dawood, K. Nomura, *Adv. Synth. Catal.* **2021**, *363*, 1970-1997.

[18] L. Ondi, G. Nagy, J. Czirok, A. Bucsai, G. Frater, *Org. Process Res. Dev.* **2016**, *20*, 1709-1716.

[19] R. R. Schrock, *J. Am. Chem. Soc.* **1974**, *96*, 6796-6797.

[20] L. J. Guggenberger, R. R. Schrock, *J. Am. Chem. Soc.* **1975**, 97, 2935-2935.

[21] J. H. Wengrovius, J. Sancho, R. R., Schrock, *J. Am. Chem. Soc*. **1981**, *103*, 3932-3934.

[22] S. Kotha, M. E. Shirbhate, G. T. Waghule, *Beilstein J. Org. Chem*. **2015**, *11*, 1274–1331.

[23] J. Tae, Y.-K. Yang, *Org. Lett.* **2003**, *5*, 741–744.

[24] S. Kotha, A. S. Chavan, M. Shaikh, *J. Org. Chem.* **2012**, *77*, 482–489.

[25] *(a)* T. Takimoto, H. Sasaki, H. Tsue, H. Takahashi, A. D. MacKerell, A. Nakamura, K. Nakano, E. Okazaki, T. Betsuyaku, R. Tachibana, K. Hioki, O. Yoluk, S. Jo, *Chem. Eur. J.* **2021**, *27*, 1648–1654.; *(b)* H. Sasaki, A. Suehiro, Y. Nakamoto, *Chem. Pharm. Bull.* **1997**, *45*, 189–193.; *(c)* H. Sasaki, T. Kitagawa, *Chem. Pharm. Bull.* **1988**, *36*, 1593–1596.; *(d)* H. Sasaki, T. Kitagawa, *Chem. Pharm. Bull.* **1988**, *36*, 1593–1596.; *(e)* H. Sasaki, R. Egi, K. Kawanishi, T. Kitagawa, T. Shingu, *Chem. Pharm. Bull.* **1989**, *37*, 1176–1178.; *(f)* H. Sasaki, A. Suehiro, Y. Nakamoto, *Chem. Pharm. Bull.* **1997**, *45*, 189–193.; *(g)* G. Cafeo, D. Garozzo, F. H. Kohnke, S. Pappalardo, M. F. Parisi, R. Pistone Nascone, D. J. Williams, *Tetrahedron* **2004**, *60*, 1895–1902.; *(h)* R. B. Ferreira, L. J. Murray, *Acc. Chem. Res.* **2019**, *52*, 447–455.

[26] A. Fürstner, A. Leitner, *Angew. Chem. Int. Ed.* **2003**, 42, 308–311.

[27] S. Kotha, G. T. Waghule, M. E. Shirbhate, *Eur. J. Org. Chem.* **2014**, 2014, 984–992.

[28] *(a)* B. S. Moore, J. L. Chen, G. M. L. Patterson, R. E. Moore, L. S. Brinen, Y. Kato, J. Clardy, *J. Am. Chem. Soc.* **1990**, 112, 4061–4063.; *(b)* B. S. Moore, J.-L. Chen, G. M. L. Patterson, R. E. Moore, *Tetrahedron* **1992**, *48*, 3001–3006.

[29] G. E. Chlipala, M. Sturdy, A. Krunic, D. D. Lantvit, Q. Shen, K. Porter, S. M. Swanson, J. Orjala, *J. Nat. Prod.* **2010**, *73*, 1529–1537.

[30] H. Nakamura, H. A. Hamer, G. Sirasani, E. P. Balskus, *J. Am. Chem. Soc.* **2012**, *134*, 18518–18521.

[31] D. Berthold, B. Breit, *Synlett* **2021**, *32*, 436–446.

[32] T. R. Hoye, P. E. Humpal, B. Moon, *J. Am. Chem. Soc.* **2000**, *122*, 4982–4983.

[33] K. C. Nicolaou, Y.-P. Sun, H. Korman, D. Sarlah, *Angew. Chem. Int. Ed.* **2010**, *49*, 5875–5878.

[34] A. B. Smith, S. A. Kozmin, D. V. Paone, *J. Am. Chem. Soc.* **1999**, *121*, 7423–7424.

[35] A. B. Smith, S. A. Kozmin, C. M. Adams, D. V. Paone, *J. Am. Chem. Soc.* **2000**, *122*, 4984–4985.

[36] H. Yamakoshi, F. Ikarashi, M. Minami, M. Shibuya, T. Sugahara, N. Kanoh, H. Ohori, H. Shibata, Y. Iwabuchi, *Org. Biomol. Chem.* **2009**, *7*, 3772.

[37] D. Berthold, B. Breit, *Chem. Eur. J.* **2018**, *24*, 16770–16773.

[38] J. J. Freudenreich, S. Bartlett, N. S. Robertson, S. L. Kidd, S. Forrest, H. F. Sore, W. R. J. D. Galloway, M. Welch, D. R. Spring, *Chem. Med. Chem.* **2020**, *15*, 1289–1293.

[39] D. V. Jarikote, P. V. Murphy, *Eur. J. Org. Chem.*, **2010**, *7*, 4959–4970.

[40] G. Chen, A. Kirschning, *Chem. Eur. J.* **2002**, *8*, 2717–2729.

[41] J. Jaunzems, B. Oelze, A. Kirschning, *Org. Biomol. Chem.* **2004**, *2*, 3448.

[42] D. T. S. Rijkers, in Synthesis of Heterocycles by Metathesis Reactions (Ed.: J. Prunet), *Springer International Publishing*, Cham, **2015**, p. 191–244.

[43] B. Sundararaju, T. Sridhar, M. Achard, G. V. M. Sharma, C. Bruneau, *Eur. J. Org. Chem*. **2013**, 2013, 6433–6442.

[44] Y. Jin, A. Zhang, Y. Huang, W. Zhang, *Chem. Commun.* **2010**, 46, 8258-8260.

[45] C. A. Hubner, *Hum. Mol. Genet.* **2002**, *11*, 2435–2445.

[46] *(a)* S. Negin, M. M. Daschbach, O. V. Kulikov, N. Rath, G. W. Gokel, *J. Am. Chem. Soc.* **2011**, *133*, 3234 —3237.; (*b*) B. Gong, Z. F. Shao, *Acc. Chem. Res.*, *2013*, *46*, 2856 —2866.; *(b)* A. J. Helsel, A. L. Brown, K. Yamato, W. Feng, L. H. Yuan, A. J. Clements, S. V. Harding, G. Szabo, Z. F. Shao, B. Gong, *J. Am. Chem. Soc.* **2008**, *130*, 15784 —15785.; *(c)* Y. J. Jeon, H. Kim, S. Jon, N. Selvapalam, D. H. Oh, I. Seo, C. S. Park, S. R. Jung, D. S. Koh, K. Kim, *J. Am. Chem. Soc.* **2004**, *126*, 15944 —15945.; *(d)* W. Si, L. Chen, X.-B. Hu, G. Tang, Z. Chen, J.-L. Hou, Z.-T. Li, *Angew. Chem. Int. Ed.* **2011**, *50*, 12564 —12568.; *(e)* X. Zhou, G. Liu, K. Yamato, Y. Shen, R. Cheng, X. Wei, W. Bai, Y. Gao, H. Li, Y. Liu, F. Liu, D. M. Czajkowsky, J. Wang, M. J. Dabney, Z. Cai, J. Hu, F. V. Bright, L. He, X. C. Zeng, Z. Shao, B. Gong, *Nat. Commun.* **2012**, *3*, 949.

[47] X. Hu, C. Yu, K. D. Okochi, Y. Jin, Z. Liu, W. Zhang, *Chem. Commun.* **2016**, *52*, 5848–5851.

[48] (*a)* S. Ito, M. Wehmeier, J. D. Brand, C. Kübel, R. Epsch, J. P. Rabe, K. Müllen, *Eur. J. Chem*. **2000**, *6*, 4327–4342; *(b)* A. J. Fleming, J. N. Coleman, A. B. Dalton, A. Fechtenkötter, M. D. Watson, K. Müllen, H. J. Byrne, W. J. Blau, *J. Phys. Chem. B*. **2003**, *107*, 37–43; *(c)* I. Fischbach, T. Pakula, P. Minkin, A. Fechtenkötter, K. Müllen, H. W. Spiess, K. Saalwächter, *J. Phys. Chem. B*. **2002**, *106*, 6408–6418.

[49] M. D. Watson, F. Jäckel, N. Severin, J. P. Rabe, K. Müllen, *J. Am. Chem. Soc.* **2004**, *126*, 1402–1407.

[50] N. G. Pschirer, W. Fu, R. D. Adams, U. H. F. Bunz, *Chem. Commun.* **2000**, 87–88.

[51] S. Beer, K. Brandhorst, J. Grunenberg, C. G. Hrib, P. G. Jones, M. Tamm, *Org. Lett.* **2008**, *10*, 981–984.

[52] B. M. Trost, Z. T. Ball, *J. Am. Chem. Soc.* **2005**, *127*, 17644–17655.

[53] B. M. Trost, M. R. Machacek, Z. T. Ball, *Org. Lett.* **2003**, *5*, 1895–1898.

[54] B. M. Trost, Z. T. Ball, *J. Am. Chem. Soc.* **2003**, *125*, 30–31.

[55] B. M. Trost, Z. T. Ball, T. Jöge, J*. Am. Chem. Soc.* **2002**, *124*, 7922–7923.

[56] S. M. Rummelt, A. Fürstner, *Angew. Chem. Int. Ed.* **2014**, *53*, 3626–3630.

[57] A. Fürstner, K. Radkowski, *Chem. Commun.* **2002**, 2182–2183.

[58] F. Lacombe, K. Radkowski, G. Seidel, A. Fürstner, *Tetrahedron* **2004**, *60*, 7315–7324.

[59] T. Matsuda, S. Kadowaki, Y. Yamaguchi, M. Murakami, *Org. Lett.* **2010**, *12*, 1056–1058.

[60] N. Barsu, M. Leutzsch, A. Fürstner, *J. Am. Chem. Soc.* **2020**, *142*, 18746–18752.

[61] P. Karier, F. Ungeheuer, A. Ahlers, F. Anderl, C. Wille, A. Fürstner, *Angew. Chem. Int. Ed.* **2019**, *58*, 248–253.

[62] X. Mo, A. Letort, D.-A. Roşca, K. Higashida, A. Fürstner, *Eur. J. Org. Chem.* **2018**, *24*, 9667–9674.

[63] A. Fürstner, K. Radkowski, J. Grabowski, C. Wirtz, R. Mynott, *J. Org. Chem.* **2000**, *65*, 8758-8762.

[64] A. Fürstner, C. Mathes, C. Lehmann, *Chem. Eur. J.***2001**, *7*, 5299-5317.

[65] Z. Meng, L. Souillart, B. Monks, N. Huwyler, J. Herrmann, R. Müller, A. Fürstner, *J. Org. Chem.* **2017**, *83*, 6977-6994.

[66] P. Karier, F. Ungeheuer, A. Ahlers, F. Anderl, C. Wille, A. Fürstner, *Angew. Chem.Int.Ed.* **2018**, *58*, 248-253.

[67] L. Löffler, C. Wirtz, A. Fürstner, *Angew. Chem. Int. Ed.* **2021**, *60*, 5316-5322.

[68] K. J. Ralston, H. C. Ramstadius, R. C. Brewster, H. S. Niblock, A. N. Hulme, *Angew. Chem. Int. Ed.*, **2015**, 54, 7086–7090.

[69] B. Niess, I. V. Hartung, L. O. Haustedt, H. M. R. Hoffmann, *Eur. J. Org. Chem.* **2006**, 1132– 1143.

[70] I. V. Hartung, B. Niess, L. O. Haustedt, H. M. R. Hoffmann, *Org. Lett.* **2002**, *4*, 3239– 3242.

[71] J. S. Lazo, C. E. Reese, A. Vogt, L. L. Vollmer, C. A. Kitchens, E. Günther, T. H. Graham, C. D. Hopkins, P. Wipf, *J. Pharmacol. Exp. Ther.* **2010**, *332*, 906– 911.

[72] W. Zhang, J. S. Moore, *J. Am. Chem. Soc.* **2004**, *126*, 12796–12796.

[73] W. Zhang, S. M. Brombosz, J. L. Mendoza, J. S. Moore, *J. Org. Chem.* **2005**, *70*, 10198–10201.

[74] C. Zhang, C. Yu, H. Long, R. J. Denman, Y. Jin, W. Zhang, *Chem. Eur. J.* **2015**, *21*, 16935–16940.

[75] C. Grave, A. D. Schlüter, *Eur. J. Org. Chem.* **2002**, 2002, 3075–3098.

[76] S. Höger, *Chem. Eur. J.* **2004**, *10*, 1320–1329.

[78] W. Zhang, J. S. Moore, *Angew. Chem. Int. Ed.* **2006**, *45*, 4416–4439.

[79] M. Iyoda, J. Yamakawa, M. J. Rahman, *Angew. Chem. Int. Ed.* **2011**, *50*, 10522–10553.

[80] H. Yang, Y. Du, S. Wan, G. D. Trahan, Y. Jin, W. Zhang, *Chem. Sci.* **2015**, *6*, 4049–4053.

[81] W. Zhang, J. S. Moore, *J. Am. Chem. Soc.* **2005**, *127*, 11863–11870.

[82] W. Zhang, J. S. Moore, *Angew. Chem. Int. Ed.* **2006**, *45*, 4416–4439.

[83] *(a)* A. Anctil, C. W. Babbitt, R. P. Raffaelle, B. J. Landi, *Environ. Sci. Technol.* **2011**, *45*, 2353–2359.; *(b)* C. Zhang, H. Long, W. Zhang, *Chem. Commun.* **2012**, *48*, 6172.

[84] C. Yu, H. Long, Y. Jin, W. Zhang, *Org. Lett.* **2016**, *18*, 2946–2949.

[85] Y. Ge, S. Huang, Y. Hu, L. Zhang, L. He, S. Krajewski, M. Ortiz, Y. Jin, W. Zhang, *Nat. Commun.* **2021**, *12*, 1136.

[86] J. Heppekausen, R. Stade, R. Goddard, A. Fürstner, *J. Am. Chem. Soc.* **2010**, *132*, 11045–11057.

[87] X. Jiang, J. D. Laffoon, D. Chen, S. Pérez-Estrada, A. S. Danis, J. Rodríguez-López, M. A. Garcia-Garibay, J. Zhu, J. S. Moore, *J. Am. Chem. Soc.* **2020**, *142*, 6493–6498.

[88] G. R. Kiel, K. L. Bay, A. E. Samkian, N. J. Schuster, J. B. Lin, R. C. Handford, C. Nuckolls, K. N. Houk, T. D. Tilley, *J. Am. Chem. Soc.* **2020**, *142*, 11084–11091.

[89] D. E. Gross, J. S. Moore, *Macromolecules* **2011**, *44*, 3685–3687.

[90] D. E. Gross, E. Discekici, J. S. Moore, *Chem. Commun.* **2012**, *48*, 4426.

[91] S. W. Sisco, J. S. Moore, *J. Am. Chem. Soc.* **2012**, *134*, 9114–9117.

[92] S. W. Sisco, J. S. Moore, *Chem. Sci.* **2014**, *5*, 81–85.

[93] S. Lee, E. Chénard, D. L. Gray, J. S. Moore, *J. Am. Chem. Soc.* **2016**, *138*, 13814–13817.

[94] X. Zhou, R. R. Thompson, F. R. Fronczek, S. Lee, *Org. Lett.* **2019**, *21*, 4680–4683.

[95] J. Hillenbrand, M. Leutzsch, A. Fürstner, *Angew. Chem. Int. Ed.* **2019**, *58*, 15690–15696.

[96] B. Wölfl, G. Mata, A. Fürstner, *Chem. Eur. J.* **2019**, *25*, 255 – 259.

[97] S. Schaubach, K. Michigami, A. Fürstner, *Synthesis* **2017**, *49*, 202 – 208.

[98] P. Persich, J. Llaveria, R. Lhermet, T. de Haro, R. Stade, A. Kondoh, A. Fürstner, *Chem. Eur. J.* **2013**, *19*, 13047 –13058.

[99] X. Xia, Z. Lao, P. Toy, *Synlett* **2019**, *30*, 1100 – 1104.

[100] A. Kirschning, P. Toy, S. Ceylan, H. Law, *Synthesis* **2016**, *49*, 145 –150.

[101] C. Raji Reddy, N. Narsimha Rao, *Tetrahedron Lett.* **2009**, *50*, 2478 – 2480.

[102] Y. Xing, G. O_Doherty, *Org. Lett.* **2009**, *11*, 1107 – 1110.

[103] E. Årstad, A. Barrett, B. Hopkins, J. Köbberling, Org. Lett. 2002, *4*, 1975 – 1977.

[104] G. Strunz, H. Finlay, *Can. J. Chem.* **1996**, *74*, 419 – 432.

[105] D. Ma, X. Lu, *Tetrahedron* **1990**, *46*, 3189 – 3198.

[106] D. Ma, X. Lu, *Tetrahedron Lett.* **1989**, *30*, 843 – 844.

[107] Y. Zhang, D. Yang, Z. Weng, *Tetrahedron* **2017**, *73*, 3853 – 3859.

[108] V. Morozova, J. Skotnitzki, K. Moriya, K. Karaghiosoff, P.Knochel, *Angew. Chem. Int. Ed.* **2018**, 57, 5516 – 5519; *Angew.Chem.* **2018**, *130*, 5614 – 5617.

[109] R. Rossi, F. Bellina, L. Mannina, *Tetrahedron Lett.* **1998**, *39*,3017 – 3020.

Chapter 2: "Canopy Catalysts"

2.1. Introduction

2.1.1 Tungsten Alkylidyne Catalysts

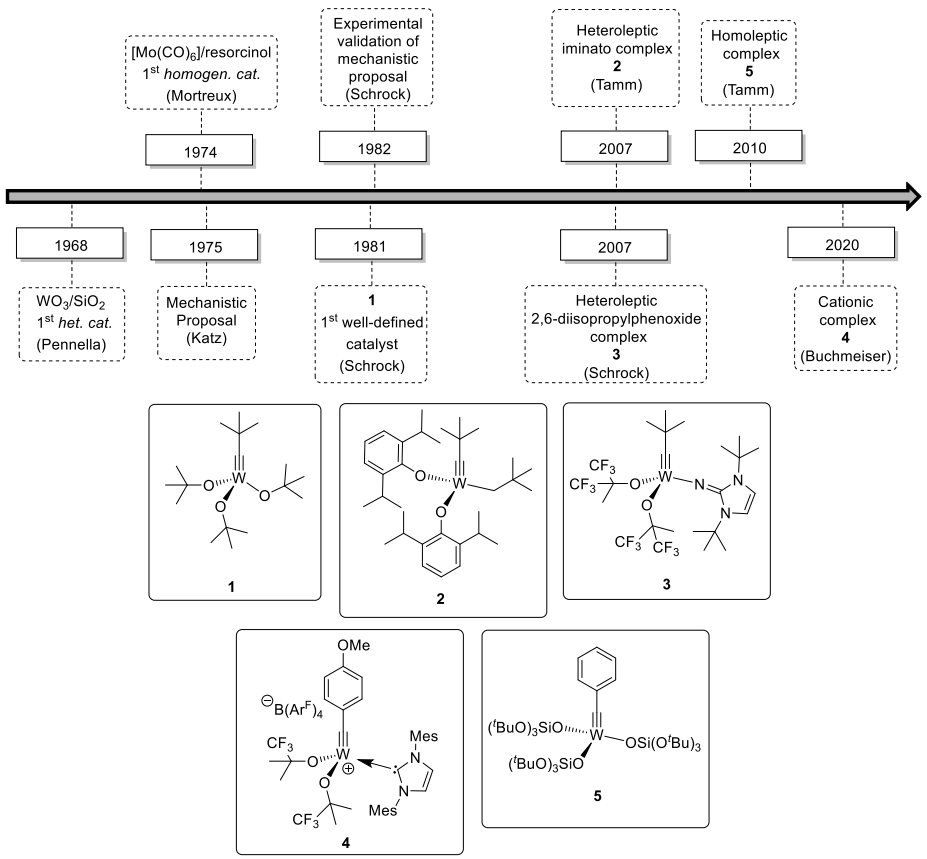

Figure 2.1. Milestones in alkyne metathesis with reference to tungsten alkylidynes.

In 1968, Penella *et al.* showed that a heterogeneous mixture of silica and tungsten trioxide at elevated temperatures can effectively scramble 2-pentyne into a mixture of 3-hexyne and 2-butyne, featuring the first-ever documented example of an alkyne metathesis reaction. Unfortunately, this initial discovery was largely overlooked, due to a competing alkyne polymerisation observed under the harsh conditions used

(Figure 2.1).[1-3] Shortly after, Mortreux and Blanchard noted that a mixture of resorcinol and $[Mo(CO)_6]$ in decalin at 160 °C gave a homogeneous catalytically competent system for alkyne metathesis (Scheme 2.1).

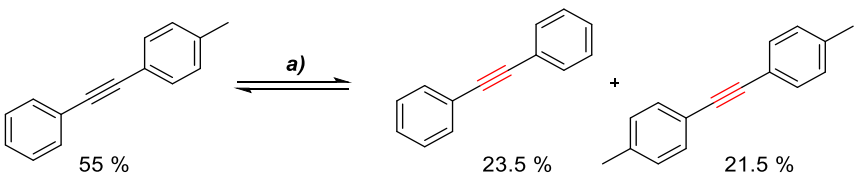

Scheme 2.1. The first example of homogeneously catalysed alkyne metathesis. *Reagents and conditions*: *(a)* $[Mo(CO)_6]$ (10 mol%), resorcinol (60 mol%), decalin, 160 °C, 3 h.

Despite numerous optimisation efforts over the years, the synthetic utility of Mortreux-type catalytic systems is rather limited due to their poor functional-group tolerance and long reaction times even at elevated temperatures.[4-27] Originally proposed by Katz in 1975 and experimentally validated later on by Schrock, the generally accepted mechanism of alkyne metathesis proceeds in a similar manner to the Chauvin cycle for alkene metathesis.[28-29] In 1981, Schrock and co-workers reported the first well-defined alkyne metathesis catalyst $[W(CCMe_3)(O^tBu)_3]$ (**1**) (Figure 2.1).[30-32] This complex can catalyse the metathesis reactions of both aliphatic and aromatic alkynes at ambient temperature with remarkable ease. This seminal discovery marked the beginning of a new era in the field of alkyne metathesis. Over the years, several different ligands were investigated to uncover the key elements to efficient alkyne metathesis catalyst design including sterically demanding phenolates (**2**), [33,34] fluorinated alkoxides (**3**), and silanols (**5**). Since alkoxides were shown to be efficient ligands for alkyne metathesis, much effort has been invested in taming the Lewis acidity of the tungsten center by installing different fluorinated alkoxides as well as heteroleptic push/pull ligand systems (**3**-**4**).[35-46] Furthermore, homoleptic siloxy-based complexes including benzylidyne **5** were also found to engage in the catalytic metathesis of conjugated diynes.[47-49]

2.1.2 Molybdenum Alkylidyne Catalysts

Along with the development of tungsten alkylidynes, Schrock and co-workers also reported the synthesis of molybdenum-based alkyne metathesis catalysts. Once again, sterically hindered fluorinated alkoxides (**6b**-**d**), 2,6-diisopropylphenoxide (**7a**) or adamantoxide (**7b**), served as competent ligands for molybdenum catalysed alkyne metathesis (Figure 2.2). Conversely, trisalkoxy complex **6a** did not react with simple internal alkynes such as diphenylacetylene or 3-heptyne.[50-53] Tamm and co-workers also investigated the effect of fluorinated alkoxides on the catalytic activity of molybdenum alkylidynes **11** in homo-metathesis reaction of 1-phenyl-1-propyne. Access to these complexes was readily achieved via a three-step sequence. Nucleophilic addition of mesityl lithium to commercially available [$Mo(CO)_6$] (**8**) and treatment of the resulting lithium enolate with tetramethylammonium bromide gave the Fischer carbene **9**. Oxidation of the latter with oxalyl bromide in CH_2Cl_2, followed by addition of bromine and DME delivered the Schrock alkylidyne **10**. Ligand exchange with LiO^tBu or fluorinated alkoxides furnished the collection of complexes of type **11a**-**d** (Scheme 2.2).

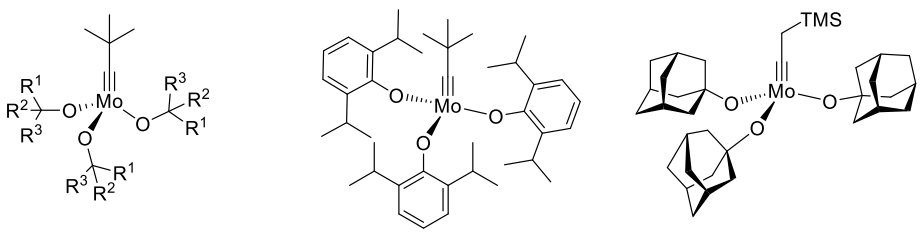

6a $R^1 = R^2 = R^3 = Me$
b $R^1 = CF_3$, $R^2 = R^3 = Me$
c $R^1 = Me$, $R^2 = R^3 = CF_3$
d $R^1 = R^2 = R^3 = CF_3$

7a **7b**

Figure 2.2. Early developed Mo-based alkyne metathesis catalysts.[50-53]

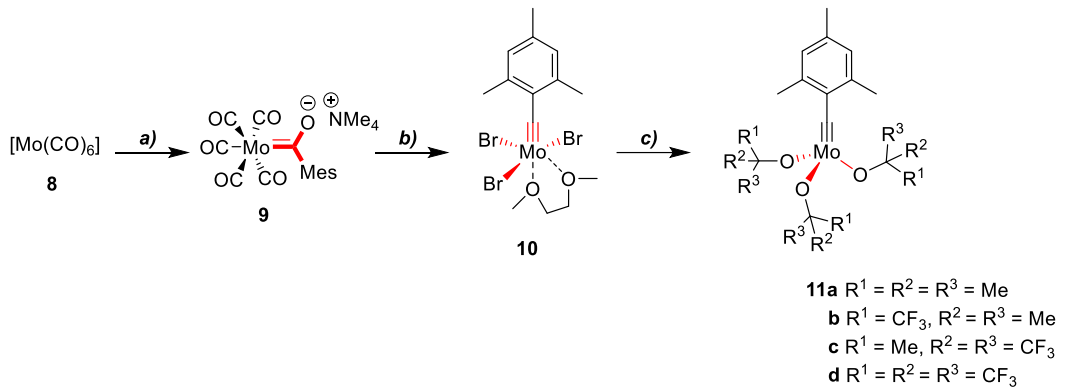

Scheme 2.2. Scalable synthesis of molybdenum alkylidyne complexes **11**.[54-56] *Reagents and conditions*: *(a)* (i) MesLi, Et_2O; (ii) NMe_4Br, H_2O; *(b)* oxalyl bromide, Br_2, CH_2Cl_2/DME, − 78 °C → RT; *(c)* LiOR.

Interestingly, all complexes examined (**11a**-**d**) were catalytically active at room temperature. Unlike the catalytically inactive complex **6a**, benzylidyne **11a** was found to be an active catalyst with a slow turnover. Whilst the introduction of a single trifluoromethyl group on the alkoxide ligands led to substantial enhancement in the catalytic performance (complex **11b**), further increase in the degree of fluorination proved to be rather detrimental for the catalytic activity (**11c**-**d**).[54-56]

In 1998, Cummins reported the synthesis of tricoordinate molybdenum (III) complexes, including the azophilic complex **14**.[57] Inspired by the work of Cummins, Fürstner and co-workers reported in 1999, the development of a new catalytic system for alkyne metathesis. Complex **14** was readily prepared from $[MoCl_3(THF)_3]$ (**12**) and lithium amide **13** (Scheme 2.3). Even though complex **14**, itself is not capable of promoting metathesis in toluene, upon treatment with an excess of CH_2Cl_2, a catalytically active mixture of complex **15** and trisamido-molybdenum (IV) chloride **16** was obtained. Subsequent mechanistic studies indicated that although both complexes in isolation can readily engage in alkyne metathesis, terminal alkylidyne complex **15a** becomes inactive after a single turnover. In addition, the mechanistic aspects behind the conversion of complex **16** into the actual catalytically competent species remain elusive.[58,59] Shortly after the initial discovery of this unique mode of activation and reactivity of Cummins reagent (**14**), Moore and co-workers documented an improved protocol for activation of the complex **14** that encompassed a reductive recycling strategy (Scheme 2.3). Activation with *gem*-dichlorides in the presence of Mg dust, led to full conversion of trisamido complex **14** to propylidyne **15b**.[60-62]

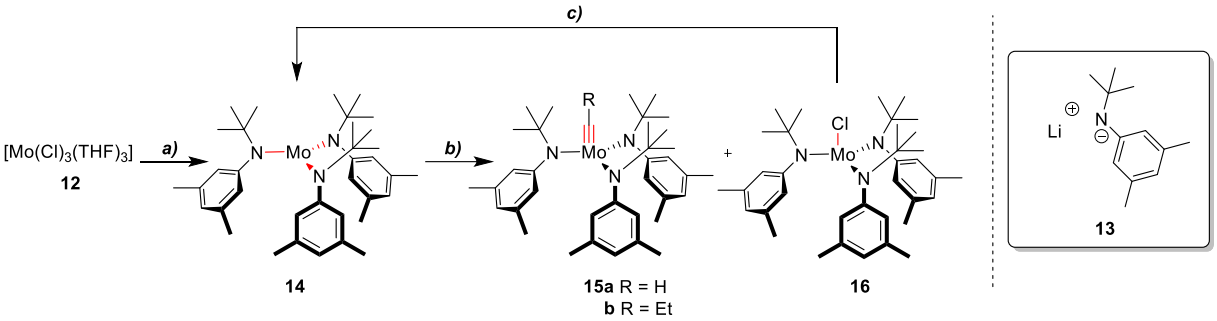

Scheme 2.3. Preparation, *gem*-dichloride activation, and reductive recycling of complex **14**.[60-62] *Reagents and conditions*: *(a)* **13**, THF, − 30 °C → RT, (**14**, 54 %); *(b)* CH_2Cl_2, toluene, RT (R = H) *or* 1,1-dichloropropane, THF, RT (R = Et); *(c)* Mg, THF.

The *in situ* catalyst system [**14**+CH_2Cl_2] can tolerate a range of functional groups, which previously proved deleterious for the catalytic activity of neopentylidyne **1**. More specifically, silyl- and thio- ethers, sulfones, amides, amines and aldehydes were well tolerated. Its superior catalytic performance over the more Lewis acidic tris(*tert*-butoxy) complex **1** is further highlighted by its extensive use in natural product syntheses.[63]

2.1.3 Molybdenum Catalysts and Precatalysts with Siloxy Ligands

In 2009, Fürstner and co-workers reported the synthesis of the first alkyne metathesis pre-catalyst **20** endowed with triphenylsilanolate ligands (Scheme 2.4 (i)). This was readily prepared via a three-step sequence from cheap commercial sodium molybdate **17**.

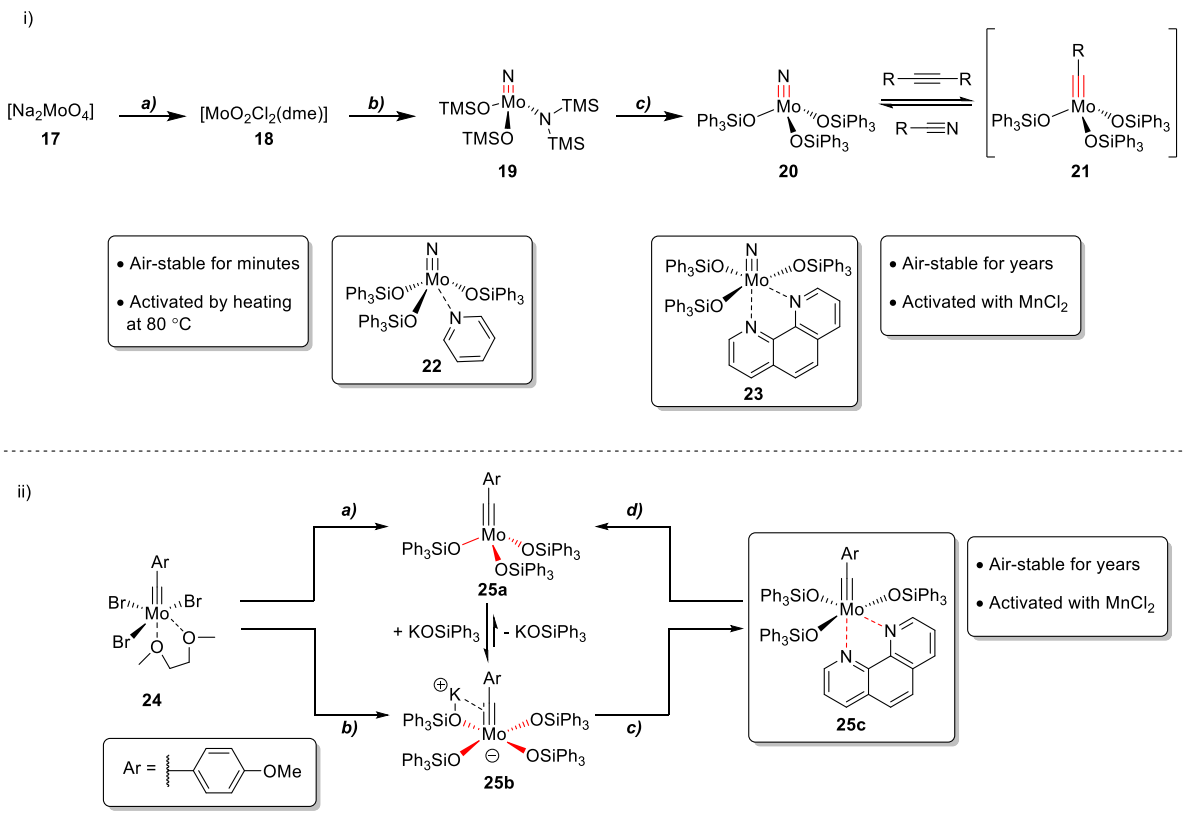

Scheme 2.4. Preparation of molybdenum-based pre-catalysts for alkyne metathesis.[64-66] *Reagents and conditions*: (i) *(a)* TMSCl, DME; *(b)* LiHMDS; *(c)* Ph_3SiOH; (ii) *(a)* $KOSiPh_3$ (3.0 equiv.), toluene; *(b)* $KOSiPh_3$ (4.0 equiv.), toluene; *(c)* 1,10-phenanthroline; *(d)* $MnCl_2$, 80 °C.

Access to dioxo complex **18** was achieved by heating salt **17** in DME with TMSCl. Treatment of the latter with excess LiHMDS gave nitrido complex **19**. Protonolysis with excess triphenylsilanol delivered pre-catalyst **20.** The user-friendliness of this pre-catalyst was greatly improved by complexation to pyridine (**22**) or 1,10-phenanthroline (**23**) (Scheme 2.4 (i)).[64] Despite its use in the synthesis of natural products, high catalyst loadings were required to release the actual active alkylidyne complex **21** and therefore achieve productive metathesis. In an attempt to harness the full potential of alkylidyne **21,** the synthesis

of complex **25a** was investigated. Prepared in a similar manner to complex **10**, tribromo complex **24** was converted to alkylidyne **25a** with triphenylsilanolate ancillary ligands via the slow and careful addition of triphenylsilanol (3.0 equiv.) in toluene. Given the high Lewis acidity of complex **24**, employing an excess of triphenylsilanol (4.0 equiv.) afforded the potassium salt **25b**. The bench-stable pre-catalyst **25c** was obtained via the addition of 1,10-phenathroline to a solution of salt **25b** in CH_2Cl_2, while its activation can be readily achieved by simply heating in toluene at 80 °C in the presence of $MnCl_2$. The excellent catalytic performance and functional group tolerance of complex **25a** in metathesis reactions is highlighted by its application in the synthesis of several challenging natural targets.[65-71]

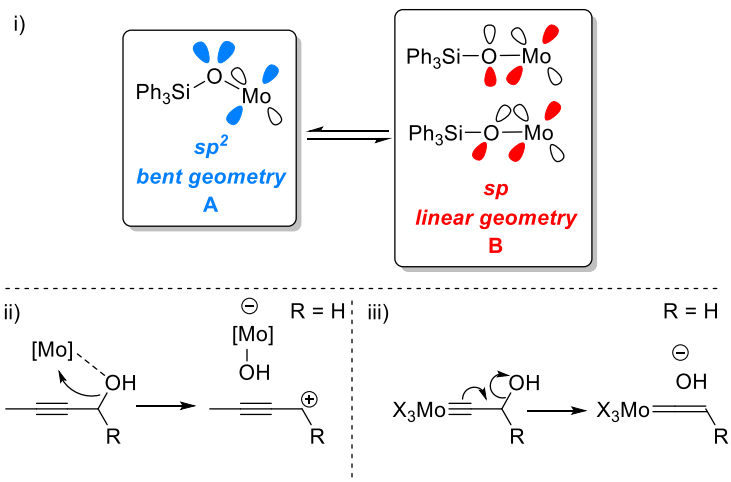

Figure 2.3. Lewis acidity modulation and deactivation of the metal centre.[65-66] (i) Conformation induced modulation of the lewis acidity of the metal centre by silanolate ligands; (ii) 1st Proposed mode of catalyst deactivation; (iii) 2nd Proposed mode of catalyst deactivation.

Although the sterically congested coordination sphere of complex **25a** shields the metal centre, disfavouring associative bimolecular decomposition without preventing the productive binding of substrates, its high catalytic activity stems from the adaptive properties of its silanolate ligands. Unlike alkoxides, silanolates are weak π- and σ- donor ligands. A change in the Si-O-Mo angle, and therefore the hybridisation of the oxygen atoms, leads to a change in the degree of π-donation of the oxygen lone pairs to the metal centre. In the bent configuration (**A**, Figure 2.3 (i)), only a single pair of electrons in p-orbitals of the oxygen can engage in $p_\pi \rightarrow d$ donation.[65-66] This in turn increases the Lewis acidity of the metal centre and therefore substrate binding. On the other hand, in the linear conformation (**B**, Figure 2.3 (i)) both orthogonal lone pairs of the oxygen donate electron density to the molybdenum d orbitals. This

reduces the Lewis acidity of the metal centre thus favouring cycloreversion and extrusion of the metathesis product.[65-66] Catalyst **25a** can tolerate a broad range of functional groups including thioesters, sulfoxides or sulfonamides, alkyl halides, azides as well as secondary and primary amines. Despite its use in the syntheses of several natural products, protic functional groups including primary or propargylic alcohols still remain a long-standing challenge. This incompatibility of complex **25a** with substrates bearing protic functional groups, has been attributed either to a competitive substrate/ligand substitution that forces the metal centre to shed its silanolate ligands or an elimination mediated decomposition (Figure 2.3 (ii)-(iii)).[67,72,73]

2.1.4. Molybdenum Alkylidyne Complexes with Chelate Ligands

In recent years, several research groups have attempted to circumvent the issues associated with monodentate ligand-based catalyst systems by utilising tridentate ligand scaffolds. As a result of the chelate effect, a tridentate ligand is more tightly bound to the metal, thus making it less likely to be displaced by a single substrate molecule. In 2011, Zhang and co-workers reported that treatment of a solution of trisamido complex **15b** in CCl_4 with amine-tethered phenol ligand **26a** gave a catalytically active mixture (Figure 2.4(i)). While the isolation of a single alkylidyne complex responsible for the observed catalytic activity was unsuccessful, increasing the Lewis acidity of the metal center (**26b**-**e**) and the steric bulk around the coordination sphere (**26f**) led to substantial improvement in the catalytic activity (Figure 2.4(i)).[74-77] In 2016, Fürstner and co-workers employed a similar approach, utilising tridentate silanolate-based ligands. *In situ* protonolysis of complex **15b** in toluene with trisilanols **27**-**28** delivered in each case, ill-defined mixtures rather than single well-defined alkylidynes (Figure 2.4(ii)).[78] Intriguingly, these elaborate mixtures consisting of partially cross-linked species are catalytically active and exhibit superior functional group tolerance compared to catalyst **25a** (Figure 2.4 (iii)). This is further illustrated by their application in a few recently reported total syntheses including that of euphorhylonal A.[79-81]

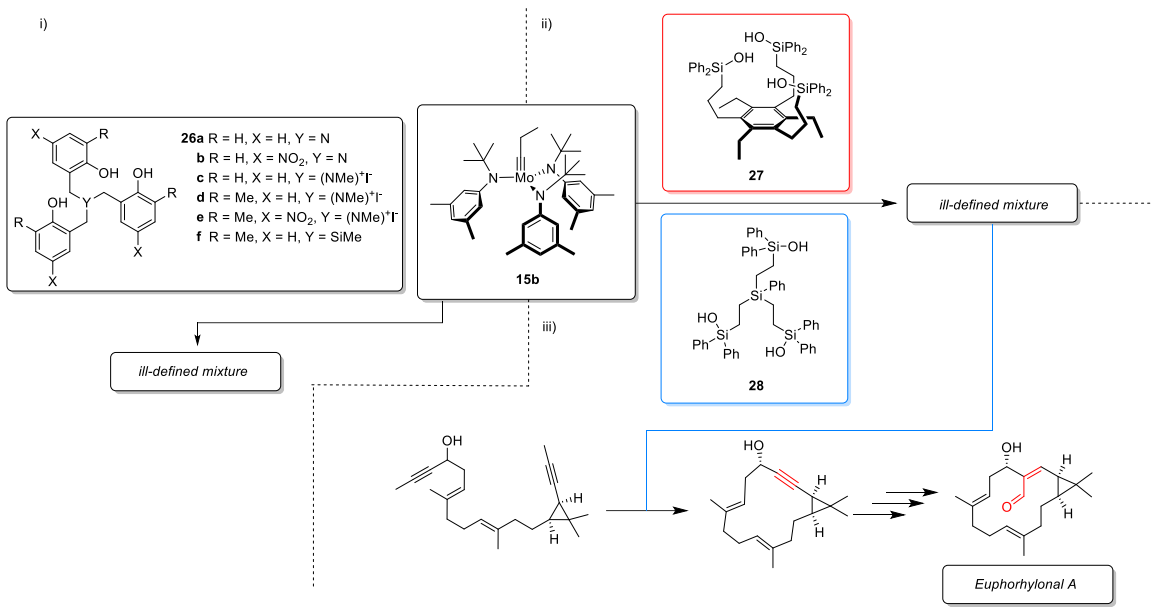

Figure 2.4. Attempts to synthesise well-defined molybdenum-based alkyne metathesis catalysts with tridentate ligands.[74-81] (i) Zhang and co-workers' contributions towards catalysts with tridentate ligands **26**; (iii) Fürstner and co-workers' contributions towards catalysts with tridentate ligand scaffolds **27**-**28**; (iv) Application of [**15b**+**28**] catalyst system in the total synthesis of euphorhylonal A.

More recently a new structurally well-defined molybdenum-based catalyst with a tripodal ligand scaffold was reported. The tridentate ligand **33** was accessible via a scalable three-step sequence from commercial 2-bromoacetophenone (**29**) (Scheme 2.5 (i)).[82] To achieve controlled protonolysis and therefore suppress the formation of any molybdate complexes during ligand complexation reactions, a more efficient and practical protonolysis protocol was also reported using precatalyst **34**. Tris(*tert*-butoxy) complex **34** was prepared on scale from complex **24** through a ligand exchange reaction with NaO^{t}Bu in THF in very good yield (Scheme 2.5 (ii)). Whilst the C_3-symmetry and required pre-organisation of ligand **33** was confirmed by X-ray crystallography, stirring a solution of precatalyst **34** in toluene with ligand **33** at ambient temperature gave the catalytically active dimeric complex [**35**·**35**] (Scheme 2.5 (ii)-(iii)).

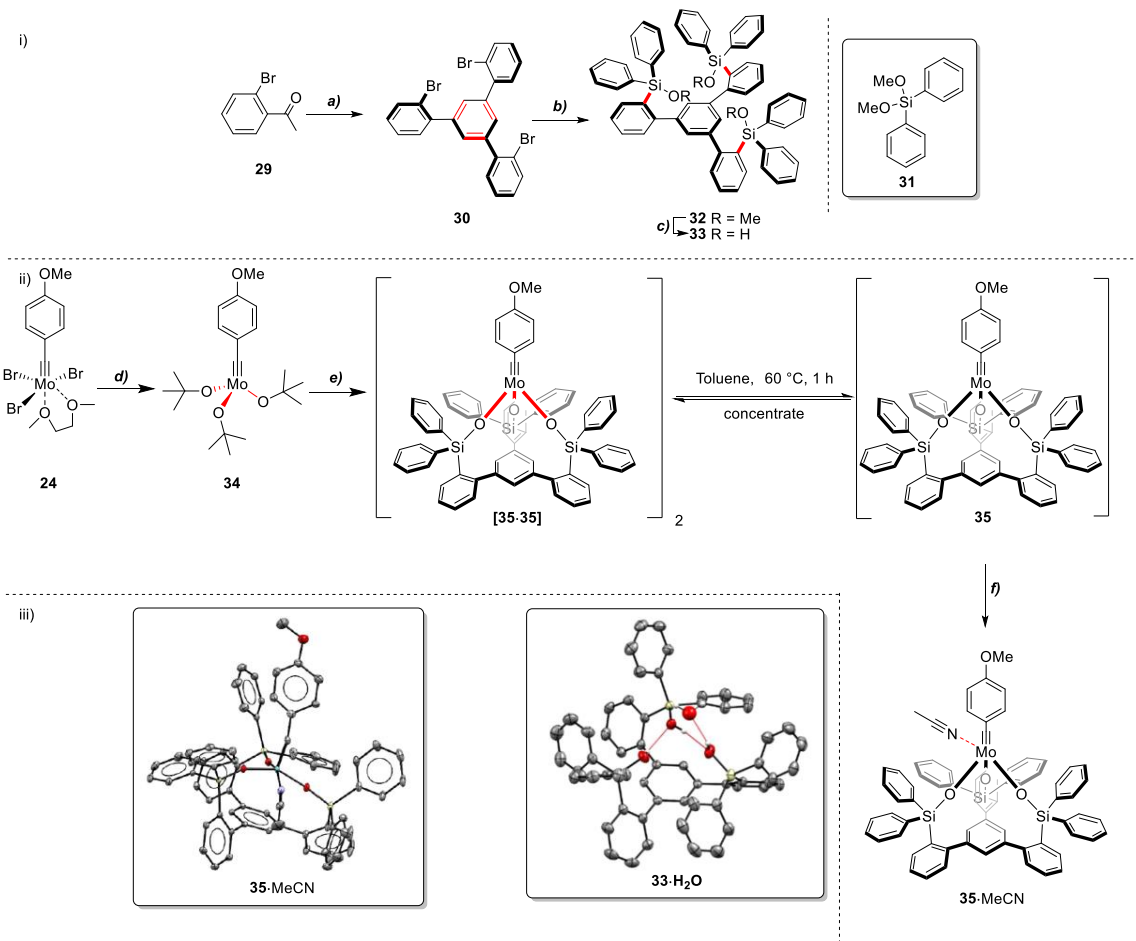

Scheme 2.5. Synthesis of well-defined molybdenum alkylidyne complex **35**.[82-83] (i) Scalable synthesis of tripodal ligand **33**, (ii) Scalable synthesis of complex **35**, (iii) Solid state structures of adduct **33**·H_2O (disorder omitted for clarity; H-atoms involved in H-bonding are shown) and adduct **35**·MeCN.[81] *Reagents and conditions*: *(a)* TfOH (neat), 130 °C, (**30**, 59%); *(b) (i)* Li^{t}Bu, Et_2O, − 125 °C, 1 h; *(ii)* **31**, Et_2O, − 125 °C → RT, 18 h (**32**, 74 %); *(c)* HCl, H_2O, 0 °C → RT, quant.; *(d)* NaO^{t}Bu, THF, RT, 18 h (**34**, 83 %); *(e)* **33**, toluene, RT, 18 h ([**35**]$_2$, 95 %); *(f)* MeCN.

Comprehensive NMR studies revealed that heating a solution of the dimeric aggregate [**35**·**35**] in toluene at 60 °C gave the monomeric complex **35**. The solid-state structure of this monomeric molybdenum alkylidyne was confirmed by X-crystallography as the adduct [**35**·MeCN]. Despite its slow initiation rate, rigid backbone and greater steric encumbrance, podand complex **35** exhibits superior functional group tolerance than both its parent complex **25a** and predecessor catalyst system [**15b**+**27**].

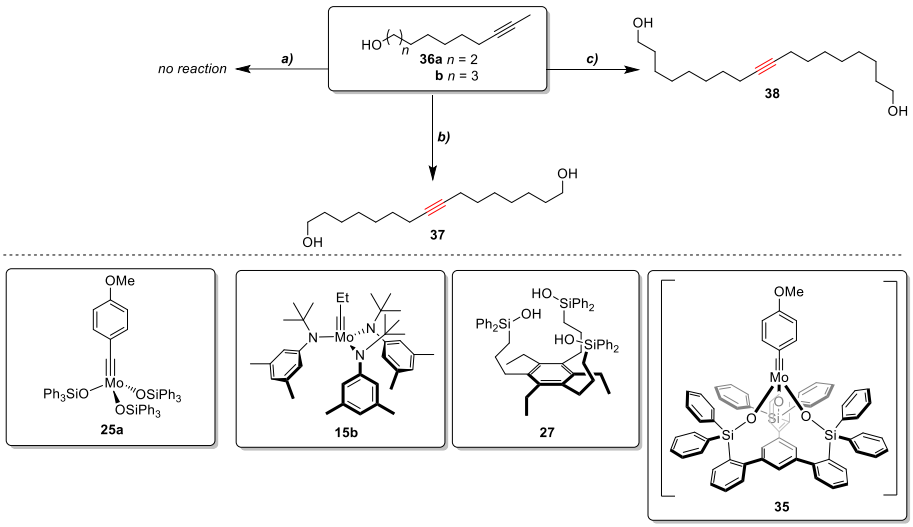

Scheme 2.6. Homo-metathesis of primary alcohols **36**.[82] *Reagents and conditions*: *(a)* **36a**, **25a** (5 mol%), toluene, RT, 5 Å MS; *(b)* **36a**, [**15b**+**27**] (5 mol%), toluene, RT, 5 Å MS, (**37**, 72 %); *(c)* **36b**, **35** (5 mol%), toluene, RT, 5 Å MS, (**38**, 91 %).

For instance, although the attempted metathesis of primary alcohol **36a** using catalyst **25a** was unsuccessful, homo-metathesis of the homologous alcohol **36b** catalysed by complex **35** afforded the diol product **38** in higher yield than that of diol **37** with the two-component catalyst system [**15b**/**27**] (Scheme 2.6).[68,78] Additionally, both primary and secondary amines as well as other substrates containing protic sites (phenol, malonate) gave homometathesis products in excellent yields (91-93 %).[82] More recently, it has been shown that the chelate effect in the tripodal ligand scaffold of complex **35** offers even a certain stability toward water, which marks a big step forward in the field of metal alkylidyne chemistry.[84] Addition of water (10 equiv.) or a primary alcohol to a solution of monodentate ligand-based complex **25a** in [D_8]-toluene results in almost instantaneous decomposition with quantitative release of Ph_3SiOH (≤5 min). Conversely under identical conditions, "canopy complex" **35** undergoes complete hydrolysis in about 9 h.[84]

2.2. Optimised Synthesis of Ligand 33

Even though the substrate scope of complex **35** was briefly explored in the past, an extensive substrate scope screen was necessary to gain a more precise and in-depth understanding of the reactivity and

functional group tolerance of this recently developed metathesis catalyst. However, this comprehensive substrate scope study had to be postponed until a critical aspect of the synthesis of ligand **33** was addressed. The strategy employed for converting 2-bromoacetophenone (**29**) into trisilanol **33**, commenced with a capricious cyclocondensation step performed in neat triflic acid at 130 °C to afford tribromide **30** in poor yield (Scheme 2.5 (i)). Moreover, ligand **33** was only obtained in an overall 44 % yield over the three-step sequence used (Scheme 2.5 (i)). This in turn highlighted the need to optimise the three-step synthetic route described in Scheme 2.5 for use on a multi-gram scale. It was envisioned that a protocol involving *in situ* generated HCl in EtOH, would serve as a safer and scalable alternative.[85] Dropwise addition of excess $SiCl_4$ to a solution of ketone **29** in EtOH at 0 °C and overnight stirring at RT, led to full conversion to the desired tribromide. Dilution of the crude reaction mixture with water, followed by filtration gave the product **30** as a yellow powdery solid in quantitative yield on first attempt (Table 2.1, entry 1). Repetition of this reaction on multi-gram scale using the same reaction conditions, delivered product **30** in almost quantitative yield (Table 2.1, entries 2-3). Due to the toxicity of $SiCl_4$, the number equivalents used for the cyclotrimerisation of aryl ketone **29** were reduced. Unfortunately, this resulted in a minor decrease in the isolated yield of cyclotrimeric product **30** (Table 2.1, entry 4).

Table 2.1. Optimisation and scale-up of the cyclotrimerisation reaction of ketone **29.**

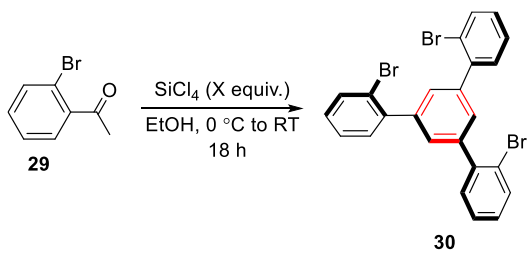

29 **30**

Entry	X (equiv.)	% Conversion	Scale (g)	% Yield
1	3.0	100	3.0	99
2	3.0	100	5.0	97
3	3.0	100	20.0	98
4	2.0	100	20.0	91

With one of the problematic aspects of the above three-step sequence rigorously resolved, the large-scale synthesis of ligand precursor **32** was examined. Previously, access to advanced intermediate **32** was achieved in 75% yield via low temperature metal-halogen exchange (−125 °C) with excess ^{t}BuLi in Et_2O,

followed by quenching with siloxane reagent **31**. The triple metalation of tribromide **29** was investigated to determine if it was possible to access this intermediate under more user-friendly conditions. Regrettably, lithium-halogen exchange at – 78 °C and subsequent dropwise addition of the electrophile **31**, furnished the triarylsilylether **32** in poor yield (Table 2.2, entry 1). Conversely, when triple lithiation was performed at −125 °C, product **32** was obtained in very good yield on multi-gram scale (Table 2.2, entries 2-4). Single-crystal X-ray diffraction of compound **32**, indicated that in the solid-state structure, the methoxy groups obstruct the scaffold from adopting a C_3-symmetric conformation (Figure 2.5).

Table 2.2. Scale-up synthesis of ligand precursor **32.**

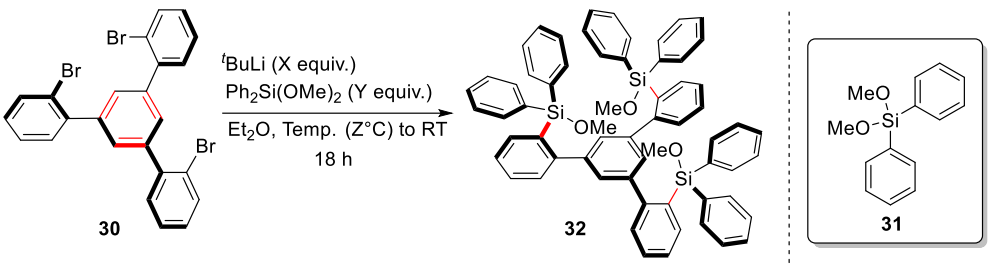

Entry	X (equiv.)	Y (equiv.)	Z (°C)	Scale (g)	% Yield
1	6.2	3.0	− 78	0.3	40
2	6.2	3.0	− 125	2.0	74
3	6.2	3.0	− 125	4.0	75
4	6.2	3.0	− 125	7.5	75

Hydrolysis of ligand precursor **32** with concentrated, aqueous HCl solution in THF at 0 °C afforded multi-gram quantities of trisilanol **33** in quantitative yield (Table 2.3, entries 1-2). As opposed to the original sequence, the refined three-step synthetic route delivered ligand **33** on multi-gram scale in an overall 74 % yield.

Table 2.3. Large-scale hydrolysis of ligand precursor **32.**

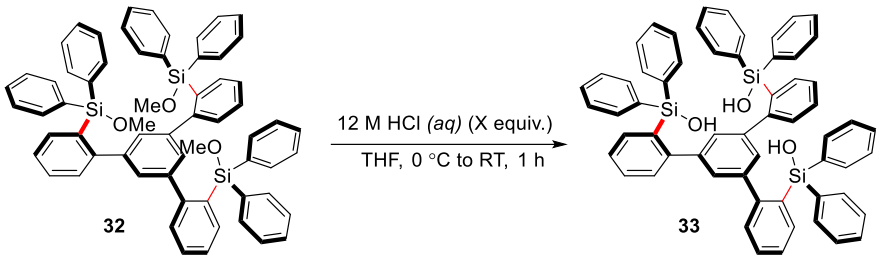

Entry	X (equiv.)	Scale (g)	% Yield
1	90.0	2.0	quant.
2	90.0	5.0	quant.

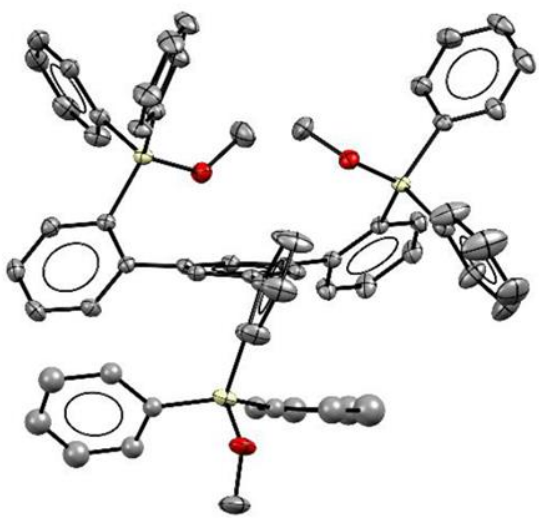

Figure 2.5. Solid-state structure of ligand precursor **33**; disorder omitted for clarity; image refined by Julius Hillenbrand.[82-83]

2.3. Functional Group Tolerance Scope of Catalyst 35

As discussed in Section 2.1.4, metathesis catalyst **35** tolerates a range of functional groups. However, its functional group tolerance has not been comprehensively examined. More specifically, the limits of its functional group and substrate tolerance with relevance to primary and propargylic alcohols as well as

other synthetically useful structural motifs are yet to be determined.[84] All the methyl-capped alkynes used in this substrate scope screen were either commercially available or obtained from the compound archive of the Fürstner group in the Max-Planck Institut für Kohlenforschung, Germany.

2.3.1 Homo-, Cross- and Ring-Closing Metathesis Reactions

All the reactions performed as part of this study were initially carried out with a catalyst loading of 5 mol% at ambient temperature in the presence of freshly activated 5 Å MS in toluene, while the progress of the reactions was monitored by TLC or GC-MS. The best yielding conditions are displayed in Tables 2.4 - 2.8.

Table 2.4. Homo metathesis reactions of alcohols with complex **35.**

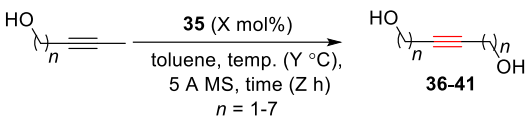

Entry	Substrate *n*		X (mol%)	Y (°C)	Z (h)	Yield (%)
1	2	**36**	5	110	18	NR [a,b]
2	3	**37**	5	110	18	NR [a,b]
3	4	**38**	5	110	18	NR [a,b]
4	5	**39**	5	RT	18	69
5	6	**40**	5	RT	18	83
6	7	**41**	5	RT	18	91

[a] Reactions also performed at RT, 40 °C, 60 °C and 90 °C. [b] Only starting material was recovered.

Table 2.5. Attempted cross metathesis reactions of alcohols (*n* = 1 - 3) with complex **35**.

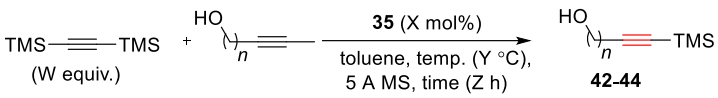

Entry	Substrate *n*		W (equiv.)	X (mol%)	Y (°C)	Z (h)	Yield (%)
1	1	**42**	1.5	5	110	18	NR [a,b]
2	2	**43**	1.5	5	110	18	NR [a,b]
3	3	**44**	1.5	5	110	18	NR [a,b]

[a] Reaction also performed at RT, 40 °C, 60 °C and 90 °C. [b] Only starting materials were recovered.

Table 2.6. Ring-Closing Alkyne metathesis natural product intermediates with complex **35.**

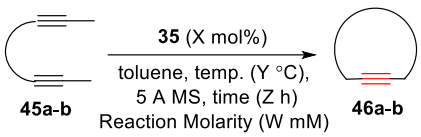

Entry	Substrate	W (mM)	X (mol%)	Y (◦C)	Z (h)	Yield (%)
1	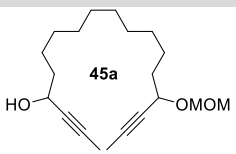	2	10	110	18	- [a]
2	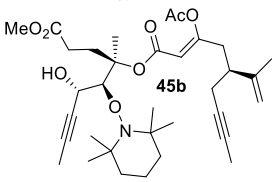	2	30	110	18	68 [b]

[a] complex mixture of linear and cyclic dimers. [b] %yield over two steps (ring-closing metathesis and reductive cleavage of the 2,2,6,6-tetramethylpiperidinyl group).

The direct comparison of the parent complex **25a** with the new catalyst **35** is particularly instructive (Table 2.4): while metathesis catalyst **25a** completely failed to promote the homo-metathesis reactions of even

higher alcohols, “canopy complex” **35** afforded the desired products (**39**-**41**) in good to excellent yields (*n* = 5-7, entries 4-6). On the other hand, homo-metathesis or cross-metathesis reactions of short-chain primary unhindered alcohols to give diols **36**-**38** or alkyne silanes **42**-**44** were unsuccessful even after overnight heating at elevated temperatures (*n* = 1-3, Table 2.4 & Table 2.5 entries 1-3). The functional group tolerance of catalyst **35** towards propargylic alcohols of catalyst **35**, however, is exemplified by the ring-closing alkyne metathesis (RCAM) reactions of polyfunctionalised acyclic diynes carrying sensitive functionalities. While the ease of assembling macrolactone **46b** in good yield over two steps, gave us confidence for more advanced synthetic applications (Table 2.6, entry 2); the RCAM reaction leading to product **45** containing two different propargylic groups, demonstrated two important attributes of complex **35**. Although treatment of diyne **45a** in refluxing toluene with molybdenum alkylidyne **35**, did not deliver the desired RCAM product **46a**, the inseparable mixture of cyclic and acyclic dimers obtained still stands as adequate proof of tolerance towards propargylic substituents. Moreover, the unexpected formation of cyclic dimeric products, highlights that the catalytical activity of complex **35** also extents to one-pot ACM/RCAM reactions.

Table 2.7. Homo metathesis reactions of methyl-capped aliphatic alkynes with complex **35**.

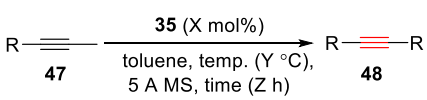

Entry	Substrate	Product	X (mol%)	Y (◦C)	Z (h)	Yield (%)
1	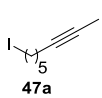 **47a**	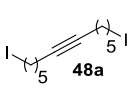 **48a**	5	RT	18	82
2	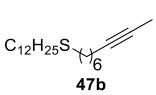 **47b**	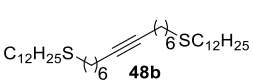 **48b**	5	RT	18	95
3	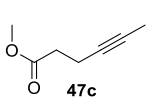 **47c**	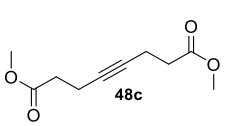 **48c**	10	90	18	79
4	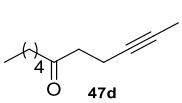 **47d**	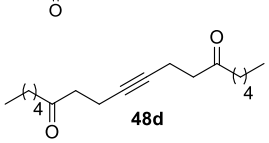 **48d**	10	110	18	– [a,b]

5	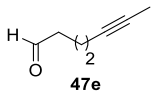 **47e**	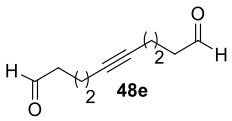 **48e**	10	110	18	– [a,c]
6	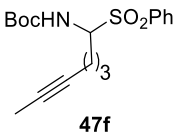 **47f**	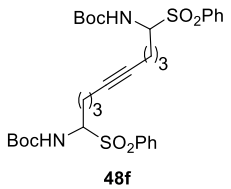 **48f**	5	RT	18	71
7	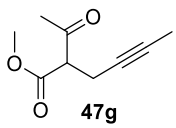 **47g**	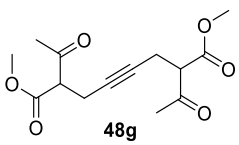 **48g**	10	90	18	79

[a] Reaction also performed at RT, 40 ◦C, 60 ◦C and 90 ◦C. [b] Only starting material was recovered. [c] Decomposition.

Given the tolerance of catalyst **35** towards phenol and malonate derivatives discussed in Section 2.1.4, substrates containing C-H acidic sites including ester **47c**, β-ketoester **47g** and α-amido sulfone **47f** were efficiently converted to the corresponding homo-metathesis products (Table 2.7, entries 3, 6-7). β-Ketoesters, which were found to be incompatible with the parent complexes **25a-d**, gave the desired product **48g** in the presence of catalyst **35** on elevated temperature (90 ◦C) in good yield. In addition, substitution-prone or coordinating substrates such as alkyl iodide **47b** and thioethers **47a** and **49a** were also well-tolerated by this catalyst (Table 2.7 & Table 2.8). Unfortunately, attempted formation of the bis-aldehyde **48e**, resulted in decomposition. This did not come as a surprise since aldehydes were previously found to be incompatible, a limitation that remains a long-standing problem. Although aromatic ketones have previously been tolerated in alkyne metathesis reaction, catalyst **35** failed to deliver aliphatic ketone derivative **48d** (Table 2.6, entry 4). It was also rewarding to find that the basic nitrogen in pyridine **49b** and sulfur-containing heterocycle **49c** were converted at ambient temperature or at 60 °C to the desired products (**50b**-**c**).

Table 2.8. Homo metathesis reactions of methyl-capped aryl/heteroaryl alkynes with complex **35**.

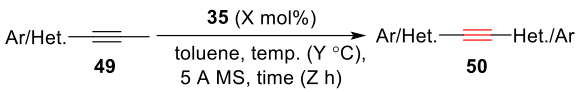

Entry	Substrate	Product	X (mol%)	Y (°C)	Z (h)	Yield (%)
1	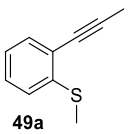 **49a**	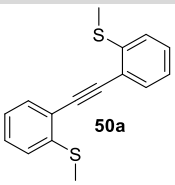 **50a**	5	60	18	47[c]
2	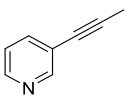 **49b**	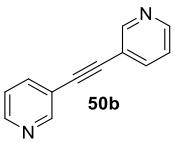 **50b**	10	60	18	62
3	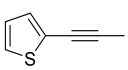 **49c**	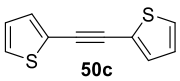 **50c**	10	RT	18	93

[a] Reaction also performed at RT, 40 °C, 60 °C and 90 °C. [b] Only starting material was recovered. [c] Full conversion confirmed by GCMS, co-elution of the product with ligand debris during chromatographic purification.

2.4. Towards the Development of a New Alkyne Metathesis Catalyst

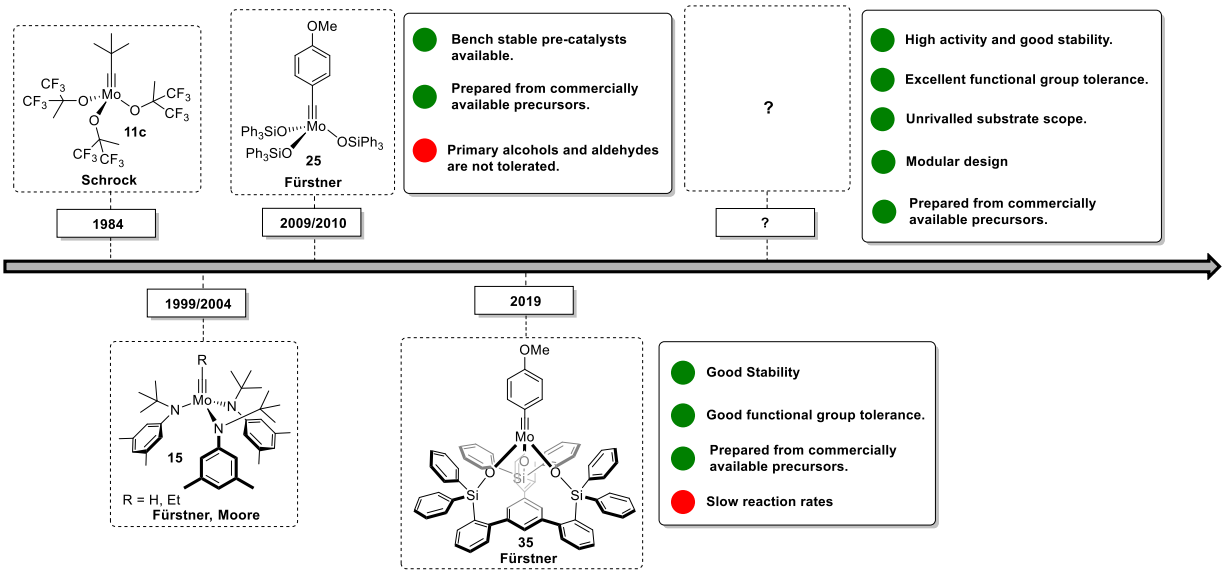

Figure 2.6. Milestones in molybdenum-catalysed alkyne metathesis.

Alkyne metathesis "canopy catalyst" **35** bears the tripodal silanolate ligand **33**. This exhibits the same catalytic activity and selectivity as seen in the parent silanolate-substituted molybdenum alkylidyne **25** but shows a significantly superior functional group tolerance (Scheme 2.6). As shown in Section 2.2, the multi-gram synthesis of ligand **33** and hence complex **35** can be readily achieved from commercially available precursors. The excellent catalytic performance of this complex is illustrated by the broad functional group tolerance discussed in Section 2.3. Catalyst **35** works well in the presence of unprotected primary alcohols and even tolerate substrates having multiple donor sites, including basic nitrogen and heterocycles. As mentioned in Section 2.1.4, complex **35** exists as a dimeric aggregate [**35**·**35**] in solution and the solid state. Although aggregation did not prove detrimental for metathesis (*vide supra* Section 2.3.1), the slow reaction rates and necessity for heating in some cases to liberate the monomeric species to achieve efficient turnover, are rather limiting and not ideal for catalysis.[82] It was envisaged that replacing the *ortho*-benzylidyne protons with more sterically demanding substituents (Figure 2.6, highlighted in blue) or substituting the phenyl groups in the periphery of the tripodal silanolate ligand framework (Figure 2.6, highlighted in red) would furnish an elegant set of strategies for mitigating these issues (Figure 2.7).

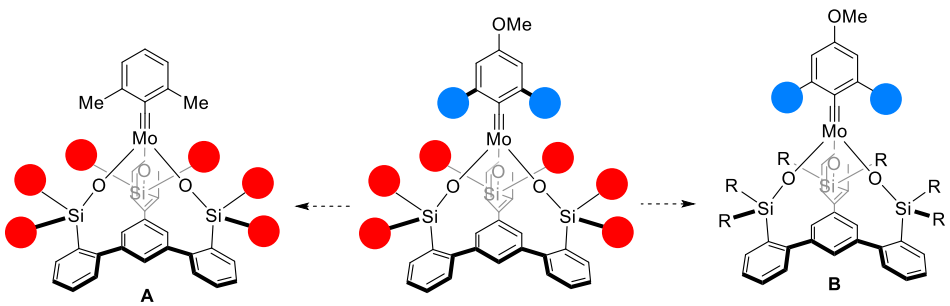

Figure 2.7. Two strategies for circumventing the issues associated with catalyst **35**. **A** = Replacement of the *ortho*-benzylidyne protons with alkyl substituents, **B** = Substitution of the phenyl groups in the periphery of the tripodal silanolate ligand framework.

2.4.1. Increasing the Steric Bulk at the *Ortho* Sites of the Benzylidyne

To explore the former strategy (**A**, Figure 2.7), the synthesis of tribromo complex **53** was investigated starting from commercial aryl bromide **51** (Scheme 2.7). Lithium-halogen exchange with excess ^{t}BuLi in Et_2O at −20 °C, followed by the addition of $[Mo(CO)_6]$ (**8**), gave the lithium enolate adduct **52**. Low-temperature oxidation of the Fischer carbene **52** with oxalyl bromide in CH_2Cl_2 and subsequent treatment with Br_2 and DME gave multi-gram quantities of the fragile complex **53**.

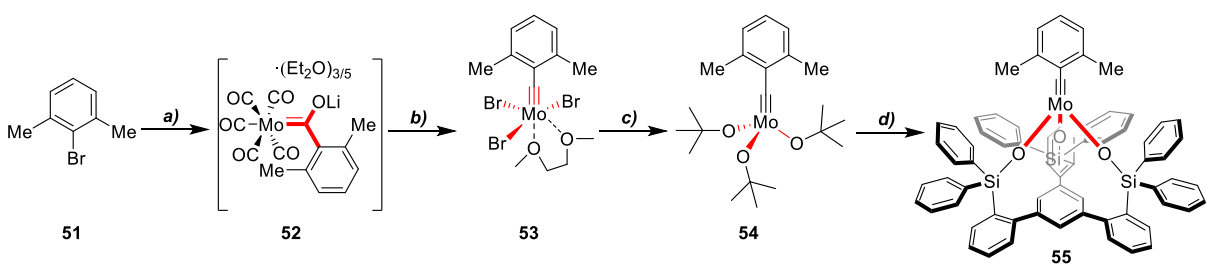

Scheme 2.7. Scalable synthesis of molybdenum alkylidyne complexes **54**. *Reagents and conditions*: *(a)* (i) ^{t}BuLi, Et_2O, − 20 °C, 3 h, (ii) $[Mo(CO)_6]$ (**8**), Et_2O, − 20 °C → RT, 6.8 g scale, (**52**, 78 %); *(b)* (i) oxalyl bromide, CH_2Cl_2, − 78 °C → − 40 °C, (ii) Br_2, DME, CH_2Cl_2, − 40 °C → RT, 2.5 g scale, (**53**, 81 %); *(c)* NaO^{t}Bu, THF, RT, 18 h, 0.8 g scale, (**54**, 83 %); *d)* **33**, toluene, RT, 5 h, (**55**, 65 %).

Conversion of the unstable cationic Fischer carbyne **53** in THF with NaO^{t}Bu afforded tris(*tert*-butoxy) complex **54** in very good yield (83 %). Complexation of ligand **33** with precatalyst **54** in toluene at ambient temperature afforded complex **55** in good yield (65 %) (Scheme 2.7). Yellow crystals suitable for single-crystal X-ray diffraction were obtained by crystallisation of benzylidyne **55** from Et_2O at – 20 °C and this confirmed its monomeric composition (Figure 2.8).

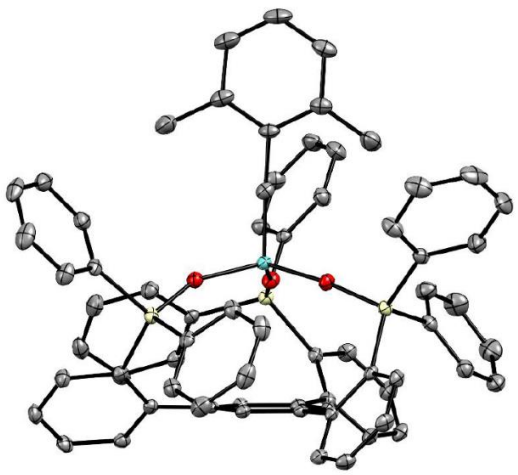

Figure 2.8. Solid-state structure of complex **55**; disorder omitted for clarity; CCDC-1987913; image refined by Julius Hillenbrand.[83]

The homo-metathesis reaction of alkyne **56** was chosen as the model reaction for determining the impact of the new ligand sphere on the catalytic activity. When homo-metathesis reactions are run in the absence of 5 Å molecular sieves, an equilibrium mixture is obtained, consisting of equimolar quantities of the homo-metathesis product (**58**) and 2-butyne (**57**) (Scheme 2.8). The conversion of the starting material (**56**) to both products (**57** & **58**) was monitored by ^{1}H NMR spectroscopy at 27 °C, upon mixing a solution of alkyne **56** in [D_8]-toluene with a solution of a complex (5 mol%) in [D_8]-toluene. The conversion-time curve obtained for catalyst **35,** indicated that the reaction reached equilibrium within 150 mins (50 % conversion, ratio of **56**:**57**:**58**; 2:1:1) (Figure 2.9). Unlike the parent catalyst **35**, a substantially slower conversion (ca. 600 mins, Figure 2.10) was observed for the monomeric complex **55** endowed with the more sterically demanding 2,6-dimethyl benzylidyne (Scheme 2.8). Given the inferior catalytic performance of complex **55** over catalyst **35**, the latter strategy in the catalyst design plan was investigated.

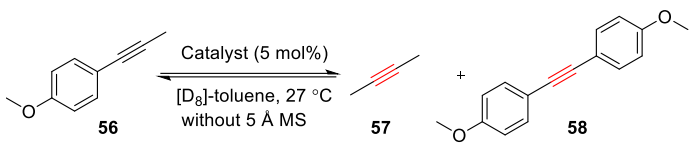

Scheme 2.8. Homo-metathesis reaction chosen for comparing the catalytic activity by ^{1}H NMR.

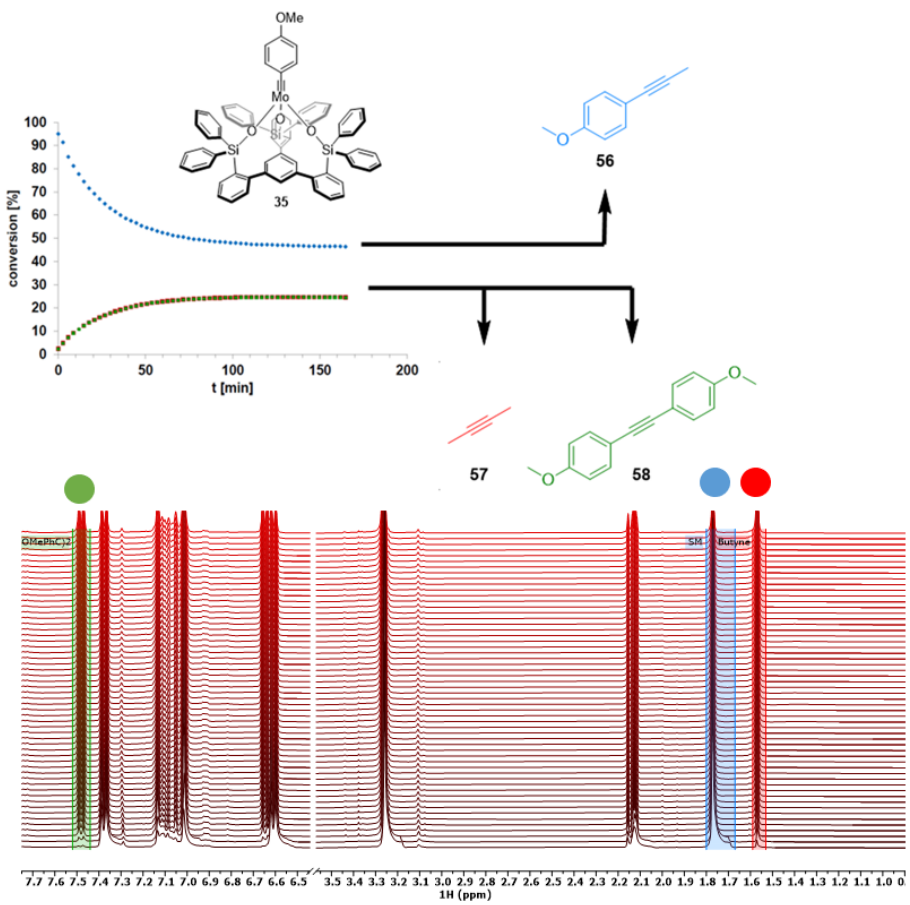

Figure 2.9. Conversion-Time plots of the homo-metathesis reactions of alkyne **56** with 5 mol% catalyst **35** in [D_8]-toluene (0.1 M) monitored by ^{1}H NMR spectroscopy at 27 °C. (Adapted with permission from ref. 84 @ copyright 2021 American Chemical Society).

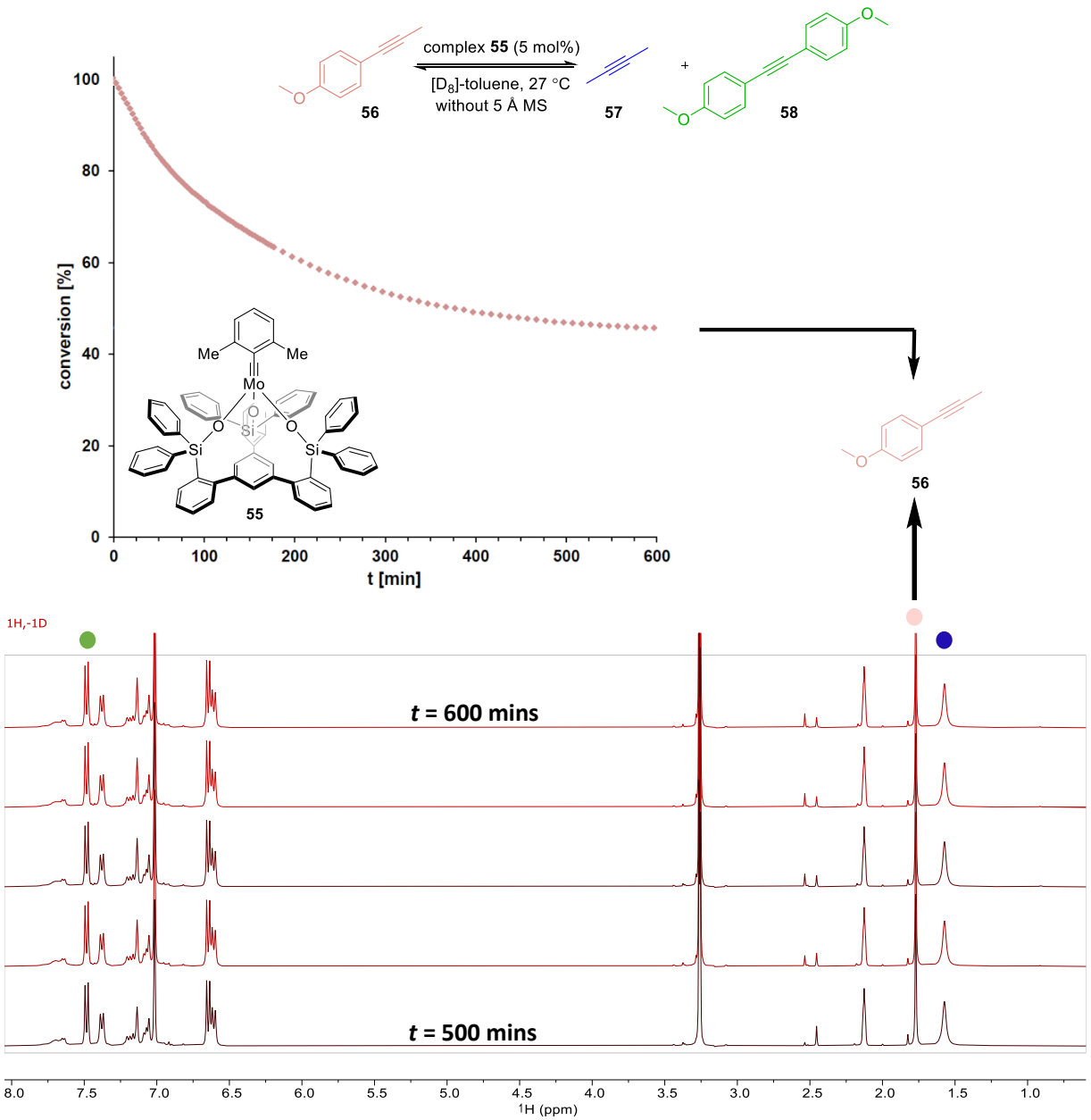

Figure 2.10. Conversion-Time plots of the homo-metathesis reactions of alkyne **56** with 5 mol% catalyst **55** in [D_8]-toluene (0.1 M) monitored by ^{1}H NMR spectroscopy at 27 °C. (Adapted with permission from ref. 84 @ copyright 2021 American Chemical Society).

2.4.2. Novel Ligand Scaffolds: Replacing the Peripheral Triphenyl Silanol Groups in the Tripodal Framework

Inspired by the pioneering work of Schrock, elegant earlier contributions from the Fürstner group and recent work of Zhang and co-workers, [50-51,78,86] four new ligand designs were conceived (Figure 2.11). It was envisioned that access to these novel ligand scaffolds can be achieved by adaptation of the modular synthetic strategy employed to access ligand **33**.

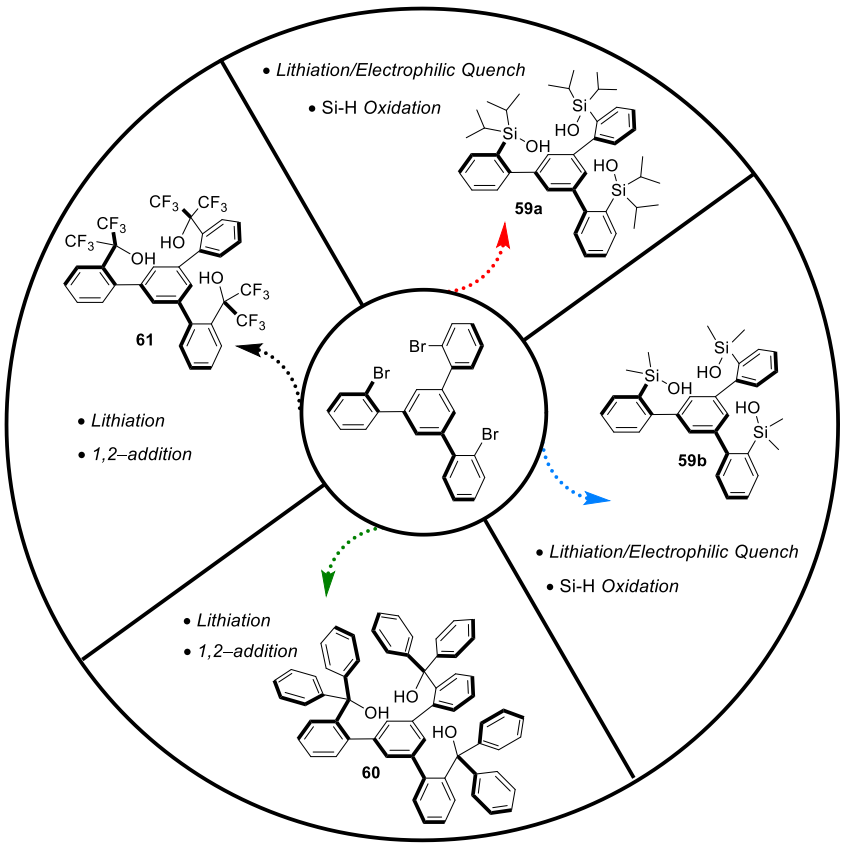

Figure 2.11. Proposed novel ligand designs and synthetic strategy.

Previously aliphatic variants of the monodentate triphenylsilanolate ligands decorating the ligand sphere of complex **25** prove to be catalytically active but significantly less effective for alkyne metathesis.

Capitalising on the rigidity of the tripodal scaffold, it anticipated that ligand designs **59a** and **59b** would possess the desired C_3-symmetry and required pre-organisation exhibited by ligand **33**. Upon complexation to the metal, due the increased electron-donating nature of an sp^3 hybridised carbon relative to its sp^2 hybridised counterparts these would furnish a pair of complexes with a less Lewis acidic metal centre.

Trisilanes **62a** and **62b** were accessible from tribromide **30** in very good to excellent yield via low-temperature lithiation using excess ^{t}BuLi in Et_2O (−125 °C), followed by electrophilic quench with $R_2Si(H)Cl$ (R = *i*Pr, Me) (Scheme 2.9). With the two trisilanes in the hand, a series of Si−H oxidation protocols were investigated.

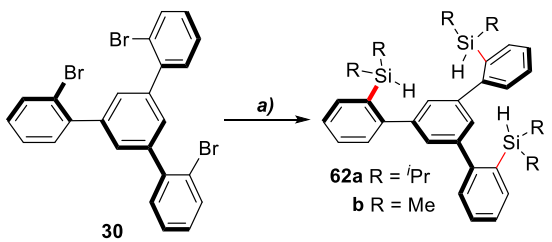

Scheme 2.9. Gram-scale synthesis of trisilanes **62a** and **62b**. *(a)* ^{t}BuLi, R_2SiHCl (R = ^{i}Pr, Me), Et_2O, − 125 °C → RT, 18 h (**62a**, 81 %, R = ^{i}Pr, 1 g scale; **62b**, 91 %, R = Me, 1 g scale).

Ruthenium catalysed Si-H oxidation or NBS mediated radical bromination followed by hydrolysis either led to no, or poor, conversion (Table 2.9, entries 1-2).[78,87] Moreover, employing TCCA as the oxidant in CH_2Cl_2 afforded the product only in 34 % yield along with large quantities of protodesilylation product **63** (Table 2.4, entry 3). Later, however, it was found that full conversion was attained just by utilising excess of *m*CPBA in THF (Table 2.9, entry 6).[84] Routine chromatography on normal phase silica sufficed to obtain ligand **59a** in analytically pure form in 81 % yield. Conversely, *m*CPBA mediated oxidation of trisilane **62b** in THF delivered product **59b** in only 25 % yield after overnight stirring at RT. When this reaction was repeated at low temperature in CH_2Cl_2, ligand **59b** was isolated in almost quantitative yield (Table 2.4, entry 8). Having successfully synthesised two out of the four designs in the proposed ligand library, the complexation reactions of trisilanols **59a**-**b** were investigated.

Table 2.9. Si–H Oxidation conditions examined.

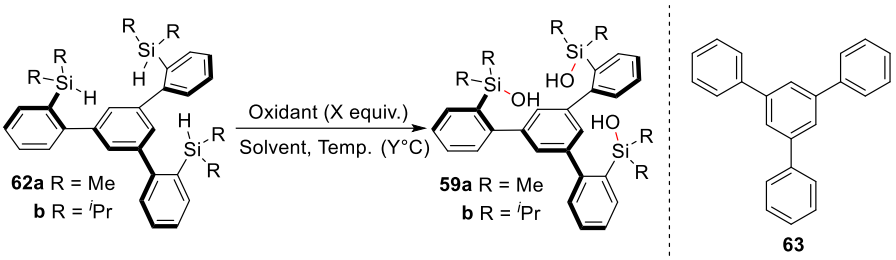

Entry	Substrate	Oxidant	X (equiv.)	Solvent	Y (°C)	Time (h)	% Yield
1	**62a**	Water	15.0	MeCN	80	8	NR[a,b]
2	**62a**	NBS	3.3	CH_2Cl_2	RT	1	9
3	**62a**	TCCA	1.25	CH_2Cl_2	RT	18	34[c]
4	**62a**	*m*CPBA	3.0	THF	RT	18	22[d]
5	**62a**	*m*CPBA	4.5	THF	RT	18	37[d]
6	**62a**	*m*CPBA	6.0	THF	RT	18	81
7	**62b**	*m*CPBA	6.0	THF	RT	18	25[d]
8	**62b**	*m*CPBA	6.0	CH_2Cl_2	0	1	94

[a] Preformed in the presence of $[Ru(p\text{-cymene})Cl_2]_2$ (10 mol%). [b] Starting material was only recovered. [c] Protodesilylation product **63** was also isolated. [d] Starting material was also recovered along with protodesilylation product **63**.

Crystallisation of ligand **59a** from a saturated solution in ether layered with *n*-pentane at RT gave crystals suitable for single-X-ray diffraction. Equally rewarding was the fact that X-ray analysis revealed that the scaffold possessed the desired C_3-symmetry and required pre-organisation (Figure 2.11). Stirring of a solution of ligand **59a** in toluene with precatalyst **34** and slow evaporation under high vacuum gave complex **64** in almost quantitative yield (Scheme 2.10 (i)).

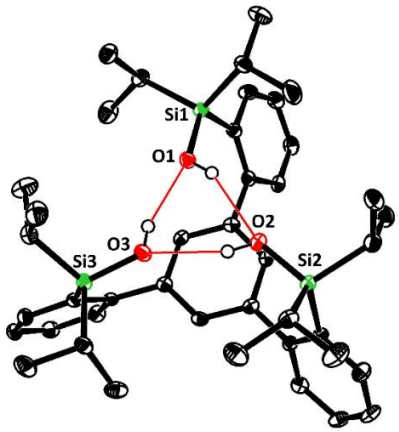

Figure 2.12. Solid-state structure of ligand **59a** (only a single molecule of the two in the unit cell is shown); only hydrogen atoms of the –OH group are not shown for clarity; the red lines indicate intramolecular hydrogen bonding. (Adapted with permission from ref. 84 @ copyright 2021 American Chemical Society).

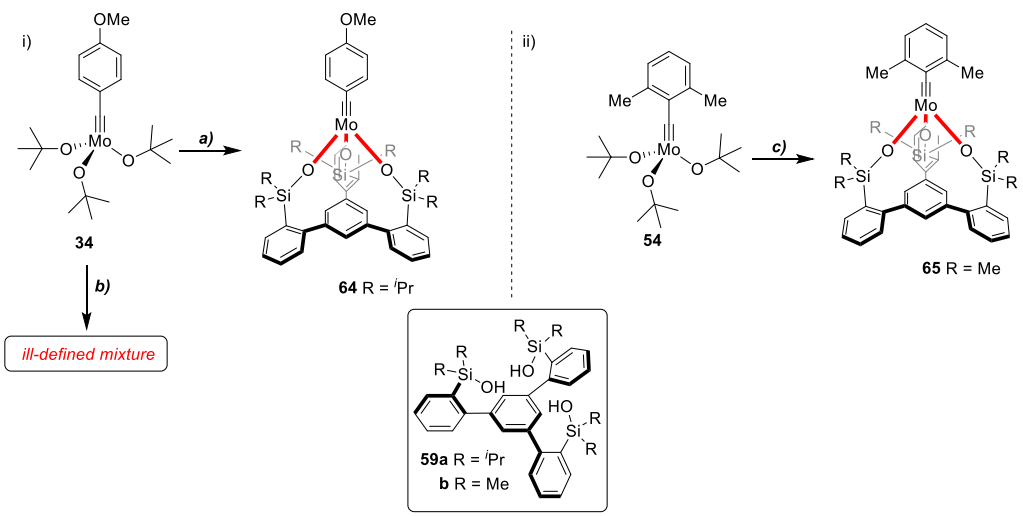

Scheme 2.10. Scalable synthesis of molybdenum complexes **64**-**65**. *Reagents and conditions*: (i) *(a)* **59a**, toluene, RT, 5 h, (**64**, 99 %); *(b)* **59b**, toluene, RT, 5 h; (ii) *(c)* **59b**, toluene, RT, 5 h, (**65**, 99 %). (Complexations conducted with Julius Hillenbrand).

Yellow crystals suitable for single-crystal X-ray diffraction grown from ether at – 30 °C, enabled confirmation of the monomeric composition of complex **64** in the solid state (Figure 2.13). Complexation

of ligand **59b** with precatalyst **34**, unfortunately afforded an ill-defined mixture of complexes (Scheme 2.10 (i)). Conversely stirring a solution of precatalyst **54** in toluene with trisilanol **59b** afforded complex **65** in quantitative yield (Scheme 2.10 (ii))**.** The monomeric nature of complex **65** was confirmed by NMR spectroscopy. ^{95}Mo NMR and ^{13}C NMR analysis indicated the presence of a minor poorly defined alkylidyne impurity; characterised by broad NMR signals with very similar chemical shifts (Figure 2.14). Having rigorously confirmed the monomeric nature and C_3-symmetry of both complexes (**64**-**65**), the synthesis of ligands **60**-**61** was explored.

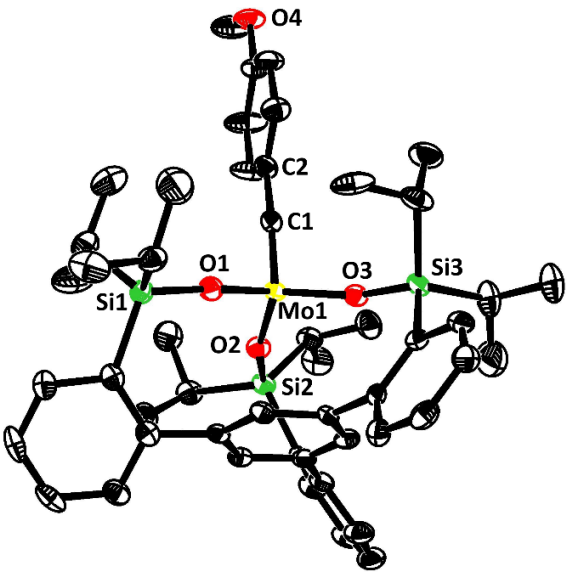

Figure 2.13. Structure of complex **64** in the solid state; hydrogen atoms are omitted for clarity; CCDC-1987911 (Adapted with permission from ref. 84 @ copyright 2021 American Chemical Society).

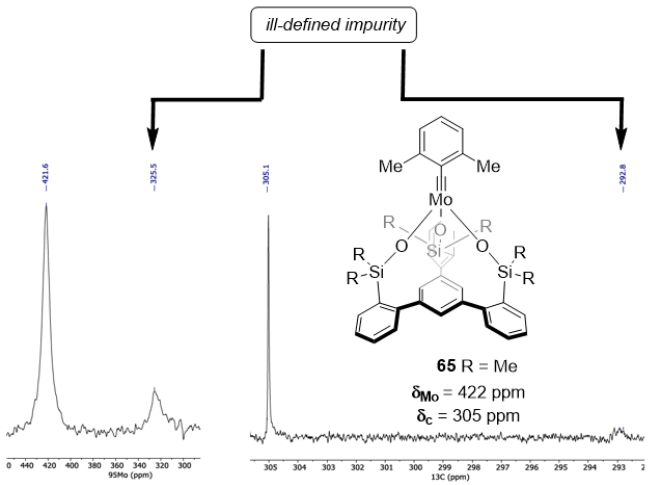

Figure 2.14. Annotated overlaid ^{95}Mo and ^{13}C NMR spectra of complex **65**. All spectra were recorded in [D_8]-toluene at 60°C.

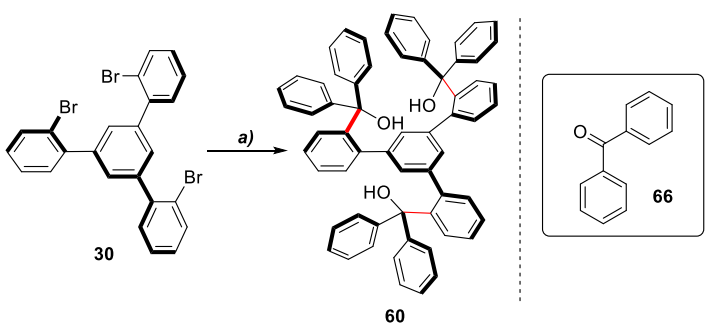

Scheme 2.11. Gram-scale synthesis of carbinol variant of ligand **33**. *(a)* ^{t}BuLi, **66**, Et_2O, − 125 °C → RT, 18 h (**60**, 75 %, 2.5 g scale).

Access to the carbinol variant of ligand **33** was possible via an initial triple lithium-halogen exchange with excess ^{t}BuLi, followed by the addition of commercially available benzophenone (**66**). Trituration of the crude product with MeOH after acidic work-up, afforded multi-gram quantities of ligand **60** in very good yield (Scheme 2.11). The ^{1}H NMR spectrum of the powdery white solid obtained, exhibited broad signals at room temperature, which were substantially different to those of trisilanol **33**.

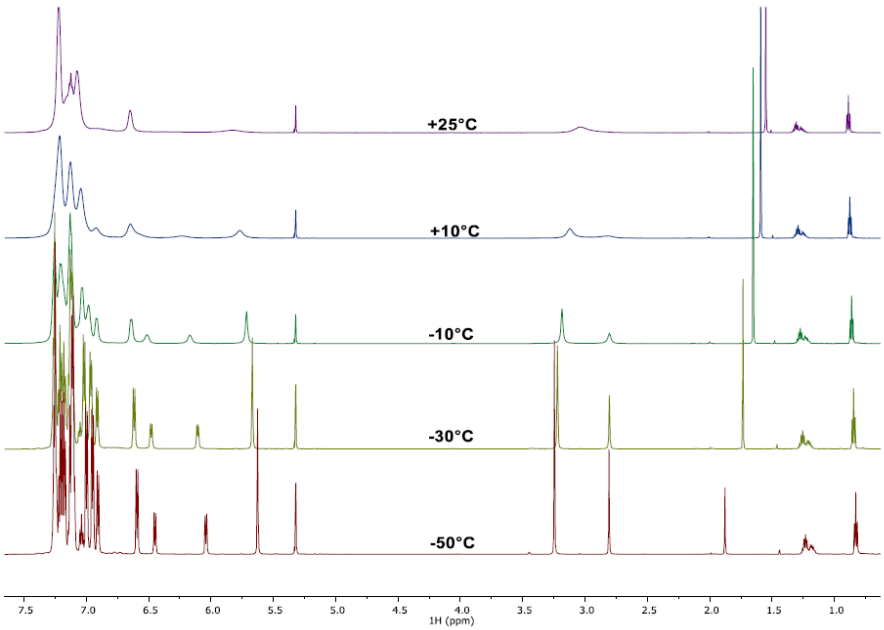

Figure 2.15. Variable-temperature (VT) NMR experiments of carbinol ligand **60** in CD_2Cl_2.

A sharp set of well-defined signals was only observed upon cooling to – 50 °C in CD_2Cl_2 (Figure 2.15). Careful analysis of the results from variable temperature NMR experiments indicated that the scaffold did not possess the required pre-organization and desired C_3-symmetry previously exhibited by ligand **33**. One of the triphenylmethanol units of the framework in solution is oriented at the opposite side of the basal plane of the molecule (See Appendix 2 for details). Single-crystal X-ray diffraction of crystals grown from CH_2Cl_2 at – 75 °, further corroborated the two-up/one-down configuration previously observed in solution (Figure 2.16 (i)). Moreover, close examination of the X-ray diffraction data proved most instructive in unravelling the source of the reduced pre-organisation of ligand **60**. Unlike trisilanol **33** (Figure 2.16 (ii)), the donor bond distances in carbinol **60** ($d(_{O–C})_{avg.}$ = 1.44(2) Å; ligand **33** ($d(_{O–Si})_{avg.}$ = 1.64(2) Å) are shorter, furnishing a shallower complexation cavity.[84] In addition, given that alcohols are generally less acidic than silanols, the hydrogen-bonding array in the solid-state structure of ligand **60** is substantially less pronounced therefore leading to this undesired arrangement. It was envisaged that the undesired configuration of triol **60** could be rectified upon complexation to the metal.

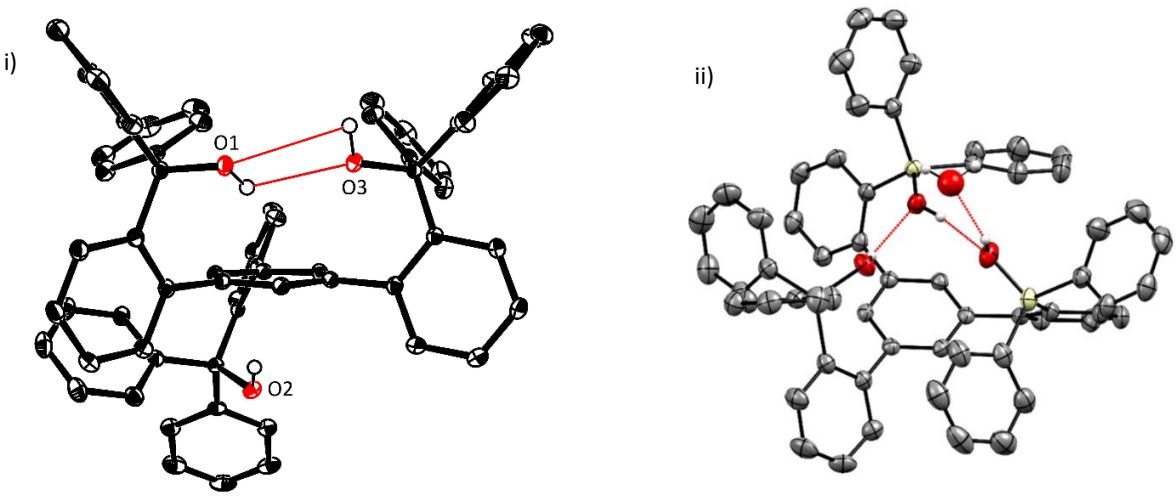

Figure 2.16. Solid state structure of ligands **33** and **60**: (i) Structure of compound **60** in the solid state; co-crystallized CH_2Cl_2 and hydrogen atoms (except for the –OH protons) are not shown for clarity; the red lines indicate intramolecular hydrogen bonds; CCDC-1987909 (Adapted with permission from ref. 84 @ copyright 2021 American Chemical Society); (ii) Solid-state structure of ligand **33**; disorder omitted for clarity; intramolecular hydrogen-bonding illustrated as red-dotted lines; CCDC-1987916; image refined by Julius Hillenbrand.[82-83]

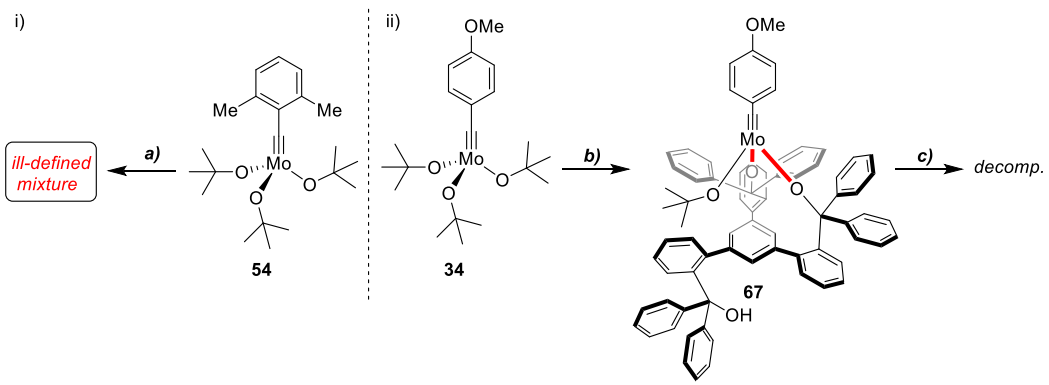

Scheme 2.12. Complexation of ligand **60** with precatalysts **34** and **54**. *Reagents and conditions*: (i) *(a)* **60**, toluene, RT, 14 h; (ii) *(b)* **60**, toluene, RT, 14 h, (**67**, 79 %); *(c)* toluene, 60 °C, 6 h. (Experiments conducted with Julius Hillenbrand)

Although stirring a solution of ligand **60** in toluene with precatalyst **54** at room temperature overnight only gave an complex mixture of cross-linked species (Scheme 2.12 (i)), complexation with precatalyst **34** afforded bidentate complex **67** in 79 % yield (Scheme 2.12 (ii)). Attempted intramolecular protonolysis of complex **67** in [D_8]-toluene at 60 °C, regrettably resulted in decomposition along with the release of isobutene (Scheme 2.12 (ii)).[84]

Influenced by the catalyst design disclosed by Schrock and co-workers in 1984, [50-51] a more Lewis acidic carbinol ligand design embellished with trifluoromethyl groups was considered. Although triple lithiation of tribromide **30** followed by a quench with hexafluoroacetone (**68**), failed to deliver the desired product (Scheme 2.13 (i)), preparation of the fluorinated ligand **61** was achieved via a revised four-step sequence featuring a late-stage bistrifluoromethylation step (Scheme 2.13 (ii)).

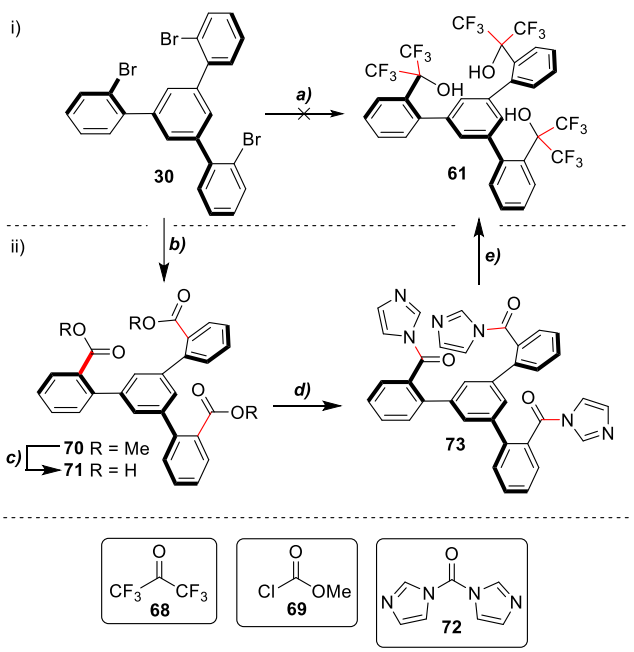

Scheme 2.13. Synthetic routes towards fluorinated carbinol ligand **61**. *Reagents and conditions*: (i) *(a)* ^{t}BuLi, Et_2O, −125 °C, 1 h then **68**, −125 °C → RT, 18 h; (ii) *(b)* ^{t}BuLi, Et_2O, −125 °C, 1 h then **69**, −125 °C → RT, 18 h (**70**, 70 %, 4 g scale); *(c)* $NaOH_{(aq)}$, THF/MeOH (1:1), 70 °C → RT, 18 h, (**71**, quant., 3.0 g scale); *(d)* **72**, CH_2Cl_2, RT, 18 h, (**66**, quant., 1.0 g scale); *(e)* See Table 2.5.

After metal-halogen exchange, the resulting trianionic organolithium intermediate was quenched with methyl chloroformate (**69**) to give multi-gram quantities of triester **70** in very good yield (70 %).

Subsequent hydrolysis on multi-gram scale delivered triacid **71** in quantitative yield. Treatment of a solution of the latter in CH_2Cl_2 with excess CDI (**72**) led to full conversion to imidazole derivative **73** after overnight stirring at room temperature. Upon removal of the solvent, simple trituration of the crude product with *n*-pentane sufficed to obtain triimidazole amide **73** as a creamy foamy solid in quantitative yield (Scheme 2.13). Utilising a modified procedure based on the work of Babadzhanova et al. (2005), activated ester **73** was converted to the fluorinated carbinol ligand **61**.[88] Employing a large excess of CsF and $TMSCF_3$ at 40 °C in THF, proved to be the most effective set of conditions for successful triple bistrifluoromethylation of acid derivative **73** (Table 2.10, entry 4, 46 %). In contrast to carbinol ligand **60**, its fluorinated variant**,** adopts mainly a C_3-symmetric configuration in CD_2Cl_2. Close inspection of ^{13}C and ^{19}F NMR spectra revealed the presence of a second minor rotameric component, which is in exchange with the major species in solution based on the 2D ROESY and ^{19}F-NOESY spectra (see Appendix 2 for more details).

Table 2.10. Trifluoromethylation conditions examined.

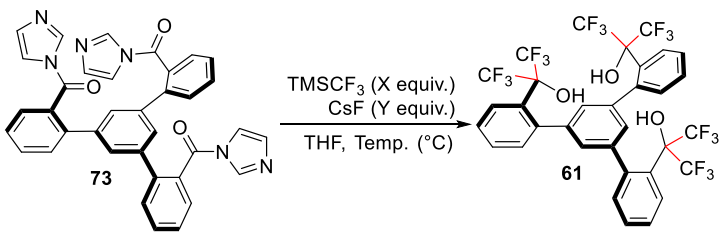

Entry	X (equiv.)	Y (equiv.)	Solvent	Temp. (◦C)	Time (h)	% Yield
1	7.5	7.5	THF	RT	18	17
2	7.5	15.0	THF	RT	18	19
3	9.0	18.0	THF	RT	18	32
4	9.0	18.0	THF	40	18	46
5	9.0	18.0	THF	80	18	42

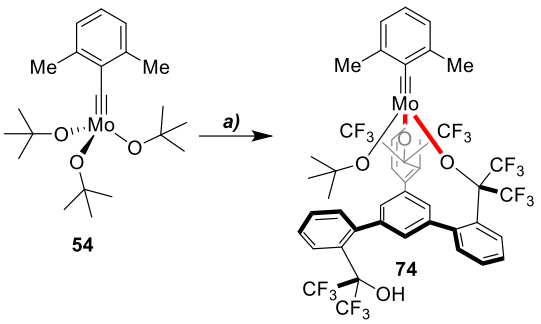

Scheme 2.14. Complexation of fluorinated carbinol ligand **61** with precatalyst **54**. *Reagents and conditions*: *(a)* **61**, toluene, RT, 18 h, (**74**, 79 %).

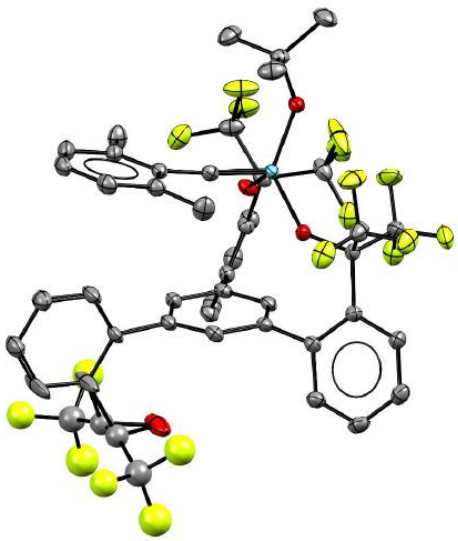

Figure 2.17. Solid-state structure of complex **74**, disorder omitted for clarity. (Structure refined by Julius Hillenbrand) [81]

Despite its C_3-symmetric configuration in solution, stirring a solution of the fluorinated carbinol ligand **61** in toluene with precatalyst **54** gave bidentate complex **74** (Scheme 2.14) as indicated by single-crystal X-ray diffraction data (Figure 2.17). Yellow crystals suitable for X-ray diffraction were grown from a saturated solution of complex **74** in benzene. Further analysis of the X-ray data revealed that the bidentate coordination environment observed is caused by the shallow bonding cavity of ligand **61.** This can be rationalised considering that a C−O bond is shorter than a Si−O bond. Since the complexation reactions of

carbinol ligands **60** and **61,** failed to deliver C_3-symmetric podand complexes, these were not investigated further.

2.4.3. Comparing the catalytic activity of molybdenum complexes: Complex 64 *versus* Complex 65

The catalytic performance of the newly prepared complexes (**64** and **65**) was evaluated using the model reaction (Scheme 2.8). Once again, upon mixing a solution of alkyne **56** in [D_8]-toluene with a solution of complex **64**/**65** (5 mol%) in [D_8]-toluene, the progress of the homo-metathesis reaction at 27 °C was monitored by ^{1}H NMR spectroscopy.

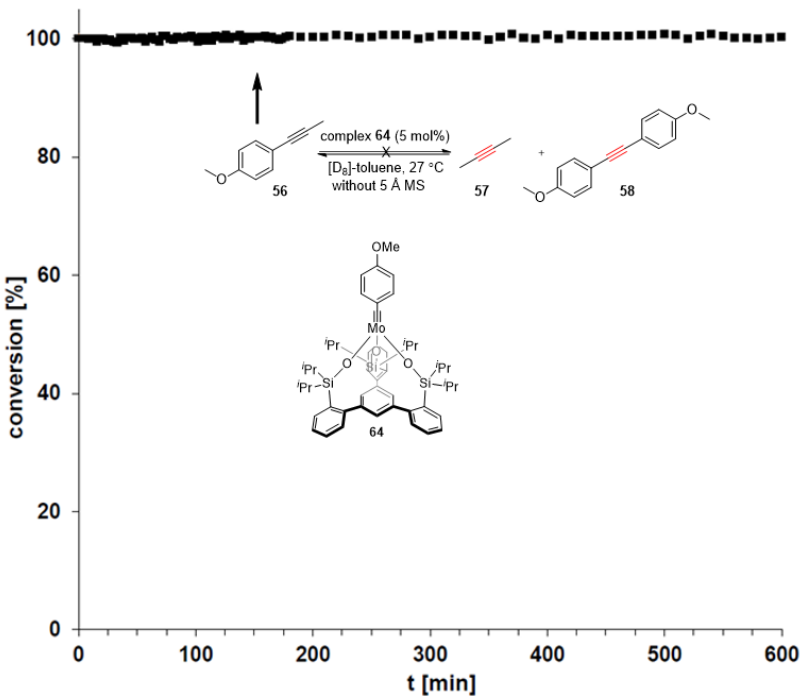

Figure 2.18. Conversion-Time plots of the homo-metathesis reactions of alkyne **56** with complex **64** (5 mol%) in [D_8]-toluene (0.1 M) monitored by ^{1}H NMR spectroscopy at 27 °C. (Adapted with permission from ref. 84 @ copyright 2021 American Chemical Society).

Complex **64** failed to effect the model reaction at 27 °C (slow conversion only in refluxing toluene) (Figure 2.18). Conversely, complex **65** outperformed even catalyst **35** (ca. 150 mins) and catalyst **25a** (≤ 10 mins). Based on the conversion-time curve obtained for complex **65**, the reaction reaches equilibrium in less than 5 mins (50 % conversion, ratio of **56**:**57**:**58**; 2:1:1) (Figure 2.19). Considering the X-ray data for the solid-state structure of complex **64** (Figure 2.13), it is evident that the cause of its poor catalytic performance is the steric block imposed by the isopropyl groups decorating its ligand sphere, which in turn prevents substrate binding to the metal centre. In addition, this dramatic difference in the catalytic performance between the two complexes has been tentatively attributed to steric effects. Overall, the results outlined above clearly demonstrate that even the subtlest difference in the ligand sphere can have a massive impact on the catalytic activity. Encouraged by the excellent catalytic performance of complex **65**, its functional group tolerance and substrate scope was briefly examined.

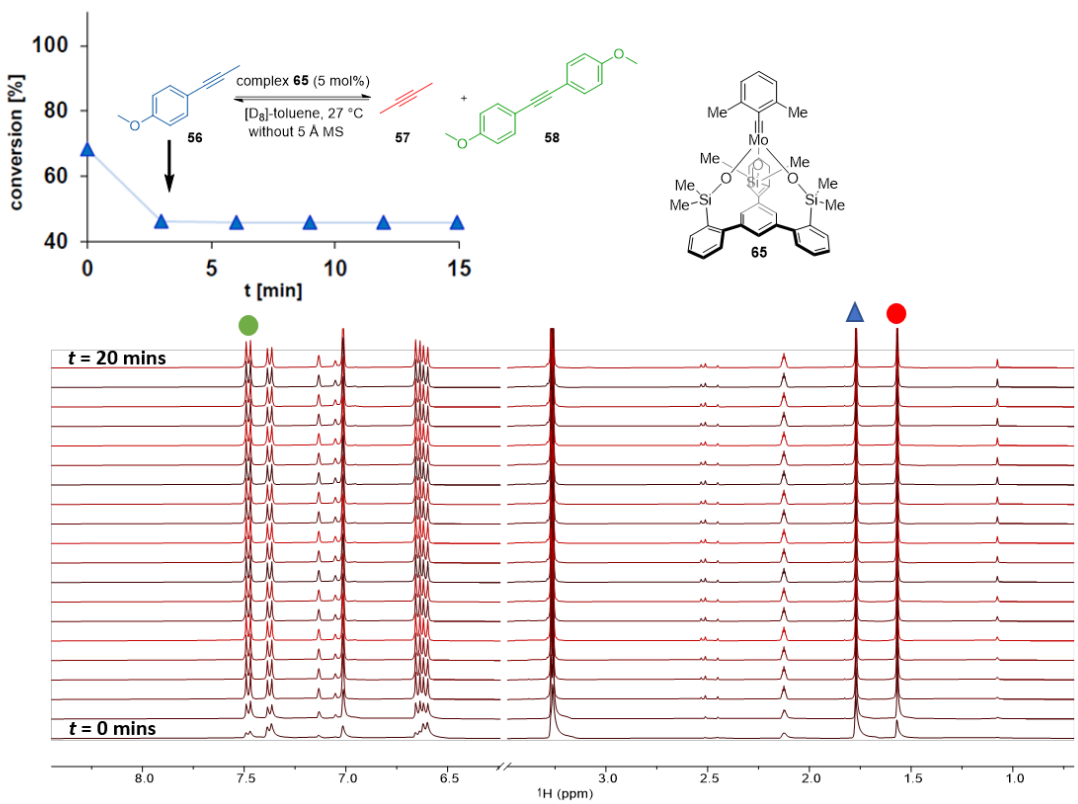

Figure 2.19. Conversion-Time plots of the homo-metathesis reactions of alkyne **56** with complex **65** (5 mol%) in [D_8]-toluene (0.1 M) monitored by ^{1}H NMR spectroscopy at 27 °C. (Adapted with permission from ref. 84 @ copyright 2021 American Chemical Society).

2.4.4. Scope and Applications of Complex 65

Although a truly comprehensive substrate and functional group compatibility scope of "canopy catalyst" **65** is beyond the scope of this short study, the collection of examples included below clearly showcases the unrivalled functional group tolerance and excellent catalytic activity of this complex. All the methyl-capped alkynes used in this screen were either commercially available or obtained from the compound archive of the Fürstner group in the Max-Planck Institut für Kohlenforschung, Germany. All the reactions performed as part of this study were initially carried out with a catalyst loading of 5 mol% at ambient temperature in the presence of freshly activated 5 Å MS in toluene, while the progress of the reactions was monitored by TLC or GCMS. The best yielding conditions are displayed.[83]

Table 2.11. Homo metathesis reactions of methyl-capped aryl/heteroaryl alkynes with complex **65**.

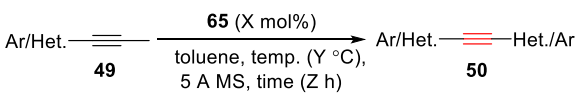

Entry	Substrate	Product	X (mol%)	Y (°C)	Z (h)	Yield (%)
1	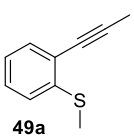 **49a**	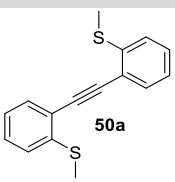 **50a**	5	90	2	81
2	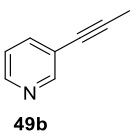 **49b**	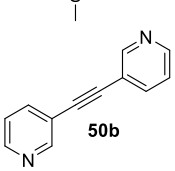 **50b**	10	90	2	75
3	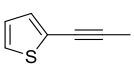 **49c**	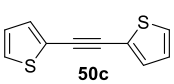 **50c**	10	RT	2	85

Substrates containing various basic donor-sites were well tolerated including potentially coordinating aromatic thioether **49a**, pyridine **49b** and thiophene **49c** (Table 2.11, entries 1-3). The tolerance towards protic functional groups was also rewarding. As discussed in Section 2.1.4, monodentate ligand-based complex **25a** failed to promote the homo-metathesis reactions of primary alcohols (Scheme 2.6), whereas

podand catalyst **65** afforded the desired products within 2 h at room temperature in very good to excellent yields (*n* = 5-8, Table 2.12, entries 1-3, 5). Homo-metathesis of secondary alcohol **75** under previously reported conditions using 10 mol% of catalyst **25a**, afforded the desired product **76** in only 34 % yield.[83] In stark contrast, using catalyst **65** (5 mol%), the diol product **76** was obtained in almost quantitative yield (Table 2.12, entry 4). Moreover, catalyst **65** smoothly converted propargylic alcohol **45a** into the monomeric macrocycle **46a** (Scheme 2.15), while catalyst **35** only gave a mixture of dimers (Table 2.6, entry 1).

Table 2.12. Homo metathesis reactions of alcohols with complex **65.**

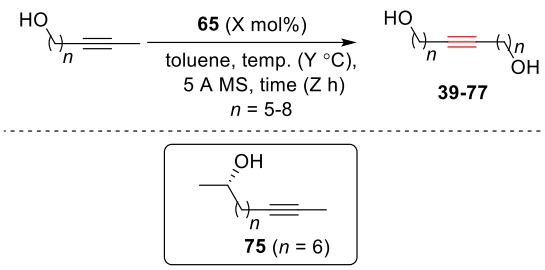

Entry	Substrate *n*		X (mol%)	Y (°C)	Z (h)	Yield (%)
1	5	**39**	5	RT	2	73
2	6	**40**	5	RT	2	71
3	7	**41**	5	RT	2	88
4	7	**76**	5	RT	2	94[a]
5	8	**77**	5	RT	2	87

[a] Chiral alcohol **75** was used as the substrate.

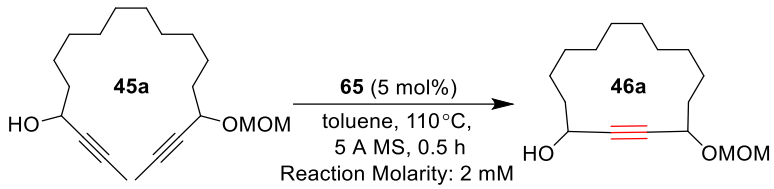

Scheme 2.15. RCAM reaction of acyclic propargyl precursor **45a** catalysed by complex **65**. *Reagents and conditions*: *(a)* **65** (5 mol%), toluene, Reaction molarity (mM): 2.0, 110 °C, 5 Å MS, 0.5 h, (**46a**, 68 %).

Table 2.13. Ring-Closing Alkyne metathesis natural product intermediates with complex **65.**

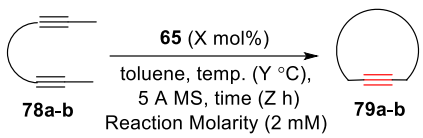

Entry	Substrate	X (mol%)	Y (°C)	Z (h)	Yield (%)
1	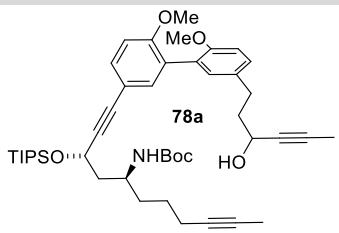	20	80	3	66
2	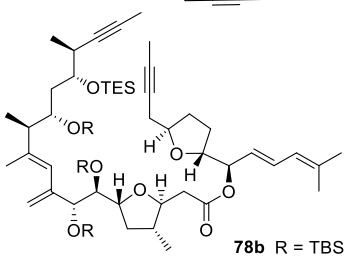	30	80	5	81

Impressive results were also obtained when catalyst **65** was used in the assembly of macrocyclic scaffolds decorated with more intricate functionality. For example, the ease of formation of **79a** and **79b**; advanced intermediates in the total synthesis of marine natural products including amphidinolide F and nor-cembranoid sinulariadiolide, further demonstrate the unrivalled functional group tolerance and catalytic activity of complex **65**. Previously, the sterically encumbered framework of the densely functionalized bisalkyne **78b** caused the preferential formation of dimers with catalyst **25a**.[89-90]

2.5. Conclusion

Although the advent of triphenylsilanolate ligand-based molybdenum alkylidyne catalysts over the recent years has certainly revolutionised the field of alkyne metathesis, some major limitations still remain. The high Lewis acidity and polarisation across the functional [Mo≡CR] unit in these Schrock alkylidynes renders them fragile in a protic environment. Moreover, substrates that can engage in ligand exchange reactions often act as catalysts poisons. Several groups attempted to address this issue utilising multidentate ligand frameworks, yet this failed to deliver well-defined complexes (Figure 2.4). More recently, a new class of alkyne metathesis catalyst endowed with the privileged tripodal silanolate ligand framework was reported; this retains the assets of the parent monodentate-ligand based complex **25a** but exhibits even better functional group tolerance. (Scheme 2.5).

Though access to the tripodal silanolate ligand **33** was previously achieved via a three-step sequence starting from commercial 2-bromoacetophenone, a capricious initial cyclocondensation step limited both the scalability and synthetic performance of the overall sequence (44 % yield over three steps). As part of a rigorous optimisation and scale-up study conducted, a rejuvenated three-step synthetic route was developed featuring a scalable early-stage cyclocondensation step (20 g scale) involving *in situ* generated HCl in EtOH. This refined sequence delivered ligand **33** on multi-gram scale in an overall 74 % yield (over three steps).

Metathesis catalyst **35** tolerates a wide range of functional groups, yet prior work had not comprehensively examined its functional group tolerance. The substrate screen conducted, established the limits of functional group and substrate tolerance of catalyst **35**. While complex **35** failed to effect the homometathesis or cross-metathesis reactions of low-molecular weight primary alcohols (*n* = 1-3, Tables 2.4-2.5), aliphatic aldehydes and ketones (Table 2.7 entries 4-5) even at elevated temperatures, the metathesis reactions of both propargylic and primary higher order alcohols afforded the corresponding diol products in good to excellent yields (Table 2.4, entries 4-6). Moreover, very good to excellent results were obtained for substrates containing functional groups such as primary alkyl halides, α-amido sulfones, aryl and alkyl thioethers, esters and ketoesters (Table 2.7). Even though complex **35** exists as a dimeric aggregate in the solid-state, this did not pose any detrimental effects for metathesis.[80] However, the slow reaction rates and need for heating at certain instances to liberate the monomeric species to achieve efficient turnover, persuaded us to investigate the development of a new alkyne metathesis catalyst.

Initially the *ortho*-benzylidyne protons in the benzylidyne complex **35** were substituted with more sterically demanding substituents in an attempt to produce a monomeric well-defined complex with superior catalytic performance. Utilising the route disclosed for the synthesis of precatalyst **34** (Scheme 2.5) and the new improved ligand complexation protocol reported by Fürstner and co-workers;[80] complex **55** endowed with 2,6-dimethyl benzylidyne unit and tripodal triphenyl silanolate ligand scaffold was prepared. This monomeric complex (**55**) was isolated in 34 % yield over four steps (Scheme 2.7). To study the impact of the sterically demanding 2,6-dimethyl benzylidyne unit on the catalytic activity, the simple homo-metathesis reaction of 1-methoxy-4-(prop-1-yn-1-yl) benzene (**56**) in the absence of 5 Å molecular sieves was chosen as the model reaction. Unfortunately, the catalytic performance of this complex (**55**) (Figure 2.10) proved significantly inferior to that of catalyst **35** (Figure 2.9).

Minor adaptation of the refined modular synthetic strategy that gave ligand **33**, delivered a small library of ligand designs, where the phenyl silanolate unit of the tripodal ligand scaffold in "canopy complex" **35** was substituted with electron-rich and sterically demanding alkyl silyl groups, phenolates and fluorinated alkoxides (Figure 2.11). Synthesis of trisilanols **59a** and **59b** was achieved in very good yield via a two-step sequence consisting of an initial lithiation using excess ^{t}BuLi in Et_2O (−125 °C), followed by electrophilic quench with $R_2Si(H)Cl$ (R = ^{i}Pr, Me) and final Si−H oxidation mediated by *m*CPBA (**59a**, 81%; **59b**, 86%). Single crystal X-ray diffraction data obtained for ligand **59a** showed that the scaffold possessed the desired C_3-symmetry and required pre-organisation (Figure 2.12). Complexation of ligand **59a** with precatalyst **34** in toluene at RT, afforded complex **64** in almost quantitative yield (Scheme 2.1 (i)), while single-crystal X-ray diffraction data, confirmed the monomeric composition complex **64** in the solid state (Figure 2.13). On the other hand, the complexation of ligand **59b** with precatalyst **34**, gave only an ill-defined mixture of complexes (Scheme 2.10 (i)). Stirring a solution of precatalyst **54** in toluene with trisilanol **59a** afforded complex **65** in quantitative yield (Scheme 2.10 (ii))**.** Even though growing crystals of complex **65** suitable for single X-ray diffraction was not possible, NMR spectroscopy confirmed the monomeric nature of this complex in solution (Figure 2.14).

Preparation of the carbinol variant of ligand **33** was possible via an initial triple lithium-halogen exchange with ^{t}BuLi, followed by the addition of commercially available benzophenone (**66**) (Scheme 2.11). Despite the relative ease of formation of carbinol ligand **60**, the reduced acidity and bond length of donor units in triol **60** gave rise to a coordination cavity, which is less preorganised and shallower than that of ligand **33**.

VT NMR experiments and single X-ray diffraction data indicated that the framework adopts a two-up/one-down configuration, both in solution and the solid-state (Figures 2.15 & 2.16). Even though it was anticipated that complexation to the metal would rectify this undesired configuration, stirring a solution of ligand **60** in toluene with precatalyst **34** at room temperature overnight only afforded a bidentate complex **67** (Scheme 2.12)**.**

Although triple lithiation on tribromide **30** and subsequent quench with hexafluoroacetone (**68**) failed to deliver the desired product, a revised sequence featuring a late-stage bistrifluoromethylation step on an activated triester (**73**) furnished the polyfluorinated ligand **61** in overall 32 % yield over four steps (Scheme 2.13; Table 2.10). Unlike ligand **60**, fluorinated triol **61** exhibits the same preorganisation and C_3-symmetry as trisilanol **33** in solution as corroborated by the NMR data (see Appendix 2 for details). Even with a more preorganised and acidic scaffold, the enlarged bonding cavity present in ligand **61** did not allow the formation of a podand complex. More specifically, stirring a solution of ligand **61** in toluene with precatalyst **34**, only gave bidentate complex **74** (Scheme 2.14). The bidentate binding motif in complex **74** was confirmed by single-crystal X-ray diffraction and NMR spectroscopy (Figure 2.17; See Appendix 3 for more details).

Since only trisilanols **59a** and **59b** delivered monomeric well-defined C_3-symmetric complexes, only the catalytic performance of alkylidynes **64** and **65** was examined. The impact of these two closely related ligand spheres on the catalytic performance was assessed using the model reaction (Scheme 2.8). While complex **64** failed to effect homo-metathesis of alkyne **56** at room temperature, catalyst **65** endowed with a methyl substituted silanolate ligand, showed superior performance to both catalyst **35** and the parent complex **25a** (Figure 2.19). The difference in the catalytic performance between these closely related complexes, highlights the impact of even the smallest change in the ligand sphere, on the catalytic activity of the "canopy complexes". Encouraged by the outstanding catalytic performance of complex **65**, its substrate scope was briefly examined.

"Canopy catalyst" **65** exhibits unique catalytic activity, and selectivity derived from tripodal silanolate ligand **59b**. Moreover, complex **65** possesses significantly superior functional group tolerance than monodentate ligand-based molybdenum alkylidyne **25a**. The unrivalled catalytic performance of this complex is illustrated by its broad functional group tolerance. Although, this catalyst is both sensitive to air and moisture, it works well in the presence of unprotected primary alcohols and even tolerates

substrates having multiple donor sites, including basic nitrogen and heterocycles (Tables 2.11-2.12). Excellent results were also obtained when catalyst **65** was employed in the synthesis of macrocyclic architectures bearing more demanding functionality (Table 2.13). In particular, the ease of formation of key intermediates in the total synthesis of marine natural products including amphidinolide F and nor-cembranoid sinulariadiolide, further highlights the unrivalled catalytic activity of complex **65**, but also underlines its potential for use with more advanced substrates.

2.6. References

[1] F. Pennella, R. L. Banks, G. C. Bailey, *Chem. Commun.* **1968,** 1548-1549.

[2] J. A. Moulijn, H. J. Reitsma, C. Boelhouwer, *J. Catal.* **1972,** *25*, 434-436.

[3] A. Mortreux, F. Petit, M. Blanchard, *J. Mol. Catal.* **1980,** *8*, 97-106.

[4] A. Mortreux, N. Dy, M. Blanchard, *J. Mol. Catal.* **1976,** *1*, 101-109.

[5] A. Mortreux, F. Petit, M. Blanchard, *Tetrahedron Lett.* **1978,** *19*, 4967-4968.

[6] A. Bencheick, M. Petit, A. Mortreux, F. Petit, *J. Mol. Catal.* **1982,** *15*, 93-101.

[7] A. Mortreux, J.C. Delgrange, M. Blanchard, B. Lubochinsky, *J. Mol. Catal.* **1977,** *2*, 73-82.

[8] J. A. K. Du Plessis, H.C.M. Vosloo, *J. Mol. Catal.* **1991,** *65*, 21-24.

[9] H. C. M. Vosloo, J. A. K. Du Plessis, *J. Mol. Catal. A: Chem.* **1998,** *133*, 205-211.

[10] S. Devarajan, D. R. M. Walton, G. J. Leigh, *J. Organomet. Chem.* **1979,** *181*, 99-104.

[11] D. Villemin, P. Cadiot, *Tetrahedron Lett.* **1982,** *23*, 5139-5140.

[12] N. Kaneta, T. Hirai, M. Mori, *Chem. Lett.* **1995,** *24*, 627-628.

[13] Kaneta, N.; Hikichi, K.; Asaka, S.; Uemura, M.; Mori, M., *Chem. Lett.* **1995,** *24*, 1055-1056.

[14] L. Kloppenburg, D. Song, U. H. F. Bunz, *J. Am. Chem. Soc.* **1998,** *120*, 7973-7974.

[15] N. G. Pschirer, U. H. F. Bunz, *Tetrahedron Lett.* **1999,** *40*, 2481-2484.

[16] R. K. Bly, K. M. Dyke, U. H. F. Bunz, *J. Organomet. Chem.* **2005,** *690*, 825-829.

[17] K. Grela, J. Ignatowska, *Org. Lett.* **2002,** *4*, 3747-3749.

[18] V. Sashuk, J. Ignatowska, K. Grela, *J. Org. Chem.* **2004,** *69* , 7748-7751.

[19] V. Huc, R. Weihofen, I. Martin-Jimenez, P. Oulié, C. Lepetit, G. Lavigne, R. Chauvin, *New J. Chem.* **2003,** *27*, 1412-1414.

[20] V. Maraval, C. Lepetit, A.-M. Caminade, J.-P. Majoral, R. Chauvin, *Tetrahedron Lett.* **2006,** *47*, 2155-2159.

[21] G. Brizius, U. H. F. Bunz, *Org. Lett.* **2002,** *4*, 2829-2831.

[22] A. Fürstner, F. Stelzer, A. Rumbo, H. Krause, *Chem. Eur. J.* **2002,** *8* , 1856-1871.

[23] A. Fürstner, K. Grela, C. Mathes, C. W. Lehmann, *J. Am. Chem. Soc.* **2000,** *122*, 11799-11805.

[24] J. R. Fritch, K. P. C . Vollhardt, *Angew. Chem., Int. Ed*. **1979,** *18*, 409-411.

[25] M. Nishida, H. Shiga, M. Mori, *J. Org. Chem.* **1998,** *63*, 8606-8608.

[26] T. Woo, E. Folga, T. Ziegler, *Organometallics* **1993,** *12*, 1289-1298.

[27] J. Sancho, R. R. Schrock, *J. Mol. Catal.* **1982,** *15*, 75-79.

[28] T. J. Katz, J. McGinnis, *J. Am. Chem. Soc.* **1975,** *97*, 1592-1594.

[29] E. O. Fischer, G. Kreis, C. G. Kreiter, J. Müller, G. Huttner, H. Lorenz, *Angew. Chem., Int. Ed*. **1973,** *12*, 564-565

[30] R. R. Schrock, *J. Am. Chem. Soc.* **1974**, *96*, 6796-6797.

[31] L. J. Guggenberger, R. R. Schrock, *J. Am. Chem. Soc.* **1975**, 97, 2935-2935.

[32] J. H. Wengrovius, J. Sancho, R. R., Schrock, *J. Am. Chem. Soc*. **1981**, *103*, 3932-3934.

[33] M. R. Churchill, J. W. Ziller, Freudenberger, R. R. Schrock, *Organometallics* **1984**, *3*, 1554-1562.

[34] R. R. Schrock, *Polyhedron* **1995**, *14*, 3177-3195.

[35] J. H. Freudenberger, R. R. Schrock, *Organometallics* **1986**, *5*, 398-400.

[36] I. Feinstein-Jaffe, S. F. Pedersen, R. R. Schrock, *J. Am. Chem. Soc.* **1983**, *105*, 7176-7177.

[37] I. Feinstein-Jaffe, J. C. Dewan, R. R. Schrock, *Organometallics* **1985**, *4*, 1189-1193.

[38] J. H. Freudenberger, R. R. Schrock, M. R. Churchill, A. L. Rheingold, J. W. Ziller, *Organometallics* **1984,** *3*, 1563-1573.

[39] M. R. Churchill, J. W. Ziller, L. McCullough, S. F. Pedersen, R. R., Schrock, *Organometallics* **1983,** *2*, 1046-1048.

[40] M. R. Churchill, J. C. Fettinger, *J. Am. Chem. Soc.* **1984,** *106*, 3356-3357.

[41] S. Beer, C. G. Hrib, P. G. Jones, K. Brandhorst, J. Grunenberg, M. Tamm, *Angew. Chem., Int. Ed*. **2007,** *46*, 8890-8894.

[42] S. Beer, K. Brandhorst, J. Grunenberg, C. G. Hrib, P. G. Jones, M. Tamm, *Org. Lett.* **2008,** *10*, 981-984.

[43] S. Beer, K. Brandhorst, C. G. Hrib, X. Wu, B. Haberlag, J. Grunenberg, P. G. Jones, M. Tamm, *Organometallics* **2009,** *28*, 1534-1545.

[44] Z. J. Tonzetich, Y. C. Lam, P. Müller, R. R. Schrock, *Organometallics* **2007,** *26*, 475-477.

[45] X. Wu, C. G. Daniliuc, C. G. Hrib, M. Tamm, *J. Organomet. Chem.* **2011,** *696*, 4147-4151.

[46] B. Haberlag, M. Freytag, Jones, P. G. Jones, M. Tamm, *Adv. Synth. Catal.* **2014,** *356*, 1255-1265.

[47] B. Haberlag, X. Wu, K. Brandhorst, J. Grunenberg, C. G. Daniliuc, P. G. Jones, M. Tamm, *Chem. Eur. J.* **2010,** *16*, 8868-8877.

[48] S. Lysenko, B. Haberlag, C. G. Daniliuc, P. G. Jones, M. Tamm, *ChemCatChem* **2011,** *3*, 115-118.

[49] S. Lysenko, J. Volbeda, P. G. Jones, M. Tamm, *Angew. Chem., Int. Ed.* **2012,** *51*, 6757-6761.

[50] L. G. McCullough, R. R. Schrock, *J. Am. Chem. Soc.* **1984,** *106*, 4067-4068.

[51] L. G. McCullough, R. R. Schrock, J. C. Dewan, J. C. Murdzek, *J. Am. Chem. Soc.* **1985,** *107*, 5987-5998.

[52] J. M. Blackwell, J. S. Figueroa, F. H. Stephens, C. C. Cummins, *Organometallics* **2003,** *22*, 3351-3353.

[53] Y.-C. Tsai, P. L. Diaconescu, C. C. Cummins, *Organometallics* **2000,** *19*, 5260-5262.

[54] D. P. Estes, C. P. Gordon, A. Fedorov, W.-C. Liao, H. Ehrhorn, C. Bittner, M. L. Zier, D. Bockfeld, K. W. Chan, O. Eisenstein, C. Raynaud, M. Tamm, C. Copéret, *J. Am. Chem. Soc.* **2017,** *139*, 17597-17607.

[55] C. Bittner, H. Ehrhorn, D. Bockfeld, K. Brandhorst, M. Tamm, *Organometallics* **2017,** *36*, 3398-3406.

[56] H. Ehrhorn, D. Bockfeld, M. Freytag, T. Bannenberg, C. E. Kefalidis, L. Maron, M. Tamm, *Organometallics* **2019,** *38*, 1627-1639

[57] C. Cummins, *Chem. Commun.* **1998**, 1777-1786.

[58] A. Fürstner, C. Mathes, C. W. Lehmann, *J. Am. Chem. Soc.* **1999,** *121*, 9453-9454.

[59] A. Fürstner, C. Mathes, C. W. Lehmann, *Chem. Eur. J.* **2001,** *7*, 5299-5317.

[60] W. Zhang, S. Kraft, J.S. Moore, *Chem. Commun.* **2003,** 832-833.

[61] W. Zhang, S. Kraft, J. S. Moore, *J. Am. Chem. Soc.* **2004,** *126*, 329-335.

[62] W. Zhang, Y. Lu, J. S.Moore, *Org. Synth.* **2007**, 163-176.

[63] A. Fürstner, P. W. Davies, *Chem. Commun.* **2005,** 2307-2320.

[64] M. Bindl, R. Stade, E. K. Heilmann, A. Picot, R. Goddard, A. Fürstner, *J. Am. Chem. Soc.* **2009,** *131*, 9468-9470.

[65] A. Fürstner, *Angew. Chem., Int. Ed*. **2013,** *52*, 2794-2819.

[66] J. Heppekausen, R. Stade, R. Goddard, A. Fürstner, *J. Am. Chem. Soc.* **2010,** *132*, 11045-11057.

[67] J. Heppekausen, R. Stade, A. Kondoh, G. Seidel, R. Goddard, A. Fürstner, *Chem. Eur. J.* **2012,** *18*, 10281-10299.

[68] S. Benson, M.-P. Collin, A. Arlt, B. Gabor, R. Goddard, A. Fürstner, *Angew. Chem., Int. Ed.* **2011,** *50*, 8739-8744.

[69] G. Valot, C. S. Regens, D. P. O'Malley, E. Godineau, H. Takikawa, A. Fürstner, *Angew. Chem., Int. Ed.* **2013,** *52*, 9534-9538.

[70] A. Ahlers, T. de Haro, B. Gabor, A. Fürstner, *Angew. Chem., Int. Ed.* **2016,** *55*, 1406-1411.

[71] P. Karier, F. Ungeheuer, A. Ahlers, F. Anderl, C. Wille, A. Fürstner, *Angew. Chem., Int. Ed*. **2019,** *58*, 248-253.

[72] C. Krempner, *Chem. Eur. J.* **2011**, 2011, 1689-1698.

[73] J. M. Mayer, *Polyhedron* **1995**, *14*, 3273-3292.

[74] K. Jyothish, W. Zhang, *Angew. Chem., Int. Ed.* **2011,** *123*, 3497-3500.

[75] D. W. Paley, D.F. Sedbrook, J. Decatur, F. R. Fischer, M. L. Steigerwald, C. Nuckolls, *Angew. Chem. Int. Ed.* **2013,** *52*, 4591-4594.

[76] K. Jyothish, Q. Wang, W. Zhang, *Adv. Synth. Catal.* **2012,** *354*, 2073-2078.

[77] H. Yang, Z. Liu, W. Zhang, *Adv. Synth. Catal.* **2013,** *355*, 885-890.

[78] S. Schaubach, K.Gebauer, F. Ungeheuer, L. Hoffmeister, M. K. Ilg, C. Wirtz, A. Fürstner, *Chem. Eur. J.* **2016**, *22*, 8494-8507.

[79] S. Schulthoff, J. Hamilton, M. Heinrich, Y. Kwon, C. Wirtz, A. Fürstner, *Angew. Chem. Int. Ed.* **2020**, *60*, 446-454.

[80] L. Löffler, C. Wirtz, A. Fürstner, *Angew. Chem. Int. Ed.* **2021**, *60*, 5316-5322.

[81] Z. Meng, A. Fürstner, *J. Am. Chem. Soc.* **2019**, 141,805 –809.

[82] J. Hillenbrand, M. Leutzsch, A. Fürstner, *Angew. Chem. Int. Ed.* **2019**, 58, 15690 – 15696; *Angew. Chem.* **2019**, 131, 15837 – 15843.

[83] J. V. Hillenbrand, Molybdän- und Wolfram-Katalysatoren mit Tripodalen Liganden für die Alkin-Metathese & Isolierung eines homoleptischen Mo(V) Alkoxid Komplexes, PhD Thesis, Max-Planck Institüt fur Kohlenforschung/Technische Universität Dortmund, Mülheim an der Ruhr/Dortmund, **2021**.

[84] J. Hillenbrand, M. Leutzsch, E. Yiannakas, C. Gordon, C. Wille, N. Nöthling, C. Copéret, A. Fürstner, *J. Am. Chem. Soc.* **2020**, *142*, 11279 – 11294.

[85] D. Trawny, M. Quennet, N. Rades, D. Lentz, B. Paulus, H. Reissig, *Chem. Eur. J.* **2015**, 21, 4667-4674.

[86] Y. Ge, S. Huang, Y. Hu, L. Zhang, L. He, S. Krajewski, M. Ortiz, Y. Jin, W. Zhang, *Nat. Comm.* **2021**, *12*, 1136.

[87] S. E. Denmark, R. C. Smith, W.-T. T. Chang, J. M. Muhuhi, *J. Am. Chem. Soc.* **2009**, *131*, 3104–3118.

[88] L. A. Babadzhanova, N. V. Kirij, Yu. L. Yagupolskii, W. Tyrra, D. Naumann, *Tetrahedron* **2005**, *61*, 1813–1819.

[89] G. Valot, C. S. Regens, D. P. O'Malley, E. Godineau, H. Takikawa, A. Fürstner, *Angew. Chem., Int. Ed.* **2013,** *52*, 9534-9538.

[90] G. Valot, D. Mailhol, C. S. Regens, D. P. O'Malley, E. Godineau, H. Takikawa, P. Philipps, A. Fürstner, *Chem. Eur. J.* **2015,** *21* (6), 2398-2408.

Chapter 3: Total synthesis of Samroiyotmycin A

3.1. Introduction

In 2013, Dramae *et al.* reported that the crude extracts of *Streptomyces* species BCC33756 collected from soil at Khao Sam Roi Yot National Park in Thailand, exhibited anti-malarial activity against *P. falciparum* K1 multi-drug resistant strain.[1] Further investigation resulted in the isolation of nine compounds. Among these, was the novel C_2-symmetric macrodiolide natural product **1** (Scheme 3.1). Apart from its unique 20-membered macrocyclic core, samroiyotmycin A (**1**), showed activity against *P. falciparum* K1 (IC_{50}: 3.65 μg mL^{-1}) and lung carcinoma cell lines (NCI-H187; IC_{50}: 24.14 μg mL^{-1}).[1]

Capitalising on the homodimerisation approach previously developed in the Hulme group, through the successful synthesis of cytotoxic protein-protein interaction (PPI) inhibitor disorazole C_1,[2] assembly of the macrocyclic ring in this promising scaffold (**1**) was considered via a late-stage a one-pot Alkyne Cross Metathesis-Ring-Closing Metathesis (ACM/RCAM) reaction. A *priori*, this approach can be applied across either the *E*-configured disubstituted alkene (C(5)C(6)/C(21)C(22)) or the *E*-enoate sites (C(3) C(4)/C(19)C(20)). Whilst considering these tactics, one must assess the potential risks. In the former case, conversion of the bis(enyne) **2** to the required *E*-configured alkenes in the absence of any protic functionality proximal to the acetylene C-atoms is a non-trivial task.[3-5] In assessing the second strategy for constructing this macrocyclic frame by a one-pot ACM/RCAM reaction of ynoate precursor **5**; the subsequent steps (ynoate-dienoate isomerisation,[6-13] bisiodination [14] and double Stille/ Negishi coupling [15,16]) were deemed fairly reliable, given the plethora of protocols in the literature for these reactions.

Although the RCAM reactions of ynoates were previously explored in the context of natural product synthesis, the formation of a bis(lactone) such as **3** from a ynoate ester such as **5** has not been reported in the literature.[17-25] Yet, the challenges associated with the plan for assembling the 20-membered core of samroiyotmycin A (**1**) by an ynoate one-pot ACM/RCAM were offset by curiosity to expand the scope of this alkyne metathesis-based approach. With this in mind, a unified plan for the construction of the required bisalkyne building blocks (**4**&**5**) was designed (Scheme 3.1 (i)).

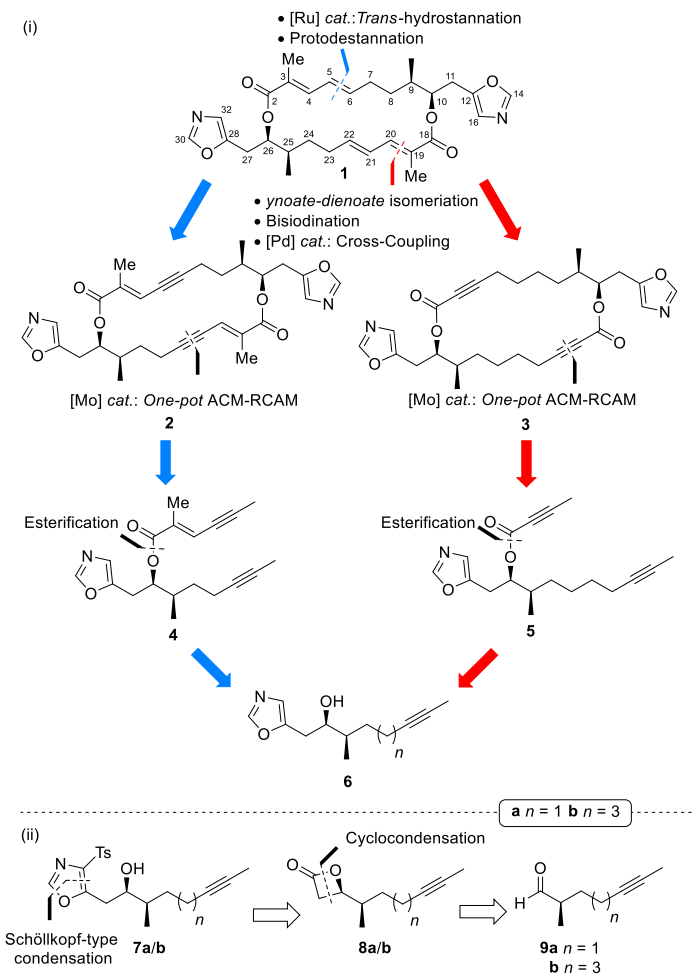

Scheme 3.1. Two conceivable convergent approaches to samroiyotmycin A based on one-pot ACM/RCAM reactions: *(i)* Ring assembly via routes based on C(5)-C(6)/C(21)-C(22) or C(3)-C(4)/C(19)-C(20) disconnections to key intermediate secondary alcohol **6**; *(ii)* Introduction of C(9)/C(10) and C(25)/C(26) stereochemistry via cyclocondensation onto α-methyl aldehydes **9a**/**b**.

The former fragments were thought to be available by esterification of secondary alcohols **6a**/**b**, after desulfonylation of 5-substituted 4-tosyloxazoles **7a**/**b**. Influenced by prior work in the Hulme group,[26] access to 4-tosyloxazoles **7a**/**b** could be achieved through a Schöllkopf-type condensation on β-lactones **8a**/**b** with anionic TosMIC. If successful, this synthetic manoeuvre would permit concurrent installation of the 1,3-oxazole unit and the hydroxy group at C(10) (Scheme 3.1 (ii)). As a key initial element of the synthetic plan, assembly of the diastereomeric β-lactones **8a**/**b** was envisaged via an asymmetric ketene cycloaddition to α-methyl aldehydes **9a**/**b**.[27] It was evident that the synthesis blueprint (Scheme

3.1 (ii)) shown above qualifies for the use of an asymmetric ketene cycloaddition on α-methyl aldehydes **9a**/**b**, since this approach enables the introduction of all stereocentres in a strictly catalyst-controlled manner, capable of overwriting any inherent bias of individual substrates. Outlined below are both parts of a synthetic study that aimed to explore two proposed one-pot ACM/RCAM strategies.

3.2. Investigating the Schöllkopf-type condensation of diastereomeric β-lactones.

To pursue this novel synthetic proposal of simultaneously introducing the 1,3-oxazole unit and set the C(9)-C(10) stereochemistry required, the Schöllkopf-type condensation of β-lactones was investigated. Although the condensation reactions of anionic TosMIC with carboxylic acid derivatives have been previously explored in the context of 5-substituted 4-tosyloxazole synthesis, [28-30] there are no prior examples of a Schöllkopf-type condensation on enantioenriched 4-substituted beta-lactones **8a**/**b** as required for the construction of heterocyclic fragments **7a**/**b**. Since the investigation of this proposed synthetic approach required the generation of α-methyl aldehydes **9a**/**b**, preliminary studies focused on the diastereoselective alkylation of *N*-acylated oxazolidinones.

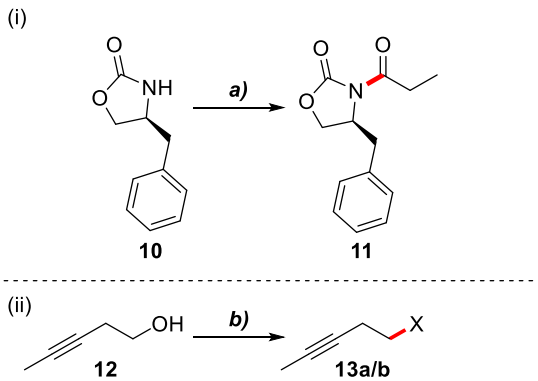

Scheme 3.2. Preparation of *N*-acyl derivative **11** and electrophiles **13a**/**b**. *Reagents and Conditions*: (i) *(a)* ^{n}BuLi, propionyl chloride, THF, − 78 °C to RT, 18 h, (**11**, 98 %); (ii) *(b)* Br_2 or I_2, PPh_3, imidazole, Et_2O-MeCN (3:1), (**13a**, X = Br, 81 %, **13b**, X = I, 91 %).

Lithiation of Evans oxazolidinone auxiliary **10** and subsequent quench with propionyl chloride, delivered *N*-acylated oxazolidinone **11** in almost quantitative yield on multi-gram scale (Scheme 3.2 (i)). Alkyl

bromide **13a** and alkyl iodide **13b** were synthesised from commercial 3-pentyn-1-ol **12** by an Appel reaction (Scheme 3.2 (ii)). With all the required precursors in hand, the diastereoselective alkylation of *N*-acyl derivative **14** was explored (Table 3.1).

Table 3.1. Conditions Screen for the diastereoselective alkylation of *N*-acyl derivative **14**.

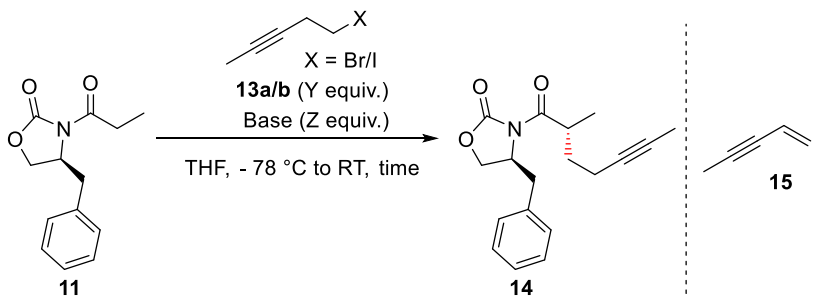

Entry	E^+ (X)	Base	Z (equiv.)	Y (equiv.)	Scale (g)	Time (h)	% Yield
1	Br	LDA	1.05	1.10	0.5	16	0
2	I	LDA	1.05	1.10	0.5	16	0
3	I	NaHMDS	1.05	5.00	1.0	4.5[a]	0

[a] At – 78 °C.

Unfortunately, none of the reaction conditions examined gave the desired product **14**. More specifically, where LDA was used as the base (Table 3.1, entries 1 and 2), this only resulted in complete collapse of the starting material amide **11** to carbamate **10** and elimination of the electrophiles (**21** and **22**) to the corresponding enyne by-product **15**. Moreover, utilising a milder base such as NaHMDS and an excess of the alkyl iodide **13b**, gave the same decomposition products (Table 3.1, entry 3). The above results prompted us to find out whether the diastereoselective alkylation of *N*-acyl oxazolidinone derivative **16** would be a better method of accessing aldehydes **9a**/**b** (Scheme 3.1).

The synthesis of *N*-acyl derivative **16** began with a KO^{t}Bu mediated isomerisation of commercially available 6-heptynoic acid to afford 5-heptynoic acid (**17**) (Scheme 3.3),[31] which was converted to the corresponding mixed anhydride with PvCl and then directly engaged in the acylation of oxazolidinone **18** to deliver multi-gram quantities of *N*-acyl oxazolidinone derivative **16** in an overall 72-74 % yield over two steps.[32] Diastereoselective methylation of the latter delivered the *N*-acyl derivative **19** in very good yield and high diastereoselectivity utilising a modified procedure based on the work of Boije af Gennäs *et al.*

(2009) (Table 3.2, entries 3 & 4).[33] With the first stereocentre set in the future C5-C16 fragment of samroiyotmycin A (**1**), the first key step of the synthesis blueprint was subsequently explored; the installation of the 1,3-oxazole unit and the concomitant setting of the stereochemistry at C(10).

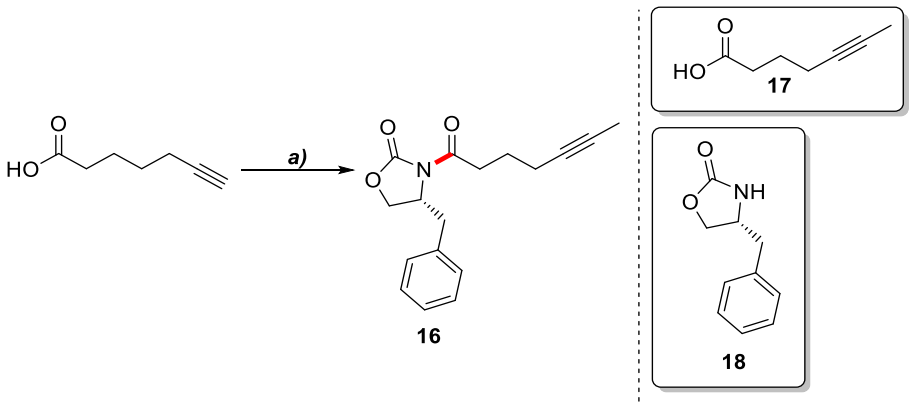

Scheme 3.3. Preparation of *N*-acyl derivative **16**. *Reagents and Conditions*: *(a) (i)* KO^{t}Bu, DMSO, 85 °C, 0.5 h; *(ii)* PvCl, TEA, **18**, LiCl, THF, − 78 °C to RT, 18 h, (**16**, 72-74 % over two steps)**.**

Table 3.2 Reaction conditions explored for the diastereoselective alkylation of *N*-acyl derivative **16**.

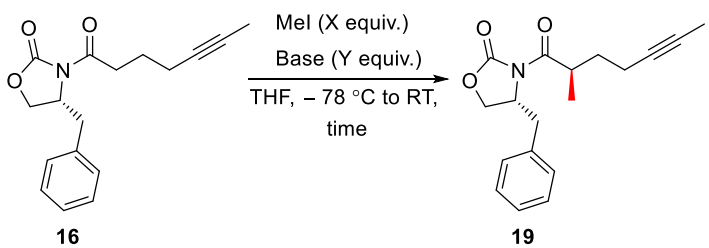

Entry	Base	Y (equiv.)	X (equiv.)	Scale (g)	T (h)[a]	% Yield	*dr*
1	LDA	1.10	1.05	0.5	4.5	0	-
2	NaHMDS	1.10	5.00	0.5	4.5	0	-
3	NaHMDS	1.50	5.00	2.5	4.5	83	> 95:5
4	NaHMDS	1.50	5.00	3.0	4.5	77	> 95:5

[a] At – 78 °C.

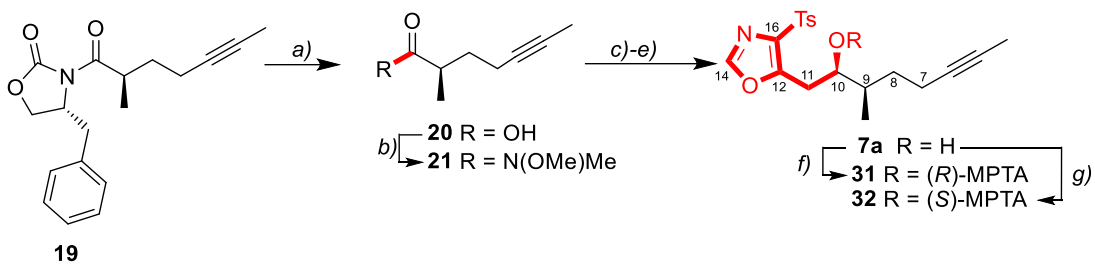

Scheme 3.4. Synthesis of chiral alcohol fragments **7a**: *(a)* LiOH, H_2O_2, THF/H_2O (1:1), 0 °C → RT, (**20**, 95 %, 93 *%ee*, 3.6 g scale); *(b)* CDI, HN(OMe)Me·HCl, CH_2Cl_2, 0 °C → RT, 18 h, (**21**, 93 %*ee*); *(c)* DIBAL-H, CH_2Cl_2, − 78 °C, 1 h; *(d)* **23** (10 mol%), $LiClO_4$, AcCl, DIPEA, CH_2Cl_2/Et_2O (2:1), − 78 °C, 18 h, (> 95:5 *dr*); (*e*) TosMIC, ^{n}BuLi, THF, − 78 °C → RT, 1 h, (**7a**, 35 %, 96:4 *dr*, over five steps from **19**); (*f*) (*S*)-(+)-MTPACl, DMAP (10 mol%), TEA, CH_2Cl_2, RT, 18 h, (**31**, 77%); (*g*) (R)-(−)-MTPACl, DMAP (10 mol%), TEA, CH_2Cl_2, RT, 18 h (**32**, 72%).

Cleavage of the auxiliary in the presence H_2O_2 gave acid **20** in almost quantitative yield (95 %) (Scheme 3.4), which was directly converted into the configurationally stable Weinreb amide **21** with minimal erosion of the enantiomeric purity as observed by HPLC. The optical purity of amide **21** was determined by HPLC on chiral stationary phase (94 %ee, Figure 3.1). The racemate of acid **20** was prepared via a three-step sequence consisting of initial alkylation of diethyl methyl malonate with 5-iodopent-2-yne (**13b**), followed by a Krapcho decarboxylation reaction and saponification. Further elaboration of racemic acid **20** also gave the racemate of amide **21** (Figure 3.1).

Inspired by the recent total syntheses of dinoflagellate-derived cytotoxic marine macrolides formosalide A and B, featuring intermolecular nucleophile-catalysed aldol lactonisation (NCAL) reactions (Figure 3.2)[34] of aldehydes with remote substitution, utilising *O*-TMS quinidine catalyst **22** (Scheme 3.5), it was envisaged that the asymmetric ketene-aldehyde cycloaddition catalysed by *O*-TMS quinine **23** would serve as an excellent way for chain elongation in a doubly diastereoselective fashion.[35] Moreover, the reliability of this method is demonstrated through the exquisite stereochemical control exerted by cinchona alkaloid catalyst **23** in intramolecular double diastereoselective, NCAL reactions of aldehyde acids (Scheme 3.6).[36]

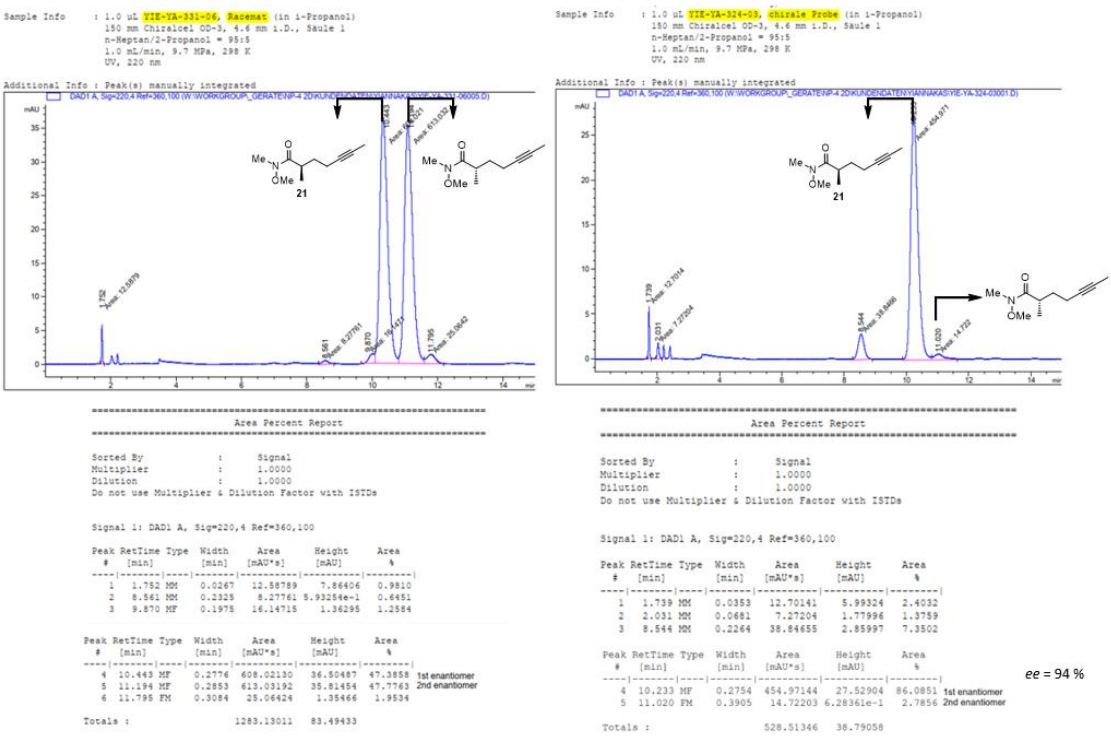

Figure 3.1. Annotated HPLC traces of racemic amide **21** (left) and crude aliquot of amide **21** (right), monitored @ 220 nm**.**

Treatment of the crude amide **21** with DIBAL-H provided the fragile α-methyl aldehyde **9a** (Scheme 3.4). Subjecting the crude aldehyde **9a** directly to cyclocondensation condensations catalysed by *O*-TMS quinine **23**, gave the thermally unstable β-lactone **8a** in excellent diastereomeric purity (> 99:1). The excellent diastereocontrol observed over the newly formed stereocentre at C(10) in this reaction furnishes the first example of a doubly diastereoselective intermolecular NCAL reaction, where the catalyst control overrides the inherent influence of an α-methyl stereogenic centre on an aldehyde. Low temperature condensation with anionic TosMIC, delivered chiral alcohol **7a** in good overall yield (35% yield over five steps) and high diastereoselectivity (96:4 *dr*) over the telescoped sequence starting from *N*-acyl amide derivative **19** (Scheme 3.4).

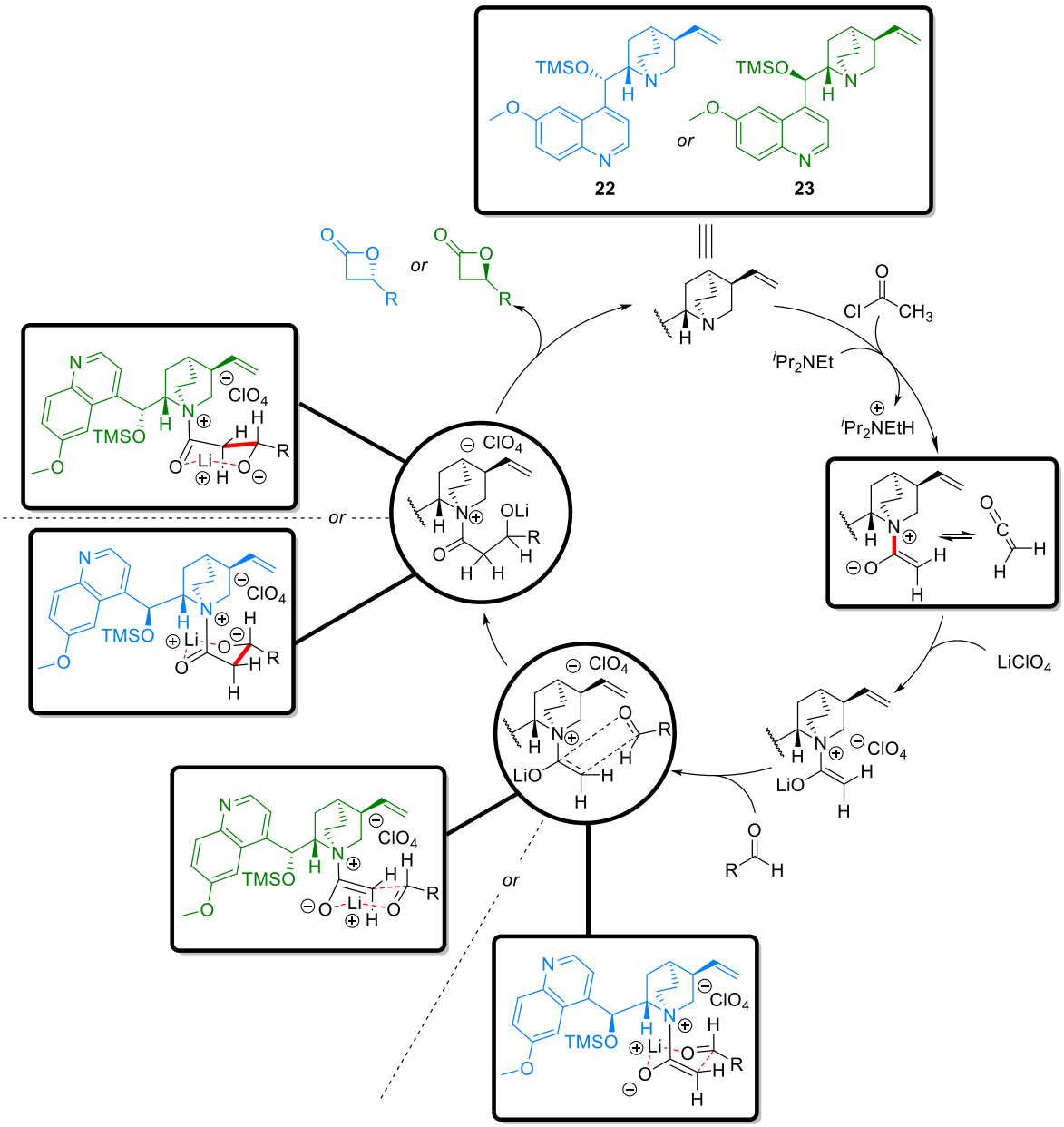

Figure 3.2. Postulated Mechanism for Alkaloid-Catalysed Asymmetric Ketene-Aldehyde Cycloaddition Reactions.

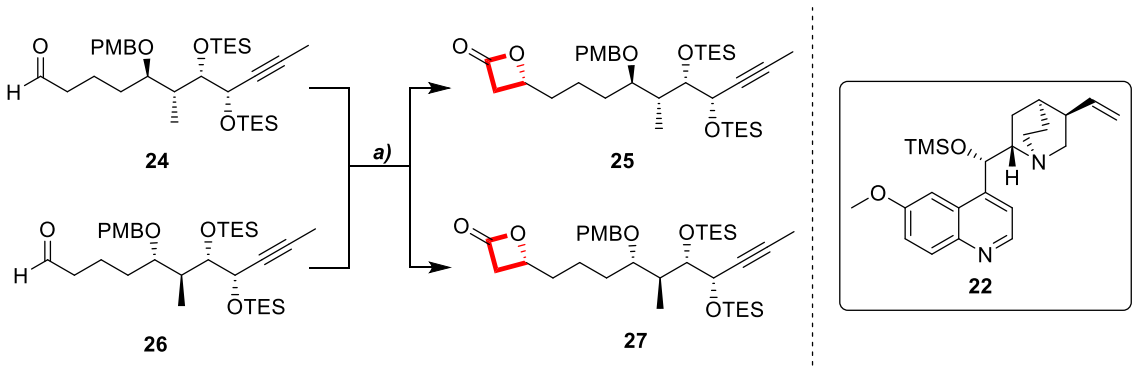

Scheme 3.5. Intermolecular NCAL reactions catalysed by *O*-TMS quinidine **22** in the total syntheses of Formosalide A and F.[35] *Reagents and Conditions*: *(a)* acetyl chloride, **22** (10 mol %), $LiClO_4$, DIPEA, CH_2Cl_2/Et_2O, −78 °C, 78 % (**25**, 95:5 *dr*), 84 % (**27**, 90:10 *dr*).

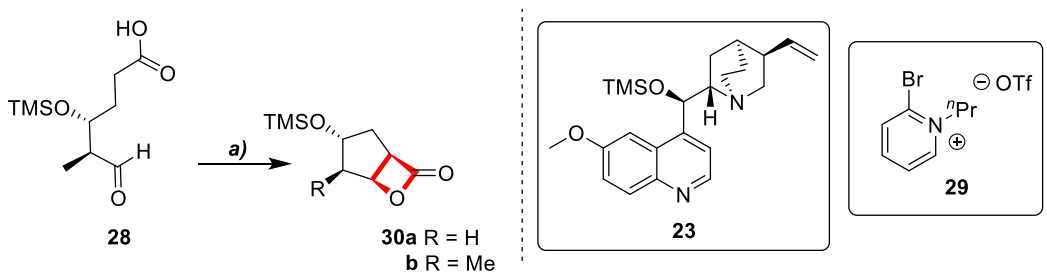

Scheme 3.6. Intramolecular NCAL reaction of ketoacid **28** catalysed by *O*-TMS quinine **23**.[36] *Reagents and Conditions*: *(a)* **23** (10 mol %), **29**, DIPEA, CH_2Cl_2, RT, (**30a**, 60 %, > 95:5 *dr*; **30b,** 55 %, 90:10 *dr*).

The configuration of the C(10)OH was confirmed by Mosher ester analysis. Developed by Dale and Mosher in the early 1970s, Mosher ester analysis provides a rigorous method for determining the absolute configuration and optical purity of chiral alcohols, by converting a pair of NMR-indistinguishable enantiomers or diastereomers into NMR-distinguishable diastereomers.[37] In this technique, the chiral alcohol of interest is converted into a pair of diastereomeric esters upon treatment with *R*- and *S*-2-methoxy-2-phenyl-2-(trifluoromethyl) acetic acid chloride (MTPA-Cl) (Scheme 3.4) or by Steglich esterification with *R*-and *S*-MTPA-OH acid [Note: Although, *R*-Mosher acid furnishes the *R*-Mosher ester, it is the *S*-Mosher acid chloride that gives rise to the *R*-Mosher ester]. The NMR spectra of the resulting diastereomeric esters are analyzed to reveal the absolute configuration of the original chiral alcohol. Dale

and Mosher proposed that the major solution-phase conformer places the proton directly attached to the stereogenic centre, trifluoromethyl and ester carbonyl moieties in the same plane (Figure 3.3 (i)).[37a]

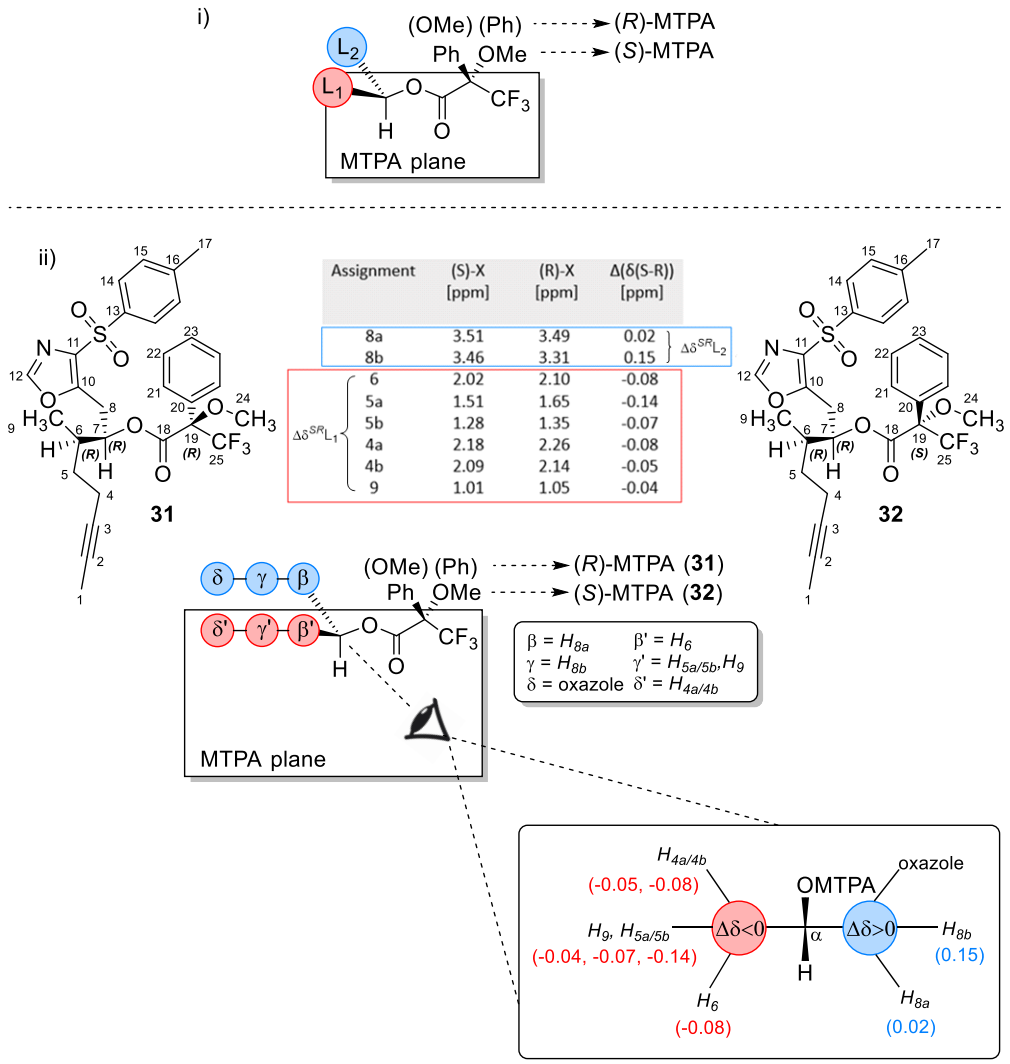

Figure 3.3. Mosher ester analysis of alcohol **7a** derivatives (**31** R=(*R*)-MTPA, **32** R=(*S*)-MTPA): *(i)* Mosher's Model; *(ii)* Table with Δ(δ(S −R)) data for the *S*- and *R*-MTPA esters **31** and **32** (arbitrary numbering scheme as shown below) and Mosher ester analysis of alcohol **7a** derivatives.

In this conformation, the protons of substituent L_2 are shielded by the phenyl ring in the (*R*)-MTPA ester, while those on L_1 remain unaffected. Conversely, in the (*S*)-MTPA derivative, it is L_1 and its protons that are shielded, whereas L_2 is unaffected. These shieldings are expressed using the parameter $\Delta\delta^{SR}$, which is the difference between the chemical shift of a given proton in the (*S*)-MTPA derivative and the chemical

shift of the same proton in the (*R*)-MTPA ester. All the protons shielded in the (*S*)-MTPA derivative will present a negative $\Delta\delta^{SR}$ value, whereas those shielded in the (*R*)-MTPA ester will present a positive $\Delta\delta^{SR}$ value (Figure 3.3 (ii)). In the case of the alcohol **7a** derivatives, the signs for each proton in L_1 and L_2 are as follows: $\Delta\delta^{SR}L_1 = \delta L_1(S) - \delta L_1(R) < 0$ and $\Delta\delta^{SR}L_2 = \delta L_2(S) - \delta L_2(R) > 0$.[38]

With a pivotal aspect of this synthetic strategy rigorously confirmed, it was clear that chiral alcohols **6** were within reach. However, the preparation of these was postponed until after the other critical steps of the proposed synthesis were validated. For proof-of-concept, 5-substituted 4-tosyloxazole **7b** was initially targeted via the same five-step telescoped sequence (Scheme 3.4). 7-Iodo-2-heptyne **36**, prepared from commercial 5-hexyn-1-ol **33** (Scheme 3.7), served as a point of departure. *N*-acylation reaction partner **37** was prepared on multi-gram scale from commercial diethyl malonate by alkylation with alkyl iodide **36** to give **38**, Krapcho decarboxylation and a final ester hydrolysis (Scheme 3.8).[32] *N*-acylation of oxazolidinone **18** using acid **37** and PvCl, followed by asymmetric alkylation with MeI, delivered *N*-acyl derivative **40** in almost quantitative yield (98 %) and high diastereoselectivity (> 95:5 *dr*).

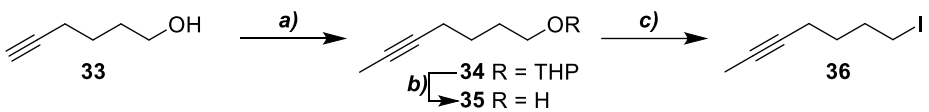

Scheme 3.7. Four-step synthesis of alkyl iodide **36.** *Reagents and Conditions*: *(a) (i)* 3,4-DHP, TsOH *(cat.)*, CH_2Cl_2, 0 °C → RT, 18 h; *(ii)* ^{n}BuLi, MeI, THF, −78 °C → RT, 18 h; *(b)* TsOH *(cat.)*, MeOH, RT, 18 h; *(c)* I_2, PPh_3, imidazole, Et_2O-MeCN (3:1), 0 °C → RT, 3 h (**36**, 95 %, 10 g scale, over four steps)**.**

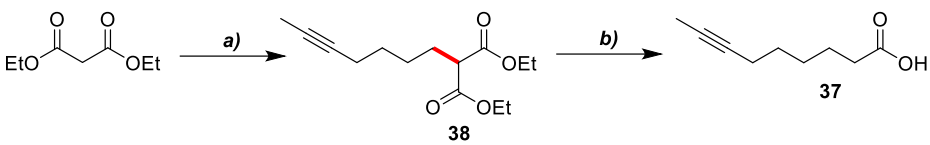

Scheme 3.8. Three-step synthesis of acid **37.** *Reagents and Conditions*: *(a)* **36**, NaH, DMF, 0 °C → RT, 18 h; *(b) (i)* LiCl, H_2O *(cat.)*, DMSO, 160 °C, 18 h; *(ii)* LiOH, THF-H_2O (3:1), RT, 18 h (**37**, 80 %, 5 g scale, over three steps)**.**

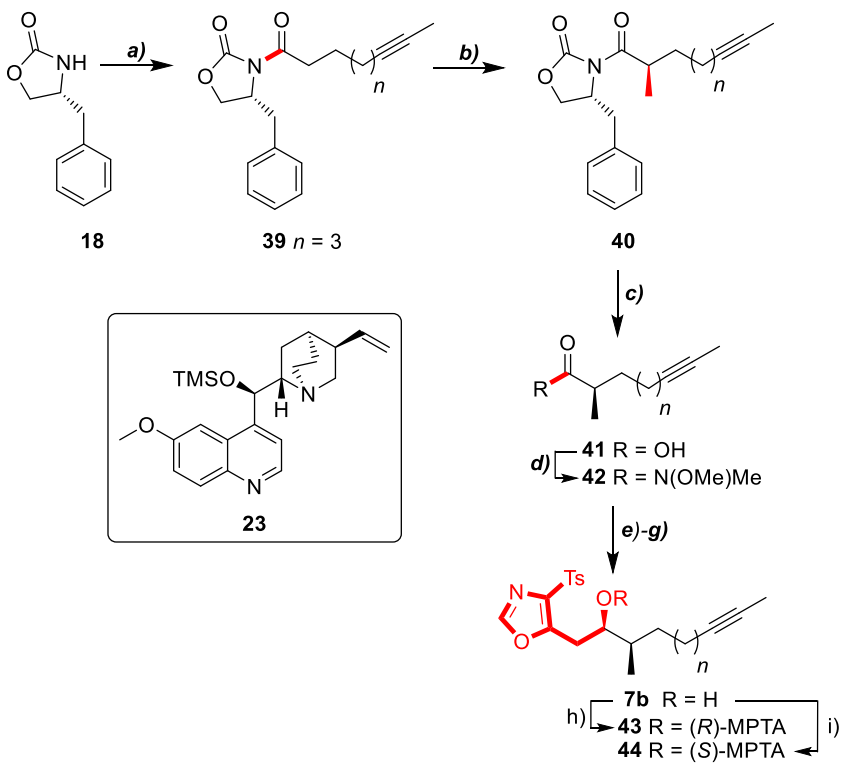

Scheme 3.9. Synthesis of chiral alcohol **7b** from Evans oxazolidinone **18**. *Reagents and Conditions*: *(a)* LiCl, PvCl, TEA, THF, − 10 °C to RT, 18 h, (**39**, 2.0 g scale, 24 % over four steps from diethyl malonate); *(b)* NaHMDS, MeI, THF, − 78 °C (**40**, 98 %, > 20:1 *dr*, 4.0 g scale); *(c)* LiOH, H_2O_2, THF/H_2O (1:1), 0 °C → RT, 18 h, (**41**, 91 %, 94 *%ee*, 4.0 g scale); *(d)* CDI, HN(OMe)Me·HCl, CH_2Cl_2, 0 °C → RT, 18 h, (**42**, 82 % over two steps from **40**, 92 *%ee*, 4.0 g scale); *(e)* DIBAL-H, CH_2Cl_2, − 78 °C, 1 h; *(f)* **23** (10 mol%), $LiClO_4$, AcCl, DIPEA, CH_2Cl_2/Et_2O (2:1), − 78 °C, 18 h, > 95:5 *dr*; *(g)* TosMIC, ^{n}BuLi, THF, − 78 °C → RT, 1 h, (**7b**, 43 % over five steps from **39**, > 95:5 *dr*); (h) (*S*)-(+)-MTPACl, DMAP (10 mol%), TEA, CH_2Cl_2, rt, 18 h, (**43**, 85 %); (*i*) (*R*)-(−)-MTPACl, DMAP (10 mol%), TEA, CH_2Cl_2, rt, 18 h, (**44**, 88 %).

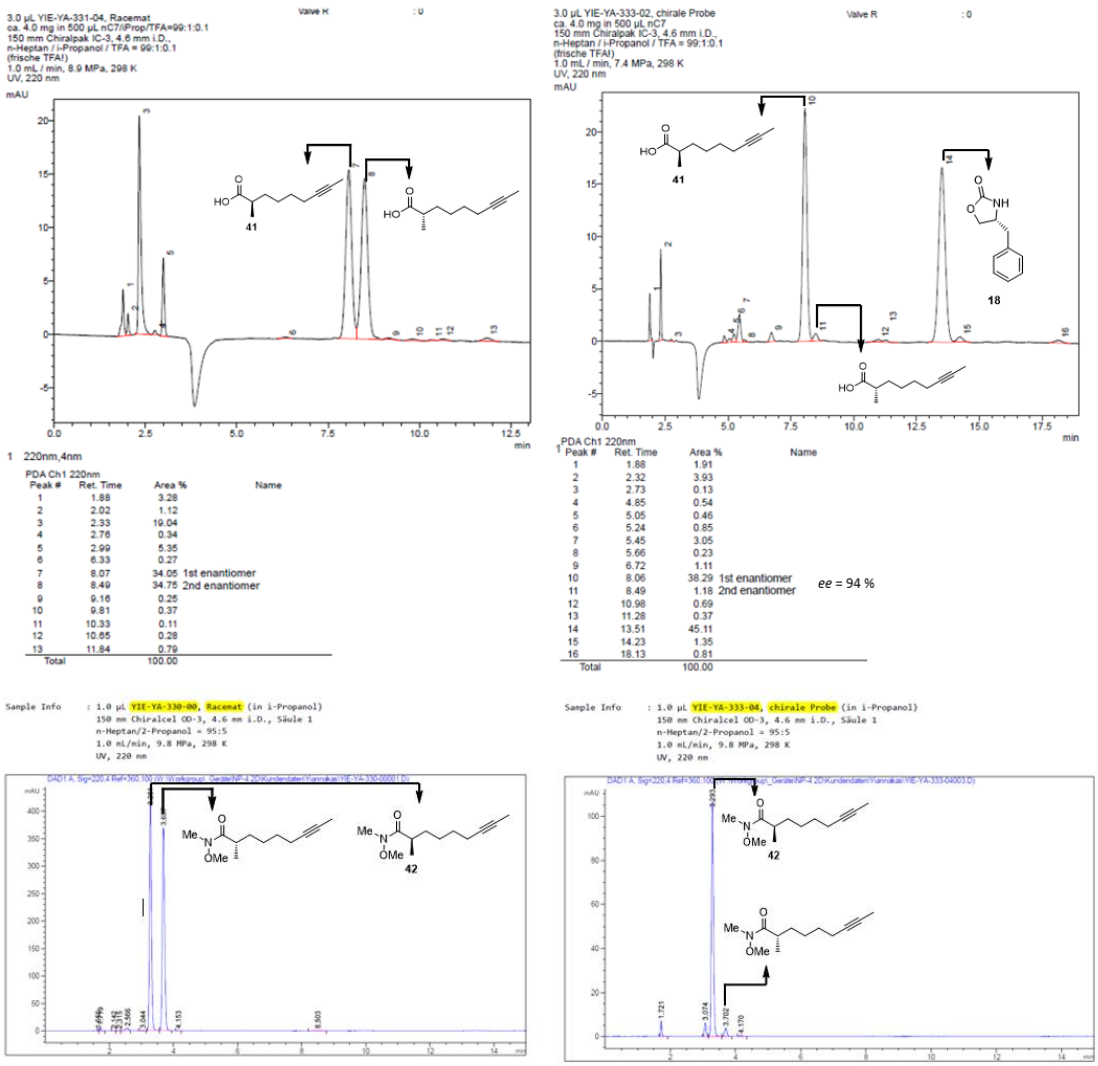

Figure 3.4. Annotated HPLC traces of racemic acid **41** (top-left) and crude aliquot of acid **41** (top-right), racemic amide **42** (bottom-left) and crude aliquot of amide **42** (bottom-right) monitored @ 220 nm**.**

Saponification of *N*-acyl derivative **40**, conversion of the resulting acid **41** (91 %) into the Weinreb amide **42** (82 % over two steps), followed by the reduction with DIBAL-H, provided aldehyde **9b**. Once again, the enantiopurity purity of the crude acid **41** (94 *%ee*, Figure 3.4) and amide **42** (92 *%ee*, Figure 3.4) was determined by HPLC on chiral stationary phase. The racemates of acid **41** and amide **42** were prepared in a similar manner to racemic acid **20** and racemic amide **21**, starting from commercial diethyl methyl malonate and alkyl iodide **36**.

The asymmetric acid chloride–aldehyde cyclocondensation in the presence of catalytic *O*-TMS quinine **23** proceeded smoothly to afford β-lactone **8b** with high diastereocontrol (> 95:5 *dr*). Equally gratifying was the fact that subsequent Schöllkopf-type condensation of the crude lactone **8b** with TosMIC, gave alcohol **7b** in 43 % yield over five steps (> 95:5 *dr*) (Scheme 3.9). Mosher ester analysis of acid derivatives **43** and **44** (Scheme 3.9), confirmed the configuration of the newly formed stereocentre at C(10)OH in fragment **7b** (Figure 3.5)**.**

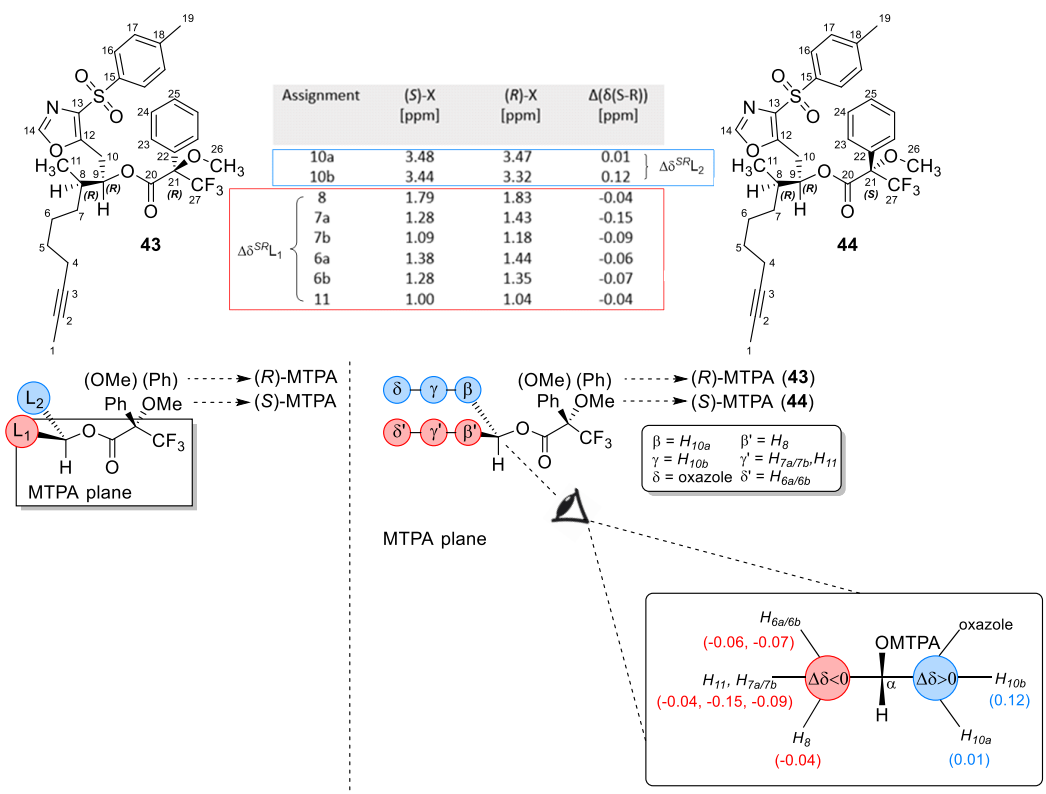

Figure 3.5. Mosher ester analysis of alcohol **7b** derivatives **43** and **44** (arbitrary numbering scheme as shown below).

3.3 Streamlined Synthesis of Fragment 7a

Having successfully validated a key aspect of the synthetic strategy, the total synthesis of this promising anti-malarial agent was investigated. For this purpose, however, it turned out more advantageous to employ Myers auxiliaries, since the pseudoephedrine amide formed post-diastereoselective electrophilic functionalisation can be directly transformed to the enantioenriched α-methyl aldehydes **9a**/**b**.[39] To streamline the synthesis of fragment **7a**/**b**, the diastereoselective alkylation of pseudoephedrine amide **46** was initially investigated (Table 3.3). Coupling of acid **17** with commercial amine **45**, gave the corresponding pseudoephedrine amide **46** in very good yield (Scheme 3.10).

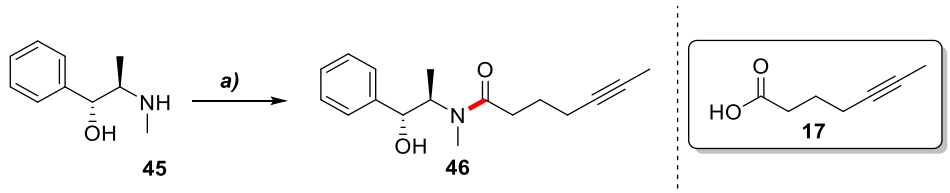

Scheme 3.10. Preparation of pseudoephedrine amide **46.** *Reagents and Conditions*: *(a)* **17**, TEA, PvCl, THF, – 10 °C → RT, 18 h, (**46**, 87 %, 5.0 g scale).

Table 3.3. Screening for reaction conditions for the diastereoselective alkylation of amide **46**.

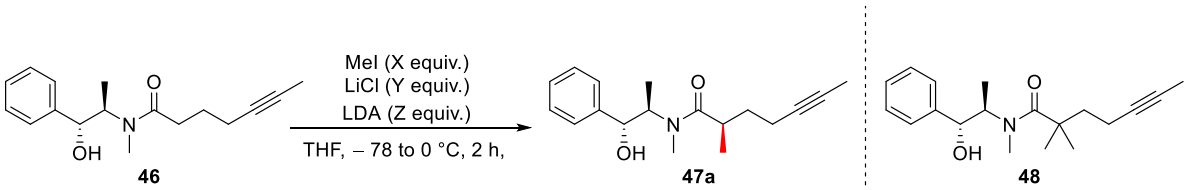

Entry	X (equiv.)	Y (equiv.)	Z (equiv.)	Scale (g)	% Yield	%Conv.of SM by GC-MS	*dr*
1	3.0	6.0	2.0	1.0	39	Full	98:2
2	3.0	6.0	2.0	1.0	56[a]	Full	98:2
3	1.5	6.0	2.0	1.0	79[a]	Full	98:2
4	1.5	6.0	2.0	4.0	41[b,c]	Full	97:3

[a] Addition of the electrophile over 30 mins. [b] Addition of the electrophile over 30 mins. [c] HPLC yield: 64 %.

Diastereoselective methylation of pseudoephedrine amide **46** on gram scale, utilising the general reaction conditions originally disclosed by Myers *et al.* (1997), afforded the α-methyl pseudoephedrine amide **47a** with excellent diastereoselectivity (Table 3.3, entry 1).[40] The diastereomeric ratio was determined by HPLC on reverse stationary phase (Figure 3.6). Despite the great diastereocontrol exhibited by this reaction over the newly formed stereocentre, due a competing second methylation reaction of amide **47** during the electrophilic fuctionalisation of the dianionic enolate of amide **46** to give **48**, the desired alkylation product **47a** was only isolated in 39 % yield.

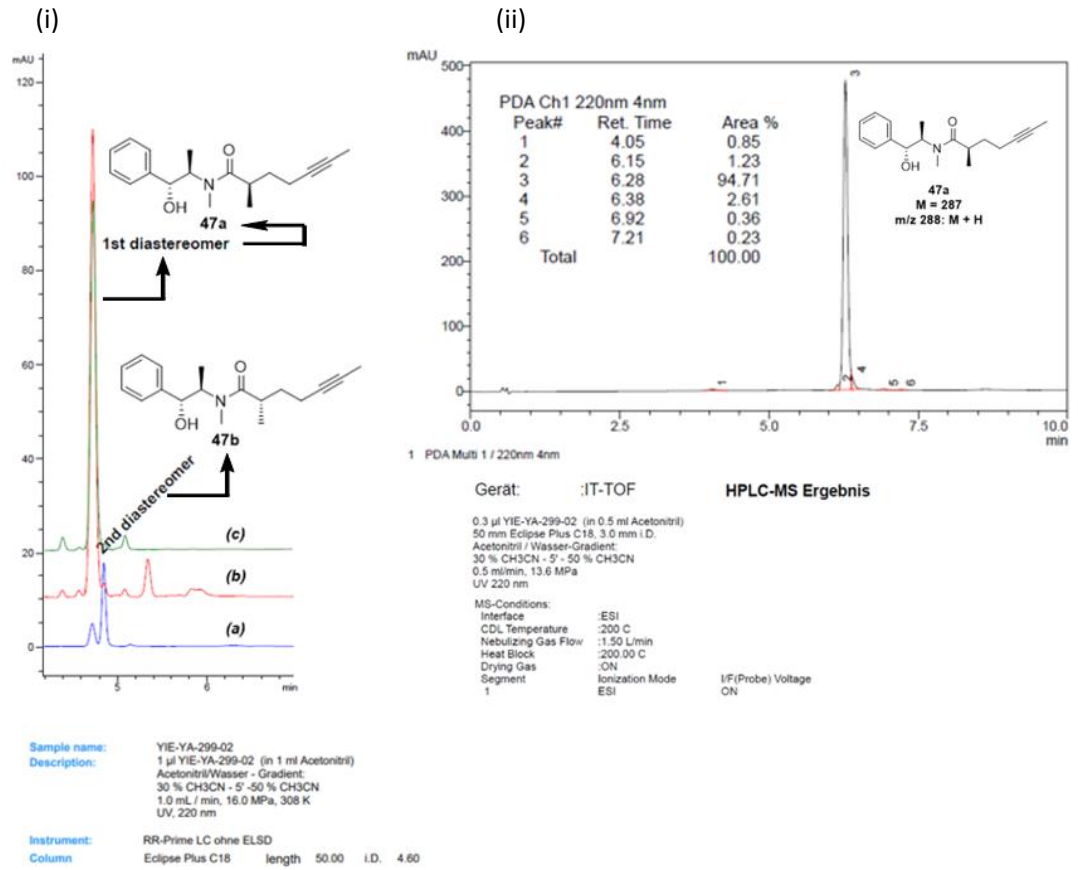

Figure 3.6. Overlaid and annotated HPLC and LCMS traces - Table 3.3, entry 1. (i) Annotated HPLC traces monitored @ 220 nm: *(a)* Annotated HPLC trace of a mixture of epimers **47a** and **47b**, prepared by stirring amide **47a** with trifluoroacetic acid in THF at reflux, followed by neutralization with sat. $NaHCO_3$ solution at RT for 24 h; *(b)* Annotated HPLC trace of crude reaction mixture aliquot (98:2 *dr*); *(c)* Annotated HPLC trace of pseudoephedrine-derivate **47a** after a single purification on normal phase silica; (ii) LCMS trace of diastereomerically pure product **47a**.

Surprisingly, slow addition along with reduction of the equivalents of MeI used, led to substantial improvement in the isolated yield of pseudoephedrine-derivative **47** (Table 3.3, entry 3), without any

impact on the diastereoselectivity of the reaction and complete suppression of sideproduct **48** formation. When this reaction was scaled up, using the improved reaction conditions, the desired product **47** was only isolated in 41 % yield with minor erosion diastereomeric purity (Table 3.3, entry 4, Figure 3.7).

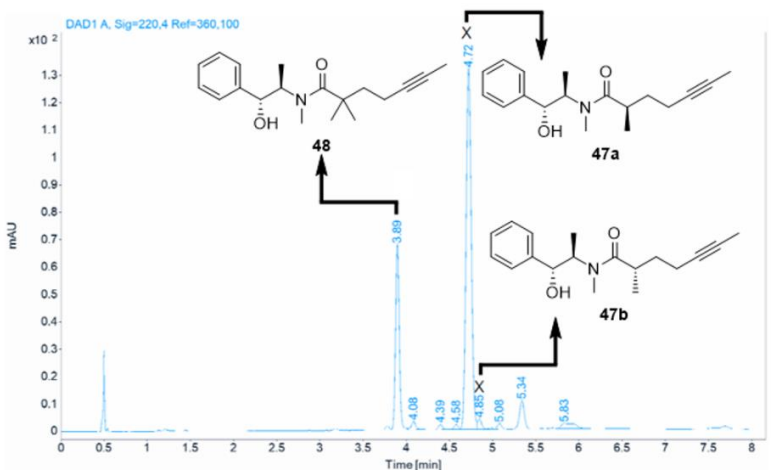

Signal: DAD1 A, Sig=220,4 Ref=360,100

RT [min]	Area	Area%	Name
3.89	202.86	23.18	
4.08	11.88	1.36	
4.39	6.83	0.78	
4.58	6.85	0.78	
4.72	557.60	63.71	1st diastereomer
4.85	12.97	1.48	2nd diastereomer
5.08	10.56	1.21	
5.34	41.53	4.75	
5.83	24.14	2.76	
Sum	875.2279		

dr = 97:3

Figure 3.7. Annotated HPLC trace of crude reaction aliquot monitored @ 220 nm - Table 3.3, entry 4.

Due to the reduced isolated yield of pseudoephedrine amide **47**, the diastereoselective alkylation of commercial propionate derivative **49** using alkyl iodide **13b** was explored as an alternative approach (Table 3.4). Among the first set of reaction conditions examined were those disclosed by Myers *et al.* (1997).[40] Regrettably, this led to elimination of the electrophile **13b** and only partial conversion to the desired product **50** (Table 3.4, entry 1). Monitoring the reaction progress by GC-MS (Table 3.4, entry 2, Figure 3.6) while slowly increasing the reaction temperature (− 78 to 0 °C) over eight hours, led to some interesting observations. Although a slow increase in temperature completely suppressed any elimination of the electrophile **13b**, no diastereoselective electrophilic functionalisation was observed at −78 °C. Upon

warming to − 10 °C over 7 h, the reaction appeared to stall at 69 % conversion. No further increase in the relative conversion was observed even after the reaction mixture was warmed to 0 °C (Figure 3.8). Based on these results, it was concluded that the enolate equivalent of pseudoephedrine amide **49** must be used in excess to attain full conversion. Employing a 2:1 ratio of pseudoephedrine amide **49** to alkyl iodide **13b** (Table 3.4, entry 3), resulted in full conversion of the starting material within two hours at 0 °C, while the desired product **50a** was isolated in 95 % yield and excellent diastereomeric purity (Figure 3.7 (ii)).

Table 3.4. Reaction conditions for the diastereoselective alkylation of pseudoephedrine amide **49**.

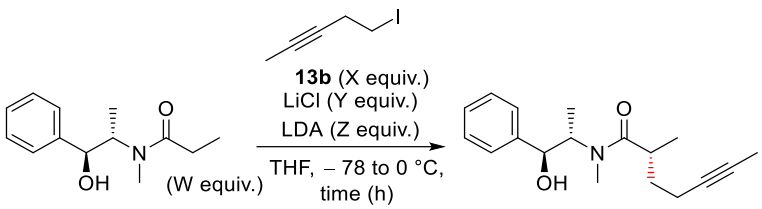

49 **50a**

Entry	W (equiv.)	X (equiv.)	Y (equiv.)	Z (equiv.)	% Conv.	Scale (g)	% Yield	*dr*[a]	Time (h)
1	1.0	3.0	1.0	2.0	60	1.0	44	99:1	2
2	1.0	3.0	1.0	2.0	69	2.0	50	99:1	8
3	2.0	1.0	2.0	4.0	100	1.0	95	99:1	2
4	2.0	1.0	2.0	4.0	100	5.0	79	99:1	2

[a] Diastereomeric ratio determined by HPLC after a single normal phase purification.

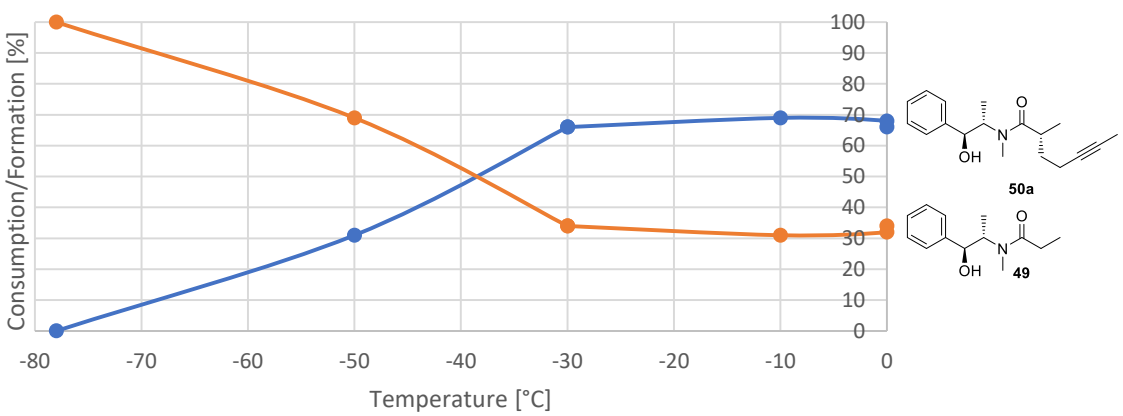

Figure 3.8. Reaction Monitoring Experiment (GC-MS): Relative % Consumption/Formation of amide **49**/**50a** with gradual increase in temperature over 8 h - Table 3.5, entry 2.

Moreover, utilising the optimized reaction conditions on larger scale, the diastereoselective alkylation of the lithium propionate enolate **49** afforded multigram quantities of pseudoephedrine amide **50a** in very good yield (79 %, Table 3.4, entry 4) with without erosion of the diastereomeric purity.

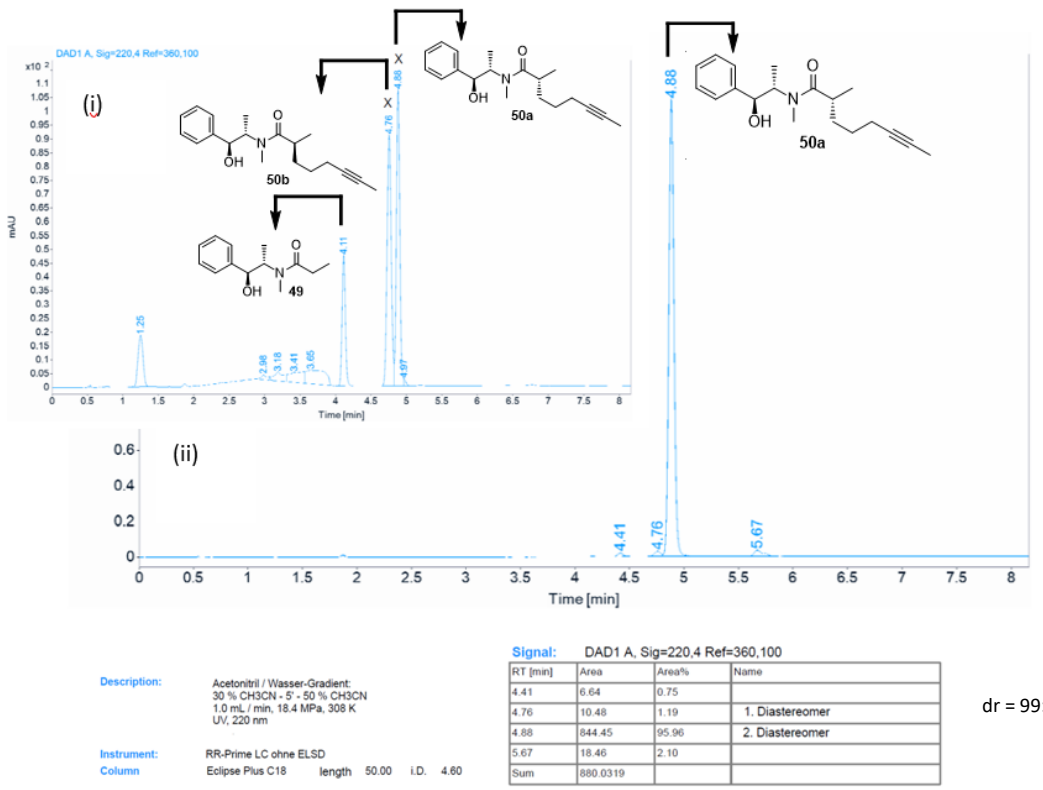

Signal: DAD1 A, Sig=220,4 Ref=360,100

RT [min]	Area	Area%	Name
4.41	6.64	0.75	
4.76	10.48	1.19	1. Diastereomer
4.88	844.45	95.96	2. Diastereomer
5.67	18.46	2.10	
Sum	880.0319		

Description: Acetonitril / Wasser-Gradient: 30 % CH3CN - 5' - 50 % CH3CN 1.0 mL / min, 18.4 MPa, 308 K UV, 220 nm

Instrument: RR-Prime LC ohne ELSD

Column: Eclipse Plus C18 length 50.00 i.D. 4.60

dr = 99:1

Figure 3.9. Annotated HPLC/LCMS traces monitored @ 220 nm. (i) Epimerized crude reaction aliquot (Table 3.4, entry 2); (ii) Isolated amide **50a** (Table 3.4, entry 3).

Reductive cleavage of the auxiliary using *in situ* generated $LiAl(OEt)_3H$ at low-temperature gave aldehyde **9a**, which was subjected crude to cyclocondensation catalysed by *O*-TMS quinine **23** to afford β-lactone **8a** (> 95:5 *dr*). Immediate condensation of crude lactone **8a** with anionic TosMIC provided chiral alcohol **7a** in good yield and high diastereomeric purity (97:3 *dr*) on multi-gram scale over a three-step telescoping sequence (52 %) (Scheme 3.11). The diastereomeric purity of the 4-tosyloxazole **7a** prepared via the above

three-step sequence (Scheme 3.11) was further validated by HPLC using a range of chiral stationary phases (see Appendix 5 for more details).

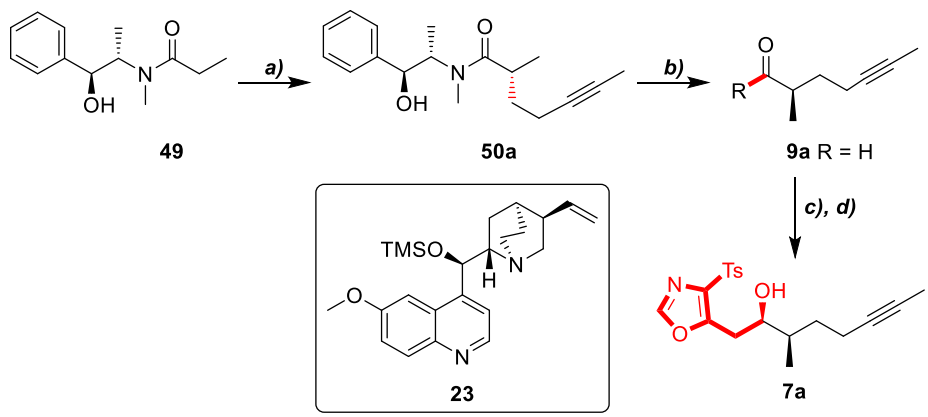

Scheme 3.11. Synthesis of chiral alcohol **7a** from pseudoephedrine propionate **49**. *Reagents and Conditions*: *(a)* LDA, LiCl, **13b**, − 78 °C → 0 °C, 2 h, (**50a**, 79 %, > 95:5 *dr*, 5.0 g scale); *(b)* $LiAlH_4$, EtOAc, THF/iso-Hexanes (4:3), − 78 °C → 0 °C, 1 h; *(c)* **23** (10 mol%), $LiClO_4$, AcCl, DIPEA, CH_2Cl_2/Et_2O (2:1), − 78 °C, 18 h, (**8a**, > 95:5 *dr*); *(d)* TosMIC, ^{n}BuLi, THF, − 78 °C → RT, 1h, (**7a**, 97:3 *dr*, 52 % over three steps from **50a**).

3.4 Streamlined Synthesis of Fragment 7b

Encouraged by the robustness of the four-step sequence developed for assembling fragment **7a**, it was envisaged that 4-tosyloxazole **7b** could also be obtained by this fragment synthesis. To confirm this hypothesis, the diastereoselective alkylation reactions of pseudoephedrine amides **51** and **49** were initially explored. Coupling of amine **45** with acid **37**, gave *N*-acyl derivative **51** in almost quantitative yield (97%) (Scheme 3.12).

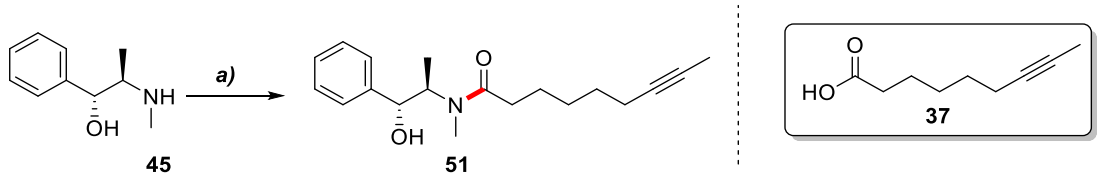

Scheme 3.12. Preparation of pseudoephedrine amide **51.** *Reagents and Conditions*: *(a)* **37**, TEA, PvCl, THF, – 10 °C → RT, 18 h, (**51**, 97 %, 1.0 g scale).

Employing the same reaction conditions previously used in the diastereoselective methylation of *N*-acyl derivative **46** (Table 3.5, entry 3), afforded amide **52** in 58 % yield and good diastereomeric purity (97:3 *dr*, Figure 3.10) (Scheme 3.13). Conversely, utilising the general reaction conditions originally reported by Myers *et al.* (1997) for the alkylation of propionate derivative **49** with alkyl iodide **36**, delivered the desired product **53a,** in almost quantitative yield and excellent diastereomeric ratio (Table 3.7, entry 1; Figure 3.11).[40] This reaction gave the *N*-acyl derivative **53a** on a multigram scale in very good to almost quantitative yield (86–98%), with high diastereoselectivity (Table 3.7, entries 2-3; Figure 3.11).

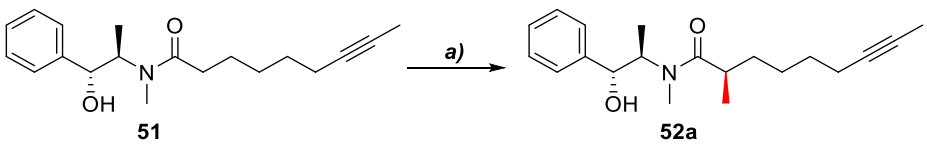

Scheme 3.13. Preparation of pseudoephedrine amide 52a. *Reagents and Conditions*: *(a)* LDA, LiCl, MeI, THF, – 78 °C → 0 °C, 2 h, (**52a**, 59 %, 97:3 *dr*, 1.5 g scale).

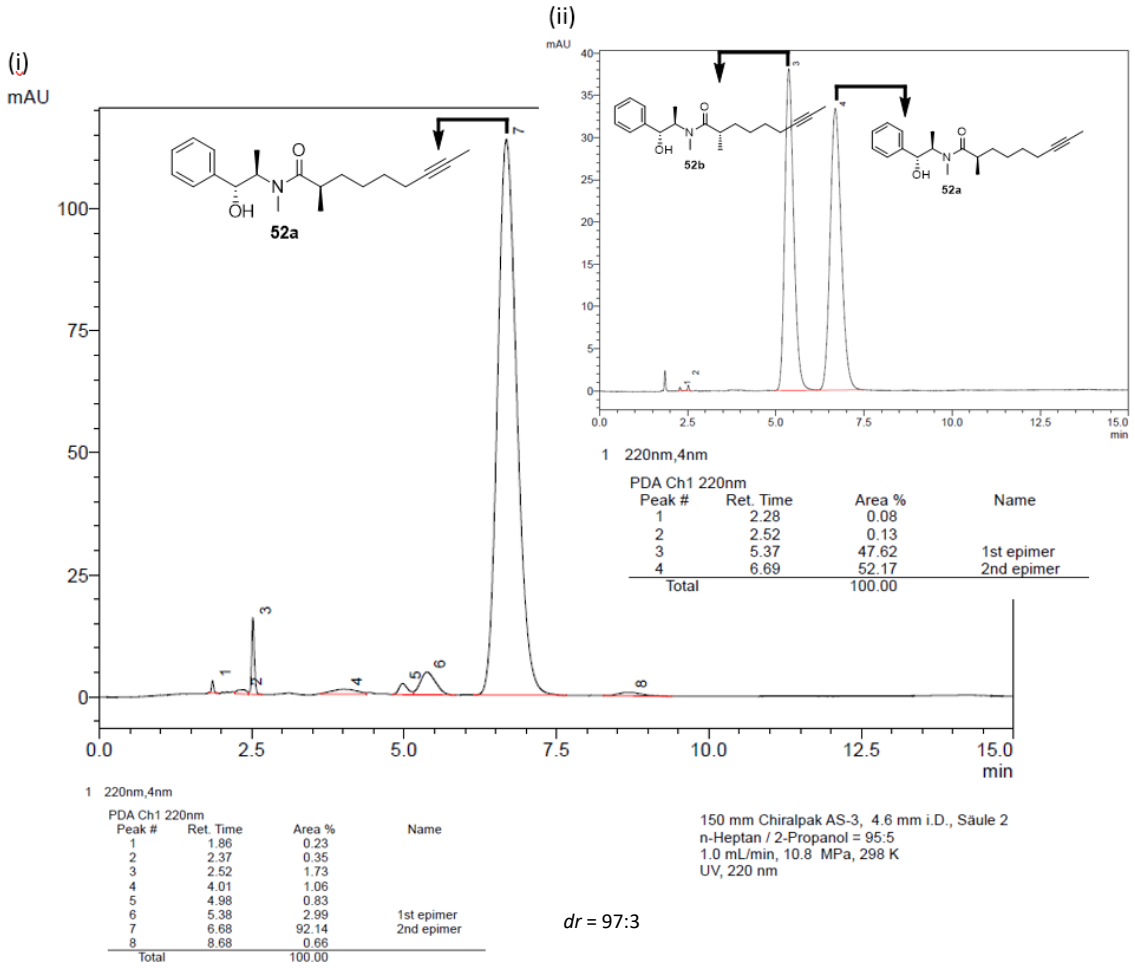

Figure 3.10. Annotated overlaid chiral HPLC traces. (i) Crude reaction mixture aliquot.; (ii) Mixture of epimers **52a** and **52b**.

Table 3.5. Diastereoselective alkylation of pseudoephedrine amide **49** with alkyl iodide **36**.

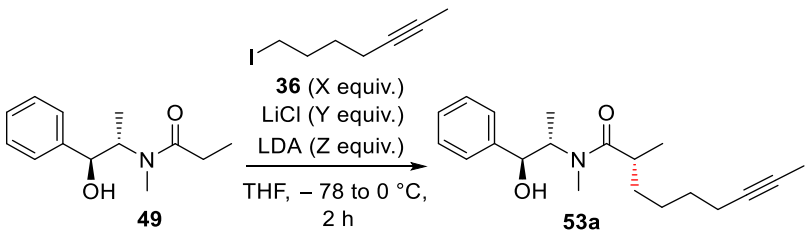

Entry	X (equiv.)	Y (equiv.)	Z (equiv.)	% Conversion	Scale (g)	% Yield	*dr*	Time (h)
1	3.0	6.0	2.0	100	1.0	98	99:1	2
2	3.0	6.0	2.0	100	2.0	86	99:1	2
3	1.5	6.0	2.0	100	3.5	98	99:1	2

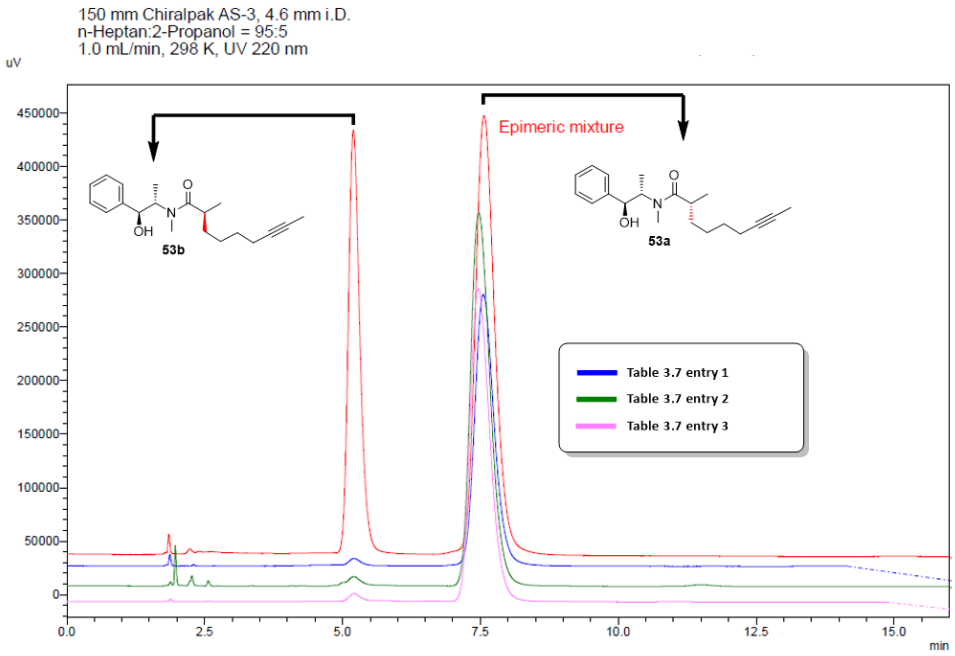

Figure 3.11. Annotated overlaid Chiral HPLC traces Table 3.7 entries 1-3.

Having established a set of optimal reaction conditions for the introduction of the alkyl branch by asymmetric alkylation, the elaboration of amide **53a** into fragment **7b** was examined. Reduction of *N*-acyl derivative **53a** using *in situ* generated $LiAl(OEt)_3H$ at low-temperature gave aldehyde **9b** (Scheme 3.13), which was subjected without purification to cyclocondensation utilising the same conditions employed in the synthesis of fragment **7a** from advanced propionate derivative **50a**. Unfortunately, this reaction only led to partial conversion of the crude aldehyde **9b** to diastereomerically pure β-lactone **8b**, even after 48 hours at − 78 °C (Figure 3.12 (ii)), while subsequent condensation with anionic TosMIC provided chiral alcohol **7b** in poor yield (12 %) over three steps but high diastereomeric purity (> 95:5 *dr*). Careful optimisation of the cycloaddition reaction conditions revealed that using an equivolume mixture of Et_2O and CH_2Cl_2 as the solvent was crucial for attaining full-conversion and high diastereoselectivity (Figure 3.12 (iii)). Condensation of the crude lactone **8b** with TosMIC, delivered fragment **7b** in an overall 24 % yield after a single purification over the three-step telescoping sequence (> 95:5 *dr*) (Scheme 3.13). The diastereomeric purity of the 4-tosyloxazole **7b** prepared via the above three-step sequence (Scheme 3.11) was further validated by HPLC using a range of chiral stationary phases (see Appendix 6 for more details).

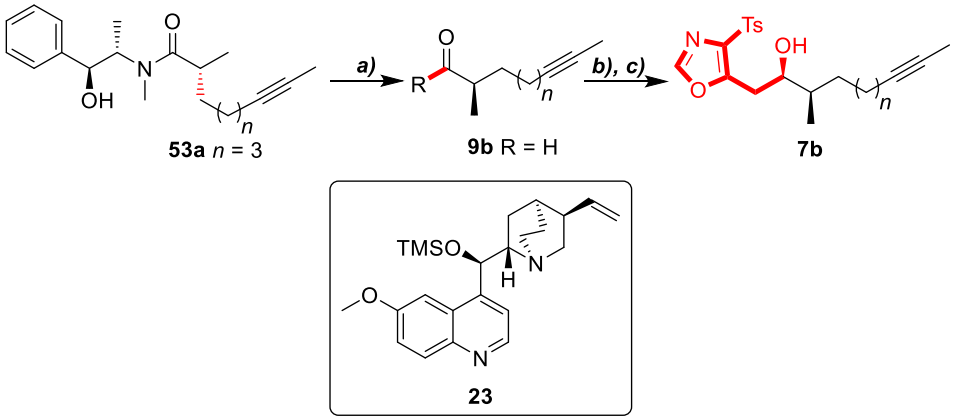

Scheme 3.13. Preparation of chiral alcohol **7b.** *Reagents and Conditions*: *(a)* $LiAlH_4$, EtOAc, THF/isohexanes (4:3), − 78 ° → 0°C, 1 h; *(b)* **23** (10 mol%), $LiClO_4$, AcCl, DIPEA, CH_2Cl_2/Et_2O (1:1), − 78 °C, 24 h, (**8b**, > 95:5 *dr*); *(c)* TosMIC, ^nBuLi, THF, − 78 °C → RT, 1h, (**7b**, > 95:5 *dr*, 52 % over three steps from **53a**).

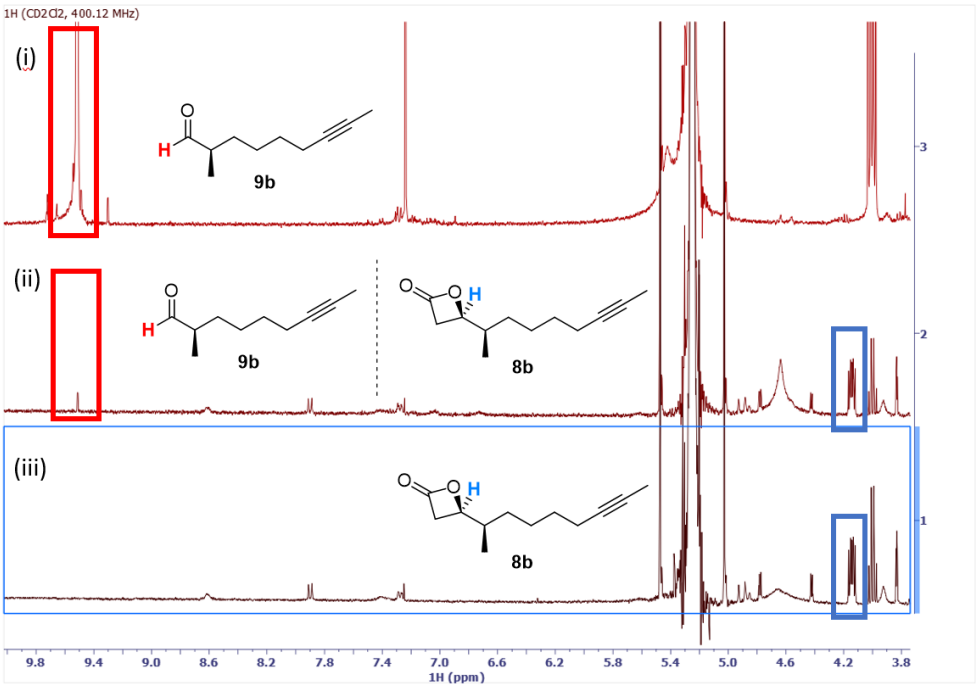

Figure 3.12. Annotated overlaid NMR spectra of crude aliquots from cyclocondensation reactions of crude aldehyde **8b**. (i) Reaction mixture at t = 0 h, (ii) Reaction mixture at t = 48 h, *Reagents and Conditions*: **23** (10 mol%), $LiClO_4$, AcCl, DIPEA, CH_2Cl_2/Et_2O (2:1), − 78 °C; (iii) Reaction mixture at t = 24 h, *Reagents and conditions*: **23** (10 mol%), $LiClO_4$, AcCl, DIPEA, CH_2Cl_2/Et_2O (1:1), − 78 °C.

3.5. Enyne Carboxylate Fragment synthesis

The synthesis of 2-methyl-2-hexen-4-ynoic acid (**55**) was previously reported by Saito *et al.*, via a nickel-mediated regio- and chemoselective carboxylation of 2,4-hexadiyne (**54**) in the presence of carbon dioxide and DBU (Scheme 3.13).[41] Despite the mild reaction conditions employed, the use of stoichiometric $Ni(COD)_2$ and super stoichiometric amount of DBU, prompted us to explore an alternative approach to acid **55**.

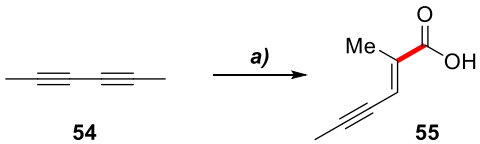

Scheme 3.14. Synthesis of eynecarboxylic acid **54** using nickel (0)-mediated carboxylation of 2,4-hexadiyne in the presence of CO_2.[38] *Reagents and Conditions*: *(a)* (i) $Ni(COD)_2$, CO_2 (1 atm), DBU, 0 °C, 3 h; (ii) H^+, 68 %.

Based on the work of Coutrot *et al.*, a simple and efficient route to 2-alkyl-2-alkenoic acids, is via a Horner-Wadsworth-Emmons (HWE) reaction (Scheme 3.15).[42] With this in mind it was considered that carboxylic acid **55** could be synthesised in a single step by a HWE reaction between commercially available 2-diethoxyphosphorylpropanoic acid (**56**) and but-2-ynal (**57**).

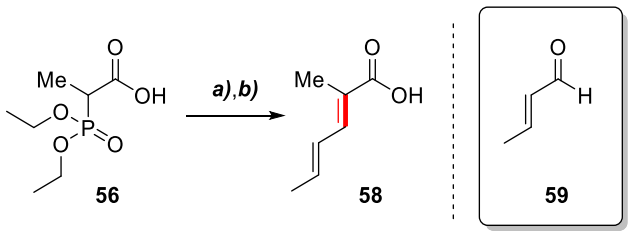

Scheme 3.15. Synthesis of (2*E*,4*E*)-2-methyl-hexa-2,4-dienoic acid (**58**) by a HWE reaction.[39] *Reagents and Conditions*: *(a)* ^{n}BuLi, THF, − 60 °C, 0.5 h; *(b)* **59**, THF, − 60 °C → RT, 3 h, 0.5 h, 73 %.

Aldehyde **57** can be prepared readily by the oxidation of the commercially available but-2-yn-1-ol (**60**) (Scheme 3.16). Despite the ease of its preparation of aldehyde **57**, Ahlers *et al.* have shown that it decomposes readily and is best isolated/stored as a solution in dichloromethane at −78 °C.[43]

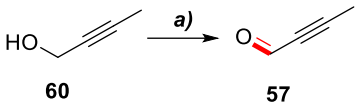

Scheme 3.16. Oxidation of But-2-yn-1-ol (**60**) to But-2-ynal (**57**).[40] *(a)* TEMPO (10 mol%), TBACl (10 mol%), NCS, CH_2Cl_2/Carbonate-Bicarbonate Buffer (1:1), RT, 7 h, 60 %.

To circumvent any issues with the instability of the aldehyde **57**, an excess of the aldehyde in crude form was used for the investigation of the proposed HWE reaction with organophosphate **56**. Therefore, a freshly prepared batch of the crude aldehyde **57** was utilised for each reaction in this synthetic study (Table 3.6). The HWE reaction of phosphonate **56** utilising a slight excess of the crude aldehyde **57** only led to poor isolated yields of the desired carboxylic acid **55** with an *E*:*Z* ratio of 90:10 determined from the crude reaction mixture by ^{1}H NMR (Table 3.6, entries 1&2). These poor yields might be attributed to decomposition of but-2-ynal (**57**) during its preparation;[43] further supported by the fact that employing aldehyde **57** in almost four-fold excess led to great improvement in the isolated yield of acid **55** (63 %, Table 3.6, entry 3) with an *E*:*Z* ratio of 90:10 (Figure 3.13). With the desired acid **55** in hand, the reductive desulfonylation of chiral alcohols **7a**/**b** was investigated.

Table 3.6. Investigating the HWE reaction of 2-diethoxyphosphorylpropanoic acid (**56**) and aldehyde **57**.

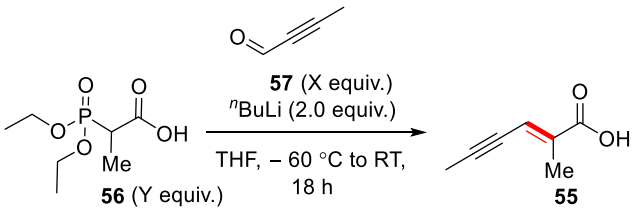

Entry	Y (equiv.)	X (equiv.)	Scale (g)	% Yield
1	1.0	1.2	1.0	34
2	1.0	1.2	2.0	23
3	1.0	3.6	1.5	63

[a] *E*:*Z* ratio of 90:10 determined by ^{1}H NMR from the crude reaction mixture.

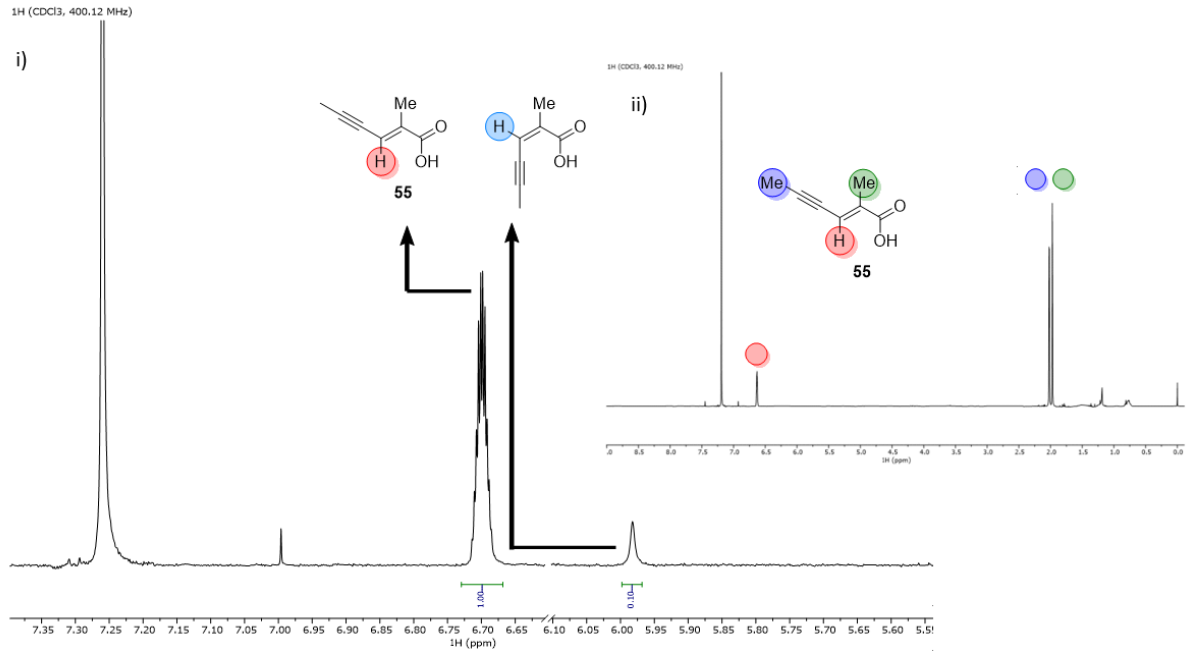

Figure 3.13. Annotated NMR spectra of the HWE reaction and acid **55**: (i) ^{1}H NMR spectrum of the crude reaction mixture (Table 3.6, entry 3, *E*/*Z* ratio: 90:10); (ii) ^{1}H NMR spectrum of acid **55** after purification.

3.6. Reductive Desulfonylation of chiral alcohols 7a & 7b.

Several feasible methods were initially assessed for the reductive desulfonylation of 4-tosyl oxazoles **7a** and **7b** (Table 3.7). Although removal of the tosyl group using metal amalgams would be considered rather harsh and detrimental for polyfunctional scaffolds similar to **7**, surprisingly sonicating fragment **7a** in THF/EtOH with Na (Hg) amalgam (Table 3.7, entry 6), gave the fragile chiral alcohol **6a**.[44] EDC-mediated Steglich esterification of the crude alcohol **6a** with acid **55** furnished the stable diyne **4** in 70 % yield over two steps and set the stage for the envisioned endgame one-pot ACM/RCAM event (Scheme 3.17). With this promising result, construction of the bisalkyne building block **5** seemed to be just a matter of two routine operations, that were, reductive cleavage of the tosyl group followed by coupling with commercial acid **61**.

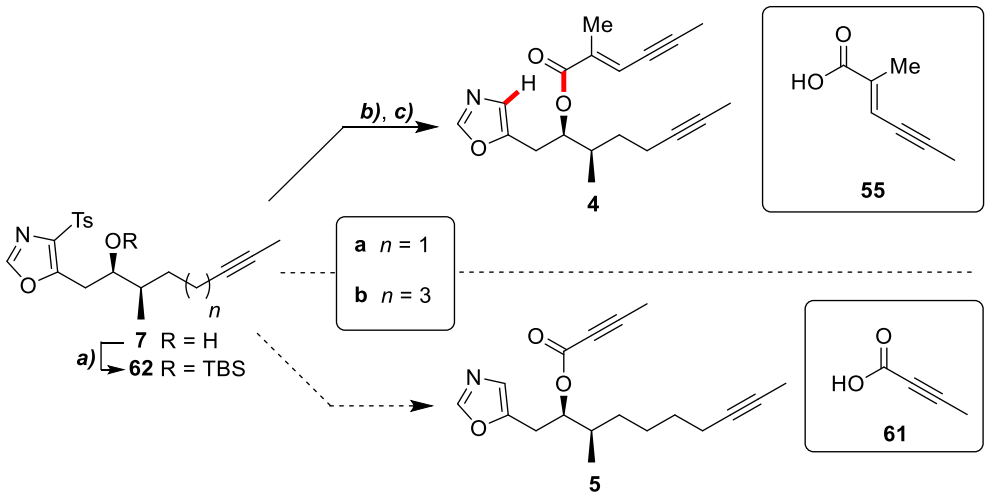

Scheme 3.17. Synthesis of bisalkyne building blocks and bisalkyne cyclic dimers: *(a)* TBSOTf, 2,6-lutidine, CH_2Cl_2, 0 °C → RT, overnight, (**63**, 73 %); *(b)* Na/Hg (10 mol % Na), Na_2HPO_4, THF/EtOH (1:1); *(c)* EDC·HCl, acid **55**, DMAP (10 mol%), CH_2Cl_2, 0 °C → RT, overnight, 70 % over two steps (**4**).

Attempted reductive removal of the *p*-tosyl group in alcohol **7b** under a variety of experimental conditions was met with failure (Table 3.7). More specifically, sonication of fragment **7b** or TBS ether **62** in THF/EtOH with Na (Hg) amalgam (2.0 - 10.0 equiv., 10 mol% Na) either failed completely or decomposed the precious material virtually instantaneously (Table 3.7, entries 2-6). Even the use of SmI_2 with DMPU, reported to be a particularly mild alternative to Na (Hg) amalgam, only led to the recovery of starting material (Table 3.11, entry 7).[44-46] This unexpected difference in behaviour between these closely related fragments (**7a**&**7b**), made the ynoate-yne one-pot ACM/RCAM strategy not feasible and enforced an adjustment in the final synthesis blueprint.

Table 3.7. Screening for reductive desulfonylation conditions.

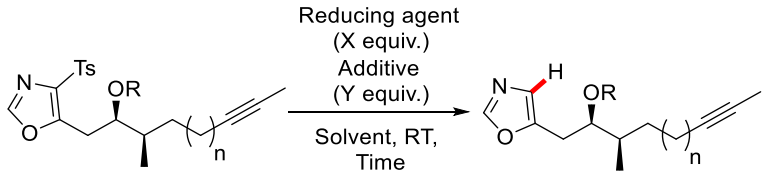

7a *n* = 1, R = H
7b *n* = 3, R = H
62 *n* = 3, R = TBS

6a
6b
63

Entry	Reducing Agent	X (equiv.)	Additive	Y (equiv.)	Solvent	Time (h)	% Relative Conversion (GCMS)		
							7a	**7b**	**61**
1	Al (Hg)	10.0	Na_2HPO_4	4.0	EtOH/THF	4	NR	NR	NR
2	Na (Hg)	2.0	Na_2HPO_4	4.0	EtOH/THF	4	traces	NR	NR
3	Na (Hg)	4.0	Na_2HPO_4	4.0	EtOH/THF	4	10	NR	NR
4	Na (Hg)	6.0	Na_2HPO_4	4.0	EtOH/THF	4	35	*decomp.*	NR
5	Na (Hg)	8.0	Na_2HPO_4	4.0	EtOH/THF	4	60	*decomp.*	NR
6	Na (Hg)	10.0	Na_2HPO_4	4.0	EtOH/THF	4	100	*decomp.*	NR
7	SmI_2	8.0	DMPU	10.0	MeOH	24	NR	NR	NR

3.7. Endgame (Part 1): One-pot Alkyne Cross Metathesis-Ring-Closing Metathesis (ACM/RCAM).

For the investigation of the one-pot ACM/RCAM reaction, the two latest generation molybdenum alkylidynes (**Mo^{E}** and **Mo^{D}**) endowed with the privileged tripodal silanolate ligand framework were recruited.[47,48] These exhibit the same catalytic activity and selectivity as seen in the parent silanolate-substituted molybdenum alkylidyne **Mo^{B}** but show a significantly superior functional group tolerance (Table 3.8).

Table 3.8. Optimisation of the one-pot ACM/RCAM of bisalkyne **4.**

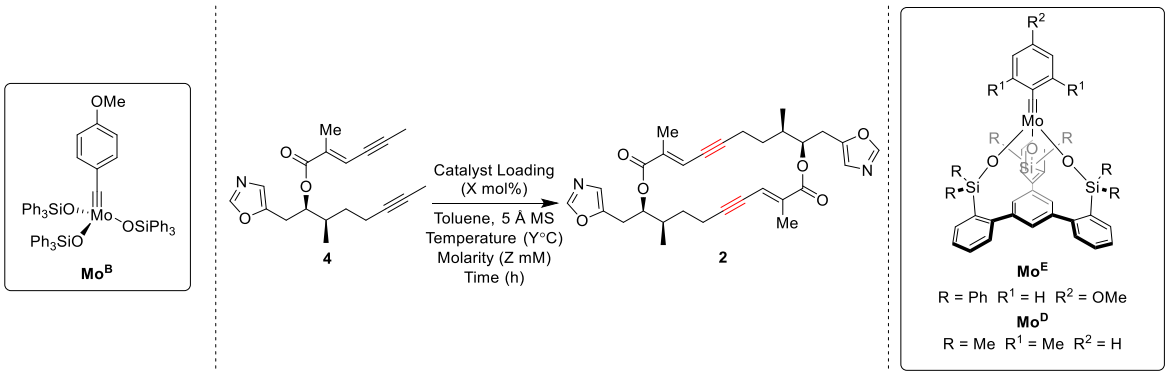

Entry	Time (h)	X (mol%)	Y (°C)	Z (mM)	% Yield
1	2	10 [a]	60	50	53
2	2	20 [a]	60	50	55
3	**1**	**20** [a]	**60**	**30**	**74**
4	1	30 [a]	60	30	71
5	3	30 [a]	60	15	71
6	18	20 [b]	80	30	50

[a] Complex **Mo^{E}**. [b] Complex **Mo^{D}**.

Following on from prior work in the Hulme group, this study of the one-pot ACM/RCAM reaction commenced by treating bisalkyne **4** with the newly developed catalyst **Mo^{E}** (10 mol%) at ambient temperature in the presence of molecular sieves (5 Å) to scavenge the released 2-butyne. Following the reaction by reverse-phase LC-MS (λ=254 nm), initially indicated no conversion even after four hours at room temperature. Later, however, it was found that full conversion to cyclobis(enyne) **2** was attained within two hours, just by raising the temperature to 60 °C (Table 3.8, entry 1). Although routine chromatography sufficed to obtain cross-dimer **2** in analytically pure form in 53 % yield, no linear dimers, higher-order oligomers nor the corresponding homo-dimeric isomer were discernible by LC-MS.

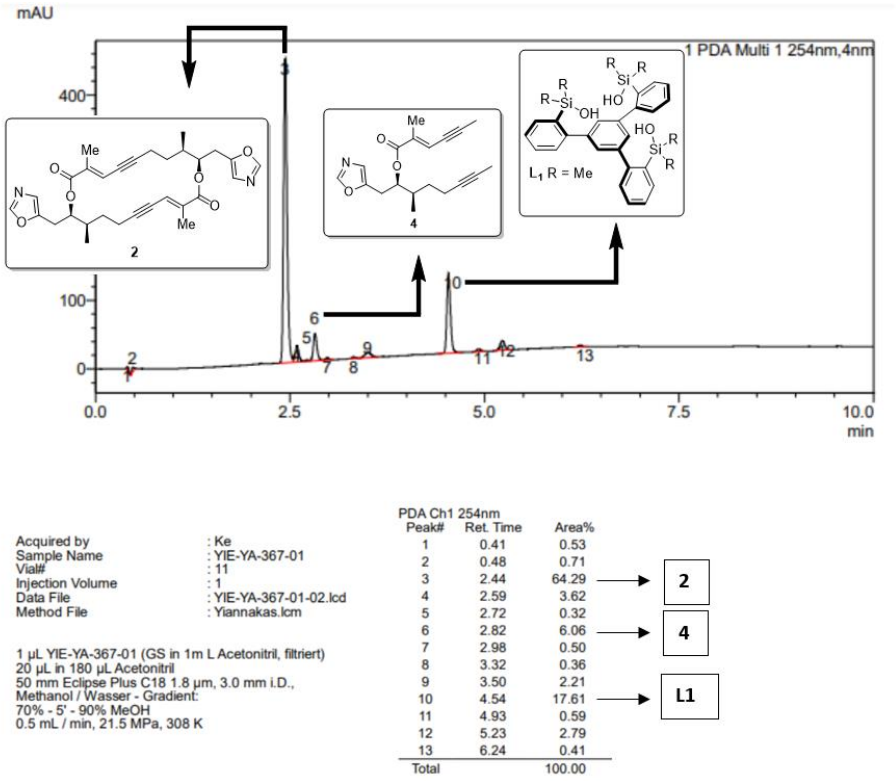

Figure 3.14. Annotated UHPLC trace of a crude aliquot of one-pot ACM/RCAM reaction of bisalkyne **4** after 50 mins at 60 °C, 20 mol% **Mo^{E}**, Reaction Molarity (mM): 30 (Reaction monitored @ 254 nm)**.**

Nonetheless, it was suspected that the likely cause of the reduced isolated yield might be a competing concentration-induced polymerisation. Gratifyingly, however, this undesired pathway, which seems to be independent of the initial catalyst loading (Table 3.8, entry 2) and can be suppressed by performing the reaction at a higher dilution. Treatment of a solution of monomer **4** in toluene (30 mM) with complex **Mo^{E}** (20 mol%) was found to be the most optimal reaction conditions (Table 3.8, entry 3) (Figure 3.14). Performing the reaction with a higher catalyst loading, only made the product isolation more tedious, and further dilution only led to prolonged reaction time without any significant improvement in the isolated yield. The remarkable functional group tolerance and robustness of catalyst **Mo^{E}**, which activates even the most demanding triple bonds under mild conditions even at the presence of two basic heterocycles, is best appreciated when compared to its predecessor molybdenum alkylidyne **Mo^{D}**. Although both complexes (**Mo$^{D\text{-}E}$**) represent the latest generation of alkyne metathesis catalysts, when complex **Mo^{D}** was used, full-conversion to the desired one-pot ACM/RCAM product **2** was only achieved after overnight heating at 80 °C. This outcome perhaps highlights that the rigidified backbone and significantly more sterically encumbered coordination sphere of the podand complex **Mo^{D}**, is responsible for its reduced reactivity, particularly for less-reactive electron-deficient substrates such as 1,3-enynes.[47] In addition, the isolation of cross-dimer **2** in the latter case, proved to be rather challenging due to co-elution of ligand debris and the desired

product (Table 3.8, entry 6). With a crucial segment of the endgame strategy confirmed, the final key steps of this total synthesis program were investigated.

3.8. Endgame (Part 2): Stereoselective Reduction

Inspired by the recent formal synthesis of (+) *Aspicilin* (**66**), [18] it was envisioned that *trans*-reduction of the newly formed internal alkynes to the required *E*-configured disubstituted alkenes in the final 20-membered macrocyclic framework, would be readily achieved via a bis*(trans*-hydrostannation-protodestannation) sequence (Scheme 3.18).

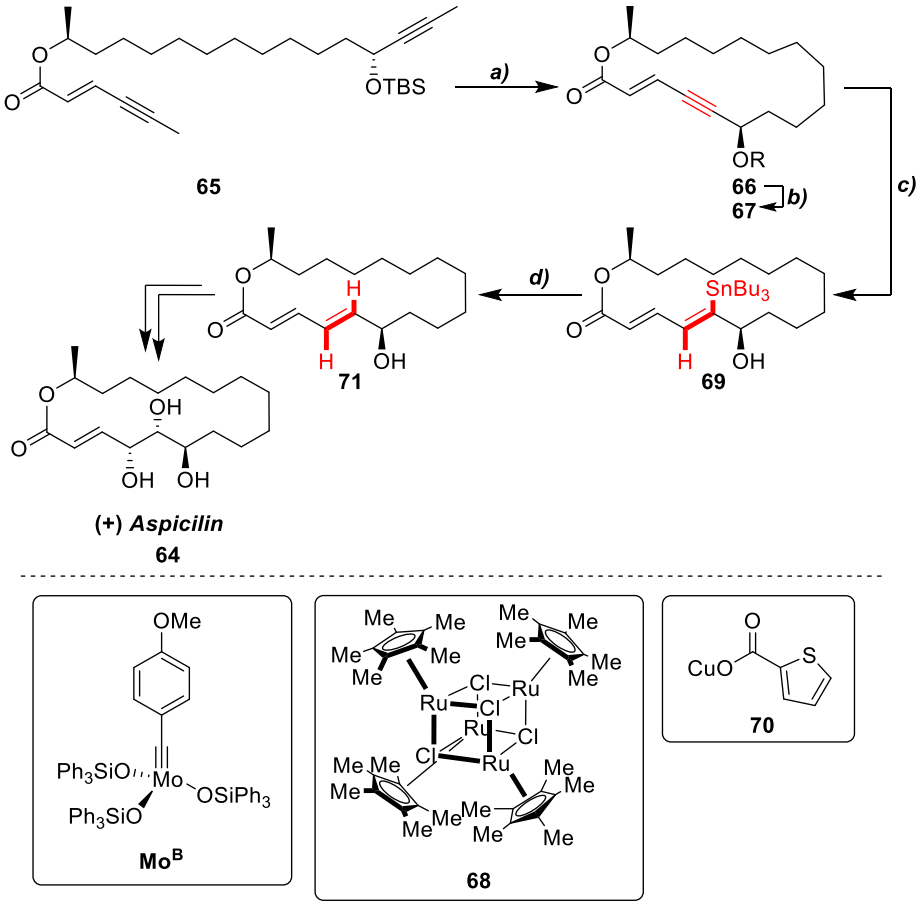

Scheme 3.18. Formal synthesis of (+) *Aspicillin* via a hydroxyl-assisted *trans*-reduction of 1,3-enynes.[18] *Reagents and conditions*: *(a)* complex **Mo^B** (10 mol%), 5 Å MS, toluene, 110 °C, (**66**, 91 %); *(b)* TBAF, THF, 0 °C → RT, 2 h, (**67**, 85 %); *(c)* tetrameric complex **68** (2 mol%), Bu_3SnH, RT, 2 h, (**71**, 66 %); *(d)* CuTC (**70**), DMF, RT, (**71**, 83 %).

However, these envisaged key steps, bore substantial risk since electron-rich arenes and 1,3-enynes often act as catalyst poisons in *trans*-hydrostannation.[49,50] This stems from the ability of these substrates to bind to the [Cp*Ru] fragment through kinetically stable η^4- or η^6-complexation, thus bringing the *trans*-hydrometallation across the alkyne triple bond to a halt as depicted by **A** and **B** (Figure 3.15 (i)). Furthermore, as illustrated by **C** and **D**, provided that the acetylene derivate bears a

protic substituent (such as an -OH group) (Scheme 3.15 (ii)), this can facilitate both the productive binding of the [Cp*Ru] and the selective proximal delivery of the $SnBu_3$ unit across the triple bond (Figure 3.15 (iii)).[49,50]

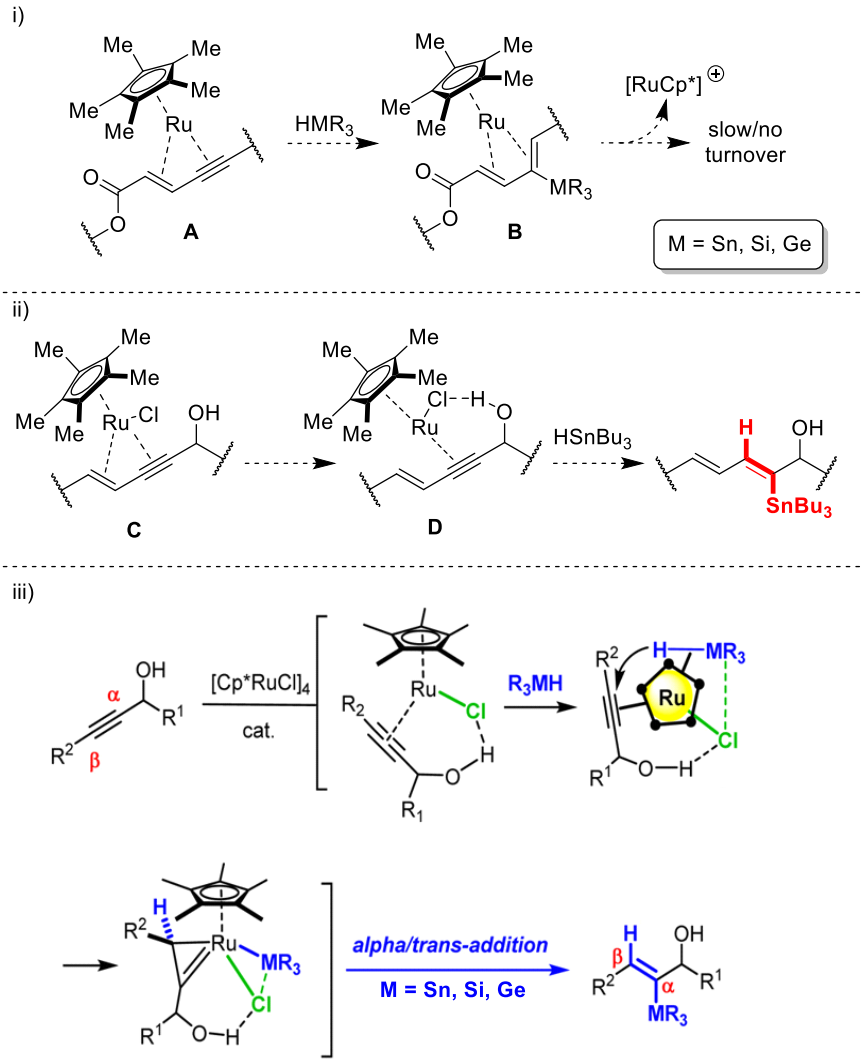

Figure 3.15. Ru-catalysed *trans*-hydrometallation: (i) Unproductive 1,3-enyne hydrometallation; (ii) Protic-group-assisted trans-hydrostannation; (iii) Postulated Mechanism of Ruthenium-Catalysed *trans*-Hydrometallation (Adapted with permission from ref. 49 @ copyright 2021 American Chemical Society).

While the presence of the electron-poor 1,3-oxazole fragments in the periphery of the macrocycle did not pose a particular concern, capitalising on the intrinsic functionality of the scaffold, it was proposed that the methyl substituents on the two dienoate units could potentially mitigate the deleterious tight binding of the [Cp*Ru] fragment (Figure 3.15 (i)). Due to the lack of any protic functionality in macrocycle **2**, a double hydrostannation reaction would lead to a statistical mixture of bis(proximally) (**72**), bis(distally) (**73**) and proximally/distally (**74**) stannylated products respectively, all of which derive from a double trans-hydrometallation process and can effectively deliver the desired *E*-configured alkenes upon protodestannation (Figure 3.16).

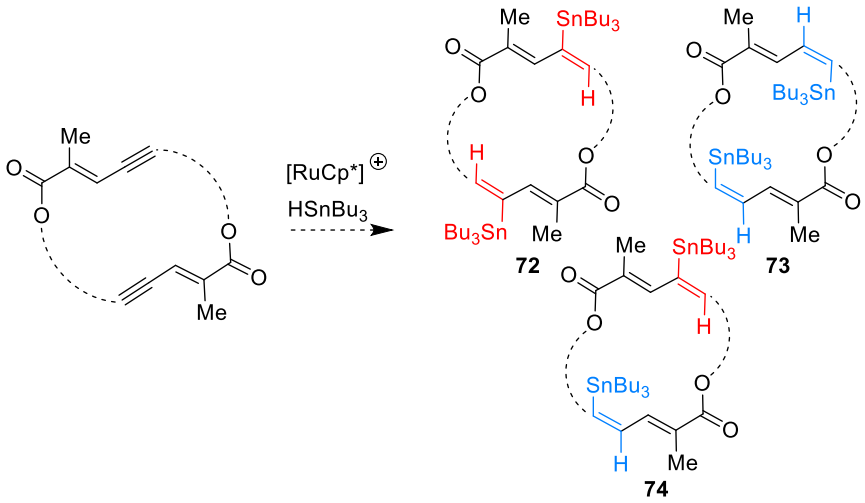

Figure 3.16. Envisaged [RuCp*]-catalysed bishydrostannation step of the endgame.[51]

Hydrostannation of bis(enyne) **2** with the aid of tetrameric ruthenium catalyst **68,** proceeded smoothly at room temperature to deliver an ill-defined mixture of stannylated products, which was not separable by flash chromatography on ordinary silica or reverse-phase HPLC. Therefore, the overall *trans*-selectivity of the double hydrostannation reaction was only determined after protodestannation has taken place. Despite the ease of forging and subsequent elaboration of the macrocyclic core, protodestannation of the alkenylstannanes was particularly taxing. Treatment of the mixture of stannanes with TFA, TBAF or even *in situ* generated HF, in both coordinating and non-coordinating media led to decomposition or no reaction (Table 3.9, entries 1-5).

Given that most synthetic methodologies available for the downstream functionalisation of alkenylstannanes rely on the reversible transmetalation of tin to copper in polar solvents, productive protodestannation must proceed via the formation of an organocuprate species in the presence of a tin scavenger and an exogeneous proton source. Subjecting a mixture of the crude stannanes and copper(I) phosphinate (**75**) to wet DMF or a solution of TFA in anhydrous DMF (Table 3.9, entries 6-7), only gave insoluble polymeric material, possibly formed through an intermolecular copper-catalysed oxidative homocoupling at the C-Sn bonds.[52] Conversely, successful protodestannation was achieved, when a solution of the alkenylstannates in DMF-MeOH (10:1), was treated with copper(I) salt (**75**) at ambient temperature (Table 3.9, entry 8). This reaction furnished the (5*E*,21*E*) isomer (**1**) as the major stereoisomer (crude HPLC ratio 78:22, (**1**): *E*/*Z* isomers, Figure 3.17), with the analytical and spectroscopic data of the purified, matching those of the natural product (Table 3.10, Figure 3.18).[1,51]

Table 3.9. Conditions attempted for the bishydrostannation – protodestannylation sequence.

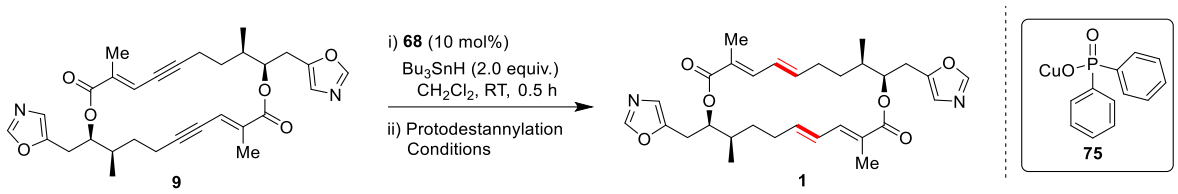

[a] Reaction performed at RT for 2 h. [b] Reaction performed at RT for 24 h. [c] Reaction performed with wet DMF with at RT for 2 h. [d] After preparative HPLC.

Entry	Reagents	Solvent	Comment	% Yield
1	TBAF (4.0 equiv.)	THF[a]	NR	0
2	TFA (4.0 equiv.)	CH_2Cl_2[a]	*decomp.*	0
3	TFA (4.0 equiv.)	THF[a]	*decomp.*	0
4	TFA (4.0 equiv.)	DMF[a]	*decomp.*	0
5	TFA (5.0 equiv.) TBAF (5.0 equiv.)	THF[b]	*decomp.*	0
6	$CuPO_2Ph_2$ (4.0 equiv.) TFA (4.0 equiv.)	DMF[a]	Polymerisation	0
7	$CuPO_2Ph_2$ (2.0 equiv.)	DMF[c]	Polymerisation	0[c]
8	$CuPO_2Ph_2$ (2.0 equiv.)	DMF/MeOH (10:1)[a,d]	Full conversion	30

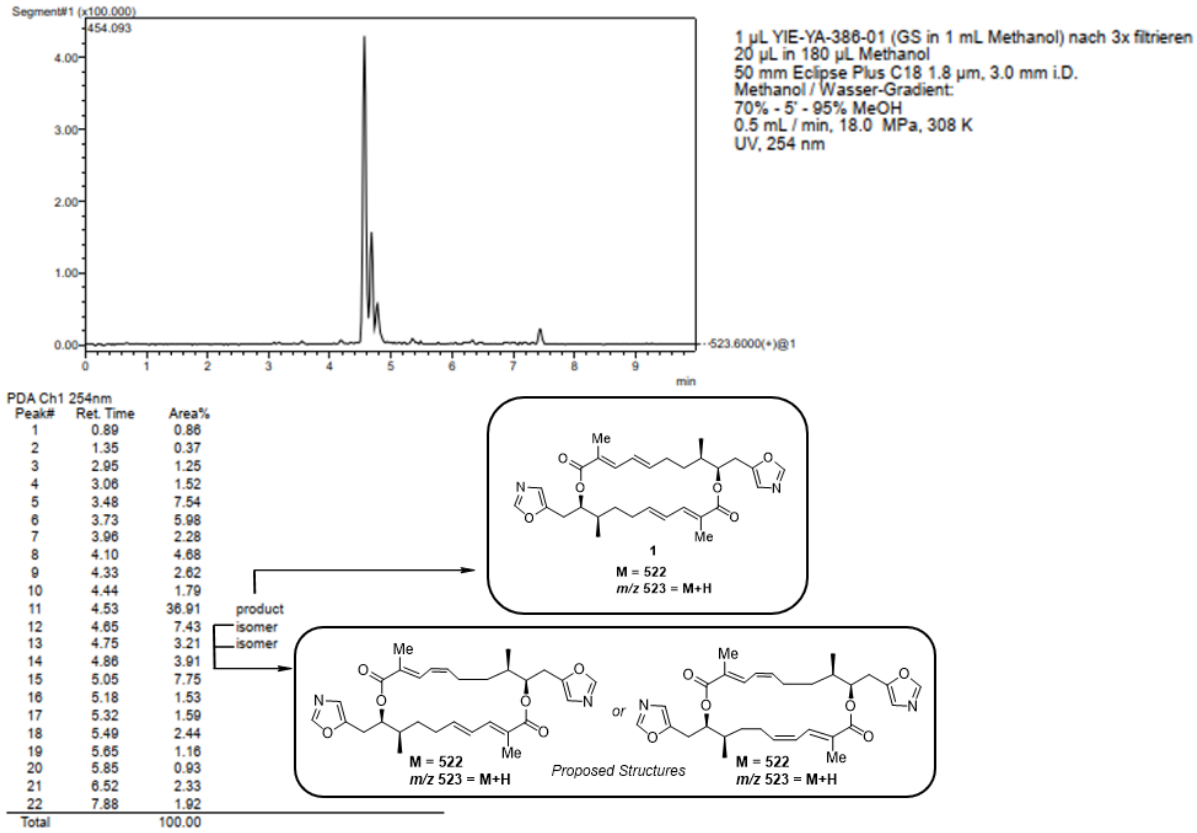

Figure 3.17. Annoted HPLC trace of a crude aliquot from the bis(*trans*-reduction) of macrocycle **2** via a bis(*trans*-hydrostannylation) – bis(protodestannylation) sequence (78:22; ratio of (5*E*,21*E*) stereoisomer (**1**) to other isomers).

Table 3.10. Comparison of NMR data between the isolated and synthetic *samroiyotmycin A* (*Peaks were mis-assigned in the original isolation paper).[1,51]

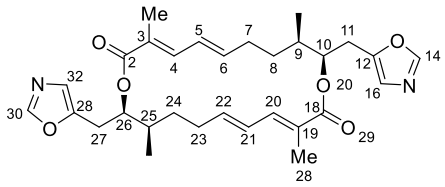

	Isolated	Synthetic		Isolated	synthetic
$[\alpha]_D$	+80.9°, c = 0.09	+76.7°, c = 0.08			
Atom	^{1}H NMR δ (ppm, *J* [Hz])		Atom	^{13}C NMR δ [ppm]	
2/18	-	-	2/18	167.7	167.7
3/19	-	-	3/19	125.8	125.7
4/20	6.94 (d, 11.2)	6.94 (dq, 11.3, 1.3)	4/20	138.4	138.3
5/21	6.27 (dd, 14.3, 11.2)	6.27 (dddd, 15.2, 11.3, 1.8, 0.8)	5/21	127.7	127.6
6/22	5.93 – 6.00 (m)	5.97 (ddd, 14.9, 9.0, 5.8)	6/22	142.6	142.5
7/23*	1.76 (d, 12.9) and 2.08 (dd, 12.9, 11.3)	2.08 (tdd, 14.2, 9.2, 1.8) and 2.46 – 2.39 (m)	7/23	29.9	29.9
8/24*	1.36- 1.45 (m) and 2.38 - 2.48 (m)	1.38 - 1.44 (m) and 2.38 -2.46 (m)	8/24	30.1	30.0
9/25	1.78 – 1.88 (m)	1.73 – 1.85 (m)	9/25	34.4	34.4
10/26	5.09 (quin, 3.8)	5.09 (ddd, 9.10, 4.2, 3.0)	10/26	75.3	75.3
11/27	2.83 – 2.95 (m)	2.87 (ddd, 15.5, 9.1, 1.0) and 2.92 (ddd, 15.6, 4.2, 1.0)	11/27	25.1	25.0
12/28	-	-	12/28	149.7	149.6
14/30	7.78 (s)	7.76 (s)	14/30	150.6	150.5
16/32	6.80 (s)	6.80 (s)	16/32	123.8	123.7
3-CH_3	1.88 (s)	1.82 (s)	3-CH_3	12.9	12.8
9-CH_3	0.98 (d, 7.1)	0.99 (d, 7.1)	9-CH_3	16.5	16.5
25-CH_3	0.98 (d, 7.0)	0.99 (d, 7.1)	25-CH_3	16.5	16.5
19-CH_3	1.88 (s)	1.82 (s)	19-CH_3	12.9	12.8

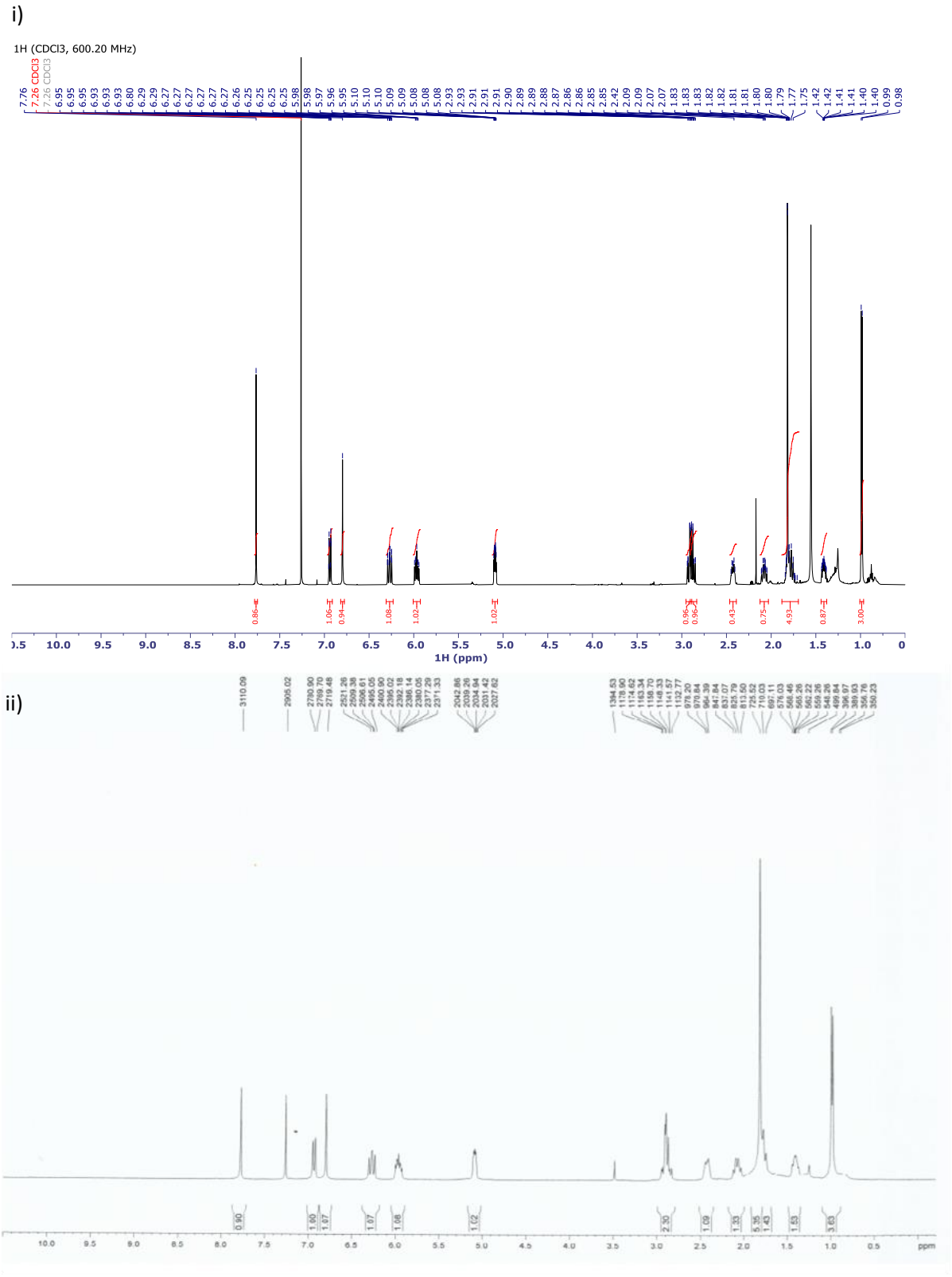

Figure 3.18. ^{1}H-NMR spectra of isolated and synthetic samroiyotmycin A (**1**): (i) ^{1}H-NMR spectrum ($CDCl_3$, 600 MHz) of synthetic samroiyotmycin A;[51] (ii) ^{1}H-NMR spectrum ($CDCl_3$, 500 MHz) of isolated samroiyotmycin A[1] (Adapted with permission from ref. 1 @ copyright 2021 Elsevier).

3.9. Conclusion

The work presented in this chapter aims to showcase through the total synthesis of samroiyotmycin A that combining one-pot ACM/RCAM reactions with a ruthenium catalysed alkyne *trans*-reduction, provides an effective way to construct macrocyclic scaffolds from simple precursors, whilst offering full control over the stereochemistry of the product diene. Capitalising on the inherent selectivity of electron-poor enynes and ynoates for cross-coupling over homodimerisation, forging of the macrocyclic ring in macrodiolide **1** was envisaged via a late-stage a one-pot ACM/RCAM reaction across either the *E*-configured disubstituted alkene (C(5)C(6)/C(21)C(22)) or the *E*-enoate sites (C(3) C(4)/C(19)C(20)).[17-18, 21,23] For this ambitious synthetic proposal, it was anticipated that the one-pot ACM/RCAM reactions of bifunctional building blocks **4** and **5** catalysed by the latest generation of alkyne metathesis catalysts **Mo^{D}** and **Mo^{E}** would give the best selectivity for the desired Head-to-Tail (H-to-T) cyclic dimers **2** and **3**. For the final elaboration of these to macrodiolide **1**, two approaches were considered (Scheme 3.1(i)). Another key element of this metathesis-based strategy (**1**) was the simultaneous installation of the 1,3-oxazole unit and setting of the stereochemistry at C10 (Scheme 3.1 (ii)) via an unprecedented-Schöllkopf-type condensation on β-lactones **8** with anionic TosMIC.

The Schöllkopf-type condensation of β-lactones was initially investigated. Since the investigation of this novel synthetic approach required the generation of α-methyl aldehydes **9 a**/**b**, preliminary studies focused on the diastereoselective alkylation of *N*-acylated oxazolidinones. After successful installation of the alkyl branch on *N*-acyl derivatives **16** and **39** via diastereoselective methylation on multi-gram scale (Table 3.2; Scheme 3.9), these were elaborated using standard methods to the fragile aldehyde **9a**/**b** (Schemes 3.4 & 3.9). It was considered that the asymmetric ketene-aldehyde cycloaddition catalysed by cinchona alkaloid catalyst **23** would serve as an excellent way for assembling β-lactones **8** in a doubly diastereoselective fashion. This reaction smoothly converted the crude aldehydes **9a**/**b** to the β-lactones **8a**/**b** with high diastereocontrol (> 95:5 *dr*). Moreover, the excellent diastereocontrol observed over the newly formed stereocentres at C(10) in these reactions provided the first set of examples of a doubly diastereoselective intermolecular NCAL reaction, whereby the catalyst control overrides the inherent influence of an α-methyl chiral centre on an aldehyde. Subsequent Schöllkopf-type condensation on the crude thermally unstable lactones **8a**/**b** with TosMIC, gave alcohols **7a** and **7b** in overall 35-43 % yield over a five-step telescoping sequence from *N*-acyl derivatives **16** and **39** respectively (96:4-99:1 *dr*). The configuration of the C(10)OH was confirmed by Mosher ester analysis (Figures 3.3 & 3.5).

To streamline the synthetic sequence developed for chiral alcohols **7a** and **7b,** it seemed more advantageous to use Myers auxiliaries, since the pseudoephedrine amides generated after

diastereoselective alkylation can be directly converted to the enantioenriched α-methyl aldehydes **9a**/**b**.[39-40] Diastereoselective electrophilic functionalisation of commercially available pseudoephedrine propionate derivative **49** using alkyl iodides **13b** and **36**, on multi-gram scale afforded amides **50a** and **53a** in 79-98 % yield and excellent diastereomeric purity (> 98:2 *dr*) (Tables 3.4-3.5). Reductive cleavage of the auxiliary at low-temperature with *in situ* generated $LiAl(OEt)_3H$ gave aldehydes **9a**/**b**, which were then subjected crude to cyclocondensation catalysed by *O*-TMS quinine **23** to afford again β-lactones **8a**/**b** (> 95:5 *dr*). Immediate, condensation of the crude lactones **8a**/**b** with anionic TosMIC provided chiral alcohols **7a**/**b** in good yield and high diastereomeric purity (97:3 *dr*) on multi-gram scale over a three-step telescoping sequence from pseudoephedrine amides **50a** and **53a** in 52-53 % yield with high diastereoselectivity (>95:5 *dr* by NMR). The diastereomeric purity determined by NMR spectroscopy for both alcohols **7a** and **7b** prepared via the above three-step sequence was corroborated by a comprehensive analytic HPLC screen using a range of chiral stationary phases (Appendices 5&6).

In the original synthetic plan, access to bisalkyne building blocks **4** and **5** was anticipated via esterification of secondary alcohols **6**, upon desulfonylation of 5-substituted 4-tosyloxazoles **7**. With the two advanced intermediates **7a**/**b** in hand, a screen of known conditions for the reductive desulfonylation of 4-tosyl oxazoles **7a** and **7b** was examined. Surprisingly sonicating fragment **7a** in THF/EtOH with Na (Hg) amalgam (Table 3.7, entry 6), furnished the fragile chiral alcohol **6a**, which proved prone to degradation on silica.[44] Esterification of the crude alcohol **6a** with acid **55** delivered the stable diyne **4** in 70 % yield over two steps (Scheme 3.17). In contrast, reductive desulfonylation of alcohol **7b** was particularly taxing. More specifically, sonication of fragment **7b** or TBS ether **62** in THF/EtOH with Na (Hg) amalgam either decomposed the precious material virtually instantaneously or failed. Furthermore, utilising SmI_2 with DMPU; a milder reducing agent, only led to the recovery of starting material.[44-46] Regrettably, this unexpected behaviour of fragment **7b** rendered the ynoate-yne one-pot ACM/RCAM strategy not feasible.

For the study of the key one-pot ACM/RCAM reaction, the two molybdenum alkylidynes **Mo^D**/**Mo^E** investigated in Chapter 2 were used.[47,48] Stirring a solution of monomer **4** in toluene (30 mM) with complex **Mo^E** (20 mol%) at 60 °C for 1 h delivered selectively the desired H-to-T dimer **2** as indicated by UHPLC (Figure 3.14). Routine chromatography on silica sufficed to obtained bis(enyne) **2** in analytically pure form in 74 % yield. Conversely, when the sterically encumbered complex **Mo^D** was used as the catalyst, overnight heating at 80 °C was necessary to attain full conversion to the bis(enyne) **4**. Moreover, dimer **4** was only isolated in 50 % yield in this case due to coelution of catalyst debris with this desired product. These results are in line with the proposed hypothesis that the inherent propensity of electron poor enynes for cross-coupling over homodimerisation would facilitate the selective formation H-to-T cyclic dimer **2**.[18,21,23]

During the double *trans*-hydrostannation reaction of bis(enyne) **4**, taking advantage of the intrinsic functionality in the macrocycle (**2**), the detrimental binding of the [RuCp*] was prevented by the steric block of the methyl substituents at the enoate units of the scaffold. On the other hand, the lack of any steering functionality in the vicinity of the alkyne sites (C(5)-C(6)/C(21)-C(22)) in macrocycle **4**, furnished an inseparable mixture of bis(proximally) (**72**), bis(distally) (**73**) and proximally/distally (**74**) stannylated products.[49,50] Elaboration of this mixture to samroiyotmycin A proved challenging. After an extensive screen of different protodestannation conditions, it was found that productive protodestannation was only achieved, when a solution of the alkenylstannates (**72**-**74**) in DMF-MeOH (10:1), was treated with copper (I) salt (**75**) at ambient temperature. The protodestannation protocol developed is thought to operate via an initial transmetallation of tin to copper, followed rapidly protodemetallation of the resulting bisorganocuprate species in the reaction medium to deliver the desired product.

In summary, over the course of this work the first total synthesis of the anti-malarial macrodiolide samroiyotmycin A (**1**) was achieved in 9 linear steps with an overall yield of 6 %. The convergent and scalable route developed, encompasses an initial diastereoselective alkylation of commercial propionate amide **49**, followed by a three-step telescoped sequence whereby the concurrent introduction of the 1,3-oxazole unit and setting of the stereochemistry at C(10)OH proceeds via an unprecedented Schöllkopf-type condensation of diastereomerically pure β-lactones. Construction of the macrocyclic core was enabled via a late stage enyne-yne one-pot ACM/RCAM reaction with the aid of "canopy catalysts" **Mo^D** and **Mo^E**. A final *trans*-hydrostannation-protodestannation sequence allowed the elaboration of bis(enyne) **4** to samroiyotmycin A. In conceptual terms, the results outlined above clearly demonstrate that the one-pot ACM/RCAM reactions when combined with ruthenium catalysed alkyne *trans*-reduction can be an versatile manifold for the assembly of complex macrocyclic scaffolds.

3.10. References

[1] A. Dramae, S. Nithithanasilp, W. Choowong, P. Rachtawee, S. Prabpai, P. Kongsaeree, P. Pittayakhajonwut, *Tetrahedron* **2013**, *69*, 8205 – 8208.

[2] K. Ralston, H. Ramstadius, R. Brewster, H. Niblock, A. Hulme, *Angew. Chem. Int. Ed.* **2015**, *54*, 7086 – 7090; *Angew. Chem.* **2015**, *127*, 7192 – 7196.

[3] S. Rummelt, A. Fürstner, *Angew. Chem. Int. Ed.* **2014**, *53*, 3626 –3630; *Angew. Chem.* **2014**, *126*, 3700 – 3704.

[4] N. Huwyler, K. Radkowski, S. Rummelt, A. Fürstner, *Eur. J.Org. Chem.* **2017**, *23* 12412 – 12419.

[5] X. Mo, A. Letort, D. Ros¸ca, K. Higashida, A. Fürstner, *Chem.Eur. J.* **2018**, *24*, 9667 – 9674.

[6] X. Xia, Z. Lao, P. Toy, *Synlett* **2019**, *30*, 1100 – 1104.

[7] A. Kirschning, P. Toy, S. Ceylan, H. Law, *Synthesis* **2016**, *49*, 145 –150.

[8] C. Raji Reddy, N. Narsimha Rao, *Tetrahedron Lett.* **2009**, *50*, 2478 – 2480.

[9] Y. Xing, G. O_Doherty, *Org. Lett.* **2009**, *11*, 1107 – 1110.

[10] E. Årstad, A. Barrett, B. Hopkins, J. Köbberling, Org. Lett. 2002, *4*, 1975 – 1977.

[11] G. Strunz, H. Finlay, *Can. J. Chem.* **1996**, *74*, 419 – 432.

[12] D. Ma, X. Lu, *Tetrahedron* **1990**, *46*, 3189 – 3198.

[13] D. Ma, X. Lu, *Tetrahedron Lett.* **1989**, *30*, 843 – 844.

[14] Y. Zhang, D. Yang, Z. Weng, *Tetrahedron* **2017**, *73*, 3853 – 3859.

[15] V. Morozova, J. Skotnitzki, K. Moriya, K. Karaghiosoff, P.Knochel, *Angew. Chem. Int. Ed.* **2018**, 57, 5516 – 5519; *Angew.Chem.* **2018**, *130*, 5614 – 5617.

[16] R. Rossi, F. Bellina, L. Mannina, *Tetrahedron Lett.* **1998**, *39*,3017 – 3020.

[17] B. Wölfl, G. Mata, A. Fürstner, *Chem. Eur. J.* **2019**, *25*, 255 – 259.

[18] S. Schaubach, K. Michigami, A. Fürstner, *Synthesis* **2017**, *49*, 202 – 208.

[19] S. Schaubach, K. Gebauer, F. Ungeheuer, L. Hoffmeister, M. K. Ilg, C. Wirtz, A. Fürstner, *Chem. Eur. J.* **2016**, *22*, 8494 – 8507.

[20] R. Lhermet, A. Fürstner, *Chem. Eur. J.* **2014**, *20*, 13188 – 13193.

[21] P. Persich, J. Llaveria, R. Lhermet, T. de Haro, R. Stade, A. Kondoh, A. Fürstner, *Chem. Eur. J.* **2013**, *19*, 13047 – 13058.

[22] J. Heppekausen, R. Stade, A. Kondoh, G. Seidel, R. Goddard, A. Fürstner, *Chem. Eur. J.* **2012**, *18*, 10281 – 10299.

[23] J. Heppekausen, R. Stade, R. Goddard, A. Fürstner, *J. Am.Chem. Soc.* **2010**, *132*, 11045 – 11057.

[24] A. Fürstner, O. Guth, A. Rumbo, G. Seidel, *J. Am. Chem. Soc.* **1999**, *121*, 11108 – 11113.

[25] A. Gollner, K.H. Altmann, J. Gertsch, J. Mulzer, *Chem. Eur. J.* **2009**, *15*, 5979 – 5997.

[26] I. Paterson, A. N. Hulme, *Tetrahedron Lett.* **1990**, *31*, 7513 – 7516.

[27] C. Zhu, X. Shen, S. G. Nelson, *J. Am. Chem. Soc.* **2004**, *126*, 5352 – 5353.

[28] N. Rajeev, T. R. Swaroop, S. M. Anil, K. R. Kiran, K. S. Rangappa, M. P. Sadashiva, *J. Chem. Sci.* **2018**, *130*, 150.

[29] S. P. J. M. van Nispen, C. Mensink, A. M. van Leusen, *Tetrahedron Lett.* **1980**, *21*, 3723 – 3726.

[30] A. M. van Leusen, B. E. Hoogenboom, H. Siderius, *Tetrahedron Lett.* **1972**, *13*, 2369 – 2372.

[31] R. Row, H. Shih, A. Alexander, R. Mehl, J. Prescher, *J. Am. Chem. Soc.* **2017**, *139*, 7370-7375.

[32] K. Moriyama, T. Sugiue, C. Nishinohara, H. Togo, *J. Org. Chem.* **2015**, *80*, 9132-9140.

[33] G. Boije af Gennäs, V. Talman, O. Aitio, E. Ekokoski, M. Finel, R. Tuominen, J. Yli-Kauhaluoma, *J. Med. Chem.* **2009**, *52*, 3969-3981.

[34] M. J. Gaunt, C. C. C. Johansson, *Chem. Rev.* **2007**, *107*, 5596–5605.

[35] S. Schulthoff, J. Y. Hamilton, M.Heinrich, Y. Kwon, C.Wirtz, A. Fürstner, *Angew. Chem. Int. Ed.* **2021**, 60, 446 – 454; *Angew. Chem.* **2021**, *133*, 450 – 458.

[36] K. Morris, K. Arendt, S. Oh, D. Romo, *Org. Lett.* **2010**, *12*, 3764 –3767.

[37] *(a)* J. A. Dale, H. S. Mosher, *J. Am. Chem. Soc.* **1973**, *95*, 512–519.; *(b)* I. Ohtani, T. Kusumi, M. O. Ishitsuka, H. Kakisawa, *Tetrahedron Lett.* **1989**, *30*, 3147–3150.; *(c)* I. Ohtani, T. Kusumi, Y. Kashman, H. Kakisawa, *J. Org. Chem.* **1991**, *56*, 1296–1298.; *(d)* I. Ohtani, T. Kusumi, Y. Kashman, H. Kakisawa, *J. Am. Chem. Soc.* **1991**, *113*, 4092–4096.

[38] *(a)* T. R. Hoye, C. S. Jeffrey, F. Shao, *Nat. Protoc.* **2007**, *2*, 2451–2458.; *(b)* S. Berger, S. Braun, *200 and More NMR Experiments: A Practical Course*, Wiley-VCH, Weinheim, **2004**.

[39] A. Myers, B. Yang, H. Chen, J. Gleason, *J. Am. Chem. Soc.* **1994**, *116*, 9361 – 9362.

[40] A. Myers, B. Yang, H. Chen, L. McKinstry, D. Kopecky, J. Gleason, *J. Am. Chem. Soc.* **1997**, *119*, 6496 – 6511.

[41] S. Saito, S. Nakagawa, T. Koizumi, K. Hirayama, Y. Yamamoto*, J. Org. Chem.* **1999**, *64*, 3975-3978.

[42] P. Coutrot, A. Ghribi, *Synthesis* **1986**, *1986*, 661-664.

[43] A. Ahlers, T. de Haro, B. Gabor, A. Fürstner, *Angew. Chem. Int. Ed.* **2015**, *55*, 1406-1411.

[44] M. Addie, R. Taylor, *J. Chem. Soc. Perkin Trans. 1* **2000**, 527 –531.

[45] G. E. Keck, K. A. Savin, M. Weglarz, *J. Org. Chem.* **1995**, 60, 3194 – 3204.

[46] S. Nanda, *Tetrahedron Lett.* **2005**, *46*, 3661 – 3663.

[47] J. Hillenbrand, M. Leutzsch, A. Fürstner, *Angew. Chem. Int. Ed.* **2019**, 58, 15690 – 15696; *Angew. Chem.* **2019**, *131*, 15837 – 15843.

[48] J. Hillenbrand, M. Leutzsch, E. Yiannakas, C. Gordon, C. Wille, N. Nöthling, C. Copéret, A. Fürstner, *J. Am. Chem. Soc.* **2020**, *142*, 11279 – 11294.

[49] D. Rosca, K. Radkowski, L. Wölf, M. Wagh, R. Goddard, W.Thiel, A. Fürstner, *J. Am. Chem. Soc.* **2017**, *139*, 2443 – 2455.

[50] A. Fürstner, *J. Am. Chem. Soc.* **2019**, *141*, 11 – 24.

[51] E. Yiannakas, M. Grimes, J. Whitelegge, A. Fürstner, A. N. Hulme, *Angew. Chem. Int. Ed.* **2021**, *60*, 18504-18508.

[52] H. Yoshida, Y. Takemoto, K. Takaki, *Chem. Comm.* **2015**, *51*, 6297-6300.

Chapter 4: Future Work

4.1. Overview:

Macrocyclic architectures have attracted considerable attention over the past two decades because of their unique properties and promising potential in a wide range of applications in drug discovery, material science and supramolecular chemistry. The rotationally restricted three-dimensional configuration of these large molecular entities offers unique conformational preorganization, which in turn accounts for their distinct properties. Access to these is usually achieved through ring-closing metathesis, macrolactamization, macroaldolisation and macrolactonisation. Although these "classic" protocols suffer from entropic penalties and undesired oligomerisation; they still remain the synthetic strategies of choice. Recent approaches for accessing complex macrocyclic frameworks from simple precursors are metathesis-based cyclooligomerisations, which are referred as one-pot alkyne/alkene cross-metathesis/ ring-closing metathesis reactions (CM/RCM or ACM/RCAM) in this thesis. A comprehensive review presented in Chapter 1, clearly demonstrates that one-pot domino metathesis reactions provide a set of versatile manifolds for the efficient construction of elaborate macrocyclic scaffolds of variable ring sizes with a wide range of properties and applications.

Despite their promising potential the practical utility of alkyne metathesis-based synthetic methodologies such as the one-pot ACM/RCAM reactions highlighted in this thesis are limited by the availability of well-defined and user-friendly alkyne metathesis catalysts due to their sensitivity to moisture and air. The advent of triphenylsilanolate ligand-based molybdenum alkylidyne catalysts over the recent years has certainly revolutionised the field of alkyne metathesis. However, the reaction of substrates containing functional groups such as primary alcohols and sterically encumbered substrates, remains a long-standing problem for catalysts of this type. Several groups have attempted to overcome this issue by developing molybdenum complexes bearing multidentate ligand frameworks; however, these failed to deliver well-defined complexes. In Chapter 2, the development of a new alkyne metathesis catalyst was investigated. The new catalyst also termed "canopy catalyst" exhibits unique catalytic activity derived from its tripodal silanolate ligand framework. The remarkable catalytic performance of this well-defined monomeric complex is exemplified by its broad functional group tolerance to a wide range of functional groups. Even though this catalyst is both sensitive to air and moisture, it works well in the presence of unprotected primary alcohols and even tolerates substrates having multiple donor sites, including basic nitrogen and heterocycles. In addition, the ease of assembling key intermediates in the total synthesis of marine natural products such as amphidinolide F and nor-cembranoid sinulariadiolide further highlight the unrivalled catalytic activity of this complex. Although the scope of alkyne metathesis does not yet rival that of alkene metathesis, the future of this transformation holds great promise. Since the discovery of this reaction, alkyne metathesis catalysts

have evolved from poorly defined *in situ* generated catalytic systems to well-defined complexes. Over the course of this transformative period, alkyne metathesis catalysts have acquired increased activity but also gained outstanding functional group tolerance, which rivals even that of the most active alkene metathesis catalysts currently available; the work presented in Chapter 2 of this thesis stands witness to this fact.

The first ever example of an alkyne-metathesis-based homodimerization approach applied in the synthesis of natural products, discussed in Chapter 1 was reported by the Hulme group in 2015.[1] Assembly of the 30-membered macrocyclic core of cytotoxic disorazole C_1, was achieved through a highly convergent, modular strategy featuring a late stage-cyclization through the one-pot ACM/RCAM reaction of a bis(enyne) precursor, followed by Lindar-reduction. To broaden the scope of this alkyne-metathesis-based synthetic methodology, the total synthesis of the anti-malarial samroiyotmycin A was investigated in Chapter 3 via an enyne-yne one-pot ACM/RCAM reaction in conjunction with a ruthenium catalysed alkyne *trans*-reduction. The first total synthesis of the C_2-symmetric anti-malarial macrodiolide samroiyotmycin A was successfully achieved in an overall 6 % yield via a 9-step linear sequence The convergent and scalable synthetic route developed for this macrocyclic scaffold proceeds via an initial diastereoselective alkylation of commercial pseudoephedrine propionate derivative, followed by a three-step telescoped sequence encompassing an unprecedented Schöllkopf-type condensation on diastereomerically pure β-lactones which allows for the simultaneous introduction of the 1,3-oxazole unit and setting of the stereochemistry at C(10)OH. Assembly of the highly decorated macrocyclic core of this macrodiolide was possible by a late stage enyne-yne one-pot ACM/RCAM reaction utilising the latest generation of "canopy catalysts" discussed in Chapter 2.[2,3] Elaboration of the resulting bis(enyne) intermediate to samroiyotmycin A was enabled by a delicate ruthenium catalysed bis(*trans*-hydrostannation-protodestannation) sequence. The results presented in Chapter 3 clearly show that b one-pot ACM/RCAM reactions when used in conjunction with stereoselective partial reduction modalities furnish a flexible and reliable tool for the construction of complex molecular architectures.

4.2. Future applications:

4.2.1 One-pot AM-RCAM Reactions - Modelling Studies and Mechanistic Analysis

Previously, Hulme and co-workers examined the one-pot ACM/RCAM reactions of a bisenyne building block en route to the total synthesis of bislactone **1a**.[1] Moreover, during the total synthesis campaign towards samroiyotmycin A, an enyne-yne one-pot ACM/RCAM reaction was investigated.

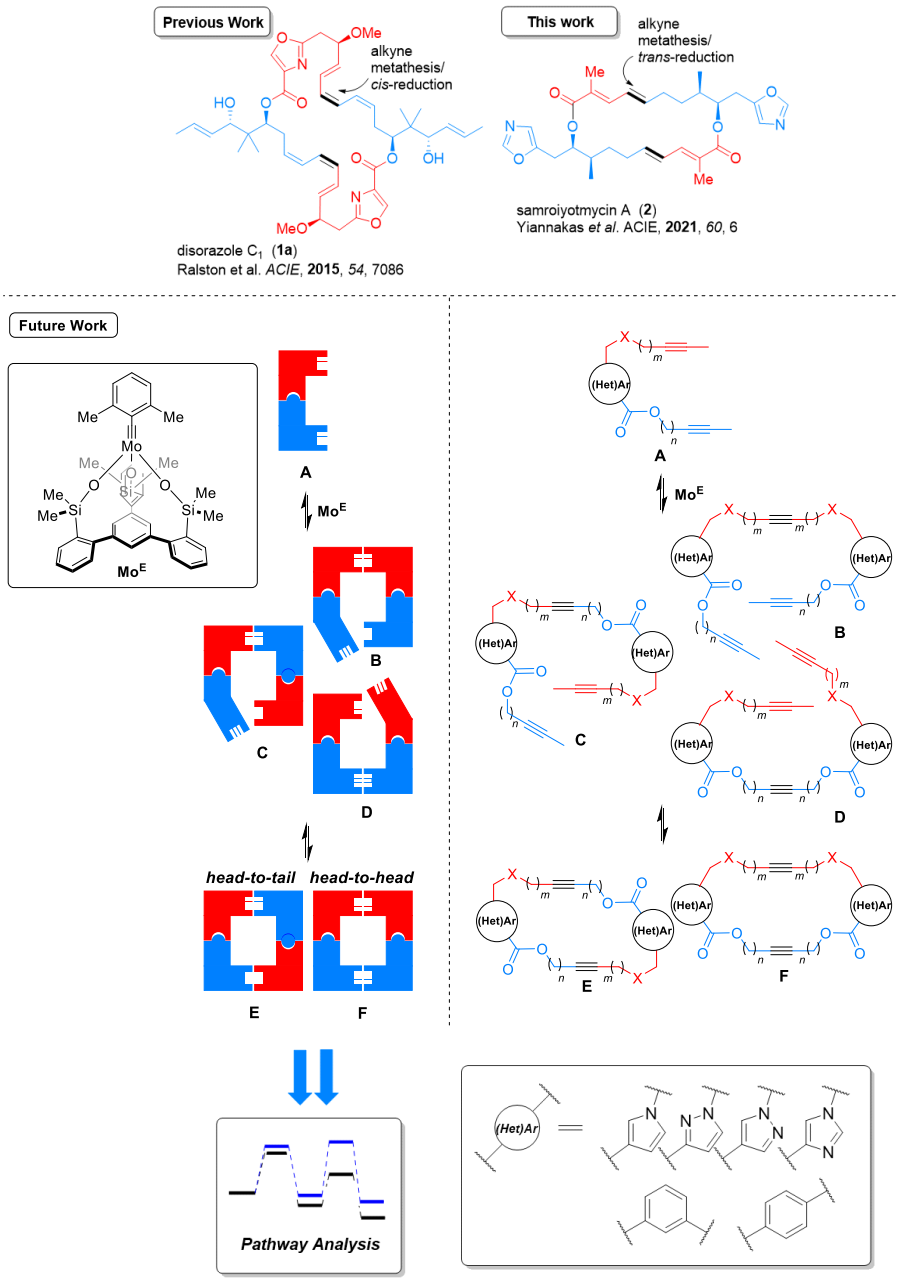

Figure 4.1 Previous, Current and Future work on one-pot ACM/RCAM reactions.

Considering the recent alkyne metathesis-based synthesis of cyclophanes reported by Tamm and co-worker,[2] future work should examine the one-pot ACM/RCAM reactions of diyne building blocks (**A**) by combining *in silico* design with experimental validation. Rigorous *in silico* studies would show which bisalkyne monomers have the highest predicted dimer/monomer (**B**-**D**) and head-to-tail (**E**)/head-to-head (**F**) alkyne metathesis coupling ratios, while chemical synthesis empowered by catalyst **Mo^{E}** would enable access to structurally novel macrocyclic scaffolds which are not covered by the patent literature. This study will form a solid basis for future pathway analysis studies aiming to elucidate the mechanistic intricacies of one-pot ACM/RCAM reactions (Figure 4.1).

‘

4.2.2 Heteroaryl disorazole C_1 Analogues

Capitalising on the unique catalytic activity and functional group tolerance of the newly developed catalyst (**Mo^{E}**) and given the success of the synthetic strategy reported in the synthesis of disorazole C_1 (**1a**), future work should seek to further explore the scope of one-pot ACM/RCAM reactions through the synthesis of heterocyclic analogues (**1b**-**d**) of the bislactone **1a** (Figure 4.2). This in turn would enable access to a new class of disorazoles with enhanced therapeutic potential. Rapid assembly of analogue libraries for biological testing could be achieved in a high-throughput combinatorial fashion utilising “canopy catalyst” **Mo^{E}**. Biological testing of these libraries of compounds on the basis of their anti-tubulin activity as well as cytotoxicity should provide a comprehensive and instructive view of the SARs in these family of natural products.

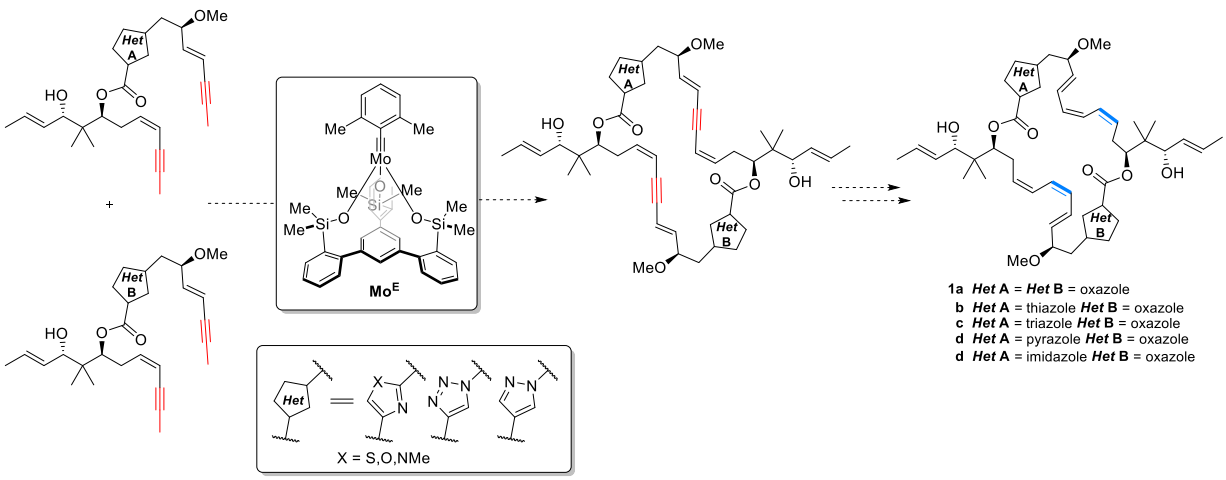

Figure 4.2. Proposed synthesis of mixed heterocyclic analogues of disorasole C_1 via one-pot ACM/RCAM reactions catalysed by complex **Mo^{E}**.

4.2.3. Diversification and Downstream Fuctionalisation: Proposed Syntheses of samroiyotmycin B, Dimethyl-and Oxo-analogues of samroiyotmycin A

As evidenced by the successful total synthesis of samroiyotmycin A (**2**) discussed in Chapter 3, combining one-pot ACM/RCAM reactions with contemporary hydrometallation chemistry provides an elegant and effective synthetic manifold for the construction of macrocyclic scaffolds.[3] The concise and scalable sequence reported for assembling this C_2-symmetric macrodiolide (**2**) should facilitate any future synthetic campaigns for exploring other members of this family but also the development of analogues with improved application profiles.

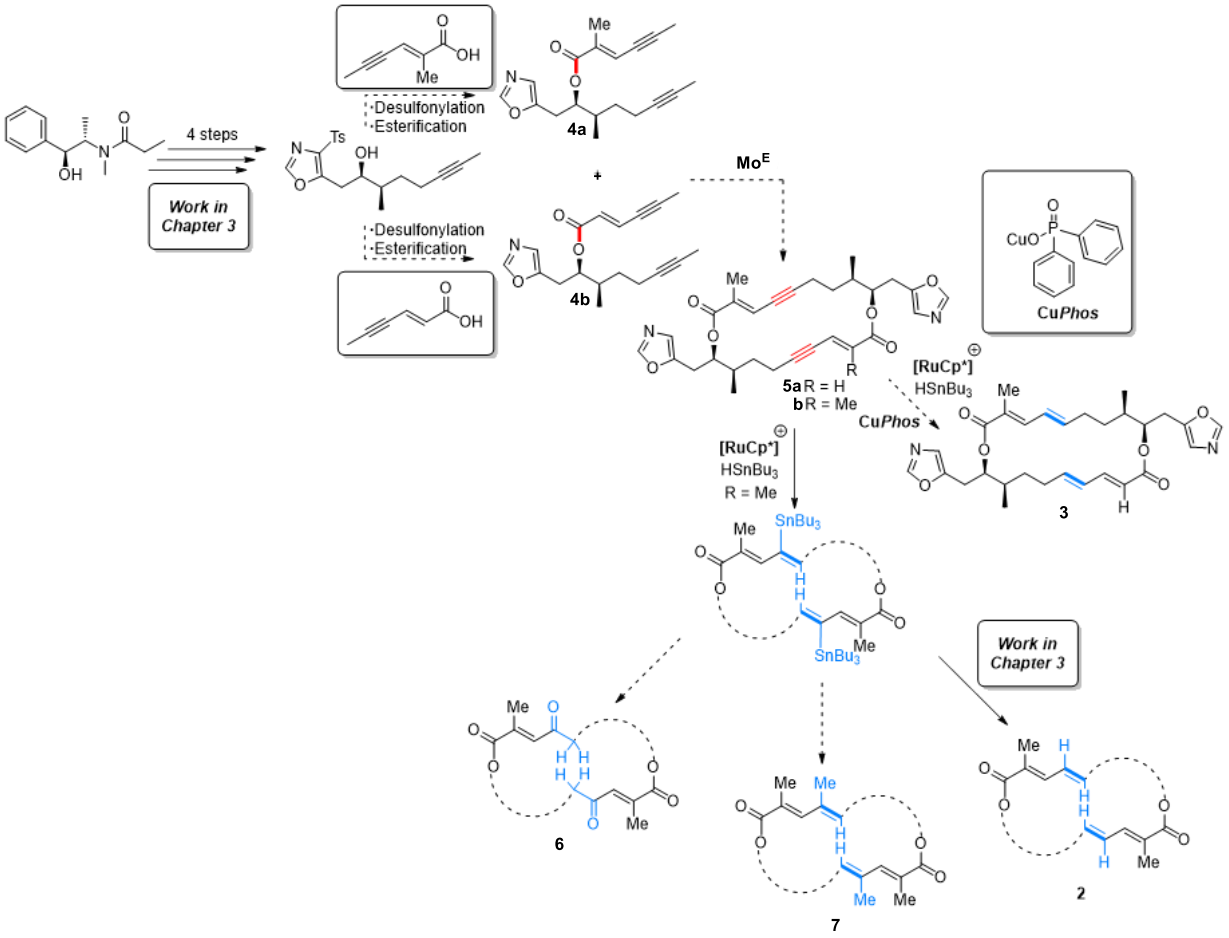

Figure 4.3. Proposed total synthesis of samroiyotmycin B (**3**) and samroiyotmycin A analogues (**6**-**7**).

By taking advantage of the propensity of the electron-poor enynes for cross-coupling over homo-metathesis, access to samroiyotmycin B (**3**) could be achieved via a novel alkyne-metathesis-based heterodimerization approach (Figure 4.3).[3,4] Minor adaptation of the robust sequence that provided building block **5a** should also enable the synthesis of bisalkyne **5b**. Forging of the macrocyclic core will be achieved via a late stage one-pot ACM/RCAM reaction between bisalkynes **5a** and **5b** utilising the "canopy catalyst" (**Mo**^{E}) developed. A final bis(*trans*-hydrostannation-protodestannation) should allow

the elaboration of bis(enyne) **5a** to samroiyotmycin B (**3**). In addition, contemporary hydrometallation chemistry should provide access to dimethyl- and oxo-analogues of samroiyotmycin A (**6**-**7**) by harnessing the reactivity of the alkyne units in macrocyclic bis(enyne) **5b**.[5-7]

4.3. References

[1] K. Ralston, H. Ramstadius, R. Brewster, H. Niblock, A. Hulme, *Angew. Chem. Int. Ed.* **2015**, *54*, 7086 – 7090; *Angew. Chem.* **2015**, *127*, 7192 – 7196.

[2] S. Beer, K. Brandhorst, J. Grunenberg, C. G. Hrib, P. G. Jones, M. Tamm, *Org. Lett.* **2008**, *10*, 981–984.

[3] E. Yiannakas, M. Grimes, J. Whitelegge, A. Fürstner, A. N. Hulme, *Angew. Chem. Int. Ed.* **2021**, *60*, 1− 6.

[4] *(a)* J. Heppekausen, R. Stade, R. Goddard, A. Fürstner, *J. Am. Chem. Soc.* **2010**, *132*, 11045–11057.; *(b)* S. Schaubach, K. Michigami, A. Fürstner, *Synthesis* **2017**, *49*, 202 – 208.; *(c)* P. Persich, J. Llaveria, R. Lhermet, T. de Haro, R. Stade, A. Kondoh, A. Fürstner, *Chem. Eur. J.* **2013**, *19*, 13047 – 13058.; *(d)* J. Heppekausen, R. Stade, R. Goddard, A. Fürstner, *J. Am.Chem. Soc.* **2010**, *132*, 11045 – 11057.

[5] P. Karier, F. Ungeheuer, A. Ahlers, F. Anderl, C. Wille, A. Fürstner, *Angew. Chem. Int. Ed.* **2019**, *58*, 248–253.

[6] H. Sommer, A. Fürstner, *Org. Lett.* **2016**, *18*, 3210–3213.

[7] H. Sommer, J. Y. Hamilton, A. Fürstner, *Angew. Chem. Int. Ed.* **2017**, *56*, 6161–6165.

Chapter 5: Experimental

5.1. General Experimental

Unless stated otherwise, all reactions were carried out under Ar in flame-dried glassware. The solvents used were purified by distillation over the drying agents indicated and were transferred under Ar: THF, Et_2O (Mg/anthracene), CH_2Cl_2, DMF (CaH_2), toluene (Na/K). Flash chromatography on silica gel (FC): Merck silica gel 60 (230–400 mesh).

NMR: Spectra were acquired on Bruker AvanceIII 300, 400, 500 MHz and an Avance Neo 600 MHz NMR spectrometers in the solvents indicated; chemical shifts (δ) are given in ppm relative to TMS, coupling constants (J) in Hz. The solvent signals were used as references and the chemical shifts converted to the TMS scale ($CDCl_3$: δ_C = 77.0 ppm; residual $CHCl_3$ in $CDCl_3$: δ_H = 7.26 ppm; CD_3OD: δ_C = 49.00 ppm, residual CD_2HOD in CD_3OD: δ_H = 3.31 ppm; $(CD_3)_2SO$: δ_C = 39.52 ppm, residual CD_2HSOCD_3 in $(CD_3)_2SO$: δ_H = 2.50 ppm). IR: Spectrum One (Perkin-Elmer) spectrometer, wavenumbers ($\tilde{\nu}$) in cm^{-1}. MS (EI): Finnigan MAT 8200 (70 eV), ESI-MS: ESQ3000 (Bruker), accurate mass determinations: Bruker APEX III FT-MS (7 T magnet) or Mat 95 XP (Finnigan). Elemental analysis: H. Kolbe, Mülheim/Ruhr. All commercially available compounds (Fluka, Lancaster, Aldrich, Fluorochem, Alfar Aeser, TCI, ChemPUR, Santa Cruz Biotechonology) were used as received, unless stated otherwise. The molecular sieves used in this investigation were dried for 24 h at 150°C (sand bath) under vacuum prior to use and were stored and transferred under argon atmosphere. Data acquired on the AVneo 600 MHz NMR spectrometer was acquired with a Bruker BBO CryoProbe, which significantly reduced the measurement time of most of the spectra, especially the 1D ^{13}C NMR data. Optical rotations were measured with a PerkinElmer Model 343 polarimeter. Melting points were recorded on a Buchi B-540 melting point apparatus. HPLC analysis was performed was conducted on a Shimadzu® Prominence HPLC/UFLC System instrument (System 1): pump LC-20AD, autosampler SIL-20AC, column oven CTO-20AC, diode array detector SPD-M20A, controller CBM-20A, ESI detector and software Labsolutions. Preparative LC was performed with a Shimadzu® LC-20A prominence system (System 2): pump LC-20AP, column oven CTO-20AC, diode array detector SPD-M20A, fraction collector FRC-10A, controller CBM-20A and software LC-solution.

Analytical HPLC methods:

- HPLC Method 1: System 1; Solvent – 98:2 *n*-Heptane (+0.1% v/v TFA)/*iso*-Propanol (+0.1% v/v TFA); Flow rate - 1 mL min^{-1}; Column - Chiralcel® OD-3, 150 mm, 3 µm, ∅ 4.6 mm at ambient temperature.
- HPLC Method 2: System 1; Solvent – 95:5 *n*-Heptane /*iso*-Propanol; Flow rate - 1 mL min^{-1}; Column - Chiralcel® OD-3, 150 mm, 3 µm, ∅ 4.6 mm at ambient temperature.

- HPLC Method 3: System 1; Solvent – 99:1 *n*-Heptane (+0.1% v/v TFA)/*iso*-Propanol (+0.1% v/v TFA); Flow rate - 1 mL min^{-1}; Column - Chiralcel® IC-3, 150 mm, 3 µm, ∅ 4.6 mm at ambient temperature.
- HPLC Method 4: System 1; Solvent – 95:5 *n*-Heptane/*iso*-Propanol; Flow rate - 1 mL min^{-1}; Column - Chiralcel® OD-3, 150 mm, 3 µm, ∅ 4.6 mm at ambient temperature.
- HPLC Method 5: System 1; Solvent – MeCN/H_2O; Flow rate - 1 mL min^{-1}; Column – Eclipse® Plus C_{18}, 50 mm, 1.8 µm, ∅ 4.6 mm at 35 °C.

Time (min)	A% MeCN	B% H_2O
0	30	70
5	50	50
10	50	50

- HPLC Method 6: System 1; Solvent – MeCN/H_2O; Flow rate – 0.5 mL min^{-1}; Column – Eclipse® Plus C_{18}, 50 mm, 1.8 µm, ∅ 3.0 mm at 35 °C.

Time (min)	A% MeCN	B% H_2O
0	30	70
5	50	50
10	50	50

- HPLC Method 7: System 1; Solvent – 95:5 *n*-Heptane/*iso*-Propanol; Flow rate - 1 mL min^{-1}; Column - Chiralpak® AS-3, 150 mm, 3 µm, ∅ 4.6 mm at ambient temperature.
- HPLC Methods 8a-f: System 1; Solvent – MeOH/H_2O; Flow rate – 1.0 mL min^{-1} at ambient temperature.

Time (min)	A% MeOH	B% H_2O
0	70	30
5	90	10
10	90	10

Method	Column
8a	Chiralpak® IB N-3, 150 mm, 3 µm, ∅ 4.6 mm
8b	Chiralpak® IA-3, 150 mm, 3 µm, ∅ 4.6 mm
8c	Chiralpak® IC-3, 150 mm, 3 µm, ∅ 4.6 mm
8d	YMC Chiral Art® Cellulose-SJ, 150 mm, 5 µm, ∅ 4.6 mm
8e	Chiralpak® AS-3R, 150 mm, 3 µm, ∅ 4.6 mm
8f	Chiracel® OZ-3R, 150 mm, 3 µm, ∅ 4.6 mm

- HPLC Methods 9a-f: System 1; Solvent – MeCN/H_2O; Flow rate – 1.0 mL min^{-1} at ambient temperature.

Time (min)	A% MeCN	B% H_2O
0	70	30
5	90	10
10	90	10

Method	Column
9a	Chiralpak® IB N-3, 150 mm, 3 µm, ∅ 4.6 mm
9b	Chiralpak® IA-3, 150 mm, 3 µm, ∅ 4.6 mm
9c	Chiralpak® IC-3, 150 mm, 3 µm, ∅ 4.6 mm
9d	YMC Chiral Art® Cellulose-SJ, 150 mm, 5 µm, ∅ 4.6 mm
9e	Chiralpak® AS-3R, 150 mm, 3 µm, ∅ 4.6 mm
9f	Chiracel® OZ-3R, 150 mm, 3 µm, ∅ 4.6 mm

- HPLC Method 10: System 1; Solvent – MeOH/H_2O; Flow rate – 0.5 mL min^{-1}; Column – Eclipse® Plus C_{18}, 50 mm, 1.8 µm, ∅ 3.0 mm at 35 °C.

Preparative HPLC methods:

- Preparative HPLC Method 1: System 2; Solvent – MeOH/H_2O; Flow rate – 0.5 mL min^{-1}; Column – Eclipse® Plus C_{18}, 50 mm, 1.8 µm, ∅ 3.0 mm at 35 °C.

Time (min)	A% MeOH	B% H_2O
0	70	30
5	90	10
10	90	10

5.2. Experimental Procedures for Chapter 2

5.2.1. Literature Known Compounds – Substrate Scope

Representative Procedure for Alkyne Homo-Metathesis:

Dodec-6-yne-1,12-diol (39)

6-Octyn-1-ol (32 mg, 23 µmol) was added to a stirred suspension of complex **35** (14 mg, 13 µmol, 5 mol%) or complex **65** (10 mg, 13 µmol, 5 mol%) and powdered molecular sieves 5Å (250 mg) in toluene (1.25 mL) at RT under argon atmosphere. The mixture was stirred for 18 h (complex **35**) or 2 h (complex **65**) at this temperature before it was filtered through a short pad of Celite® which was carefully rinsed with ethyl acetate (20 mL). The combined filtrates were evaporated under reduced pressure and the residue was purified by flash chromatography on silica to give the title compound as a colorless oil (16 mg, 69%; 18.0 mg, 73%). ^{1}H NMR (400 MHz, $CDCl_3$): δ = 3.64 – 3.54 (m, 4H), 2.14 – 2.03 (m, 4H), 1.58 – 1.33 (m, 12H). ^{13}C NMR (101 MHz, $CDCl_3$): δ = 80.2, 62.9, 32.3, 28.8, 24.9, 18.7. The analytical and spectroscopic data agree with those reported in the literature.[1]

Tetradec-7-yne-1,14-diol (40)

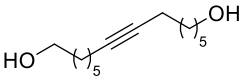

Prepared analogously to diol **39** with either complex **35** (14 mg, 13 µmol, 5 mol%) or complex **65** (10 mg, 13 µmol, 5 mol%) at 23°C; white waxy solid (18 mg, 66%; 20.1 mg, 71%). ^{1}H NMR (400 MHz, $CDCl_3$): δ = 3.58 (t, *J* = 6.6 Hz, 4H), 2.09 (m, 4H), 1.58 – 1.26 (m, 16 H); ^{13}C NMR (101 MHz, $CDCl_3$): δ = 80.2, 62.9, 32.7, 29.0, 28.6, 25.3, 18.7. The analytical and spectroscopic data are in agreement with those reported in the literature.[2]

Hexadec-8-yne-1,16-diol (41)

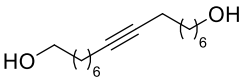

Prepared analogously to diol **39** with either complex **35** (14 mg, 13 µmol, 5 mol%) or complex **65** (10 mg, 13 µmol, 5 mol%) at 23°C; white waxy solid (25.0 mg, 83%; 28 mg, 88%). ^{1}H NMR (400 MHz, $CDCl_3$): δ = 3.57 (t, J = 6.6 Hz, 4H), 2.19 – 1.96 (m, 4H), 1.62 – 1.13 (m, 20H); ^{13}C NMR (101 MHz, $CDCl_3$): δ = 80.2, 63.0, 32.7, 29.0, 28.9, 28.8, 25.7, 18.7. The analytical and spectroscopic data agree with those reported in the literature.[3]

4-(Methoxymethoxy)cyclotetradec-2-yn-1-ol (46a)

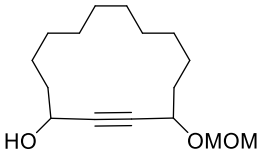

To a stirred suspension of 15-(methoxymethoxy)octadeca-2,16-diyn-4-ol **45a** (10 mg, 30 µmol) and powdered molecular sieves 5Å (200 mg) in toluene (13 mL) at 110°C was added a solution of complex **65** (2.2 mg, 3.0 µmol, 10 mol%) in toluene (2.0 mL) under argon atmosphere. The mixture was stirred for 2 h at this temperature before it was cooled to ambient temperatures and filtered through a short pad of Celite® and rinsed with ethyl acetate (20 mL). The filtrate was evaporated under reduced pressure and the residue was purified by flash chromatography on silica gel (hexanes/t-butyl methyl ether 8:2 to 7:3) to give the title compound as an oil (5 mg, 68%). 1H NMR (400 MHz, $CDCl_3$) δ = 4.92 (dd, *J* = 6.8, 5.0 Hz, 1H), 4.60 (dd, *J* = 6.8, 1.6 Hz, 1H), 4.55 – 4.35 (m, 2H), 3.38 (d, *J* = 0.7 Hz, 3H), 1.79 – 1.62 (m, 4H), 1.57 – 1.25 (m, 16H); ^{13}C NMR (101 MHz, $CDCl_3$) δ = 94.3, 87.1, 87.1, 84.1, 83.9, 66.3, 66.2, 63.1, 63.0, 55.8, 37.2, 37.1, 35.1, 35.0, 26.6, 26.5, 25.9, 25.9, 25.8, 25.8, 23.9, 23.8, 22.5, 22.4, 22.3, 22.3. The analytical and spectroscopic data agree with those reported in the literature.[2]

Compound 46b

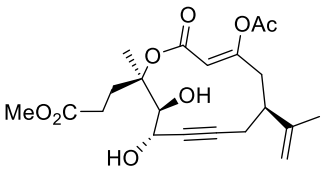

Diyne **45b** (50 mg, 83 µmol) was added to a stirred suspension of complex **35** (28 mg, 25 µmol, 30 mol%) and powdered molecular sieves 5Å (20 mg) in toluene (42 mL) at 110°C under Ar. The mixture was stirred for 45 min at this temperature before it was filtered through a short pad of Celite®, which was carefully rinsed with ethyl acetate (100 mL). The combined filtrates were evaporated under reduced pressure and the residue was purified by flash chromatography on silica (hexanes/ethyl acetate,3:1). Zinc dust (217 mg, 332 µmol) was added to a solution of this compound in HOAc/THF/H_2O (0.3 mL, 3:1:1). The suspension was vigorously stirred for 3 h at RT before all insoluble materials were filtered off through a pad of Celite. The filtrate was diluted with sat. aq. $NaHCO_3$ (10 mL), the aqueous phase was extracted with ethyl acetate (3 x 20 mL), the combined organic layers were washed with brine, dried over $MgSO_4$, filtered and concentrated. The residue was purified by flash chromatography on silica (hexanes/ethyl acetate, 2:1 to 1:1) to afford the title compound as a colourless oil (23 mg, 68% over two steps). ^{1}H NMR (400 MHz, $CDCl_3$): δ = 5.61 (s, 1H), 4.82 (q, *J* = 1.6 Hz, 1H), 4.78 – 4.73 (m, 1H), 4.58 (q, *J* = 2.3 Hz, 1H), 4.18 – 4.11 (m, 1H), 3.84 – 3.77 (m, 1H), 3.75 (d, *J* = 1.7 Hz, 1H), 3.72 (s, 3H), 3.42 (dd, *J* = 14.4, 5.0 Hz, 1H), 3.06 (d, *J* = 14.6 Hz, 1H), 2.74 – 2.69 (m, 1H), 2.67 (d, *J* = 1.9 Hz, 1H), 2.63 (d, *J* = 1.4 Hz, 1H), 2.48 (tt, *J* = 9.0, 4.6 Hz, 1H), 2.39 (dd, *J* = 4.1, 1.7 Hz, 1H), 2.34 (dd, *J* = 4.1, 1.7 Hz, 1H), 2.30 (dd, *J* = 8.8, 3.0 Hz, 1H), 2.11 (s, 3H), 2.05 (dd, *J* = 16.2, 8.4 Hz, 1H), 1.71 (s, 3H), 1.69 (t, *J* = 1.0 Hz, 3H). ^{13}C NMR (101 MHz, $CDCl_3$): δ = 172.9, 168.1, 165.1, 163.2, 144.9, 114.2, 112.9, 85.7, 83.2, 81.4, 71.6, 67.3, 52.4, 44.7, 42.6, 40.1, 33.6, 25.8, 24.0, 21.2, 20.1. The analytical and spectroscopic data agree with those reported in the literature.[4]

1,10-Bis(dodecylthio)dec-5-yne (48b)

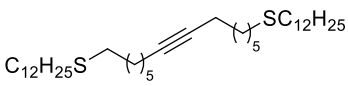

Prepared analogously to diol **39** with complex **35** (14 mg, 13 µmol, 5 mol%) at 23°C; white solid (64 mg, 95%). ^{1}H NMR (400 MHz, CD_2Cl_2): δ = 2.46 – 2.42 (m, 8H), 2.10 – 2.06 (m, 4H),1.54 – 1.46 (m, 16H), 1.30 – 1.18 (m, 32H), 0.83 – 0.79 (m, 6H). ^{13}C NMR (101 MHz, CD_2Cl_2): δ = 80.5, 32.6, 32.5, 32.5, 30.7, 30.4, 30.3, 30.2, 30.1, 30.0, 29.9, 29.9, 29.5, 29.4, 28.7, 23.3, 19.2, 14.5. The analytical and spectroscopic data agree with those reported in the literature.[2]

Dimethyl oct-4-ynedioate (48c)

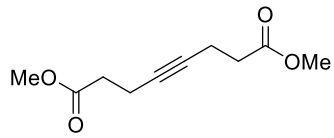

Prepared analogously to diol **39** with complex **35** (14 mg, 13 µmol, 5 mol%) at 23°C; colorless oil (28 mg, 72%). ^{1}H NMR (400 MHz, $CDCl_3$): δ = 3.63 (s, 6H), 2.56 – 2.27 (m, 8H). ^{13}C NMR (101 MHz, $CDCl_3$): δ = 171.5, 77.9, 50.7, 32.7, 13.7. The analytical and spectroscopic data agree with those reported in the literature.[5]

1,2-Bis(2-(methylthio)phenyl)ethyne (50a)

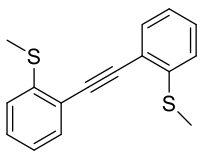

Prepared analogously to diol **39** with complex **35** (14 mg, 13 µmol, 5 mol%) or **65** (10 mg, 13 µmol, 5 mol%) at 90°C; white solid (15 mg, 47%; 31 mg, 92%). ^{1}H NMR (400 MHz, $CDCl_3$): δ = 7.57 – 7.53 (m, 2H), 7.33 – 7.28 (m, 2H), 7.21 – 7.18 (m, 2H), 7.14 – 7.10 (m, 2H), 2.52 (s, 6H). ^{13}C NMR (101 MHz, $CDCl_3$): δ = 141.6, 132.6, 128.9, 124.2, 121.4, 92.2, 77.2, 15.3. The analytical and spectroscopic data agree with those reported in the literature.[5]

1,2-Di(pyridin-3-yl)ethyne (50b)

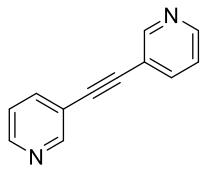

Prepared analogously to diol **39** with either complex **35** (14 mg, 13 µmol, 5 mol%) or complex **65** (10 mg, 13 µmol, 5 mol%) at 90°C; pale yellow solid (14 mg, 62%; 17 mg, 76%). ^{1}H NMR (400 MHz, $CDCl_3$): δ = 8.86 – 8.77 (m, 2H), 8.67 – 8.55 (m, 2H), 7.87 (dt, *J* = 6.1 Hz, 2H), 7.35 (m, 2H); ^{13}C NMR (101 MHz, $CDCl_3$): δ = 151.8, 148.6, 138.96, 123.3, 119.8, 89.2. The analytical and spectroscopic data agree with those reported in the literature.[5]

1,2-Di(thiophen-2-yl)ethyne (50c)

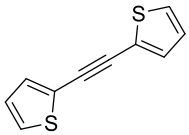

Prepared analogously to diol **39** with either complex **35** (14 mg, 13 µmol, 5 mol%) or complex 65 (10 mg, 13 µmol, 5 mol%) at 23°C; white solid (22 mg, 94%; 20 mg, 85%). ^{1}H NMR (400 MHz, $CDCl_3$): δ = 7.33 – 7.27 (m, 4H), 7.02 (dd, *J* = 5.2, 3.7 Hz, 2H); ^{13}C NMR (101 MHz, $CDCl_3$): δ = 132.1, 127.6, 127.1, 122.9, 86.2. The analytical and spectroscopic data agree with those reported in the literature.[5]

1,2-Bis(4-methoxyphenyl)ethyne (58)

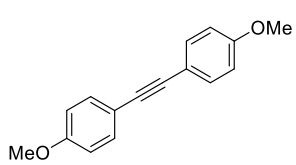

Prepared analogously to diol **39** with complex **35** (14 mg, 13 µmol, 5 mol%) at 23°C; white solid (27 mg, 92%). ^{1}H NMR (400 MHz, $CDCl_3$): δ = 7.45 (d, *J* = 8.8 Hz, 3H), 6.87 (d, *J* = 8.8 Hz, 4H), 3.82 (s, 6H); ^{13}C NMR (101 MHz, $CDCl_3$): δ = 159.5, 133.0, 115.9, 114.1, 88.1, 55.4. The analytical and spectroscopic data are in agree with those reported in the literature.[6]

(2*S*,17*S*)-octadec-9-yne-2,17-diol (76)

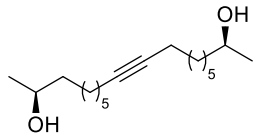

Prepared analogously to diol **39** with complex **65** (9.2 mg, 13 µmol, 5 mol%) at 23°C; pale yellow oil (33 mg, 94%). ^{1}H NMR (400 MHz, $CDCl_3$): δ = 3.83 – 3.70 (m, 2H), 2.18 – 2.08 (m, 4H), 1.66 (s, 2H), 1.53 – 1.24 (m, 20H), 1.17 (d, *J* = 6.2 Hz, 6H); ^{13}C NMR (101 MHz, $CDCl_3$): δ = 80.3, 68.2, 39.4, 29.3, 29.2, 28.9, 25.8, 23.6, 18.8. The analytical and spectroscopic data agree with those reported in the literature.[2]

Compound 79a

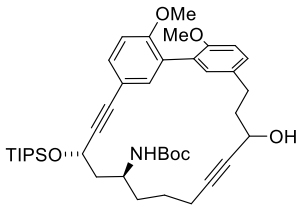

To a stirred suspension of diyne **78a** (17 mg, 23 µmol) and powdered molecular sieves 5Å (200 mg) in toluene (10 mL) at 80°C was added a solution of complex **65** (3.4 mg, 4.6 µmol, 20 mol%) in toluene (2.0 mL) under argon atmosphere. The mixture was stirred for 3 h at this temperature before it was cooled to ambient temperatures and filtered through a short pad of Celite® and rinsed with ethyl acetate (20 mL). The filtrate was evaporated under reduced pressure and the residue was purified by flash chromatography on silica gel (hexanes/*t*-butyl methyl ether 6:4 to 7:3) to give the title compound as an oil (11 mg, 66%). ^{1}H NMR (mixture of conformers 400 MHz, $CDCl_3$): δ = 7.39 – 7.27 (m, 2H), 7.21 – 7.13 (m, 1H), 7.07 (d, *J* = 2.3 Hz, 1H), 6.93 – 6.83 (m, 2H), 5.17 – 5.08 (m, 1H), 4.90 – 4.81 (m, 1H), 4.71 (ddd, *J* = 19.1, 10.5, 3.4 Hz, 1H), 4.51 (d, *J* = 8.2 Hz, 1H), 4.07 (ddd, *J* = 16.1, 9.9,

4.0 Hz, 1H), 3.93 (d, *J* = 20.6 Hz, 1H), 3.79 (dd, *J* = 14.1, 2.8 Hz, 7H), 3.65 (q, *J* = 2.0 Hz, 1H), 2.93 – 2.65 (m, 2H), 2.42 – 2.16 (m, 1H), 2.17 – 1.88 (m, 2H), 1.88 – 1.53 (m, 2H), 1.41 (d, *J* = 9.3 Hz, 9H), 1.22 – 0.95 (m, 18H). The analytical and spectroscopic data agree with those reported in the literature.[2]

Compound 79b

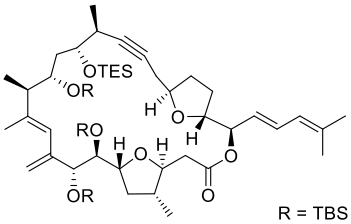

To a stirred suspension of diyne **78b** (8.1 mg, 7.3 µmol) and powdered molecular sieves 5Å (30 mg) in toluene (3.5 mL) at 80°C was added a solution of complex **65** (1.8 mg, 2.2 µmol, 30 mol%) in toluene (1.0 mL) under argon atmosphere. The mixture was stirred for 5 h at this temperature before it was filtered through a short pad of Celite® and rinsed with ethyl acetate (10 mL). The filtrate was evaporated under reduced pressure and the residue was purified by flash chromatography on silica gel (hexanes/*t*-butyl methyl ether 97:3 to 9:1) to give the title compound as an oil (6 mg, 81%). ^{1}H NMR (600 MHz, C_6D_6, broad signals due to slowly equilibrating conformers): δ = 6.65 (m, 1H), 6.48 (s, 1H), 5.77 (m, 1H), 5.48 (m, 1H), 5.43 (m, 1H), 5.10 (s, 1H), 5.04 (s, 1H), 4.26 (bs, 1H), 4.15 (s, 1H), 4.12 (m, 1H), 4.10 (m, 1H), 4.03 (m, 1H), 4.00 (m, 1H), 3.80 (d, *J* = 7 Hz, 1H), 3.58 (bs, 1H), 2.86 (m, 1H), 2.82 (m, 1H), 2.73 (bs, 1H), 2.57 (m, 1H), 2.53 (m, 1H), 2.40 (m, 1H), 2.33 (d, *J* = 13 Hz, 1H), 2.18 (m, 1H), 2.13 (m, 3H), 2.07 (m, 1H), 2.06 (m, 1H), 1.83 (m, 1H), 1.60 (m, 1H), 1.57 (m, 1H), 1.54 (s, 3H), 1.48 (s, 3H), 1.45 (m, 3H), 1.43 (m, 1H), 1.34 (m, 3H), 1.29 (s, 9H), 1.13 (m, 1H), 1.07 (m, 9H), 1.05 (s, 9H), 1.01 (s, 9H), 0.82 (m, 3H), 0.70 (q, *J* = 8 Hz, 6H), 0.49 (s, 3H), 0.43 (s, 3H), 0.25 (s, 3H), 0.22 (s, 3H), 0.13 (s, 3H), 0.12 (s, 3H); ^{13}C NMR (151 MHz, $CDCl_3$, broad signals due to slowly equilibrating rotamer): δ = 169.2, 147.3, 140.9, 137.2, 132.1, 129.4, 126.0, 125.0, 115.0, 83.8, 83.1, 81.4, 80.3, 80.0, 79.4, 77.8, 76.3, 73.9, 72.6, 47.7, 38.8, 37.8, 33.0, 31.3, 27.8, 27.0, 26.9, 26.3, 26.0, 19.2, 18.7, 18.4, 18.3, 17.6, 16.4, 16.3, 14.4, 7.3, 5.6, –3.8, –3.9, –4.3, –4.3. The analytical and spectroscopic data agree with those reported in the literature.[7]

5.2.2. Novel Compounds – Substrate Scope

Please refer to Appendix 1 for the NMR spectra.

1,12-Diiodododec-6-yne (48a)

Prepared analogously with complex **35** (14 mg, 13 µmol, 5 mol%) at 23°C; pale orange oil (43 mg, 82%). ^{1}H NMR (400 MHz, $CDCl_3$): δ = 3.21 (t, *J* = 7.0 Hz, 4H), 2.17 (m, 4H), 1.85 (m, 4H), 1.50 (m, 8H). ^{13}C NMR (101 MHz, $CDCl_3$): δ = 80.1, 33.1, 29.7, 27.9, 18.6, 6.9. IR (film): ṽ 2931, 2855, 1606, 1509, 1456, 1428, 1368, 1347, 1333, 1290, 1246, 1202, 1164, 1120, 1077, 1032, 891, 832, 805, 765, 723, 593, 532, 503 cm^{-1}. HRMS-CI (m/z): calcd. for $C_{12}H_{21}I_2^+$ [M+H]$^+$, 418.9727; found, 418.9728.

Di-*tert*-butyl (1,10-bis(phenylsulfonyl)dec-5-yne-1,10-diyl)dicarbamate (48f)

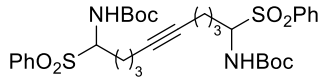

Prepared analogously with complex **35** (14 mg, 13 µmol, 5 mol%) at 23°C; white solid (62 mg, 76%). ^{1}H NMR (Diastereomer 1, 600 MHz, C_6D_6): δ = 8.15 – 8.10 (m, 4H), 7.09 – 7.03 (m, 6H), 6.38 (d, *J* = 10.7 Hz, 2H), 5.19 (td, *J* = 10.4, 5.1 Hz, 2H), 2.52 – 2.37 (m, 1H), 2.13 – 2.02 (m, 4H), 1.97 – 1.90 (m, 3H), 1.52 – 1.34 (m, 4H), 1.15 (s, 18H); ^{1}H NMR (Diastereomer 2, 600 MHz, C_6D_6): δ = 8.08 (dt, *J* = 7.4, 1.9 Hz, 4H), 6.99 (td, *J* = 5.8, 5.1, 2.9 Hz, 6H), 5.30 (d, *J* = 10.8 Hz, 2H), 5.13 (td, *J* = 10.9, 3.5 Hz, 2H), 2.52 – 2.46 (m, 1H), 1.93 (td, *J* = 5.1, 3.9, 2.1 Hz, 4H), 1.85 (d, *J* = 4.2 Hz, 1H), 1.30 – 1.21 (m, 4H), 1.16 (s, 18H); ^{13}C NMR (Diastereomer 1, 151 MHz, C_6D_6): δ = 154.3, 138.1, 133.1, 129.7, 128.5, 80.3, 79.4, 71.2, 27.7, 26.4, 24.4, 18.3; ^{13}C NMR (Diastereomer 2, 151 MHz, C_6D_6): δ = 153.9, 138.1, 133.0, 129.5, 128.6, 80.0, 79.5, 70.7, 27.7, 25.4, 24.5, 17.9. IR (film): $\tilde{\nu}$ 3339, 2977, 2933, 1718, 1514, 1447, 1393, 1367, 1307, 1284, 1242, 1164, 1138, 1081, 1048, 1025, 999, 864, 812, 776, 754, 732, 715, 687, 592, 545, 517, 498, 428 cm^{-1}; HRMS-ESI (m/z): calcd. for $C_{32}H_{44}N_2O_8S_2Na^+$ $[M+Na]^+$, 671.2431; found, 671.2435.

Dimethyl 2,7-diacetyloct-4-ynedioate (48g)

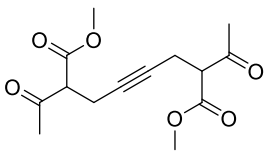

Prepared analogously to diol **39** with catalyst **35** (28 mg, 0.025 mmol, 10 mol%) at 90°C; colorless oil (28 mg, 79%). ^{1}H NMR (400 MHz, $CDCl_3$): δ = 3.75 (s, 6H), 3.65 – 3.56 (m, 2H), 2.67 – 2.61 (m, 4H), 2.27 (s, 6H); ^{13}C NMR (101 MHz, $CDCl_3$): δ = 201.4, 168.8, 78.4, 58.5, 52.8, 29.6, 17.9; IR (film): $\tilde{\nu}$ = 2956, 2163, 2002, 1745, 1719, 1435, 1361, 1266, 1226, 1151, 1004, 904, 510, 424 cm^{-1}; HRMS-ESI (m/z): calcd. for $C_{14}H_{18}O_6Na^+$ $[M+Na]^+$, 305.0996; found, 305.0997.

Octadec-9-yne-1,18-diol (77)

Prepared analogously to diol **39** with either complex **35** (14 mg, 13 µmol, 5 mol%) or complex **65** (9.7 mg, 13 µmol, 5 mol%) at 23°C; white solid (32 mg, 91%; 30.7 mg, 87%). ^{1}H NMR (400 MHz, $CDCl_3$): δ = 3.63 (t, *J* = 6.6 Hz, 4H), 2.19 – 2.06 (m, 4H), 1.61 – 1.42 (m, 8H), 1.37 – 1.27 (m, 16H); ^{13}C NMR (101 MHz, $CDCl_3$): δ = 80.4, 63.2, 32.9, 29.5, 29.3, 29.2, 28.9, 25.8, 18.9; IR (film): $\tilde{\nu}$ = 3260, 2930, 2851, 1460, 1414, 1052, 1023, 995, 725, 420 cm^{-1}; HRMS-ESI (*m/z*): calcd. for $C_{18}H_{34}O_{32}$ $[M]^+$, 283.2632; found, 283.2633.

5.2.3. Ligands and Ligand Precursors

Please refer to Appendix 2 for the NMR spectra.

1,3,4-Tris-2'-bromophenylbenzene (30)

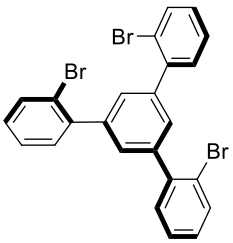

A two-necked, round-bottomed flask was equipped with a magnetic stir bar and a gas inlet connected to an argon-vacuum manifold. The flame-dried flask was filled with argon and charged with a solution of 2-bromoacetophenone (**29**) (20 g, 100 mmol) in EtOH (164 mL). The flask was cooled to 0°C, connected to a bubbler containing aqueous KOH solution and silicon tetrachloride (34.5 mL, 301 mmol) was added dropwise over 1 min. The resulting yellow mixture was stirred for 1.5 h at 0°C and then allowed to warm to ambient temperature. After 24 h, the mixture was again cooled to 0°C and the reaction quenched with water (800 mL). The orange-yellow slurry obtained was extracted with $CHCl_3$ (3 x 250 mL). The combined extracts were dried over $MgSO_4$, filtered and concentrated under reduced pressure. The red syrup obtained was triturated with hexanes (100 mL) and filtered with suction to give the title compound as a yellow flaky solid (16 g, 90%). ^{1}H NMR (400 MHz, $CDCl_3$): δ = 7.69 (dd, *J* = 8.0, 1.2 Hz, 3H), 7.50 (s, 3H), 7.46 (dd, *J* = 7.6, 1.7 Hz, 3H), 7.38 (td, *J* = 7.5, 1.2 Hz, 3H), 7.22 (ddd, *J* = 8.0, 7.4, 1.8 Hz, 3H). ^{13}C NMR (100 MHz, $CDCl_3$): δ = 141.9, 140.4, 133.2, 131.5, 129.6, 128.9, 127.4, 122.7. The analytical and spectroscopic data agree with those reported in the literature.[8]

(5'-(2-(Methoxydiphenylsilyl)phenyl)-[1,1':3',1''-terphenyl]-2,2''-diyl)bis(methoxydiphenyl silane) (32)

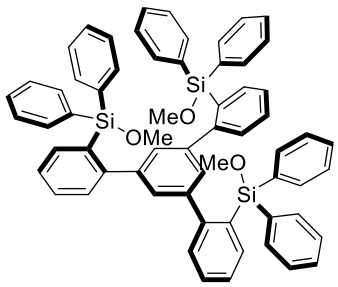

A three-necked, round-bottomed flask was equipped with a magnetic stir bar and a gas inlet connected to an argon-vacuum manifold. The flame-dried flask was filled with argon and charged with 1,3,4-tris-2'-bromophenylbenzene **30** (4.0 g, 7.4 mmol). Et_2O (90 mL) was added, and the stirred suspension was cooled to −125°C. A solution of ^{t}BuLi (28.3 mL, 45.3 mmol, 1.7 M in *n*-pentane) was added over 10 min while the suspension was stirring. The mixture was allowed to warm to ambient temperature and stirring was continued for 1.5 h. The obtained brown suspension was again cooled to −125°C and a solution of diphenyldimethoxysilane **31** (5.2 mL, 22 mmol) in Et_2O (30 mL) was added dropwise over 15 min. The reaction mixture was allowed to warm to ambient temperature and stirred for 12 h. The reaction was carefully quenched with water and the mixture was transferred into a separation funnel. The organic phase was separated, and the aqueous solution was extracted with CH_2Cl_2 (3 x 50 mL). The combined organic layers were dried over $MgSO_4$, filtered, and then concentrated in under reduced pressure.

Hexanes (50 mL) was added to precipitate the title compound as a white solid (7.5 g, 75%). ^{1}H NMR (500 MHz, $CDCl_3$): δ = 7.62 (dd, *J* = 7.4, 1.4 Hz, 3H), 7.38 (td, *J* = 7.5, 1.5 Hz, 3H), 7.35 (dd, *J* = 7.6, 1.3 Hz, 12H), 7.30 (td, *J* = 7.4, 1.3 Hz, 3H), 7.24 (tt, *J* = 7.4, 1.4 Hz, 6H), 7.14 (t, *J* = 7.5, 7.1 Hz, 12H), 6.98 (dd, *J* = 7.6, 1.3 Hz, 3H), 6.95 (s, 3H), 3.01 (s, 9H); ^{13}C NMR (126 MHz, $CDCl_3$): δ = 149.6, 141.5, 137.3, 135.2, 135.1, 131.6, 130.9, 129.6, 129.4, 129.2, 127.5, 125.7, 50.9; ^{29}Si NMR (99 MHz, $CDCl_3$): δ = −11.6; IR (film): ṽ = 3045, 2930, 2830, 1582, 1557, 1471, 1427, 1409, 1263, 1183, 1108, 1082, 998, 877, 830, 760, 735, 697, 621, 499, 477, 411 cm^{-1}; HRMSESI (m/z): calc'd. for $C_{36}H_{54}O_3Si_3Na^+$[M+Na]$^+$, 965.3273; found, 965.3286; CCDC-1987913.

Ligand 33

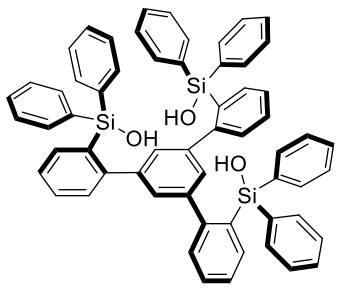

A two-necked, round-bottomed flask was equipped with a magnetic stir bar and a dropping funnel. The flask was charged with compound **32** (5.0 g, 5.3 mmol) and THF (120 mL). The solution was cooled to 0°C before concentrated aqueous HCl (39.5 mL, 474 mmol) was added dropwise. The mixture was allowed to warm to ambient temperature and stirring was continued for 1 h. After cooling to 0°C, the mixture was carefully neutralized by dropwise addition of saturated aqueous $NaHCO_3$ solution. The organic phase was separated and the aqueous solution extracted with CH_2Cl_2 (3 x 100 mL). The combined organic layers were washed with water (200 mL), dried over $MgSO_4$, filtered and concentrated under reduced pressure to give the title compound as a white solid (4.7 g, quant.). ^{1}H NMR (400 MHz, $CDCl_3$): δ = 7.55 – 7.51 (m, 12H), 7.48 – 7.43 (m, 3H), 7.30 – 7.22 (m, 12H), 7.21 – 7.13 (m, 12H), 6.92 – 6.87 (m, 6H), 4.36 (s, 3H); ^{13}C NMR (126 MHz, $CDCl_3$): δ = 149.0, 143.8, 137.5, 137.0, 134.6, 133.9, 130.1, 129.7, 129.4, 128.6, 127.9, 126.0; IR (film): $\tilde{\nu}$ = 3046, 1582, 1471, 1427, 1263, 1204, 1112, 1087, 997, 900, 824, 762, 735, 698, 622, 471, 411 cm^{-1}. HRMS-ESI (*m/z*): calcd. for $C_{60}H_{48}O_3Si_3Na^+$ [M+Na]$^+$, 923.2803; found, 923.2818; CCDC-1987916.

5'-(2-(Diisopropylsilyl)phenyl)-[1,1':3',1"-terphenyl]-2,2"-diyl)bis(diisopropyl silane) (62a)

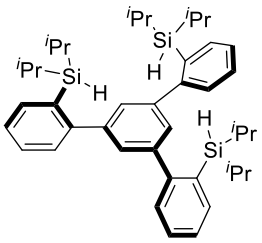

A two-necked, round-bottomed flask was equipped with a magnetic stir bar and a gas inlet connected to an argon-vacuum manifold. The flame-dried flask was filled with argon and charged with 1,3,4-tris-2'- bromophenylbenzene (**30**) (1.5 g, 2.6 mmol) and Et_2O (58 mL). The resulting mixture was cooled to −125°C and a solution of ^{t}BuLi (11 mL, 17 mmol, 1.7 M in *n*-pentane) was added dropwise. The reaction mixture was allowed to warm to ambient temperature and stirring continued for 1 h. After cooling to −125°C, diisopropylchlorosilane (2.9 mL, 17 mmol) was added dropwise and the resulting

mixture was allowed to warm to ambient temperature while stirring overnight. The reaction was carefully quenched with water, the solvent was removed *in vacuo*, and the residue was purified by flash chromatography on silica gel (hexanes/ethyl acetate, 4:1) to give the title compound as a pale-yellow foam (1.5 g, 81%). ^{1}H NMR (500 MHz, $CDCl_3$): δ = 7.57 (ddd, *J* = 7.3, 1.5, 0.6 Hz, 3H), 7.41 (td, *J* = 7.7, 7.1, 1.5 Hz, 3H), 7.36 (ddd, *J* = 7.7, 1.5, 0.6 Hz, 3H), 7.32 (td, *J* = 7.3, 1.5 Hz, 3H), 7.20 (s, 3H), 3.87 (t, *J* = 3.7 Hz, 3H), 1.07 (heptd, *J* = 7.2, 3.7 Hz, 6H), 0.95 (d, *J* = 7.2 Hz, 18H), 0.89 (d, *J* = 7.3 Hz, 18H); ^{13}C NMR (126 MHz, $CDCl_3$): δ = 149.7, 142.6, 135.8, 129.6, 129.4, 128.7, 125.9, 77.2, 77.0, 76.7, 19.2, 18.9, 11.6; ^{29}Si NMR (99 MHz, $CDCl_3$): δ = 2.1; IR (film): ṽ = 3051, 2939, 2889, 2862, 2132, 1583, 1557, 1461, 1409, 1383, 1364, 1259, 1122, 1098, 1065, 1001, 919, 877, 811, 773, 734, 686, 656, 631, 603, 527, 481, 458 cm^{-1}; HRMS-ESI (m/z): calculated for $C_{42}H_{61}Si_3$ $[M+H]^+$, 649.4076; found, 649.4068.

(5'-(2-(Dimethylsilyl)phenyl)-[1,1':3',1''-terphenyl]-2,2''-diyl)bis(dimethylsilane) (62b)

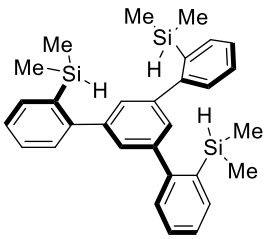

A two-necked, round-bottomed flask was equipped with a magnetic stir bar and a gas inlet connected to an argon-vacuum manifold. The flame-dried flask was filled with argon and charged with 1,3,4-tris-2'-bromophenylbenzene (**30**) (1.0 g, 1.8 mmol) and Et_2O (39 mL). The resulting mixture was cooled to −125°C. A solution of ^{t}BuLi (7.1 mL, 11 mmol, 1.7 M in *n*-pentane) was added dropwise and the resulting mixture was allowed to warm to ambient temperature. After stirring at ambient temperature for 1 h, the mixture was cooled to −125°C and dimethylchlorosilane (1.3 mL, 11 mmol) was added dropwise. The mixture was allowed to warm to ambient temperature and stirred overnight. The reaction was carefully quenched with water and the solvent was removed under reduced pressure. The residue was purified by flash chromatography on silica (hexanes/ethyl acetate, 4:1) to give the title compound as a pale-yellow foam (0.8 g, 91%). ^{1}H NMR (500 MHz, $CDCl_3$): 7.55 – 7.50 (m, 3H), 7.36 – 7.30 (m, 3H), 7.28 – 7.24 (m, 6H), 7.16 (s, 3H), 4.34 (hept, *J* = 3.8 Hz, 3H), 0.05 (d, *J* = 3.8 Hz, 18H). ^{13}C NMR (126 MHz, $CDCl_3$): δ = 148.94, 143.03, 135.84, 135.03, 129.41, 129.11, 128.81, 126.44, - 2.80. ^{29}Si NMR (99 MHz, $CDCl_3$): δ = –19.1. IR (film): ṽ = 3051, 2956, 2117, 1583, 1558, 1468, 1409, 1247, 1124, 1100, 1063, 893, 833, 967, 707, 524, 426, 448 cm^{-1}; HRMS-ESI (m/z): calculated for $C_{30}H_{36}Si_3$ $[M]^{\cdot+}$,480.2123; found, 480.2125.

Ligand 59a

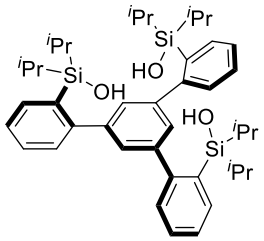

A round bottomed flask equipped with a stir bar was charged with compound **62a** (0.8 g, 1.3 mmol) and THF (14 mL). *m*CPBA (1.8 g, 7.8 mmol, 77% *w/w*) was added portionwise and the resulting mixture was stirred at ambient temperature overnight before it was concentrated under reduced pressure. The residue was purified by flash chromatography on silica gel (hexanes/ethyl acetate, 4:1) to give the title compound as a white powdery solid (0.8 g, 87%). ^{1}H NMR (400 MHz, $CDCl_3$): δ = 7.48 (dd, *J* = 7.4, 1.6 Hz, 3H), 7.40 – 7.29 (m, 6H), 7.29 – 7.25 (m, 3H), 7.21 (s, 3H), 2.97 (s, 3H), 1.12 (ddt, *J* = 13.5, 8.4, 6.5 Hz, 6H), 0.99 (d, *J* = 7.2 Hz, 18H), 0.95 (d, *J* = 7.4 Hz, 18H); ^{13}C NMR (101 MHz, $CDCl_3$): δ = 149.3, 143.6, 135.0, 134.3, 130.2, 128.5, 127.7, 126.0, 18.1, 17.9, 14.1; ^{29}Si NMR (99 MHz, $CDCl_3$): δ = 7.7; IR (film): ṽ = 3473, 3044, 2943, 2864, 2182, 2021, 1966, 1583, 1557, 1462, 1410, 1381, 1363, 1259, 1242, 1023, 1088, 1064, 997, 950, 919, 884, 760, 740, 738, 720, 653, 633, 495, 467 cm^{-1}; HRMS-ESI (m/z): calculated for $C_{42}H_{59}O_3Si_3$-[M-H]$^-$, 695.3778; found, 695.3777.

Ligand 59b

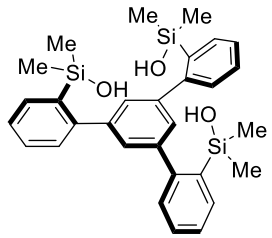

A one-neck round bottomed flask equipped with a stir bar was charged with compound **62b** (1.0 g, 2.1 mmol) and CH_2Cl_2 (28 mL). The resulting mixture was cooled to 0°C. *m*CPBA (1.5 g, 6.9 mmol, 77% w/w) was added portionwise and the resulting mixture stirred at ambient temperature for 4 h. The mixture was diluted with CH_2Cl_2 (370 mL), carefully transferred to a separation funnel, and washed with sat. $NaHCO_3$ (3 x 150 mL) and brine (3 x 100 mL). The organic phase was dried over $MgSO_4$, filtered and concentrated under reduced pressure to give the title compound as a pale colourless fluffy solid (1.0 g, 94%). ^{1}H NMR (500 MHz, $CDCl_3$): δ = 7.55 (d, *J* = 8.4 Hz, 3H), 7.43 – 7.34 (m, 6H), 7.33 – 7.28 (m, 6H), 3.30 (s, 3H), 0.31 (s, 18H); ^{13}C NMR (126 MHz, $CDCl_3$): δ = 147.9, 143.8, 137.9, 134.2, 129.6, 128.9, 127.9, 126.4, 2.1; ^{29}Si NMR (99 MHz, $CDCl_3$): δ = 6.9. IR (film): ṽ = 3262, 3050, 2898, 1699, 1558, 1409, 1430, 1408, 1252, 1161, 1126, 1065, 830, 778, 759, 694, 664, 623, 580, 530, 460, 440 cm^{-1}; HRMS-ESI (m/z): calculated for $C_{30}H_{35}O_3Si_3^-$[M-H]$^-$, 527.1900; found, 527.1908.

Ligand 60

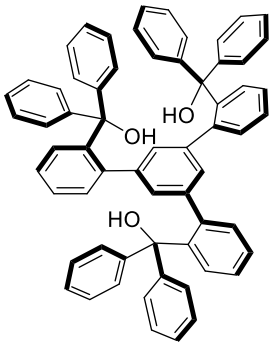

A two-necked, round-bottomed flask was equipped with a magnetic stir bar and a gas inlet connected to an argon-vacuum manifold. The flame-dried flask was filled with argon and charged with compound **30** (2.0 g, 3.9 mmol). Et_2O (78 mL) was added, and the resulting bright yellow mixture was cooled to –125°C. A solution of ^{t}BuLi (14 mL, 23 mmol, 1.6 M in *n*-pentane) was added over 10 min and the mixture was allowed to warm to ambient temperature. After stirring for another 1 h, the heterogeneous dark brown mixture was again cooled to –125°C. A solution of benzophenone **66** (2.0 g, 11 mmol) in Et_2O (10 mL) was added and the resulting mixture was allowed to warm to ambient temperature while stirring overnight. The reaction was carefully quenched with water and the solution transferred into a separation funnel. The organic phase was separated and the aqueous solution was extracted with CH_2Cl_2 (3 x 100 mL). The combined organic layers were dried over $MgSO_4$, filtered and concentrated under reduced pressure. The residue was purified by trituration with ice-cold MeOH (3 x 20 mL) to afford the title compound as a pale pink powdery solid (2.5 g, 78%). ^{1}H NMR (600 MHz, CD_2Cl_2): δ = 7.25 (m, 8H), 7.21 (m, 4H), 7.18 (m, 4H), 7.12 (m, 12H), 7.04 (t, *J* = 7.7 Hz, 1H), 7.00 (d, *J* = 7.6 Hz, 4H), 6.95 (d, *J* = 7.7 Hz, 4H), 6.91 (d, *J* = 7.4 Hz, 2H), 6.59 (d, *J* = 7.9 Hz, 2H), 6.45 (d, *J* = 7.9 Hz, 1H), 6.04 (d, *J* = 7.5 Hz, 1H), 5.62 (d, *J* = 1.6 Hz, 2H), 3.25 (s, 2H), 2.81 (s, 1H); ^{13}C NMR (151 MHz, CD_2Cl_2): δ = 147.6, 147.5, 147.1, 144.4, 143.9, 141.2, 140.7, 139.3, 139.2, 133.8, 132.5, 129.9, 129.6, 129.4, 129.2, 128.2, 127.9, 127.9, 127.8, 127.6, 127.4, 127.3, 127.1, 127.0, 126.8, 126.3, 126.1, 126.0, 83.0, 82.9; IR (film): $\tilde{\nu}$ = 3537, 3057, 1980, 1587, 147, 1445, 1414, 1317, 1262, 1154, 1014, 896, 750, 728, 706, 636, 583, 508, 446, 416 cm^{-1}; HRMS-ESI (m/z): calculated for $C_{63}H_{48}O_3Na^+$ $[M+Na]^+$, 875.3496; found, 875.3491; CCDC-1987909.

1,3,5-Tris(2-methoxycarbonylphenyl)benzene (70)

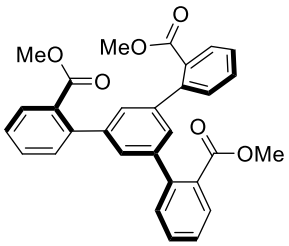

A two neck round-bottomed flask equipped with a stir bar was charged with 1,3,5-tris(2′-bromophenyl)benzene **30** (4.0 g, 7.4 mmol) and Et_2O (155 mL). The bright yellow mixture was cooled to - 125°C. A solution of ^{t}BuLi (28 mL, 45 mmol, 6.2 equiv., 1.6 M in pentane) was added over 10 mins and the reaction mixture was allowed to warm to rt. After stirring at rt for 1 h, the heterogeneous dark brown mixture, was again cooled to - 125 °C. Methyl chloroformate (3.4 mL, 44 mmol, 6.0 equiv.) was added dropwise and the resulting mixture was allowed to warm to rt and then stirred for 17 h. The reaction was carefully quenched by adding water and was transferred in a separation funnel. The organic phase was separated and the aqueous solution was extracted with CH_2Cl_2 (3 x 100 mL). The combined organic layers were dried over $MgSO_4$, filtered and concentrated under

reduced pressure. The residue obtained was purified by flash column chromatography (SiO_2, 100 g, 55 mm Ø, 0 - 50 % EtOAc/iso-Hexane, ca. 75 mL fractions). This gave the product as an orange-brown syrup (2.5 g, 70%). ^{1}H NMR (400 MHz, $CDCl_3$): δ = 7.85 – 7.79 (m, 3H), 7.56 – 7.49 (m, 3H), 7.44 – 7.38 (m, 6H), 7.24 (s, 3H), 3.69 (s, 9H); ^{13}C NMR (101 MHz, $CDCl_3$): δ = 169.1, 141.9, 141, 131.2, 131.1, 130.8, 127.3, 127.2, 52.0; IR (film): $\tilde{\nu}$ = 2950, 1703, 1593, 1432, 1290, 1270, 1124,1094, 1043, 960, 780, 709, 696, 621, 585, 517 cm^{-1}; HRMS-ESI (m/z): calc'd. for $C_{30}H_{24}O_6Na^+$ $[M+Na]^+$, 503.1461; found, 503.1465.

1,3,5-Tris(2-carboxyphenyl)benzene (71)

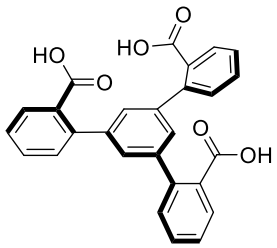

A round-bottomed flask equipped with a stir bar and a reflux condenser was charged with a solution of 1,3,5-tris(2-methoxycarbonylphenyl)benzene (1.6 g, 3.3 mmol) in THF/MeOH (50:50, 56 mL) and aqueous NaOH (24 mL, 59 mmol, 2.5 M, 18 equiv.). The resulting mixture was heated under reflux overnight (73 °C) with vigorous stirring for 24 h. The solvent was removed under reduced pressure. The brown residue obtained, was treated with concentrated hydrochloric acid (30 mL, 6 M) and the thick brown slurry formed was stirred at rt for 0.5 h. The slurry was filtered under suction. The beige brown cake obtained was washed with water (30 mL) and then allowed to dry under strong suction for 2 h. This gave the product as a powdery beige brown solid (1.3 g, 93 %). ^{1}H NMR (400 MHz, DMSO): δ = 7.72 – 7.69 (m, 3H), 7.61 – 7.58 (m, 3H), 7.55 – 7.52 (m, 3H), 7.49 – 7.45 (m, 3H), 7.38 (s, 3H); ^{13}C NMR (101 MHz, DMSO): δ = 169.6, 139.6, 139.4, 132.4, 130.4, 130.1, 128.6, 127.1, 126.9; IR (film): $\tilde{\nu}$ = 3036, 1868, 1594, 1572, 1487, 1454, 1404,1261, 1138, 1098, 1071, 874, 799, 750, 709, 686, 640, 621, 589, 521, 412 cm^{-1}; HRMS-ESI (m/z): calc'd. for $C_{27}H_{17}O_6^-$ $[M-H]^-$, 437.1031; found, 437.1034.

1,3,5-Tris(2-imidazolecarbonylphenyl)benzene (73)

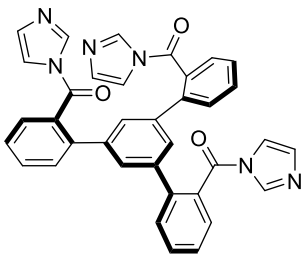

A two neck round-bottomed flask equipped with a stir bar was charged with 1,3,5-tris(2-carboxyphenyl)benzene (1.0 g, 2.3 mmol) and 1,1'-carbonyldiimidazole (1.7 g, 10 mmol, 4.5 equiv.). THF (101 mL) was added and the resulting mixture was stirred overnight at rt. The solvent was then removed under reduced pressure and the residue was dissolved CH_2Cl_2 (200 mL), washed with brine (3 x 100 mL), dried over $MgSO_4$, filtered and then concentrated under reduced pressure. The residue obtained was triturated with pentane (200 mL). The resulting mixture was concentrated under reduced pressure. This gave the product as a cream coloured foamy solid (1.3 g, 97 %). ^{1}H NMR (400 MHz, $CDCl_3$): δ = 7.81 (s, 3H), 7.71 (m, 3H), 7.66 – 7.57 (m, 6H), 7.43 – 7.38 (m, 3H), 7.32 (m, 3H), 7.16 (m, 3H), 7.04 (m, 3H); ^{13}C NMR (101 MHz, $CDCl_3$): δ = 136.8, 133.9, 131.1, 129.9, 129.7, 127.7, 127.4, 127.1, 120.7, 116.1; IR (film): $\tilde{\nu}$ = 3122, 2539, 2469, 2211, 2194, 2177, 2153,

2076, 2009, 1995, 1964, 1937, 1711, 1466, 1369, 1291, 1238, 1180, 1093, 1061, 1015, 902, 827, 747, 710, 696, 673, 650, 621, 557, 526, 482, 430, 419 cm^{-1}; HRMS-ESI (m/z): calc'd. for $C_{36}H_{25}N_6O_3^+$ $[M+H]^+$, 589.1982; found, 589.1983.

1,3,5-Tris[2-(1,1,1,3,3,3-hexafluoropropan-2-ol)phenyl]benzene (61)

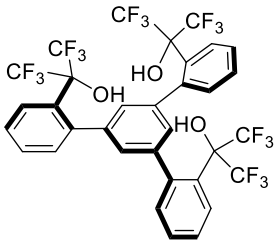

A two-neck round-bottomed flask equipped with a stir bar and a reflux condenser was charged with 1,3,5-tris(2-imidazolecarbonylphenyl)benzene (1.5 g, 2.6 mmol), CsF (7.2 g, 48 mmol, 18 equiv.) and THF (102 mL). To the resulting suspension, $TMSCF_3$ (3.5 mL, 24 mmol, 9.0 equiv.) was added. The resulting mixture was heated at 40 °C for 24 h. After that the solvent was removed *in vacuo* and the residue was purified by flash column chromatography (SiO_2, 100g, 55 mm Ø, 0-40 % EtOAc/iso-Hexane, ca. 20 mL fractions). This gave the product as a pale-yellow solid (1.0 g, 46%). ^1H NMR (600 MHz, CD_2Cl_2): δ = 7.72 (d, *J* = 7.9 Hz, 3H), 7.52 – 7.47 (m, 3H), 7.49 – 7.44 (m, 3H), 7.35 – 7.32 (m, 3H), 7.13 (s, 3H), 4.46 (s, 3H);^{13}C NMR (151 MHz, CD_2Cl_2): δ = 141.4, 141.4, 132.5, 129.1, 127.9, 127.5, 126.7, 126.6, 122.6 (q, *J* = 288.1, 287.5 Hz), 79.8 (hept, *J* = 30.5 Hz); ^{19}F NMR (565 MHz, CD_2Cl_2): δ = -75.8, -75.6 (q, *J* = 8.2 Hz), -75.4 (q, *J* = 8.3 Hz), -75.2; IR (film): $\tilde{\nu}$ = 3520, 1592, 1496, 1444, 1419, 1256, 1200, 1153, 1128, 1102, 1048, 965, 948, 924, 888, 757, 728, 690, 688, 648, 622, 529, 490, 434 cm^{-1}; HRMS-ESI (m/z): calc'd. for $C_{33}H_{17}F_{18}O_3^-$ $[M-H]^-$, 803.0895; found, 803.0897.

5.2.4. Complexes

For the work presented in this section, complexation experiments were conducted with Julius Hillenbrand at the MPI. Advanced NMR spectroscopic measurements were carried out in close collaboration with Dr. Markus Leutzsch at the NMR facility of the MPI. The single crystal structure analysis was carried out by Nils Nöthling, Dr. Richard Goddard and Jörg Rust at the MPI, while some of the X-ray structures presented were refined by Julius Hillenbrand. For all single crystal X-ray data both raw and processed cf. refs 9-10. Please refer to Appendix 3 for the NMR spectra. Unless otherwise stated NMR spectra were acquired at RT.

Complex 54

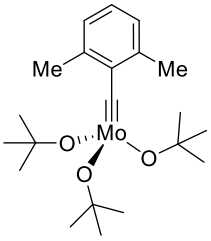

A Schlenk flask was equipped with a magnetic stir bar and was flame dried under vacuum. The flask was filled with argon and charged with Mo(≡CAr)Br_3(dme) (**53**, Ar = 2,6-dimethylphenyl) (1.1 g, 1.9 mmol)[11] and THF (21 mL). A solution of NaO^tBu (0.6 g, 5.7 mmol) in THF (5 mL) was added dropwise at 23°C and stirring was continued for 14 h before the solvent was removed under reduced pressure to

obtain a dark brown solid. A second, flame dried 250 mL Schlenk flask was equipped with a magnetic stir bar and a Celite® (2 cm) packed argon frit. The dark brown solid was suspended in *n*-pentane (4 x 15 mL) and was filtered through the Celite® pad. The resulting filtrate was concentrated under reduced pressure and the residue was dried under vacuum (10^{-3} mbar) to give the crude complex **54** as a brown solid. The mixture was dissolved in minimum of *n*-pentane (20 mL) and filtered via cannula into a flame dried 50 mL Schlenk flask under Ar. The brown/purple solution was stored for 6 h on dry ice (–85°C) to give red/purple crystals. The brown supernatant solution was filtered off via cannula and the solvent of this solution was removed under reduced pressure to give the pure complex **54**. ^{1}H NMR (400 MHz, C_6D_6): δ = 6.90 (dd, *J* = 7.3, 0.8 Hz, 2H), 6.80 (dd, *J* = 8.2, 6.8 Hz, 2H), 2.86 (s, 6H), 1.44 (s, 27H); ^{13}C NMR (101 MHz, C_6D_6): δ = 297.1, 145.5, 139.4, 127.4, 127.1, 78.7, 33.2, 32.3; IR (film): $\tilde{\nu}$ = 2969, 2923, 1461, 1359, 1383, 1236, 1162, 1099, 1025, 946, 895, 765, 788, 732, 640, 575, 591, 475, 412 cm^{-1}; Elemental analysis (%) calc'd for $C_{21}H_{36}MoO_3$: C 58.32, H 8.39, Mo 22.19; found: C 58.32, H 8.66, Mo 21.77; HRMS: not detectable (decomp.).

Complex 55[9-10]

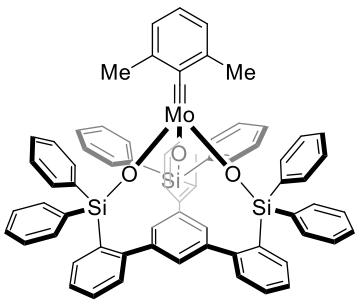

A Schlenk flask was equipped with a magnetic stir bar and flame dried under vacuum. The flask was filled with argon and charged with ligand **33** (0.39 g, 0.43 mmol), which was azeotropically dried with benzene (3 x 5 mL) to remove residual water. Toluene (32 mL) was added and the mixture vigorously stirred for 10 min to obtain a clear solution. Then a solution of complex **54** (0.19 g, 0.44 mmol) in toluene (6 mL) was added dropwise and stirring was continued for 6 h at ambient temperature. The solvent was removed under reduced pressure and the yellow/orange solid was washed with *n*-pentane (3 x 5 mL) and Et2O (3 x 5 mL) to give a yellow/orange powder containing only the monomeric complex **55** (0.31 g, 65%). Yellow crystals suitable for single-crystal X-ray diffraction were grown from a concentrated Et_2O solution at –20°C. ^{1}H NMR (400 MHz, $C_6D_5CD_3$): δ = 7.81 – 7.76 (m, 12H), 7.76 – 7.72 (m, 3H), 7.23 (s, 3H), 7.13 – 7.00 (m, 24H), 6.87 – 6.81 (m, 3H), 6.37 (s, 3H), 1.95 (s, 6H); ^{13}C NMR (101 MHz, $C_6D_5CD_3$): δ = 312.2, 149.2, 144.8, 143.8, 138.6, 137.5, 137.1, 134.8, 134.6, 130.1, 129.7, 129.4, 128.7, 127.6, 127.2, 125.8, 125.6, 19.7; ^{29}Si NMR (79 MHz, $C_6D_5CD_3$): δ = −9.4; ^{95}Mo NMR (26 MHz, 60°C, $C_6D_5CD_3$): δ = 466.8; ^{1}H-DOSY NMR ($C_6D_5CD_3$): *Dpredicted.* = 5.56·10^{-10} m^2/s^{-2}; *Dexp.* = 5.56·10^{-10} m^2/s^{-2}; IR (film): $\tilde{\nu}$ 1428, 1112, 1086, 1020, 1032, 997, 875, 849, 736, 772, 443, 413 cm^{-1}. HRMS-ESI (m/z): calc'd for $C_{69}H_{55}MoO_3Si_3^+$ [M+H]$^+$, 1113.2508; found, 1113.2510. Elemental analysis (%) calc'd for $C_{69}H_{54}MoO_3Si_3$: C 74.57, H 4.90, Mo 8.63; found: C 74.45, H 5.06, Mo 9.13; CCDC-1987913.

Complex 64[9-10]

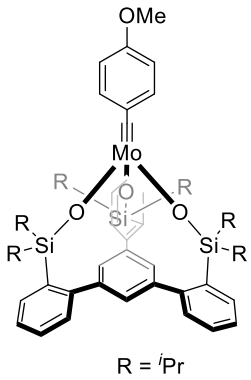

A Schlenk flask was equipped with a magnetic stir bar and was flame dried under vacuum. The flask was filled with argon and charged with ligand **59b** (0.26 g, 0.38 mmol), which was azeotropically dried with benzene (3 x 5 mL) to remove residual water. Toluene (28 mL) was added and the mixture vigorously stirred for 10 min to obtain a clear solution. Then a solution of complex **34** (0.16 g, 0.37 mmol) in toluene (6 mL) was added dropwise at 23°C and stirring continued for 3 h. The solvent was removed under reduced pressure to give a yellow/orange powder containing only monomeric complex **64** (0.34 g, 99%). Yellow crystals suitable for single-crystal X-ray diffraction were grown from a concentrated Et_2O solution at –30°C. ^{1}H NMR (400 MHz, $C_6D_5CD_3$): δ = 7.45 – 7.38 (m, 6H), 7.28 – 7.21 (m, 3H), 7.17 (td, *J* = 6.6, 5.6, 3.7 Hz, 6H), 7.13 – 7.06 (m, 2H), 6.54 (d, *J* = 8.8 Hz, 2H), 3.16 (s, 3H), 1.29 (hept, *J* = 7.1 Hz, 6H), 1.24 (d, *J* = 6.8 Hz, 18H), 1.11 (d, *J* = 7.1 Hz, 18H); ^{13}C NMR (101 MHz, $C_6D_5CD_3$): δ = 303.3, 158.7, 149.6, 143.6, 140.9, 135.0, 133.8, 130.8, 129.6, 128.3 (t, *J* = 23.8 Hz), 127.6, 125.9, 112.7, 54.1, 18.1, 17.7, 15.0; ^{29}Si NMR (79 MHz, $C_6D_5CD_3$): δ = 10.2; ^{95}Mo NMR (26 MHz, 60°C, $C_6D_5CD_3$): δ = 358.0; ^{1}H-DOSY NMR ($C_6D_5CD_3$): *Dpredicted.* = $6.08\cdot10^{-10}$ m^2/s^{-2}; *Dexp.* = $6.80\cdot10^{-10}$ m^2/s^{-2}. IR (film): $\tilde{\nu}$ = 2941, 2862, 1591, 1503, 1462, 1408, 1259, 1243, 1171, 1088, 1017, 919, 875, 799, 757, 738, 722, 671, 651, 627, 518, 471 cm^{-1}; HRMS-ESI (m/z): calc'd for $C_{50}H_{65}MoO_4Si_3^+$ $[M+H]^+$, 911.3239; found, 911.3241; Elemental analysis (%) calc'd for $C_{50}H_{64}MoO_4Si_3$: C 66.05, H 7.09, Mo 10.55, Si 9.27; found: C 62.02, H 6.82, Mo 9.93, Si 8.72; CCDC-1987911.

Complex 65[9-10]

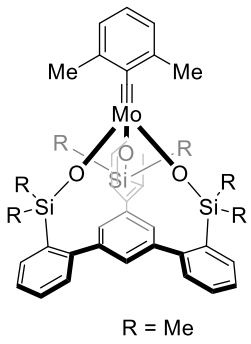

A Schlenk flask was equipped with a magnetic stir bar and flame dried under vacuum. The flask was filled with argon and charged with ligand **59a** (0.50 g, 0.89 mmol), which was azeotropically dried with benzene (3 x 5 mL) to remove residual water. Toluene (70 mL) was added and the mixture was vigorously stirred for 10 min to obtain a clear solution. Then a solution of complex **54** (0.40 g, 0.93 mmol) in toluene (14 mL) was added dropwise and stirring was continued for 4 h at ambient temperature. The solvent was removed under reduced pressure and the crude solid was extracted with *n*-pentane (5 x 5 mL) to give a yellow/orange powder containing monomeric complex **65** and a minor (oligomeric) impurity (0.55 g, 84%). ^{1}H NMR (400 MHz, $C_6D_5CD_3$): δ 7.44 (s, 3H), 7.43 – 7.40 (m, 3H), 7.25 – 7.13 (m, 9H), 6.77 (d, *J* = 7.5 Hz, 2H), 6.71 – 6.62 (m, 1H), 2.63 (s, 6H), 0.41 (s, 18H); ^{13}C NMR (101 MHz, $C_6D_5CD_3$): δ = 304.7, 148.4, 145.0, 144.2, 138.4, 138.0, 134.2, 130.1, 128.7, 127.9, 127.1, 126.4, 126.3, 20.3, 3.0; ^{29}Si NMR (79 MHz, $C_6D_5CD_3$): δ = 9.4; ^{95}Mo

NMR (26 MHz, 60°C, $C_6D_5CD_3$): δ = 421.8; ^{1}H-DOSY NMR ($C_6D_5CD_3$): *Dpredicted.* = $6.69 \cdot 10^{-10}$ m^2/s_{-2}; *Dexp.* = $7.09 \cdot 10^{-10}$ m^2/s; IR (film): $\tilde{\nu}$ = 2964, 2037, 1259, 1124, 1094, 1020, 987, 886, 877, 832, 806, 781, 759, 743, 728, 695, 653, 633, 605, 592, 581, 562, 529, 518, 509, 493, 474, 463, 454, 430, 412 cm^{-1}; HRMS-ESI (m/z): calc'd for $C_{39}H_{43}MoO_3Si_3^+$ $[M+H]^+$, 741.1569; found, 741.1569.

Complex 67[9-10]

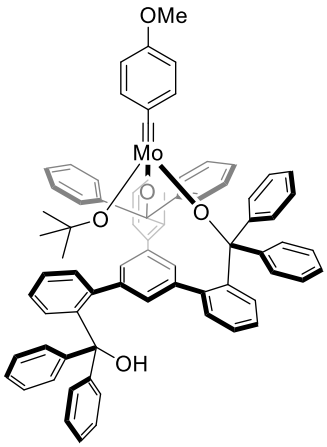

A Schlenk flask was equipped with a magnetic stir bar and flame dried under vacuum. The flask was filled with argon and charged with ligand **60** (0.15 g, 0.18 mmol), which was azeotropically dried with benzene (3 x 5 mL) to remove residual water. Toluene (13 mL) was added and the mixture vigorously stirred for 10 min to obtain a clear solution. A solution of complex **34** (0.1 g, 0.20 mmol) in toluene (3 mL) was added dropwise and stirring continued for 14 h. The solvent was removed *in vacuo* and the brown residue was washed with *n*-pentane (3 x 5 mL) to give complex **67** as a bright brown powder (0.16 g, 82%). ^{1}H NMR (600 MHz, $C_6D_5CD_3$): 7.71 (dd, *J* = 7.5, 1.5 Hz, 1H), 7.57 (dd, *J* = 8.4, 1.3 Hz, 4H), 7.38 (dd, *J* = 8.4, 1.3 Hz, 4H), 7.32 – 7.29 (m, 4H), 7.28 (td, *J* = 7.4, 1.3 Hz, 1H), 7.11 (dd, *J* = 8.4, 7.0 Hz, 4H), 7.04 – 7.00 (m, 9H), 6.97 – 6.89 (m, 8H), 6.89 – 6.84 (m, 5H), 6.75 (t, *J* = 1.7 Hz, 1H), 6.71 (d, *J* = 1.7 Hz, 2H), 6.66 (dd, *J* = 7.6, 1.5 Hz, 2H), 6.36 – 6.27 (m, 2H), 5.46 – 5.40 (m, 2H), 3.66 (s, 1H), 3.09 (s, 3H), 1.46 (s, 9H); ^{13}C NMR (151 MHz, $C_6D_5CD_3$): δ = 287.1, 158.3, 149.3, 149.0, 148.7, 145.2, 144.9, 144.5, 141.2, 141.1, 139.2, 138.8, 133.9, 132.5, 131.0, 130.8, 130.0, 129.3, 128.7, 128.5, 127.7, 127.6, 127.5, 127.5, 127.5, 127.4, 127.0, 126.7, 126.5, 126.1, 126.1, 125.7, 112.1, 94.2, 83.6, 82.7, 53.9, 32.8; ^{95}Mo NMR (26 MHz, 60°C, $C_6D_5CD_3$): δ = 118.3; ^{1}H-DOSY NMR ($C_6D_5CD_3$): *Dpredicted.* = $5.50 \cdot 10^{-10}$ m^2/s^{-2}; *Dexp.* = $5.58 \cdot 10^{-10}$ m^2/s^{-2}; IR (film): $\tilde{\nu}$ = 3533, 3058, 2968, 1593, 1503, 1445, 1360, 1283, 1243, 1168, 1040, 1013, 922, 908, 828, 804, 787, 755, 729, 696, 637, 607, 591, 515, 498, 454, 430, 412 cm^{-1}; HRMS-ESI (m/z): calc'd for $C_{75}H_{62}MoO_5Na^+$ $[M+Na]^+$, 1163.3544; found, 1163.3551; Elemental analysis (%) calc'd for $C_{75}H_{62}MoO_5$: C 79.07, H 5.49, Mo 8.42; found: C 79.25, H 5.66, Mo 8.12.

Complex 74[9-10]

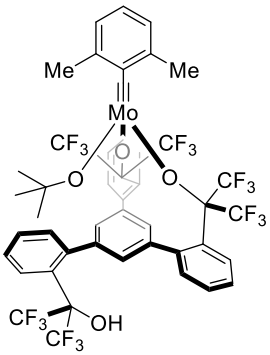

A Schlenk flask was equipped with a magnetic stir bar and flame dried under vacuum. The flask was filled with argon and charged with ligand **61** (0.31 g, 0.37 mmol), which was azeotropically dried with benzene (3 x 5 mL) to remove residual water. Toluene (13 mL) was added and the mixture vigorously stirred for 10 min to obtain a clear solution. A solution of complex **54** (0.16 g, 0.38 mmol) in toluene (3 mL) was added dropwise and stirring continued for 14 h. The solvent was removed *in vacuo* and the brown residue was washed with *n*-pentane (3 x 5 mL) to give complex **74** as a bright brown powder (0.32 g, 79%).^{1}H NMR (400 MHz, C_6D_6) δ 7.82 – 7.65 (m, 3H), 7.24 – 7.17 (m, 3H), 7.08 (dd, *J* = 7.6, 1.7 Hz, 2H), 7.02 – 6.85 (m, 6H), 6.74 – 6.62 (m, 3H), 6.58 (td, *J* = 7.5, 1.2 Hz, 1H), 5.73 (dd, *J* = 7.7, 1.5 Hz, 1H), 3.87 (s, 1H), 2.42 (s, 6H), 1.37 (s, 9H). The complex decomposes over time in C_6D_6 during the 13C NMR spectrum acquisition. Although the bidentate nature of the complex was confirmed by single X-ray diffraction from crystals grown from *n*-pentane.

5.2.5. References Experimental Chapter 2

[1] L. G. Ulysse, J. Chmielewski, *Bioorg. Med. Chem. Lett.* **1998**, *8*, 3281.

[2] S. Schaubach, K. Gebauer, F. Ungeheuer, L. Hoffmeister, M. K. Ilg, C. Wirtz, A. Fürstner, *Chem. Eur. J.* **2016,** *22*, 8494.

[3] D. Obando, Y. Koda, N. Pantarat, S. Lev, X. Zuo, J. Bijosono Oei, F. Widmer, J. T. Djordjevic, T. C. Sorrell, K. A. Jolliffe, *ChemMedChem* **2018**, *13*, 1421.

[4] Z. Meng, A. Fürstner, *J. Am. Chem. Soc.* **2019**, *141*, 805-809.

[5] J. Heppekausen, R. Stade, R. Goddard, A. Fürstner, *J. Am. Chem. Soc.* **2010,** *132*, 11045.

[6] G. Jin, X. Zhang, S. Cao, *Org. Lett.* **2013,** *15*, 3114.

[7] G. Valot, C. S. Regens, D. P. O'Malley, E. Godineau, H. Takikawa, A. Fürstner, *Angew. Chem. Int. Ed.* **2013,** *52*, 9534.

[8] D. Trawny, M. Quennet, N. Rades, D. Lentz, B. Paulus, H. Reissig, *Chem. Eur. J.* **2015**, *21*, 4667-4674.

[9] J. Hillenbrand, M. Leutzsch, E. Yiannakas, C. Gordon, C. Wille, N. Nöthling, C. Copéret, A. Fürstner, *J. Am. Chem. Soc.* **2020**, *142*, 11279 – 11294.

[10] J. V. Hillenbrand, Molybdän- und Wolfram-Katalysatoren mit Tripodalen Liganden für die Alkin-Metathese & Isolierung eines homoleptischen Mo(V) Alkoxid Komplexes, PhD Thesis, Max-Planck Institüt fur Kohlenforschung/Technische Universität Dortmund, Mülheim an der Ruhr/Dortmund, **2021**.

[11] J. Heppekausen, R. Stade, A. Kondoh, G. Seidel, R. Goddard, A. Fürstner, *Chem. Eur. J.* **2012,** *18*, 10281.

5.3. Experimental Procedure for Chapter 3

5.3.1. Literature Known Compounds

(*S*)-4-Benzyl-3-propionyloxazolidin-2-one (11)

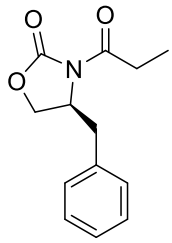

A three-neck jacketed glass reaction vessel equipped with a magnetic stir bar, a pressure equalizing addition funnel and a gas inlet connected to an argon-vacuum manifold, was charged with solution of (*S*)-4-benzyloxazolidin-2-one (5.0 g, 28 mmol) in THF (100 mL). The reaction mixture was cooled to - 78 °C and ^{n}BuLi (18 mL, 65 mmol, 1.1 equiv., 1.6 M in n-hexanes) was added dropwise. After 1 h of stirring at - 78 °C, propionyl chloride (2.7 mL, 30 mmol, 1.1 equiv.) was added and the resulting mixture was allowed to warm to rt overnight. The reaction mixture was diluted with NH_4Cl (200 mL, sat. aq.) and then extracted with EtOAc (3 x 150 mL). The combined organic extracts were washed with brined (150 mL), dried over $MgSO_4$, filtered and then concentrated under reduced pressure. This gave the product as a white solid (6.4 g, 99%). ^{1}H NMR (400 MHz, $CDCl_3$): δ = 7.36 – 7.31 (m, 2H), 7.30 – 7.25 (m, 1H), 7.23 – 7.19 (m, 2H), 4.71 – 4.64 (m, 1H), 4.28 – 4.11 (m, 2H), 3.31 (dd, *J* = 13.4, 3.3 Hz, 1H), 3.07 – 2.85 (m, 2H), 2.77 (dd, *J* = 13.4, 9.6 Hz, 1H), 1.21 (t, *J* = 7.3 Hz, 3H); ^{13}C NMR (101 MHz, $CDCl_3$) δ 174.1, 153.5, 135.4, 129.4, 129.0, 127.4, 66.3, 55.3, 38.0, 29.2, 8.3; Lit. $[a]_D^{20}$= + 59 (c = 7.6, $CHCl_3$), $[a]_D^{20}$= + 59.1 (c = 1.13, $CHCl_3$), The ^{1}H and ^{13}C NMR spectroscopic data agree with those reported in the literature.[1]

5-Bromopent-2-yne (13a)

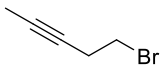

A tin-foil covered one-neck round-bottomed flask equipped with a stir bar, was charged with a solution of 4-pentyn-1-ol **12** (3.8 g, 45 mmol) in Et_2O/MeCN (3:1, 176 mL), imidazole (1.5 g, 45 mmol, 1.5 equiv.) and PPh_3 (12 g, 45 mmol, 1.5 equiv.). The resulting mixture was cooled to 0 °C and bromine (2.1 mL, 45 mmol, 1.5 equiv) was added in the small portions over 5 mins. The reaction mixture was then allowed to warm to rt and stirred for 2 h. The reaction mixture was then diluted with Et_2O (200 mL) and quenched with $NaHCO_3$ (100 mL, sat. aq.). The aqueous phase was then extracted with with Et_2O (2 x 100 mL) and then combined organic extracts were washed with $Na_2S_2O_3$ (100 mL, sat.aq.), dried over $MgSO_4$, filtered and then concentrated under reduced pressure (300 mbar) at rt in the abscence of light. The residue obtained was purified by flash column chromatography (200 g, SiO_2, 110 mm Ø, pentane). This gave the desired product as a pale yellow oil (3.6 g, 81%). ^{1}H NMR (600 MHz, $CDCl_3$): δ = 3.43 (t, *J* = 7.3 Hz, 2H), 2.72 (tq, *J* = 7.4, 2.5 Hz, 2H), 1.78 (t, *J* = 2.5 Hz, 3H); ^{13}C NMR (101 MHz, $CDCl_3$): δ = 78.1, 76.2, 23.5, 9.8, 3.6. The ^{1}H and ^{13}C NMR spectroscopic data agree with those reported in the literature.[2]

5-Iodopent-2-yne (13b)

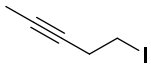

A tin-foil covered one-neck round-bottomed flask equipped with a stir bar, was charged with a solution of 4-pentyn-1-ol **12** (5.0 g, 59 mmol) in Et_2O/MeCN (3:1, 300 mL), imidazole (6.1 g. 89 mmol, 1.5 equiv.) and PPh_3 (23 g, 89 mmol, 1.5 equiv.). The resulting mixture was cooled to 0 °C and iodine (23 g, 89 mmol, 1.5 equiv) was added in the small portions over 5 mins. The reaction mixture was then allowed to warm to rt and stirred for 2 h. The reaction mixture was then diluted with Et_2O (240 mL) and quenched with $NaHCO_3$ (150 mL, sat. aq.). The aqueous phase was then extracted with with Et_2O (2 x 150 mL) and then combined organic extracts were washed with $Na_2S_2O_3$ (200 mL, sat.aq.), dried over $MgSO_4$, filtered and then concentrated under reduced pressure (300 mbar) at rt in the abscence of light. The residue obtained was purified by flash column chromatography (300 g, SiO_2, 110 mm Ø, pentane). This gave the desired product as a pale yellow oil (11 g, 91 %). ^{1}H NMR (400 MHz, $CDCl_3$): δ = 3.20 (t, *J* = 7.4 Hz, 2H), 2.72 (tq, *J* = 7.4, 2.5 Hz, 2H), 1.78 (t, *J* = 2.5 Hz, 3H); ^{13}C NMR (101 MHz, $CDCl_3$) δ 77.9, 77.8, 24.1, 3.6, 2.6. The ^{1}H and ^{13}C NMR spectroscopic data agree with those reported in the literature.[3]

6-Heptynoic acid (17)

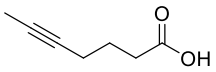

A two-neck round round-bottomed flask equipped with a magnetic stir bar, a reflux condenser and a gas inlet connected to an argon-vacuum manifold, was charged with solution of 6-heptynoic acid (6 g, 48 mmol) in DMSO (89 mL) and KOtBu (11 g, 101 mmol, 2.1 equiv.). The reaction mixture was heated at 85 °C for 0.5 h. After that, the reaction mixture was allowed to cool to rt and then quenched with HCl (100 mL, 1 M, aq). The resulting mixture was extracted with Et_2O (3 x 100 mL). The combined organic extracts were dried over $MgSO_4$, filtered and then concentrated under reduced pressure. The residue obtained was purified by flash column chromatography (SiO_2, 100 g, 90 mm ⌀, 0-50% EtOAc/iso-Hexane, ca. 20 mL fractions). This gave the product as white crystalline solid (5 g, 76 %). ^{1}H NMR (400 MHz, $CDCl_3$): δ = 11.0 (brs, 1H), 2.49 (t, *J* = 7.4 Hz, 2H), 2.22 (tq, *J* = 7.4, 2.5 Hz, 2H), 1.86 – 1.79 (m, 2H), 1.77 (t, *J* = 2.5 Hz, 3H); ^{13}C NMR (101 MHz, $CDCl_3$) δ 178.0, 77.7, 77.2, 33.9, 23.9, 18.1, 3.4. The ^{1}H and ^{13}C NMR spectroscopic data agree with those reported in the literature.[4]

(1*S*,2*S*,4*S*,5*R*)-2-((*R*)-(6-Methoxyquinolin-4-yl)((trimethylsilyl)oxy)methyl)-5-vinylquinuclidine (23)

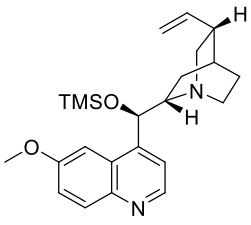

A flame dried two neck round bottomed flask equipped with with a magnetic stir bar and a gas inlet connected to an argon-vacuum manifold, was charged with a solution of quinine (3.0 g, 9.2 mmol) in CH_2Cl_2 (90 mL) and TEA (3.8 mL, 28 mmol, 3.0 equiv.). TMSCl (1.4 mL, 11 mmol, 1.2 equiv.) was added dropwise and the resulting mixture was stirred overnight. The reaction mixture was then quenched with $NaHCO_3$ (40 mL, sat. aq.) and the aqueous layer was extracted with CH_2Cl_2 (3 x 30 mL). The combined organic extracts were then dried over $MgSO_4$, filtered and then concentrated under reduced pressure. The residue obtained was purified by flash column chromatography (SiO_2, 100 g, 55 mm ø, 0-30 % MeOH/EtOAc, ca. 20 mL). This gave the product as a white powdery solid (3 g, 83 %). ^{1}H NMR (400 MHz, DMSO): δ = 8.67 (s, 1H), 7.93 (d, *J* = 9.2 Hz, 1H), 7.62 – 7.20 (m, 3H), 5.83 (d, *J* = 17.3 Hz, 1H), 5.48 (s, 1H), 5.07 – 4.80 (m, 2H), 3.89 (s, 3H), 3.25 – 2.61 (m, 5H), 2.40 – 2.05 (m, 1H), 1.93 – 1.07 (m, 5H), -0.05 (s, 9H). ^{13}C NMR (101 MHz, DMSO): δ = 173.4, 157.9, 147.4, 144.8, 143.7, 141.7, 131.8, 127.0, 121.8, 118.8, 114.5, 101.4, 73.5, 59.1, 56.5, 55.6, 42.4, 39.6, 27.74, 27.72, 27.5, 24.3, 9.0. The ^{1}H and ^{13}C NMR spectroscopic data agree with those reported in the literature.[5]

7-Iodohept-2-yne (36)

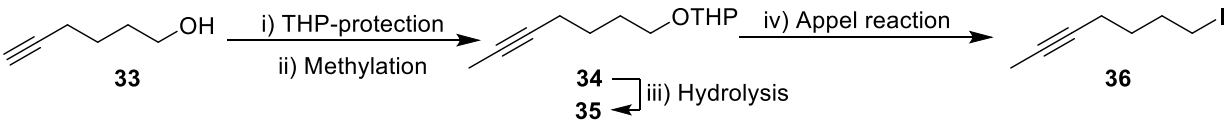

Step 1 (THP-protection):

A three-neck round bottom flask equipped with a stir bar, an argon bridge and a rubber septum, was charged with TsOH (0.2 g, 1 mmol, 1 mol%) and a solution of 5-hexyn-1-ol (10 g, 97 mmol) in CH_2Cl_2 (125 mL). The flask was cooled to 0 °C over an ice-bath and 3,4-DHP (10 mL, 106 mmol, 1.1 equiv.) was added dropwise. The resulting mixture was allowed to warm to rt and then stirred overnight. After that the reaction mixture was directly passed through a silica plug (SiO_2, 100 g, 120 mm Ø, CH_2Cl_2, ca. 75 mL fractions). Fractions containing the desired protected alcohol were combined and concentrated under reduced pressure. This gave the THP-ether as a colourless oil (17 g). The crude THP-ether was used in the next step without any further purification.

Step 2 (Methylation):

A three-neck round bottom flask equipped with a stir bar, an argon bridge and a pressure equalising dropping funnel, was charged with a solution of the crude THP-ether (17 g, 97 mmol) in THF (345 mL). The reaction mixture was cooled to - 78 °C and ^{n}BuLi (79 mL, 127 mmol, 1.6 M, 1.1 equiv., in *n*-hexanes) was added dropwise. After stirring at - 78 °C for 1 h, MeI (9 mL, 145 mmol, 1.5 equiv.) was added dropwise and the resulting mixture was allowed to warm to rt overnight. After that the reaction mixture was quenched with brine (1000 mL) and then extracted with Et_2O (3 x 250 mL). The combined organic extracts were dried over $MgSO_4$, filtered and then concentrated under reduced pressure. This gave the desired product as a pale orange oil (14 g), which was utilized in the next step without purification.

Step 3 (Hydrolysis):

A two-neck round bottom flask equipped with an argon bridge, a stir bar and a rubber septum, was charged with a solution of the crude THP-protected alcohol in MeOH (150 mL) and TsOH (0.4 g, 2.0 mmol, 2.0 mol%). The reaction mixture was stirred overnight at rt. After that the reaction mixture was quenched with $NaHCO_3$ and then diluted with H_2O (850 mL). The resulting mixture was extracted with Et_2O (3 x 250 mL) and the combined organic extracts were dried over $MgSO_4$, filtered and then concentrated under reduced pressure. This afforded the alcohol as a colourless oil (10 g), which was used in the next step without purification.

Step 4 (Appel Reaction):

A tin-foil wrapped round bottom flask equipped with a stir bar was charged with a solution of the alcohol in Et_2O/MeCN (3:1, 400 mL) was added along with PPh_3 (38 g, 145 mmol, 1.5 equiv.) and imidazole (10 g, 145 mmol, 1.5 equiv.). The mixture was cooled to 0 °C over an ice-bath and iodine (37 g, 145 mmol, 1.5 equiv.) was added portion wise. After that, the cooling bath was removed and resulting mixture was stirred at rt for 2 h. The reaction mixture was then diluted with Et_2O (600 mL), quenched with $NaHCO_3$ (100 mL, sat. aq.) and washed twice with $Na_2S_2O_3$ (2 x 200 mL, sat. aq.). The organic phase was then dried over $MgSO_4$, filtered and then concentrated under reduced pressure at rt. The residue obtained was then passed through a silica plug (SiO_2, 100 g, 120 mm Ø, *n*-pentane, ca. 75 mL fractions). This afforded alkyl iodide **36** as a colourless oil (21 g, 95 % over four steps). ^{1}H NMR (400 MHz, $CDCl_3$): δ = 3.14 (t, *J* = 7.8 Hz, 2H), 2.09 (tp, *J* = 7.8, 2.6 Hz, 2H), 1.92 – 1.81 (m, 2H), 1.71 (t, *J* = 2.6 Hz, 3H), 1.57 – 1.45 (m, 2H); ^{13}C NMR (101 MHz, $CDCl_3$): δ = 78.8, 76.6, 32.9, 30.2, 18.2, 6.8, 3.9. The ^{1}H and ^{13}C NMR spectroscopic data agree with those reported in the literature.[6]

Non-7-ynoic acid (37)

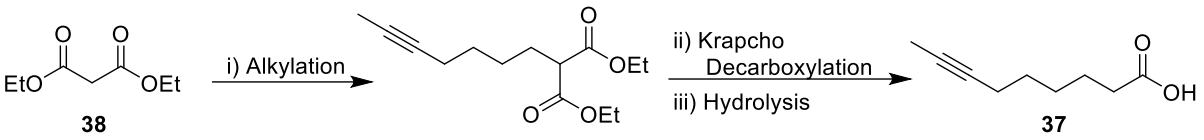

Step 1 (Alkylation):

A two-neck round bottom flask equipped with a stir bar, rubber septum and an argon bridge was charged with NaH (0.8 g, 34 mmol, 1.1 equiv.) and DMF (89 mL). The resulting suspension was cooled to 0°C over an ice-bath. Diethyl malonate **38** (5.3 g, 32 mmol) was added, and the resulting mixture was stirred for 0.5 h at 0 °C. After that 7-iodohept-2-yne **36** (7.5 g, 34 mmol, 1.1 equiv.) was added and reaction mxture was allowed to warm to rt and then stirred overnight. The reaction mixture was quenched with brine (400 mL) and then extracted with Et_2O (4 x 125 mL). The combined organic extracts were then dried over $MgSO_4$, filtered and then concentrated under reduced pressure. The yellow oil obtained was carried forward without any purification.

Step 2 (Krapcho Decarboxylation):

A round bottom flask equipped with a reflux condenser and a stir bar was charged with a solution of the crude diethyl 2-(hept-5-yn-1-yl)malonate in DMSO (57 mL), water (0.23 mL, 13 mmol, 0.4 equiv.) and LiCl (3.0 g, 71 mmol, 2.2 equiv.). The resulting mixture was heated at 160 °C overnight. Upon cooling to rt, the reaction mixture was diluted with brine (600 mL) and extracted with Et_2O (3 x 150 mL). The combined organic extracts were dried over $MgSO_4$, filtered and then concentrated under reduced pressure. The brown oil obtained was then carried forward without any purification.

Step 3 (Hydrolysis):

A round bottom flask equipped with a stir bar was charged with a solution of the crude ethyl non-7-ynoate in THF (115 mL) and the flask was cooled to 0 °C. A solution of LiOH (2.3 g, 97 mmol, 3.0 equiv.) in water (115 mL) was added and the resulting mixture was allowed to warm to rt and then stirred overnight. The THF was removed under reduced pressure and the aqueous fraction obtained was acidified to pH 1 with conc. HCl. The resulting mixture was extracted with EtOAc (3 x 100 mL) and the combined organic extracts were dried over $MgSO_4$, filtered and then concentrated under reduced pressure. This gave the acid **37** as a white solid (4 g, 80 % over three steps). ^{1}H NMR (400 MHz, $CDCl_3$): δ = 2.36 (t, *J* = 7.5 Hz, 2H), 2.17 – 2.09 (m, 2H), 1.77 (t, *J* = 2.5 Hz, 3H), 1.69 – 1.60 (m, 2H), 1.54 – 1.38 (m, 4H); ^{13}C NMR (101 MHz, $CDCl_3$): δ = 180.7, 79.4, 76.1, 34.4, 29.1, 28.6, 24.7, 18.9, 3.9; mp: 50-51 °C; (IR (film): $\tilde{\nu}$ = 2936, 2907, 2858, 1688, 1468, 1439, 1410, 1298, 1275,1252, 1206, 1198, 918 cm^{-1}; HRMS-

EI (*m/z*): calc'd. for $C_9H_{14}O_2[M]^{+\cdot}$, 155.1066; found, 155.1064. The ^1H and ^{13}C NMR spectroscopic data agree with those reported in the literature.[7]

(*E*)-2-Methylhex-2-en-4-ynoic acid (55)

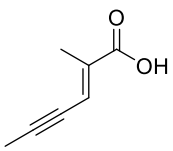

A two-neck round round-bottomed flask equipped with a magnetic stir bar with a magnetic stir bar, a glass stopper and a gas inlet connected to an argon-vacuum manifold equipped with a bubbler containing aqueous KOH, was charged with solution of 2-butyn-1-ol **60** (4.0 mL, 52 mmol) in CH_2Cl_2 (350 mL) and aq. pH 8.6 buffer (15 g of $NaHCO_3$ and 2.4 g of K_2CO_3 in 350 mL of H_2O). TBACl (1.5 g, 5.2 mmol, 10 mol%), TEMPO (0.83 g, 5.2 mmol, 10 mol%) and NCS (11 g, 82 mmol, 1.6 equiv.) were successively added. The resulting biphasic mixture was vigorously stirred at rt for 7 h. The aqueous layer was extracted with CH_2Cl_2 (300 mL), the combined organic layers were washed with brine, dried over $MgSO_4$ and then concentrated under reduced pressure (300 mbar) at rt. This gave but-2-ynal as a light orange liquid (2 g, 50 %), which was directly engaged in the next step. ^1H NMR (400 MHz, CD_2Cl_2): δ = 9.13 (q, *J* = 1.0 Hz, 1H), 2.07 (d, *J* = 1.0 Hz, 3H). The ^1H NMR spectroscopic data agree with those reported in the literature.[8]

A three-neck jacketed vessel equipped with a magnetic stir bar, a gas inlet connected to an argon-vacuum manifold, a ground-glass joint thermometer adapter connected to low temperature thermometer and a rubber septum was charged with THF (45 mL). The reaction vessel was cooled to – 60 °C and ^{n}BuLi (9.2 mL, 15 mmol, 2.0 equiv.) was added. A solution of 2-(diethoxyphosphoryl)propanoic acid **56** (1.5 g, 7.8 mmol, 1.0 equiv.) in THF (7 mL) was added dropwise and the mixture was stirred at – 60 °C for 0.5 h. A solution of the crude but-2-ynal in THF (10 mL) was added and the resulting mixture was stirred at – 60 °C for 0.5 h, before it was warmed to rt and then stirred overnight. The reaction mixture was then quenched with dilute HCl (20 mL, 1.0 M, aq.) and extracted with Et_2O (3 x 100 mL). The combined organic yellow slurry obtained was then diluted with water (100 mL) and extracted with EtOAc (3 x 150 mL). The combined organic layers were dried over $MgSO_4$, filtered and then concentrated under reduced pressure. The residue was purified by flash column chromatography (SiO_2, 100 g, 55 mm ø, 0-40% EtOAc/iso-Hexanes, ca. 20 mL). This gave product **55** as a white solid (0.6 g, 63 %) (*E*:*Z* ratio of 90:10; determined from the crude reaction mixture by ^1H NMR). ^1H NMR (400 MHz, $CDCl_3$): δ = 9.81 (brs, 1H), 6.70 (qt, *J* = 2.5, 1.3 Hz, 1H), 2.09 (dd, *J* = 2.5, 0.7 Hz, 3H), 2.04 (dd, *J* = 1.3, 0.7 Hz, 3H); ^{13}C NMR (101 MHz, $CDCl_3$): δ = 171.6, 136.9, 122.9, 100.8, 77.2, 14.9, 5.1. The ^1H and ^{13}C NMR spectroscopic data agree with those in the literature.[9]

5.3.2. Novel Compounds

Please refer to Appendix 4 for the NMR spectra in this section. Unless otherwise stated NMR spectra were acquired at RT.

(*R*)-4-Benzyl-3-(hept-5-ynoyl) oxazolidin-2-one (16)

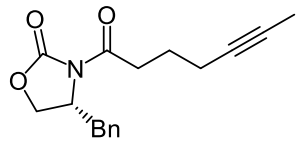

A three-neck jacketed glass reaction vessel equipped with a magnetic stir bar, a pressure equalizing addition funnel and a gas inlet connected to an argon-vacuum manifold, was charged with solution of 6-heptynoic acid **17** (4.6 g, 37 mmol) in THF (100 mL) and TEA (13 mL, 39 mmol, 1.1 equiv.). The reaction mixture was then cool to - 10°C and PvCl (4.4 mL, 36 mmol, 1.1 equiv.) dropwise. The white slurry immediately formed was stirred at this temperature for 1 h. Then, LiCl (1.7 g, 40 mmol, 1.2 equiv.) and (R)-4-(phenylmethyl)-2-oxazolidinone (6.2 g, 34 mmol) were added in one portion. The resulting mixture was allowed to warm to rt and then stirred overnight. The reaction mixture was quenched with $NaHCO_3$ (200 mL, sat. aq.) and extracted with EtOAc (3 x 150 mL). The combined organic layers were washed with brine (150 mL), dried $MgSO_4$, filtered and then concentrated under reduced pressure. The residue was purified by flash column chromatography (SiO_2, 100 g, 55 mm ø, 0-40% EtOAc/iso-Hexanes, ca. 20 mL). This gave the product as a pale yellow oil (7 g, 72 %).^{1}H NMR (400 MHz, $CDCl_3$): δ = 7.36 – 7.31 (m, 2H), 7.30 – 7.25 (m, 1H), 7.23 – 7.17 (m, 2H), 4.67 (ddt, *J* = 9.6, 7.4, 3.4 Hz, 1H), 4.26 – 4.13 (m, 2H), 3.30 (dd, *J* = 13.3, 3.4 Hz, 1H), 3.16 – 2.97 (m, 2H), 2.77 (dd, *J* = 13.3, 9.6 Hz, 1H), 2.26 (tq, *J* = 7.4, 2.5 Hz, 2H), 1.93 – 1.82 (m, 2H), 1.78 (t, *J* = 2.5 Hz, 3H);^{13}C NMR (101 MHz, $CDCl_3$): δ = 173.3, 153.9, 135.8, 129.9, 129.4, 127.8, 78.5, 76.9, 66.5, 55.8, 38.4, 34.9, 23.9, 18.6, 3.9; $[\alpha]_D^{20}$= − 59.1 (c = 1.13, $CHCl_3$); IR (film): $\tilde{\nu}$ = 3029, 2919,1779,1699, 1604, 1631, 1496, 1480, 1453, 1386, 1352, 1324, 1290, 1251, 1210, 1110, 1076, 1052, 1012, 932, 843, 762, 748, 703, 666. 671, 621, 595, 506, 438, 416 cm-1; HRMS-ESI+ (*m/z*): calc'd. for $C_{17}H_{20}N_1O_3$ $[M+H]^{+,}$ 286.1436; found, 286.1437.

(*R*)-4-Benzyl-3-((*R*)-2-methylhept-5-ynoyl)oxazolidin-2-one (19)

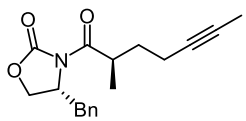

A three-neck jacketed vessel equipped with a stir bar, a gas inlet connected to an argon-vacuum manifold, a ground-glass joint thermometer adapter connected to low temperature thermometer and a rubber septum was charged with a solution of (*R*)-4-benzyl-3-(hept-5-ynoyl)oxazolidin-2-one **16** (2.0 g, 7.0 mmol) in THF (40 mL). The reaction mixture was cooled to –78 °C. A solution of NaHMDS (7.1 mL, 11 mmol, 1.5 equiv., 1.5 M solution in THF) was added dropwise. The resulting pale yellow mixture was stirred for 1 h at - 78 °C. The reaction mixture was then treated with MeI (2.2 mL, 35 mmol, 5.0 equiv.) and stirred for additional 4.5 h at -78 °C. The yellow reaction was quenched with AcOH (4.0 mL) and warmed up to room temperature. The yellow slurry obtained was then diluted with water (100 mL) and extracted with EtOAc (3 x 150 mL). The combined organic layers were dried over $MgSO_4$, filtered and then concentrated under reduced pressure. The residue was purified by flash column chromatography (SiO_2, 100 g, 55 mm ø, 0-40% EtOAc/iso-Hexanes, ca. 20 mL). This gave the product as a colourless oil (2.3 g, 77 %). ^{1}H NMR (400 MHz, $CDCl_3$) δ 7.36 – 7.31 (m, 2H), 7.30 – 7.26 (m, 1H), 7.24 – 7.19 (m, 2H), 4.68 (ddt, *J* = 9.6, 7.4, 3.2 Hz, 1H), 4.25 – 4.13 (m, 2H), 3.93 – 3.80 (m, 1H), 3.26 (dd, *J* = 13.3, 3.2 Hz, 1H), 2.77 (dd, *J* = 13.3, 9.6 Hz, 1H), 2.25 – 2.08 (m, 2H), 1.97 (ddt, J = 13.3, 7.4, 6.9 Hz, 1H), 1.75 (t, *J* = 2.5 Hz, 3H), 1.68 – 1.56 (m, 1H), 1.33 – 1.16 (m, 3H); ^{13}C NMR (101 MHz, $CDCl_3$) δ 176.7, 153.0, 135.3, 129.5, 128.9, 127.4, 78.1, 76.4, 66.1, 55.3, 37.9, 36.9, 32.3, 17.5, 16.6, 3.5; $[\alpha]_D^{20}$= − 47.3 (*c* = 1.02, $CHCl_3$); IR (film): $\tilde{\nu}$ = 3030, 2971, 2920, 2857, 2857, 1779, 1696, 1604, 1481, 1481, 1455, 1386, 1350, 1290, 1247; 1212, 1105, 1075, 1049, 1015, 974, 924, 762, 746, 703, 507 cm^{-1}; HRMS-EI (*m/z*): calc'd. for $C_{18}H_{21}NO_3$ $[M]^{+\cdot}$, 299.1515; found, 299.1515.

(2*R*,3*R*)-3-Methyl-1-(4-tosyloxazol-5-yl)oct-6-yn-2-ol (7a)

(2*R*,3*R*)-3-methyl-1-(4-tosyloxazol-5-yl)oct-6-yn-2-ol **7a** was prepared by a five-step telescoped sequence starting from (*R*)-4-benzyl-3-((*R*)-2-methylhept-5-ynoyl)oxazolidin-2-one **19** .

Step 1 (Hydrolysis):

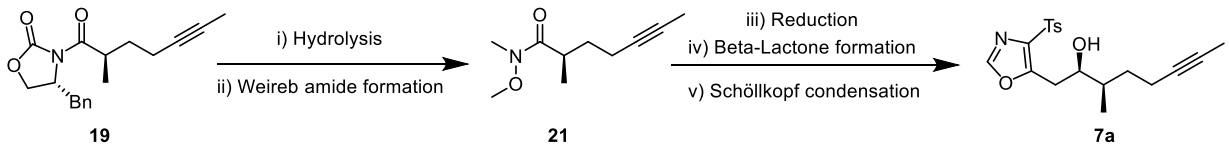

(*R*)-2-Methylhept-5-ynoic acid (20)

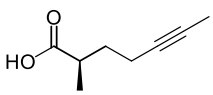

A one-neck round-bottomed flask equipped with a stir bar, was charged with a solution of (*R*)-4-benzyl-3-((*R*)-2-methylhept-5-ynoyl)oxazolidin-2-one **19** (3.6 g, 12 mmol) in THF-H_2O (50 mL, 1:1). The reaction mixture was cooled to 0 °C, before H_2O_2 (4.7 mL, 48 mmol, 4.0 equiv., 35 % w/w, aq.) and LiOH (0.57 g, 24 mmol, 2.0 equiv.) were added. The resulting mixture was allowed to warm to rt and then stirred overnight. After that the THF was evaporated under reduced pressure and the aqueous fraction obtained was extracted with CH_2Cl_2 (2 x 50 mL). The aqueous solution was then acidified with dilute HCl (1 M,aq) to pH ~1 and re-extracted with CH_2Cl_2 (4 x 50 mL). The combined organic extracts were dried over $MgSO_4$, filtered and then concentrated under reduced pressure. This gave the product as a colourless oil (2 g, 95 %, 93 %*ee*). ^{1}H NMR (400 MHz, $CDCl_3$): δ = 2.72 – 2.58 (m, 1H), 2.21 (tp, *J* = 7.4, 2.4 Hz, 2H), 1.91 (dtd, *J* = 13.4, 7.4, 6.9 Hz, 1H), 1.77 (t, *J* = 2.4 Hz, 3H), 1.59 (dtd, *J* = 13.4, 7.4, 6.5 Hz, 1H), 1.21 (d, *J* = 7.4 Hz, 3H). ^{13}C NMR (101 MHz, $CDCl_3$): δ = 182.4, 78.3, 76.9, 38.5, 32.8, 17.10, 17.06, 3.9. $[\alpha]_D^{20}$ = −51.8 (c = 1.05, $CHCl_3$); IR (film): $\tilde{\nu}$ = 2974, 2921, 2660, 1702, 1465, 1418, 1379, 1287, 1244, 1203, 1181, 1125, 1061, 939, 801, 638, 538, 467, 409 cm^{-1}; HRMS-CI (*m/z*): calc'd. for $C_8H_{13}O_2$ $[M+H]^+$, 141.0910; found, 141.0909; R_t (Minor Enantiomer, HPLC Method 1) = 5.42 min; R_t (Major Enantiomer, HPLC Method 1) = 5.96 min.

Step 2 (Weinreb amide formation):

(*R*)-*N*-Methoxy-*N*,2-dimethylhept-5-ynamide (21):

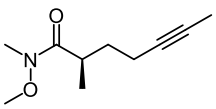

A two-neck round round-bottomed flask equipped with a magnetic stir bar, a glass stopper and a gas inlet connected to an argon-vacuum manifold, was charged with solution of acid **20** (1.6 g, 11mmol) in CH_2Cl_2 (56 mL). Upon cooling to 0 °C, 1,1-carbonyldiimidazole (2.4 g, 14 mmol, 1.2 equiv.) was added and the resulting mixture was stirred at this temperature for 0.5 h. After that *N,O*-dimethylhydroxylamine-hydrochloride (2.9 g, 30 mmol, 2.5 equiv.) was added and the reaction mixture was allowed to stir at rt overnight. The slurry obtained was then filtered and the filtrate was washed with dilute HCl (30 mL, 1 M, aq.). The organic phase was then dried over $MgSO_4$, filtered, and then concentrated under reduced pressure. The residue obtained (2.0 g, a mixture of the desired amide **21** and residual Weinreb amine) was then progressed to the next step without any further purification, due concerns about potential racemization. ^{1}H NMR (400 MHz, $CDCl_3$): δ = 3.72 (s, 3H), 3.67 (s, 3H), 3.19 (s, 3H), 3.08 (s, 3H), 2.22 – 2.08 (m, 2H), 1.89 (ddt, *J* = 13.4, 8.4, 6.9 Hz, 1H), 1.76 (t, *J* = 2.6 Hz, 3H), 1.57 – 1.44 (m, 1H), 1.12 (d, *J* = 6.9 Hz, 3H). ^{13}C NMR (101 MHz, $CDCl_3$) δ 79.2, 76.3, 61.8, 61.0, 36.6, 34.5, 33.0, 17.7, 17.2, 3.9. HRMS-EI (*m/z*): calc'd. for $C_{10}H_{17}NO_2$ $[M]^{+\cdot}$, 183.1253; found, 183.1254; 94 %*ee*; R_t (Minor Enantiomer, HPLC Method 2) = 10.43 min; R_t (Major Enantiomer, HPLC Method 2) = 11.02 min.

Step 3 & 4 (Weinreb Amide reduction & Cyclocondensation):

A three-neck jacketed vessel equipped with a stir bar, a gas inlet connected to an argon-vacuum manifold, a ground-glass joint thermometer adapter connected to low temperature thermometer and a rubber septum was charged with a solution of the crude amide **21** (2.0 g, 12 mmol) in CH_2Cl_2 (56 mL). The reaction mixture was cooled to –78 °C and DIBAL-H (16 mL, 16 mmol, 1.5 equiv., 1.0 M in *n*-hexanes) was added dropwise. The resulting mixture stirred for 1 h at this temperature, before it was quenched with Rochelle salt (50 mL, sat.aq.). The slurry immediately formed was allowed to warm to rt. The biphasic mixture obtained was then separated and the aqueous layer was extracted with CH_2Cl_2 (3 x 50 mL). The combined organic extracts were dried over $MgSO_4$, filtered, and then concentrated under reduced pressure (300 mbar) at rt. The crude aldehyde **9a** was engaged to the next without any purification. A three-neck jacketed vessel equipped with a stir bar, a gas inlet connected to an argon-vacuum manifold, a

ground-glass joint thermometer adapter connected to low temperature thermometer and a rubber septum was charged with a solution of lithium perchlorate (1.1 g, 11 mmol, 0.9 equiv.) in Et_2O (17 mL) and a solution of TMS*q* (0.4 g, 1.1 mmol, 10 mol%) in CH_2Cl_2 (34 mL). The mixture was stirred for 0.5 h at rt and then cooled to –78 °C. DIPEA (4.7 mL, 27 mmol, 2.3 equiv.) was added, followed by a solution of the crude aldehyde **9a** in CH_2Cl_2 -Et_2O (51 mL, 2:1). A solution of AcCl (1.1 mL, 16 mmol, 1.3 equiv.) in CH_2Cl_2 (9 mL) was added via syringe pump over 5 h and the resulting mixture was stirred at –78 °C for 24 h. The reaction mixture was diluted with Et_2O (50 mL) and then allowed to warm to rt. The yellow suspension obtained was then filtered through a silica plug eluting with Et_2O (100 mL) and the filtrate obtained was concentrated under reduced pressure (300 mbar) at rt. This afforded the crude beta-lactone **8a** as a pale-yellow oil (96:4 *dr*), which was subjected to the next step without any purification.

Step 5 (Schöllkopf Condensation):

A three-neck jacketed vessel equipped with a stir bar, a gas inlet connected to an argon-vacuum manifold, a ground-glass joint thermometer adapter connected to low temperature thermometer and a rubber septum, was charged with a solution of TosMIC (2.2 g, 11 mmol, 1.0 equiv.) in THF (120 mL). The solution was cooled to –78 °C and ^{n}BuLi (7.5 mL, 12 mmol, 1.0 equiv., 1.6 M in n-hexane) was added dropwise. The pale-yellow solution obtained was stirred at –78 °C for 0.5 h, before a solution of the crude beta-lactone **8a** in THF (20 mL) was added. The resulting mixture was stirred at –78 °C for an hour and then warmed to rt. The reaction was then quenched with HCl (20 mL, 1.0 M, aq.) and extracted with EtOAc (3 x 100 mL). The combined organic extracts were dried over $MgSO_4$, filtered and then concentrated under reduced pressure. The dark brown oily residue obtained was purified by flash column chromatography (SiO_2, 100 g, 55 mm ø, 0-100% EtOAc/iso-Hexanes, ca. 20 mL). This gave the product **7a** as an orange viscous oil (1.5 g, 35 % yield over 5 steps, 96:4 *dr*). ^{1}H NMR (400 MHz, $CDCl_3$): δ = 7.90 – 7.83 (m, 2H), 7.69 (s, 1H), 7.32 – 7.24 (m, 2H), 3.88 (ddt, *J* = 9.6, 6.8, 3.6 Hz, 1H), 3.27 (dd, *J* = 14.8, 9.6 Hz, 1H), 3.13 (dd, *J* = 14.8, 3.6 Hz, 1H), 2.36 (s, 3H), 2.26 – 2.03 (m, 2H), 1.94 (d, *J* = 6.6 Hz, 1H), 1.79 – 1.59 (m, 4H), 1.38 (dddd, *J* = 13.3, 8.4, 7.1, 6.8 Hz, 1H), 0.94 (d, *J* = 6.8 Hz, 3H); ^{13}C NMR (101 MHz, $CDCl_3$): δ = 155.4, 150.2, 145.5, 137.4, 137.2, 130.4, 128.6, 79.2, 76.6, 73.7, 38.3, 32.6, 31.5, 22.2, 16.9, 13.7, 3.9; $[\alpha]_D^{20}$= + 21.0 (c = 2.41, $CHCl_3$); IR (film): $\tilde{\nu}$ = 3527, 3128, 2921, 1595, 1517, 1494, 1449, 1402, 1382, 1342, 1305, 1245, 1217, 1147, 1085, 1059, 1017, 854, 815, 709, 697, 663, 601, 540, 502 cm^{-1}; HRMS-ESI+ (*m/z*): calc'd. for $C_{19}H_{23}NO_4SNa$ $[M+Na]^+$, 384.1240; found, 384.1241.

5-((2*R*,3*R*)-3-Methyl-2-((*R*)-2,2,2-trifluoro-1-methoxy-1-phenylethoxy)oct-6-yn-1-yl)-4-tosyloxazole (31)

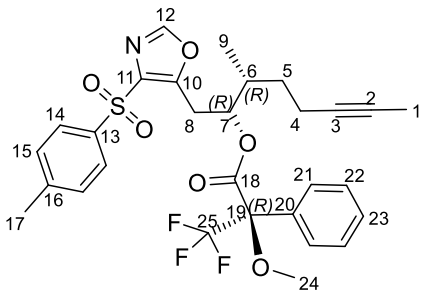

A Schleck tube equipped a magnetic stir bar was charged with a solution of (2*R*,3*R*)-3-methyl-1-(4-tosyloxazol-5-yl)oct-6-yn-2-ol **7a** (45 mg, 0.12 mmol, 1.5 equiv.) in CH_2Cl_2 (1 mL), DMAP (1.0 mg, 6.3 µmol, 10 mol%) and TEA (35 µL, 0.25 µmol, 3.0 equiv.). (S)-(+)-MTPACl (12 µL, 63 µmol) was added and the resulting mixture was stirred overnight at rt. After that the solvent was evaporated under reduced pressure. The residue was purified by flash column chromatography (SiO_2, 10 g, 20 mm ø, 0-50% EtOAc/iso-Hexanes, ca. 5 mL). This gave the product as a pale yellow oil (28 mg, 77 %).^{1}H NMR (600 MHz, $CDCl_3$): δ = 7.94 – 7.90 (m, 2H), 7.44 (s, 1H), 7.38 – 7.32 (m, 6H), 7.31 – 7.27 (m, 2H), 5.49 (ddd, *J* = 9.2, 4.4, 3.2 Hz, 1H), 3.51 – 3.47 (m, 4H), 3.31 (dd, *J* = 15.3, 9.2 Hz, 1H), 2.43 (s, 3H), 2.30 – 2.22 (m, 1H), 2.18 – 2.07 (m, 1H), 1.71 (t, *J* = 2.5 Hz, 3H), 1.65 (dddd, *J* = 13.2, 8.3, 6.9, 4.9 Hz, 1H), 1.35 (dddd, *J* = 13.2, 9.2, 6.9, 6.1 Hz, 1H), 1.05 (d, *J* = 6.9 Hz, 3H); ^{13}C NMR (151 MHz, $CDCl_3$): δ = 166.0, 152.5, 149.9, 145.1, 136.8, 136.7, 131.8, 129.9, 129.5, 129.5, 128.5, 128.4, 128.24, 128.21, 127.13, 127.06, 126.0, 123.14 (q, *J* = 288.7 Hz), 84.6, 77.7, 77.2, 77.0, 76.8, 76.5, 55.4, 35.2, 31.0, 27.1, 21.7, 16.3, 14.0, 3.4; IR (film): $\tilde{\nu}$ =3130, 2923, 1746, 1595, 1515, 1495, 1451, 1386, 1329, 1291, 1248, 1169, 1148, 1120, 1083, 1018, 998, 933, 815, 766, 719, 697, 662, 601, 540 cm^{-1}; $[\alpha]_D^{20}$= + 9.7 (c = 1.31, $CHCl_3$); HRMS-ESI+ (*m/z*): calc'd. for $C_{29}H_{30}F_3NO_6SNa$ $[M+Na]^+$, 600.1638; found, 600.1640.

5-((2*R*,3*R*)-3-Methyl-2-((*S*)-2,2,2-trifluoro-1-methoxy-1-phenylethoxy)oct-6-yn-1-yl)-4-tosyloxazole (32)

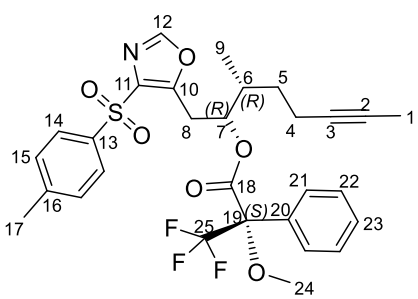

A Schleck tube equipped a magnetic stir bar was charged with a solution of (2*R*,3*R*)-3-methyl-1-(4-tosyloxazol-5-yl)oct-6-yn-2-ol **7a** (45 mg, 100 µmol, 1.5 equiv.) in CH_2Cl_2 (1.0 mL), DMAP (1 mg, 6 µmol, 10.0 mol%) and TEA (35 µL, 300 µmol, 3.0 equiv.). (R)-(-)-MTPACl (12 µL, 63 µmol) was added and the resulting mixture was stirred overnight at rt. After that the solvent was evaporated under reduced pressure. The residue

was purified by flash column chromatography (SiO_2, 10 g, 20 mm ø, 0-50% EtOAc/iso-Hexanes, ca. 5 mL). This gave the product as a pale yellow oil (26 mg, 72 %).^{1}H NMR (600 MHz, $CDCl_3$): δ = 7.94 – 7.90 (m, 2H), 7.44 (s, 1H), 7.38 – 7.32 (m, 6H), 7.31 – 7.27 (m, 2H), 5.49 (ddd, *J* = 9.2, 4.4, 3.2 Hz, 1H), 3.51 – 3.47 (m, 4H), 3.31 (dd, *J* = 15.3, 9.3 Hz, 1H), 2.43 (s, 3H), 2.30 – 2.22 (m, 1H), 2.18 – 2.07 (m, 1H), 1.71 (t, *J* = 2.5 Hz, 3H), 1.65 (dddd, *J* = 13.3, 8.3, 7.0, 4.9 Hz, 1H), 1.35 (dddd, *J* = 13.2, 9.2, 6.9, 6.1 Hz, 1H), 1.05 (d, *J* = 6.9 Hz, 3H); ^{13}C NMR (151 MHz, $CDCl_3$): δ = 166.0, 152.5, 149.9, 145.1, 136.8, 136.7, 131.8, 129.9, 129.5, 129.5, 128.5, 128.4, 128.2, 128.2, 127.1, 127.1, 126.0, 123.3 (q, *J* = 288.5 Hz), 84.6, 77.7, 77.2, 77.0, 76.8, 76.5, 55.4, 35.2, 31.0, 27.1, 21.7, 16.3, 14.0, 3.4; IR (film): $\tilde{\nu}$ = 3129, 2923, 1746, 1595, 1515, 1494, 1451, 1385, 1329, 1291, 1248, 1169, 1148, 1120, 1083, 1018, 997, 932, 815, 765, 719, 697, 662, 601, 540 cm^{-1}; $[\alpha]_D^{20}$= - 14.1 (c = 1.22, $CHCl_3$); HRMS-ESI+ (*m/z*): calc'd. for $C_{29}H_{30}F_3NO_6SNa$ $[M+Na]^+$, 600.1638; found, 600.1641.

(*R*)-4-Benzyl-3-(non-7-ynoyl)oxazolidin-2-one (39)

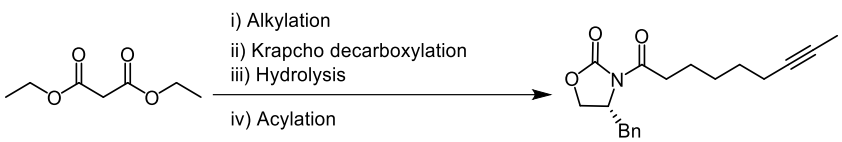

39

Step 1 (Alkylation):

A two-neck round bottom flask equipped with a stir bar, rubber septum and an argon bridge was charged with NaH (0.4 g, 14 mmol, 1.1 equiv.) and DMF (38 mL). The resulting suspension was cooled to 0°C over an ice-bath. Diethyl malonate (2.2 g, 13 mmol) was added, and the resulting mixture was stirred for 0.5 h at 0 °C. After that 7-iodohept-2-yne **36** (3.0 g, 14 mmol, 1.1 equiv.) was added and reaction mixture was allowed to warm to rt and then stirred overnight. The reaction mixture was quenched with brine (200 mL) and then extracted with Et_2O (4 x 100 mL). The combined organic extracts were then dried over $MgSO_4$, filtered and then concentrated under reduced pressure. The yellow oil obtained was carried forward without any purification.

Step 2 (Krapcho Decarboxylation):

A round bottom flask equipped with a reflux condenser and a stir bar was charged with a solution of the crude diethyl 2-(hept-5-yn-1-yl)malonate in DMSO (24 mL), water (0.1 mL, 5.6 mmol, 0.4 equiv.) and LiCl (1.3 g, 30 mmol, 2.2 equiv.). The resulting mixture was heated at 160 °C overnight. Upon cooling to rt, the reaction mixture was diluted with brine (250 mL) and extracted with Et_2O (3 x 100 mL). The combined

organic extracts were dried over $MgSO_4$, filtered and then concentrated under reduced pressure. The brown oil obtained was then carried forward without any purification.

Step 3 (Hydrolysis):

A round bottom flask equipped with a stir bar was charged with a solution of the crude ethyl non-7-ynoate in THF (115 mL) and the flask was cooled to 0 °C. A solution of LiOH (2.3 g, 97 mmol, 3.0 equiv.) in water (115 mL) was added and the resulting mixture was allowed to warm to rt and then stirred overnight. The THF was removed under reduced pressure and the aqueous fraction obtained was acidified to pH 1 with conc. HCl. The resulting mixture was extracted with EtOAc (3 x 100 mL) and the combined organic extracts were dried over $MgSO_4$, filtered and then concentrated under reduced pressure. This gave the acid **37** as a white solid, which was used directly in the next step.

Step 4 (Acylation):

A three-neck jacketed glass reaction vessel equipped with a magnetic stir bar, a pressure equalizing addition funnel and a gas inlet connected to an argon-vacuum manifold, was charged with solution of the crude 7-nonynoic acid **48** (6.0 g, 13 mmol) in THF (70 mL) and TEA (4.8 mL, 34 mmol, 2.6 equiv.). The reaction mixture was then cool to - 10°C and PvCl (1.6 mL, 13 mmol, 1.0 equiv.) dropwise. The white slurry immediately formed was stirred at this temperature for 1 h. Then, a solution of (*R*)-4-benzyloxazolidin-2-one (2.2 g, 12 mmol, 1.0 equiv.) and TEA (2.3 mL, 17 mmol, 3.0 equiv.) in THF (7.4 mL) was added. The resulting mixture was allowed to warm to rt and then stirred overnight. The reaction mixture was quenched with $NaHCO_3$ (100 mL, sat. aq.) and extracted with EtOAc (3 x 100 mL). The combined organic layers were washed with brine (100 mL), dried $MgSO_4$, filtered and then concentrated under reduced pressure. The residue was purified by flash column chromatography (SiO_2, 100 g, 55 mm ø, 0-50% EtOAc/iso-Hexanes, ca. 20 mL). This gave the product **39** as a pale yellow oil (1.0 g, 24 %). ^{1}H NMR (400 MHz, $CDCl_3$): δ = 7.32 – 7.22 (m, 2H), 7.24 – 7.19 (m, 1H), 7.16 – 7.10 (m, 2H), 4.67 – 4.52 (m, 1H), 4.17 – 4.09 (m, 2H), 3.23 (dd, *J* = 13.3, 3.3 Hz, 1H), 2.97 – 2.78 (m, 2H), 2.76 – 2.64 (m, 1H), 2.08 (tq, J = 7.0, 2.6 Hz, 2H), 1.70 (t, J = 2.6 Hz, 3H), 1.68 – 1.59 (m, 2H), 1.52 – 1.35 (m, 4H).; ^{13}C NMR (151 MHz, $CDCl_3$): δ = 173.3, 153.5, 135.3, 129.4, 128.9, 127.4, 79.0, 75.6, 66.2, 55.2, 37.9, 34.9, 28.8, 28.3, 23.8, 18.6, 3.5; IR (film): $\tilde{\nu}$ = 3029, 2923, 2859, 1776, 1698, 1604, 1497, 1480, 1454, 1386, 1351, 1329, 1291, 1212, 1198, 1156, 1111, 1078, 1051, 1016, 921, 844, 762, 746, 703, 621, 595, 504 cm^{-1}; $[\alpha]_D^{20}$= -43.9 (c = 1.48, $CHCl_3$); HRMS-ESI+ (*m/z*): calc'd. for $C_{19}H_{23}NO_3Na$ $[M+Na]^+$,336.1570; found 336.1566.

(*R*)-4-Benzyl-3-((*R*)-2-methylnon-7-ynoyl)oxazolidin-2-one (40)

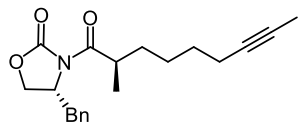

A three-neck jacketed vessel equipped with a stir bar, a gas inlet connected to an argon-vacuum manifold, a ground-glass joint thermometer adapter connected to low temperature thermometer and a rubber septum was charged with a solution of (*R*)-4-benzyl-3-(non-7-ynoyl)oxazolidin-2-one **39** (4.0 g, 13 mmol) in THF (75 mL). The reaction mixture was cooled to –78 °C. A solution of NaHMDS (13 mL, 19 mmol, 1.5 equiv., 1.5 M solution in THF) was added dropwise. The resulting pale yellow mixture was stirred for 1 h at - 78 °C. The reaction mixture was then treated with MeI (4.0 mL, 63.8 mmol, 5.0 equiv.) and stirred for additional 4.5 h at -78 °C. The yellow reaction was quenched with AcOH (7.3 mL) and warmed up to room temperature. The yellow slurry obtained was then diluted with water (200 mL) and extracted with EtOAc (3 x 250 mL). The combined organic layers were dried over $MgSO_4$, filtered and then concentrated under reduced pressure. The residue was purified by flash column chromatography (SiO_2, 100 g, 55 mm ø, 0-40% EtOAc/iso-Hexanes, ca. 20 mL). This gave the product as a colourless oil (4.1 g, 98 %). ^{1}H NMR (400 MHz, $CDCl_3$) δ = 7.26 (ddt, m, 2H), 7.23 – 7.20 (m, 1H), 7.17 – 7.11 (m, 2H), 4.61 (ddt, *J* = 9.6, 7.3, 3.3 Hz, 1H), 4.18 – 4.04 (m, 2H), 3.73 – 3.58 (m, 1H), 3.20 (dd, *J* = 13.3, 3.3 Hz, 1H), 2.70 (dd, *J* = 13.3, 9.6 Hz, 1H), 2.12 – 2.00 (m, 2H), 1.70 (t, *J* = 2.5 Hz, 4H), 1.52 – 1.25 (m, 5H), 1.16 (d, *J* = 6.8 Hz, 3H); ^{13}C NMR (101 MHz, $CDCl_3$) δ = 177.7, 153.5, 135.8, 129.9, 129.4, 127.8, 79.5, 76.1, 66.5, 55.8, 38.4, 38.1, 33.3, 29.4, 26.9, 19.1, 17.8, 3.9; $[\alpha]_D^{20}$= − 62.2 (*c* = 1.03, $CHCl_3$); IR (film): $\tilde{\nu}$ = 3065, 3028, 2934, 2861, 1780, 1697, 1650, 1494, 1481, 1454, 1386, 1350, 1290, 1237, 1211, 1107, 1015, 972, 762, 747, 703, 522, 509, 411 cm^{-1}; HRMS-GC-EI (*m/z*): calc'd. for $C_{20}H_{25}NO_3$ $[M]^{+\cdot}$, 327.1828; found, 327.1830.

(2*R*,3*R*)-3-M/ethyl-1-(4-tosyloxazol-5-yl)dec-8-yn-2-ol (7b)

(2*R*,3*R*)-3-methyl-1-(4-tosyloxazol-5-yl)dec-8-yn-2-ol **7b** was prepared by a five-step telescoped sequence starting from (*R*)-4-benzyl-3-((*R*)-2-methylnon-7-ynoyl)oxazolidin-2-one **40**.

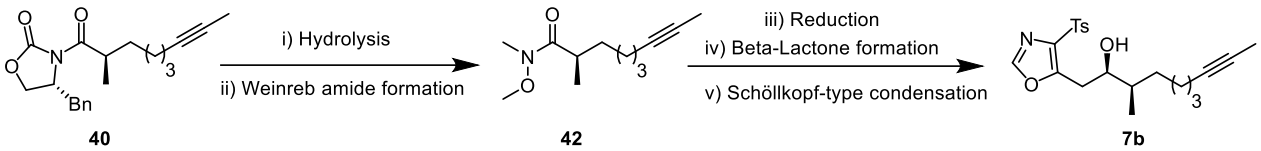

40 **42** **7b**

Steps 1-2 (Hydrolysis and Amidation):

A round-bottom flask equipped with a stir bar, was charged with a solution of (*R*)-4-benzyl-3-((*R*)-2-methylnon-7-ynoyl)oxazolidin-2-one **40** (4.2 g, 13 mmol) in THF-H_2O (45 mL, 1:1). The reaction mixture was cooled to 0 °C, before H_2O_2 (5.0 mL, 51.8 mmol, 4.0 equiv., 35 % w/w, aq.) and LiOH (0.6 g, 26 mmol, 2.0 equiv.) were added. The resulting mixture was allowed to warm to rt and then stirred overnight. After that the THF was evaporated under reduced pressure and the aqueous fraction obtained was extracted with CH_2Cl_2 (3 x 50 mL). The aqueous solution was then acidified with dilute HCl (1 M,aq) to pH 1 and re-extracted with CH_2Cl_2 (4 x 50 mL). The combined organic extracts were dried over $MgSO_4$, filtered and then concentrated under reduced pressure. This gave the product as a colourless oil (2.0 g, 91 %, 94 %*ee*). ^{1}H NMR (400 MHz, $CDCl_3$): δ = 2.47 – 2.34 (m, 2H), 2.13 – 2.01 (m, 2H), 1.71 (t, *J* = 2.6 Hz, 3H), 1.69 – 1.55 (m, 1H), 1.48 – 1.29 (m, 4H), 1.12 (d, *J* = 7.0 Hz, 3H); R_t (Minor Enantiomer, HPLC Method 3) = 8.49 min; R_t (Major Enantiomer, HPLC Method 3) = 8.06 min.

A two-neck round round-bottomed flask equipped with a magnetic stir bar, a glass stopper and a gas inlet connected to an argon-vacuum manifold, was charged with solution of the crude acid **41** (1.6 g, 11 mmol) in CH_2Cl_2 (56 mL). Upon cooling to 0 °C, 1,1-carbonyldiimidazole (2.6 g, 16 mmol, 1.2 equiv.) was added and the resulting mixture was stirred at this temperature for 0.5 h. After that *N,O*-dimethylhydroxylamine-hydrochloride (3.2 g, 32 mmol, 2.5 equiv.) was added and the reaction mixture was allowed to rt overnight. The slurry obtained was then filtered and the filtrate was washed with dilute HCl (30 mL, 1 M, aq.). The organic phase was then dried over $MgSO_4$, filtered, and then concentrated under reduced pressure. This afforded the amide **42** as a colourless oil (2.2 g, 82% over two steps, 92 %*ee*). ^{1}H NMR (400 MHz, $CDCl_3$): δ = 3.69 (s, 3H), 3.19 (s, 3H), 2.16 – 2.06 (m, 2H), 1.77 (t, *J* = 2.5 Hz, 3H), 1.70 – 1.32 (m, 7H), 1.11 (d, *J* = 6.8 Hz, 3H); ^{13}C NMR (101 MHz, $CDCl_3$) δ = 178.6, 79.6, 75.9, 61.9, 35.5, 33.8, 32.7, 29.6, 27.3, 19.1, 17.9, 3.9; IR (film): $\tilde{\nu}$ = 2935, 2860, 1661, 1462, 1415, 1385, 1318, 1176, 1118, 1089, 995, 741, 711, 599, 526, 437 cm^{-1}; $[\alpha]_D^{20}$ = – 17.2 (*c* = 1.14,

$CHCl_3$); HRMS-ESI+ (*m/z*): calc'd. for $C_{12}H_{21}NO_2Na$ $[M+Na]^+$, 234.1464; found, 234.1464; R_t (Minor Enantiomer, HPLC Method 4) = 3.70 min; R_t (Major Enantiomer, HPLC Method 4) = 3.29 min.

Steps 3-4 (Weinreb Amide Reduction & Cyclocondesation):

A three-neck jacketed vessel equipped with a stir bar, a gas inlet connected to an argon-vacuum manifold, a ground-glass joint thermometer adapter connected to low temperature thermometer and a rubber septum was charged with a solution of the crude amide **13b** (2.2 g, 11 mmol) in CH_2Cl_2 (60 mL). The reaction mixture was cooled to –78 °C and DIBAL-H (11 mL, 11 mmol, 1.0 equiv., 1.0 M in *n*-hexane) was added dropwise. The resulting mixture stirred for 1 h at this temperature, before it was quenched with Rochelle salt (50 mL, sat.aq.). The slurry immediately formed was allowed to warm to rt. The biphasic mixture obtained was then separated and the aqueous layer was extracted with CH_2Cl_2 (3 x 50 mL). The combined organic extracts were dried over $MgSO_4$, filtered, and then concentrated under reduced pressure (300m mbar) at rt. The crude aldehyde **9b** was engaged to the next without any purification. A three-neck jacketed vessel equipped with a stir bar, a gas inlet connected to an argon-vacuum manifold, a ground-glass joint thermometer adapter connected to low temperature thermometer and a rubber septum was charged with a solution of lithium perchlorate (1.2 g, 11 mmol, 1.0 equiv.) in Et_2O (17 mL) and a solution of TMS*q* **14** (0.42 g, 1.1 mmol, 10 mol%) in CH_2Cl_2 (35 mL). The mixture was stirred for 0.5 h at rt and then cooled to –78 °C. DIPEA (4.7 mL, 27 mmol, 2.3 equiv.) was added, followed by a solution of the crude aldehyde **9b** in CH_2Cl_2 - Et_2O (51 mL, 2:1). A solution of AcCl (1.1 mL, 16 mmol, 1.3 equiv.) in CH_2Cl_2 (9 mL) was added via syringe pump over 5 h and the resulting mixture was stirred at –78 °C for 24 h. The reaction mixture was diluted with Et_2O (50 mL) and then allowed to warm to rt. The yellow suspension obtained was then filtered through a silica plug eluting with Et_2O (100 mL) and the filtrate obtained was concentrated under reduced pressure (300 mbar) at rt. This afforded the crude beta-lactone **8b** as a pale-yellow oil (> 99:1 dr), which was subjected to the next step without any purification.

Step 5 (Schöllkopf Condensation):

A three-neck jacketed vessel equipped with a stir bar, a gas inlet connected to an argon-vacuum manifold, a ground-glass joint thermometer adapter connected to low temperature thermometer and a rubber septum, was charged with a solution of TosMIC (2.0 g, 10 mmol, 1.0 equiv.) in THF (41 mL). The solution was cooled to –78 °C and ^{n}BuLi (6.6 mL, 12 mmol, 1.0 equiv., 1.6 M in *n*-hexanes) was added dropwise. The pale-yellow solution obtained was stirred at –78 °C for 0.5 h, before a solution of the crude beta-lactone **8b** in THF (20 mL) was added. The resulting mixture was stirred at –78 °C for an hour and then warmed to rt. The reaction was then quenched with HCl (20 mL, 1.0 M, aq.) and extracted with EtOAc (3 x 100 mL). The combined organic extracts were dried over $MgSO_4$,

filtered and then concentrated under reduced pressure. The dark brown oily residue obtained was purified by flash column chromatography (SiO_2, 100 g, 55 mm ø, 0-100% EtOAc/iso-Hexanes, ca. 20 mL). This gave the product **7b** as an orange viscous oil (2.2 g, 43 % yield over 5 steps, > 95:5 dr). ^{1}H NMR (400 MHz, $CDCl_3$): δ = 8.00 – 7.86 (m, 2H), 7.75 (s, 1H), 7.40 – 7.28 (m, 2H), 3.91 (dq, *J* = 9.8, 4.6 Hz, 1H), 3.37 – 3.24 (m, 1H), 3.18 (dd, *J* = 9.8, 3.5 Hz, 1H), 2.43 (s, 3H), 2.15 (ddt, *J* = 6.9, 4.6, 2.6 Hz, 2H), 1.88 (d, *J* = 6.4 Hz, 1H), 1.78 (t, *J* = 2.6 Hz, 3H), 1.53 – 1.17 (m, 7H), 1.01 (d, *J* = 6.9 Hz, 3H); ^{13}C NMR (101 MHz, $CDCl_3$): δ = 155.5, 149.5, 146.4, 137.9, 136.2, 130.4, 128.6, 79.6, 76.1, 74.2, 40.8, 33.5, 31.5, 28.5, 25.6, 22.7, 19.1, 14.1, 3.9; $[\alpha]_D^{20}$= + 24.7 (c = 2.84, $CHCl_3$); IR (film): ῦ = 3527, 3129, 2932,2859, 1594, 1517, 1494, 1460, 1402, 1381, 1323, 1305, 1244, 1216, 1146, 1085, 1060, 1017, 932, 860, 814, 754, 706, 696, 661, 600, 439, 494 cm^{-1}; HRMS-ESI+ (m/z): calc'd. for $C_{21}H_{27}N_1O_4S_1Na^+$ $[M+Na]^+$, 412.1556; found, 412.1557.

(2*R*,3*R*)-3-Methyl-1-(4-tosyloxazol-5-yl)dec-8-yn-2-yl (*R*)-3,3,3-trifluoro-2-methoxy-2-phenyl propanoate (43)

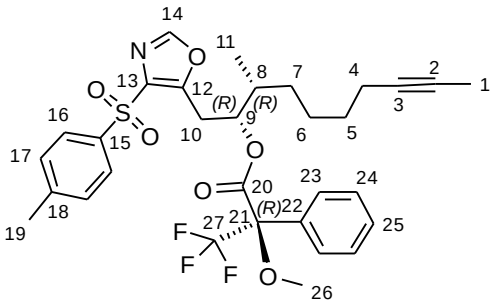

A Schleck tube equipped a magnetic stir bar was charged a solution of (2*R*,3*R*)-3-methyl-1-(4-tosyloxazol-5-yl)dec-8-yn-2-ol **7b** (39 mg, 97 µmol, 1.5 equiv.) in CH_2Cl_2 (1 mL), DMAP (1 mg, 6 µmol, 10 mol%) and TEA (20 µL, 200 µmol, 3.0 equiv.). (S)-(+)-MTPACl (12 µL, 65 µmol) was added and the resulting mixture was stirred overnight at rt. After that the solvent was evaporated under reduced pressure. The residue was purified by flash column chromatography (SiO_2, 10 g, 20 mm ø, 0-50% EtOAc/iso-Hexanes, ca. 5 mL). This gave the product as a pale yellow oil (33 mg, 85 %).^{1}H NMR (600 MHz, $CDCl_3$): δ = 7.94 – 7.89 (m, 2H), 7.47 (s, 1H), 7.39 – 7.33 (m, 5H), 7.33 – 7.28 (m, 2H), 5.48 (ddd, *J* = 9.2, 4.3, 3.4 Hz, 1H), 3.47 (dd, *J* = 15.3, 4.3 Hz, 1H), 3.45 (q, *J* = 1.2 Hz, 3H), 3.32 (dd, *J* = 15.3, 9.2 Hz, 1H), 2.43 (s, 3H), 2.12 (m, 2H), 1.86 – 1.79 (m, 1H), 1.77 (t, *J* = 2.6 Hz, 3H), 1.50 – 1.38 (m, 4H), 1.38 – 1.32 (m, 1H), 1.18 (dddd, *J* = 15.3, 10.2, 6.9 Hz, 1H), 1.04 (d, *J* = 6.9 Hz, 3H); ^{13}C NMR (151 MHz, $CDCl_3$): δ = 166.0, 152.6, 149.9, 145.1, 136.8, 136.7, 131.7, 129.9, 129.5, 128.5, 128.2, 127.2, 126.0 – 120.3 (q, *J* = 289.0 Hz) , 124.1, 122.2, 120.3, 84.8– 84.2 (q, *J* = 28.0 Hz) 78.9, 77.5, 75.7, 55.3, 36.7, 31.8, 29.0, 27.2, 26.4, 21.7, 18.6, 14.4, 3.4; IR (film): *ῦ* = 3134, 2937, 2859, 1746, 1595, 1515, 1495, 1451, 1386, 1329, 1292, 1252, 1169, 1149, 1121, 1084, 1018, 996, 932, 814, 766, 719, 697, 662, 601, 540, 505, 411 cm^{-1}; $[\alpha]_D^{20}$= + 15.4 (c = 1.14, $CHCl_3$); HRMS-ESI+ (*m/z*): calc'd. for $C_{31}H_{34}F_3NO_6SNa^+$ $[M+Na]^+$, 628.1951; found, 628.1956.

(2*R*,3*R*)-3-Methyl-1-(4-tosyloxazol-5-yl)dec-8-yn-2-yl (*S*)-3,3,3-trifluoro-2-methoxy-2-phenyl propanoate (44)

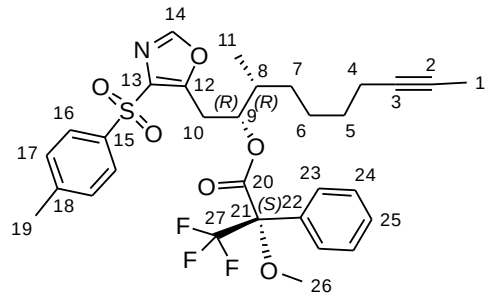

A Schleck tube equipped a magnetic stir bar was charged a solution of 2*R*,3*R*)-3-methyl-1-(4-tosyloxazol-5-yl)dec-8-yn-2-ol **7b** (39 mg, 97 µmol, 1.5 equiv.) in CH_2Cl_2 (1 mL), DMAP (1 mg, 6 µmol, 10 mol%) and TEA (20 µL, 200 µmol, 3.0 equiv.). (*R*)-(-)-MTPACl (12 µL, 65 µmol) was added and the resulting mixture was stirred overnight at rt. After that the solvent was evaporated under reduced pressure. The residue was purified by flash column chromatography (SiO_2, 10 g, 20 mm ø, 0-50% EtOAc/iso-Hexanes, ca. 5 mL). This gave the product as a pale yellow oil (34 mg, 88 %).^{1}H NMR (600 MHz, $CDCl_3$): δ = 7.93 – 7.89 (m, 2H), 7.65 (s, 1H), 7.37 – 7.27 (m, 7H), 5.50 (ddd, *J* = 8.6, 4.9, 3.3 Hz, 1H), 3.48 (dd, *J* = 15.5, 4.9 Hz, 1H), 3.44 (dd, *J* = 15.5, 8.6 Hz, 1H), 3.44 – 3.41 (m, 3H), 2.41 (s, 3H), 2.11 – 2.06 (m, 2H), 1.77 (t, *J* = 2.6 Hz, 3H), 1.37 (qd, *J* = 6.9, 4.9, 2.6 Hz, 2H), 1.33 – 1.24 (m, 2H), 1.14 – 1.06 (m, 1H), 1.00 (d, *J* = 6.9 Hz, 3H); ^{13}C NMR (151 MHz, $CDCl_3$): δ = 165.9, 152.7, 149.9, 145.1, 136.9, 136.7, 131.9, 129.9, 129.9, 129.6, 128.4, 128.2, 127.1, 126.1 – 121.4 (q, *J* = 289.0 Hz) , 124.2, 122.3, 120.4, 84.7– 84.2 (q, *J* = 28.0 Hz) 78.9, 77.3, 75.7, 55.3, 36.6, 31.6, 28.9, 27.4, 26.4, 21.7, 18.6, 14.2, 3.4; IR (film): $\tilde{\nu}$ = 3134, 2937, 2859, 1746, 1595, 1515, 1495, 1451, 1386, 1329, 1292, 1252, 1169, 1149, 1121, 1084, 1018, 996, 932, 814, 766, 719, 697, 662, 601, 540, 505, 487 cm^{-1}; $[\alpha]_D^{20}$= - 4.5 (c = 1.10, $CHCl_3$); HRMS-ESI+ (*m/z*): calc'd. for $C_{31}H_{34}F_3NO_6SNa$ $[M+Na]^+$, 628.1951; found, 628.1956.

(*R*)-*N*-((1*R*,2*R*)-1-Hydroxy-1-phenylpropan-2-yl)-N,2-dimethylhept-5-ynamide (46)

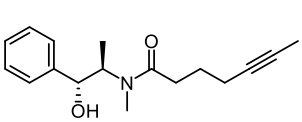

A three-neck jacketed glass reaction vessel equipped with a magnetic stir bar, a pressure equalizing addition funnel and a gas inlet connected to an argon-vacuum manifold, was charged with solution of 6-heptynoic acid (4.8 g, 38 mmol) in THF (50 mL) and TEA (16 mL, 114 mmol, 3.0 equiv.). The reaction mixture was then cool to - 10°C and PvCl (5.6 mL, 46 mmol, 1.2 equiv.) dropwise. The white slurry immediately formed was stirred at this temperature for 1 h. Then, a solution of (1*R*,2*R*)-2-(methylamino)-1-phenylpropan-1-ol **45** (8.3 g, 50 mmol, 1.3 equiv.) and TEA (16 mL, 114 mmol, 3.0 equiv.) in THF (50 mL) was added. The resulting mixture was allowed to warm to rt and then stirred overnight. The reaction mixture was quenched with $NaHCO_3$ (200 mL, sat. aq.) and extracted with EtOAc (3 x 150 mL). The combined organic layers were washed with brine (150 mL), dried $MgSO_4$, filtered and then concentrated under reduced pressure. The residue was purified by flash column chromatography (SiO_2, 100 g, 55 mm ø, 0-100% EtOAc/iso-Hexanes, ca. 20 mL). This gave the product as a pale-yellow oil (8.1 g, 86 %). ^{1}H NMR (600 MHz, DMSO): δ = 7.39 – 7.35 (m, 3H, major), 7.34 (dq, *J* = 7.8, 1.2 Hz, 2H, major), 7.33 – 7.31 (m, 2H, minor), 7.29 – 7.26 (m, 1H, major), 7.25 (dd, *J* = 3.3, 2.6 Hz, 1H, minor), 5.46 (d, *J* = 4.1 Hz, 1H, major), 5.25 (d, *J* = 4.3 Hz, 1H, minor), 4.64 (d, *J* = 8.0 Hz, 1H, minor), 4.53 (dd, *J* = 8.0, 4.3 Hz, 1H, minor), 4.49 (dd, J = 8.3, 4.1 Hz, 1H, major,minor), 3.91 (dq, *J* = 8.3, 6.8 Hz, 1H, major), 2.83 (s, 3H, minor), 2.76 (s, 3H, major), 2.37 (td, *J* = 7.4, 3.8 Hz, 2H, major), 2.29 (td, *J* = 7.3, 2.5 Hz, 2H, minor), 2.09 (ddtt, *J* = 9.8, 7.2, 4.7, 2.4 Hz, 3H, major, minor), 1.73 - 1.74 (t, *J* = 2.6 Hz, 3H, major, minor), 1.65 – 1.57 (m, 2H, major, minor), 0.91 (d, J = 6.8 Hz, 3H, major), 0.83 (d, *J* = 6.9 Hz, 3H, minor); ^{13}C NMR (151 MHz, DMSO): δ = 172.0 , 171.7, 143.5, 143.5, 128.0, 127.8, 127.3, 127.0, 126.8, 126.8, 79.07, 79.05, 75.92, 75.86, 73.77, 73.69, 57.2, 53.3, 32.0, 31.6, 29.6, 26.6, 24.6, 24.3, 17.8, 17.6, 15.3, 15.0, 3.1; ṽ = 3369, 3062, 3028, 2969, 2936, 2918, 1617, 1481, 1452, 1405, 1356, 1376, 1330, 1260, 1236, 1201, 1117, 1074, 1049, 1027, 1001, 838, 761, 702, 607, 519 cm^{-1}; $[\alpha]_D^{20}$= - 73.4 (c = 1.44, EtOH); HRMS-ESIpos (m/z): calc'd. for $C_{17}H_{23}N_1O_2Na_1$ $[M+Na]^+$, 296.16209; found, 296.16206.

(*R*)-*N*-((1*R*,2*R*)-1-Hydroxy-1-phenylpropan-2-yl)-*N*,2-dimethylhept-5-ynamide (47a)

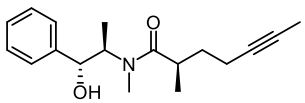

A three-neck jacketed vessel equipped with a stir bar, a gas inlet connected to an argon-vacuum manifold, a ground-glass joint thermometer adapter connected to low temperature thermometer and a rubber septum, was charged with a solution of lithium chloride (0.9 g, 20 mmol, 4.3 equiv.) and diisopropylamine (2.9 mL, 20 mmol, 4.3 equiv.) in THF (77 mL). Upon cooling of the mixture to 0 °C, ^{n}BuLi (4.8 mL, 7.6 mmol, 2.1 equiv., 1.6 M in *n*-hexanes) was added dropwise and the mixture was stirred at this temperature for 1 h. After that the reaction mixture was cooled to - 78 °C and a solution of *N*-((1*R*,2*R*)-1-hydroxy-1-phenylpropan-2-yl)-N-methylhept-5-ynamide **46** (1.0 g, 3.7 mmol, 1.0 equiv.) in THF (6 mL) was added dropwise. The mixture was then stirred for 1 h at - 78 °C, before it was warmed to 0 °C. MeI (0.5 mL, 7.3 mmol, 2.0 equiv.) was added and the resulting mixture was then stirred for 2 h at 0 °C. The reaction mixture was then quenched with NH_4Cl (100 mL, sat. aq.) and then extracted with EtOAc (3 x 100 mL). The combined organic extracts were dried over $MgSO_4$, filtered and then concentrated under reduced pressure. The orange oily residue obtained was then purified by flash column chromatography (SiO_2, 100 g, 55 mm ø, 0-100% EtOAc/iso-Hexanes, ca. 20 mL). This afforded the product as a thick pale yellow syrup (1.4 g, 95 %, 99:1 *dr*). ^{1}H NMR (600 MHz, DMSO, mixture of rotamers): δ = 7.36 – 7.30 (m, 5H, major), 7.30 – 7.27 (m, 3H, minor), 7.26 – 7.23 (m, 1H, major), 7.21 – 7.18 (m, 1H, minor), 5.46 (d, *J* = 3.9 Hz, 1H, major), 5.30 (d, *J* = 4.6 Hz, 1H, minor), 4.68 (s, 1H, minor), 4.54 (dd, *J* = 7.5, 4.6 Hz, 1H, minor), 4.48 (dd, *J* = 8.2, 3.8 Hz, 1H, major), 4.12 – 4.04 (m, 1H, major), 3.01 – 2.93 (m, 1H, major), 2.85 (s, 3H, minor), 2.76 (s, 4H, major), 2.06 – 1.98 (m, 1H, major), 1.98 – 1.93 (m, 1H, minor), 1.91 – 1.86 (m, 1H, major), 1.86 – 1.79 (m, 1H, major), 1.71 (t, *J* = 2.6 Hz, 3H, minor), 1.63 (t, *J* = 2.6 Hz, 4H, minor), 1.62 – 1.55 (m, 2H, minor), 1.34 – 1.21 (m, 2H, major), 0.91 (d, *J* = 6.6 Hz, 3H, major, minor), 0.91 (d, *J* = 6.8 Hz, 4H, major, minor), 0.90 (d, *J* = 7.1 Hz, 3H, major,minor), 0.87 (d, *J* = 7.0 Hz, 3H, minor); ^{13}C NMR (151 MHz, DMSO): δ = 176.0, 175.5, 144.1, 144.0, 128.6, 128.2, 127.8, 127.4, 127.3, 127.1, 79.7, 79.2, 76.5, 76.2, 74.3, 74.1, 57.6, 53.7, 34.7, 34.0, 33.7, 33.7, 30.4, 27.4, 17.8, 17.5, 16.5, 16.4, 15.9, 14.5, 3.5, 3.4; ṽ = 3367, 3062, 3028, 2970, 2919, 2873, 1613, 1451, 1409, 1374, 1338, 1308, 1258, 1233, 1200, 1111, 1080, 1050, 1028, 1001, 838, 764, 702, 671, 608, 527, 463 cm^{-1}; $[\alpha]_D^{20}$= + 121.3 (c = 1.55, EtOH); HRMS-ESIpos (m/z): calc'd. for $C_{18}H_{25}N_1O_2Na_1$ $[M+Na]^+$, 310.17774; found, 310.17758; R_t (Minor Diastereomer, HPLC Method 5) = 4.85 min; R_t (Major Diastereomer, HPLC Method 5) = 4.72 min.

(*R*)-*N*-((1*S*,2*S*)-1-Hydroxy-1-phenylpropan-2-yl)-*N*,2-dimethylhept-5-ynamide (50a)

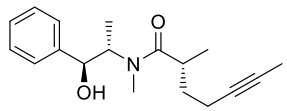

A three-neck jacketed vessel equipped with a stir bar, a gas inlet connected to an argon-vacuum manifold, a ground-glass joint thermometer adapter connected to low temperature thermometer and a rubber septum, was charged with a solution of lithium chloride (0.9 g, 20 mmol, 4.3 equiv.) and diisopropylamine (2.9 mL, 20 mmol, 4.3 equiv.) in THF (77 mL). Upon cooling of the mixture to 0 °C, ^{n}BuLi (12 mL, 12 mmol, 4.3 equiv., 1.6 M in *n*-hexanes) was added dropwise and the mixture was stirred at this temperature for 1 h. After that the reaction mixture was cooled to - 78 °C and a solution of *N*-((1*S*,2*S*)-1-hydroxy-1-phenylpropan-2-yl)-*N*-methylpropionamide **49** (2.2 g, 10 mmol, 2.1 equiv.) in THF (33 mL) was added dropwise. The mixture was then stirred for 1 h at - 78 °C, before it was warmed to 0 °C. 5-Iodopent-2-yne **13b** (1.0 g, 4.7 mmol) was added and the resulting mixture was then stirred for 2 h at 0 °C. The reaction mixture was then quenched with NH_4Cl (100 mL, sat. aq.) and then extracted with EtOAc (3 x 100 mL). The combined organic extracts were dried over $MgSO_4$, filtered and then concentrated under reduced pressure. The orange oily residue obtained was then purified by flash column chromatography (SiO_2, 100 g, 55 mm ø, 0-100% EtOAc/iso-Hexanes, ca. 20 mL). This afforded the product as a thick pale yellow syrup (1.4 g, 95 %, 99:1 *dr*). ^{1}H NMR (600 MHz, DMSO, mixture of rotamers): δ = 7.38 – 7.35 (m, 3H, major), 7.33 – 7.30 (m, 3H, major), 7.29 – 7.27 (m, 3H, minor), 7.26 – 7.23 (m, 2H, major), 7.21 – 7.18 (m, 1H, minor), 5.41 (d, *J* = 3.7 Hz, 1H, major), 5.28 (d, *J* = 4.6 Hz, 1H, minor), 4.67 (s, 1H, minor), 4.54 (dd, *J* = 7.7, 4.5 Hz, 1H, minor), 4.51 (dd, *J* = 8.1, 3.7 Hz, 1H, major), 3.99 – 3.93 (m, 1H, major), 2.85 (s, 3H, major), 2.84 – 2.79 (m, 1H, minor), 2.77 – 2.73 (m, 1H, major), 2.72 (s, 3H, minor), 1.96 (dddt, *J* = 14.7, 9.6, 7.3, 2.6 Hz, 4H, major, minor), 1.84 – 1.75 (m, 1H, major), 1.66 – 1.58 (m, 1H, minor), 1.35 – 1.25 (m, 2H, major, minor), 0.91 (d, *J* = 5.7 Hz, 3H, major), 0.90 (s, 3H, major), 0.86 (d, *J* = 6.9 Hz, 3H, minor), 0.80 (d, *J* = 6.8 Hz, 3H, minor); ^{13}C NMR (151 MHz, DMSO, mixture of romatmers): δ = 175.3, 174.9, 143.4, 143.3, 127.9, 127.5, 127.1, 126.7, 126.7, 126.4, 79.1, 78.7, 75.7, 75.4, 73.8, 65.2, 56.7, 53.4, 33.9, 33.7, 33.6, 32.8, 32.8, 29.9, 26.7, 17.2, 16.8, 15.9, 15.2, 14.0, 13.9, 2.9; $[a]_D^{20}$= + 23.8 (c = 1.00, EtOH); mp: 67-69 °C; (IR (film): ṽ = 3364, 2974, 2917, 2849, 1614, 1517, 1483, 1450, 1408, 1374, 1350, 1302, 1245, 1233, 1198, 1140,1108, 1082, 1051, 1026, 1001, 924, 900, 860, 762, 702, 610, 540 cm^{-1}; HRMS-ESI+ (*m/z*): calc'd. for $C_{18}H_{25}NO_2Na$ $[M+Na]^+$, 310.1777; found, 310.1780; R_t (Minor Diastereomer, HPLC Method 6) = 4.78 min; R_t (Major Diastereomer, HPLC Method 6) = 4.88 min.

(2*R*,3*R*)-3-Methyl-1-(4-tosyloxazol-5-yl)oct-6-yn-2-ol 7a was prepared by a three-step sequence starting from (*R*)-*N*-((1*S*,2*S*)-1-hydroxy-1-phenylpropan-2-yl)-*N*,2-dimethylhept-5-ynamide 50a:

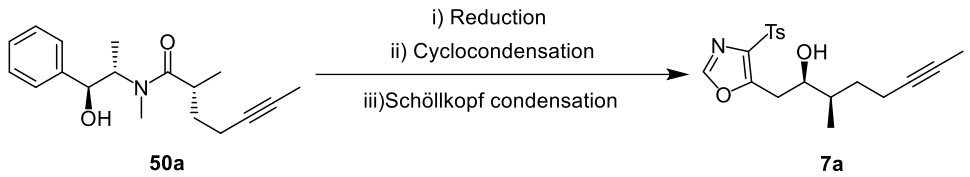

A three-neck jacketed vessel equipped with a stir bar, a gas inlet connected to an argon-vacuum manifold, a ground-glass joint thermometer adapter connected to low temperature thermometer and a rubber septum was charged with $LiAlH_4$ (0.7 g, 19 mmol, 2.3 equiv.) and *iso*-hexane (43 mL). The vessel was cooled to 0 °C and ethyl acetate (2.7 mL, 28 mmol, 3.4 equiv) was added via a syringe pump over a period of 1.5 h. The resulting suspension of lithium triethoxyaluminum hydride was cooled to −78 °C. A solution of amide **50a** (2.3 g, 8.1 mmol, 1.0 equiv) in THF (30mL) was added via a syringe pump over 5 min, and the reaction mixture was warmed to 0 °C. After being stirred for 1 h at 0 °C, the reaction mixture was transferred by cannula to an ice-cold solution of trifluoroacetic acid (5 mL, 33 mmol, 10 equiv) in dilute HCl (80 mL, 1.0 M, aq).The resulting biphasic mixture was diluted with dilute HCl (140 mL, 1.0 M, aq.) and the layers were separated. The aqueous layer was extracted with CH_2Cl_2 (3 × 100 mL). The combined organic layers were neutralized with $NaHCO_3$ (100 mL, sat., aq.). The aqueous layer (pH 7−8) was separated and extracted with CH_2Cl_2 (100 mL). The combined organic extracts were dried over $MgSO_4$ filtered and concentrated under reduced pressure (300 mbar) at rt. This gave the crude aldehyde **9a** as pale-yellow oil. Due to concerns about potential oxidation and racemization, the crude aldehyde **9a** was subjected to the next step without any purification. A three-neck jacketed vessel equipped with a stir bar, a gas inlet connected to an argon-vacuum manifold, a ground-glass joint thermometer adapter connected to low temperature thermometer and a rubber septum was charged with a solution of lithium perchlorate (1.1 g, 11 mmol, 0.9 equiv.) in Et_2O (17 mL) and a solution of **23** (0.4 g, 1.1 mmol, 10 mol%) in CH_2Cl_2 (35 mL). The mixture was stirred for 0.5 h at rt and then cooled to –78 °C. DIPEA (4.5 mL, 26 mmol, 2.25 equiv.) was added, followed by a solution of the crude aldehyde **9a** in CH_2Cl_2-Et_2O (26 mL, 2:1). A solution of AcCl (1.3 mL, 19 mmol, 1.3 equiv.) in CH_2Cl_2 (9 mL) was added via syringe pump over 5 h and the resulting mixture was stirred at –78 °C for 24 h. The reaction mixture was diluted with Et_2O (50 mL) and then allowed to warm to rt. The yellow suspension obtained was then filtered through a silica plug eluting with Et_2O (100 mL) and the filtrate obtained was concentrated under reduced pressure (300 mbar) at rt. This afforded the crude β-lactone **8a** as a pale-yellow oil (> 20:1 dr by NMR), which was subjected to the next

step without any purification. A three-neck jacketed vessel equipped with a stir bar, a gas inlet connected to an argon-vacuum manifold, a ground-glass joint thermometer adapter connected to low temperature thermometer and a rubber septum, was charged with a solution of TosMIC (0.8 g, 3.8 mmol, 1.0 equiv.) in THF (13 mL). The solution was cooled to - 78 °C and ^{n}BuLi (2.5 mL, 4.0 mmol, 1.0 equiv., 1.6 M in *n*-hexanes) was added dropwise. The pale-yellow solution obtained was stirred at - 78 °C for 0.5 h, before a solution of the crude β-lactone **8a** in THF (20 mL) was added. The resulting mixture was stirred at –78 °C for an hour and then warmed to rt. The reaction was then quenched with HCl (20 mL, 1.0 M, aq.) and extracted with EtOAc (3 x 100 mL). The combined organic extracts were dried over $MgSO_4$, filtered and then concentrated under reduced pressure. The dark brown oily residue obtained was purified by flash column chromatography (SiO_2, 100 g, 55 mm ø, 0-100% EtOAc/iso-Hexanes, ca. 20 mL). This gave the product **7a** as an orange viscous oil (1.5 g, 52 % yield over 3 steps, 97:3 *dr*). The spectroscopic data are in agreement with those obtained previously for (2*R*,3*R*)-3-methyl-1-(4-tosyloxazol-5-yl)oct-6-yn-2-ol **7a**. The diastereomeric purity of (2*R*,3*R*)-3-methyl-1-(4-tosyloxazol-5-yl)oct-6-yn-2-ol **7a** prepared via this three-step sequence was further validated by HPLC using a range of chiral stationary phases (see Appendix 5 for more details); R_t (Major Diastereomer, HPLC Method 8c) = 9.46 min, R_t (Minor Diastereomer, HPLC Method 8c) = 11.16 min.

N-((1*R*,2*R*)-1-Hydroxy-1-phenylpropan-2-yl)-*N*-methylnon-7-ynamide (46)

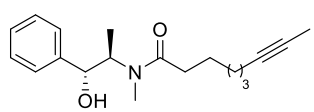

A three-neck jacketed glass reaction vessel equipped with a magnetic stir bar, a pressure equalizing addition funnel and a gas inlet connected to an argon-vacuum manifold, was charged with solution of acid **37** (0.9 g, 5.6 mmol) in THF (7 mL) and TEA (2.3 mL, 17 mmol, 3.0 equiv.). The reaction mixture was then cool to - 10°C and PvCl (0.8 mL, 6.7 mmol, 1.2 equiv.) dropwise. The white slurry immediately formed was stirred at this temperature for 1 h. Then, a solution of (1*R*,2*R*)-2-(methylamino)-1-phenylpropan-1-ol **45** (1.2 g, 7.3 mmol, 1.3 equiv.) and TEA (2.3 mL, 16.8 mmol, 3.0 equiv.) in THF (7 mL) was added. The resulting mixture was allowed to warm to rt and then stirred overnight. The reaction mixture was quenched with $NaHCO_3$ (50 mL, sat. aq.) and extracted with EtOAc (3 x 100 mL). The combined organic layers were washed with brine (50 mL), dried $MgSO_4$, filtered and then concentrated under reduced pressure. The residue was purified by flash column chromatography (SiO_2, 50 g, 55 mm ø, 0-100% EtOAc/iso-Hexanes, ca. 20 mL). This gave the product as a pale-yellow oil (1.6 g, 97 %). ^{1}H NMR (600 MHz, DMSO, mixture of rotamers): δ = 7.38 – 7.35 (m, 2H, major), 7.34 (q, *J* = 1.2 Hz, 2H, major), 7.32 (*d*, *J* = 4.7 Hz, 2H, major), 7.32 – 7.29 (m, 2H, minor), 7.29 – 7.26 (m, 1H, minor), 7.26 – 7.22 (m, 1H, major), 5.44 (d, *J* = 4.2 Hz, 1H, major), 5.25 (d,

J = 4.3 Hz, 1H, minor), 4.68 – 4.61 (m, 1H, major), 4.53 (dd, *J* = 8.1, 4.3 Hz, 1H, major), 4.49 (dd, J = 8.1, 4.2 Hz, 1H, minor), 3.90 (dq, *J* = 8.2, 6.8 Hz, 1H, major), 2.82 (s, 3H, major), 2.76 (s, 3H, major), 2.28 (tt, *J* = 15.1, 7.6 Hz, 2H, major), 2.20 (p, *J* = 6.5 Hz, 2H, minor), 2.08 (tq, *J* = 7.2, 2.5 Hz, 3H, major, minor), 1.73 (t, *J* = 2.5 Hz, 3H, major), 1.72 (t, *J* = 2.6 Hz, 3H, minor), 1.47 – 1.38 (m, 4H, major, minor), 1.41 – 1.35 (m, 4H, major, minor), 1.30 (ddtd, *J* = 10.3, 8.8, 5.1, 2.0 Hz, 4H, major, minor), 0.91 (d, *J* = 6.8 Hz, 3H, major), 0.83 (d, *J* = 6.9 Hz, 3H, minor); ^{13}C NMR (151 MHz, DMSO): δ = 172.3, 172.2, 143.6, 143.6, 128.1, 127.9, 127.3, 127.1, 126.9, 126.8, 79.3, 79.2, 75.6, 75.6, 74.0, 73.8, 57.1, 53.4, 33.0, 32.5, 29.8, 28.5, 28.4, 28.2, 28.1, 26.7, 24.4, 24.2, 18.0, 15.4, 14.1, 3.1; ṽ = 3381, 3061, 3029, 2933, 2859, 1614, 1452, 1404, 1374, 1333, 1311, 1257, 1200, 1117, 1076, 1050, 1026 838, 756, 701, 671, 665, 607, 586, 521 cm^{-1}; $[\alpha]_D^{20}$= + 68.6 (c = 1.26, EtOH); HRMS-ESI+ (m/z): calc'd. for $C_{19}H_{28}N_1O_2$ $[M+H]^+$, 302.2114; found, 302.2114.

(*R*)-*N*-((1*R*,2*R*)-1-Hydroxy-1-phenylpropan-2-yl)-N,2-dimethylnon-7-ynamide (52a)

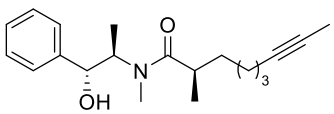

A three-neck jacketed vessel equipped with a stir bar, a gas inlet connected to an argon-vacuum manifold, a ground-glass joint thermometer adapter connected to low temperature thermometer and a rubber septum, was charged with a solution of lithium chloride (1.3 g, 32 mmol, 6.0 equiv.) and diisopropylamine (1.7 mL, 12 mmol, 2.3 equiv.) in THF (10 mL). Upon cooling of the mixture to 0 °C, ^{n}BuLi (6.9 mL, 11 mmol, 2.1 equiv., 1.6 M in *n*-hexanes) was added dropwise and the mixture was stirred at this temperature for 1 h. After that the reaction mixture was cooled to - 78 °C and a solution of *N*-((1*R*,2*R*)-1-hydroxy-1-phenylpropan-2-yl)-*N*-methylnon-7-ynamide **51** (1.0 g, 3.7 mmol, 1.0 equiv.) in THF (8 mL) was added dropwise. The mixture was then stirred for 1 h at − 78 °C, before it was warmed to 0 °C. MeI (0.66 mL, 10.6 mmol, 2.0 equiv.) was added and the resulting mixture was then stirred for 2 h at 0 °C. The reaction mixture was then quenched with NH_4Cl (100 mL, sat. aq.) and then extracted with EtOAc (3 x 100 mL). The combined organic extracts were dried over $MgSO_4$, filtered and then concentrated under reduced pressure. The orange oily residue obtained was then purified by flash column chromatography (SiO_2, 100 g, 55 mm ø, 0-100% EtOAc/iso-Hexanes, ca. 20 mL). This afforded the product as a thick pale-yellow syrup (1.0 g, 59 %, 97:3 *dr*). ^{1}H NMR (600 MHz, DMSO, mixture of rotamers): δ = 7.37 – 7.32 (m, 4H, major), 7.32 – 7.27 (m, 4H, minor), 7.27 – 7.23 (m, 1H, major), 7.22 – 7.19 (m, 1H, minor), 5.45 (d, *J* = 3.9 Hz, 1H, major), 5.33 (d, *J* = 4.6 Hz, 1H, minor), 4.69 (s, 1H, minor), 4.57 (dd, *J* = 7.3, 4.7 Hz, 1H, minor), 4.51 (dd, *J* = 7.9, 3.9 Hz, 1H, major), 3.98 (p, *J* = 6.9 Hz, 1H, major), 2.83 (s, 3H, minor), 2.76 (s, 3H, major), 2.76 – 2.71 (m, 1H, major), 2.62 – 2.55 (m, 1H, minor), 2.03 (dtt, *J* = 7.4, 5.1, 2.6 Hz, 4H, major, minor), 1.71 (t, *J* = 2.6 Hz, 3H, minor), 1.67 (t, *J* = 2.6 Hz, 3H, major), 1.42 (ddd, *J* = 10.8, 9.1, 6.8 Hz, 1H, major), 1.39 – 1.36 (m, 1H, minor), 1.35

– 1.27 (m, 4H, major, minor), 1.24 – 1.16 (m, 3H, major), 1.13 – 1.06 (m, 3H, minor), 0.93 (d, *J* = 6.7 Hz, 3H, major), 0.89 (d, *J* = 6.9 Hz, 3H, minor), 0.89 (d, *J* = 6.8 Hz, 3H, minor), 0.88 (d, *J* = 6.6 Hz, 3H, major); ^{13}C NMR (151 MHz, DMSO): δ = 175.8, 175.4, 143.6, 143.5, 128.0, 127.7, 127.2, 126.8, 126.8, 126.5, 79.3, 79.1, 75.6, 75.5, 73.8, 73.7, 57.0, 53.3, 39.9, 39.7, 39.6, 39.4, 39.3, 39.2, 39.0, 34.8, 34.3, 33.7, 33.1, 30.0, 28.7, 28.5, 27.0, 26.0, 25.8, 17.9, 17.9, 17.5, 17.2, 15.5, 14.0, 3.1, 3.0; ṽ = 3370, 3061, 3029, 2935, 2856, 1613, 1450, 1404, 1365, 1311, 1199, 1109, 1075, 1049, 1025, 838, 750, 702, 665, 664, 591, 549, 521 cm^{-1}; $[\alpha]_D^{20}$= + 121.3 (c = 1.55, EtOH); HRMS-ESI+ (m/z): calc'd. for $C_{20}H_{30}N_1O_2$ [M+H]$^+$, 316.2271; found, 316.2275; R_t (Minor Diastereomer, HPLC Method 7) = 5.38 min, R_t (Major Diastereomer, HPLC Method 7) = 6.68 min.

(*R*)-*N*-((1*S*,2*S*)-1-Hydroxy-1-phenylpropan-2-yl)-*N*,2-dimethylnon-7-ynamide (53a)

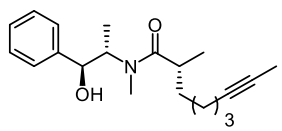

A three-neck jacketed vessel equipped with a stir bar, a gas inlet connected to an argon-vacuum manifold, a ground-glass joint thermometer adapter connected to low temperature thermometer and a rubber septum, was charged with a solution of lithium chloride (4.6 g, 109 mmol, 6.0 equiv.) and diisopropylamine (5.7 mL, 41 mmol, 2.3 equiv.) in THF (30 mL). Upon cooling of the mixture to 0 °C, ^{n}BuLi (24 mL, 38 mmol, 2.1 equiv., 1.6 M in *n*-hexane) was added dropwise and the mixture was stirred at this temperature for 1 h. After that the reaction mixture was cooled to - 78 °C and a solution of N-((1*S*,2*S*)-1-hydroxy-1-phenylpropan-2-yl)-*N*-methylpropionamide **49** (4.0 g, 18 mmol, 1.0 equiv.) in THF (30 mL) was added dropwise. The mixture was then stirred for 1 h at - 78 °C, before it was warmed to 0 °C. 7-iodohept-2-yne **S3** (6.0 g, 27 mmol. 1.5 equiv.) was added and the resulting mixture was then stirred for 2 h at 0 °C. The reaction mixture was then quenched with NH_4Cl (100 mL, sat. aq.) and then extracted with EtOAc (3 x 100 mL). The combined organic extracts were dried over $MgSO_4$, filtered and then concentrated under reduced pressure. The orange oily residue obtained was then purified by flash column chromatography (SiO_2, 100 g, 55 mm ø, 0-100% EtOAc/iso-Hexanes, ca. 20 mL). This afforded the product as a thick pale yellow syrup (5.6 g, 98 %, 99:1 *dr*). ^{1}H NMR (600 MHz, DMSO, mixture of rotamers (1:1)): δ 7.35 – 7.30 (m, 4H, rotamer a), 7.30 – 7.25 (m, 4H, rotamer b), 7.25 – 7.22 (m, 1H, rotamer a), 7.21 – 7.18 (m, 1H, rotamer b), 5.42 (d, *J* = 3.9 Hz, 1H, rotamer a), 5.29 (d, *J* = 4.2 Hz, 1H, rotamer b), 4.68 (s, 1H, rotamer b), 4.54 (dd, *J* = 7.7, 4.6 Hz, 1H, rotamer a), 4.51 (dd, *J* = 7.5, 3.9 Hz, 1H, rotamer b), 3.94 (p, *J* = 6.9 Hz, 1H, rotamer a), 2.83 (s, 3H, rotamer b), 2.73 (s, 3H, rotamer a), 2.68 – 2.57 (m, 2H, rotamer a, rotamer b), 2.03 (qt, *J* = 6.8, 2.6 Hz, 4H, rotamer a, rotamer b), 1.71 (t, *J* = 2.6 Hz, 3H, rotamer a), 1.67 (t, *J* = 2.6 Hz, 3H, rotamer b), 1.52 – 1.42 (m, 2H, rotamer a, rotamer b), 1.37 – 1.27 (m, 4H, rotamer a, rotamer b), 1.19 – 1.08 (m, 4H, rotamer a, rotamer b), 0.95

(d, *J* = 6.8 Hz, 3H, rotamer a), 0.88 (d, *J* = 6.9 Hz, 3H, rotamer a), 0.85 (d, *J* = 7.0 Hz, 3H, rotamer b), 0.81 (d, *J* = 6.8 Hz, 3H, rotamer b); ^{13}C NMR (151 MHz, DMSO, mixture of rotamers): δ = 176.2 (rotamer a), 175.9 (rotamer b), 144.1 (rotamer b), 144.0 (rotamer a), 128.5 (rotamer a), 128.2 (rotamer b), 127.7 (rotamer a), 127.4 (rotamer b), 127.3 (rotamer a), 127.1 (rotamer b), 79.9 (rotamer a), 79.7 (rotamer b), 76.1 (rotamer b), 76.0 (rotamer a), 74.4v(rotamer a), 74.3 (rotamer b), 57.2 (rotamer a), 53.6 (rotamer b), 35.2 (rotamer b), 35.0 (rotamer a), 33.7 (rotamer b), 33.4 (rotamer a), 30.4 (rotamer b), 29.4 (rotamer a), 29.1 (rotamer b), 27.7 (rotamer a), 26.6 (rotamer b), 26.5 (rotamer a), 18.6 (rotamer a), 18.5 (rotamer b), 18.4 (rotamer a), 17.9(rotamer b), 16.0 (rotamer a), 14.5 (rotamer b), 3.6 (rotamer a), 3.5 (rotamer b); $[a]_D^{20}$= + 44.0 (c = 1.05, EtOH); IR (film): $\tilde{\nu}$ = 3367, 3061, 3029, 2968, 2934, 2859, 1617, 1452, 1409, 1374, 1308, 1199, 1109, 1083, 1051, 1027, 756, 702, 671, 666, 591, 549, 526 cm^{-1}; HRMS-GC-EI (*m/z*): calc'd. for $C_{20}H_{25}NO_3$ [M] $^{+\cdot}$, 327. 1828; found, 327. 1830; R_t (Minor Diastereomer, HPLC Method 7) = 5.21 min, R_t (Major Diastereomer, HPLC Method 7) = 7.46 min.

(2*R*,3*R*)-3-Methyl-1-(4-tosyloxazol-5-yl)dec-8-yn-2-ol 7b was also prepared by a three-step sequence starting from (*R*)-*N*-((1S,2S)-1-hydroxy-1-phenylpropan-2-yl)-*N*,2-dimethylnon-7-ynamide 53a.

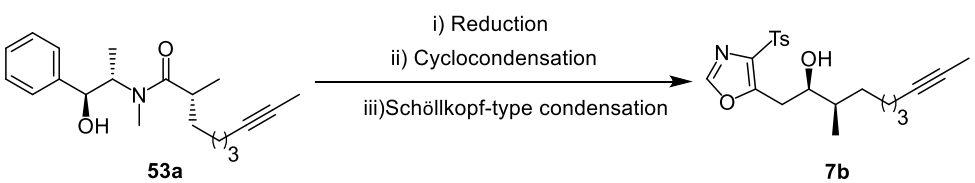

Reduction & Cyclocondensation:

A three-neck jacketed vessel equipped with a stir bar, a gas inlet connected to an argon-vacuum manifold, a ground-glass joint thermometer adapter connected to low temperature thermometer and a rubber septum was charged with $LiAlH_4$ (1.5 g, 41 mmol, 2.3 equiv.) and iso-hexane (96 mL). The vessel was cooled to 0 °C and ethyl acetate (6.0 mL, 60 mmol, 3.4 equiv) was added via a syringe pump over a period of 1.5 h. The resulting suspension of lithium triethoxyaluminum hydride was cooled to −78 °C. A solution of amide 18b (5.6 g, 18 mmol, 1.0 equiv) in THF (65 mL) was added via a syringe pump over 5 min, and the reaction mixture was warmed to 0 °C. After being stirred for 1 h at 0 °C, the reaction mixture was transferred by cannula to an ice-cold solution of trifluoroacetic acid (14 mL, 177 mmol, 10 equiv) in dilute HCl (80 mL, 1.0 M, aq).The resulting biphasic mixture was diluted with dilute HCl (140 mL, 1.0 M, aq.) and the layers were separated. The aqueous layer was extracted with CH_2Cl_2 (3 × 100 mL). The combined

organic layers were neutralized with $NaHCO_3$ (100 mL, sat., aq.). The aqueous layer (pH 7–8) was separated and extracted with CH_2Cl_2 (100 mL). The combined organic extracts were dried over $MgSO_4$, filtered and concentrated under reduced pressure (300 mbar) at rt. This gave the crude aldehyde **9b** as pale yellow oil. Due to concerns about potential oxidation and racemization, the crude aldehyde **9b** was subjected to the next step without any purification. A three-neck jacketed vessel equipped with a stir bar, a gas inlet connected to an argon-vacuum manifold, a ground-glass joint thermometer adapter connected to low temperature thermometer and a rubber septum was charged with a solution of lithium perchlorate (1.9 g, 18 mmol, 1.0 equiv.) in Et_2O (28 mL) and a solution of TMS*q* (0.7 g, 1.8 mmol, 10 mol%) in CH_2Cl_2 (56 mL). The mixture was stirred for 0.5 h at rt and then cooled to –78 °C. DIPEA (7.7 mL, 44 mmol, 2.5 equiv.) was added, followed by a solution of the crude aldehyde **9b** in CH_2Cl_2 -Et_2O (42 mL, 2:1). A solution of AcCl (2.3 mL, 33 mmol, 1.3 equiv.) in CH_2Cl_2 (15 mL) was added via syringe pump over 5 h and the resulting mixture was stirred at –78 °C for 24 h. The reaction mixture was diluted with Et_2O (100 mL) and then allowed to warm to rt. The yellow suspension obtained was then filtered through a silica plug eluting with Et_2O (100 mL) and the filtrate obtained was concentrated under reduced pressure (300 mbar) at rt. This afforded the crude beta-lactone **8b** as a pale yellow oil (> 95:5 dr by NMR), which was subjected to the next step without any purification.

Schöllkopf Condesation:

A three-neck jacketed vessel equipped with a stir bar, a gas inlet connected to an argon-vacuum manifold, a ground-glass joint thermometer adapter connected to low temperature thermometer and a rubber septum, was charged with a solution of TosMIC (2.5 g, 12mmol, 1.0 equiv.) in THF (42 mL). The solution was cooled to –78 °C and ^{n}BuLi (8.1 mL, 13 mmol, 1.1 equiv., 1.6 M in *n*-hexanes) was added dropwise. The pale-yellow solution obtained was stirred at –78 °C for 0.5 h, before a solution of the crude beta-lactone **8b** in THF (20 mL) was added. The resulting mixture was stirred at –78 °C for an hour and then warmed to rt. The reaction was then quenched with HCl (20 mL, 1.0 M, aq.) and extracted with EtOAc (3 x 100 mL). The combined organic extracts were dried over $MgSO_4$, filtered and then concentrated under reduced pressure. The dark brown oily residue obtianed was purified by flash column chromatography (SiO_2, 100 g, 55 mm ø, 0-100% EtOAc/iso-Hexanes, ca. 20 mL). This gave the product as an orange viscous oil (1.7 g, 24 % yield over 3 steps, > 95:5 dr). The spectroscopic data are in agreement with those obtained previously for (2*R*,3*R*)-3-methyl-1-(4-tosyloxazol-5-yl)dec-8-yn-2-ol **7b**. The diastereomeric purity of (2*R*,3*R*)-3-methyl-1-(4-tosyloxazol-5-yl)dec-8-yn-2-ol **7b** prepared via this three-step sequence was further validated by HPLC using a range of chiral stationary phases (see Appendix 6 for more details).

5-((2*R*,3*R*)-2-((*tert*-butyldimethylsilyl)oxy)-3-methyldec-8-yn-1-yl)-4-tosyloxazole (62)

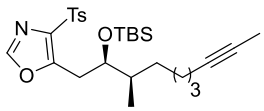

A Schleck tube equipped a magnetic stir bar was charged a solution of (2*R*,3*R*)-3-methyl-1-(4-tosyloxazol-5-yl)dec-8-yn-2-ol **7b** (130 mg, 33 µmol) in CH_2Cl_2 (2 mL) and 2,6-lutidine (78 µL, 67 µmol, 2.0 equiv.). The reaction mixture was cooled to 0 ◦C and *tert*-butyldimethylsilyl triflate (120 µL, 50 µmol, 1.5 equiv.) was added dropwise and the resulting mixture was allowed to warm to rt overnight. After that the solvent was removed under reduced pressure and the residue obtained was purified by flash column chromatography (SiO_2, 10 g, 20 mm ø, 0-25% EtOAc/iso-Hexanes, ca. 5 mL). This gave the product **62** as a pale yellow oil (120 mg, 71 %).^{1}H NMR (400 MHz, $CDCl_3$): δ = 7.95 – 7.88 (m, 2H), 7.73 (s, 1H), 7.38 – 7.30 (m, 2H), 4.07 (m, 1H), 3.27 – 3.09 (m, 2H), 2.43 (s, 3H), 2.23 – 1.99 (m, 2H), 1.78 (t, *J* = 2.5 Hz, 3H), 1.49 – 1.25 (m, 6H), 1.19 – 1.03 (m, 1H), 0.97 (d, *J* = 6.8 Hz, 3H), 0.81 (s, 9H), -0.00 (s, 3H), -0.24 (s, 3H); ^{13}C NMR (101 MHz, $CDCl_3$): δ = 155.5, 149.5, 144.8, 137.4, 136.3, 129.9, 128.1, 79.2, 75.5, 74.5, 40.2, 31.8, 29.9, 28.7, 26.9, 25.7, 22.8, 19.3, 17.9, 15.7, 2.6, -4.7, -5.1; $[\alpha]_D^{20}$= + 41.4 (c = 1.08, $CHCl_3$); IR (film): $\tilde{\nu}$ = 3128, 2929, 2857, 1595, 1516, 1495, 1462, 1404, 1385, 1362, 1329, 1305, 1291, 1252, 1224, 1148, 1106, 1080, 1043, 1018, 1006, 920, 863, 837, 812, 776, 736, 706, 697, 661, 601, 540, 493 cm^{-1}; HRMS-ESI+ (*m/z*): calc'd. for $C_{27}H_{41}O_4NSSiNa$ $[M+Na]^+$, 526.2417; found, 526.2416.

(2*R*,3*R*)-3-Methyl-1-(oxazol-5-yl)oct-6-yn-2-yl (*E*)-2-methylhex-2-en-4-ynoate (4):

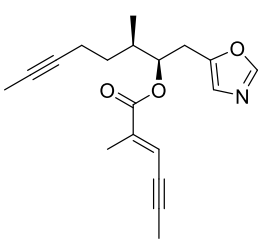

A Schlenck tube was charged with freshly prepared Na-Hg amalgam (5.0 g, 2.6 mmol Na, 10.0 equiv., 10 mol% Na), a solution of (2*R*,3*R*)-3-methyl-1-(4-tosyloxazol-5-yl)oct-6-yn-2-ol **7a** (0.3 g, 0.3 mmol) in EtOH/THF (1:1, 5 mL) and Na_2HPO_4 (0.2 g, 1.0 mmol, 4.0 equiv.). The resulting mixture was sonicated for 2 h. The reaction mixture was then diluted with EtOAc (20 mL), and then carefully decanted into water (10 mL). The aqueous phase was extract with EtOAc (2 x 10 mL), The combined organic extracts were dried over $MgSO_4$, filtered and then concentrated under reduced pressure. This gave the crude (2*R*,3*R*)-3-methyl-1-(oxazol-5-yl)oct-6-yn-2-ol **6a** as a cloudy syrup, which was used directly in the next step.

A Schlenk tube equipped with a magnetic stir bar was charged with a solution of the crude(2*R*,3*R*)-3-methyl-1-(oxazol-5-yl)oct-6-yn-2-ol in CH_2Cl_2 (3 mL), DMAP (3 mg, 26 µmol, 10 mol%) and (*E*)-2-methylhex-2-en-4-ynoic acid **55** (13 mg, 100 µmol, 0.5 equiv.). The resulting mixture was cooled to 0°C. EDC·HCl (49 mg, 0.26 mmol, 1.0 equiv.) was added and the reaction mixture was allowed to warm to rt and stirred overnight. The solvent was then evaporated under reduced pressure and the residue obtained was purified by flash column chromatography (SiO_2, 10 g, 20 mm ø, 0-50% EtOAc/iso-Hexanes, ca. 5 mL). This gave the product **4** as a pale-yellow oil (24 mg, 73 %). ^{1}H NMR (400 MHz, $CDCl_3$): δ = 7.77 (s, 1H), 6.82 (d, *J* = 1.0 Hz, 1H), 6.57 (tt, *J* = 2.6, 1.3 Hz, 1H), 5.17 (ddd, *J* = 7.6, 5.4, 4.0 Hz, 1H), 3.07 – 2.89 (m, 2H), 2.26 – 2.08 (m, 2H), 2.07 (d, *J* = 0.7 Hz, 3H), 2.00 (dd, *J* = 1.4, 0.7 Hz, 3H), 1.90 (dddt, *J* = 8.1, 6.8, 4.0, 1.4 Hz, 1H), 1.74 (t, *J* = 2.5 Hz, 3H), 1.66 – 1.53 (m, 1H), 1.41 – 1.27 (m, 1H), 0.98 (d, *J* = 6.8 Hz, 3H); ^{13}C NMR (101 MHz, $CDCl_3$) δ = 166.7, 150.7, 149.1, 137.8, 124.0, 120.9, 99.7, 78.4, 76.8, 76.3, 74.6, 35.0, 32.2, 27.9, 16.6, 15.2, 14.0, 5.0, 3.6; IR (film): $\tilde{\nu}$ = 2968, 2920, 2850, 2222, 2147, 1709, 1617, 1510, 1438, 1386, 1346, 1256, 1122, 1177, 969, 825, 742, 642, 485, 457, 432, 412 cm^{-1}; $[\alpha]_D^{20}$= + 26.5 (c = 0.78, $CHCl_3$); HRMS-CI (*m/z*): calc'd. for $C_{19}H_{24}NO_3$ $[M+H]^+$, 314.1751; found, 314.1752.

(3*E*,9*R*,10*R*,13*E*,19*R*,20*R*)-3,9,13,19-Tetramethyl-10,20-bis(oxazol-5-ylmethyl)-1,11-dioxacycloicosa-3,13-dien-5,15-diyne-2,12-dione (2):

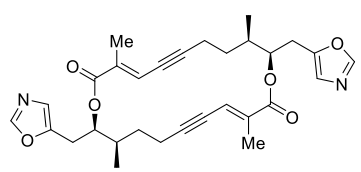

(2*R*,3*R*)-3-Methyl-1-(oxazol-5-yl)oct-6-yn-2-yl-(*E*)-2-methylhex-2-en-4-ynoate **4** (16 mg, 51 µmol) was added to a stirred suspension of complex **64a** (8 mg, 10 µmol, 20 mol%) and powdered molecular sieves 5Å (325 mg) in toluene (4 mL) at 23 °C under argon atmosphere. The mixture was heated at 60 °C stirred for 1 h, before it was filtered through a short pad of Celite® and rinsed with ethyl acetate (30 mL). The filtrate was evaporated and the residue was purified by by flash column chromatography (SiO_2, 10 g, 20 mm ø, 0-100% EtOAc/iso-Hexanes, ca. 5 mL) to give the product as a white solid (10 mg, 74 %). ^{1}H NMR (400 MHz, $CDCl_3$): δ = 7.76 (s, 2H), 6.81 (s, 2H), 6.48 (dt, *J* = 2.8, 1.3 Hz, 2H), 5.15 (ddd, *J* = 8.9, 4.8, 3.1 Hz, 2H), 2.98 – 2.83 (m, 4H), 2.63 (ddt, *J* = 17.1, 6.1, 2.8 Hz, 2H), 2.34 (ddt, *J* = 17.1, 11.6, 2.8 Hz, 2H), 2.25 – 2.12 (m, 2H), 1.99 – 1.74 (m, 8H), 1.47 – 1.35 (m, 2H), 1.03 (d, J = 7.1 Hz, 6H); ^{13}C NMR (101 MHz, $CDCl_3$) δ 166.4, 150.6, 149.5, 138.1, 123.7, 120.7, 103.0, 78.2, 75.7, 34.5, 29.8, 24.5, 18.4, 16.6, 15.2; IR (film): ν̃ = 3127, 2958, 2923, 2852, 2357, 2209, 2171, 2145, 2056, 1706, 1614, 1511, 1459, 1435, 1385, 1364, 1342, 1257, 1170, 1123, 1097, 1008, 970, 918, 896, 825, 798, 787, 743, 661, 641,

536, 496, 480, 469, 450, 420, 407 cm^{-1}; $[\alpha]_D^{20}$= 11.5 (c = 0.2, $CHCl_3$); HRMS-ESI+ (*m/z*): calc'd. for $C_{30}H_{35}N_2O_6$ $[M+H]^+$, 519.2490; found, 519.2487.

Samroiyotmycin A (1)

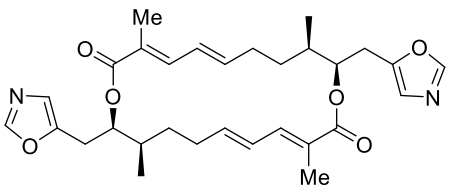

A solution of macrocycle **2** (6.5 mg, 13 µmol) in CH_2Cl_2 (1.0 mL) was added to $[RuCp^*Cl]_4$ (**23**) (1.4 mg, 1 µmol, 10 mol%) with vigorous stirring. A solution of Bu_3SnH (8.4 µL, 25 µmol, 2.0 equiv.) in CH_2Cl_2 (0.1 mL) was added dropwise and the reaction mixture was stirred at rt for 0.5 h. After that, the solvent was removed under reduced pressure and the residue obtained was dissolved in DMF/MeOH (10:1, 0.5 mL). $CuPO_2Ph_2$ (**24**) (20 µg, 68 µmol, 2.0 equiv.) was added and the resulting mixture was stirred for 0.5 h at rt. The solvent was removed under reduced pressure and the residue was purified by preparative HPLC (50 mm Eclipse Plus C_{18} 1.8 µm, 3.0 mm i.d. Methanol / Water-Gradient:70% - 5' - 95% MeOH, 0.5 mL / min, 18.0 MPa, 308 K, UV, 254 nm). This afforded Samroiyotmycin A (**1**) as a white solid (2 mg, 31 %). ^{1}H NMR (600 MHz, $CDCl_3$): δ = 7.76 (s, 2H), 6.94 (dq, *J* = 11.3, 1.3 Hz, 2H), 6.80 (s, 2H), 6.27 (dddd, *J* = 15.2, 11.3, 1.8, 0.8 Hz, 2H), 5.97 (ddd, *J* = 14.9, 9.0, 5.8 Hz, 2H), 5.09 (ddd, *J* = 9.1, 4.2, 3.0 Hz, 2H), 2.92 (ddd, *J* = 15.6, 4.2, 1.0 Hz, 2H), 2.87 (ddd, *J* = 15.5, 9.1, 0.9 Hz, 2H), 2.46 – 2.39 (m, 2H), 2.08 (tdd, *J* = 14.2, 9.2, 1.8 Hz, 2H), 1.86 – 1.74 (m, 10H), 1.44 – 1.38 (m, 2H), 0.99 (d, *J* = 7.1 Hz, 6H); ^{13}C NMR (151 MHz, $CDCl_3$): δ = 167.7, 150.5, 149.6, 142.5, 138.3, 127.6, 125.7, 123.7, 75.3, 34.4, 30.0, 29.9, 25.0, 16.5, 12.8; IR (film): ṽ = 2958, 2922, 2853, 1700, 1634, 1607, 1510, 1460, 1388, 1364, 1312, 1288, 1239, 1102, 1193, 1156, 1102, 1012, 972, 922, 825, 746, 648 cm^{-1}; Lit. $[\alpha]_D^{20}$= + 80.9 (c = 0.09, MeOH), $[\alpha]_D^{20}$= + 76.7 (c = 0.08, MeOH); HRMS-ESI+ (*m/z*): calc'd. for $C_{30}H_{38}N_2O_6$ $[M+Na]^+$, 545.2622; found, 545.2620; R_t (Minor Isomer 1, HPLC Method 10) = 4.75 min, R_t (Minor Isomer 2, HPLC Method 10) = 4.65 min, R_t (samroiyotmycin A (**1**), HPLC Method 10) = 4.53 min; R_t (samroiyotmycin A (**1**), Preparative HPLC Method 1) = 4.53 min. The ^{1}H and ^{13}C NMR spectroscopic data are in agreement with those reported in the literature.[10]

5.3.3 References Experimental Chapter 3

[1] T. Speltz, S. Fanning, C. Mayne, C. Fowler, E. Tajkhorshid, G. Greene, T. Moore*, Angew. Chem. Int. Ed.* **2016**, *55*, 4252-4255.

[2] M. Fuchs, A. Fürstner, *Angew. Chem. Int. Ed.* **2015**, *54*, 3978-3982.

[3] Z. Meng, A. Fürstner, *J. Am. Chem. Soc.* **2020**, *142*, 11703–11708

[4] W. Fang, B. Breit, *Angew. Chem. Int. Ed.* **2018**, *57*, 14817-14821.

[5] C. Zhu, X. Shen, S. Nelson, *J. Am. Chem. Soc.*, **2004**, *126*, 5352-5353.

[6] Z. Meng, A. Fürstner, *J. Am. Chem. Soc.* **2020**, *142*, 11703–11708.

[7] J. Robinson, H. Flohr, U. Kempe, W. Panhorst, J. Rétey, Liebigs *Ann. Chem.* **1983**, *2*, 181-203.

[8] D. Mailhol, J. Willwacher, N. Kausch-Busies, E. Rubitski, Z. Sobol, M. Schuler, M. Lam, S. Musto, F. Loganzo, A. Maderna, A. Fürstner, *J. Am. Chem. Soc.* **2014**, *136*, 15719-15729.

[9] S. Saito, S. Nakagawa, T. Koizumi, K. Hirayama and Y. Yamamoto, *J. Org. Chem.* **1999**, *64*, 3975-3978.

[10] A. Dramae, S. Nithithanasilp, W. Choowong, P. Rachtawee, S. Prabpai, P. Kongsaeree and P. Pittayakhajonwut, *Tetrahedron* **2013**, *69*, 8205-8208.

Appendices:

Appendix 1: NMR spectra - Section 5.2.2. Novel Compounds – Substrate Scope

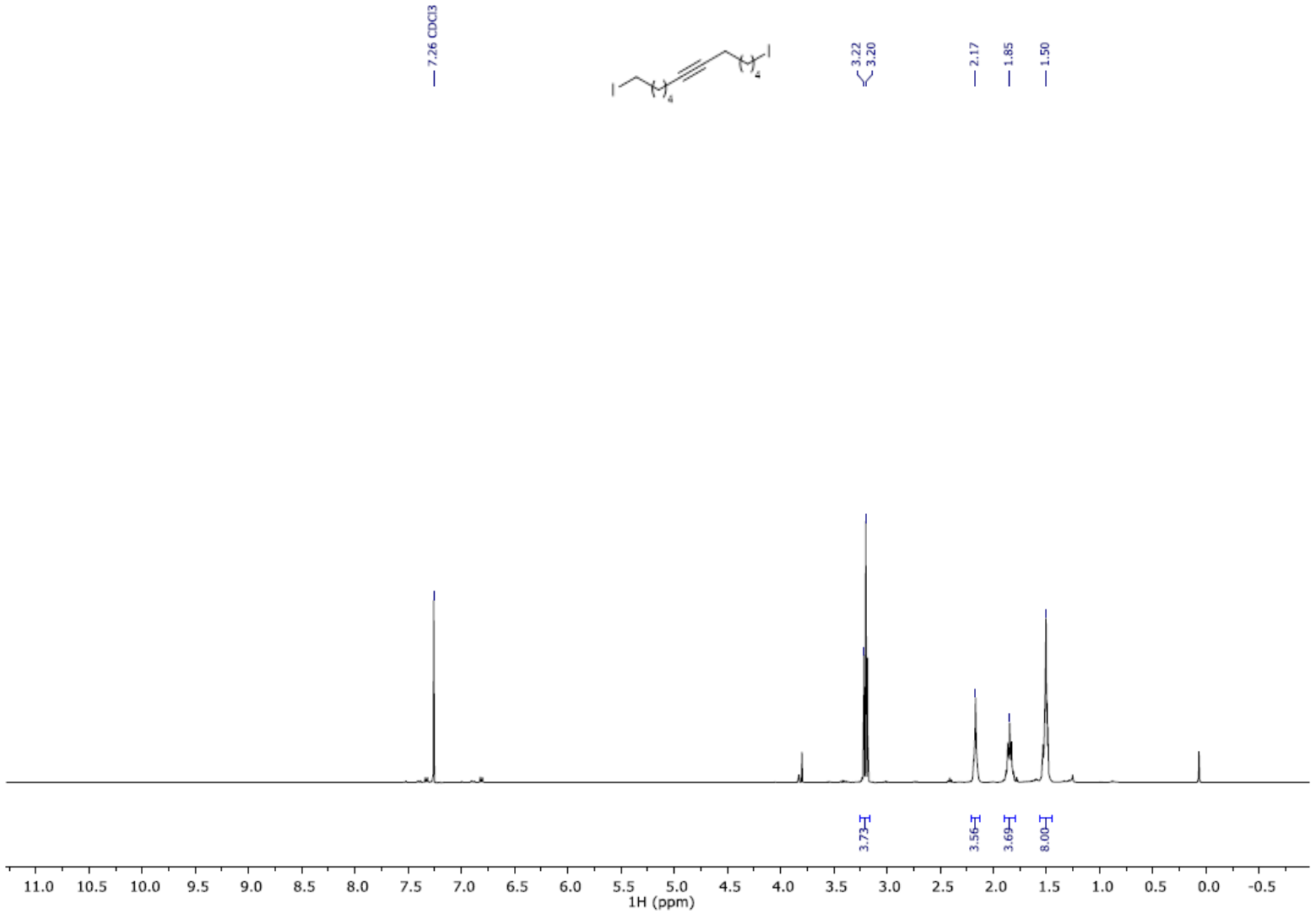
7.26 CDCl3
3.22
3.20
2.17
1.85
1.50
3.73
3.56
3.69
8.00
11.0 10.5 10.0 9.5 9.0 8.5 8.0 7.5 7.0 6.5 6.0 5.5 5.0 4.5 4.0 3.5 3.0 2.5 2.0 1.5 1.0 0.5 0.0 -0.5
1H (ppm)

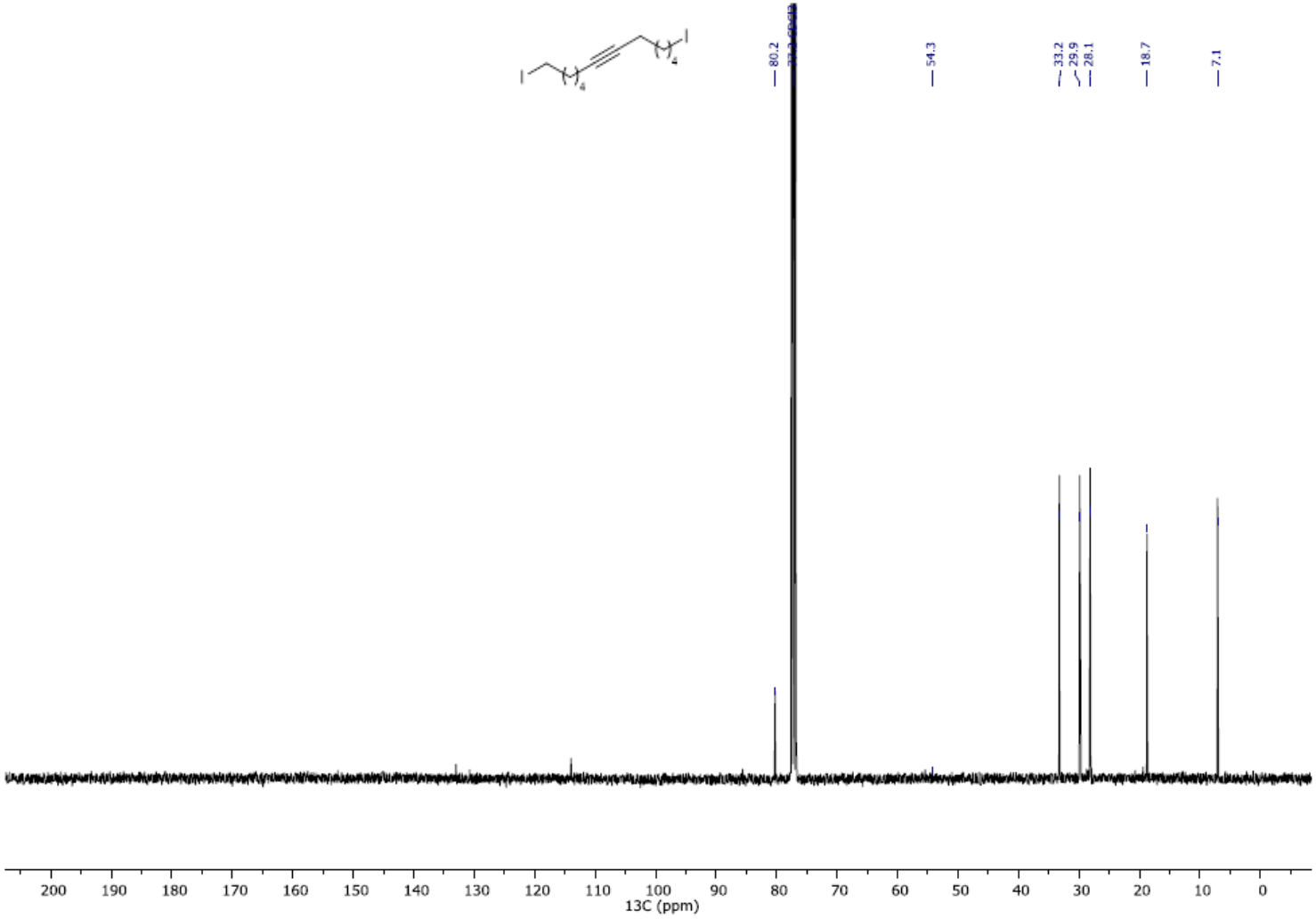
80.2
54.3
33.2
29.9
28.1
18.7
7.1
200
190
180
170
160
150
140
130
120
110
100
90
80
70
60
50
40
30
20
10
0
13C (ppm)

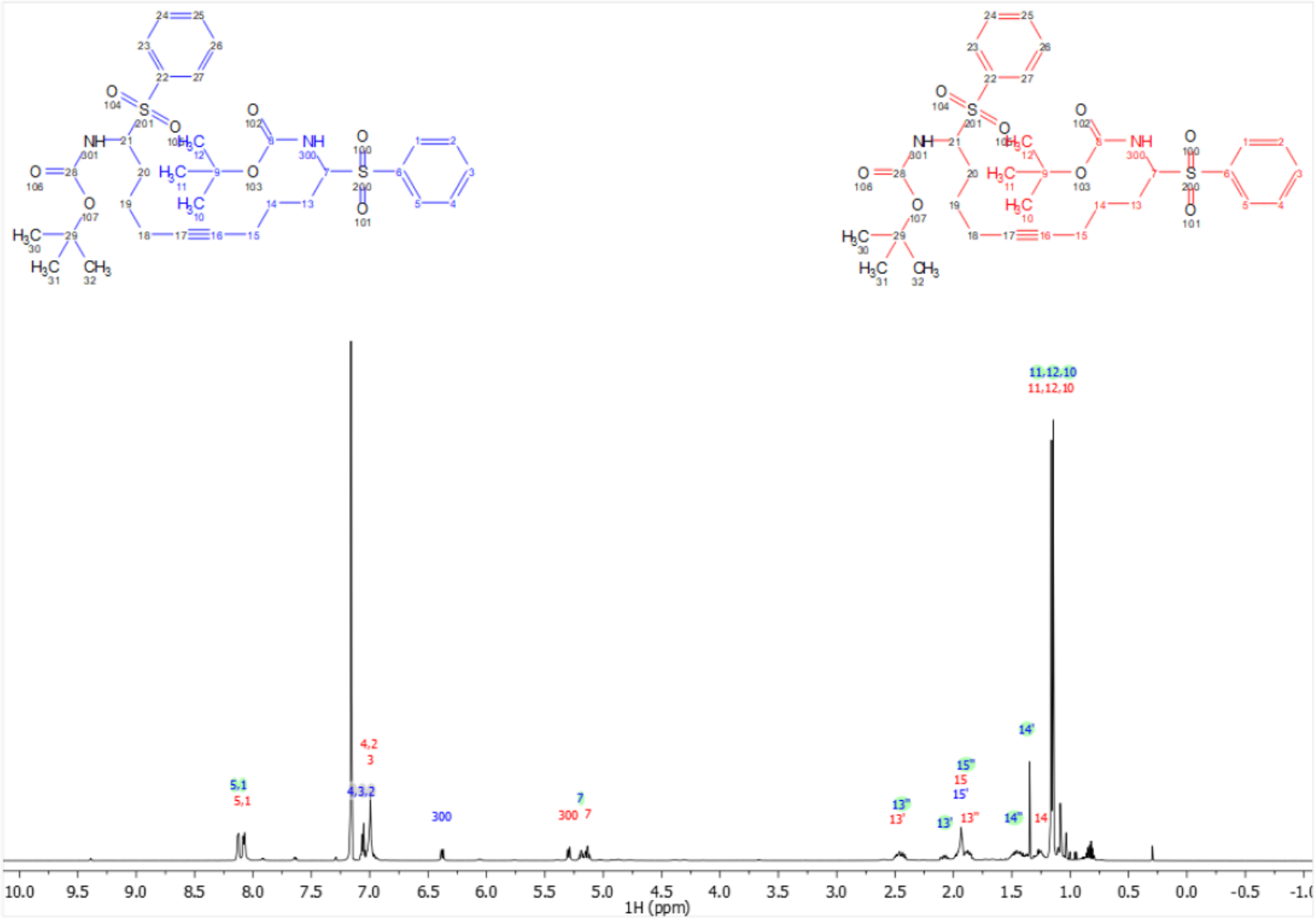
11,12,10
11,12,10
14'
15"
15
15'
4,2
3
5,1
5,1
4,3,2
300
7
300 7
13"
13'
13'
13"
14"
14
1H (ppm)

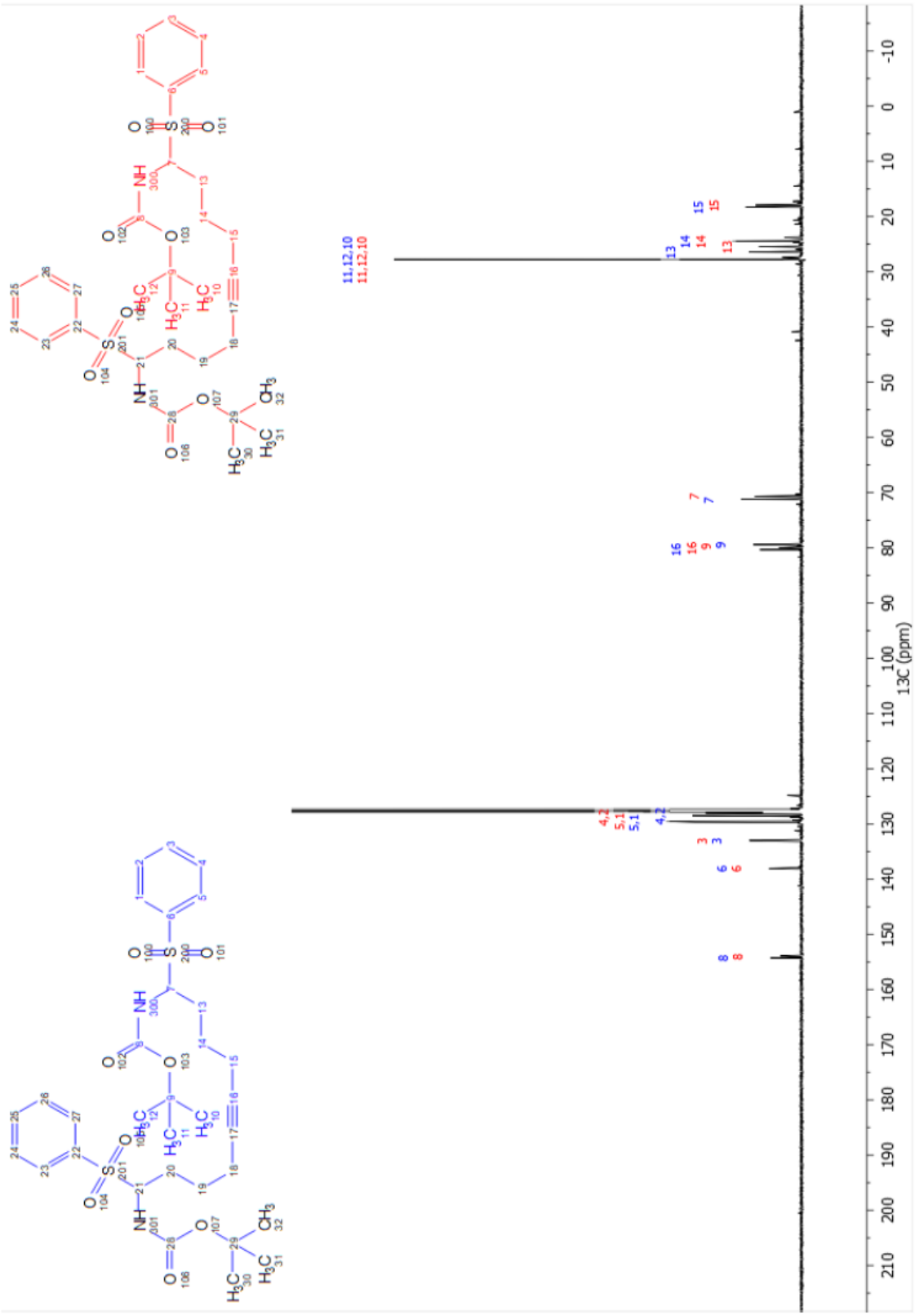
13C (ppm)

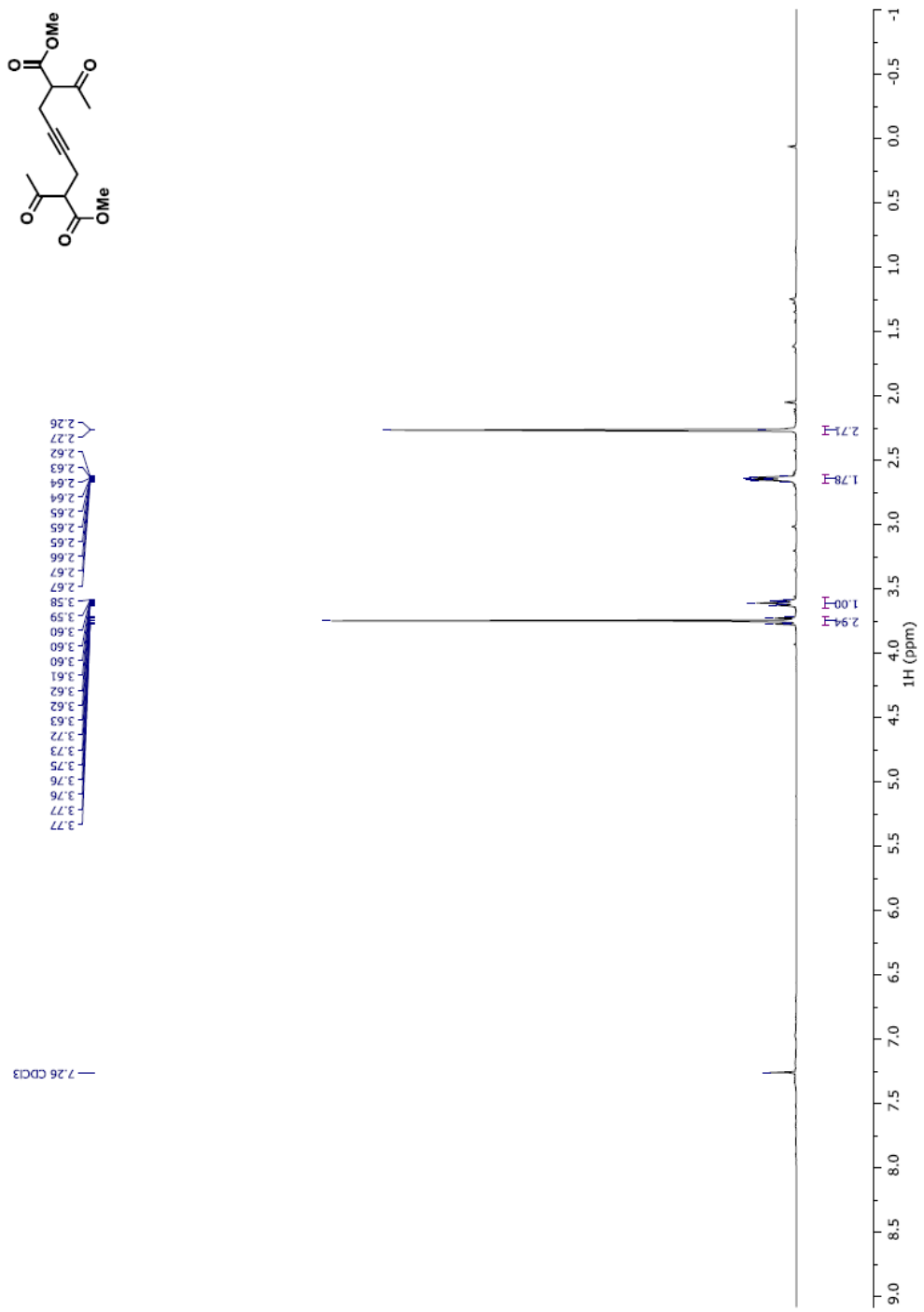
OMe
O
O
O
O
OMe
2.26
2.27
2.62
2.63
2.64
2.64
2.65
2.65
2.65
2.66
2.67
2.67
3.58
3.59
3.60
3.60
3.60
3.61
3.62
3.62
3.63
3.72
3.73
3.75
3.76
3.76
3.77
3.77
7.26 CDCl3
2.71
1.78
1.00
2.94
9.0
8.5
8.0
7.5
7.0
6.5
6.0
5.5
5.0
4.5
4.0
3.5
3.0
2.5
2.0
1.5
1.0
0.5
0.0
-0.5
-1
1H (ppm)

OMe
O
O
O
OMe
O
O
17.9
29.6
52.8
58.5
78.4
77.2 CDCl3
168.8
201.4
13C (ppm)

HO
OH
7.26 CDCl3
3.64
3.63
3.61
2.15
2.14
2.14
2.13
2.12
2.12
2.11
1.59
1.58
1.57
1.56
1.56
1.54
1.54
1.52
1.50
1.50
1.48
1.48
1.47
1.46
1.46
1.45
1.43
1.41
1.39
1.37
1.36
1.36
1.35
1.34
1.34
1.33
1.33
1.32
1.30
1.29
1.29
1.28
1.27
1.25
0.06 grease
15.65
7.65
4.18
4.00
1H (ppm)

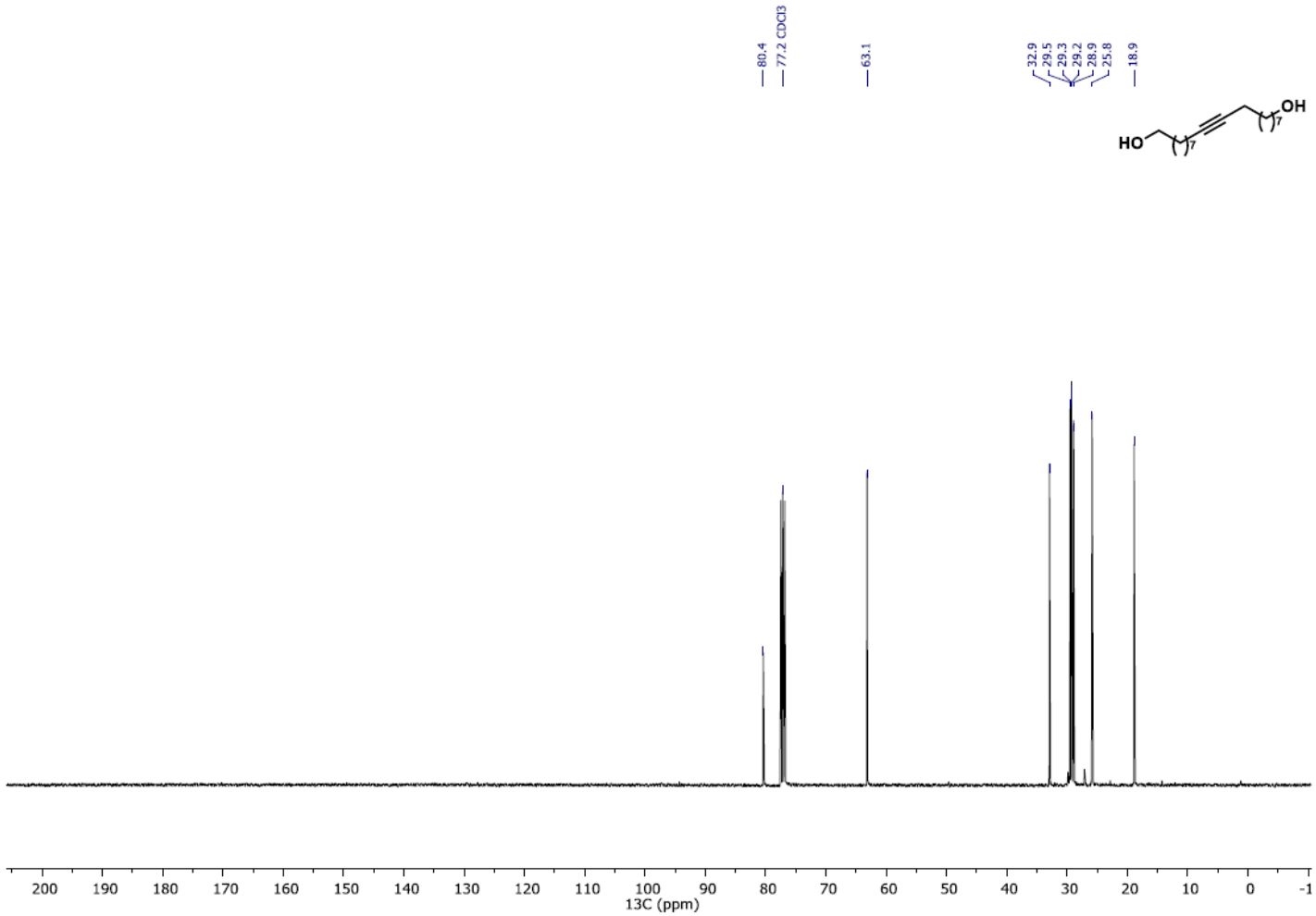
80.4
77.2 CDCl3
63.1
32.9
29.5
29.3
29.2
28.9
25.8
18.9
HO
OH
7
7
200 190 180 170 160 150 140 130 120 110 100 90 80 70 60 50 40 30 20 10 0 -1
13C (ppm)

Appendix 2: NMR spectra - Section 5.2.3. Ligands and Ligand Precursors

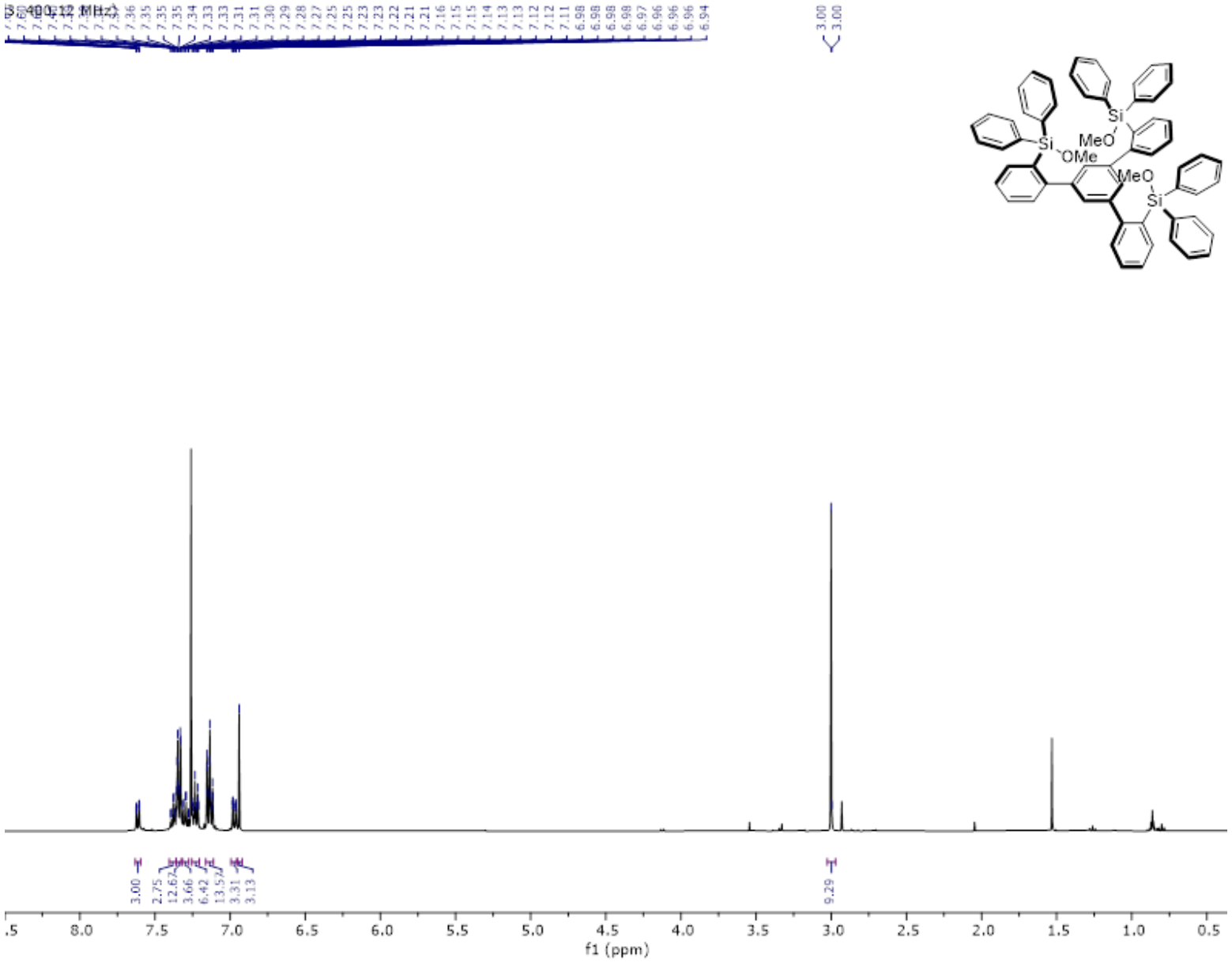
Si
MeO
Si
OMe
MeO
Si
f1 (ppm)

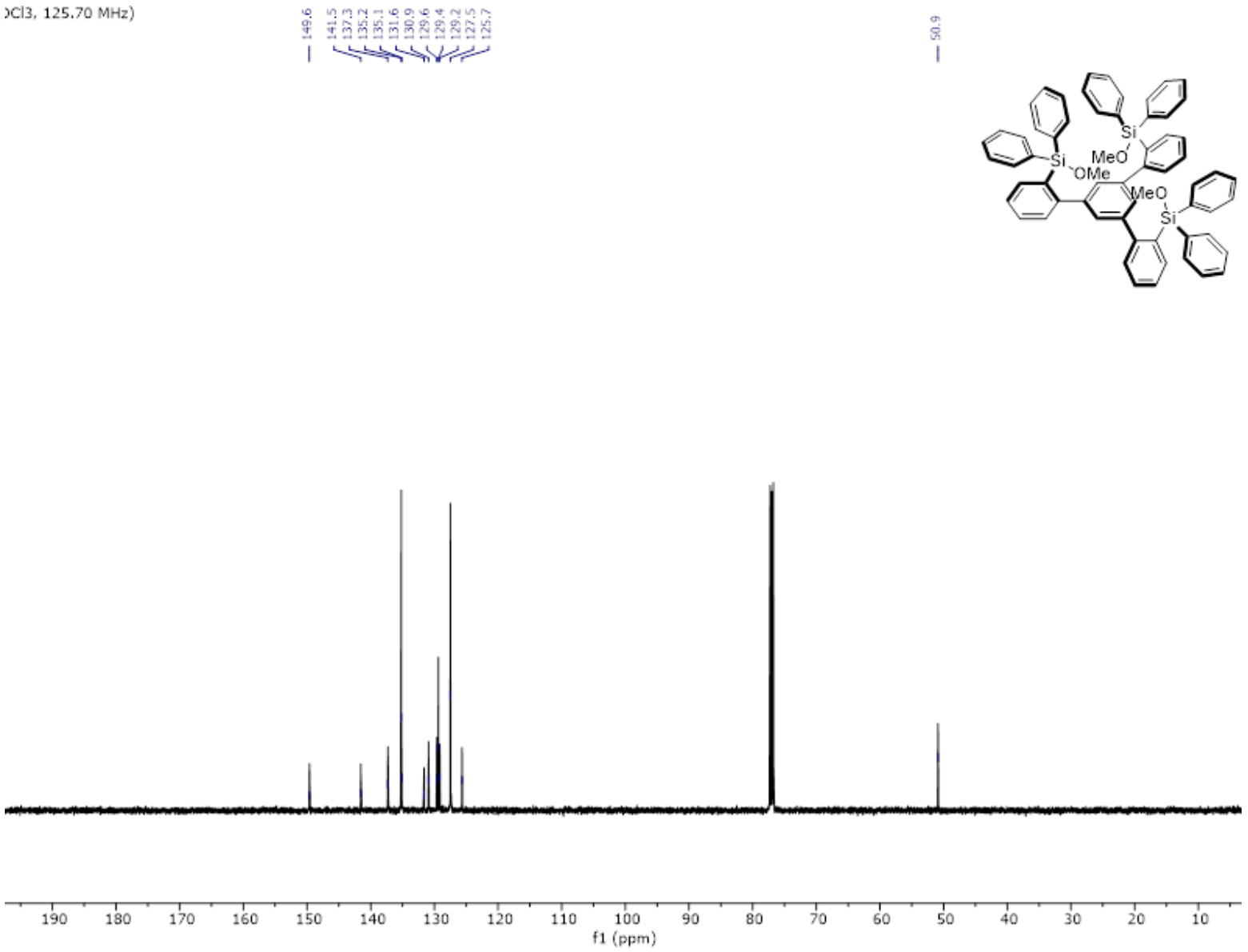
)Cl3, 125.70 MHz)
149.6
141.5
137.3
135.2
135.1
131.6
130.9
129.6
129.4
129.2
127.5
125.7
50.9
Si
MeO
Si
OMe
MeO
Si
190
180
170
160
150
140
130
120
110
100
90
80
70
60
50
40
30
20
10
f1 (ppm)

MeO
MeO
OMe
Si
Si
Si
-11.6
120 100 80 60 40 20 0 -20 -40 -60 -80 -100 -120 -140 -160 -180 -200 -220 -240 -260 -280 -300 -320 -340 -360 -380 -400 -420
29Si (ppm)

HO
Si
HO
Si
OH
Si
4.36
6.88
6.89
6.89
6.90
6.90
7.14
7.14
7.15
7.16
7.16
7.16
7.18
7.18
7.18
7.25
7.25
7.25
7.26 CDCl3
7.26
7.27
7.27
7.45
7.46
7.46
7.47
7.47
7.52
7.52
7.53
7.53
7.54
7.54
7.54
3.21
6.00
13.53
20.83
2.94
12.91
1H (ppm)

77.2 CDCl3
126.0
127.9
128.6
129.4
129.7
130.1
133.9
134.6
137.0
137.5
143.8
149.0
13C (ppm)

Me
Si
H
Me
Me
Si
H
Me
Me
Si
H
0.07 grease
0.14
0.15
1.55 H2O
2.17 acetone
4.42
4.43
4.44
4.44
4.45
4.46
4.47
7.26
7.26 CDCl3
7.34
7.34
7.35
7.36
7.36
7.36
7.36
7.37
7.37
7.37
7.37
7.37
7.38
7.41
7.42
7.43
7.43
7.43
7.44
7.45
7.62
7.62
7.62
7.62
7.63
7.63
7.63
7.63
7.63
17.95
3.02
4.68
2.88
3.40
10.0
9.5
9.0
8.5
8.0
7.5
7.0
6.5
6.0
5.5
5.0
4.5
4.0
3.5
3.0
2.5
2.0
1.5
1.0
0.5
0.0
-0.5
-1.0
1H (ppm)

Me
Me
Si
H
H
Si
Me
Me
Me
Me
Si
H
-2.6
77.2 CDCl3
126.6
129.0
129.3
129.6
135.2
136.0
143.2
149.1
200
190
180
170
160
150
140
130
120
110
100
90
80
70
60
50
40
30
20
10
0
-10
13C (ppm)

Me
Me
Si
H
H
Si
Me
Me
Me
Me
Si
H
-19.1
-90
-80
-70
-60
-50
-40
-30
-20
-10
0
10
20
29Si (ppm)
30
40
50
60
70
80
90
100
110
120
130
140

0.07 grease
0.88
0.89
0.89
0.90
0.90
0.95
0.96
1.02
1.03
1.03
1.04
1.04
1.05
1.05
1.05
1.06
1.06
1.06
1.07
1.07
1.08
1.08
1.08
1.08
1.09
1.09
1.10
1.11
1.55 H2O
3.67
3.68
3.68
3.86
3.87
3.87
4.05
4.05
4.06
7.20
7.26
7.26 CDCl3
7.31
7.31
7.32
7.33
7.34
7.34
7.35
7.36
7.36
7.36
7.37
7.37
7.37
7.39
7.39
7.40
7.41
7.41
7.41
7.42
7.42
7.56
7.56
7.56
7.56
7.57
7.57
7.57
7.57
0.18
0.18
0.18
0.19
0.01
0.17
0.34
1.00
0.98
10.0
9.5
9.0
8.5
8.0
7.5
7.0
6.5
6.0
5.5
5.0
4.5
4.0
3.5
3.0
2.5
2.0
1.5
1.0
0.5
0.0
-0.5
-1.0
1H (ppm)

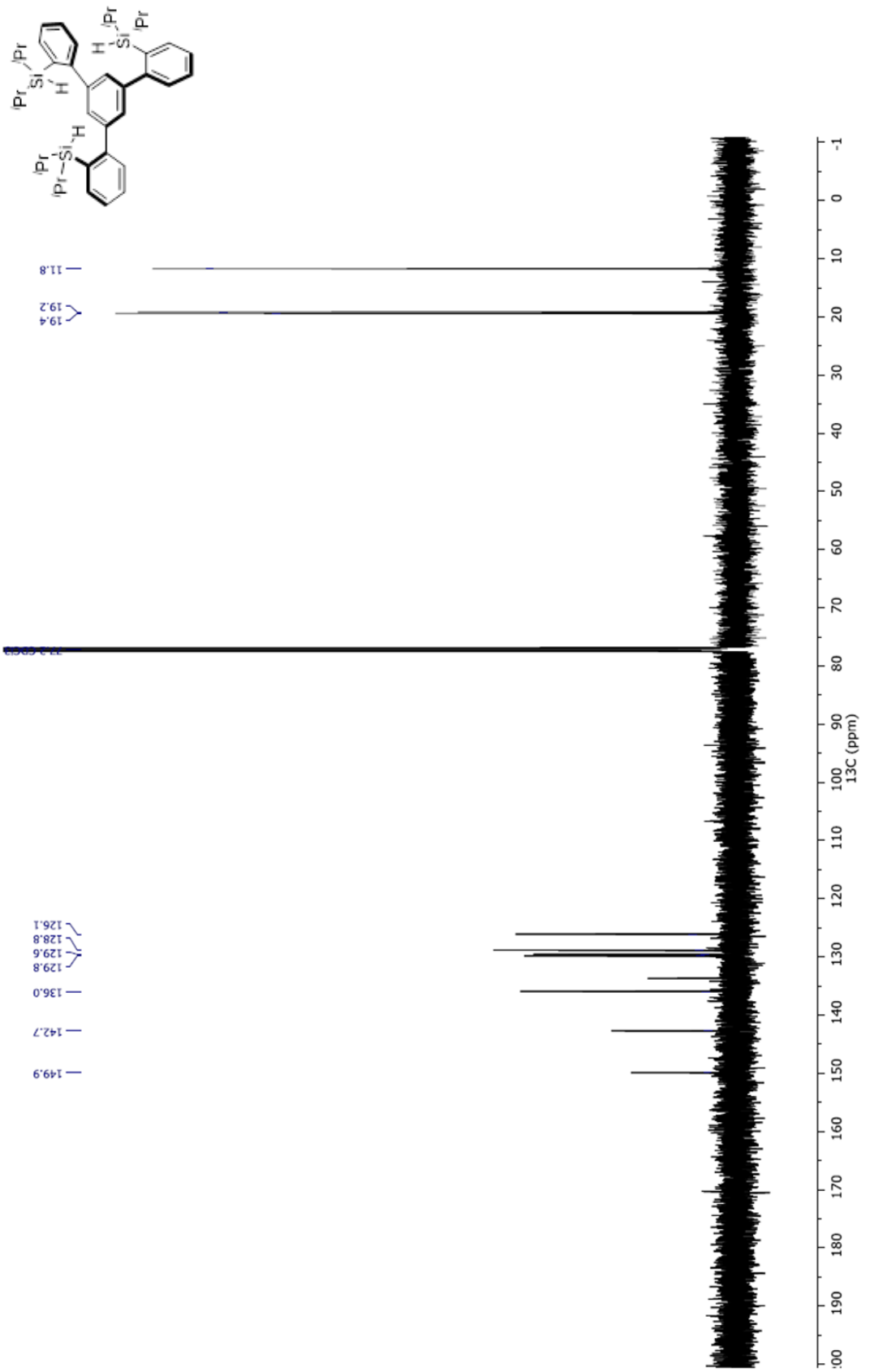
11.8
19.4
19.2
126.1
128.8
129.6
129.8
136.0
142.7
149.9
13C (ppm)

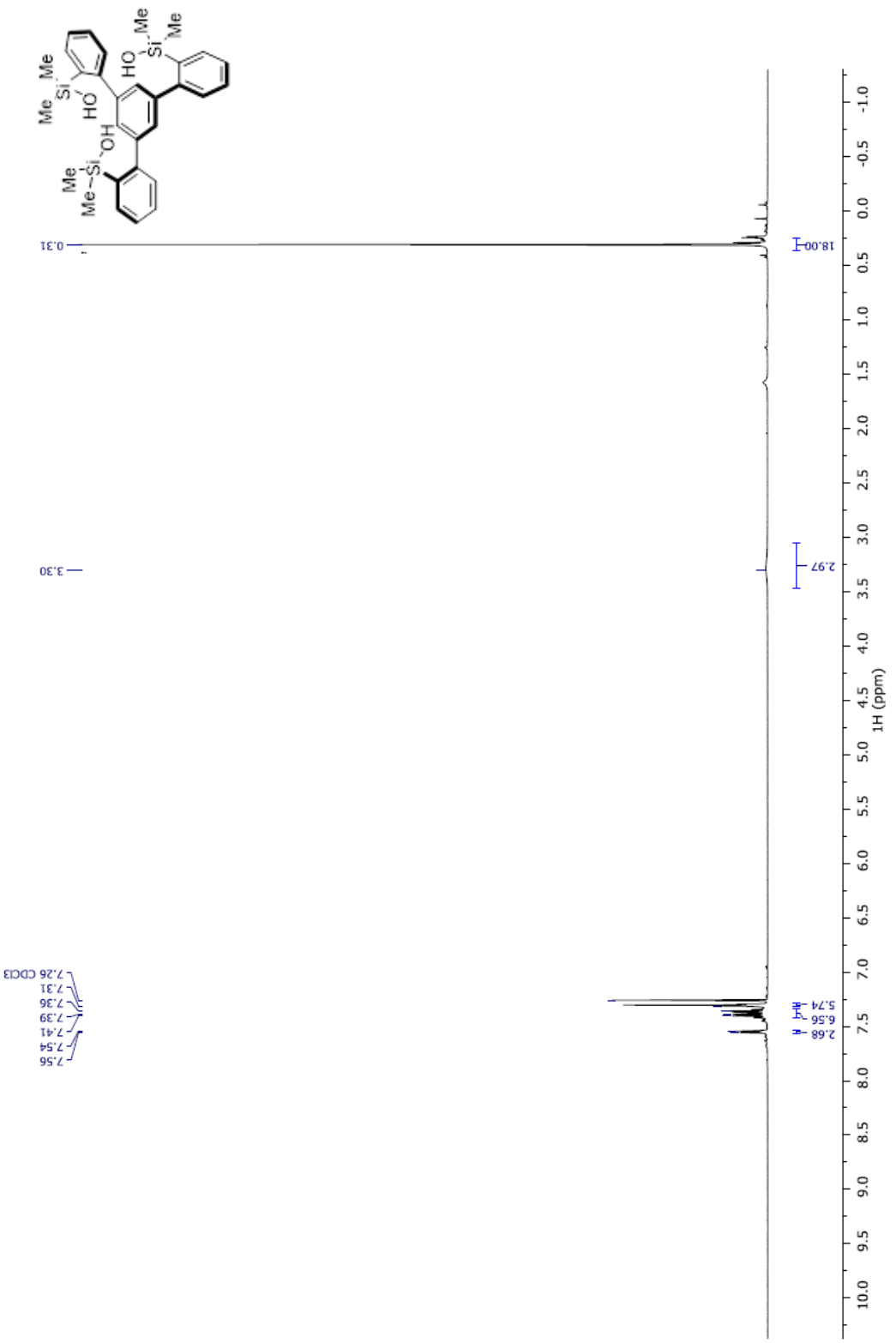
Me
Me
Si
HO
HO
Si
Me
Me
Si
OH
Me
Me
Si
Me
0.31
3.30
7.26 CDCl3
7.56
7.54
7.41
7.39
7.36
7.31
18.00
2.97
5.74
6.56
2.68
10.0
9.5
9.0
8.5
8.0
7.5
7.0
6.5
6.0
5.5
5.0
4.5
4.0
3.5
3.0
2.5
2.0
1.5
1.0
0.5
0.0
-0.5
-1.0
1H (ppm)

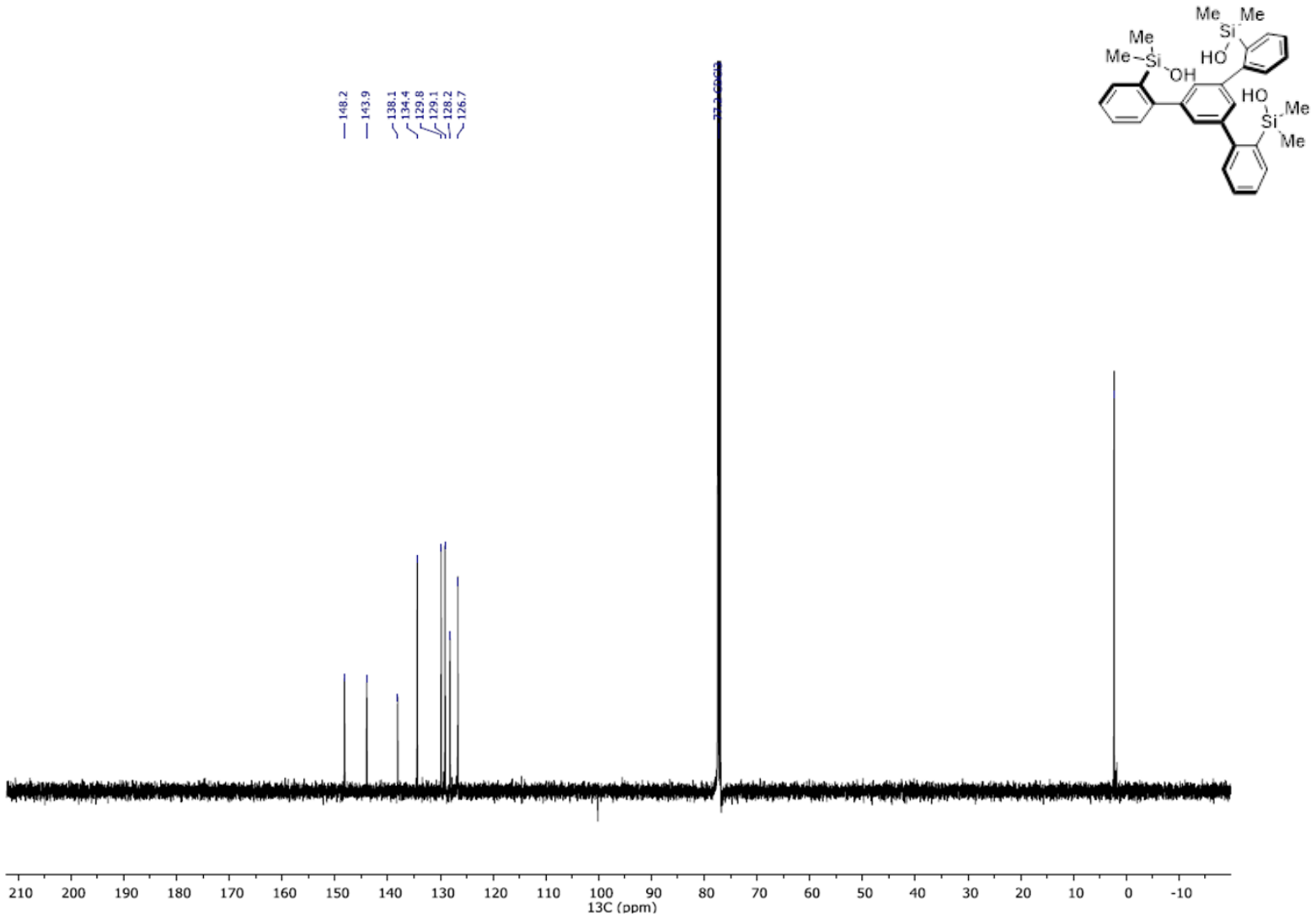
148.2
143.9
138.1
134.4
129.8
129.1
128.2
126.7
77.3
Me
Me
Si
HO
Me
Me
Si
OH
HO
Si
Me
Me
210
200
190
180
170
160
150
140
130
120
110
100
90
80
70
60
50
40
30
20
10
0
-10
13C (ppm)

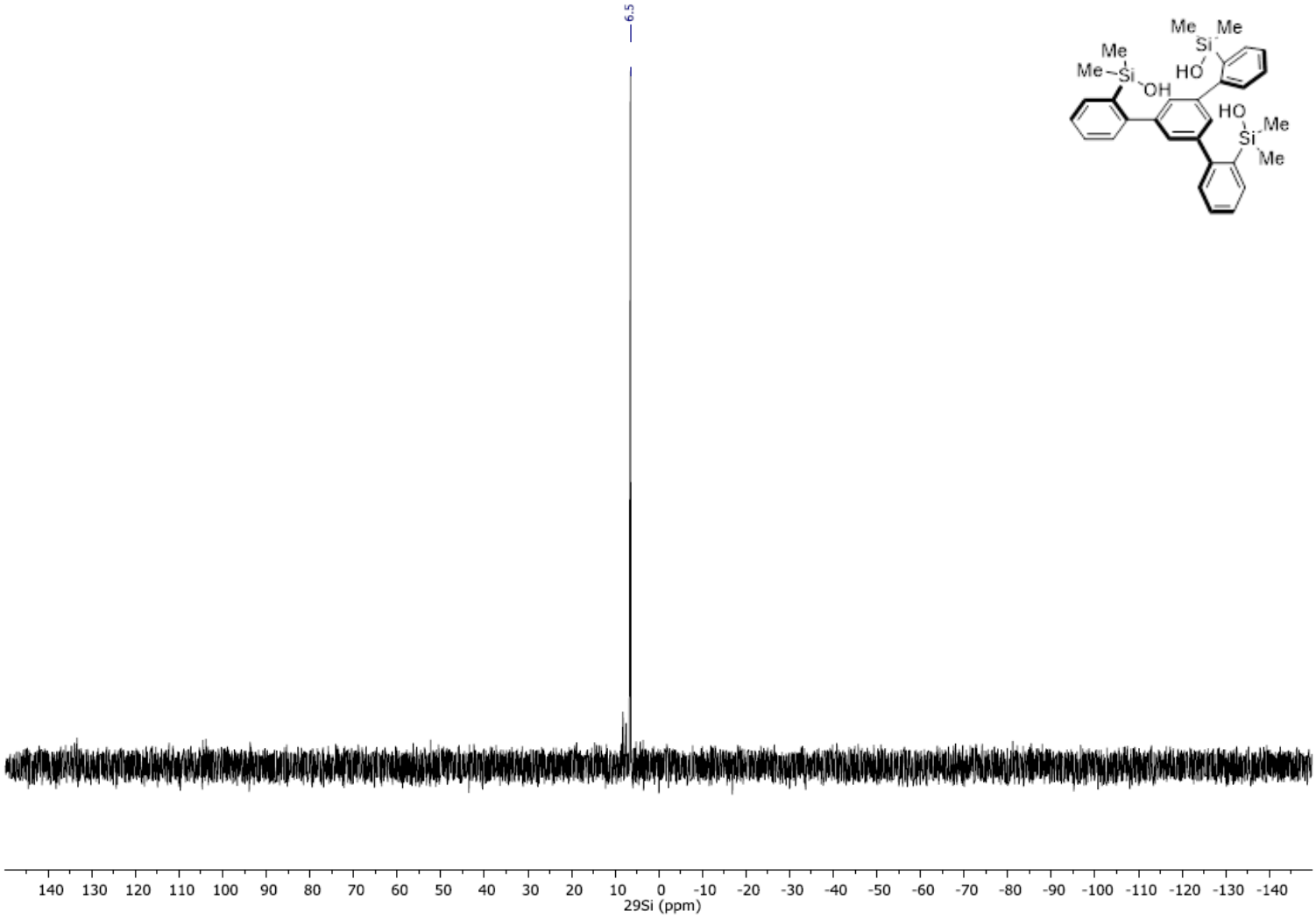
6.5
Me
Me
Si
HO
Me
Me
Si
OH
HO
Me
Si
Me
140 130 120 110 100 90 80 70 60 50 40 30 20 10 0 -10 -20 -30 -40 -50 -60 -70 -80 -90 -100 -110 -120 -130 -140
29Si (ppm)

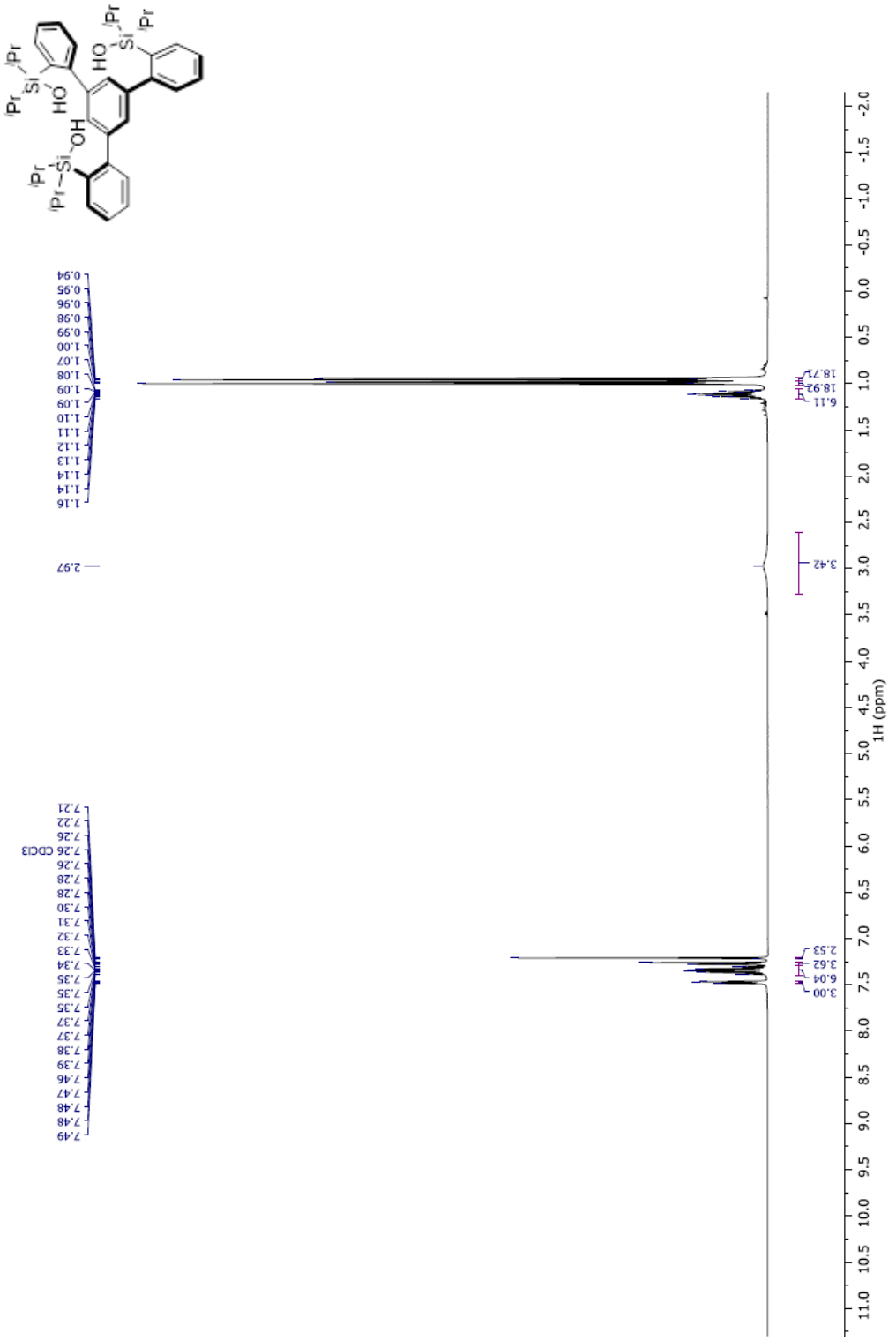
1H (ppm)
CDCl3

14.1
17.9
18.1
77.2 CDCl3
126.0
127.7
128.5
130.2
134.3
135.0
143.6
149.3
13C (ppm)

iPr
Si
iPr
iPr
HO
iPr
Si
iPr
HO
OH
iPr
Si
iPr
7.7
8
-4
0
2
4
6
8
10
12
14
16
18
20
22
24
26
28
30
32
34
36
-2
-6
-8
-10
29Si (ppm)

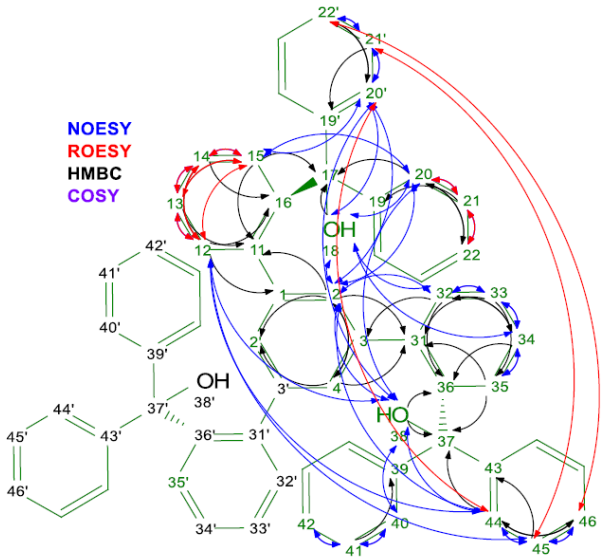

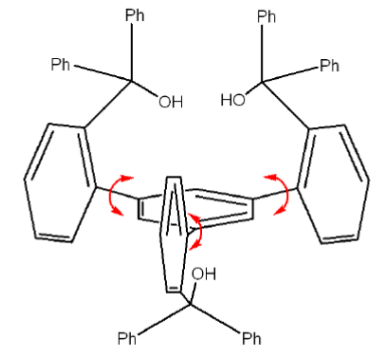

C2-symmetry with conformational exchange

Although this molecule might be expected to have 3-fold symmetry, the NMR results clearly indicate that a 2-fold symmetry is present in CD_2Cl_2 at low temperature (-50°C). The axis of symmetry is indicated by the numbering of the atoms (e.g. 2 and 2'). This symmetry is clearly visible through 2:1 integrals for corresponding 1Hs (e.g. 38OH:18:OH = 2:1). Importantly, this molecule shows int-slow dynamics (on the NMR timescale) which causes the lines to broadened at ambient temperature. At low T, one can differentiate the exchanging nuclei.The symmetry, dynamic exchange and

^{1}H ROESY NMR CD_2Cl_2, –50°C

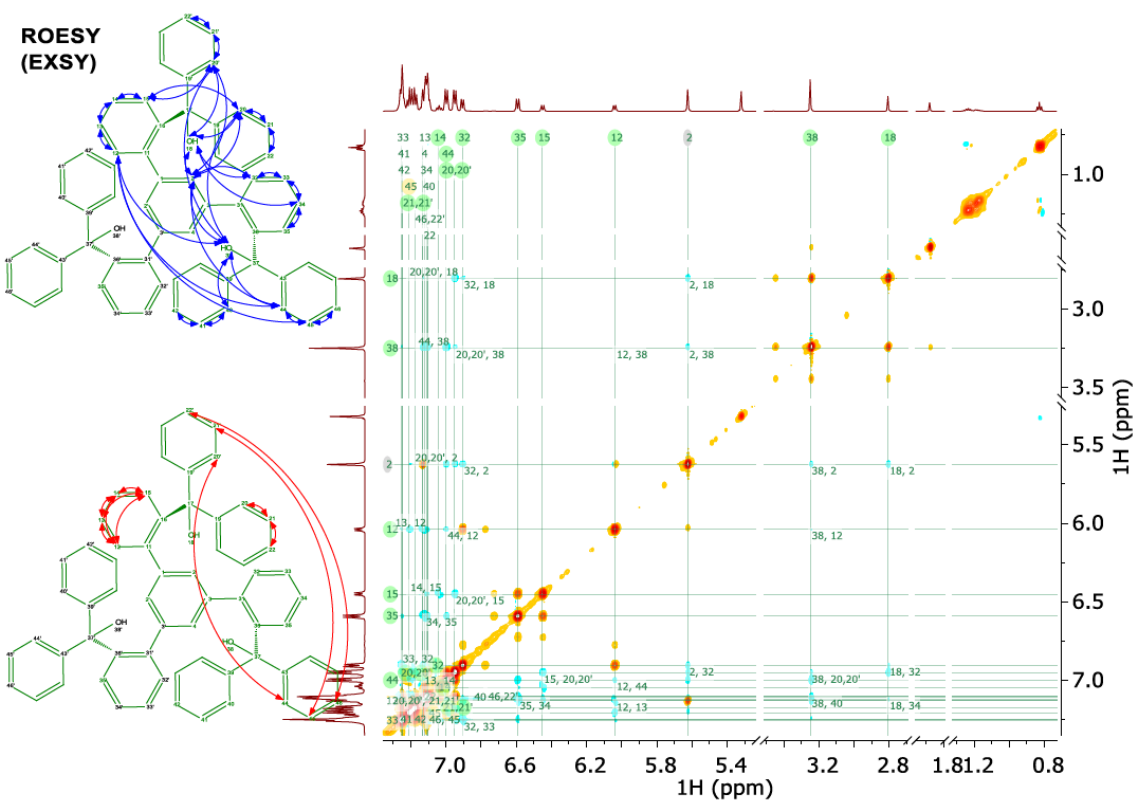

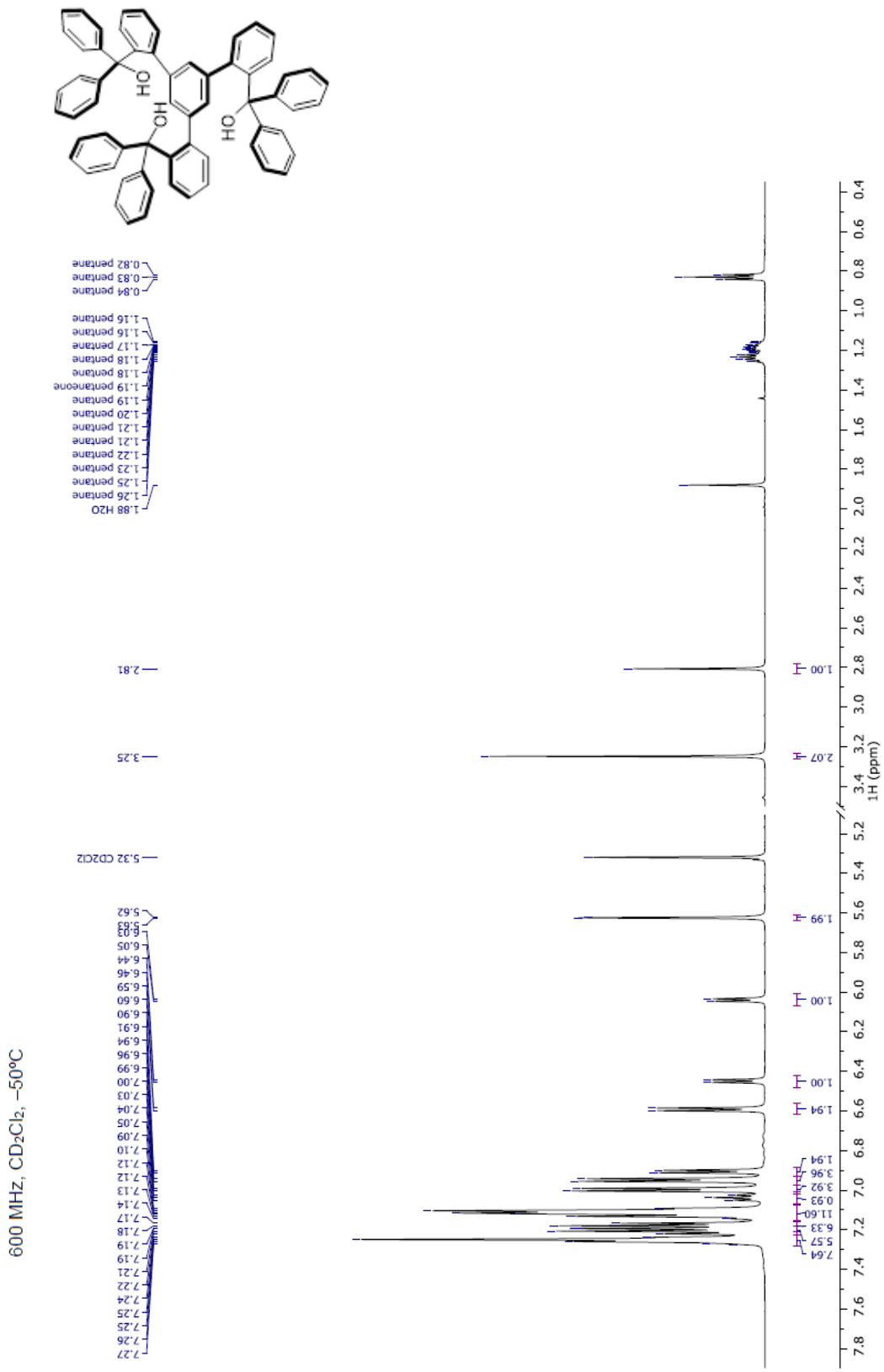
600 MHz, CD2Cl2, –50°C
1H (ppm)

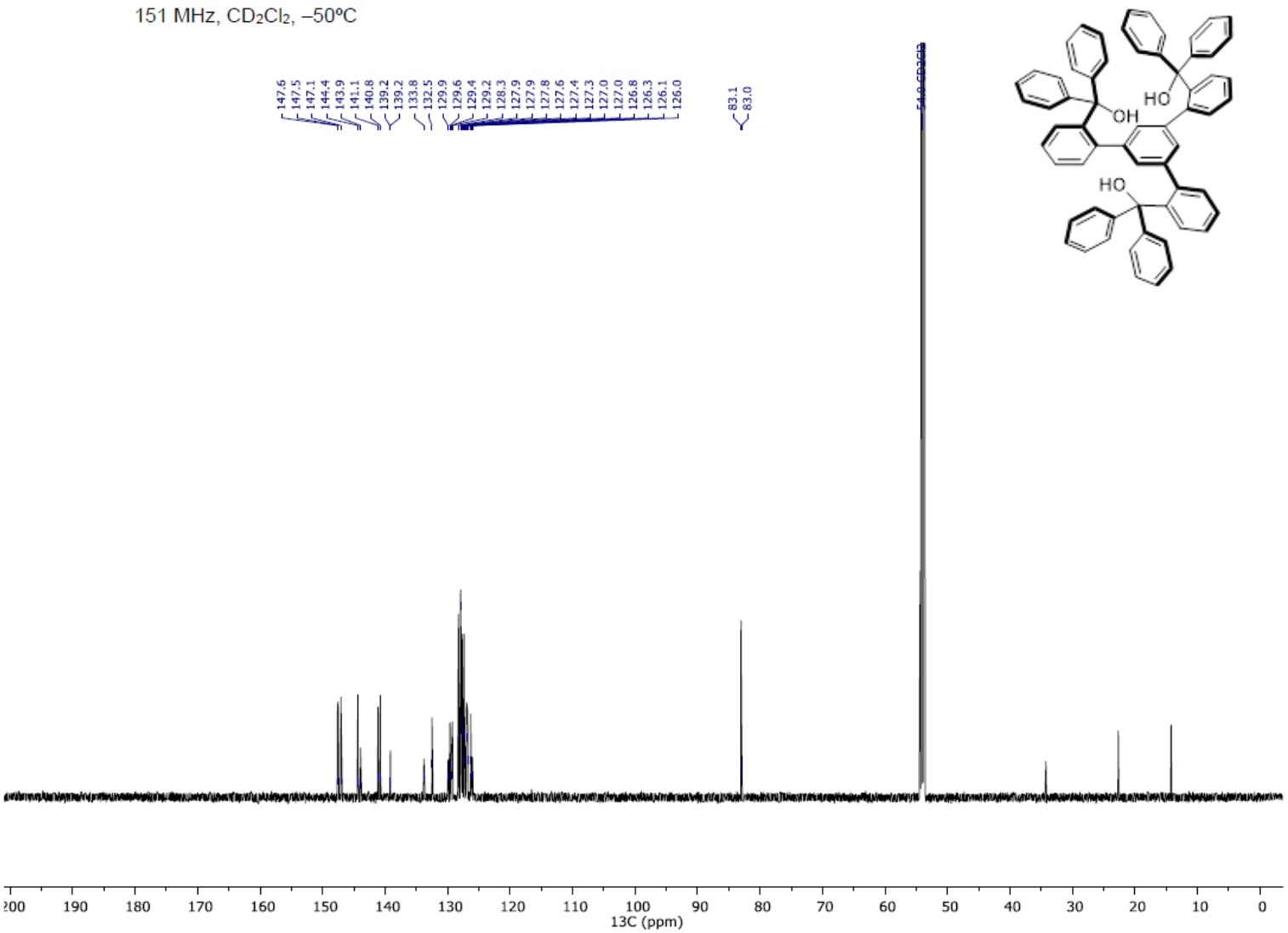
151 MHz, CD2Cl2, –50°C
147.6
147.5
147.1
144.4
143.9
141.1
140.8
139.2
139.2
133.8
132.5
129.9
129.6
129.4
129.2
128.3
127.9
127.9
127.8
127.6
127.4
127.3
127.0
127.0
126.8
126.3
126.1
126.0
83.1
83.0
HO
OH
HO
200
190
180
170
160
150
140
130
120
110
100
90
80
70
60
50
40
30
20
10
0
13C (ppm)

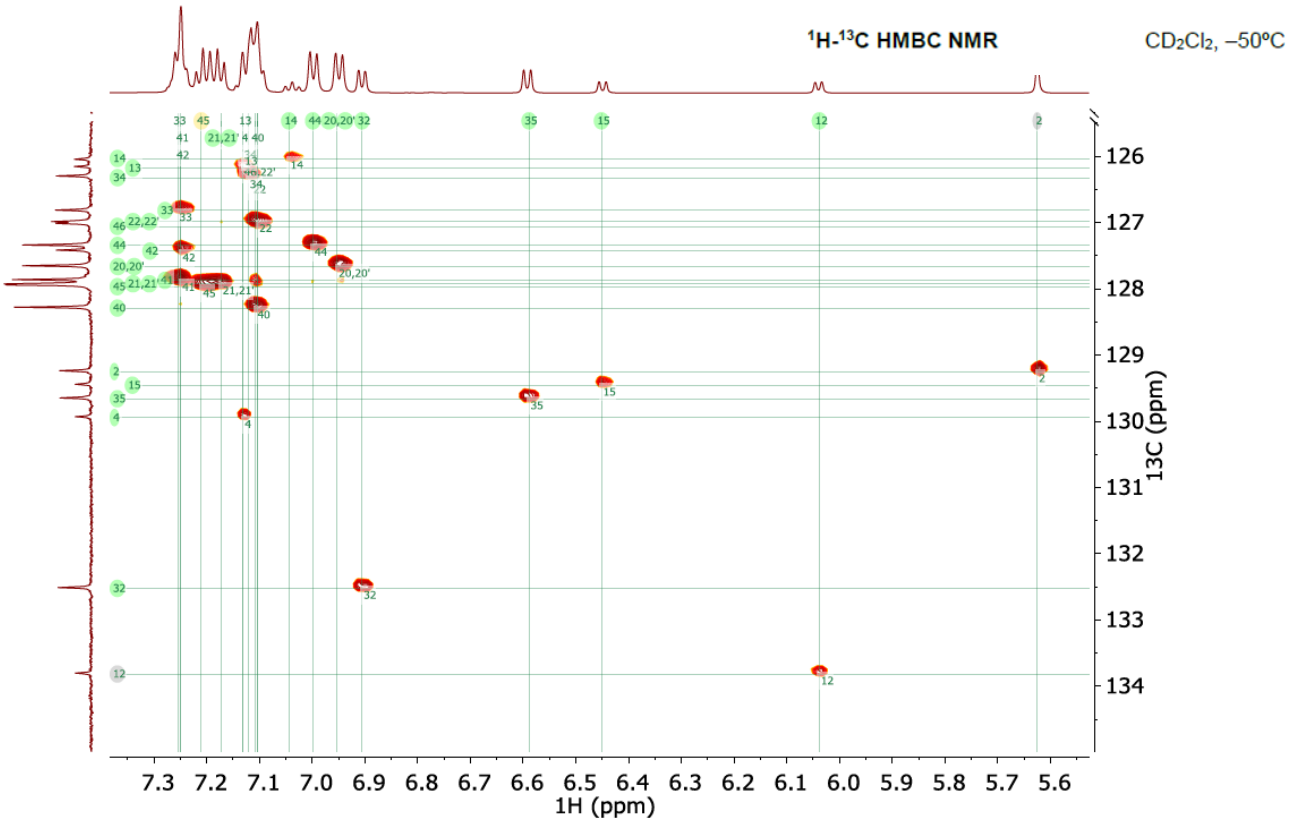
^{1}H-^{13}C HMBC NMR
CD_2Cl_2, –50°C
1H (ppm)
13C (ppm)

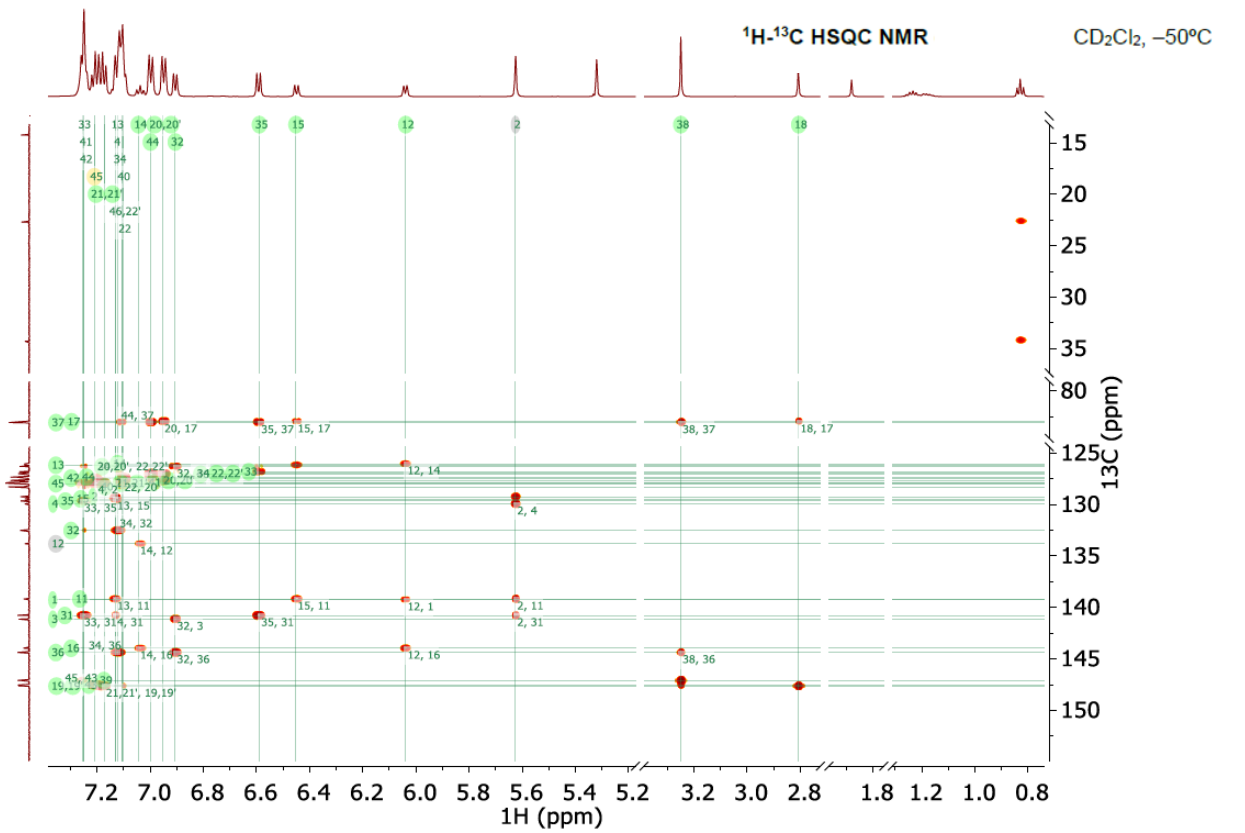
^{1}H-^{13}C HSQC NMR
CD_2Cl_2, –50°C
1H (ppm)
13C (ppm)

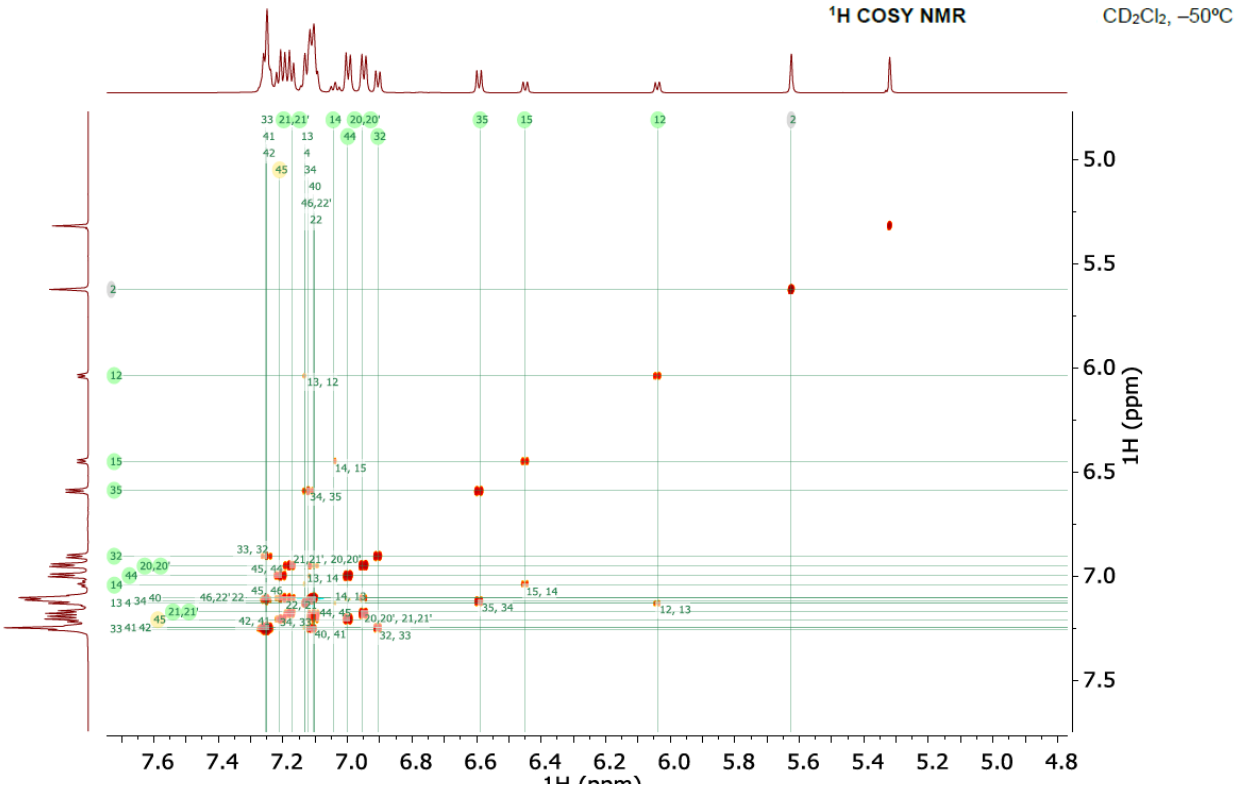
¹H COSY NMR
CD₂Cl₂, –50°C
1H (ppm)

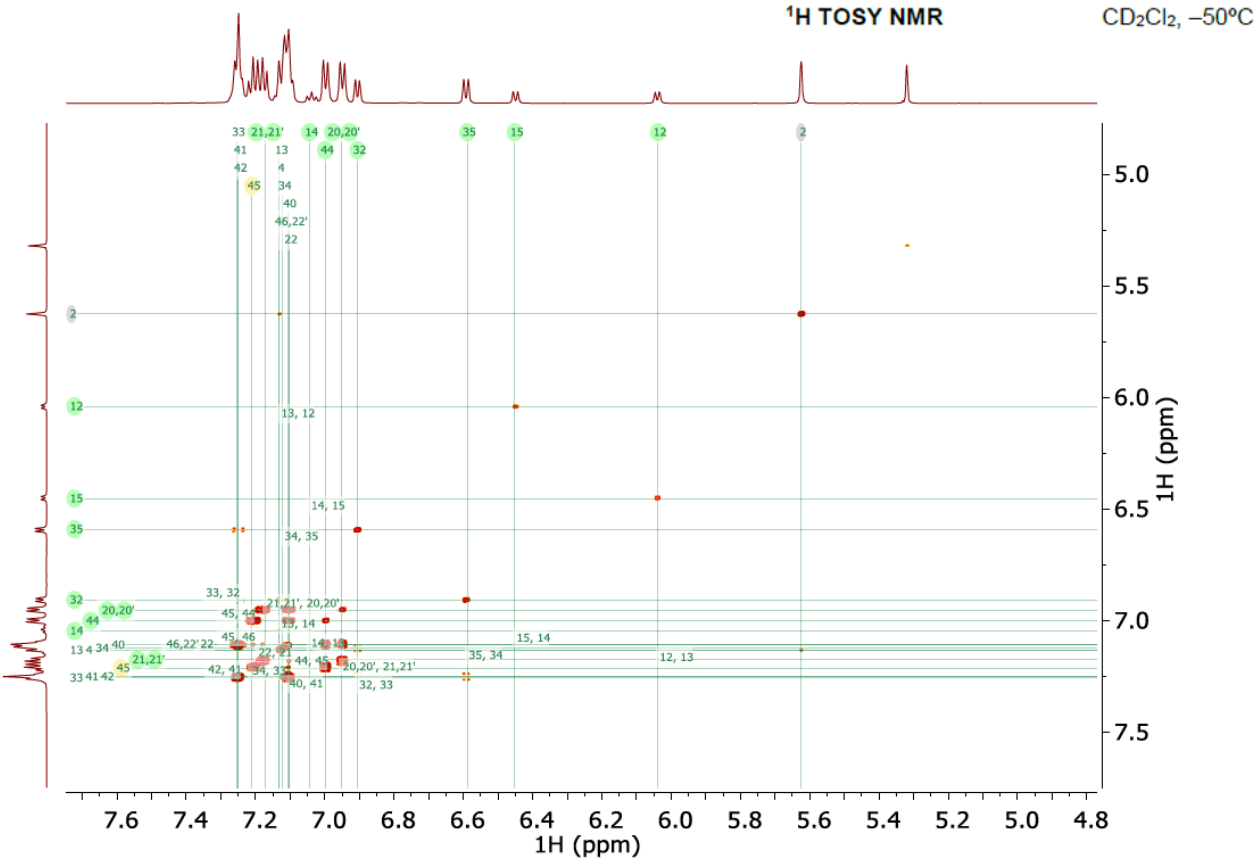
¹H TOSY NMR
CD₂Cl₂, –50°C
1H (ppm)

400.12 MHz)

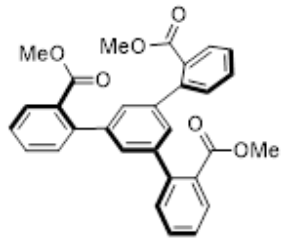
MeO
O
MeO
O
O
OMe

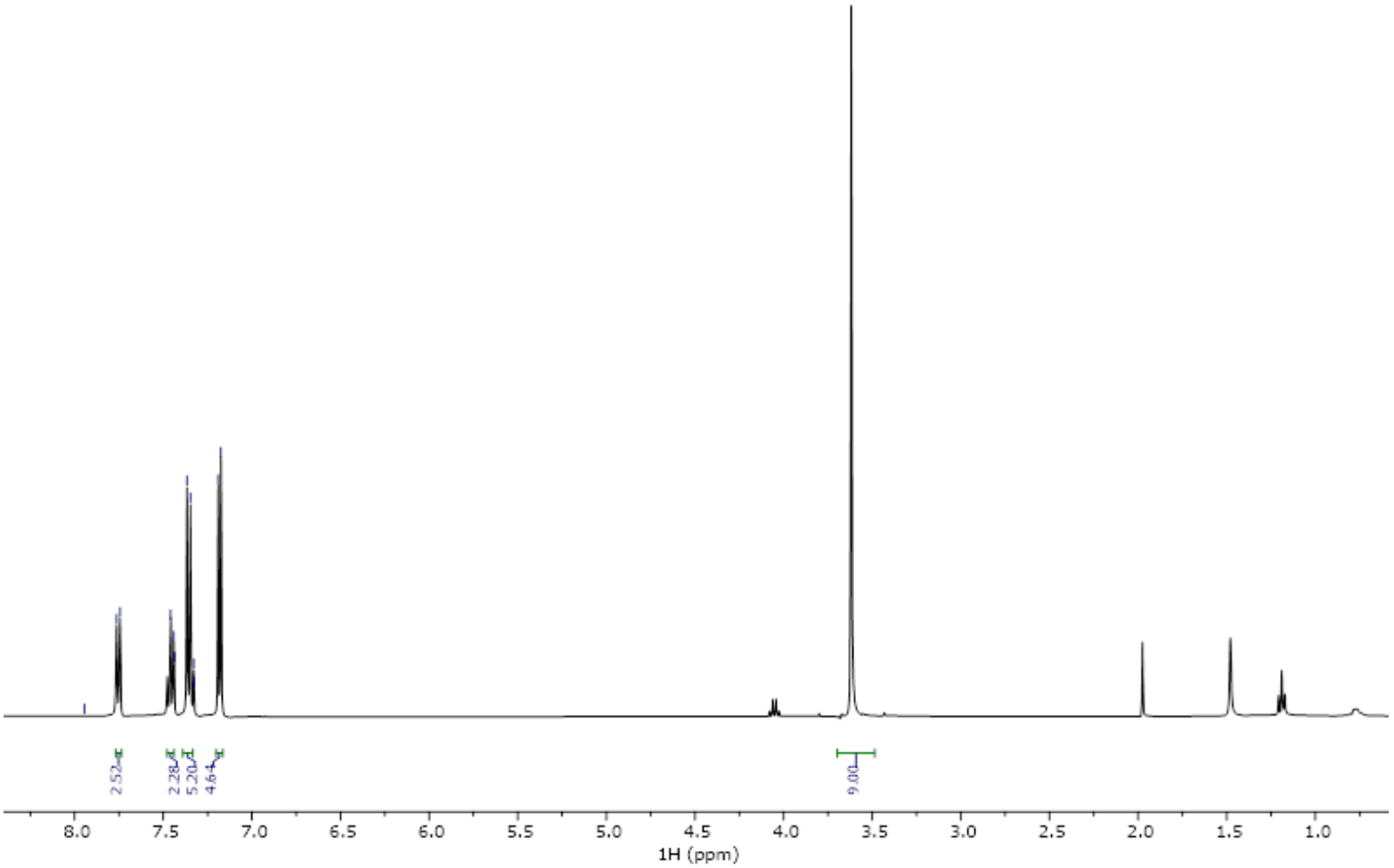
2.52
2.28
5.20
4.61
9.00
8.0
7.5
7.0
6.5
6.0
5.5
5.0
4.5
4.0
3.5
3.0
2.5
2.0
1.5
1.0
1H (ppm)

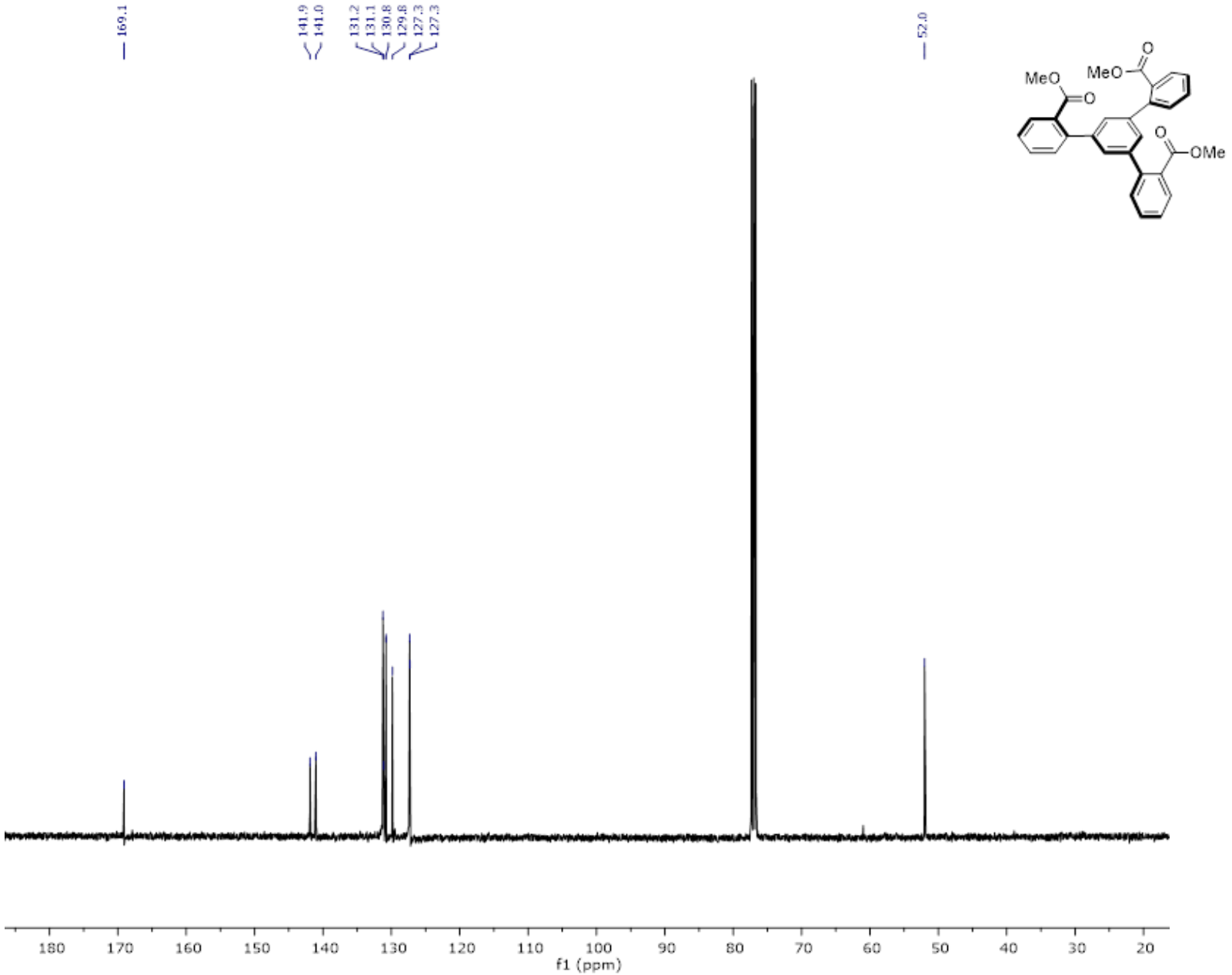
169.1
141.9
141.0
131.2
131.1
130.8
129.8
127.3
127.3
52.0
MeO
O
MeO
O
O
OMe
180
170
160
150
140
130
120
110
100
90
80
70
60
50
40
30
20
f1 (ppm)

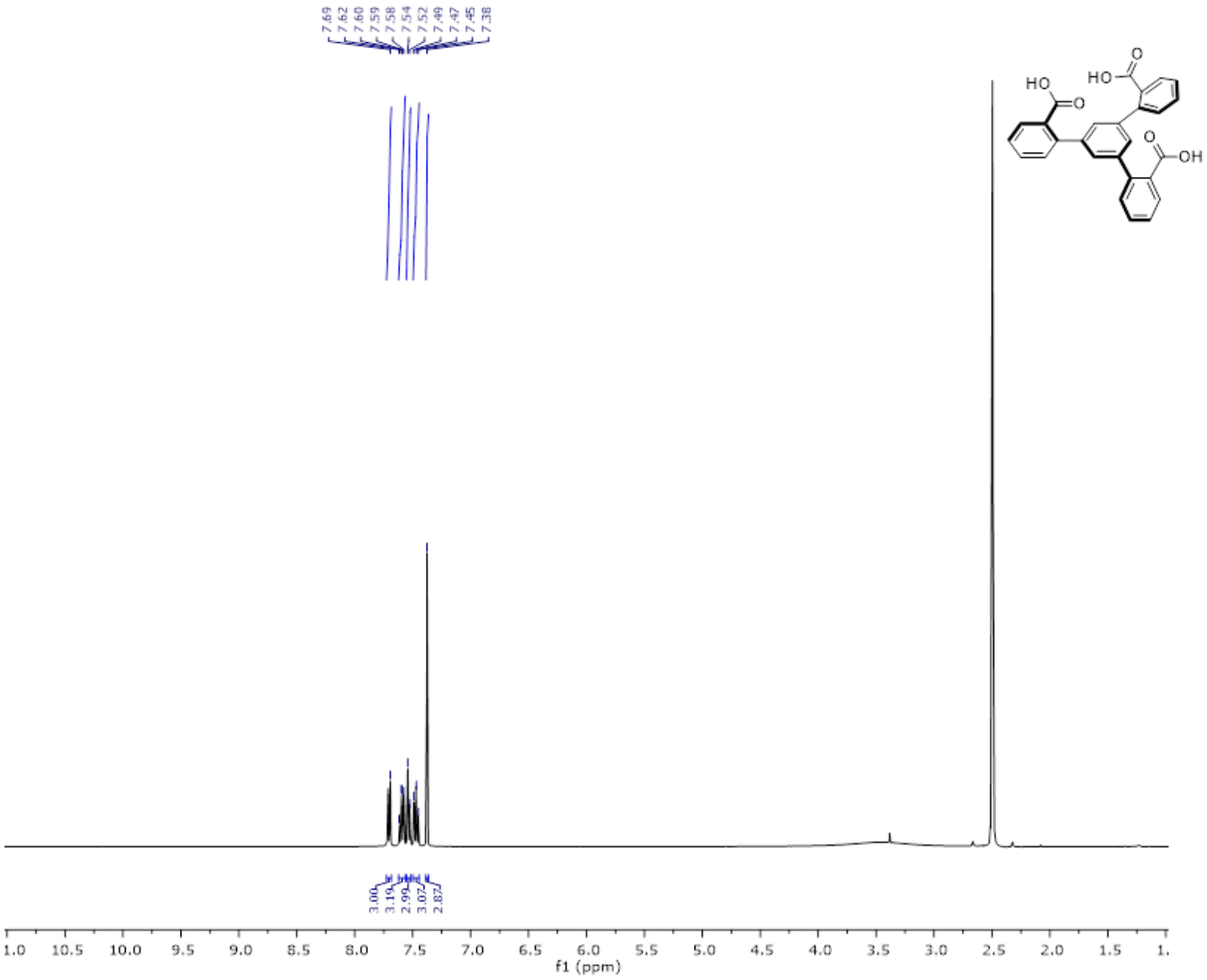
7.69
7.62
7.60
7.59
7.58
7.54
7.52
7.49
7.47
7.45
7.38
HO
O
HO
O
O
OH
3.00
3.19
2.99
3.07
2.87
1.0
10.5
10.0
9.5
9.0
8.5
8.0
7.5
7.0
6.5
6.0
5.5
5.0
4.5
4.0
3.5
3.0
2.5
2.0
1.5
f1 (ppm)

170.5
170.5
140.5
140.3
133.3
131.2
131.0
129.5
127.9
127.8
f1 (ppm)

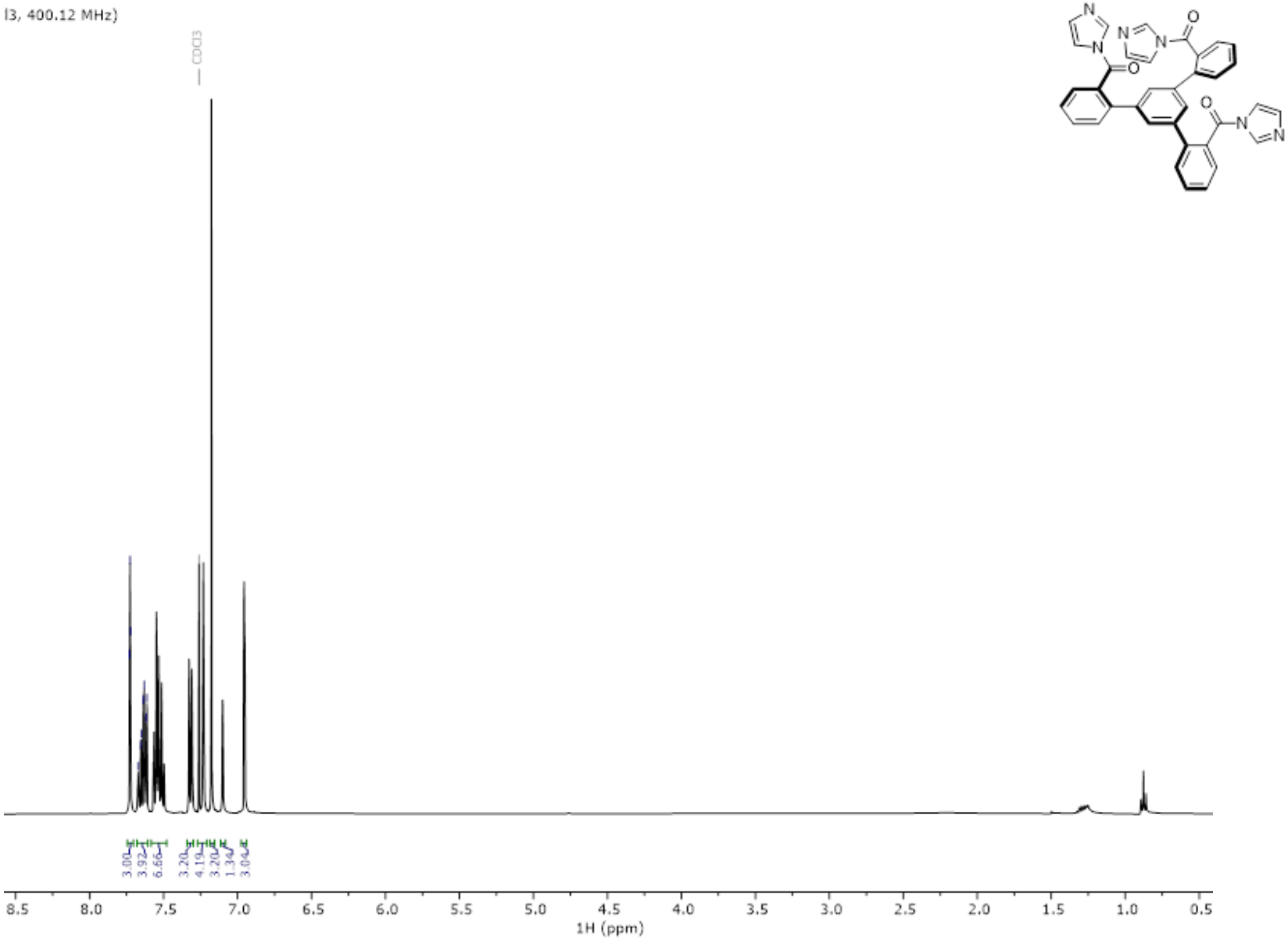
l3, 400.12 MHz)
CDCl3
3.00
3.92
6.66
3.20
4.19
3.20
1.34
3.04
8.5
8.0
7.5
7.0
6.5
6.0
5.5
5.0
4.5
4.0
3.5
3.0
2.5
2.0
1.5
1.0
0.5
1H (ppm)

Cl3, 100.63 MHz)

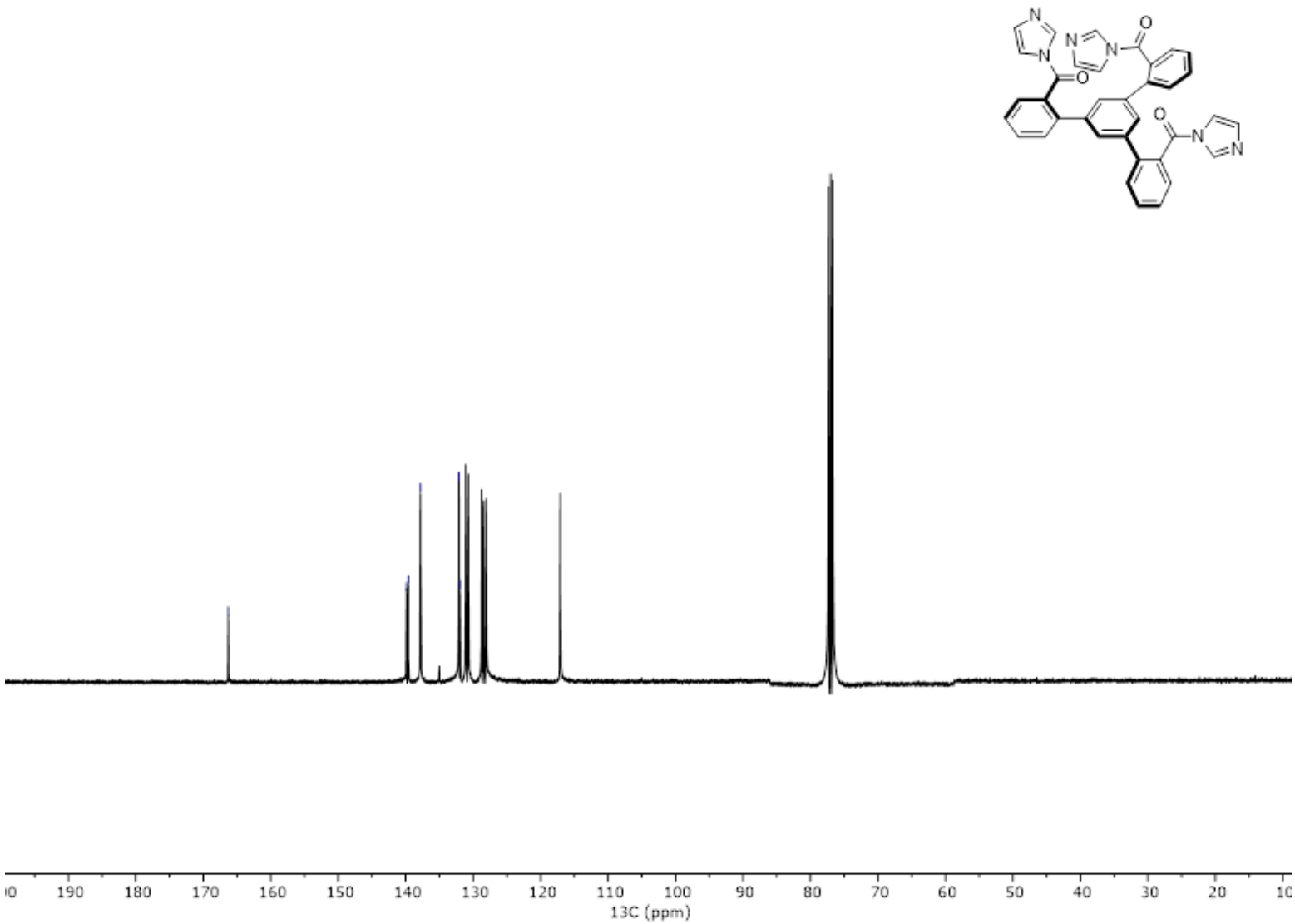

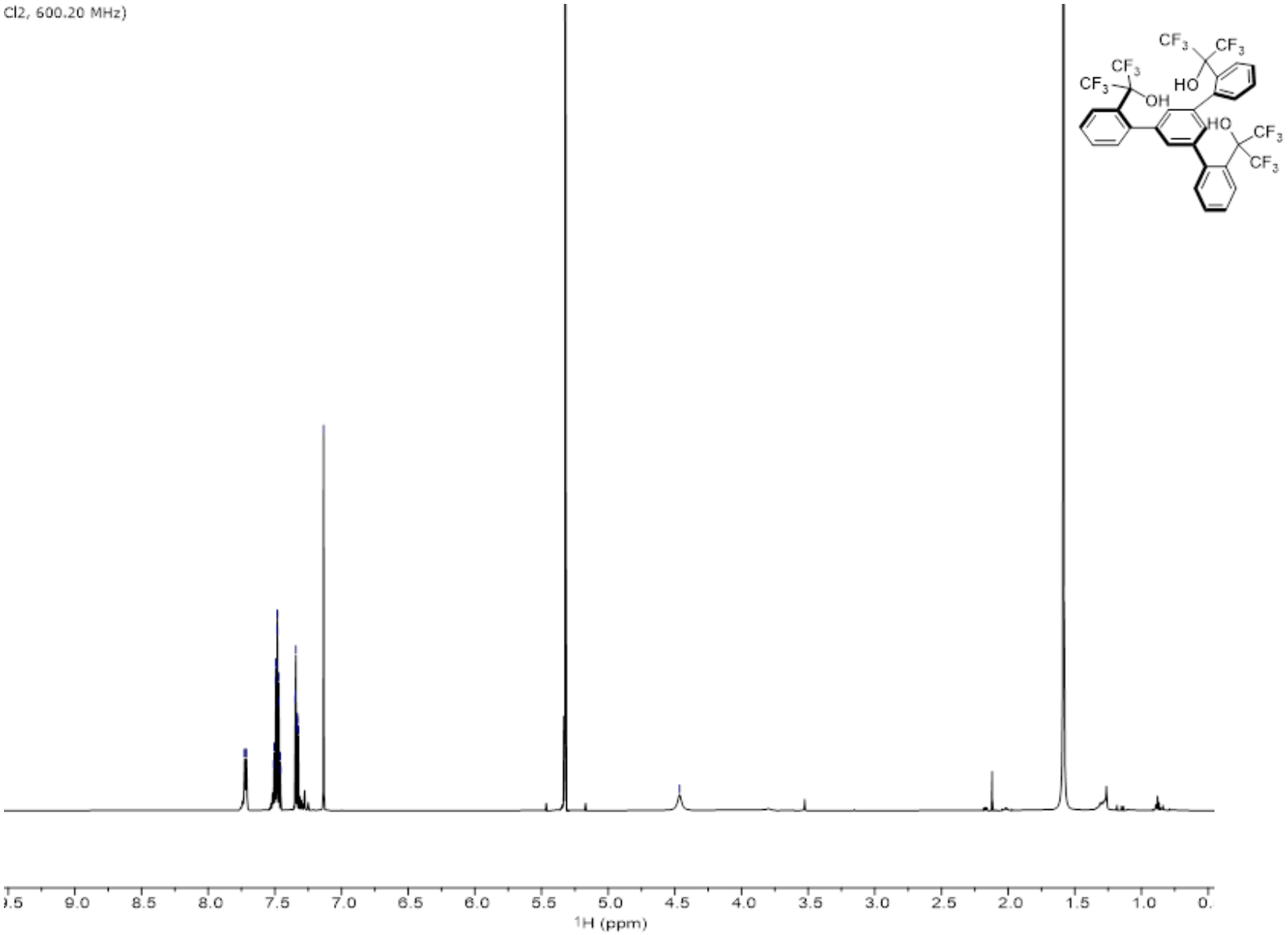
Cl2, 600.20 MHz)
CF3
CF3
CF3
CF3
HO
OH
HO
CF3
CF3
9.5
9.0
8.5
8.0
7.5
7.0
6.5
6.0
5.5
5.0
4.5
4.0
3.5
3.0
2.5
2.0
1.5
1.0
0.
1H (ppm)

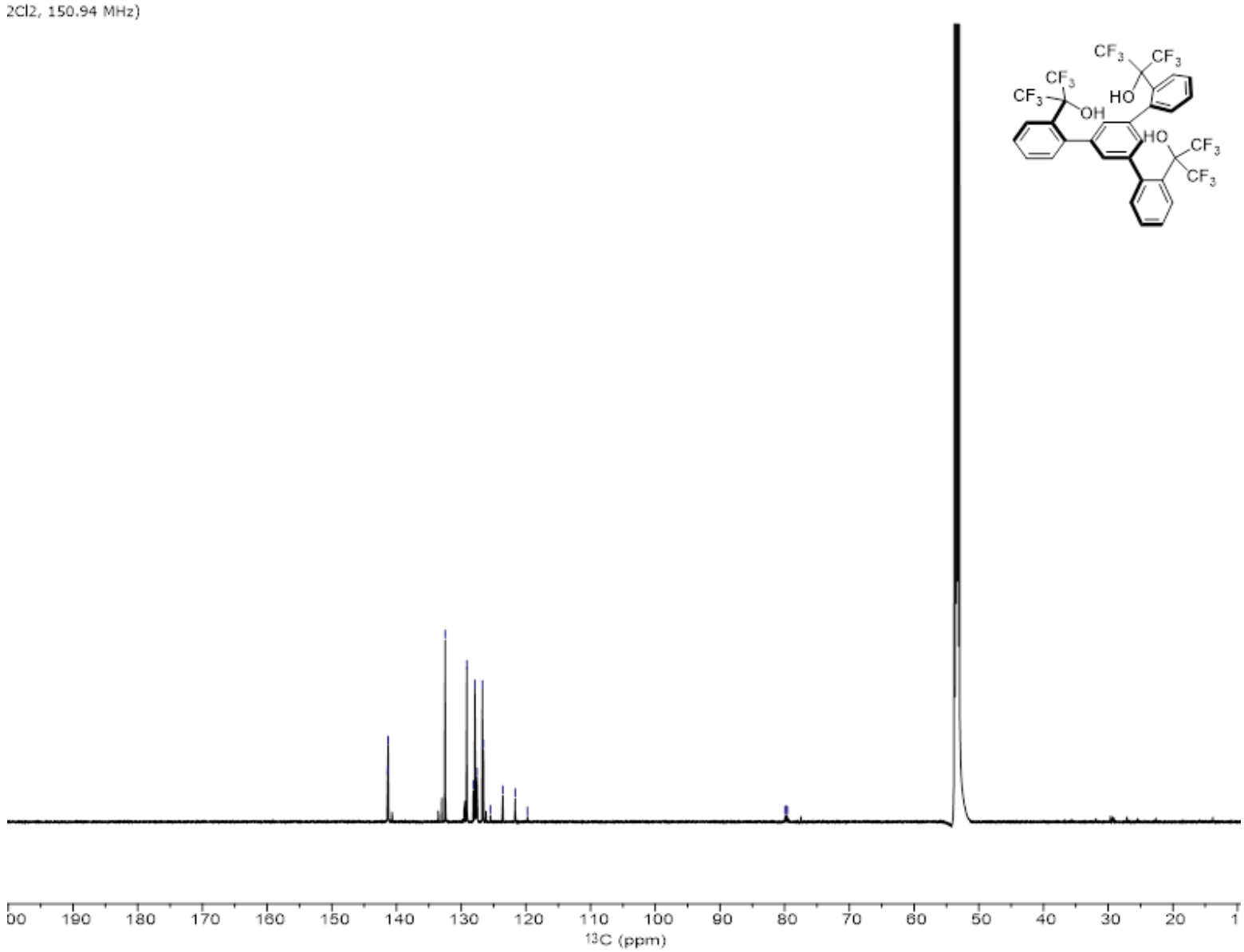
2Cl2, 150.94 MHz)
CF3
CF3
HO
CF3
CF3
OH
HO
CF3
CF3
00
190
180
170
160
150
140
130
120
110
100
90
80
70
60
50
40
30
20
1
13C (ppm)

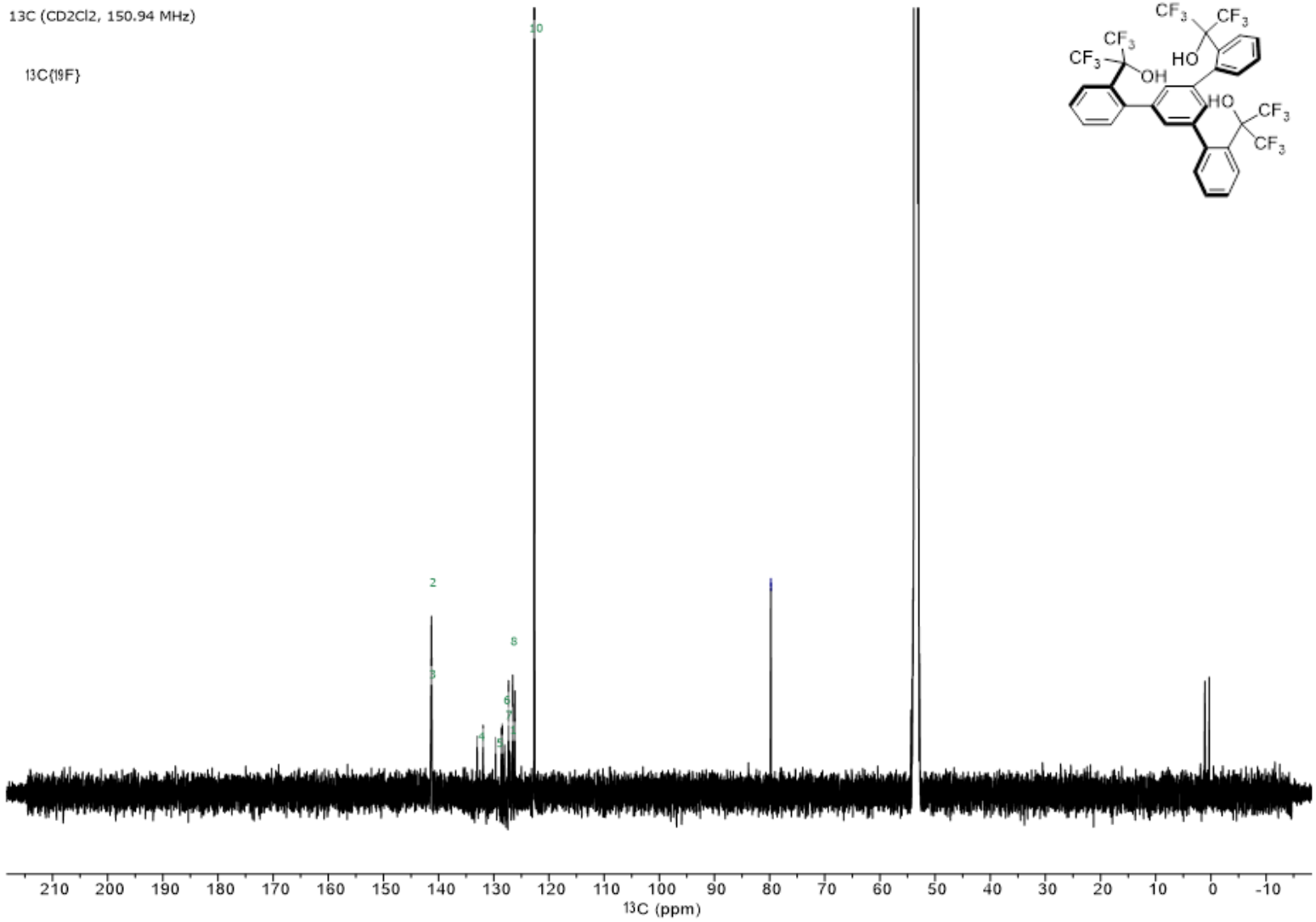
13C (CD2Cl2, 150.94 MHz)
13C{19F}
CF3
CF3
CF3
HO
OH
HO
CF3
CF3
10
2
8
3
6
210 200 190 180 170 160 150 140 130 120 110 100 90 80 70 60 50 40 30 20 10 0 -10
13C (ppm)

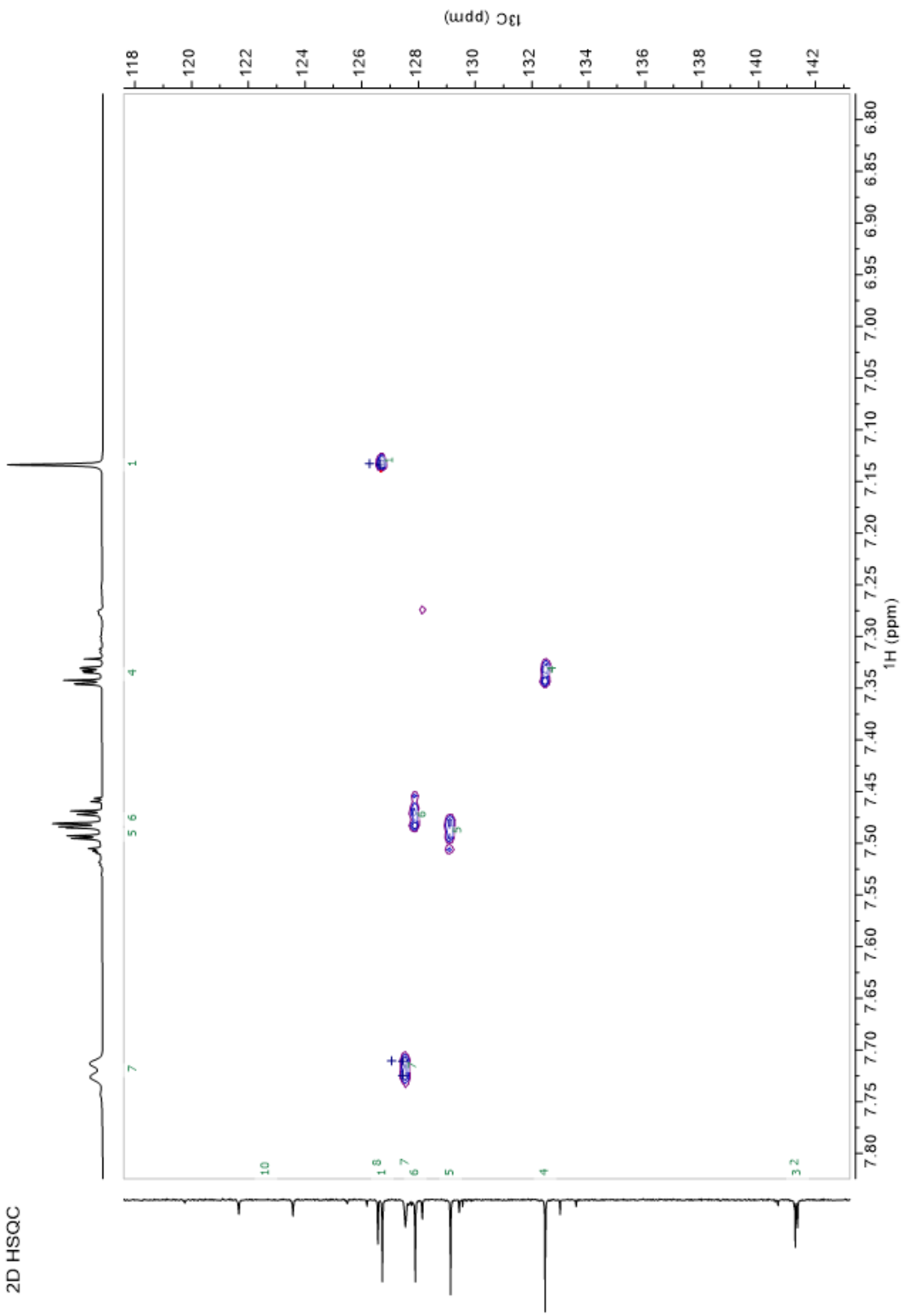
2D HSQC
13C (ppm)
1H (ppm)

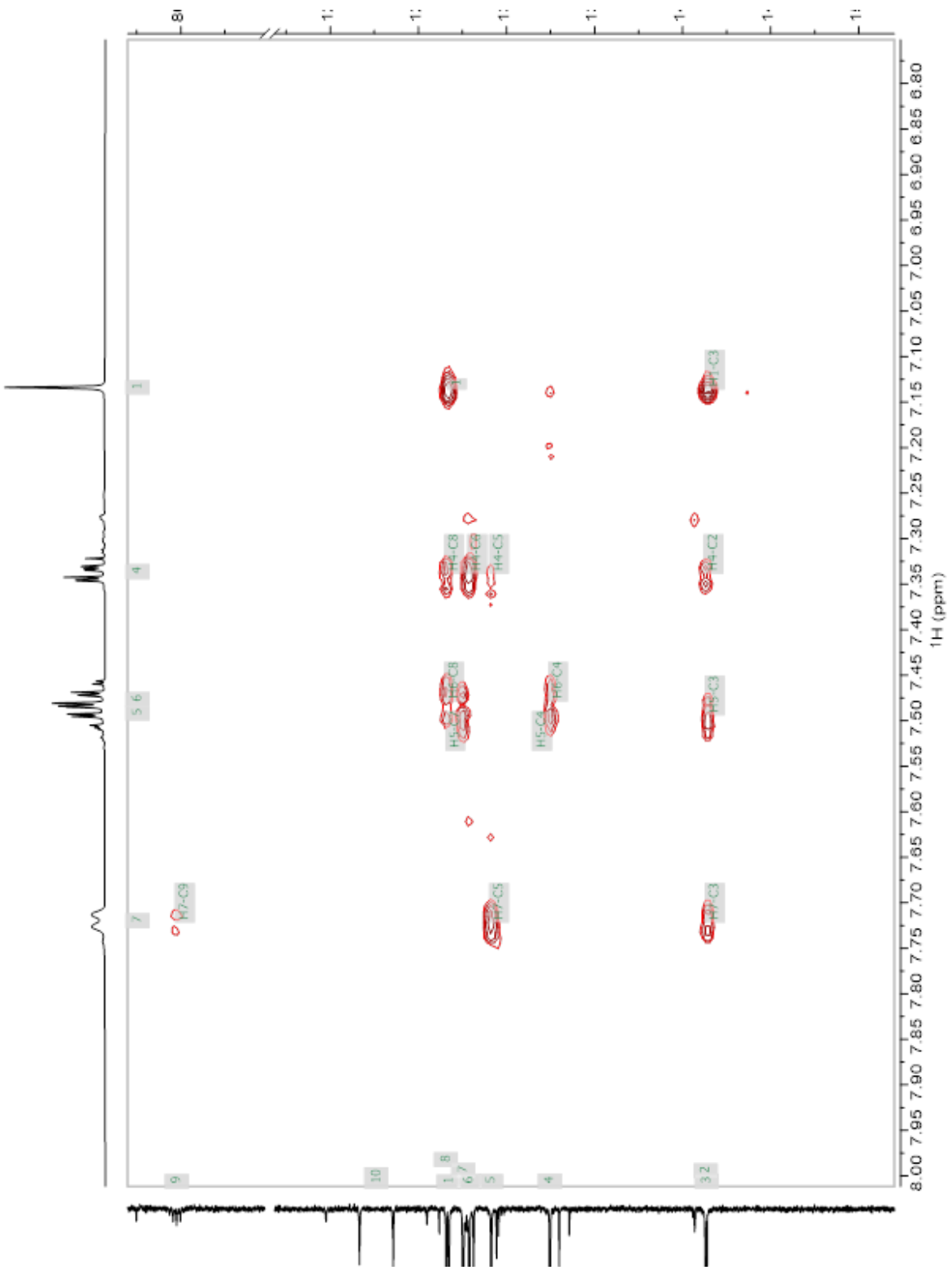
1H (ppm)

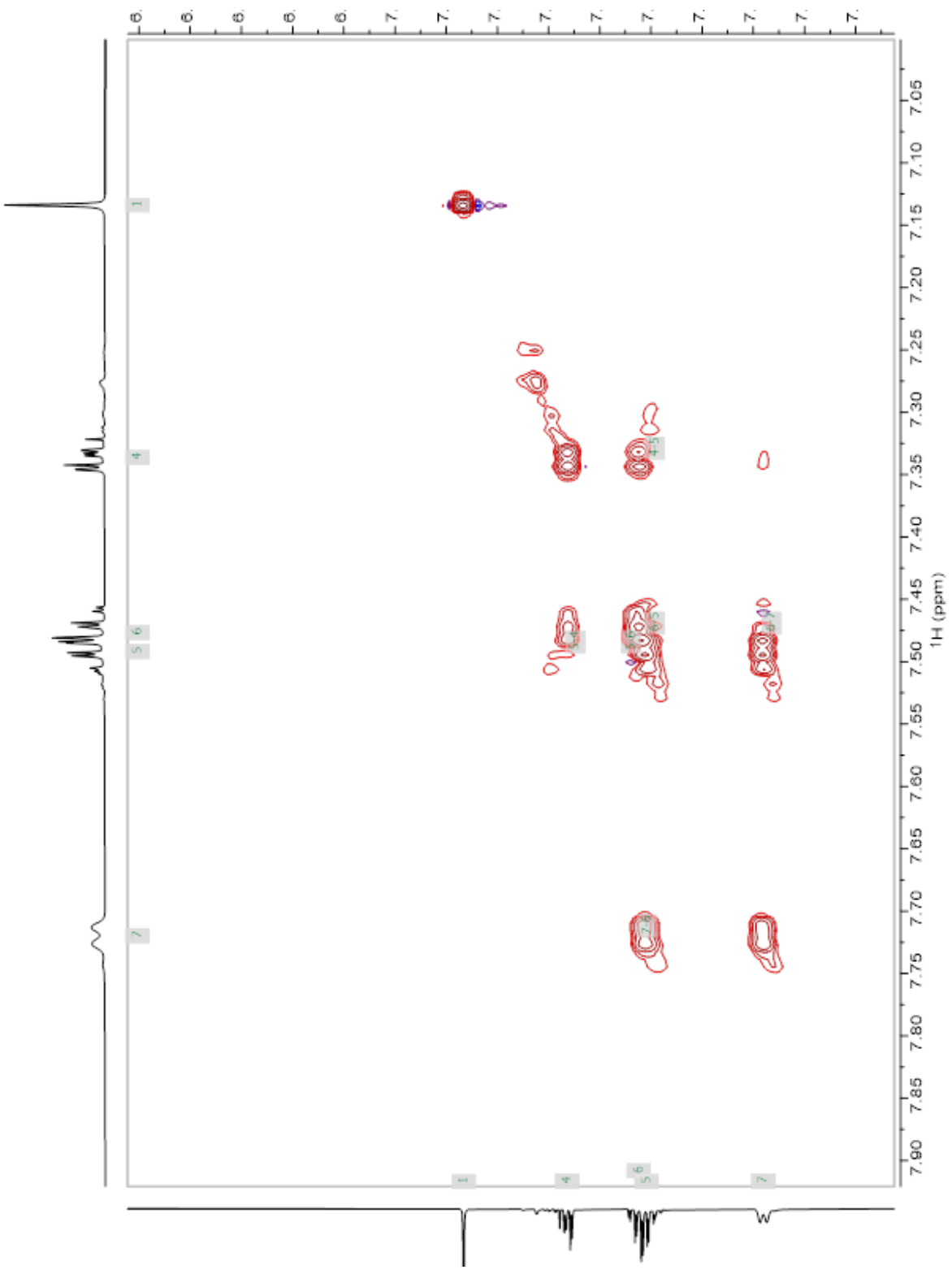
1H (ppm)

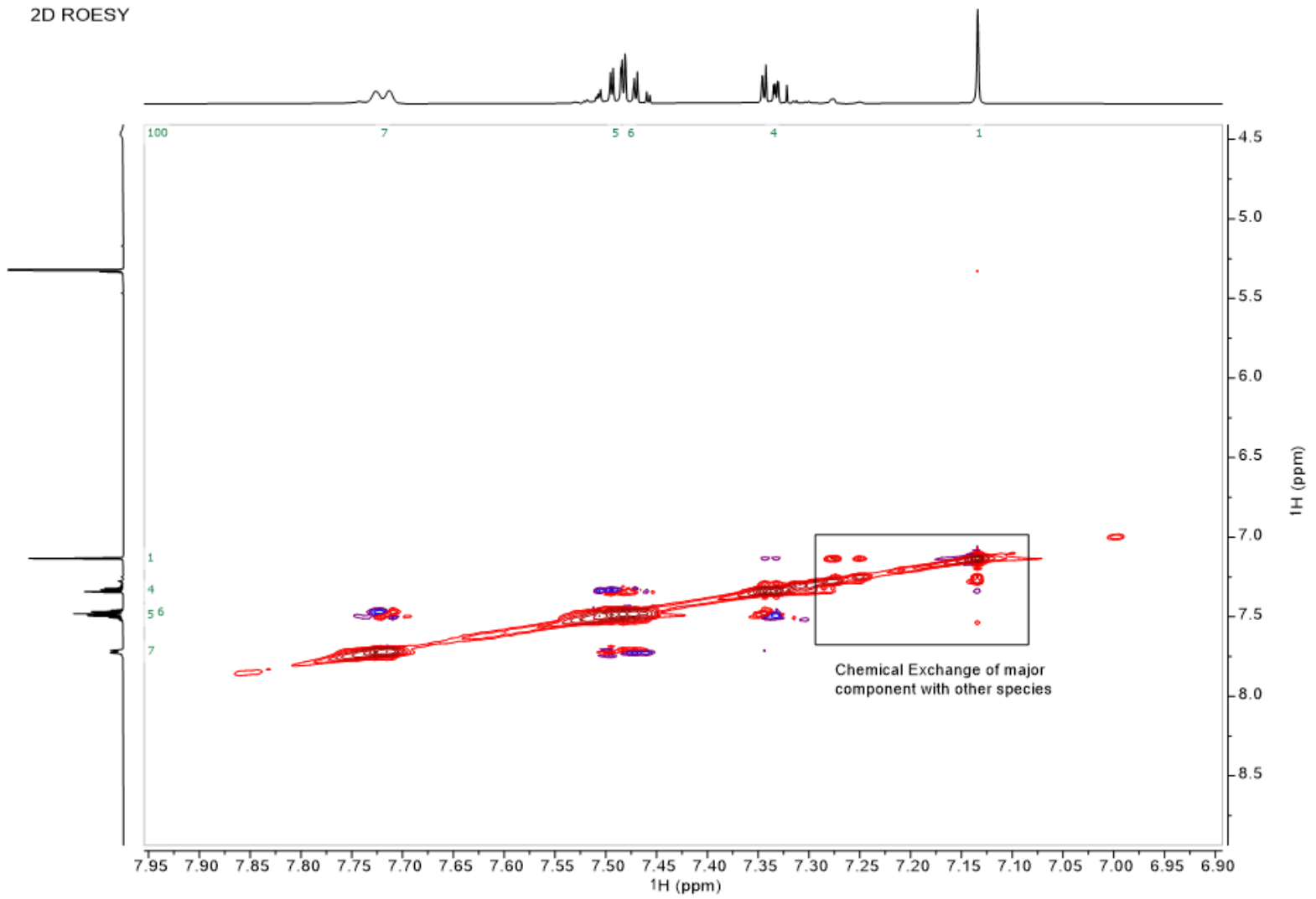
2D ROESY
100
7
5 6
4
1
1
4
5 6
7
Chemical Exchange of major
component with other species
7.95 7.90 7.85 7.80 7.75 7.70 7.65 7.60 7.55 7.50 7.45 7.40 7.35 7.30 7.25 7.20 7.15 7.10 7.05 7.00 6.95 6.90
1H (ppm)
4.5
5.0
5.5
6.0
6.5
7.0
7.5
8.0
8.5
1H (ppm)

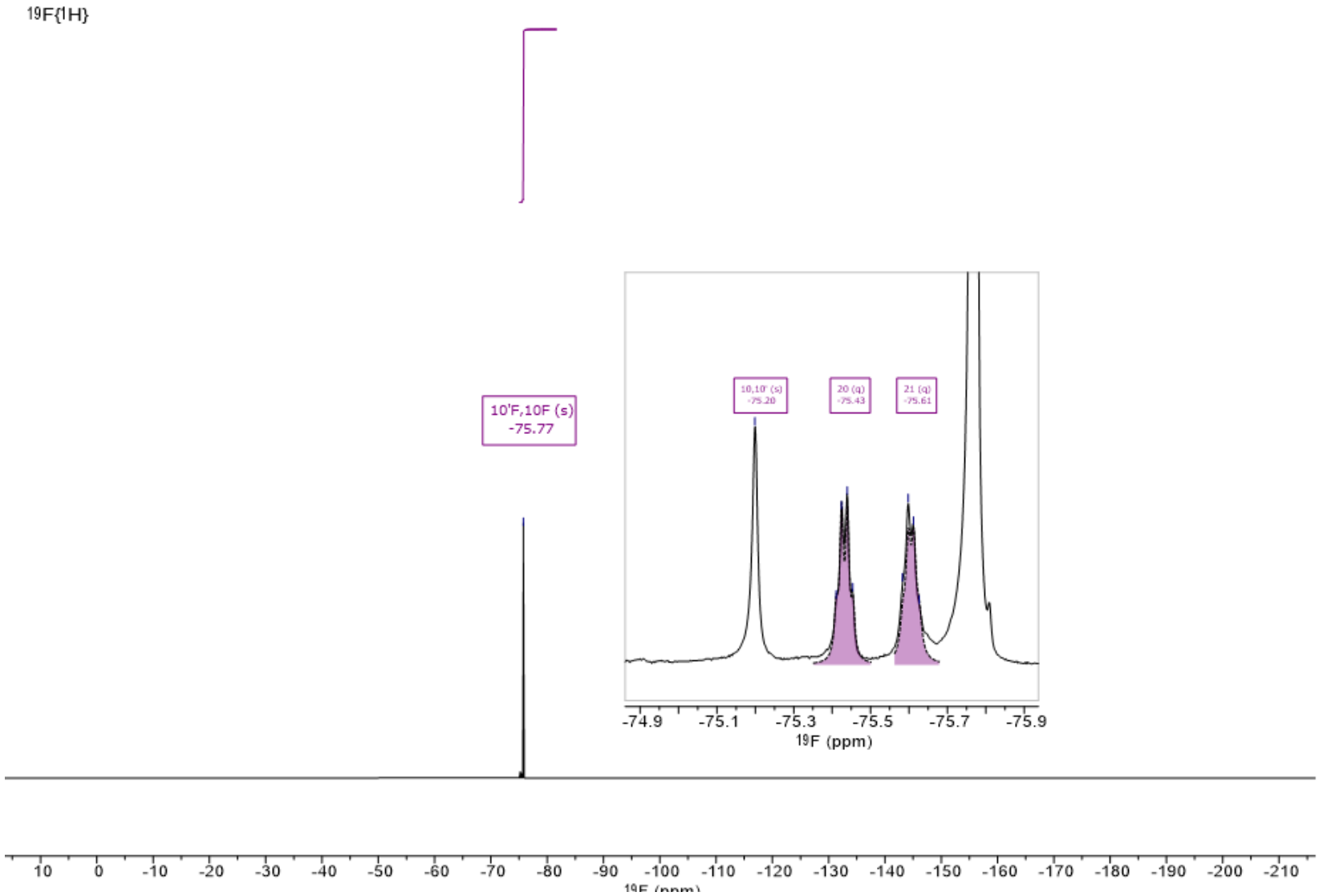
19F{1H}
10'F,10F (s)
-75.77
10,10' (s)
-75.20
20 (q)
-75.43
21 (q)
-75.61
-74.9
-75.1
-75.3
-75.5
-75.7
-75.9
19F (ppm)
10
0
-10
-20
-30
-40
-50
-60
-70
-80
-90
-100
-110
-120
-130
-140
-150
-160
-170
-180
-190
-200
-210

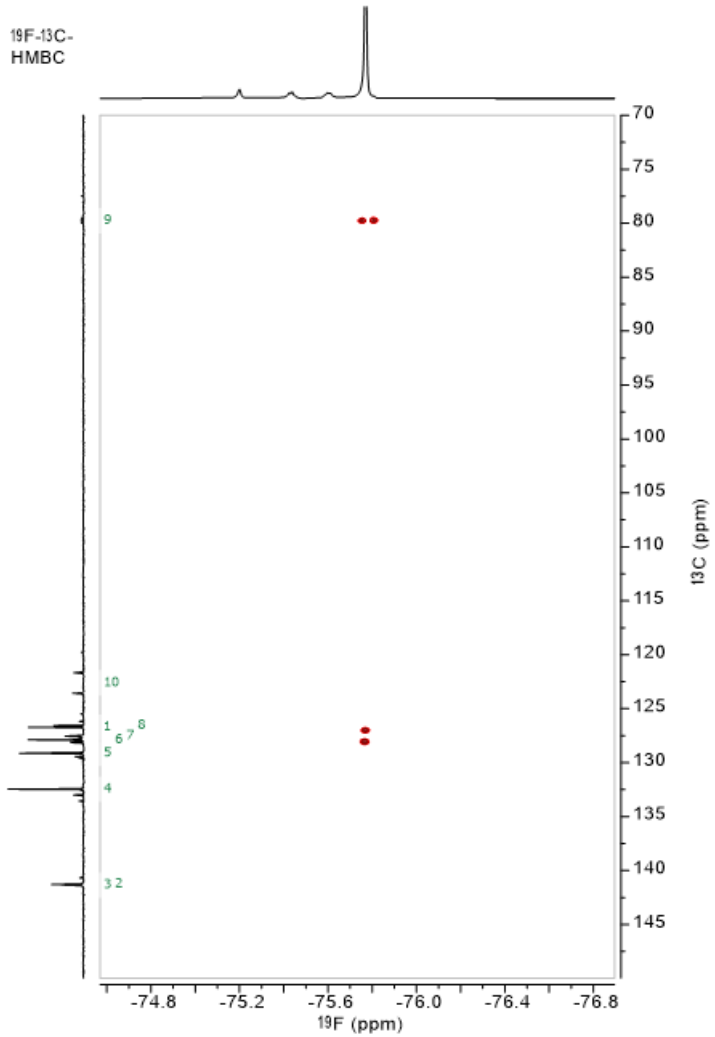
19F-13C-
HMBC
9
10
1
6
7
8
5
4
3
2
-74.8
-75.2
-75.6
-76.0
-76.4
-76.8
19F (ppm)
70
75
80
85
90
95
100
105
110
115
120
125
130
135
140
145
13C (ppm)

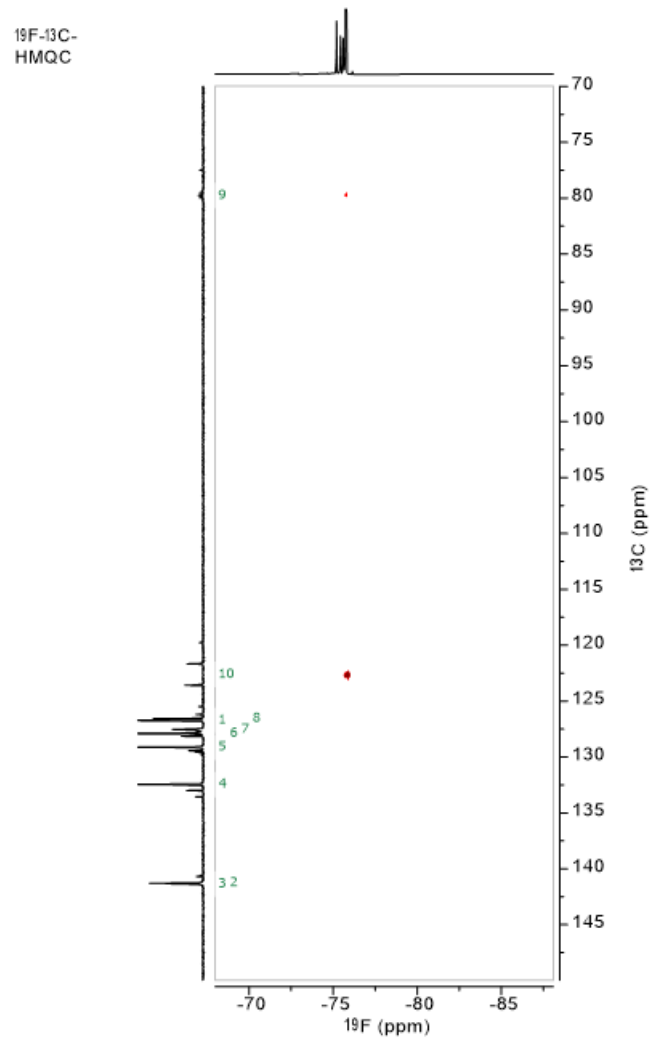
19F-13C-
HMQC
9
10
1
6
7
8
5
4
3
2
-70
-75
-80
-85
19F (ppm)
70
75
80
85
90
95
100
105
110
115
120
125
130
135
140
145
13C (ppm)

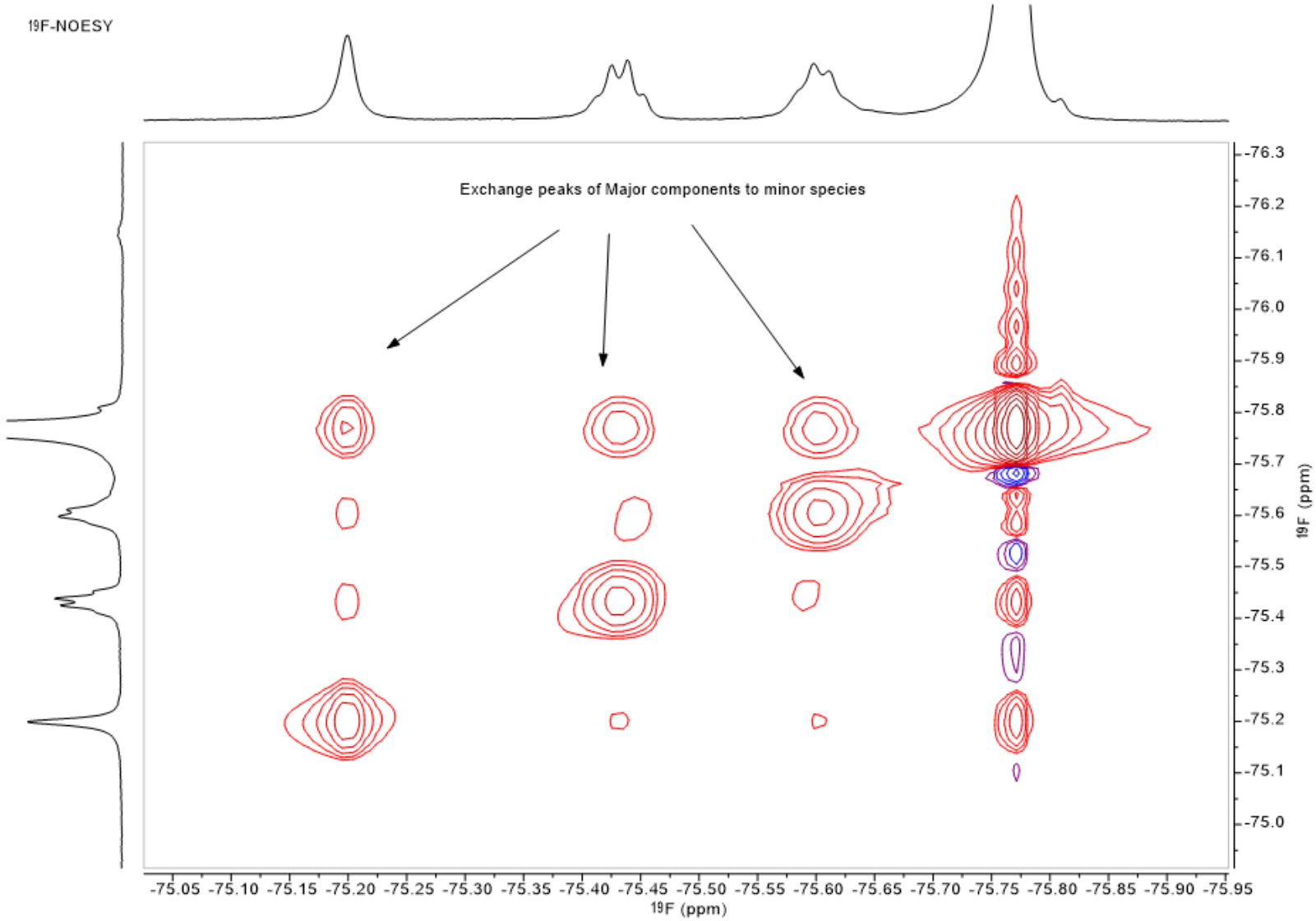
19F-NOESY
Exchange peaks of Major components to minor species
-76.3
-76.2
-76.1
-76.0
-75.9
-75.8
-75.7
-75.6
-75.5
-75.4
-75.3
-75.2
-75.1
-75.0
19F (ppm)
-75.05 -75.10 -75.15 -75.20 -75.25 -75.30 -75.35 -75.40 -75.45 -75.50 -75.55 -75.60 -75.65 -75.70 -75.75 -75.80 -75.85 -75.90 -75.95
19F (ppm)

Appendix 3: NMR spectra - Section 5.2.4. Complexes

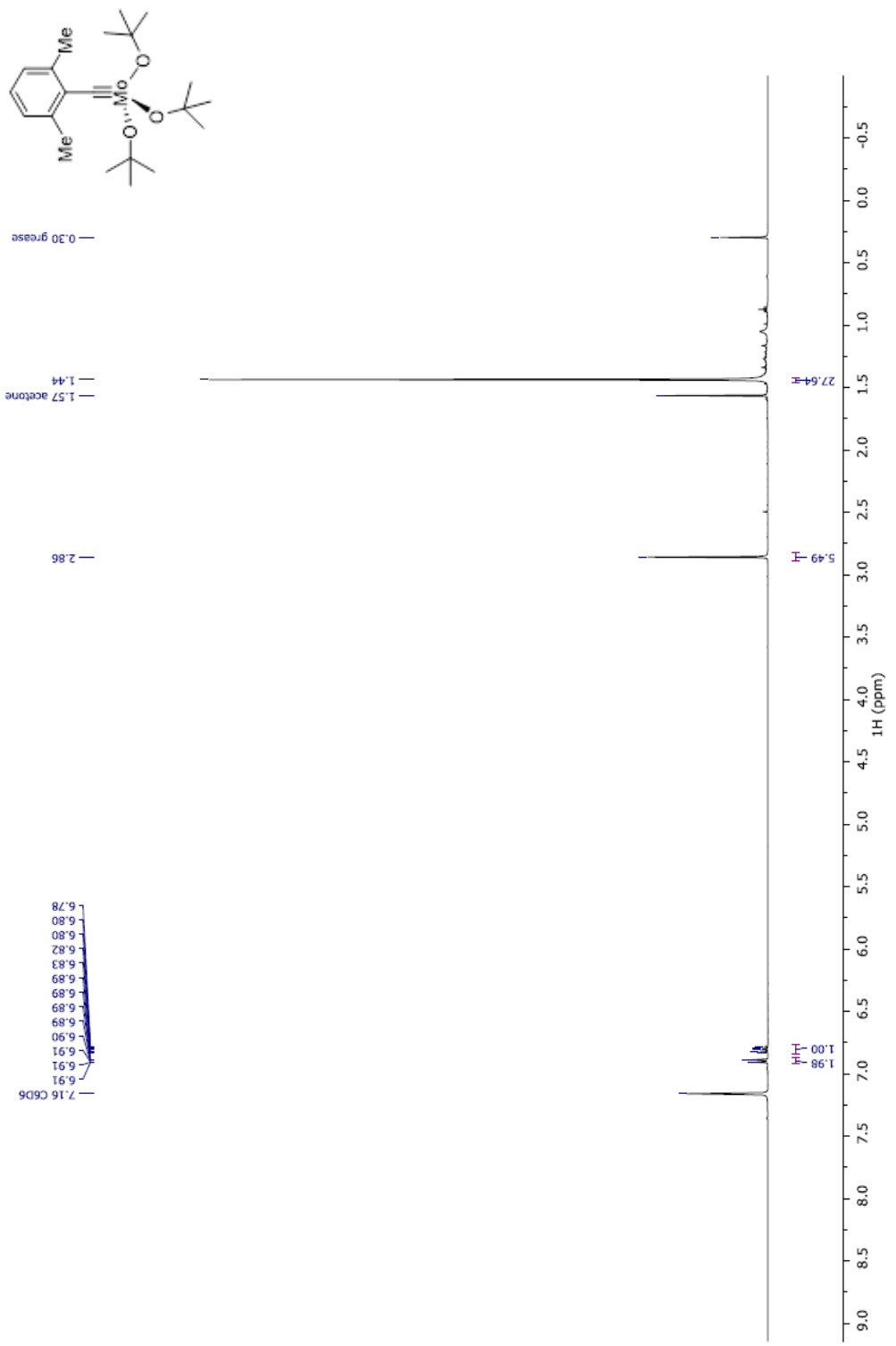
Me
Me
Mo
O
O
O
0.30 grease
1.44
1.57 acetone
2.86
7.16 C6D6
6.78
6.80
6.80
6.82
6.83
6.89
6.89
6.89
6.89
6.90
6.91
6.91
6.91
1.98
1.00
5.49
27.64
1H (ppm)

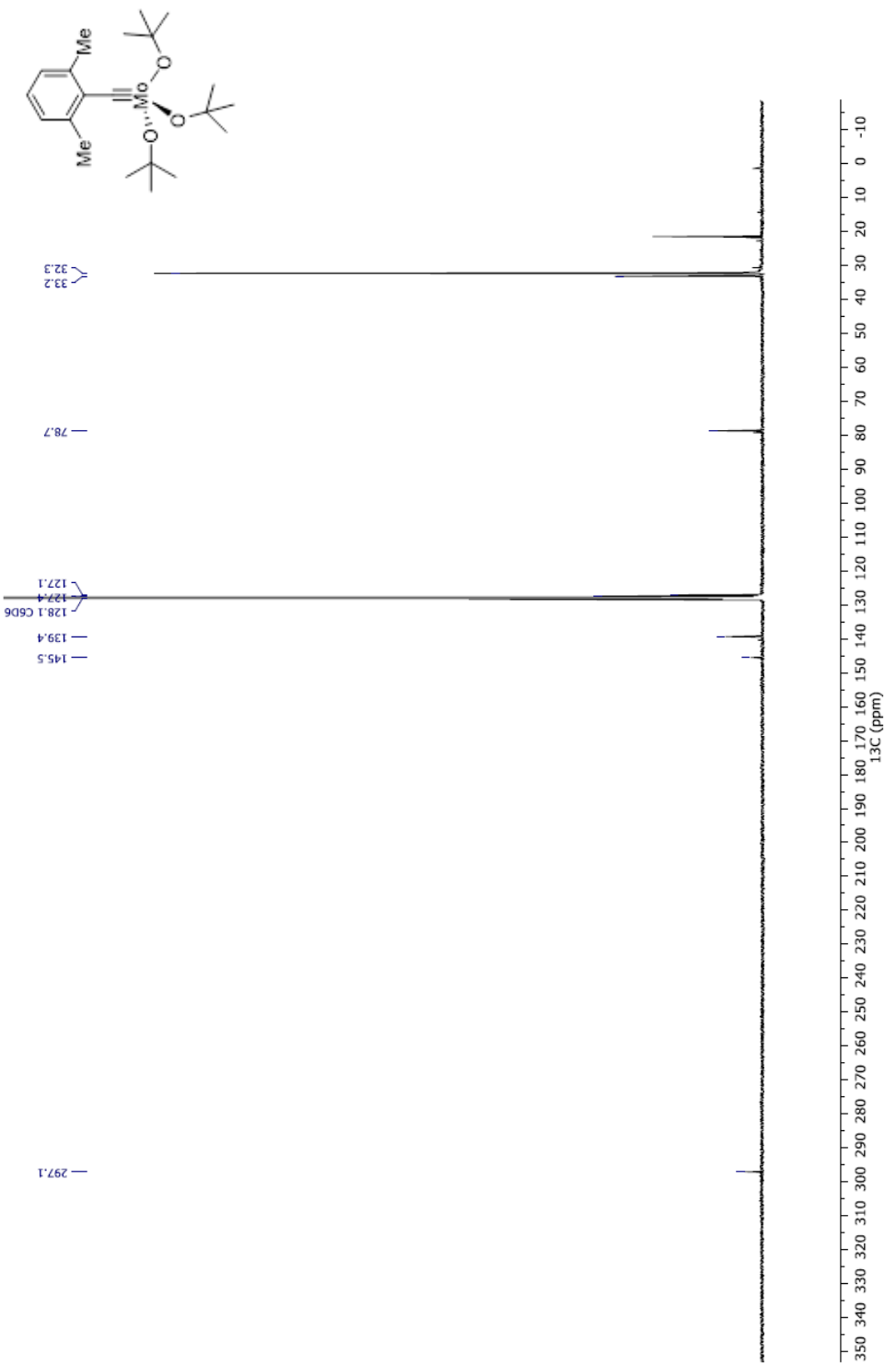
Me
Me
Mo
O
O
O
297.1
145.5
139.4
128.1 C6D6
127.4
127.1
78.7
33.2
32.3
350 340 330 320 310 300 290 280 270 260 250 240 230 220 210 200 190 180 170 160 150 140 130 120 110 100 90 80 70 60 50 40 30 20 10 0 -10
13C (ppm)

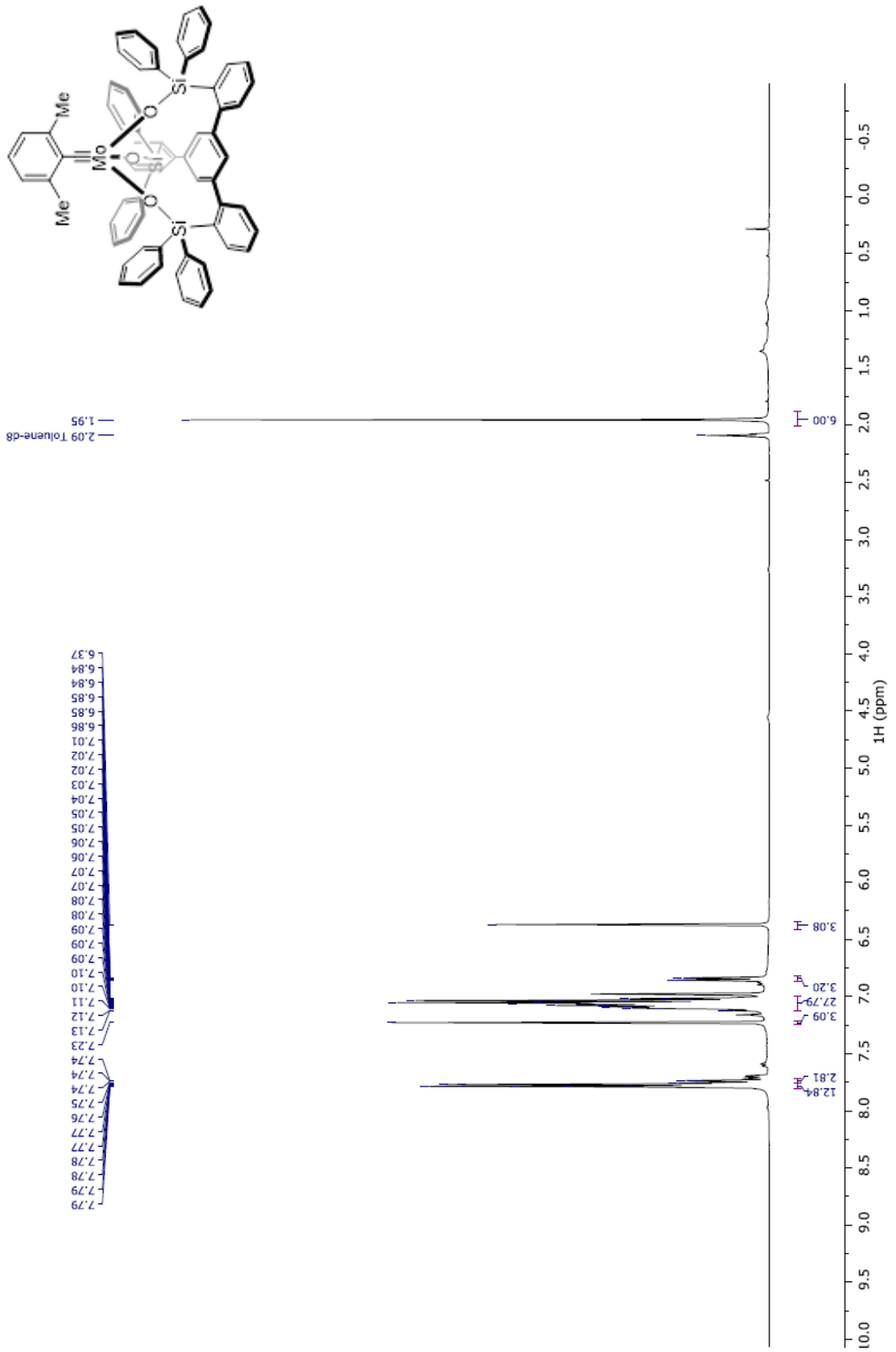
Me
Me
Mo
O
O
Si
Si
1.95
2.09 Toluene-d8
6.00
3.08
3.20
27.79
3.09
2.81
12.84
1H (ppm)

312.6
149.6
145.3
144.2
139.0
137.9
137.5
135.2
135.0
130.5
130.1
129.8
129.1
128.1
127.7
127.7
126.2
126.0
20.4 Toluene-d8
20.1
Me
Mo
Me
O
O
Si
Si
13C (ppm)

Me
Me
Mo
O
O
Si
Si
Si
-9.4
160 150 140 130 120 110 100 90 80 70 60 50 40 30 20 10 0 -10 -20 -30 -40 -50 -60 -70 -80 -90 -100 -110 -120 -130 -140 -150 -160 -170 -180
29Si (ppm)

26 MHz, $C_6D_5CD_3$, 60ºC

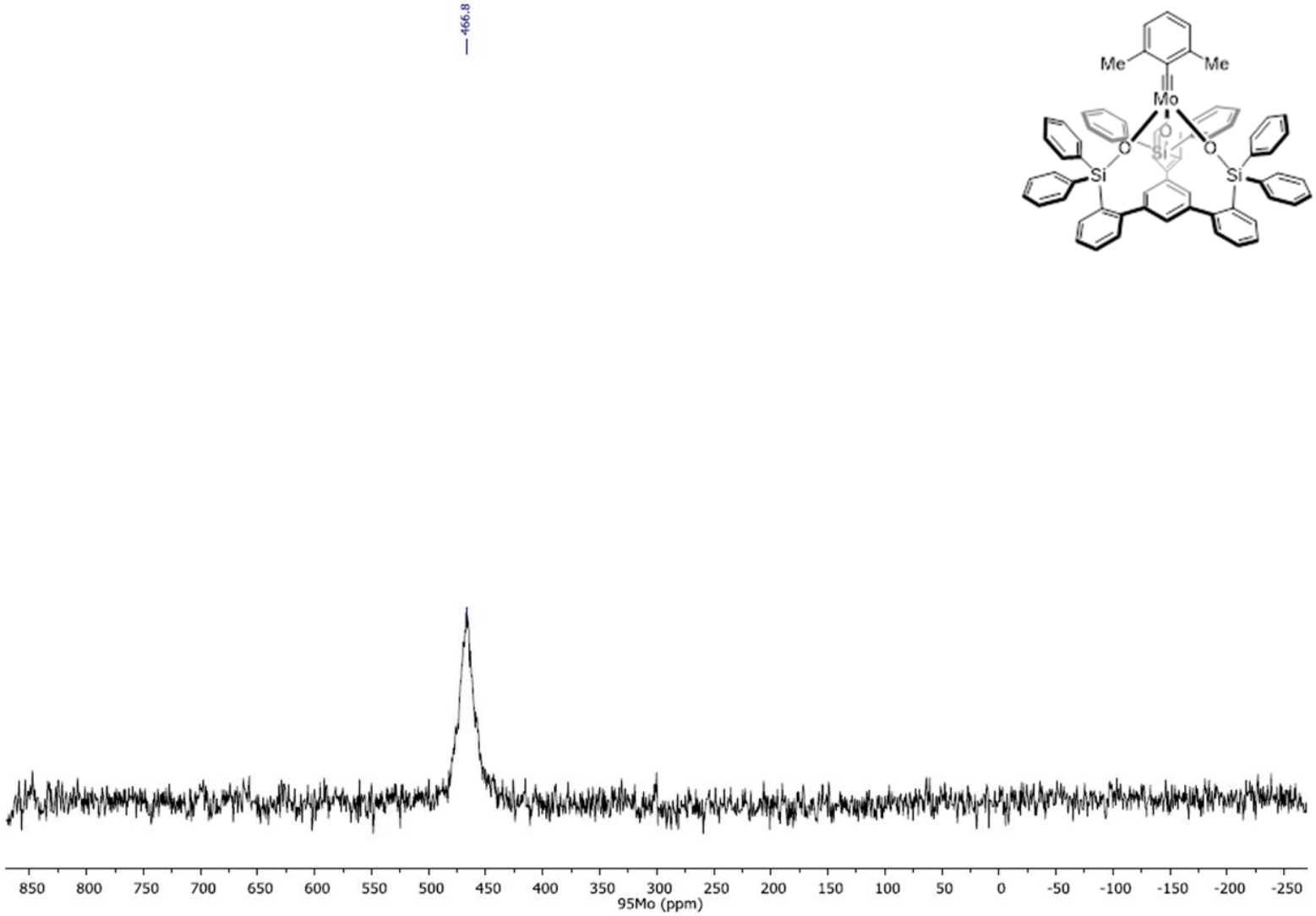

OMe
Mo
O
Si
R
R = iPr
1H (ppm)
2.09 Toluene-d8
3.16
6.06
3.01
6.20
2.28
1.66
3.00
6.96
17.84
17.71

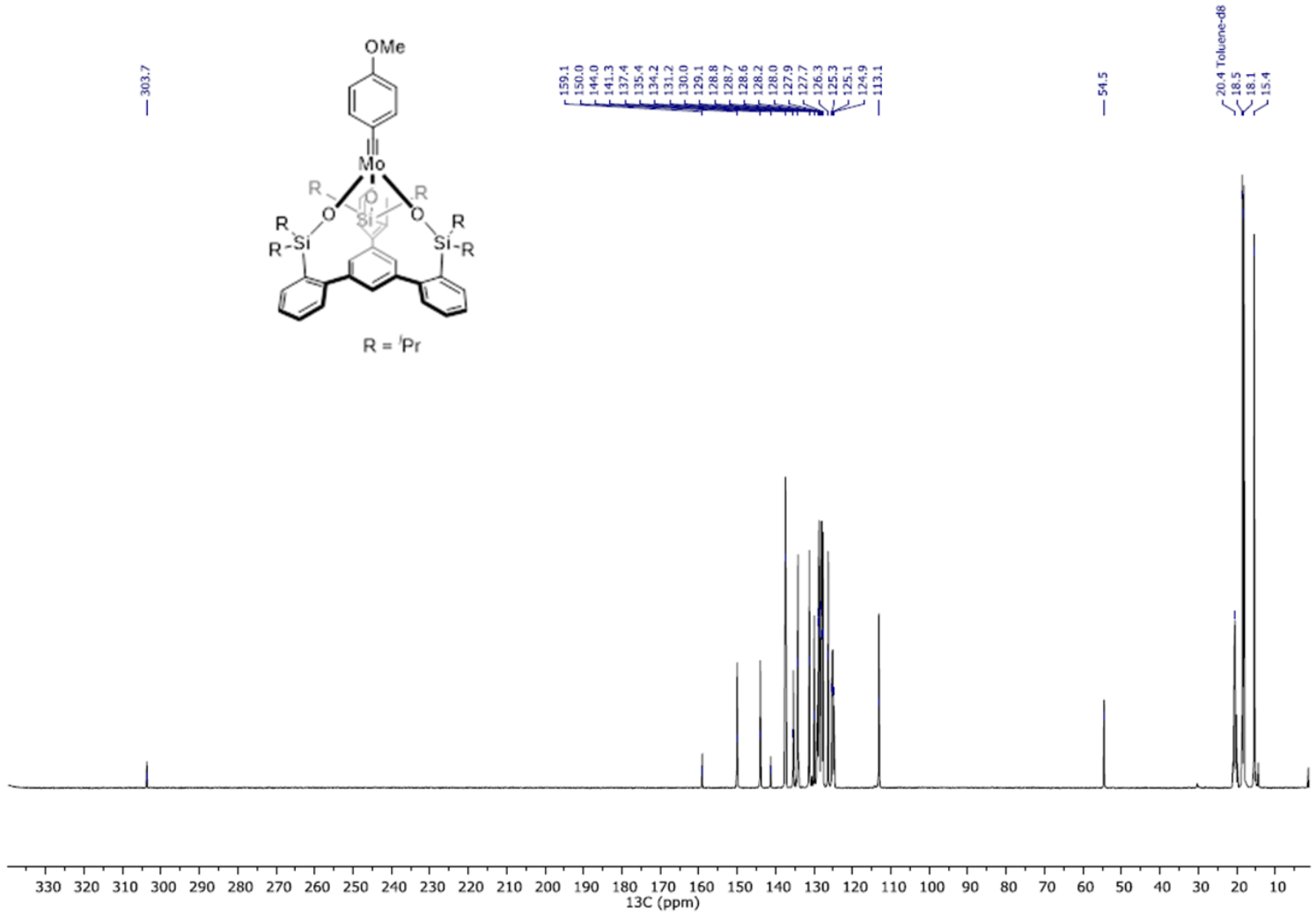
OMe
Mo
R
O
Si
R = iPr
303.7
159.1
150.0
144.0
141.3
137.4
135.4
134.2
131.2
130.0
129.1
128.8
128.7
128.6
128.2
128.0
127.9
127.7
126.3
125.3
125.1
124.9
113.1
54.5
20.4 Toluene-d8
18.5
18.1
15.4
330 320 310 300 290 280 270 260 250 240 230 220 210 200 190 180 170 160 150 140 130 120 110 100 90 80 70 60 50 40 30 20 10
13C (ppm)

OMe
Mo
O
R
Si
R
R = iPr
10.2
160 150 140 130 120 110 100 90 80 70 60 50 40 30 20 10 0 -10 -20 -30 -40 -50 -60 -70 -80 -90 -100 -110 -120 -130 -140 -150 -160 -170 -180
29Si (ppm)

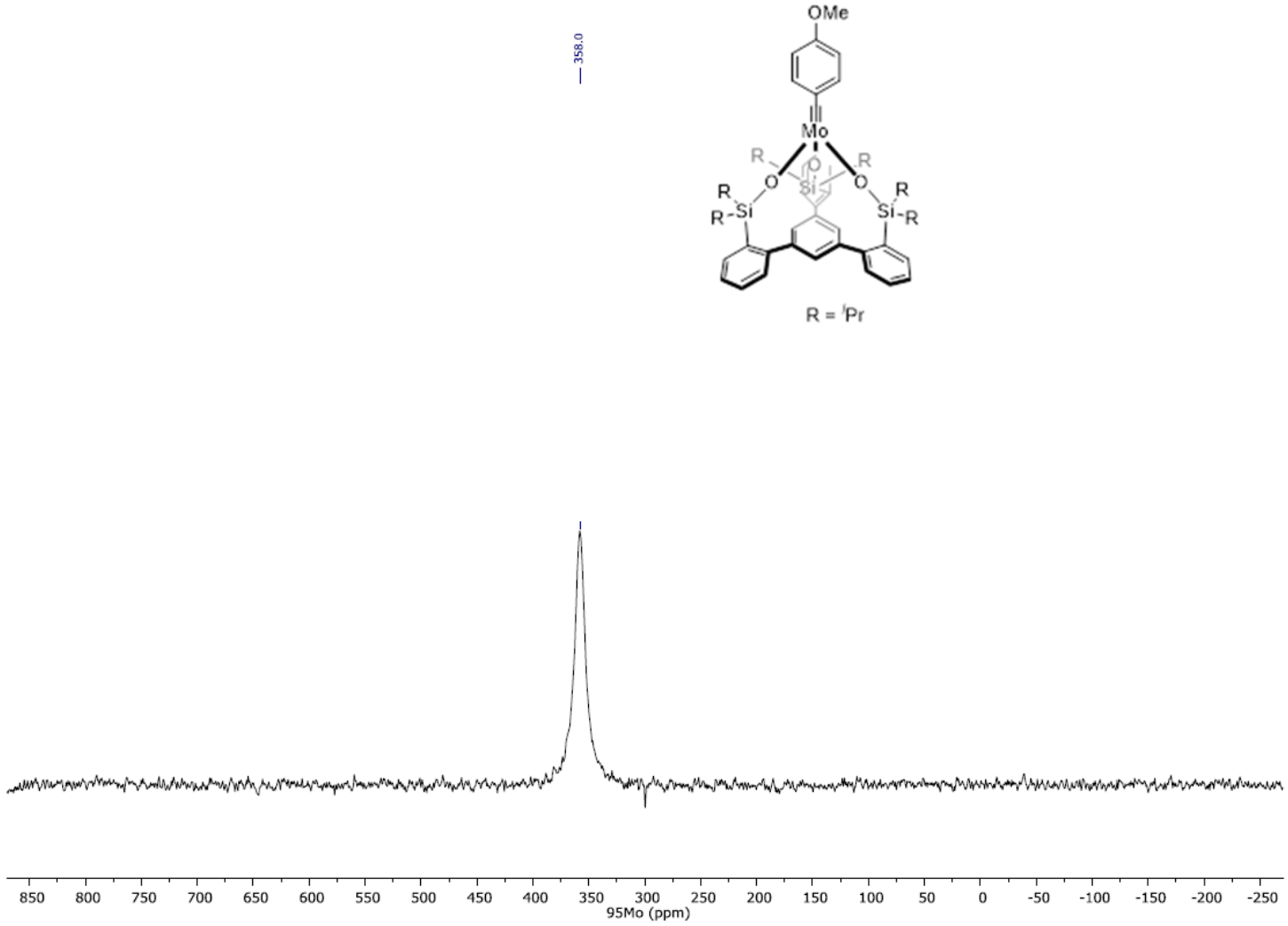
358.0
OMe
Mo
R
O
Si
R
R = iPr
850 800 750 700 650 600 550 500 450 400 350 300 250 200 150 100 50 0 -50 -100 -150 -200 -250
95Mo (ppm)

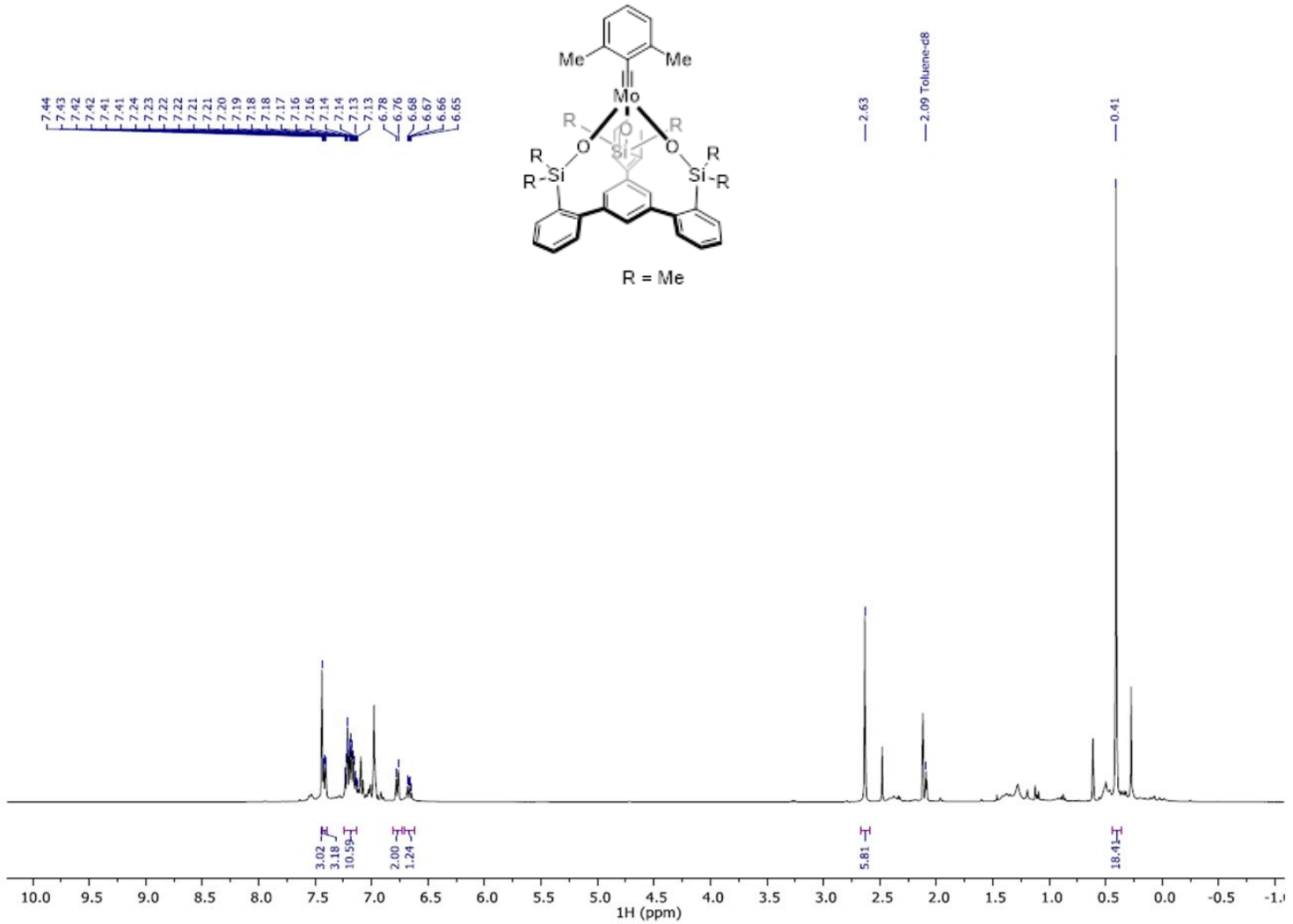
7.44
7.43
7.42
7.42
7.41
7.41
7.24
7.23
7.22
7.22
7.21
7.21
7.20
7.19
7.18
7.18
7.17
7.16
7.16
7.14
7.14
7.13
6.78
6.76
6.68
6.67
6.66
6.65
Me
Me
Mo
R
O
O
R
Si
R
R
Si
R
O
R
Si
R
R = Me
2.63
2.09 Toluene-d8
0.41
3.02
3.18
10.59
2.00
1.24
5.81
18.41
10.0
9.5
9.0
8.5
8.0
7.5
7.0
6.5
6.0
5.5
5.0
4.5
4.0
3.5
3.0
2.5
2.0
1.5
1.0
0.5
0.0
-0.5
1H (ppm)

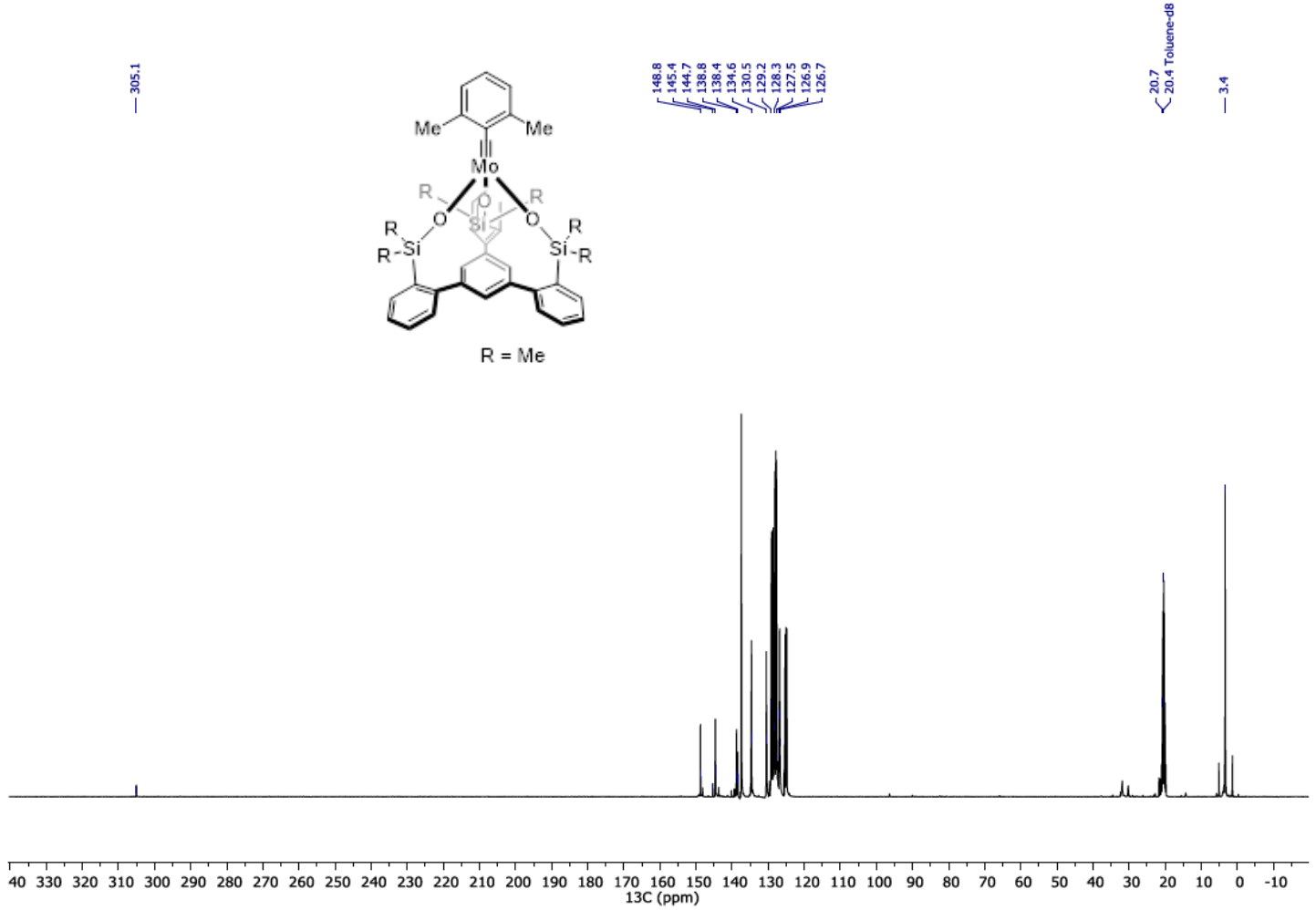
305.1
148.8
145.4
144.7
138.8
138.4
134.6
130.5
129.2
128.3
127.5
126.9
126.7
20.7
20.4 Toluene-d8
3.4
Me
Me
Mo
R
O
Si
R
R = Me
40 330 320 310 300 290 280 270 260 250 240 230 220 210 200 190 180 170 160 150 140 130 120 110 100 90 80 70 60 50 40 30 20 10 0 -10
13C (ppm)

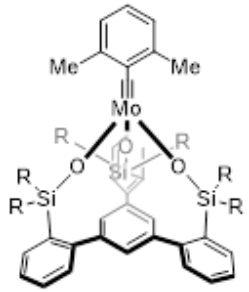
Me
Me
Mo
R
O
R
O
Si
R
R-Si
O
Si-R
R

R = Me

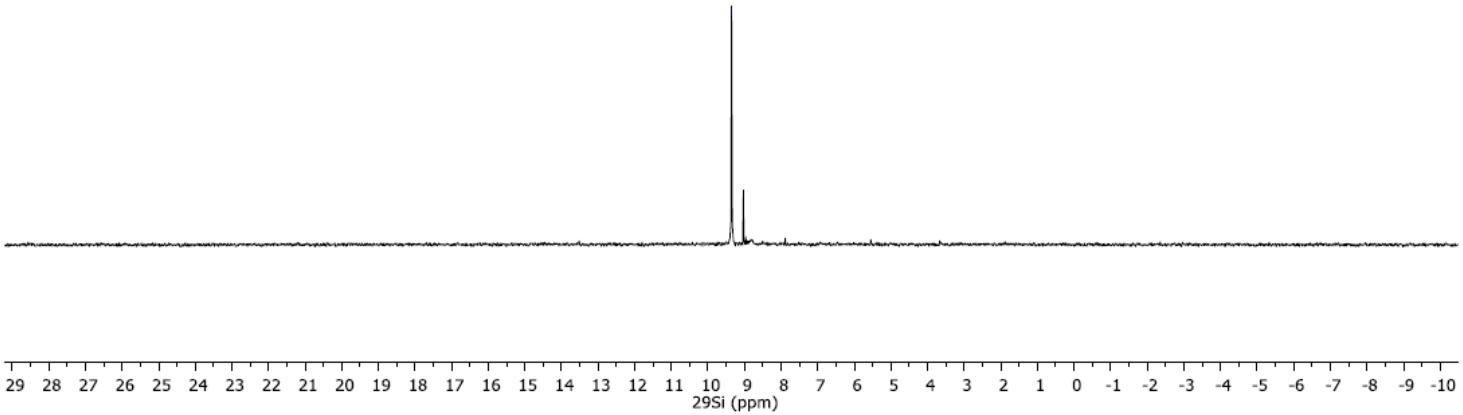
9.4
29 28 27 26 25 24 23 22 21 20 19 18 17 16 15 14 13 12 11 10 9 8 7 6 5 4 3 2 1 0 -1 -2 -3 -4 -5 -6 -7 -8 -9 -10
29Si (ppm)

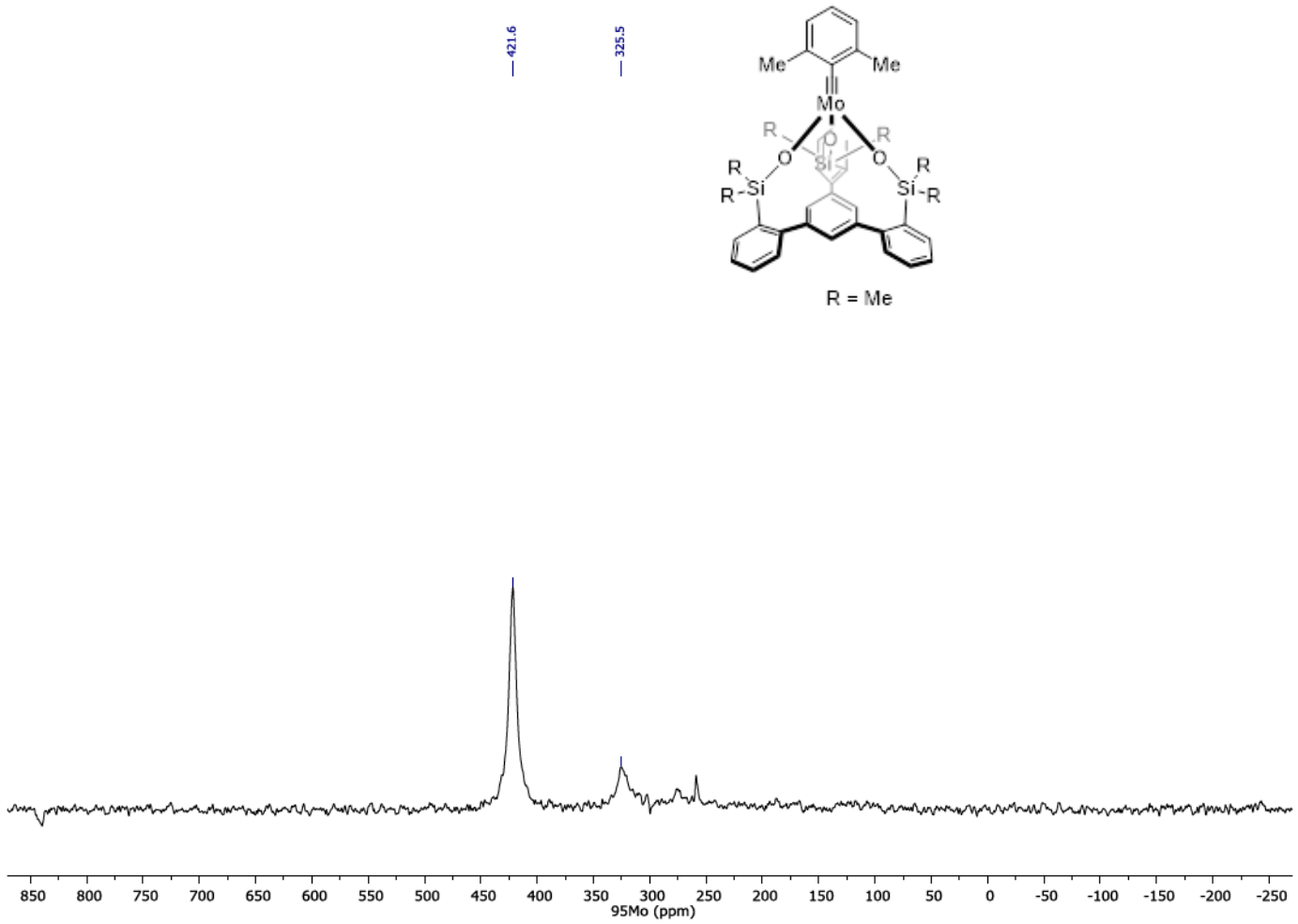
421.6
325.5
Me
Me
Mo
R
O
O
R
R
Si
Si
R
R
R = Me
850 800 750 700 650 600 550 500 450 400 350 300 250 200 150 100 50 0 -50 -100 -150 -200 -250
95Mo (ppm)

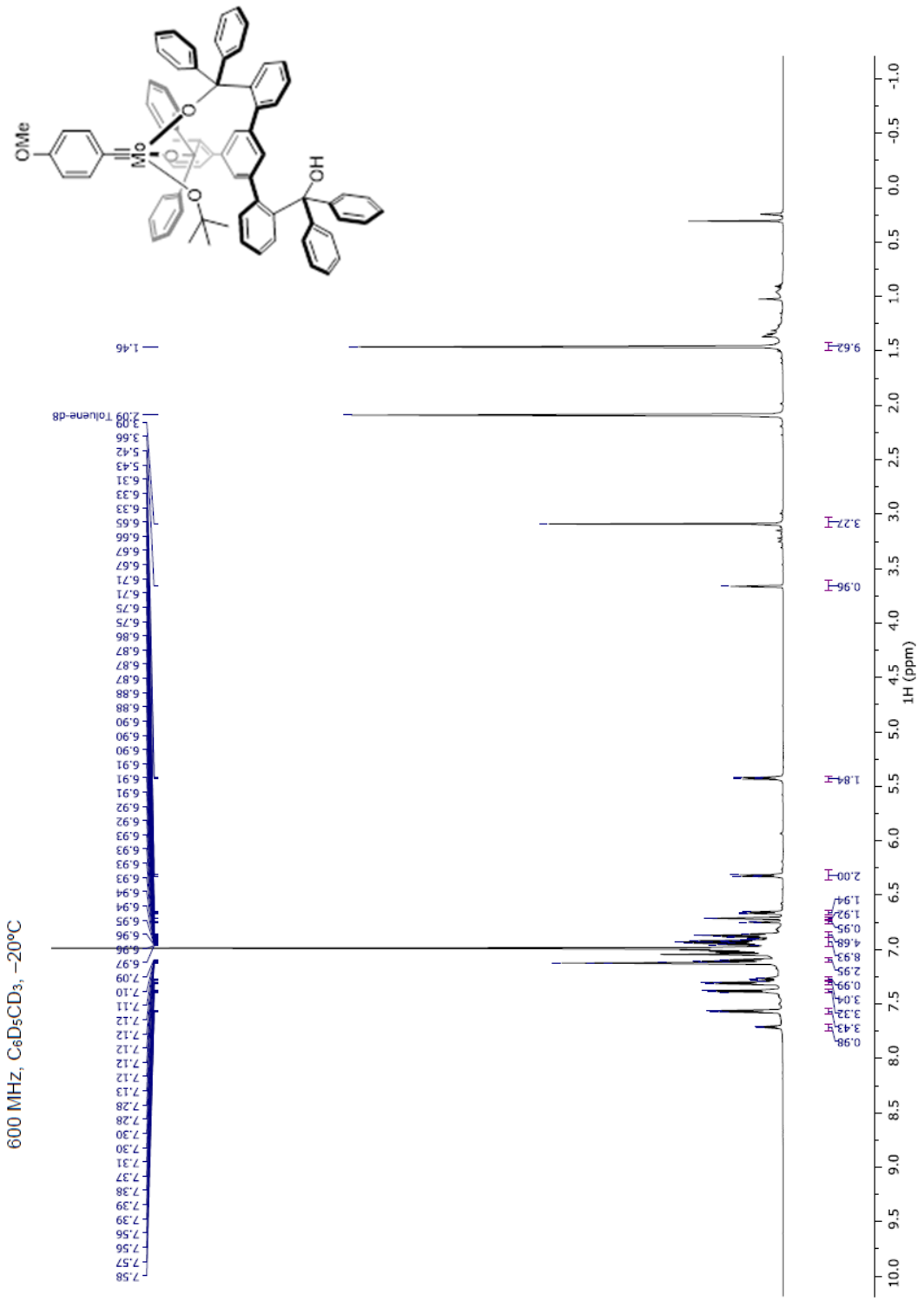
600 MHz, C6D5CD3, –20°C
OMe
Mo
OH
1H (ppm)

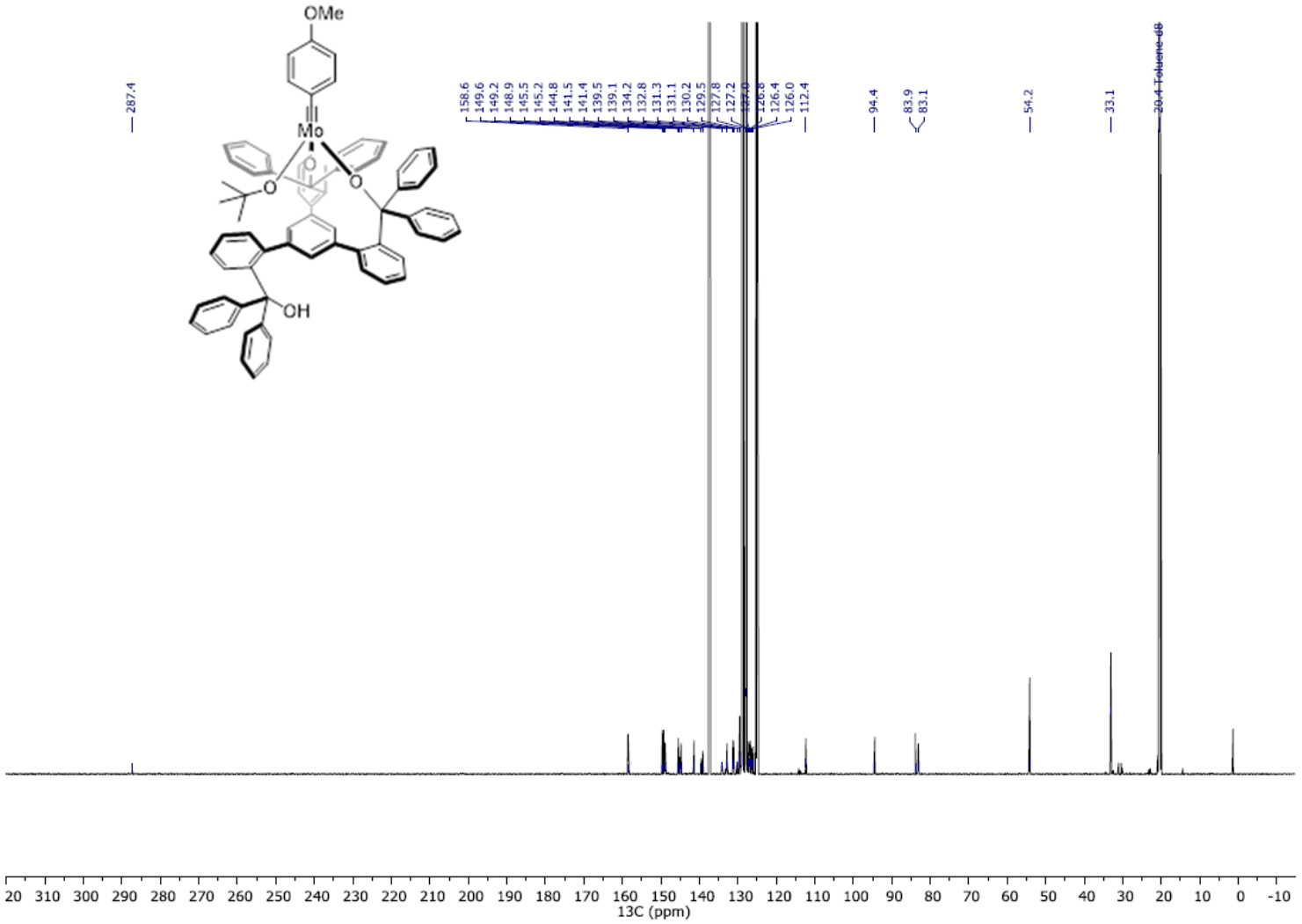
OMe
Mo
O
O
O
OH
287.4
158.6
149.6
149.2
148.9
145.5
145.2
144.8
141.5
141.4
139.5
139.1
134.2
132.8
131.3
131.1
130.2
129.5
127.8
127.2
126.8
126.4
126.0
112.4
94.4
83.9
83.1
54.2
33.1
20.4 Toluene-d8
20 310 300 290 280 270 260 250 240 230 220 210 200 190 180 170 160 150 140 130 120 110 100 90 80 70 60 50 40 30 20 10 0 -10
13C (ppm)

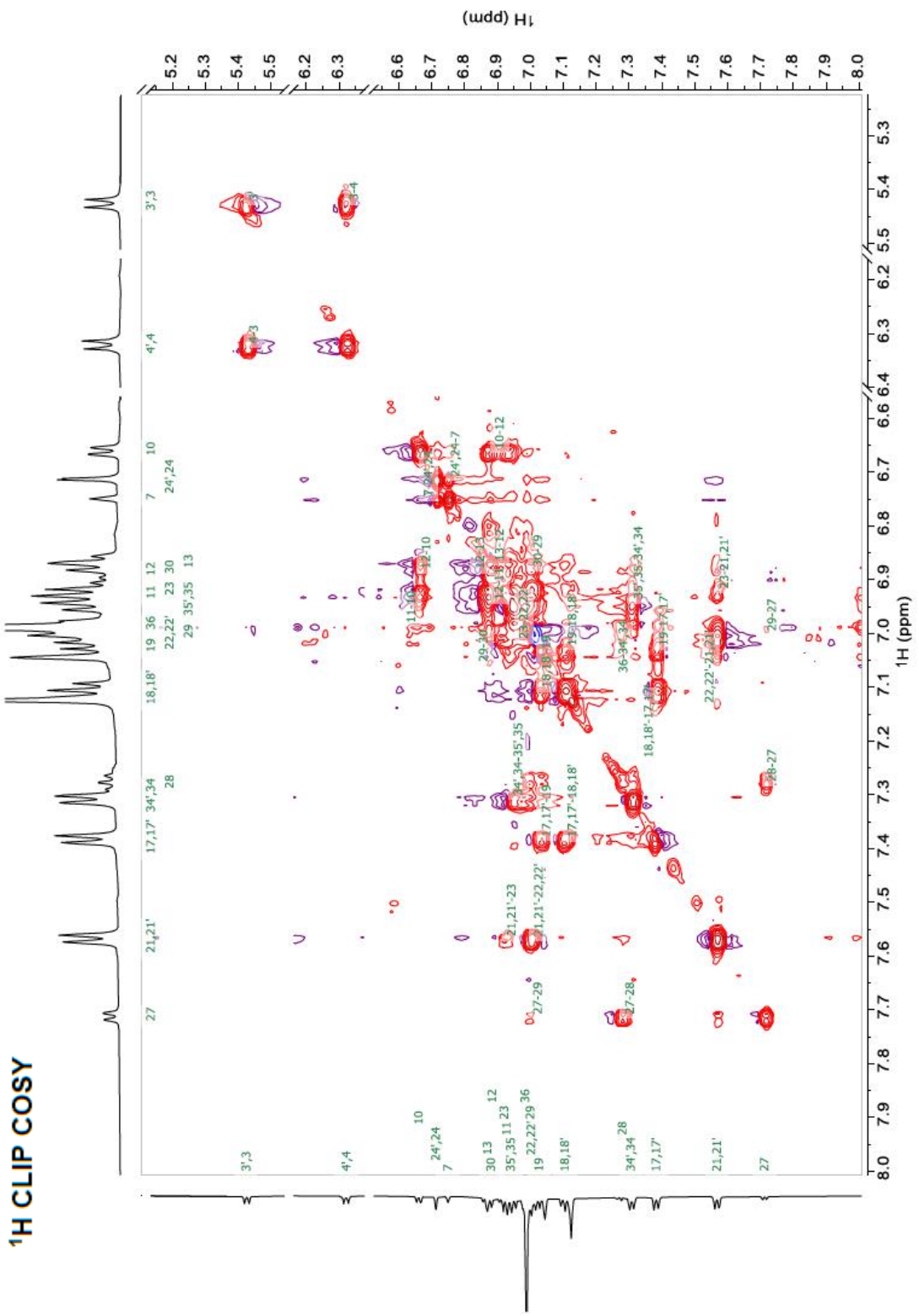
^{1}H CLIP COSY
^{1}H (ppm)
^{1}H (ppm)

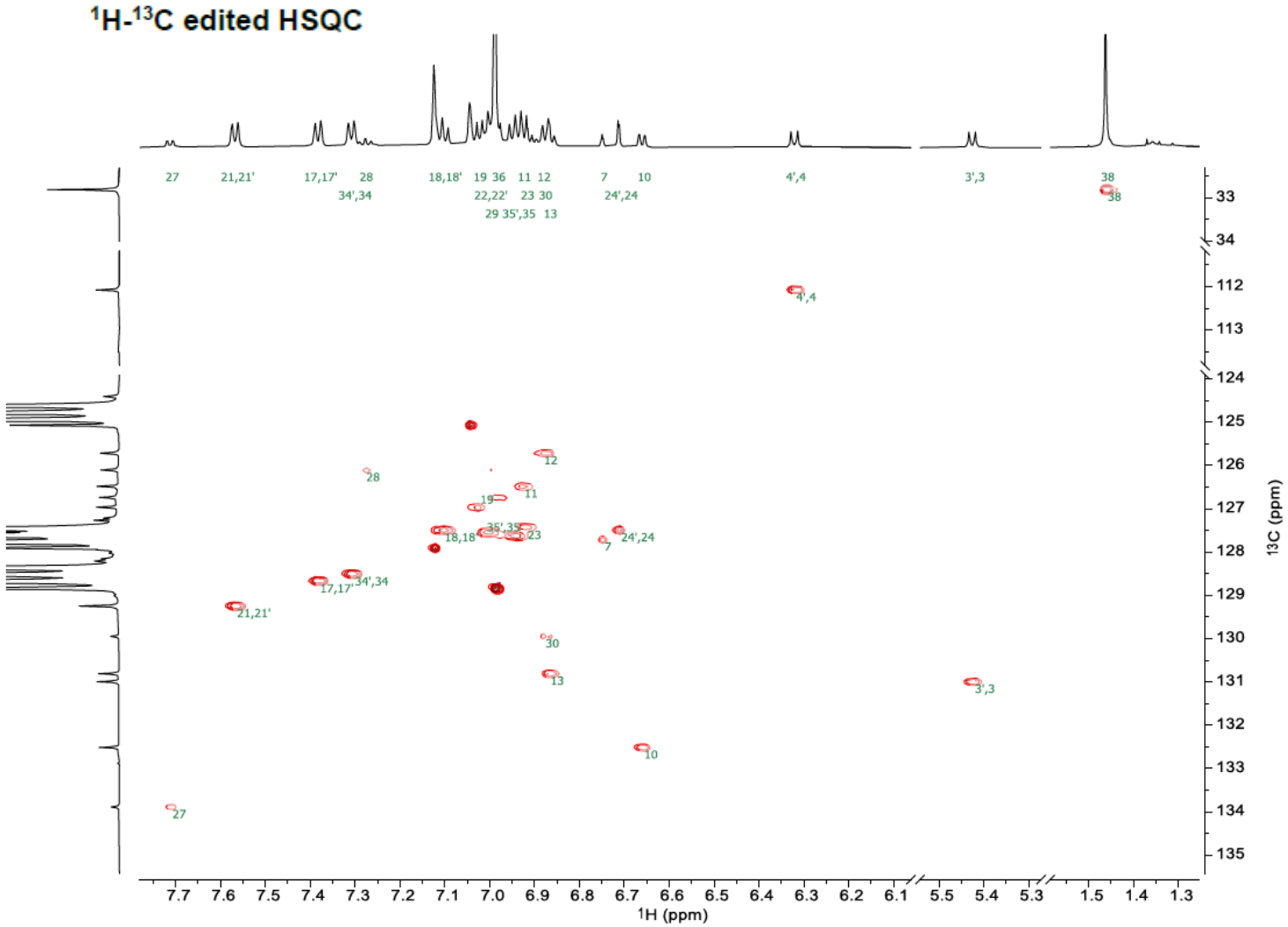
^{1}H-^{13}C edited HSQC
27
21,21'
17,17'
28
34',34
18,18'
19
36
11
12
22,22'
23
30
29
35',35
13
7
10
24',24
4',4
3',3
38
^{1}H (ppm)
^{13}C (ppm)

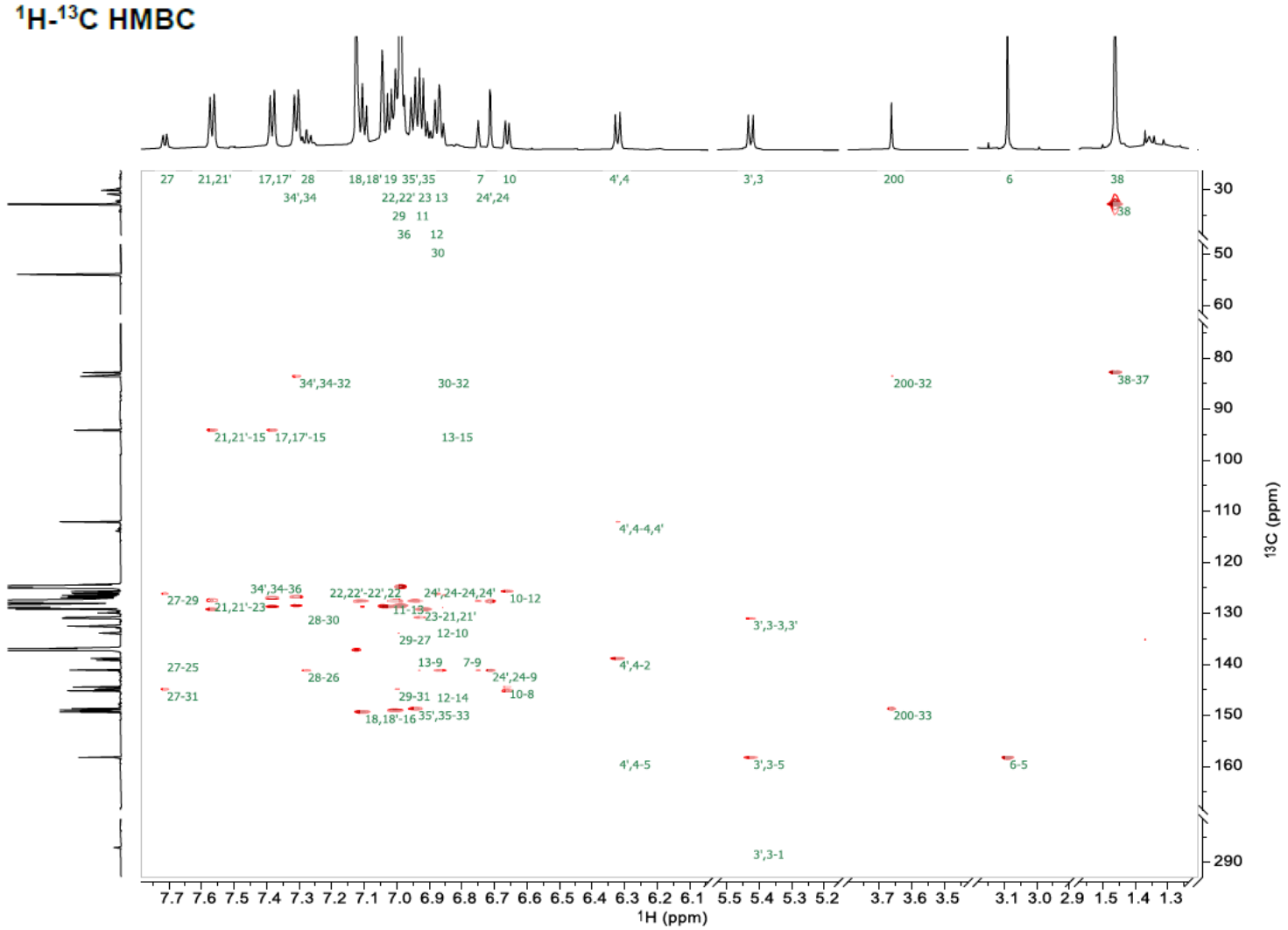
^{1}H-^{13}C HMBC
27
21,21'
17,17'
28
34',34
18,18'
19
35',35
22,22'
23
13
29
11
36
12
30
7
10
24',24
4',4
3',3
200
6
38
38
34',34-32
30-32
200-32
38-37
21,21'-15
17,17'-15
13-15
4',4-4,4'
34',34-36
22,22'-22',22
24',24-24,24'
10-12
27-29
21,21'-23
11-19
23-21,21'
28-30
12-10
3',3-3,3'
29-27
27-25
13-9
7-9
4',4-2
28-26
24',24-9
27-31
10-8
29-31
12-14
200-33
18,18'-16
35',35-33
4',4-5
3',3-5
6-5
3',3-1
7.7 7.6 7.5 7.4 7.3 7.2 7.1 7.0 6.9 6.8 6.7 6.6 6.5 6.4 6.3 6.2 6.1 5.5 5.4 5.3 5.2 3.7 3.6 3.5 3.1 3.0 2.9 1.5 1.4 1.3
^{1}H (ppm)
30 50 60 80 90 100 110 120 130 140 150 160 290
^{13}C (ppm)

OMe
Mo
O
O
OH
118.3
800
750
700
650
600
550
500
450
400
350
300
250
200
150
100
50
0
-50
-100
-150
-200
95Mo (ppm)

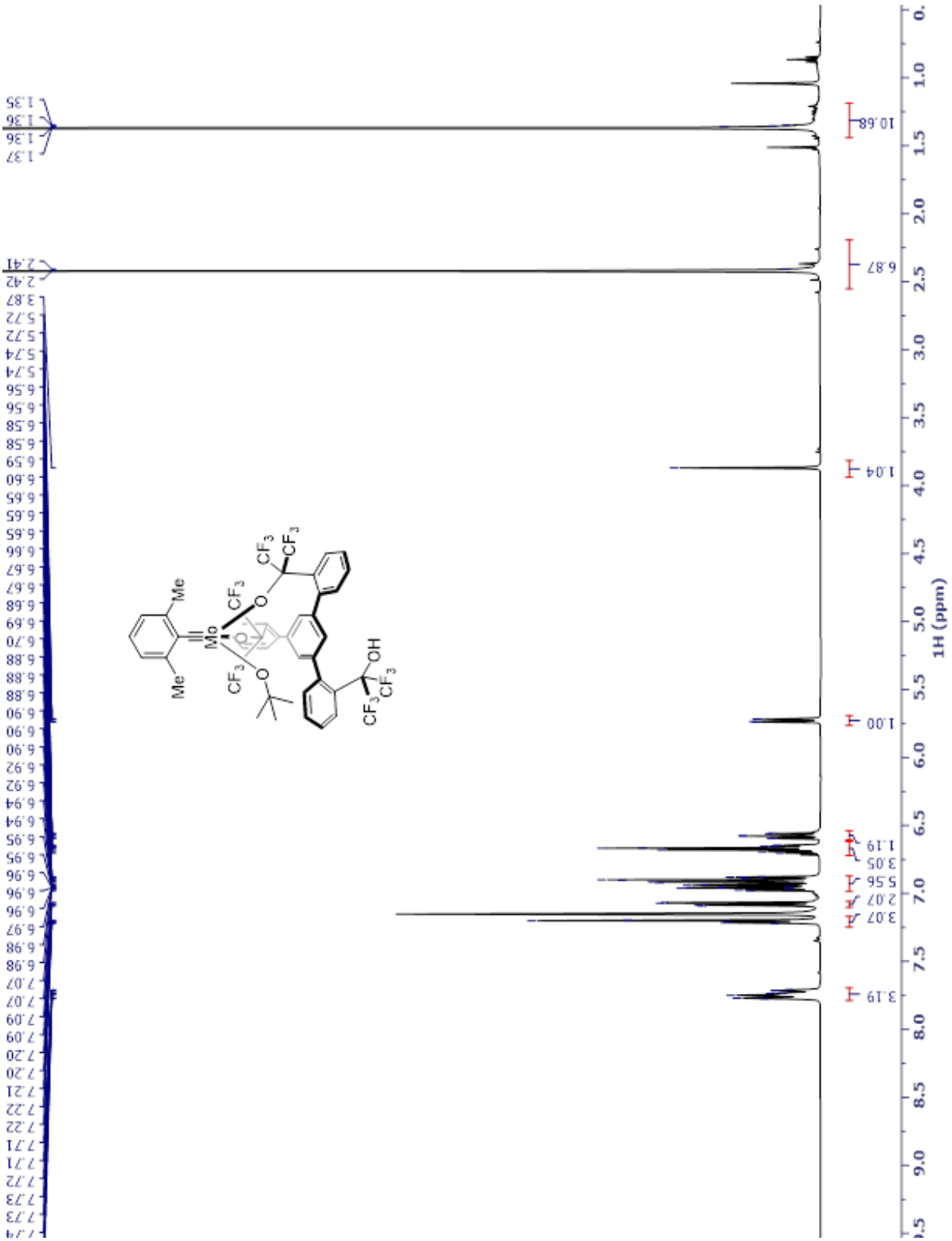
Me
Mo
CF3
CF3
CF3
CF3
CF3
OH
Me
1H (ppm)

Appendix 4: NMR spectra - Section 5.3.2. Novel Compounds

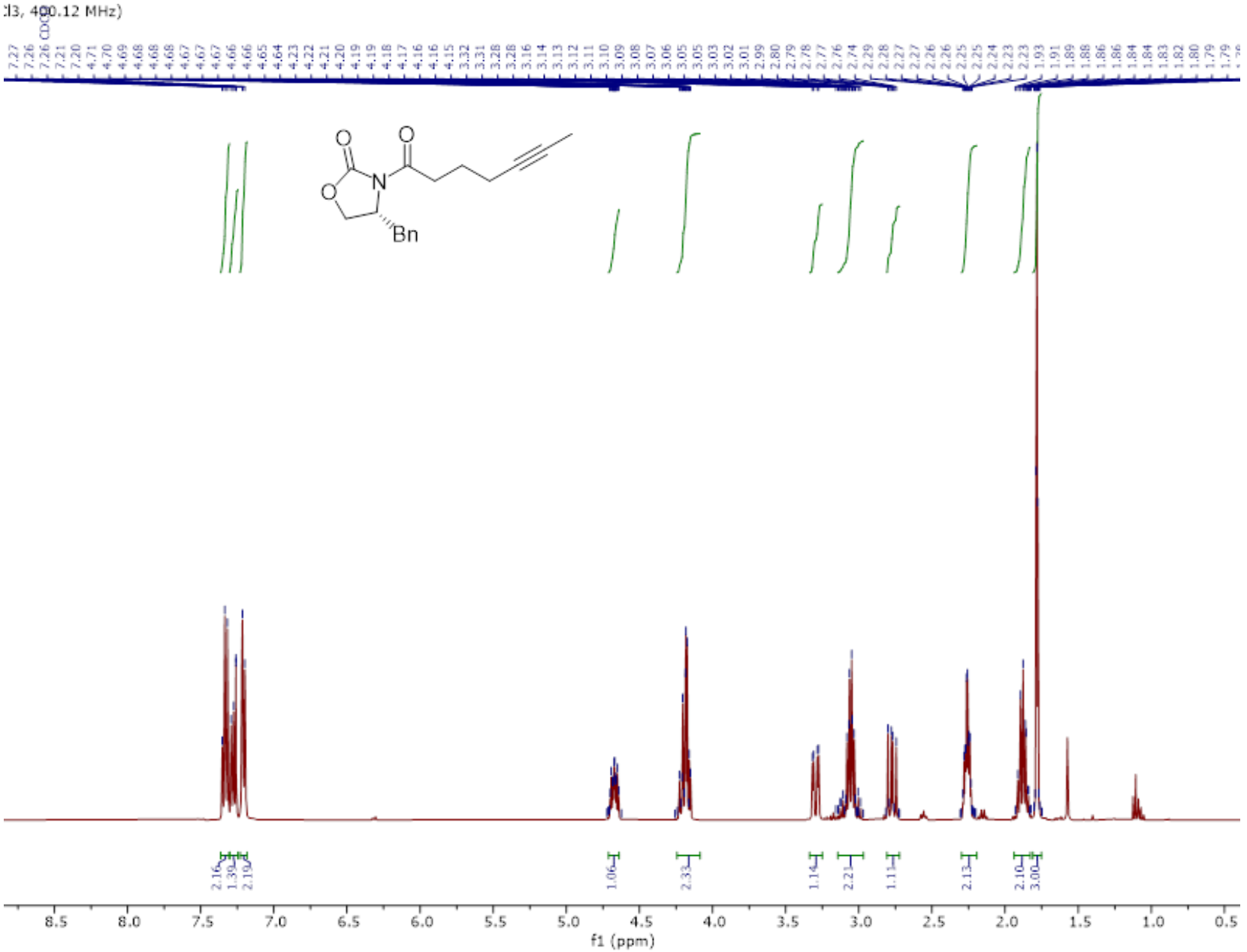
Bn
f1 (ppm)

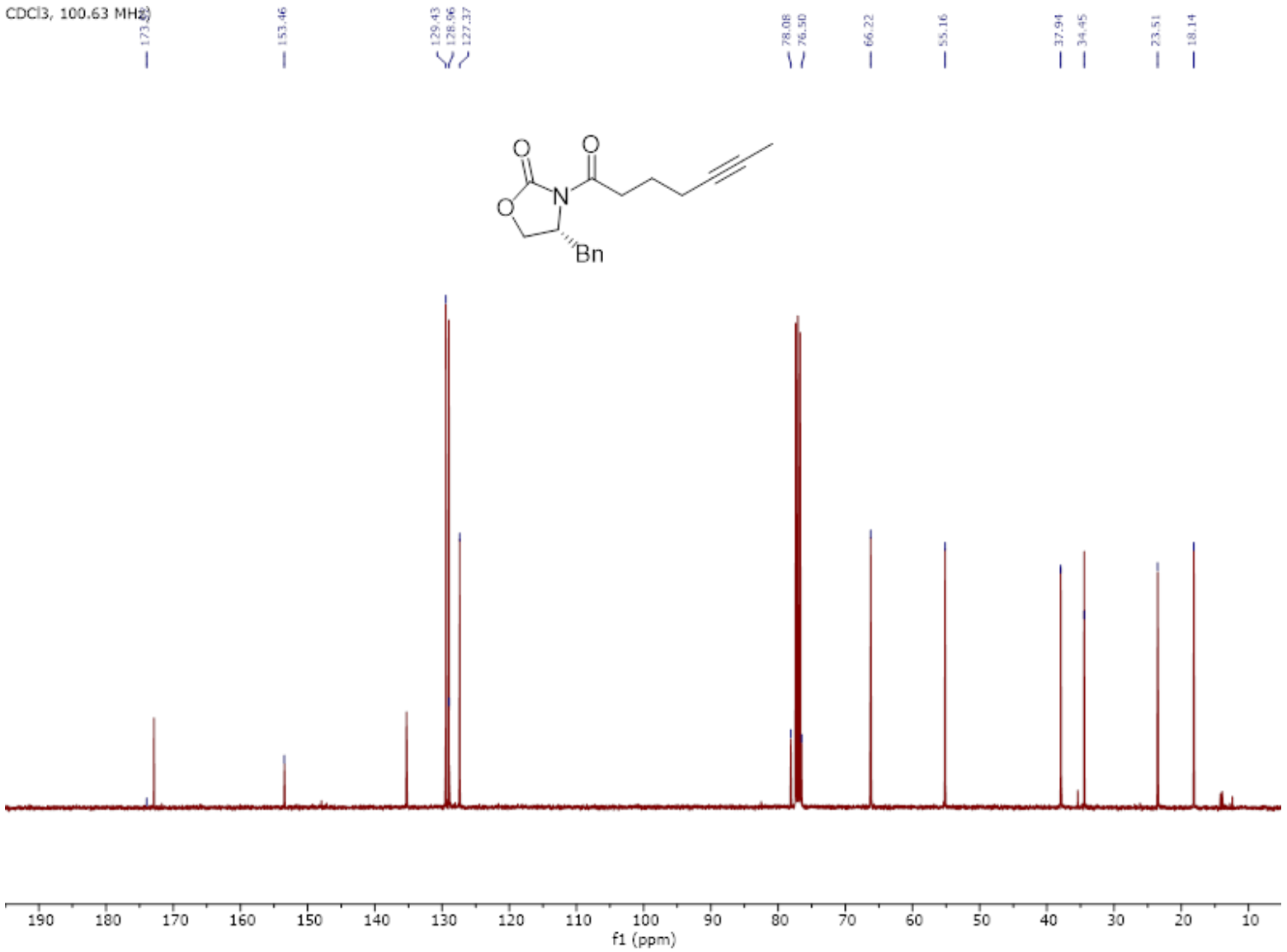
CDCl3, 100.63 MHz
173.3
153.46
129.43
128.96
127.37
78.08
76.50
66.22
55.16
37.94
34.45
23.51
18.14
O
O
N
O
Bn
190
180
170
160
150
140
130
120
110
100
90
80
70
60
50
40
30
20
10
f1 (ppm)

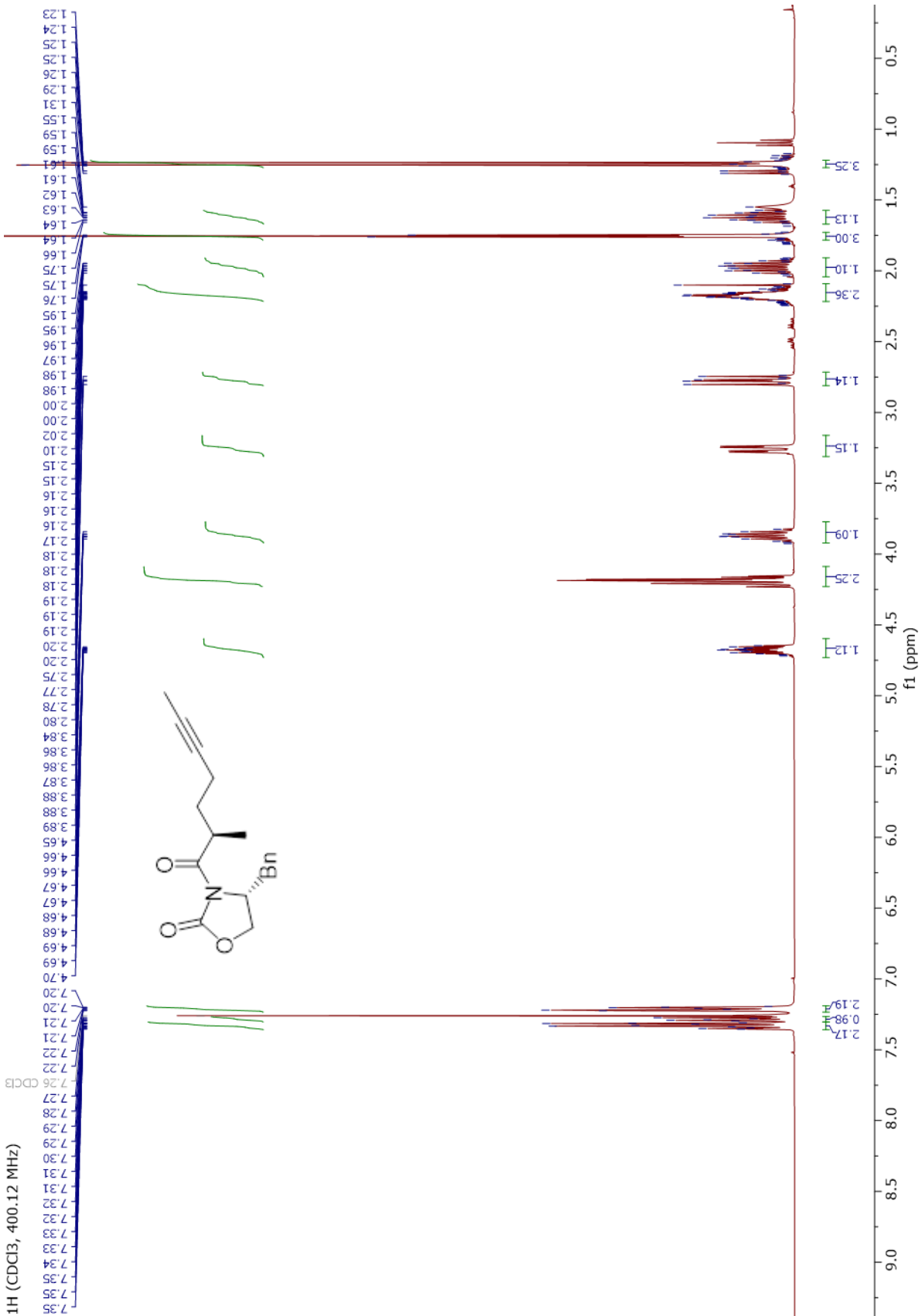
1H (CDCl3, 400.12 MHz)
f1 (ppm)
Bn
O
N
O
O

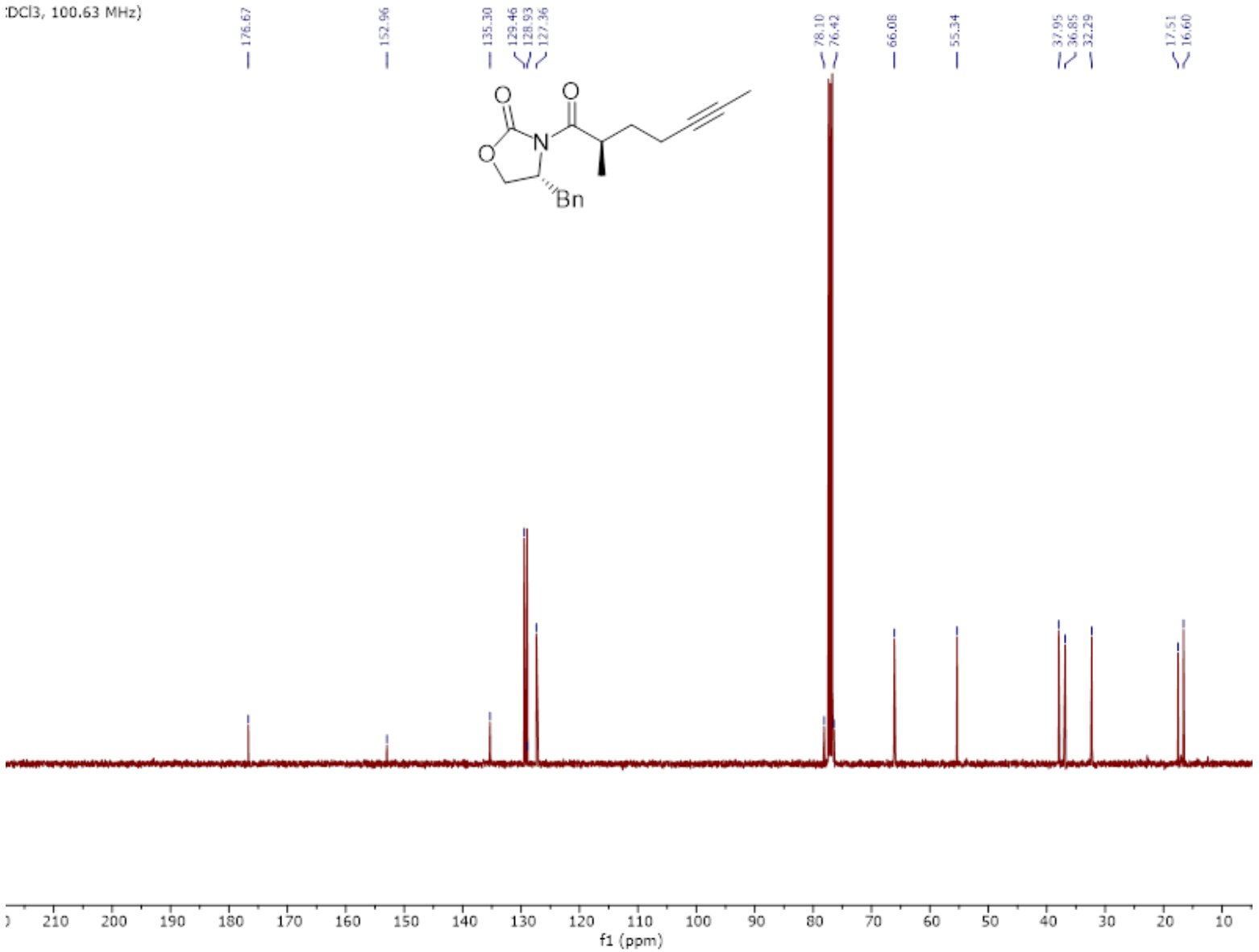
:DCl3, 100.63 MHz)
176.67
152.96
135.30
129.46
128.93
127.36
78.10
76.42
66.08
55.34
37.95
36.85
32.29
17.51
16.60
O
O
N
O
Bn
210
200
190
180
170
160
150
140
130
120
110
100
90
80
70
60
50
40
30
20
10
f1 (ppm)

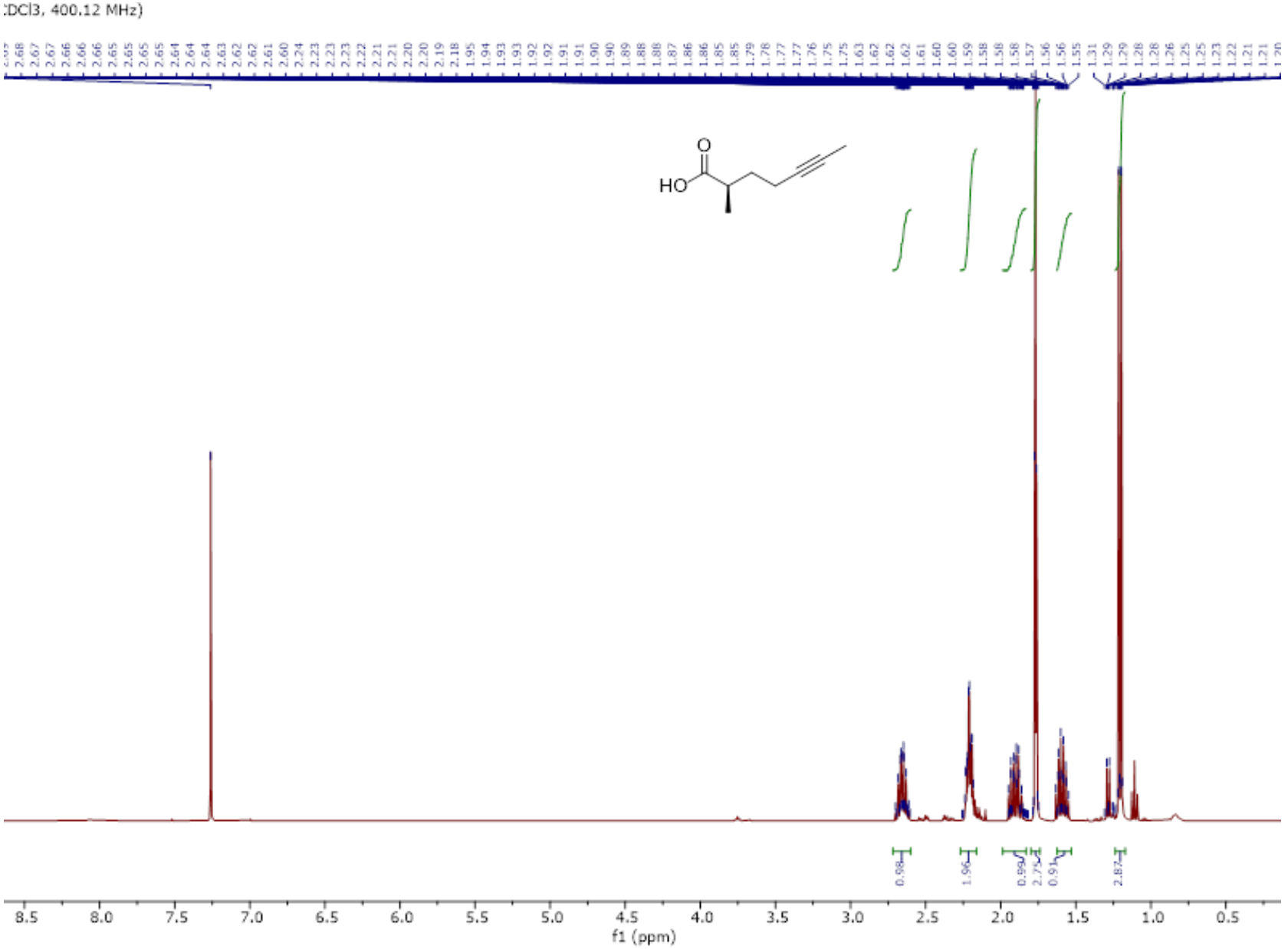
:DCl3, 400.12 MHz)
O
HO
0.98
1.96
0.99
2.75
0.91
2.87
8.5
8.0
7.5
7.0
6.5
6.0
5.5
5.0
4.5
4.0
3.5
3.0
2.5
2.0
1.5
1.0
0.5
f1 (ppm)

13C (CDCl3, 100.62 MHz)

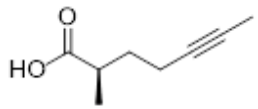

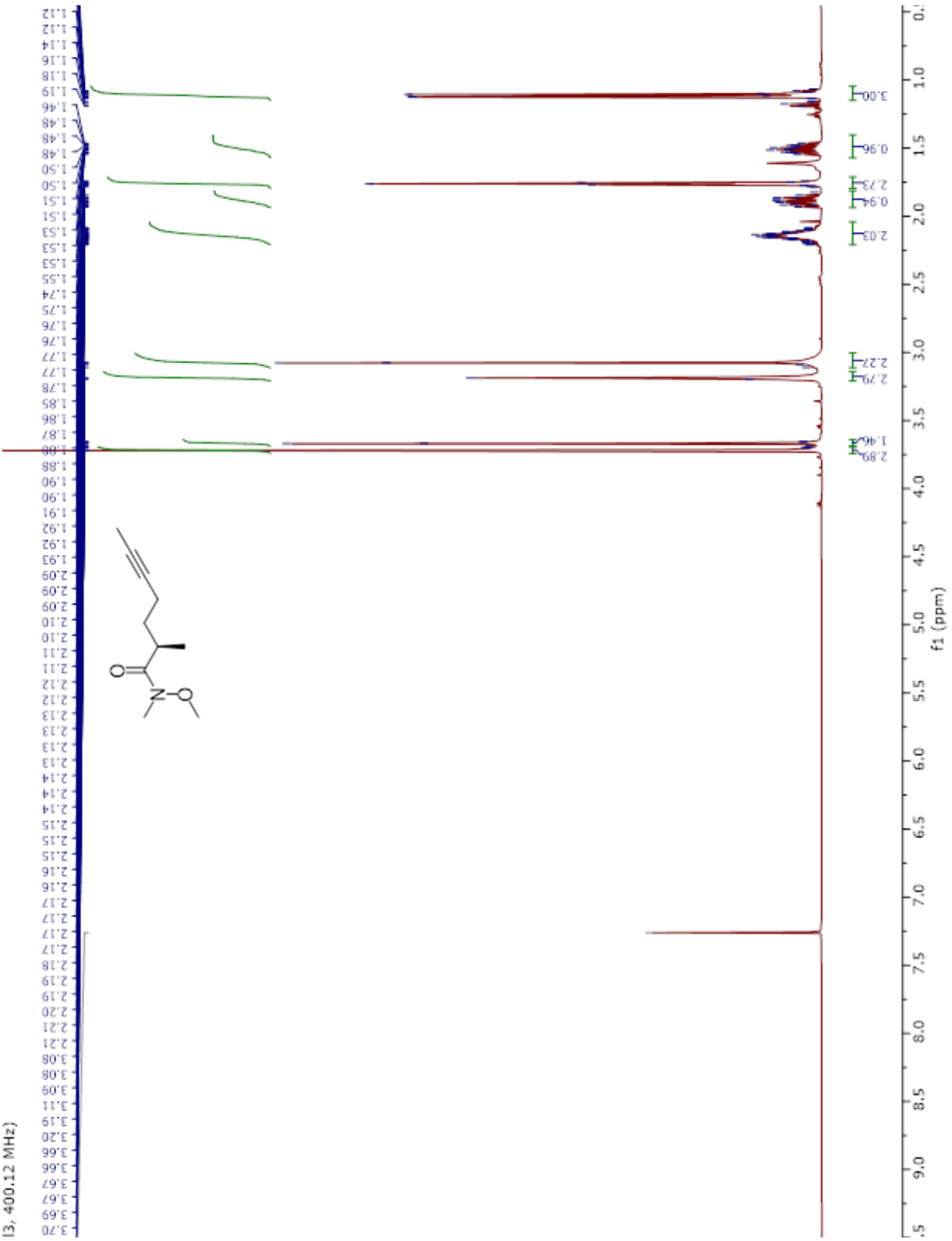
13, 400.12 MHz)
f1 (ppm)
3.00
0.96
2.73
0.94
2.03
2.27
2.79
1.46
2.89

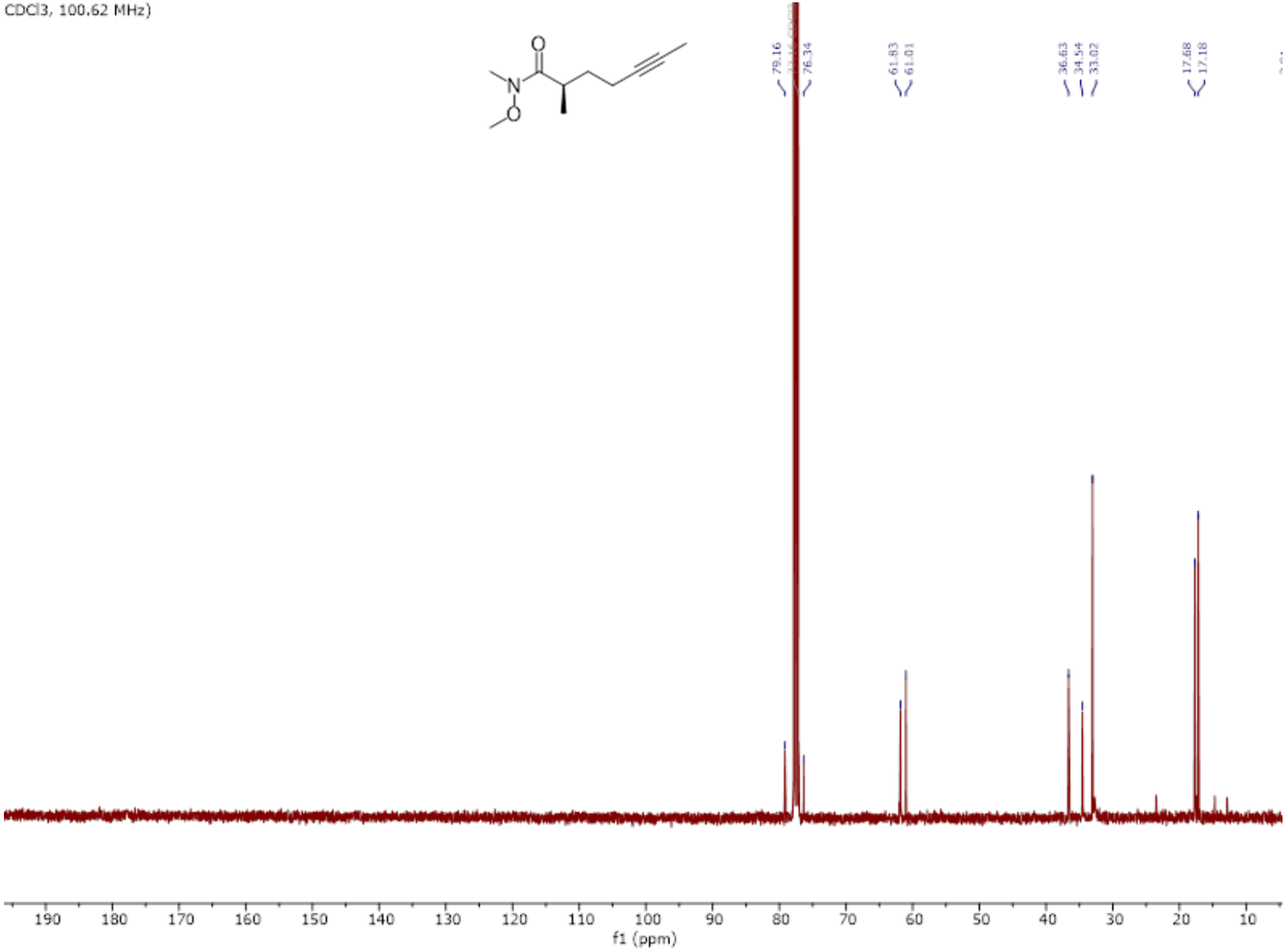
CDCl3, 100.62 MHz)
79.16
76.34
61.83
61.01
36.63
34.54
33.02
17.68
17.18
190
180
170
160
150
140
130
120
110
100
90
80
70
60
50
40
30
20
10
f1 (ppm)

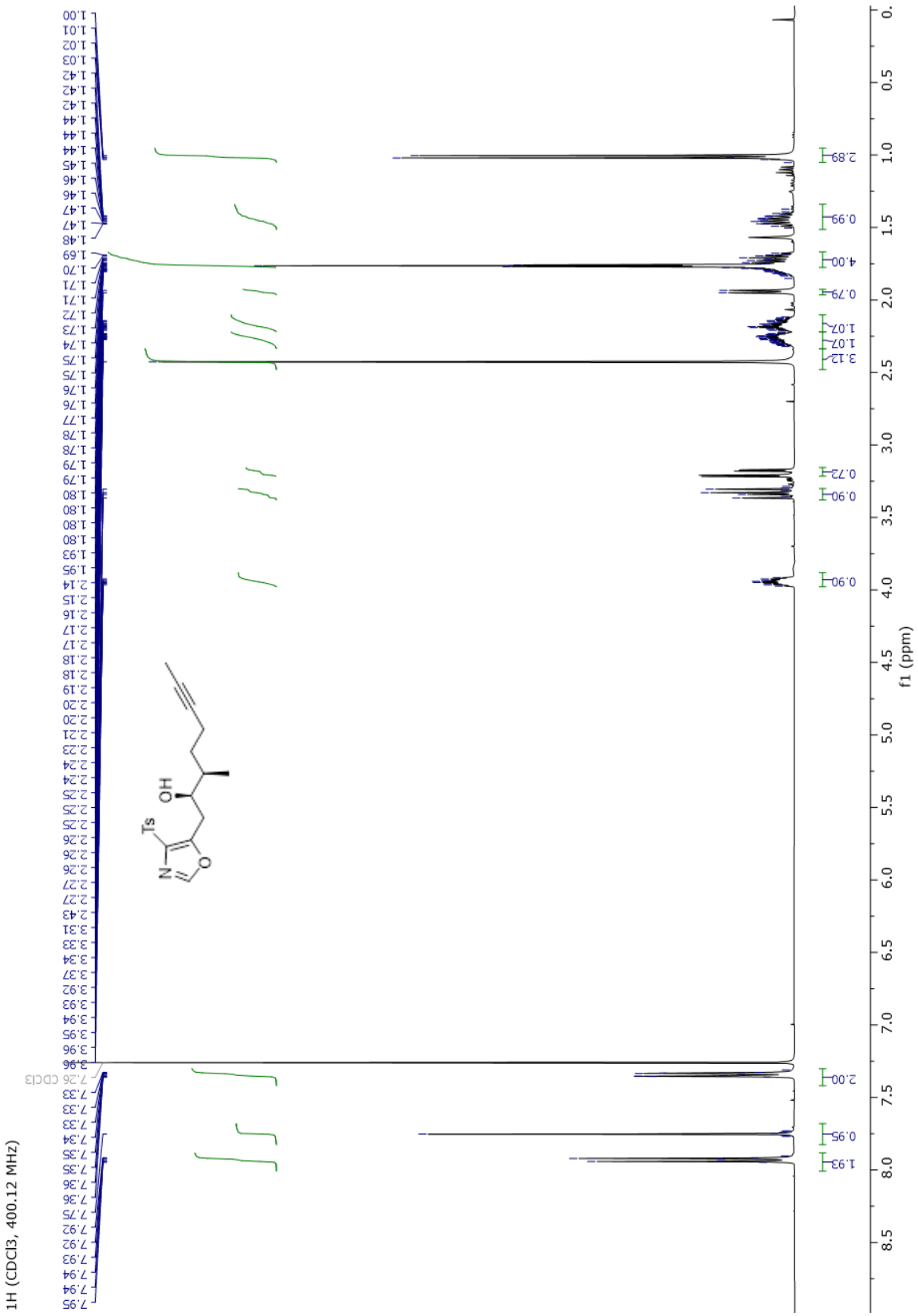
1H (CDCl3, 400.12 MHz)
f1 (ppm)
7.26 CDCl3
OH
Ts
N
O

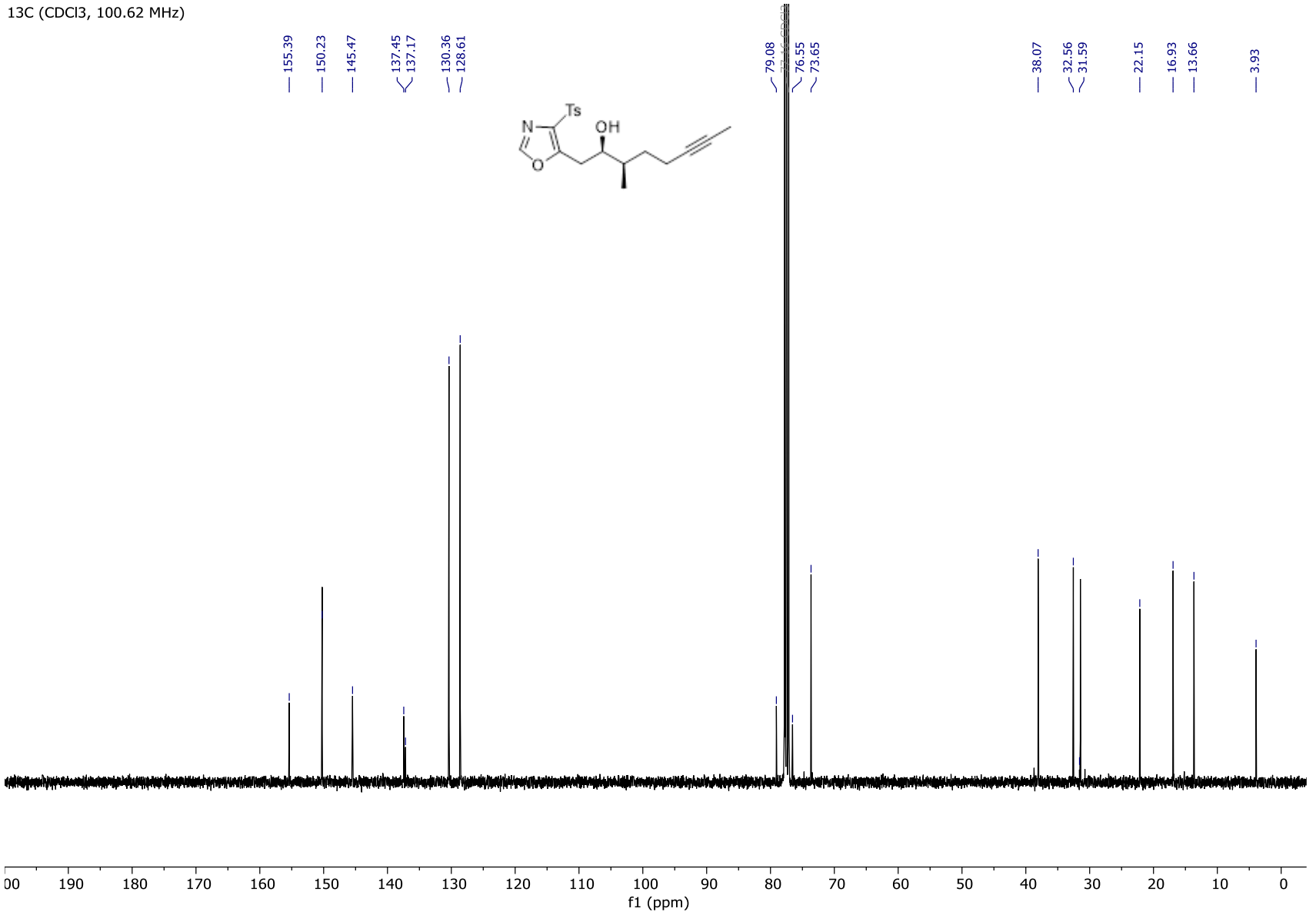
13C (CDCl3, 100.62 MHz)
155.39
150.23
145.47
137.45
137.17
130.36
128.61
79.08
76.55
73.65
38.07
32.56
31.59
22.15
16.93
13.66
3.93
Ts
N
O
OH
f1 (ppm)

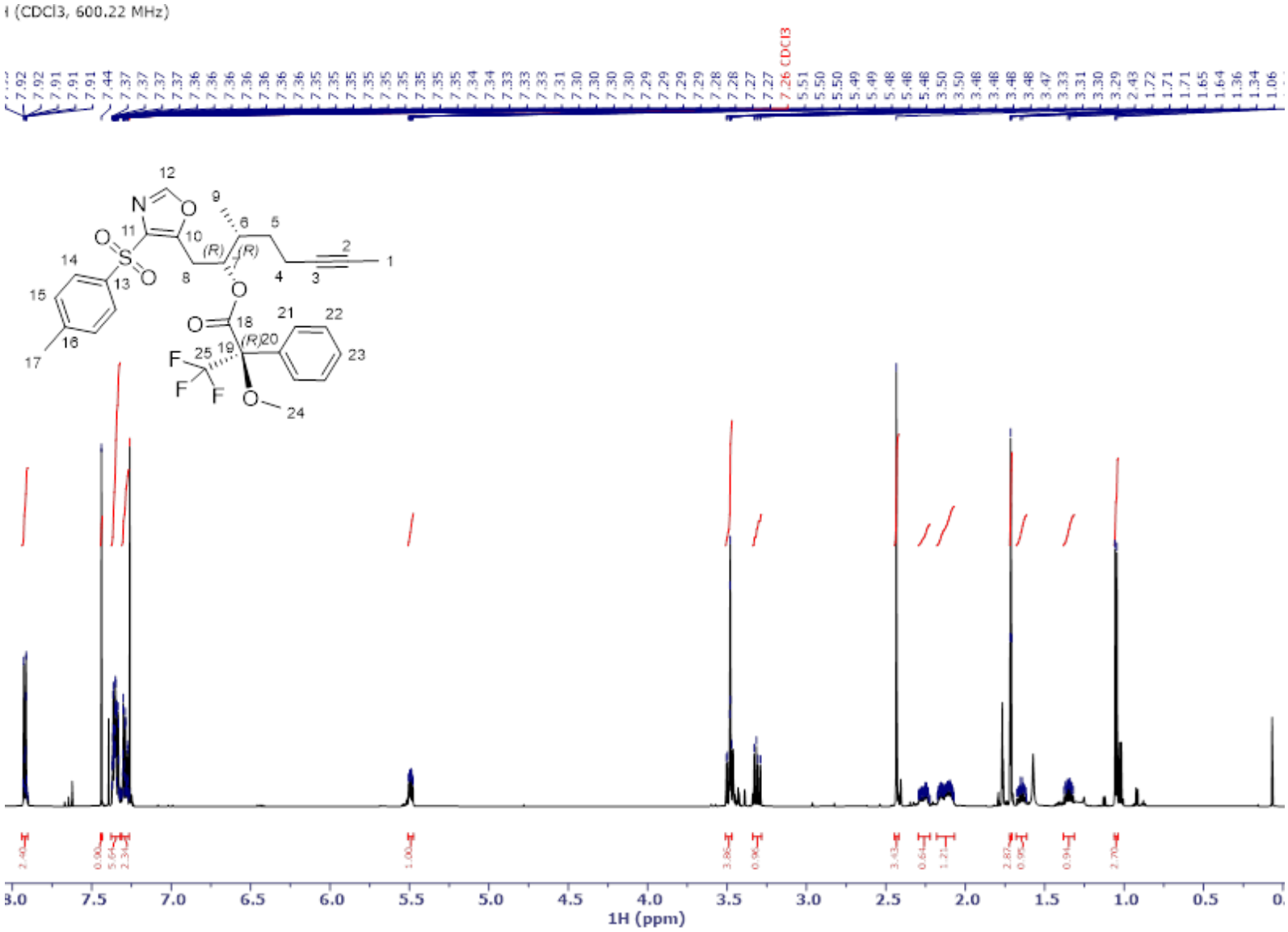
(CDCl3, 600.22 MHz)
7.26 CDCl3
1H (ppm)

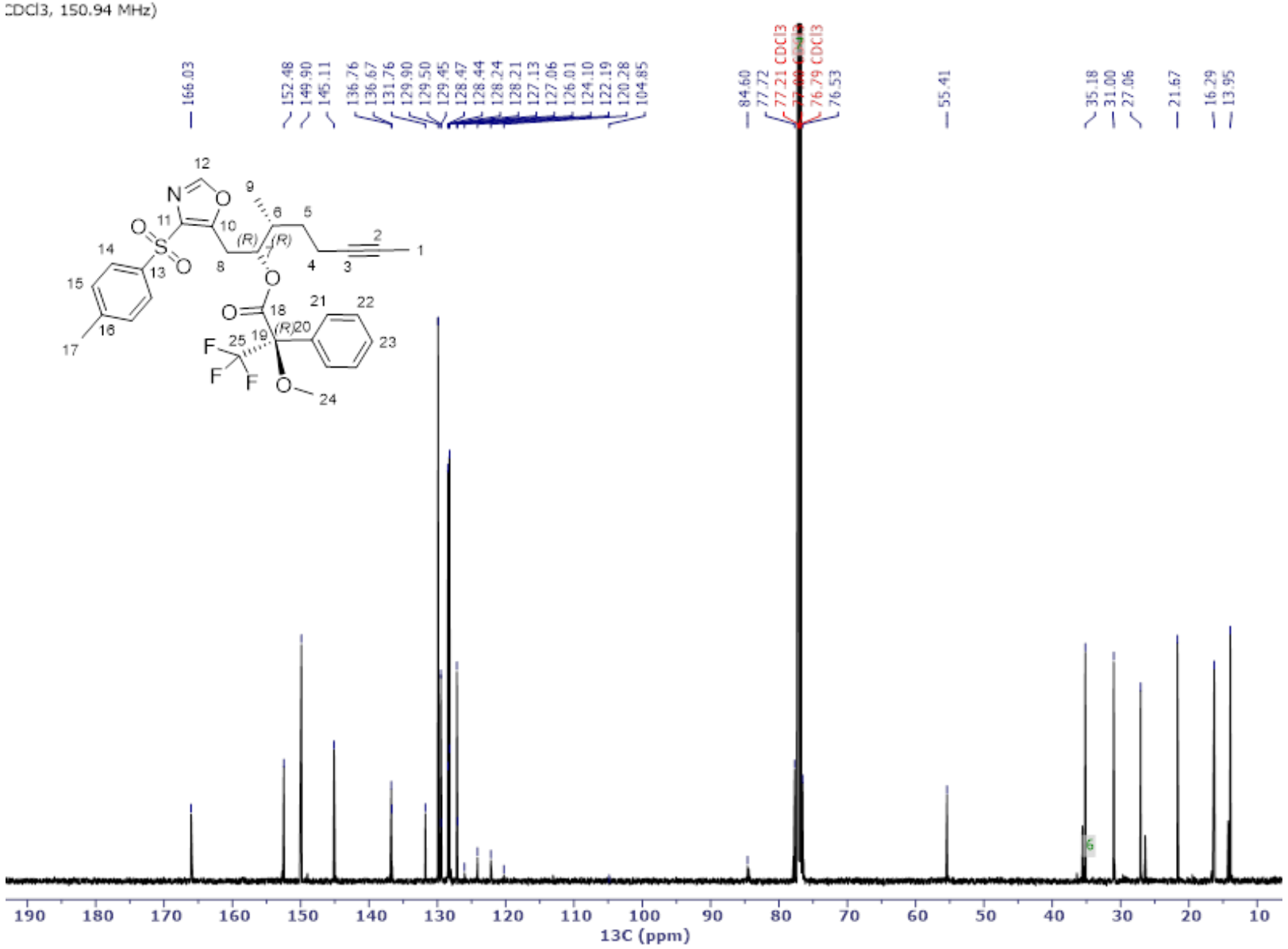
CDCl3, 150.94 MHz)
166.03
152.48
149.90
145.11
136.76
136.67
131.76
129.90
129.50
129.45
128.47
128.44
128.24
128.21
127.13
127.06
126.01
124.10
122.19
120.28
104.85
84.60
77.72
77.21 CDCl3
76.79 CDCl3
76.53
55.41
35.18
31.00
27.06
21.67
16.29
13.95
13C (ppm)

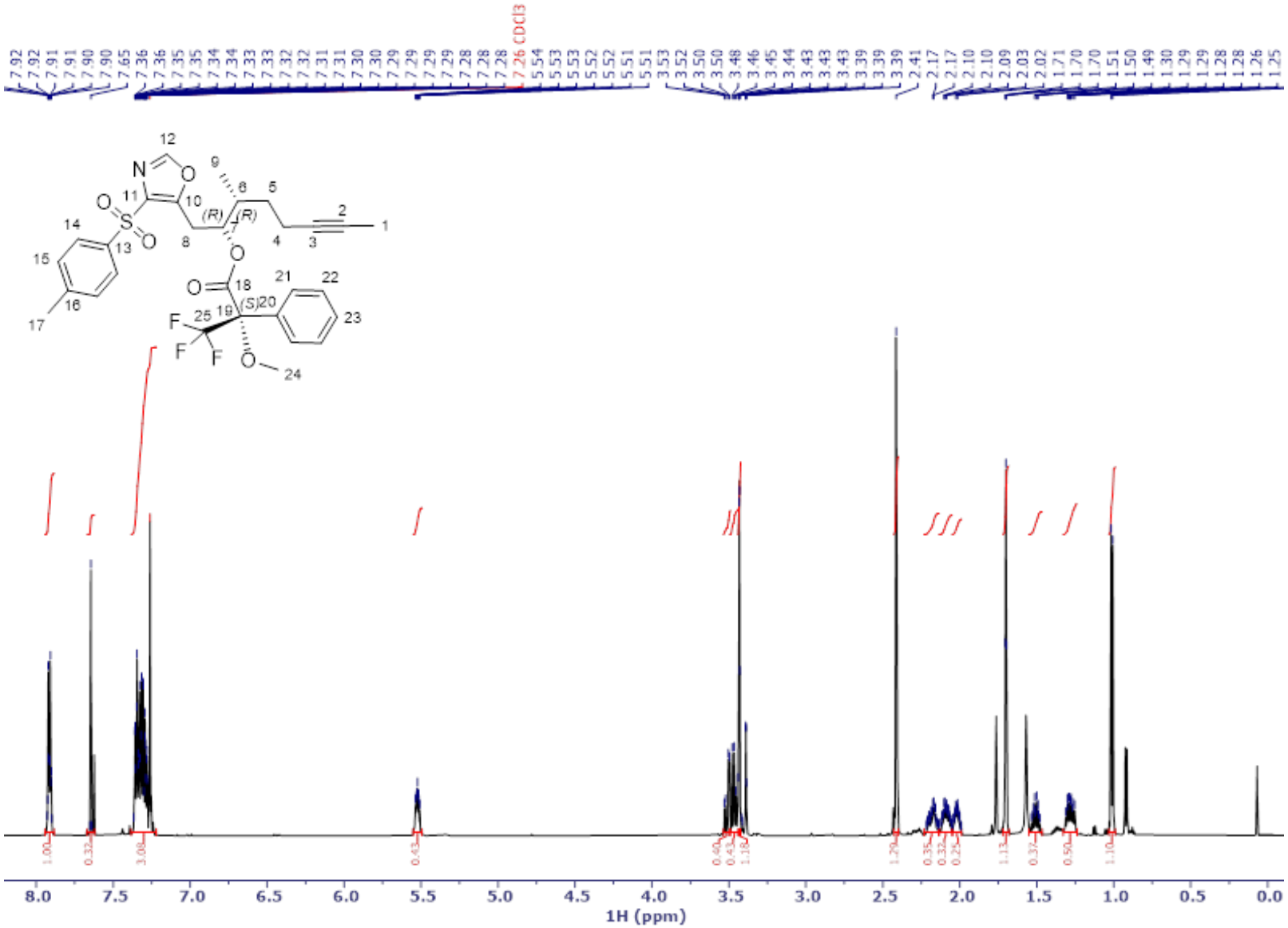
CDCl3, 600.22 MHz)
CDCl3
(R)
(R)
(S)
1H (ppm)

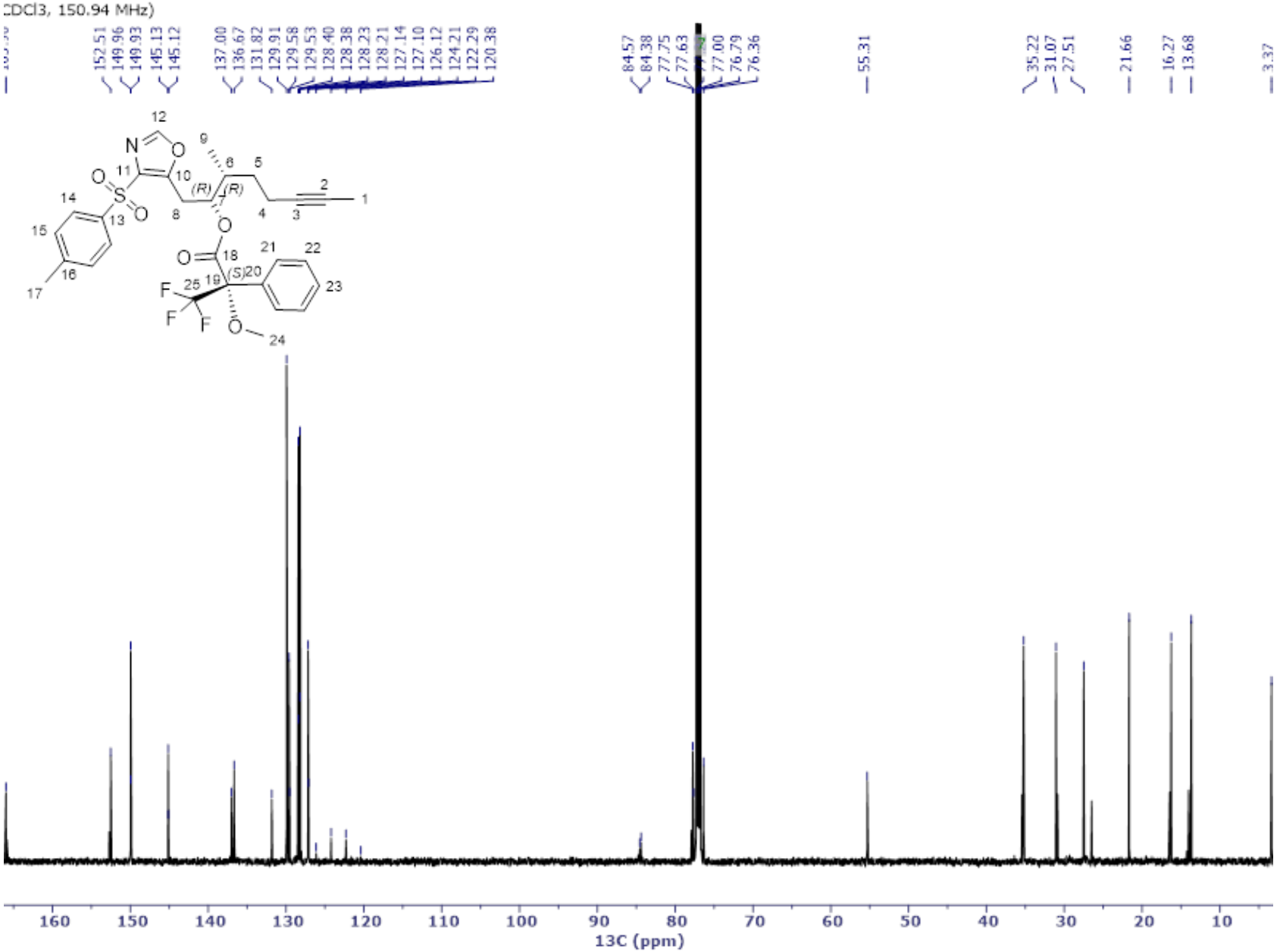
CDCl3, 150.94 MHz)
152.51
149.96
149.93
145.13
145.12
137.00
136.67
131.82
129.91
129.58
129.53
128.40
128.38
128.23
128.21
127.14
127.10
126.12
124.21
122.29
120.38
84.57
84.38
77.75
77.63
77.00
76.79
76.36
55.31
35.22
31.07
27.51
21.66
16.27
13.68
3.37
160
150
140
130
120
110
100
90
80
70
60
50
40
30
20
10
13C (ppm)

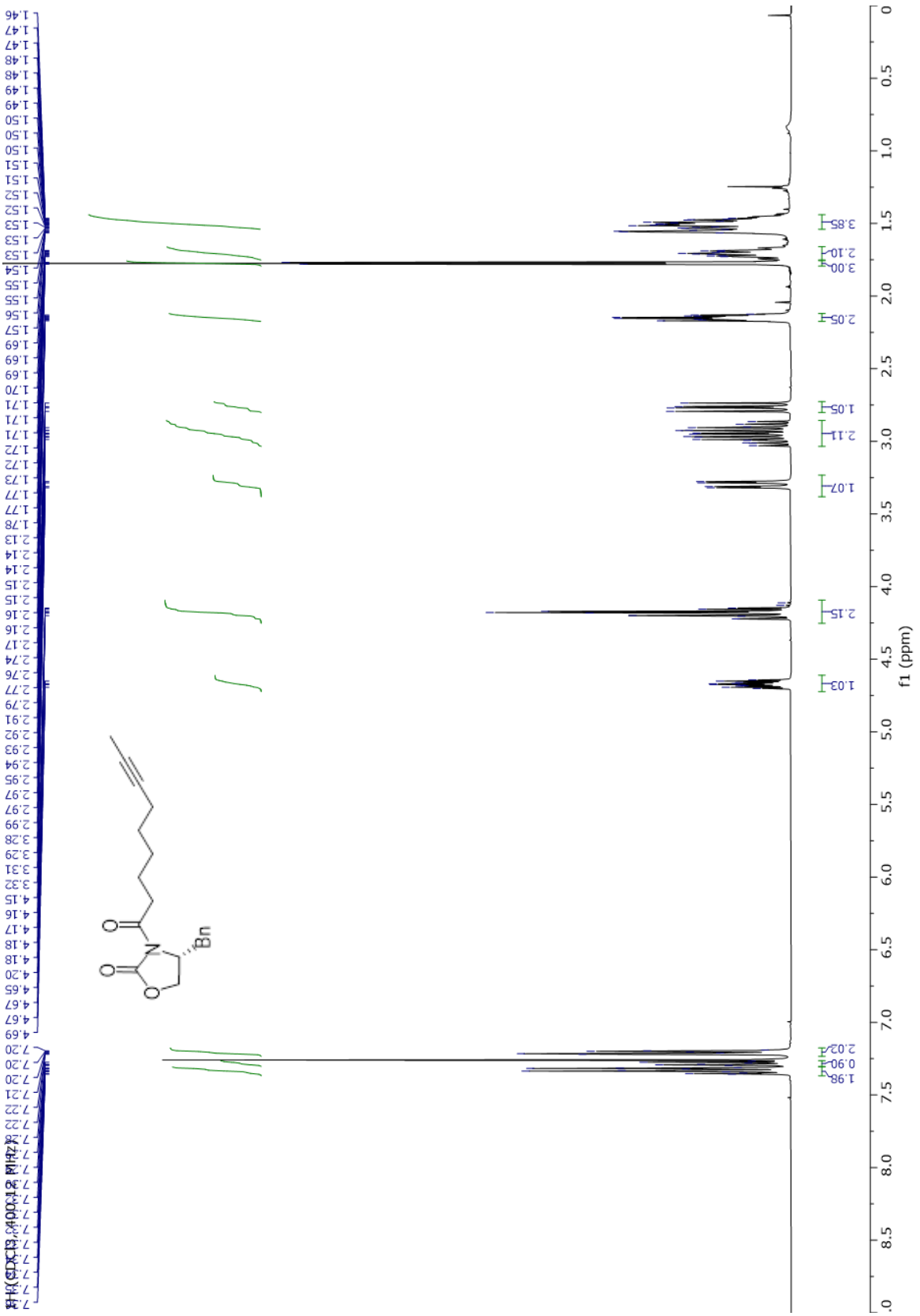
Bn
f1 (ppm)

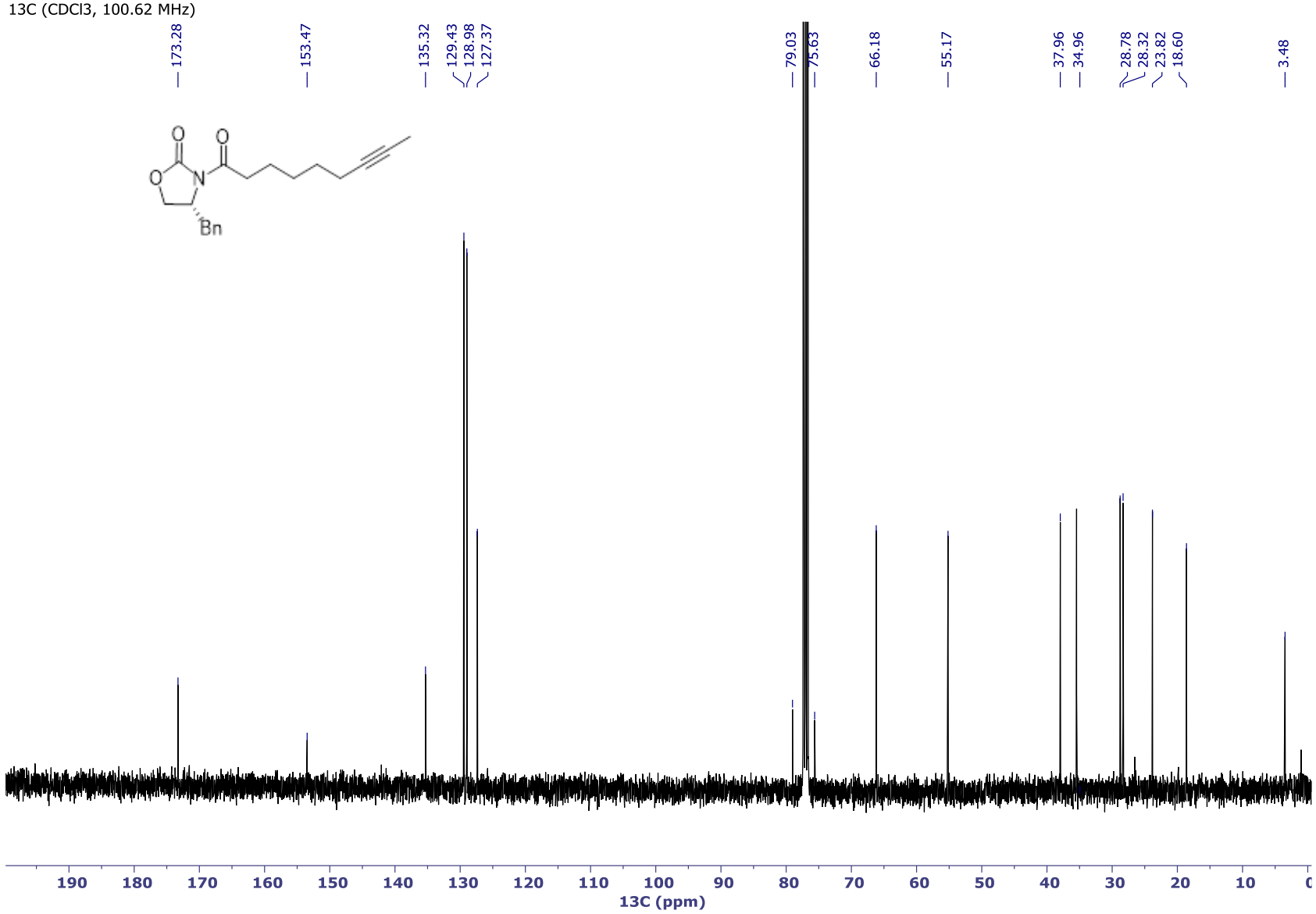
13C (CDCl3, 100.62 MHz)
173.28
153.47
135.32
129.43
128.98
127.37
79.03
75.63
66.18
55.17
37.96
34.96
28.78
28.32
23.82
18.60
3.48
O
O
O
N
Bn
190
180
170
160
150
140
130
120
110
100
90
80
70
60
50
40
30
20
10
0
13C (ppm)

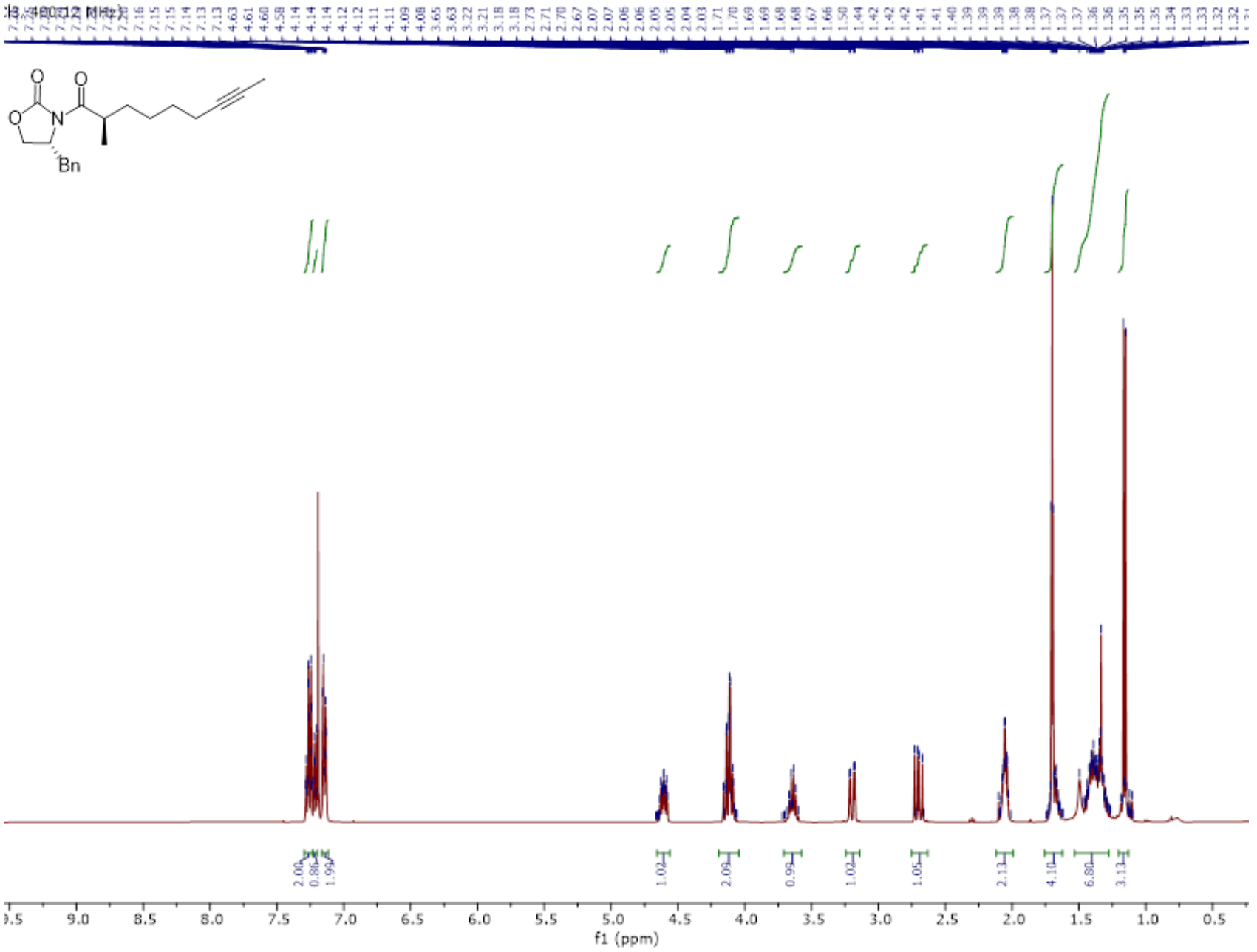
O
O
O
N
Bn
f1 (ppm)

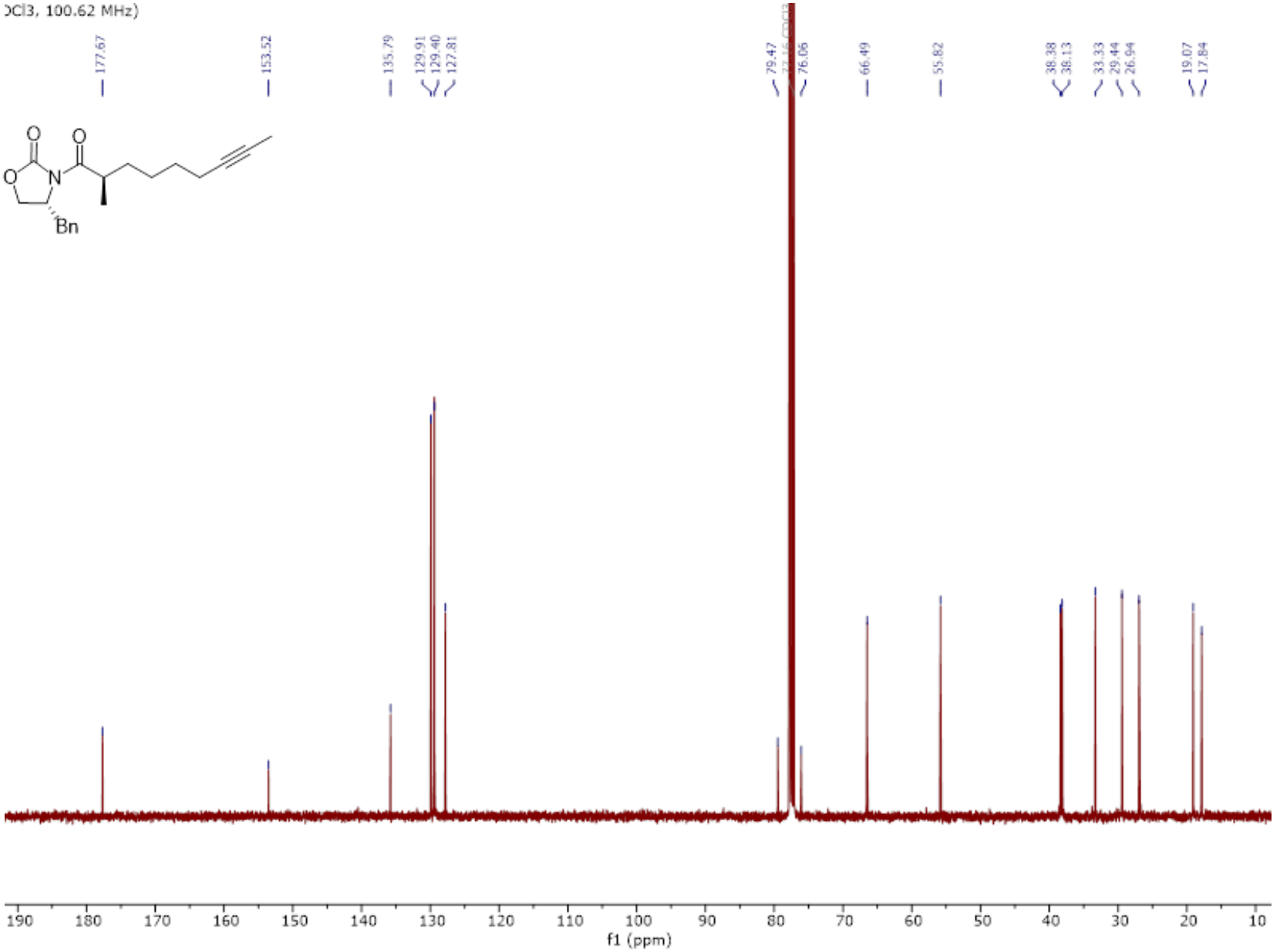
CDCl3, 100.62 MHz)
177.67
153.52
135.79
129.91
129.40
127.81
79.47
77.16
76.06
66.49
55.82
38.38
38.13
33.33
29.44
26.94
19.07
17.84
O
O
O
N
Bn
190
180
170
160
150
140
130
120
110
100
90
80
70
60
50
40
30
20
10
f1 (ppm)

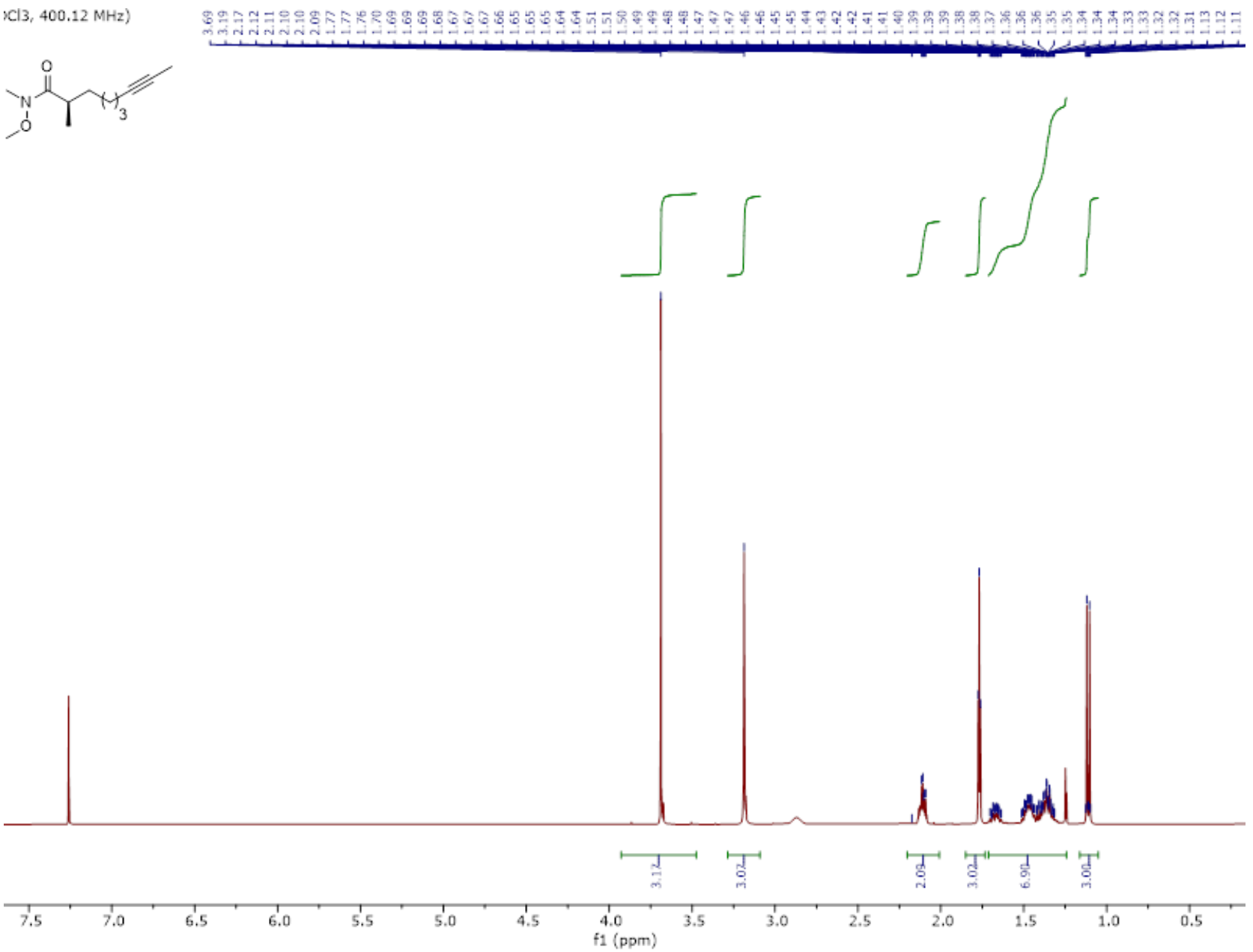
)Cl3, 400.12 MHz)
O
N
O
3
3.69 3.19 2.17 2.12 2.11 2.10 2.10 2.09 1.77 1.76 1.70 1.69 1.69 1.69 1.68 1.67 1.67 1.67 1.66 1.65 1.65 1.64 1.64 1.51 1.51 1.50 1.49 1.49 1.48 1.48 1.47 1.47 1.47 1.46 1.46 1.45 1.45 1.44 1.43 1.42 1.42 1.41 1.41 1.40 1.39 1.39 1.39 1.38 1.38 1.37 1.36 1.36 1.36 1.35 1.35 1.34 1.34 1.34 1.33 1.33 1.32 1.32 1.31 1.13 1.12 1.11
3.17
3.07
2.09
3.02
6.90
3.00
7.5 7.0 6.5 6.0 5.5 5.0 4.5 4.0 3.5 3.0 2.5 2.0 1.5 1.0 0.5
f1 (ppm)

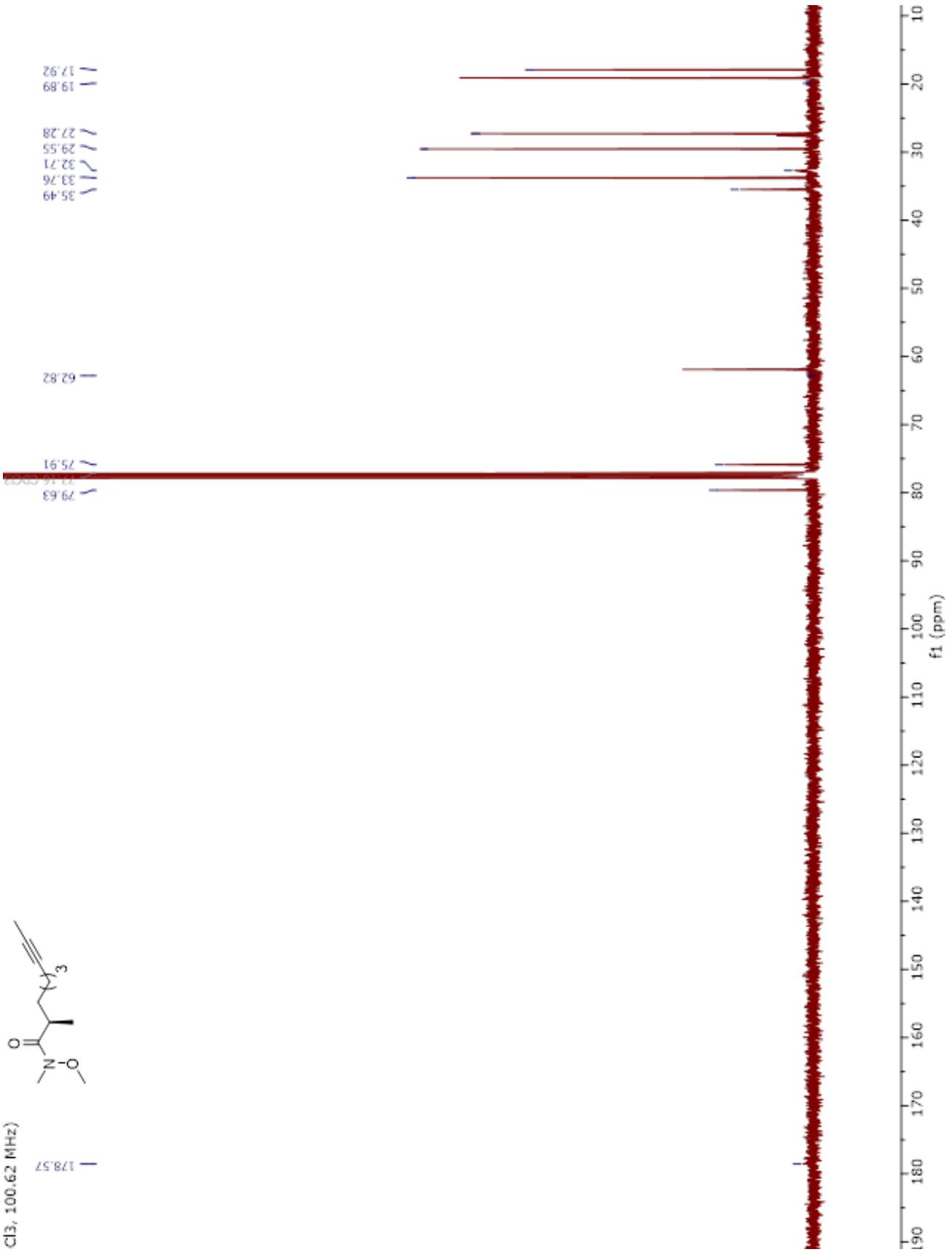
17.92
19.89
27.28
29.55
32.71
33.76
35.49
62.82
75.91
79.63
178.57
CDCl3, 100.62 MHz)
f1 (ppm)

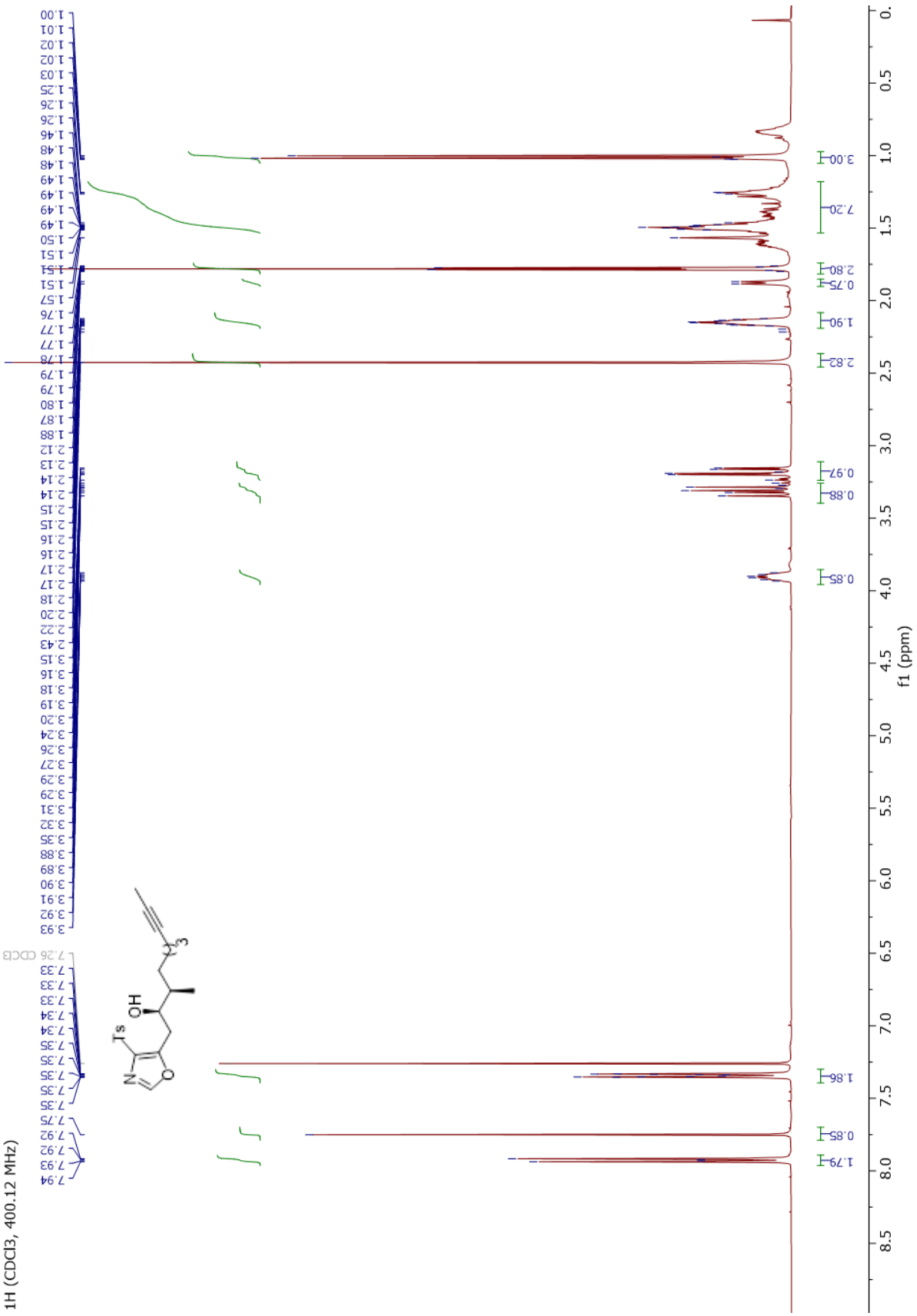
1H (CDCl3, 400.12 MHz)
f1 (ppm)
3.00
7.20
2.80
0.75
1.90
2.82
0.97
0.88
0.85
1.86
0.85
1.79

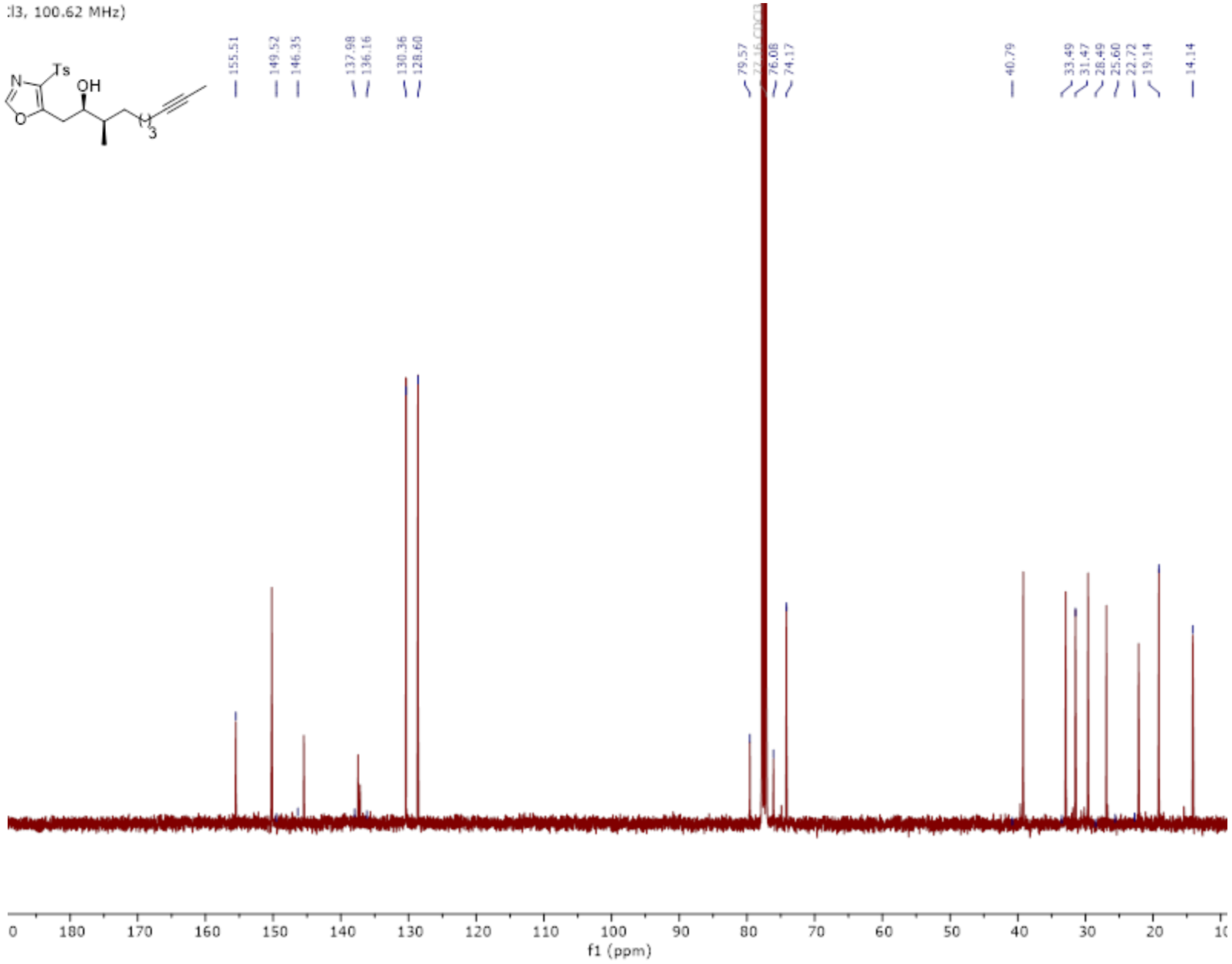
:l3, 100.62 MHz)
Ts
N
OH
O
3
155.51
149.52
146.35
137.98
136.16
130.36
128.60
79.57
77.16 CDCl3
76.08
74.17
40.79
33.49
31.47
28.49
25.60
22.72
19.14
14.14
0
180
170
160
150
140
130
120
110
100
90
80
70
60
50
40
30
20
10
f1 (ppm)

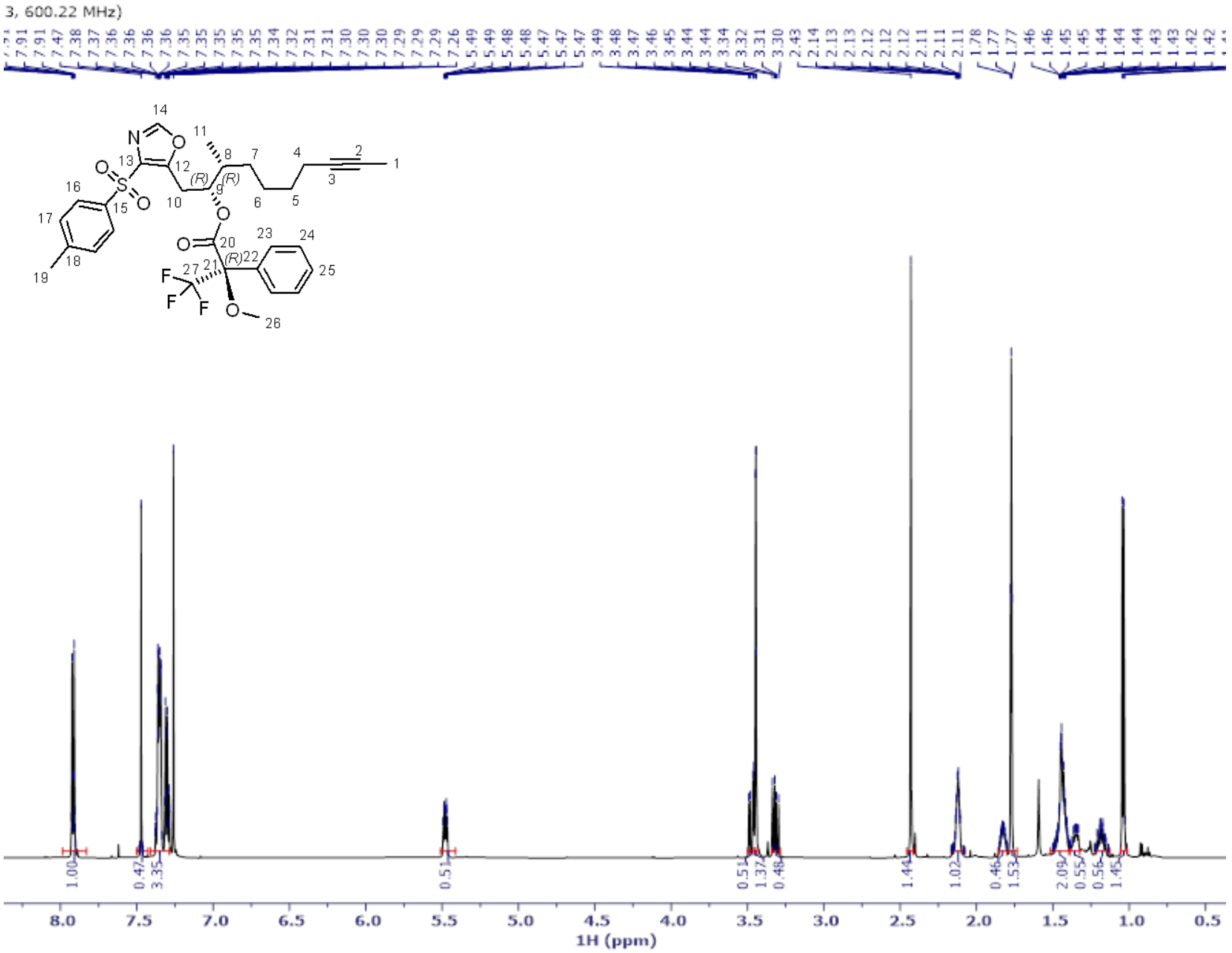
3, 600.22 MHz)
1H (ppm)

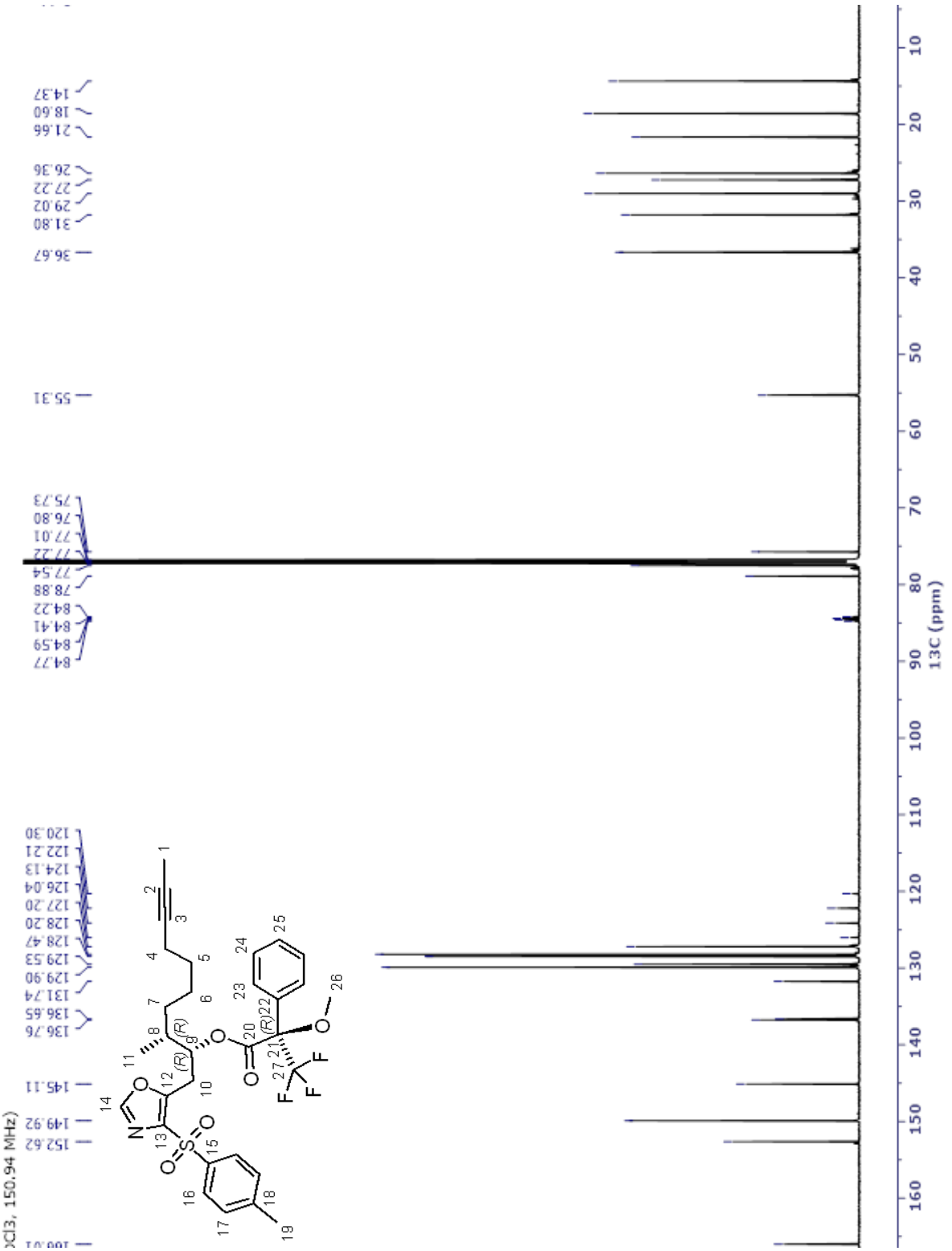
13C (ppm)
CDCl3, 150.94 MHz)

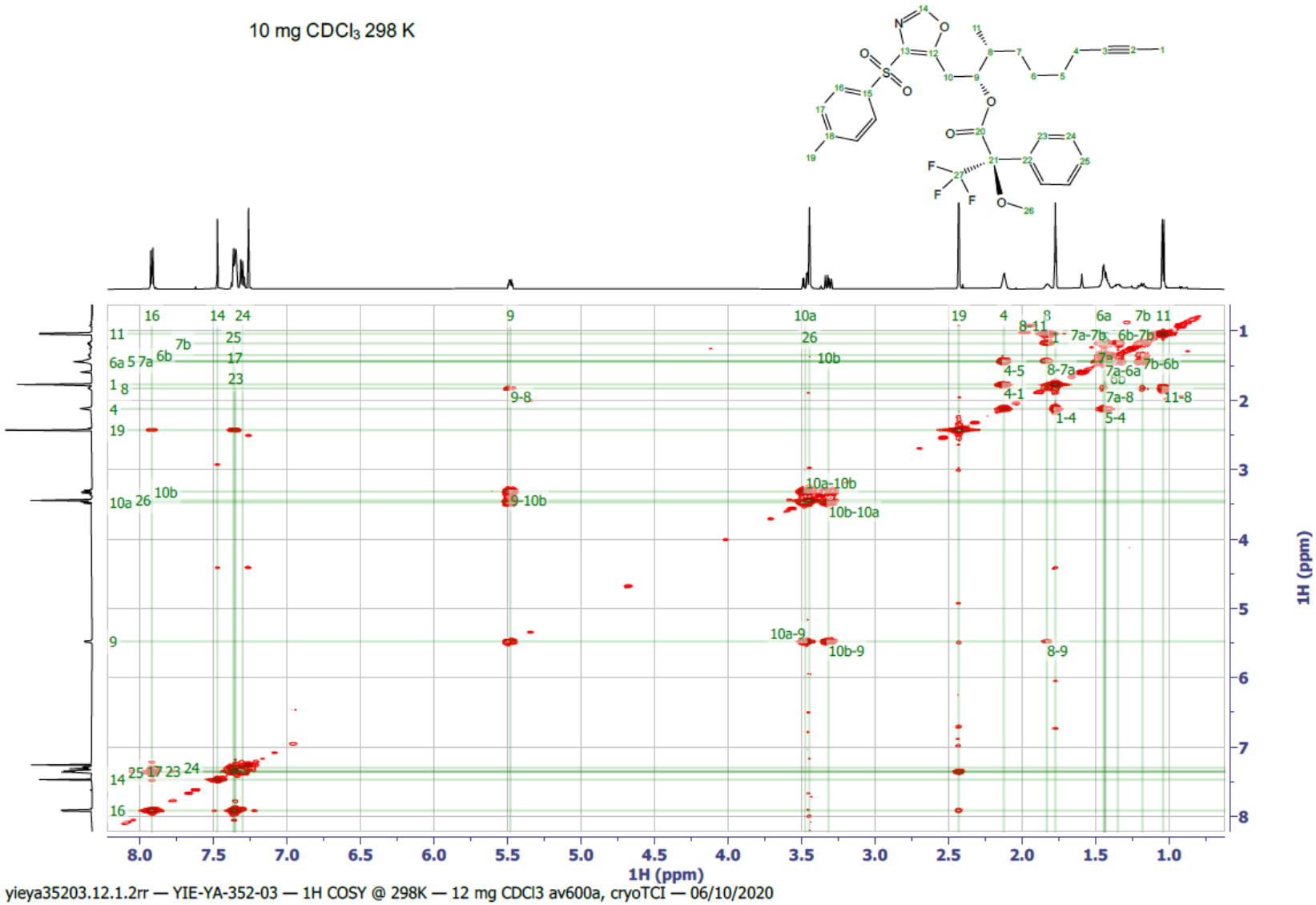
10 mg CDCl3 298 K
1H (ppm)
1H (ppm)
yieya35203.12.1.2rr — YIE-YA-352-03 — 1H COSY @ 298K — 12 mg CDCl3 av600a, cryoTCI — 06/10/2020

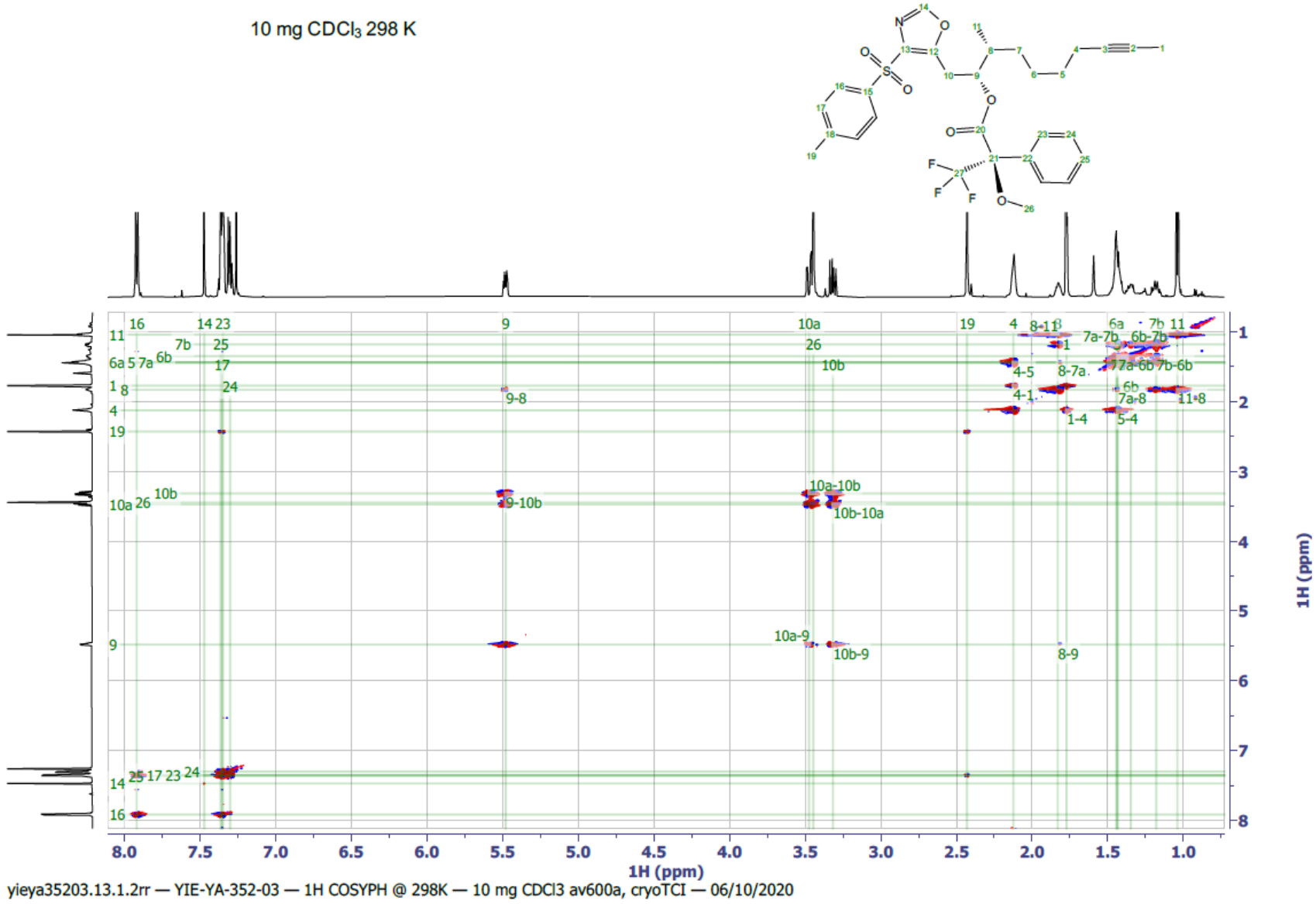
10 mg CDCl3 298 K
1H (ppm)
1H (ppm)
yieya35203.13.1.2rr — YIE-YA-352-03 — 1H COSYPH @ 298K — 10 mg CDCl3 av600a, cryoTCI — 06/10/2020

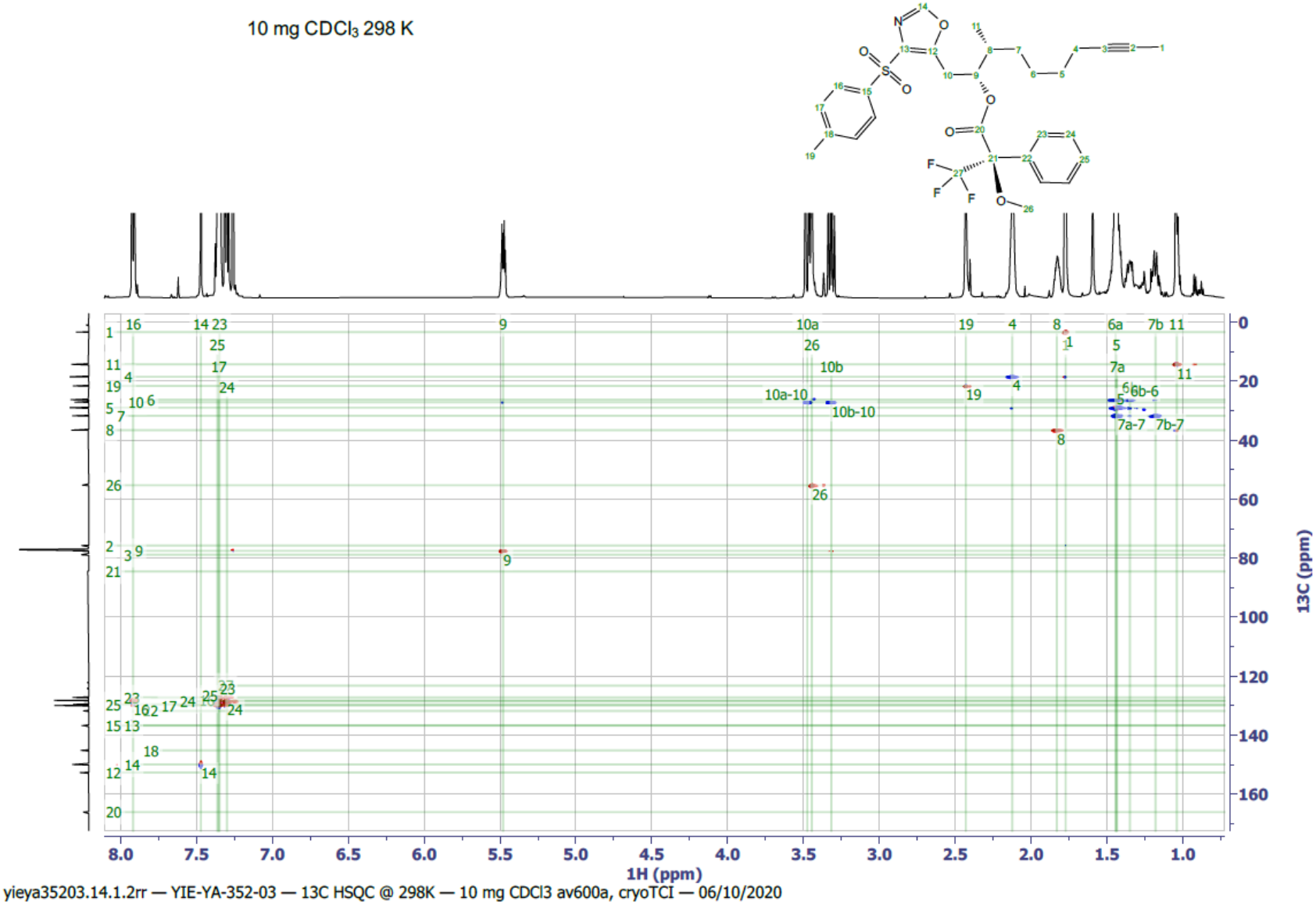
10 mg CDCl3 298 K
1H (ppm)
13C (ppm)
yieya35203.14.1.2rr — YIE-YA-352-03 — 13C HSQC @ 298K — 10 mg CDCl3 av600a, cryoTCI — 06/10/2020

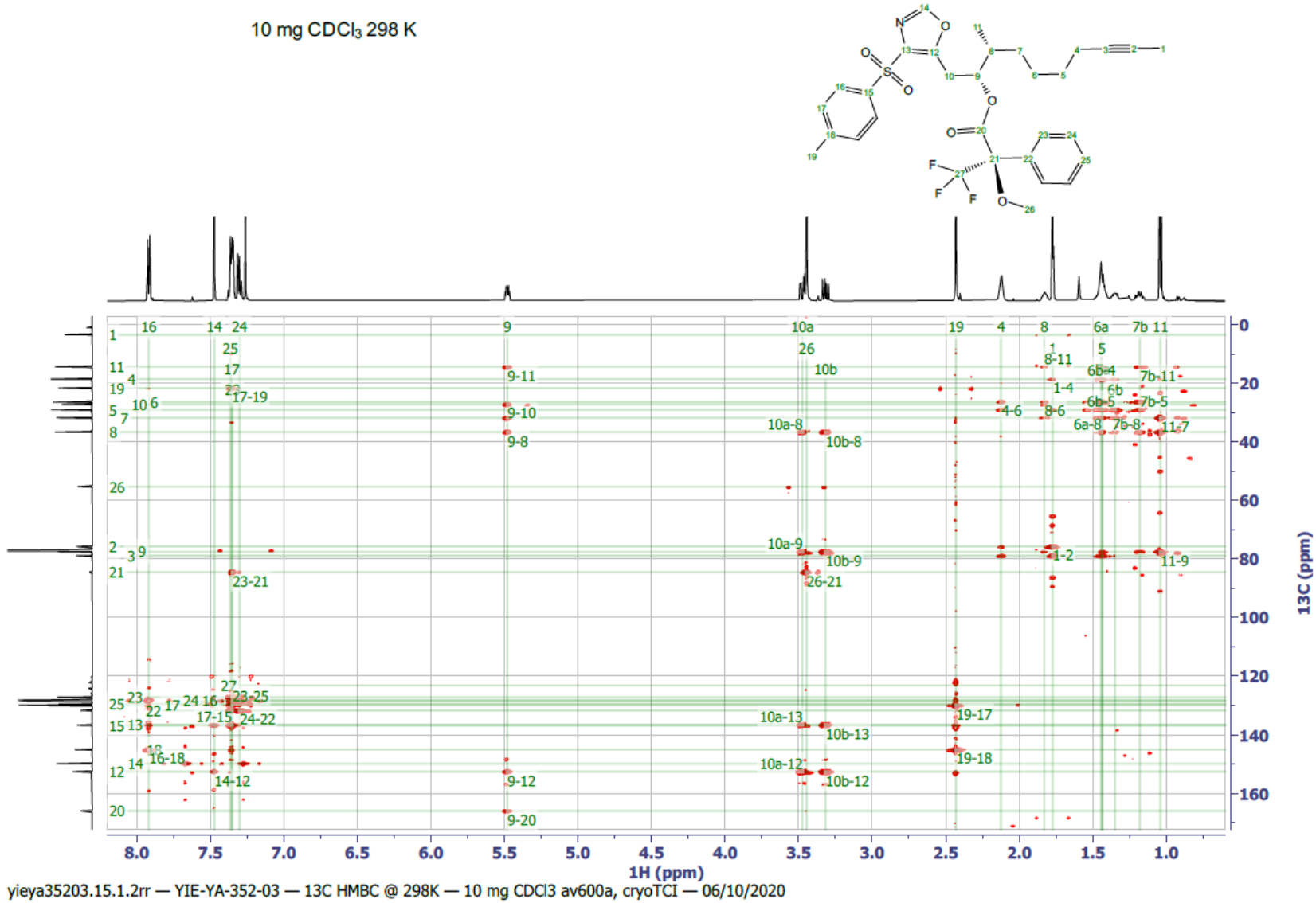
10 mg CDCl3 298 K
1H (ppm)
13C (ppm)
yieya35203.15.1.2rr — YIE-YA-352-03 — 13C HMBC @ 298K — 10 mg CDCl3 av600a, cryoTCI — 06/10/2020

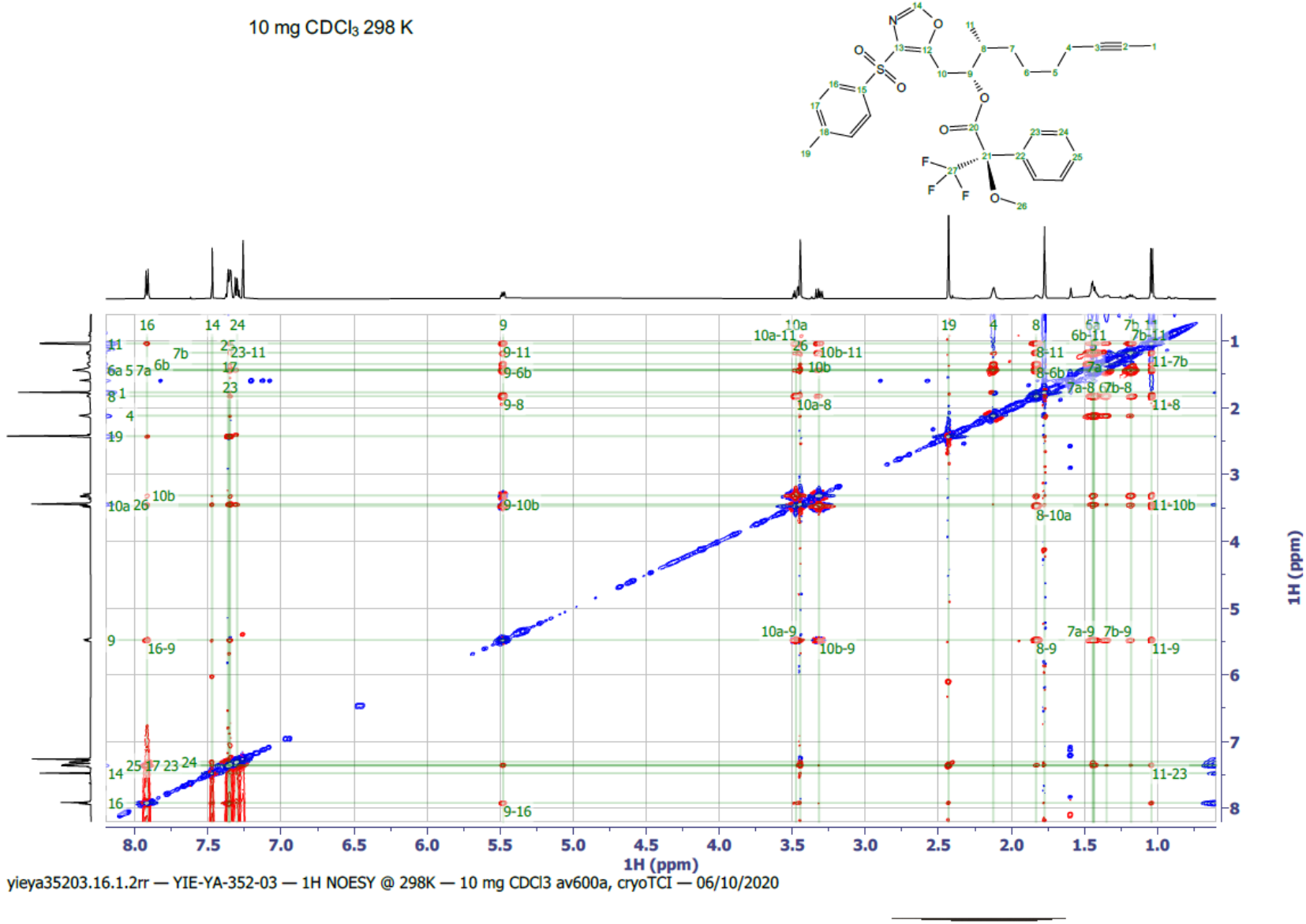
10 mg CDCl3 298 K
1H (ppm)
yieya35203.16.1.2rr — YIE-YA-352-03 — 1H NOESY @ 298K — 10 mg CDCl3 av600a, cryoTCI — 06/10/2020

10 mg $CDCl_3$ 298 K

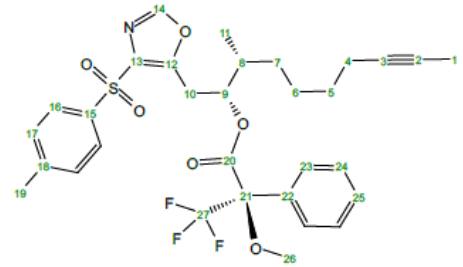

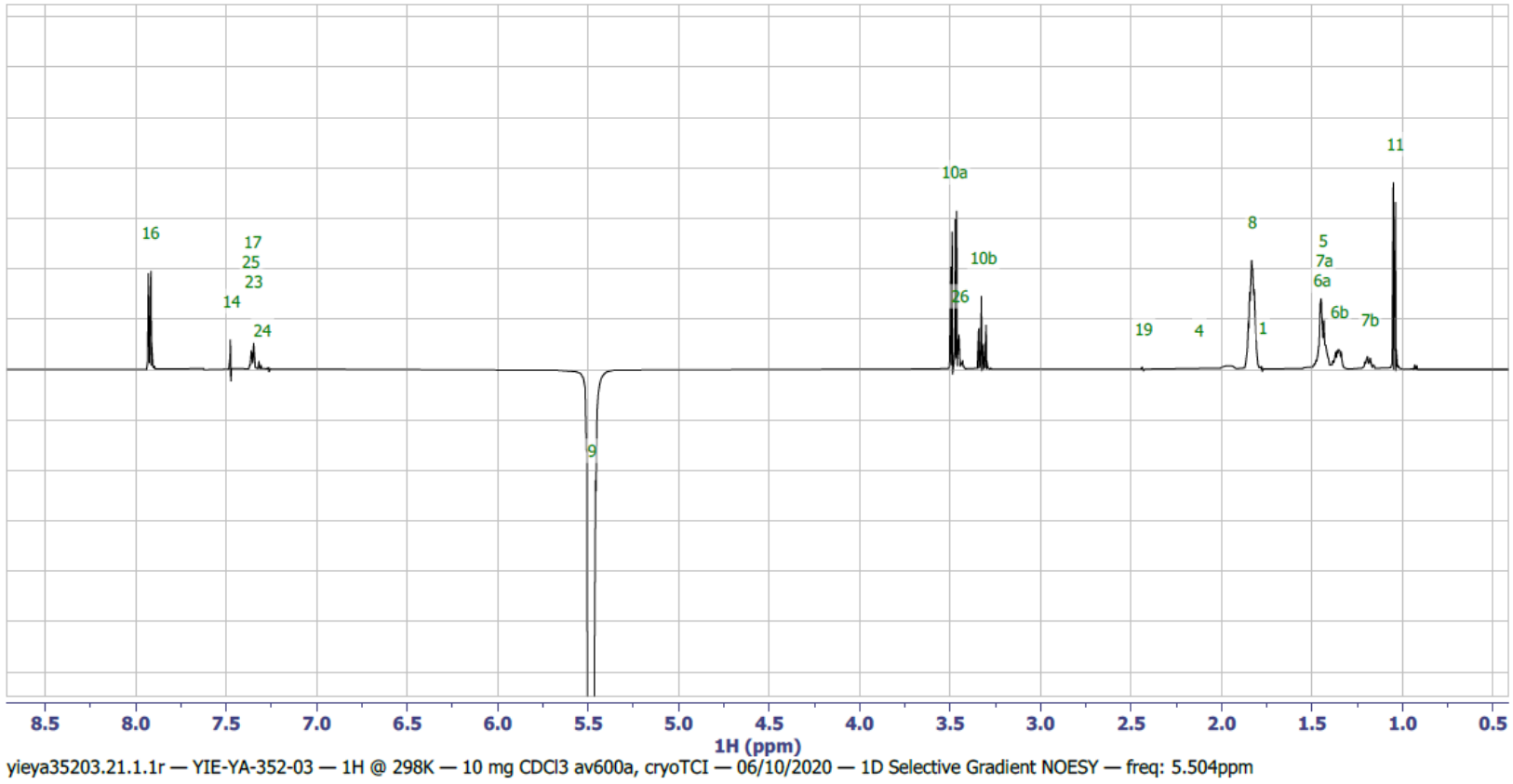

yieya35203.21.1.1r — YIE-YA-352-03 — 1H @ 298K — 10 mg CDCl3 av600a, cryoTCI — 06/10/2020 — 1D Selective Gradient NOESY — freq: 5.504ppm

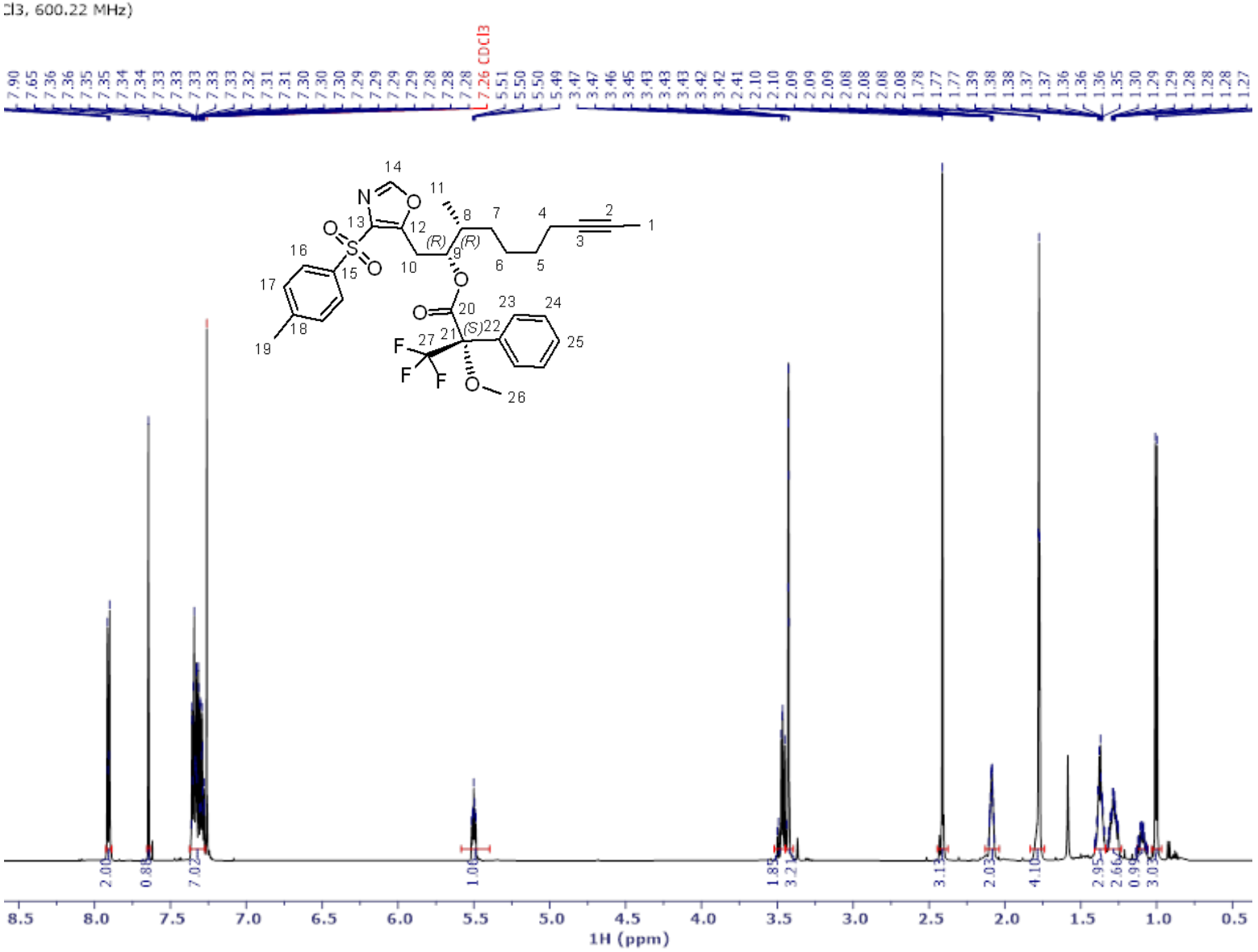
CDCl3
1H (ppm)

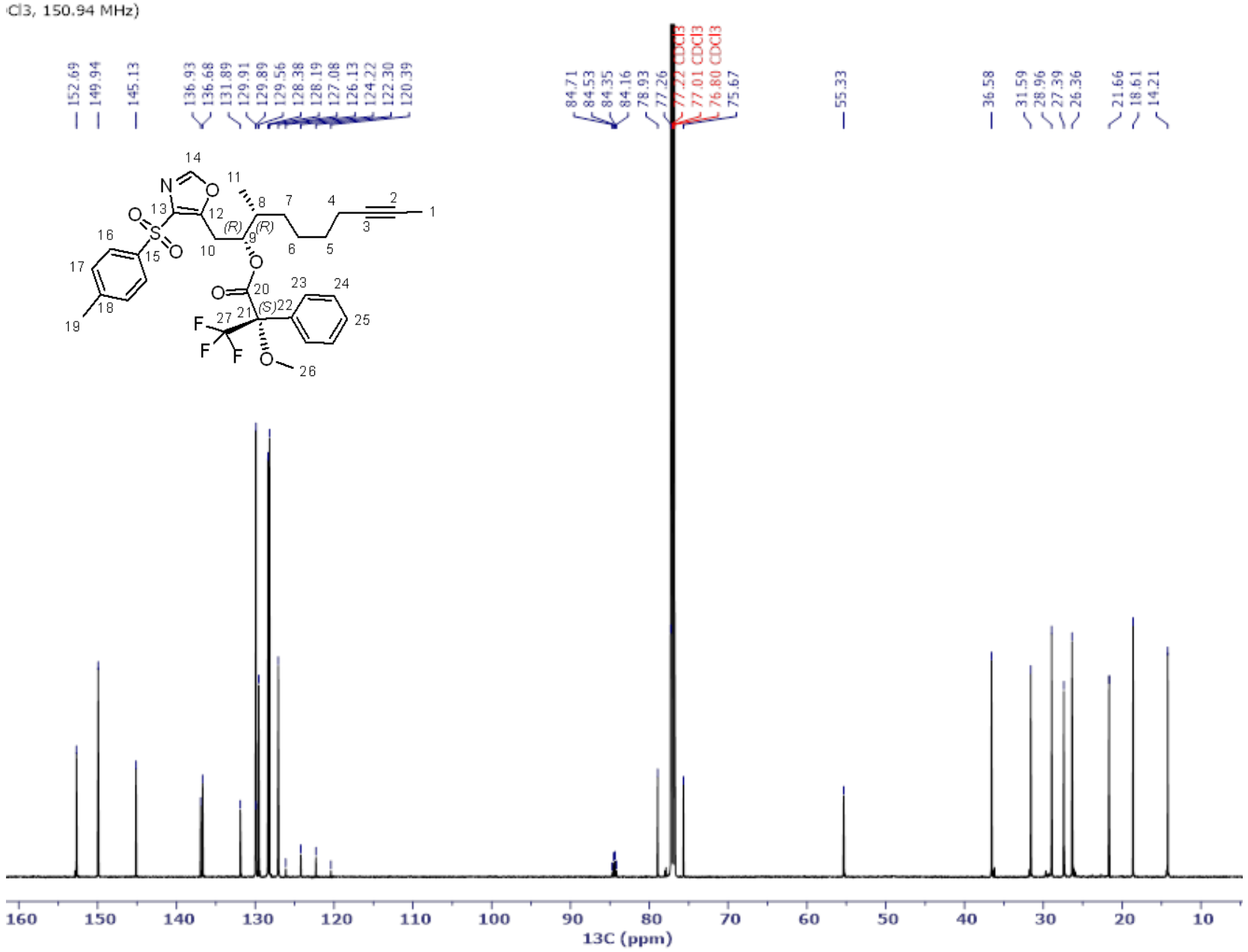
Cl3, 150.94 MHz)
152.69
149.94
145.13
136.93
136.68
131.89
129.91
129.89
129.56
128.38
128.19
127.08
126.13
124.22
122.30
120.39
84.71
84.53
84.35
84.16
78.93
77.26
77.22 CDCl3
77.01 CDCl3
76.80 CDCl3
75.67
55.33
36.58
31.59
28.96
27.39
26.36
21.66
18.61
14.21
13C (ppm)

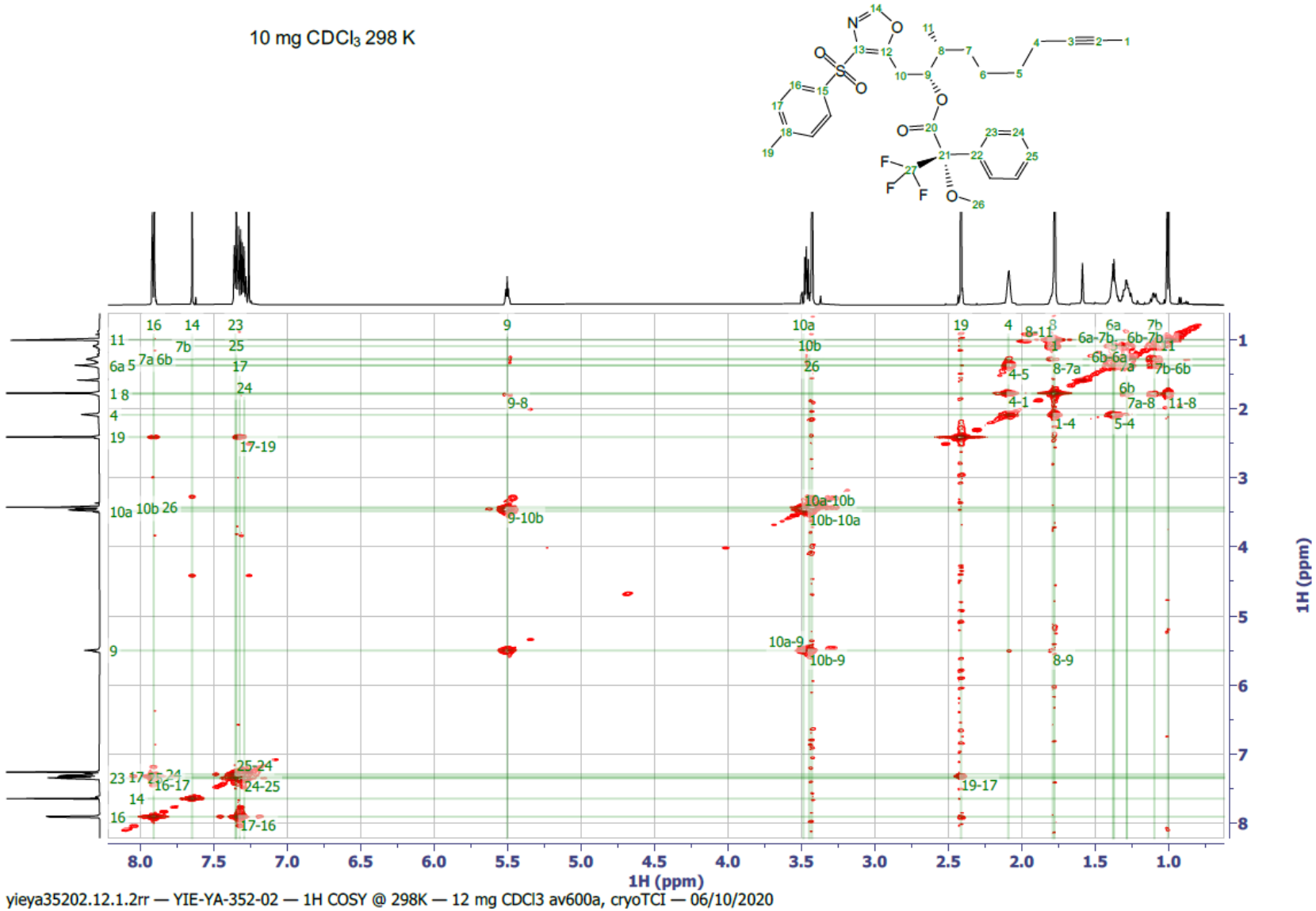
10 mg CDCl3 298 K
1H (ppm)
yieya35202.12.1.2rr — YIE-YA-352-02 — 1H COSY @ 298K — 12 mg CDCl3 av600a, cryoTCI — 06/10/2020

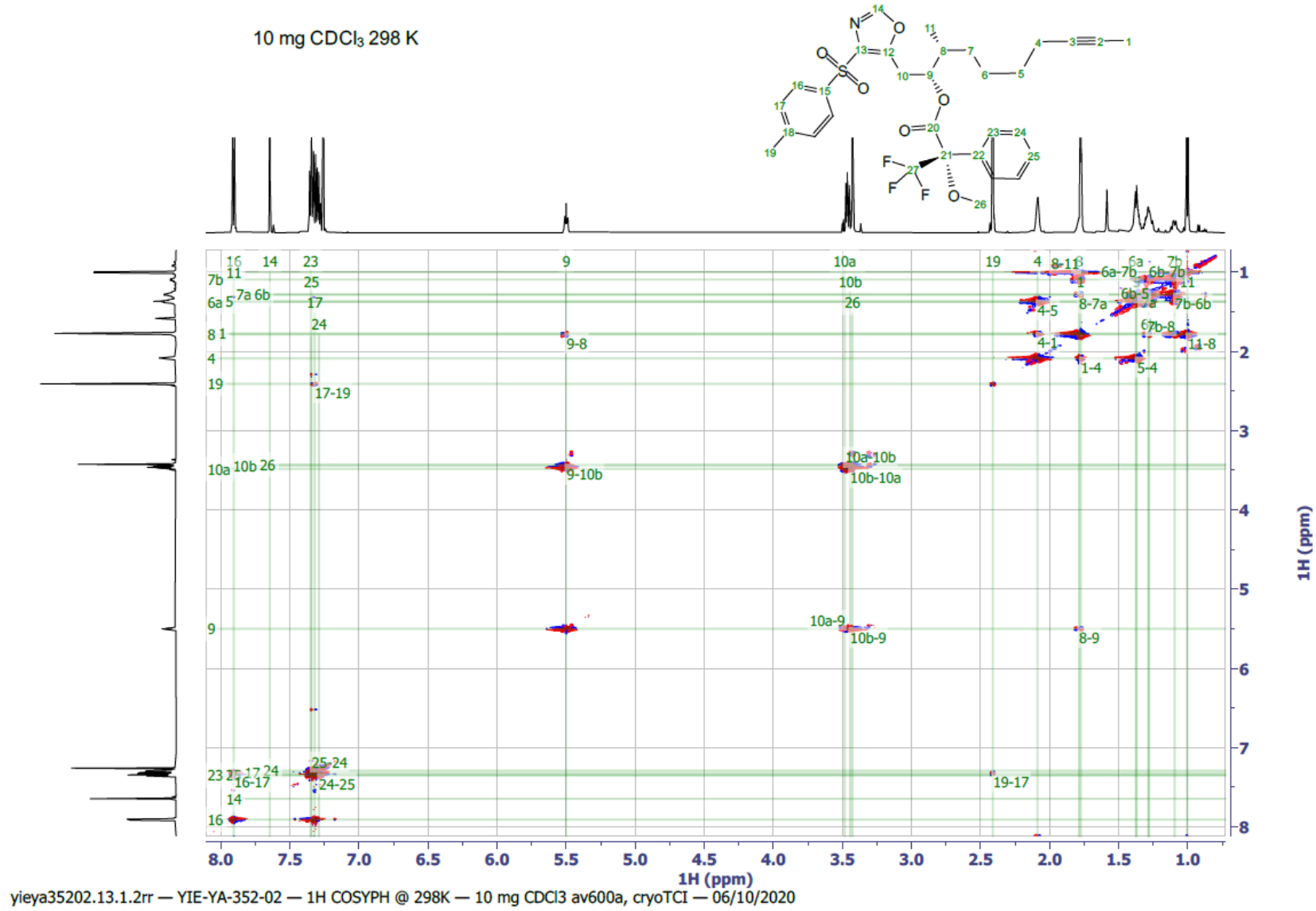
10 mg CDCl3 298 K
1H (ppm)
yieya35202.13.1.2rr — YIE-YA-352-02 — 1H COSYPH @ 298K — 10 mg CDCl3 av600a, cryoTCI — 06/10/2020

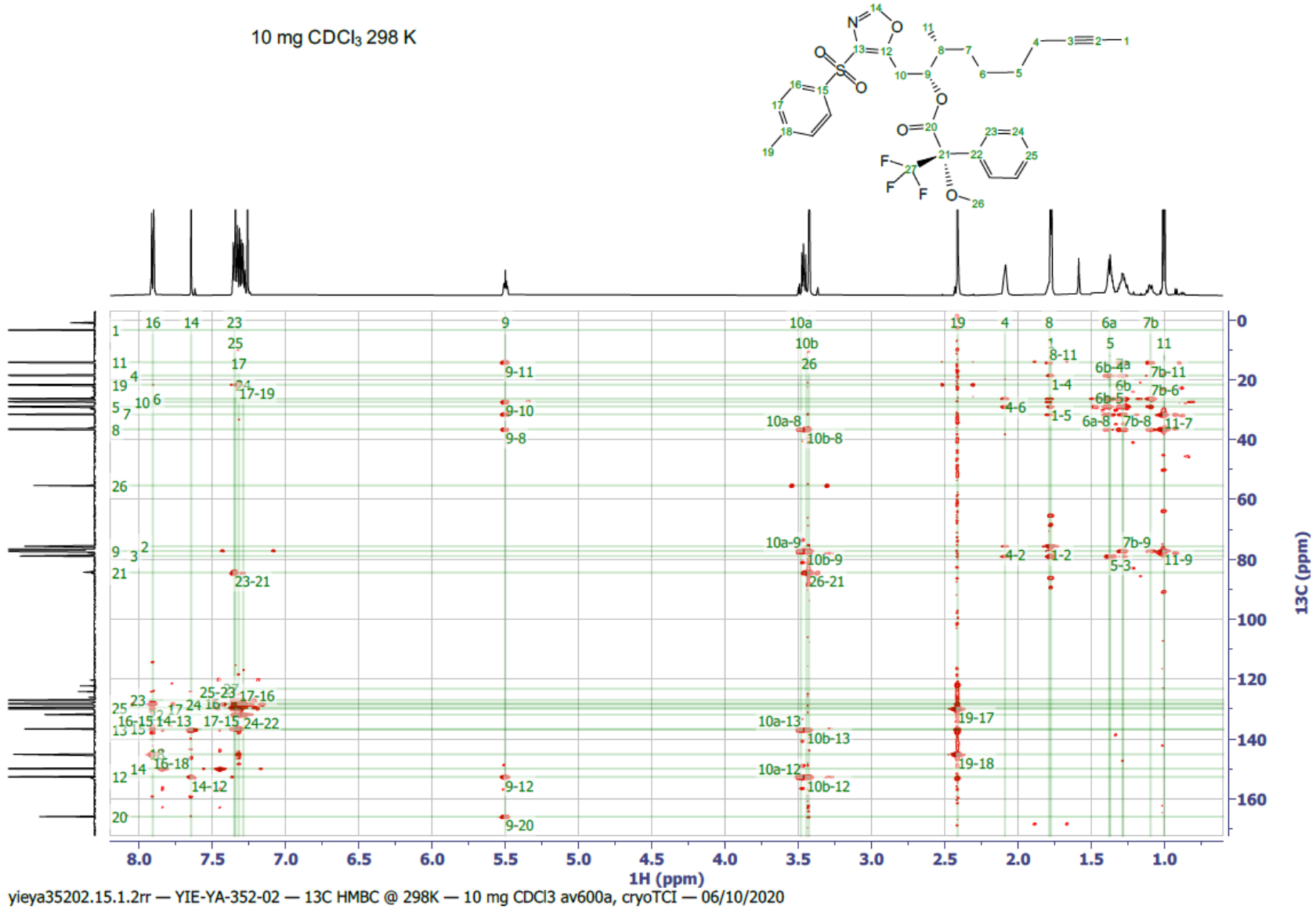
10 mg CDCl3 298 K
1H (ppm)
13C (ppm)
yieya35202.15.1.2rr — YIE-YA-352-02 — 13C HMBC @ 298K — 10 mg CDCl3 av600a, cryoTCI — 06/10/2020

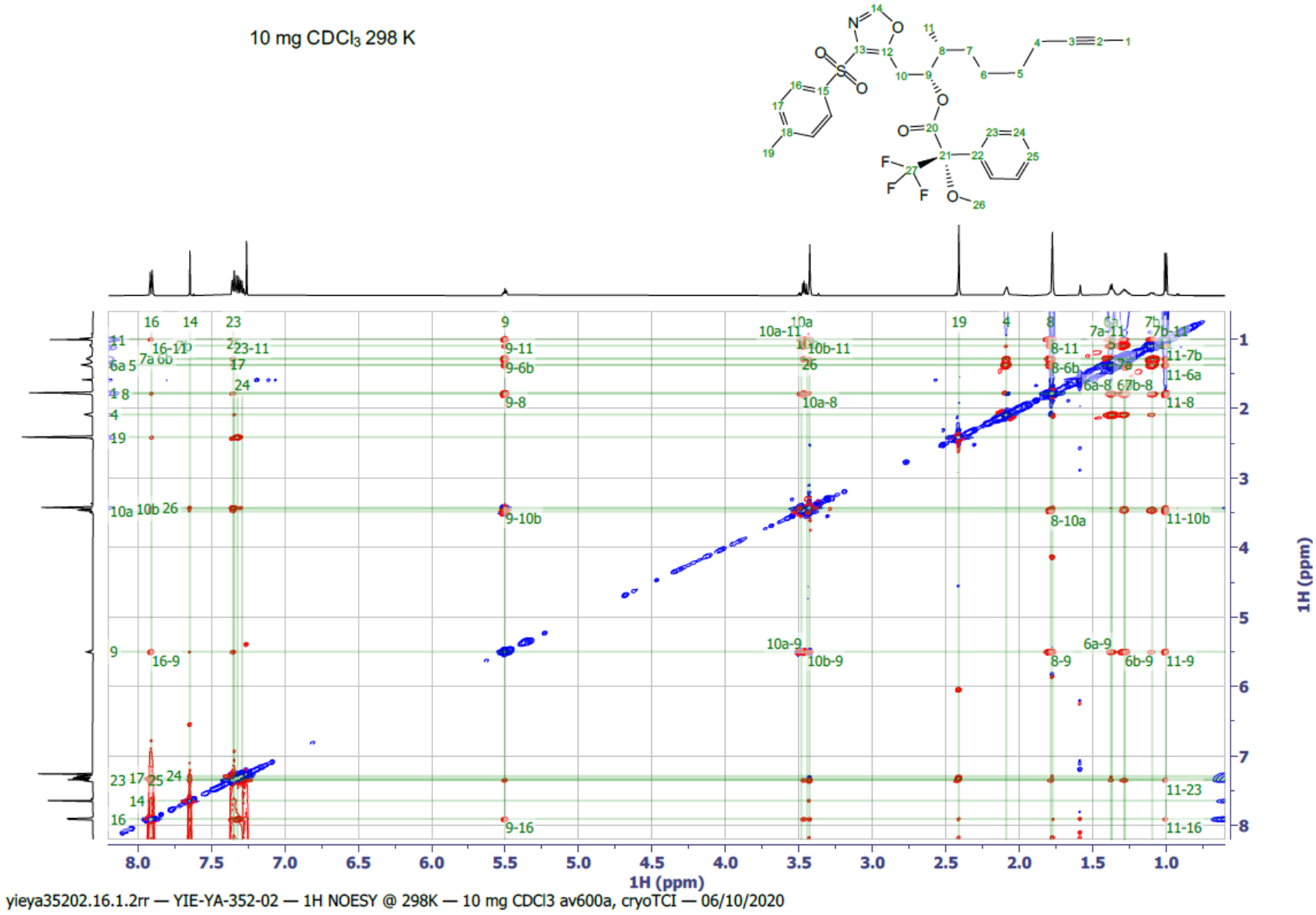
10 mg CDCl3 298 K
1H (ppm)
1H (ppm)
yieya35202.16.1.2rr — YIE-YA-352-02 — 1H NOESY @ 298K — 10 mg CDCl3 av600a, cryoTCI — 06/10/2020

10 mg $CDCl_3$ 298 K

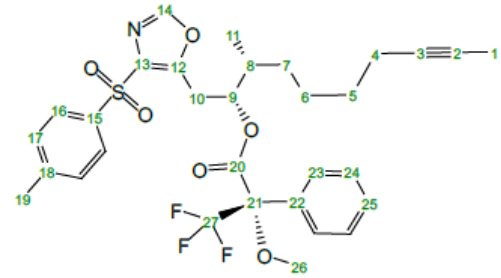

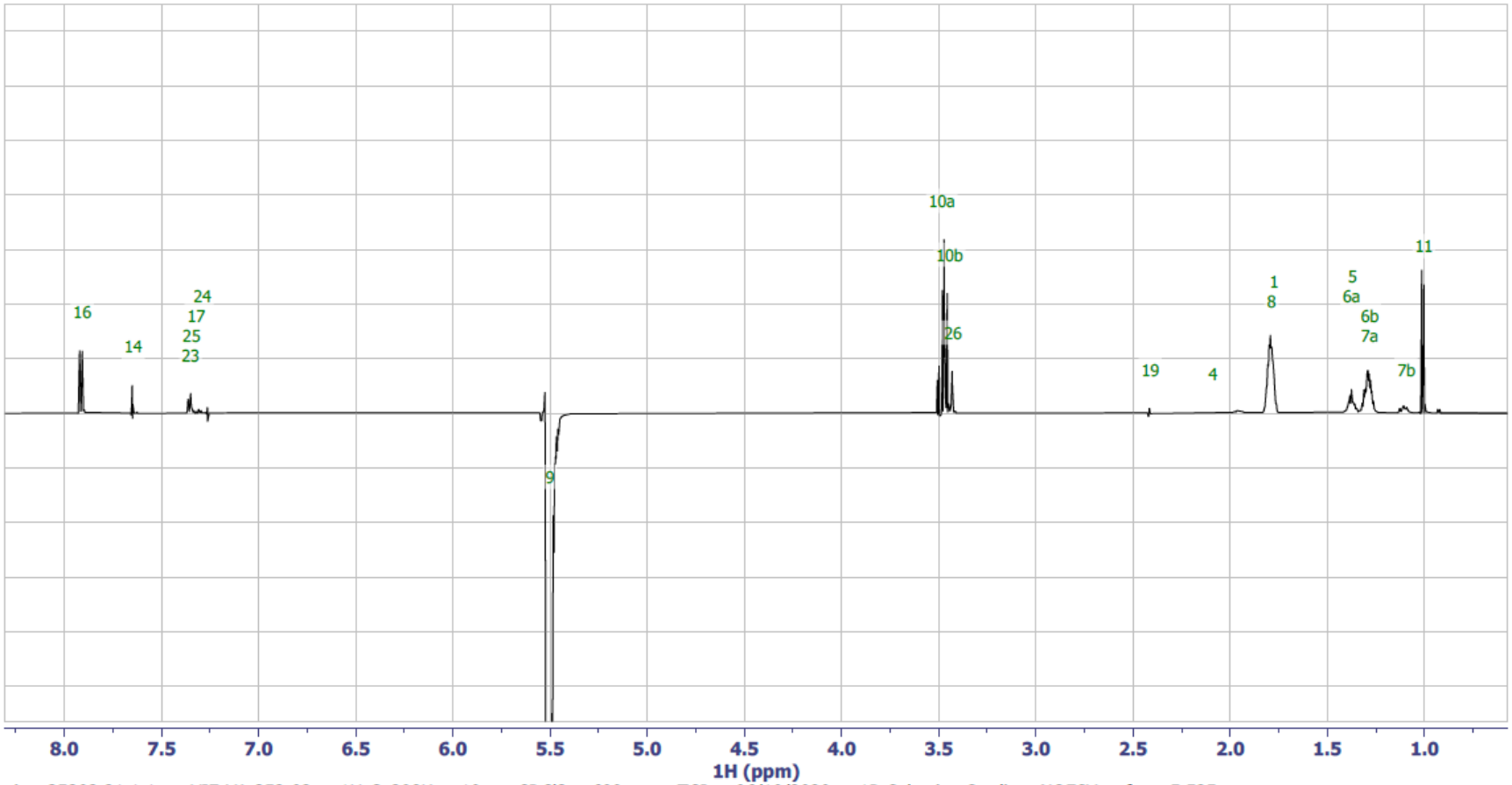

yieya35202.21.1.1r — YIE-YA-352-02 — 1H @ 298K — 10 mg CDCl3 av600a, cryoTCI — 06/10/2020 — 1D Selective Gradient NOESY — freq: 5.525ppm

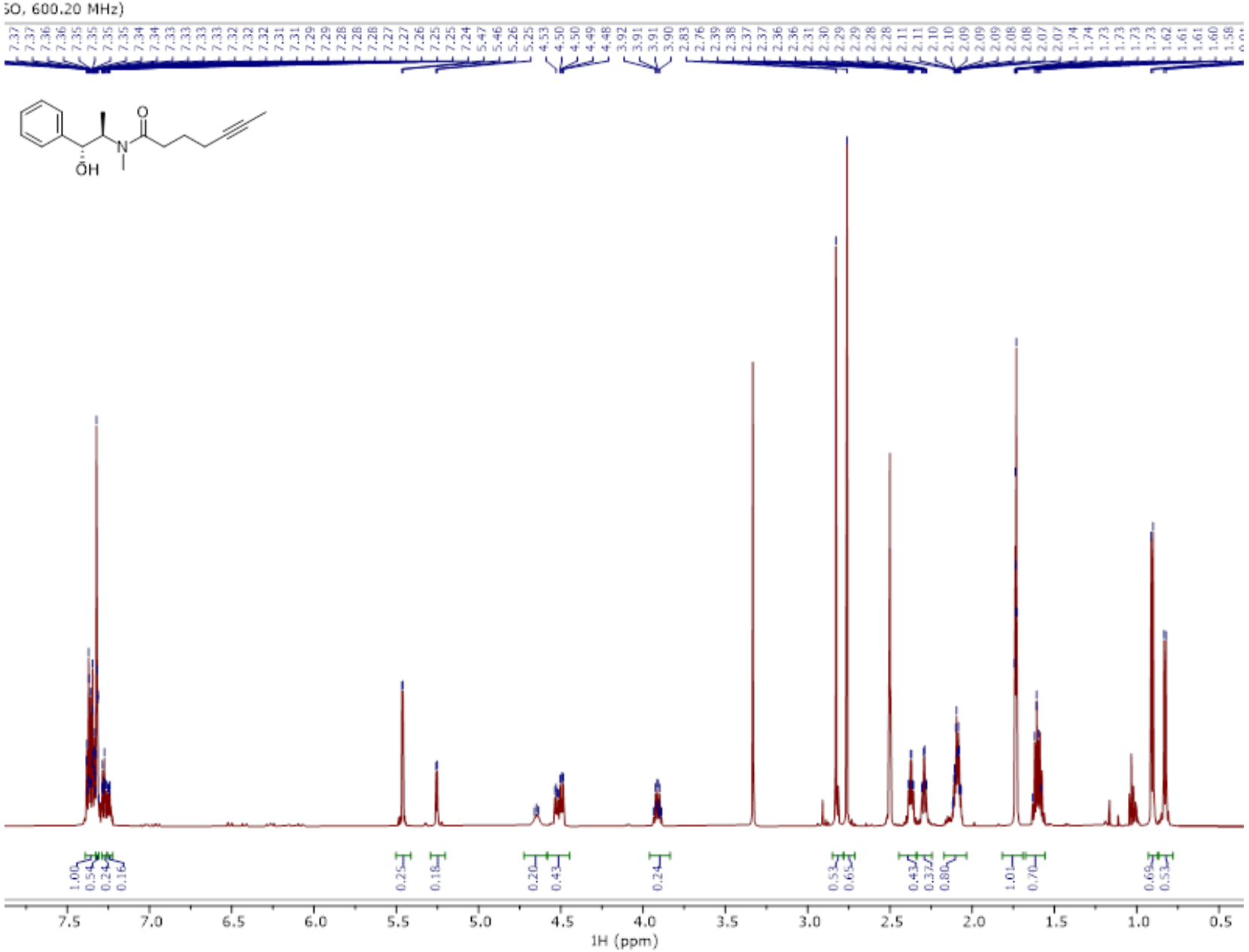
SO, 600.20 MHz)
OH
N
O
1H (ppm)

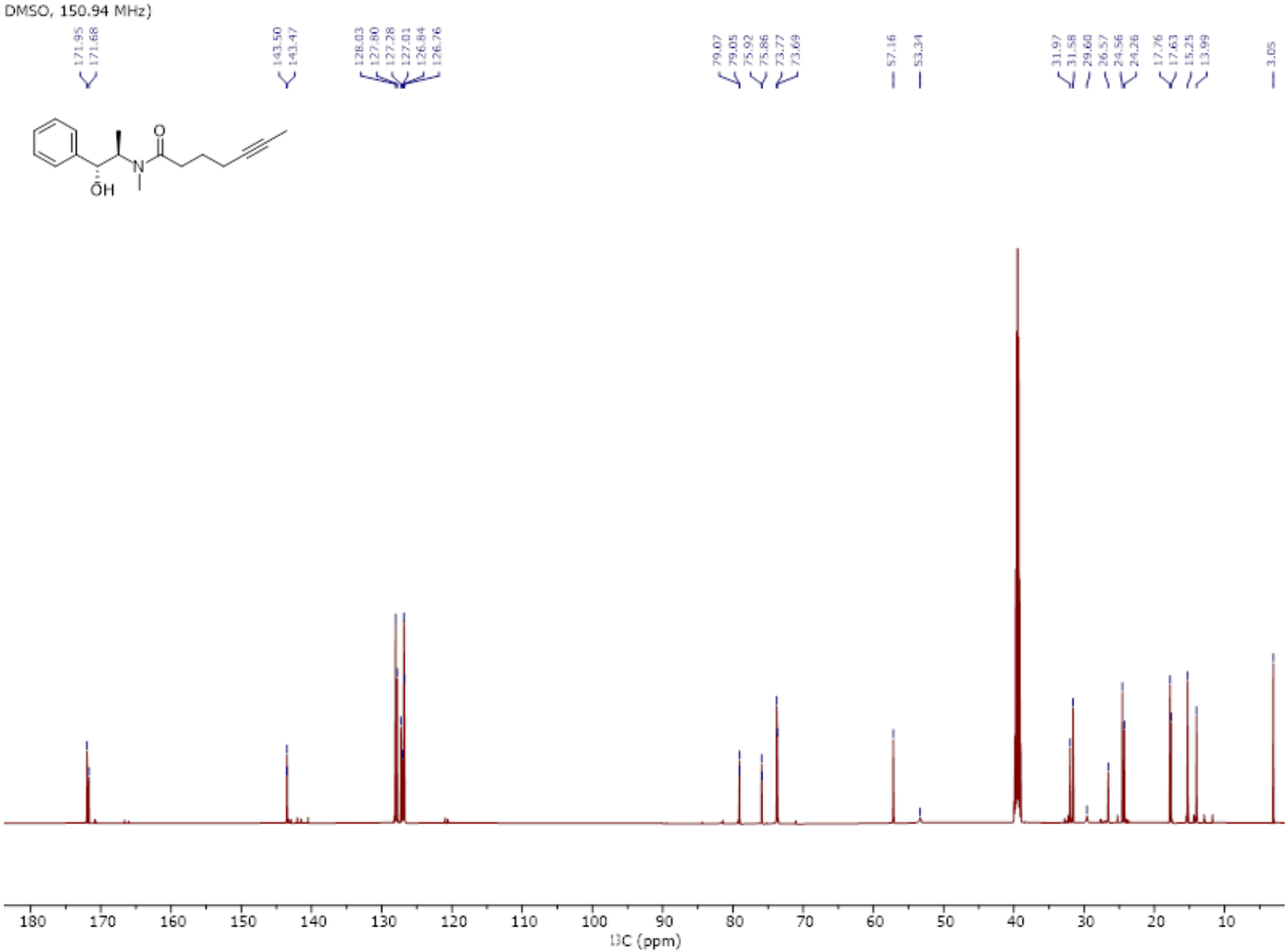
DMSO, 150.94 MHz)
171.95
171.68
143.50
143.47
128.03
127.80
127.28
127.01
126.84
126.76
79.07
79.05
75.92
75.86
73.77
73.69
57.16
53.34
31.97
31.58
29.60
26.57
24.56
24.26
17.76
17.63
15.25
13.99
3.05
O
N
OH
180
170
160
150
140
130
120
110
100
90
80
70
60
50
40
30
20
10
13C (ppm)

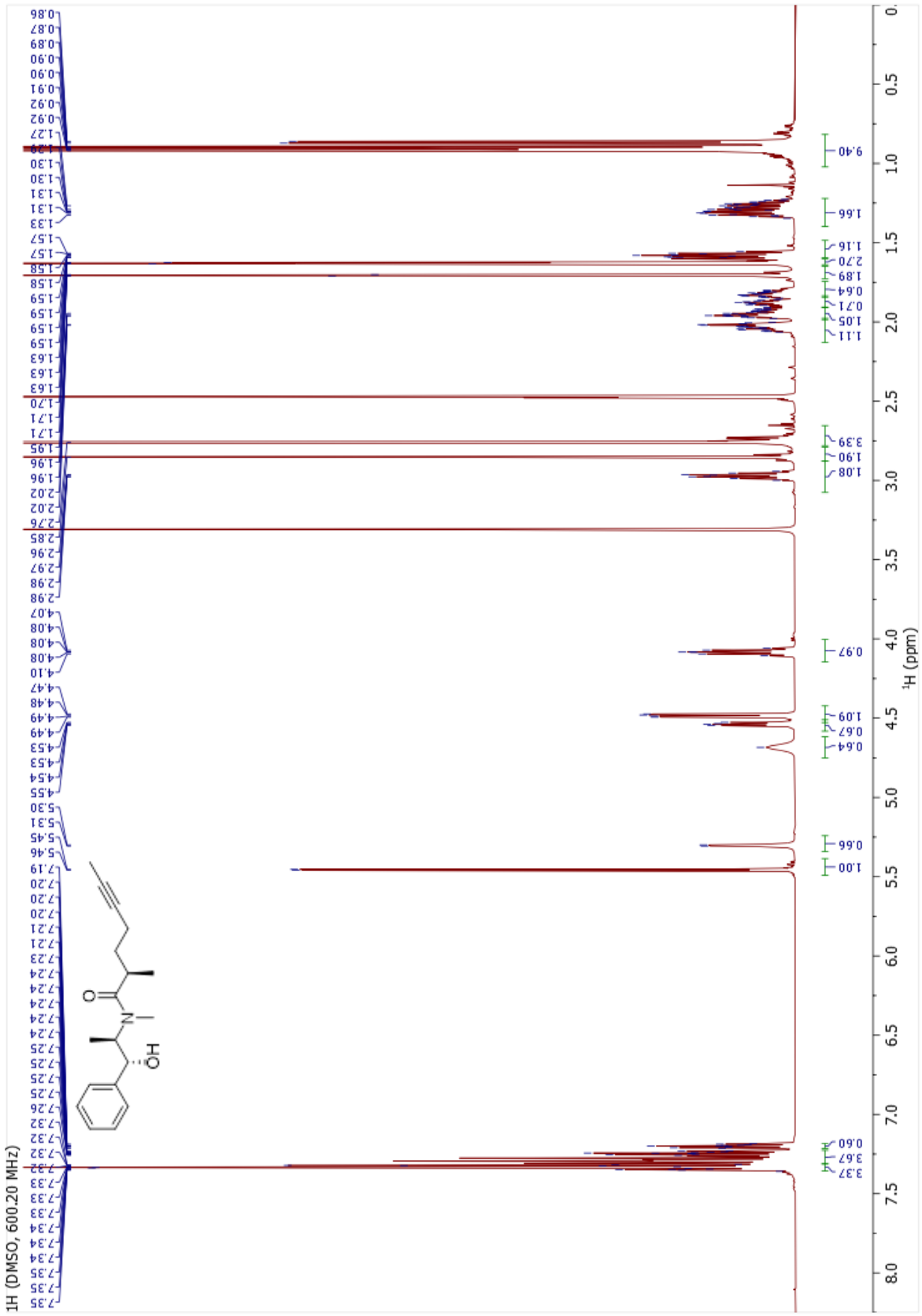
1H (DMSO, 600.20 MHz)
¹H (ppm)
OH
N
O

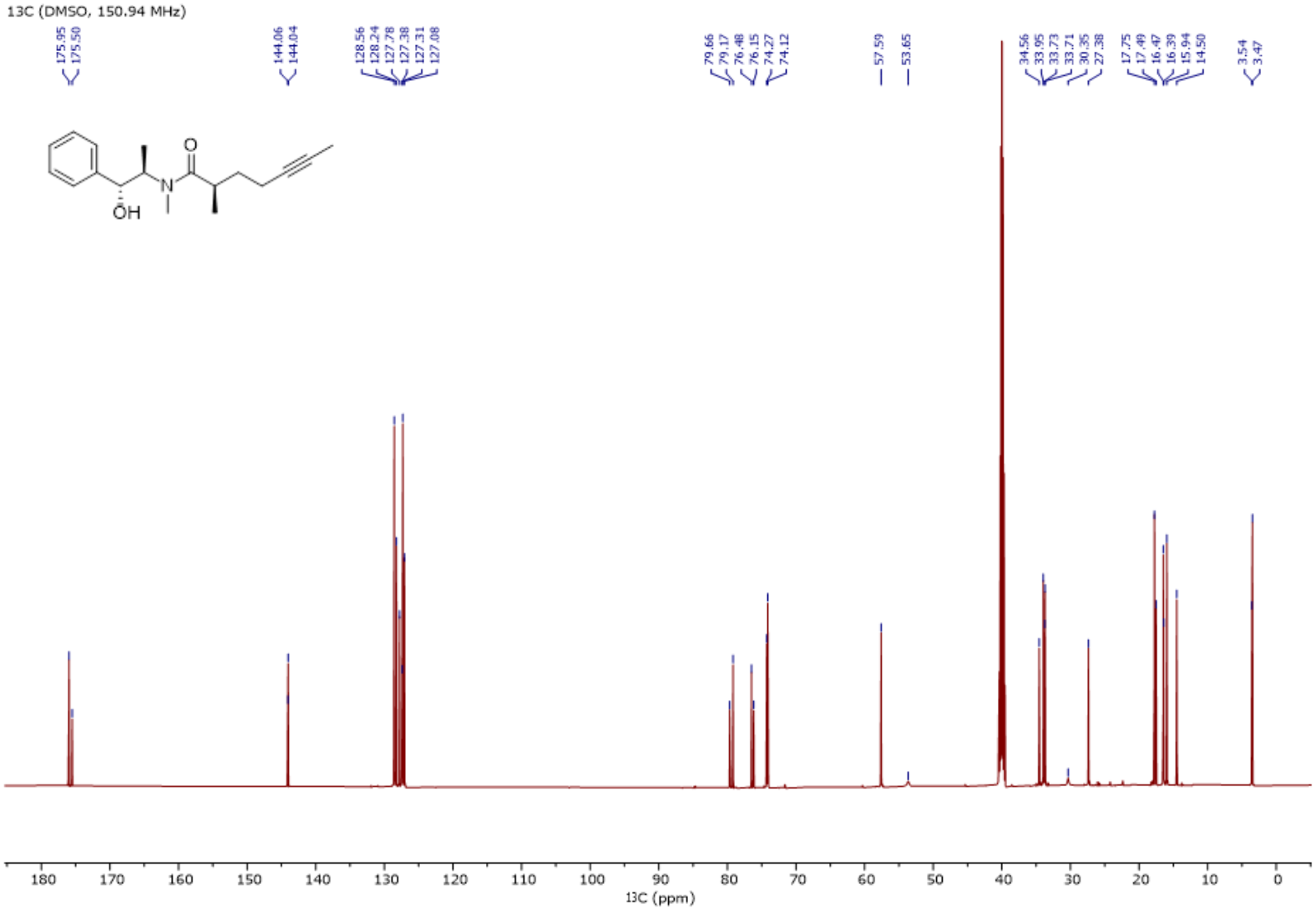
13C (DMSO, 150.94 MHz)
175.95
175.50
144.06
144.04
128.56
128.24
127.78
127.38
127.31
127.08
79.66
79.17
76.48
76.15
74.27
74.12
57.59
53.65
34.56
33.95
33.73
33.71
30.35
27.38
17.75
17.49
16.47
16.39
15.94
14.50
3.54
3.47
OH
O
N
180
170
160
150
140
130
120
110
100
90
80
70
60
50
40
30
20
10
0
13C (ppm)

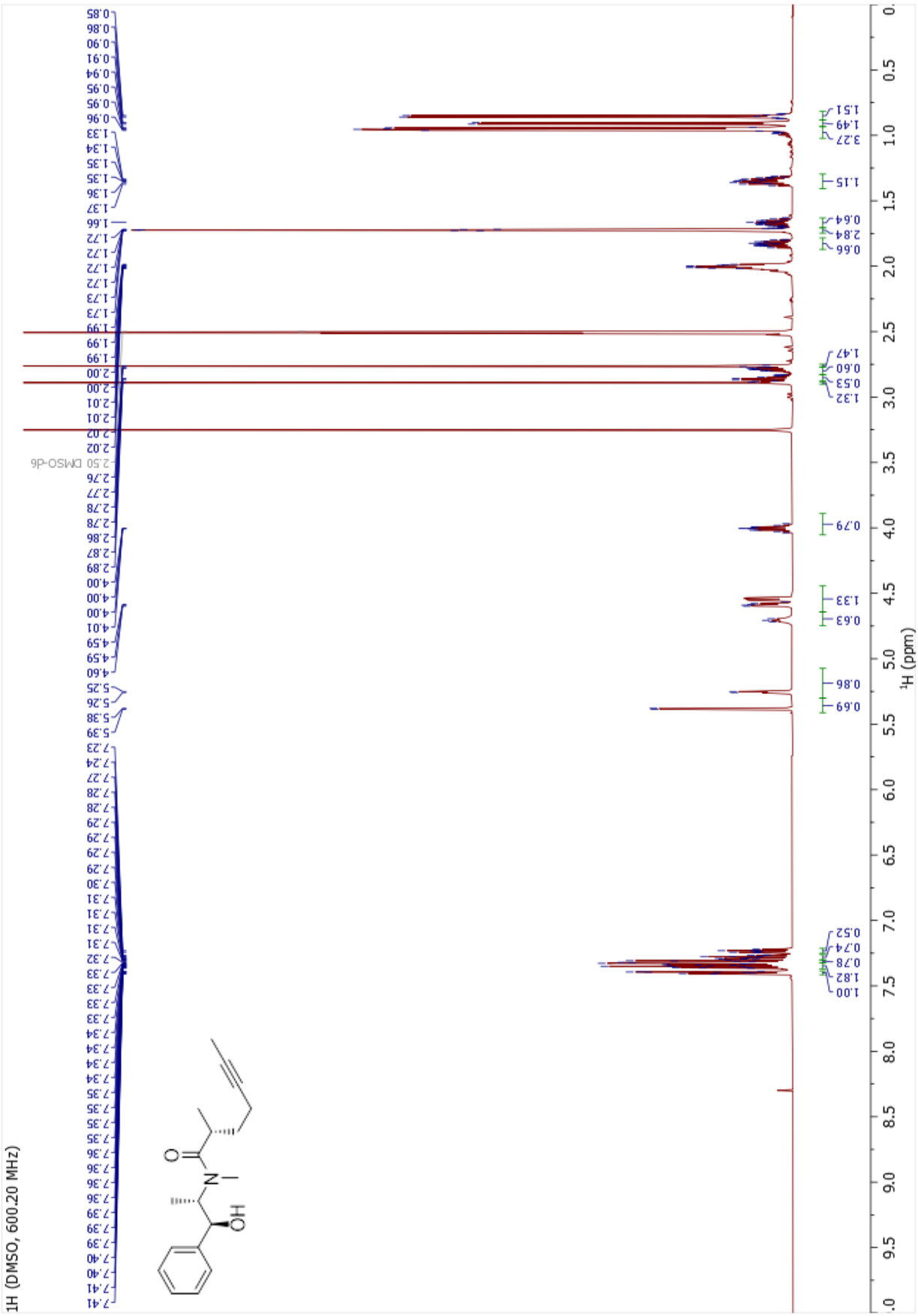
1H (DMSO, 600.20 MHz)
DMSO-d6
1H (ppm)

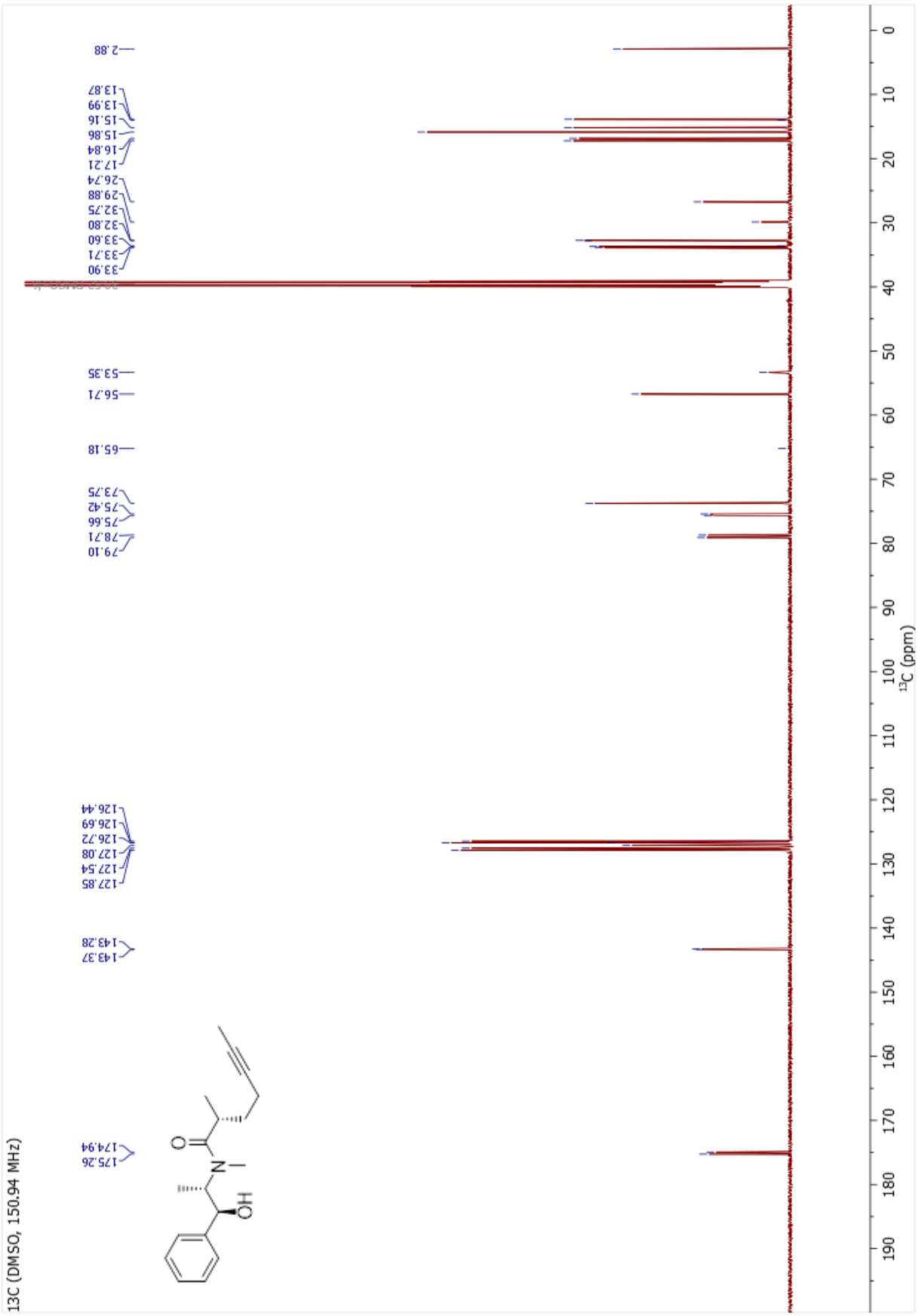
13C (DMSO, 150.94 MHz)
2.88
13.87
13.99
15.16
15.86
16.84
17.21
26.74
29.88
32.75
32.80
33.60
33.71
33.90
53.35
56.71
65.18
73.75
75.42
75.66
78.71
79.10
126.44
126.69
126.72
127.08
127.54
127.85
143.28
143.37
174.94
175.26
OH
N
O
^{13}C (ppm)

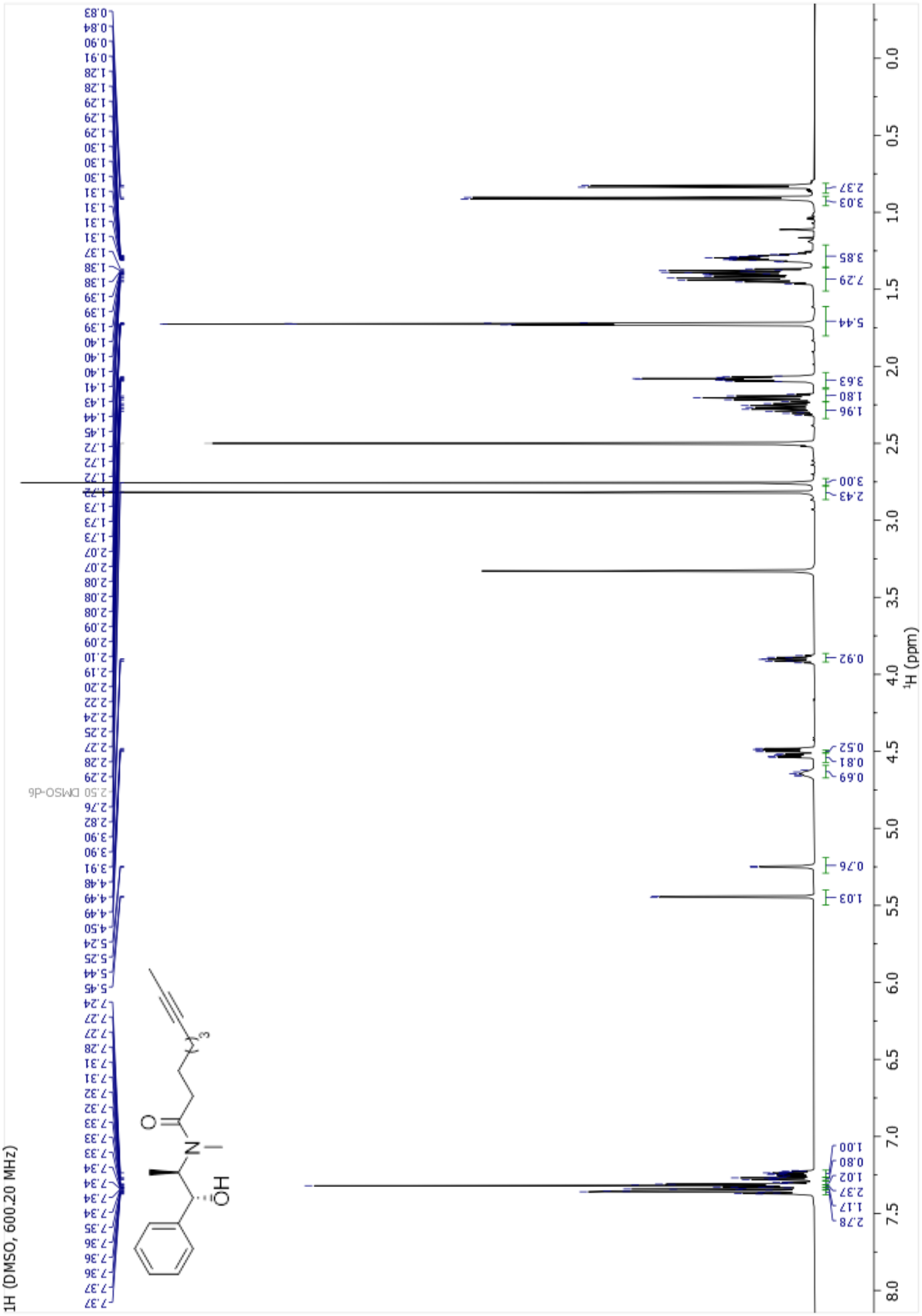
1H (DMSO, 600.20 MHz)
DMSO-d6
OH
N
O
3
2.78
1.17
2.37
1.02
0.80
1.00
0.76
1.03
0.92
0.52
0.81
0.69
3.00
2.43
1.96
1.80
3.63
5.44
7.29
3.85
3.03
2.37
1H (ppm)

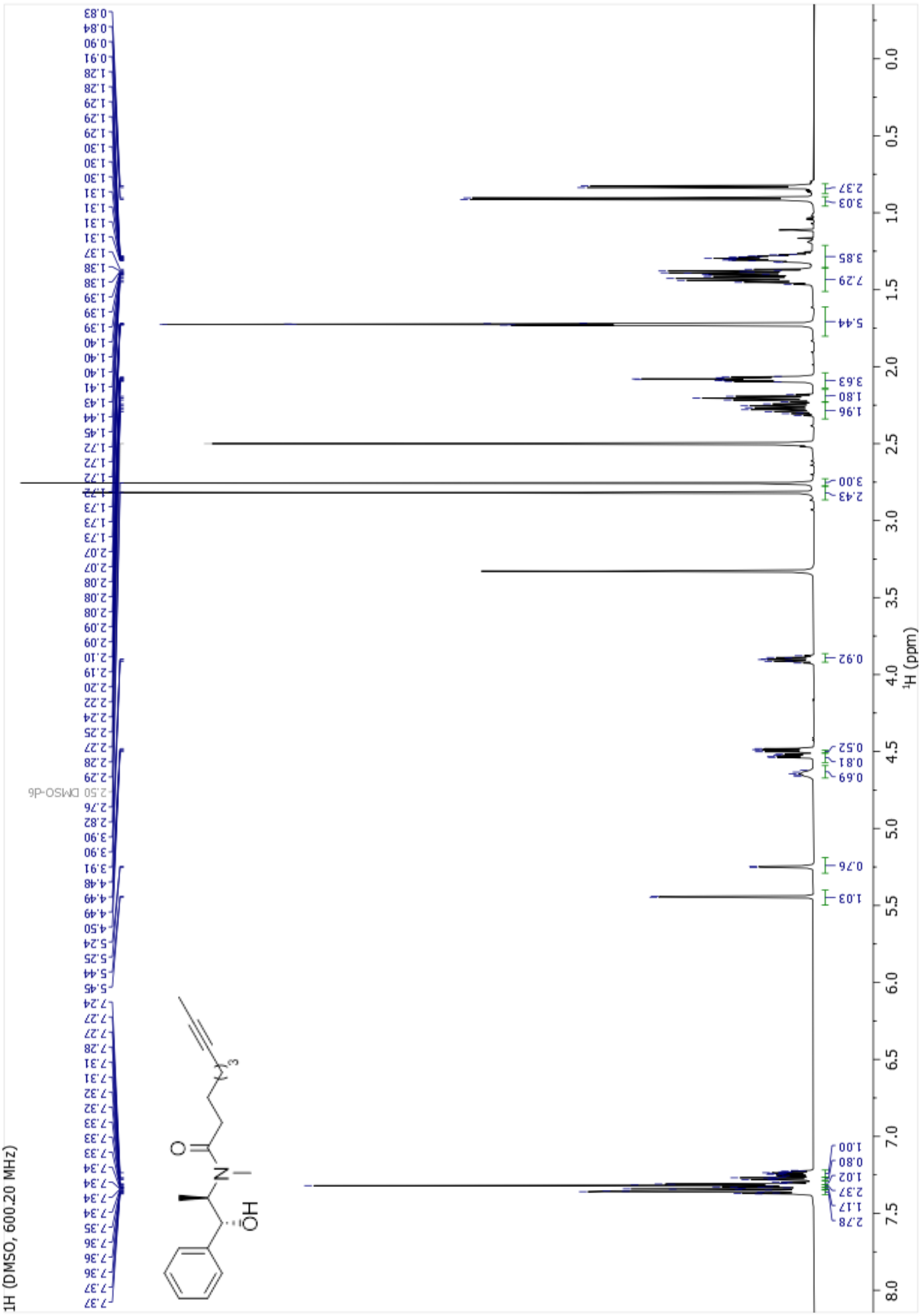
1H (DMSO, 600.20 MHz)
DMSO-d6
1H (ppm)

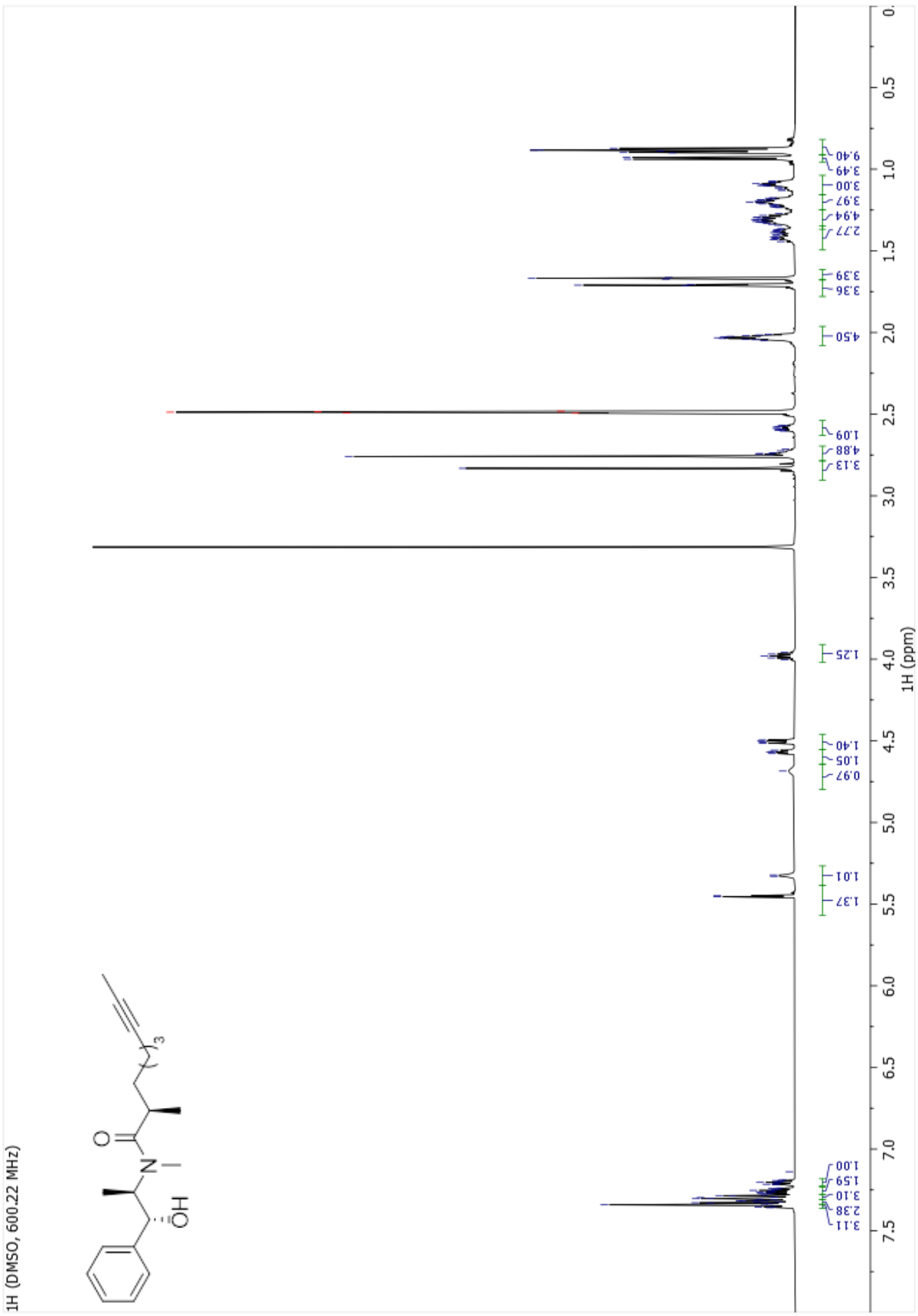
1H (DMSO, 600.22 MHz)
1H (ppm)

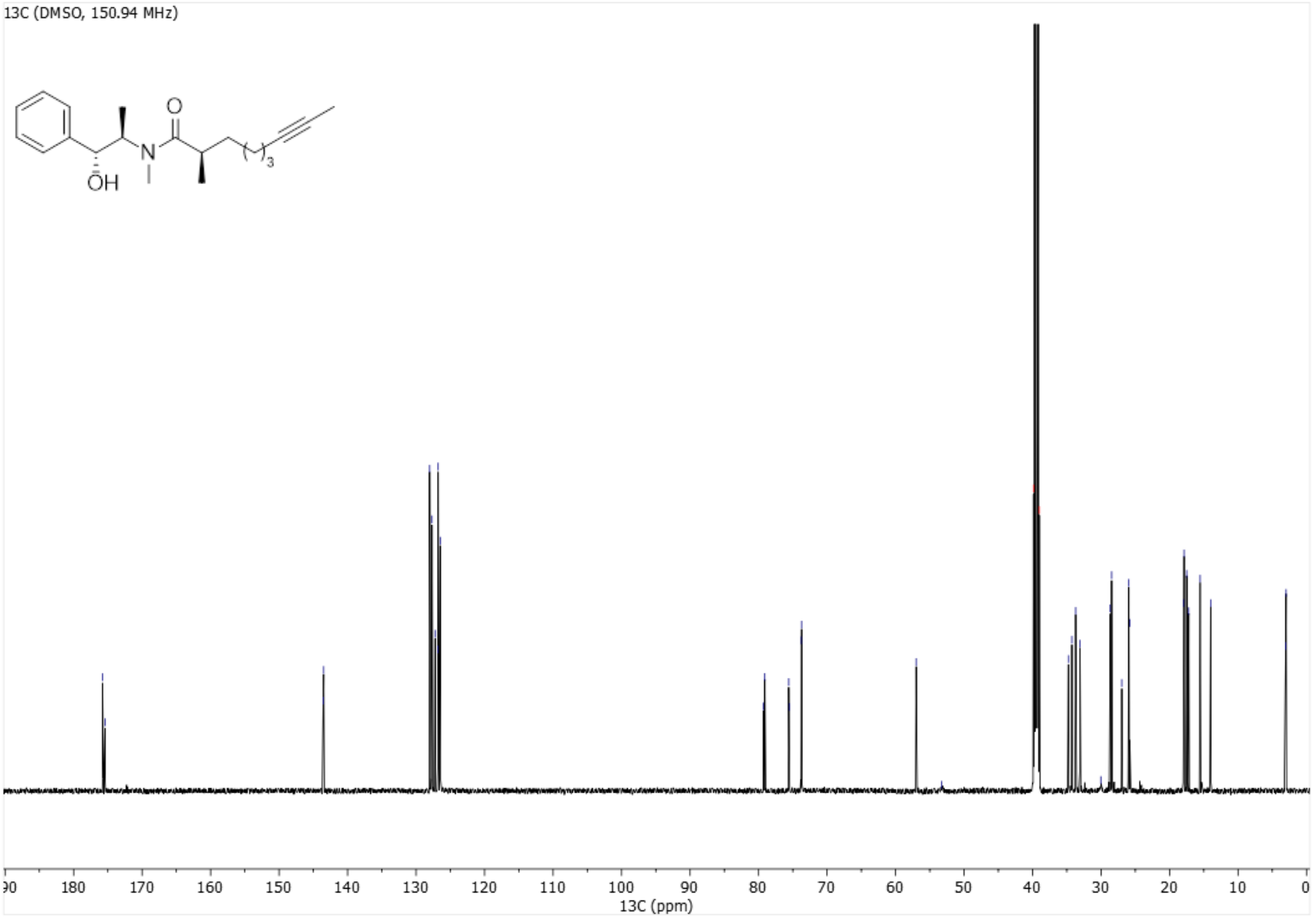
13C (DMSO, 150.94 MHz)
O
N
OH
3
90
180
170
160
150
140
130
120
110
100
90
80
70
60
50
40
30
20
10
0
13C (ppm)

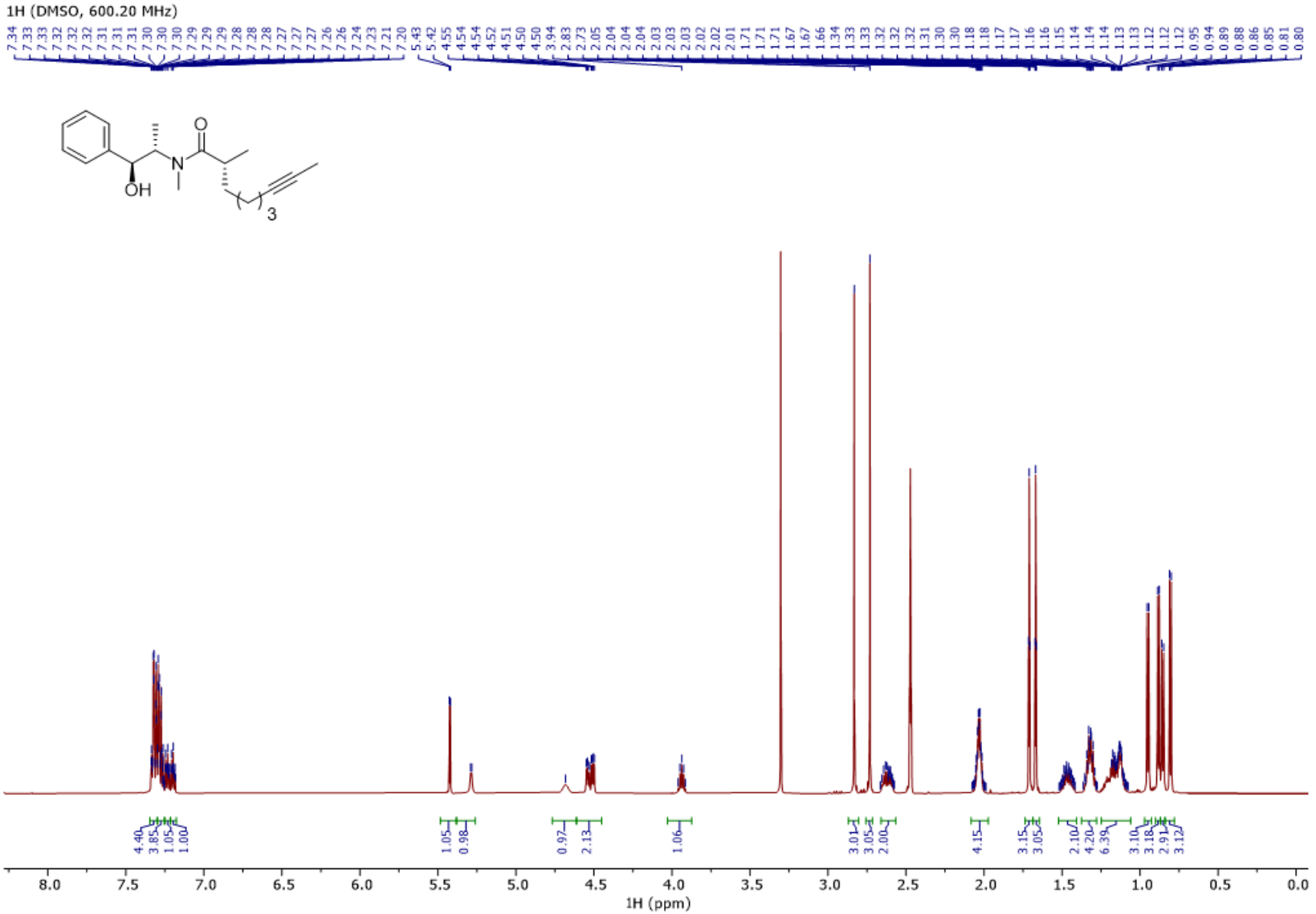
1H (DMSO, 600.20 MHz)
OH
N
O
3
1H (ppm)

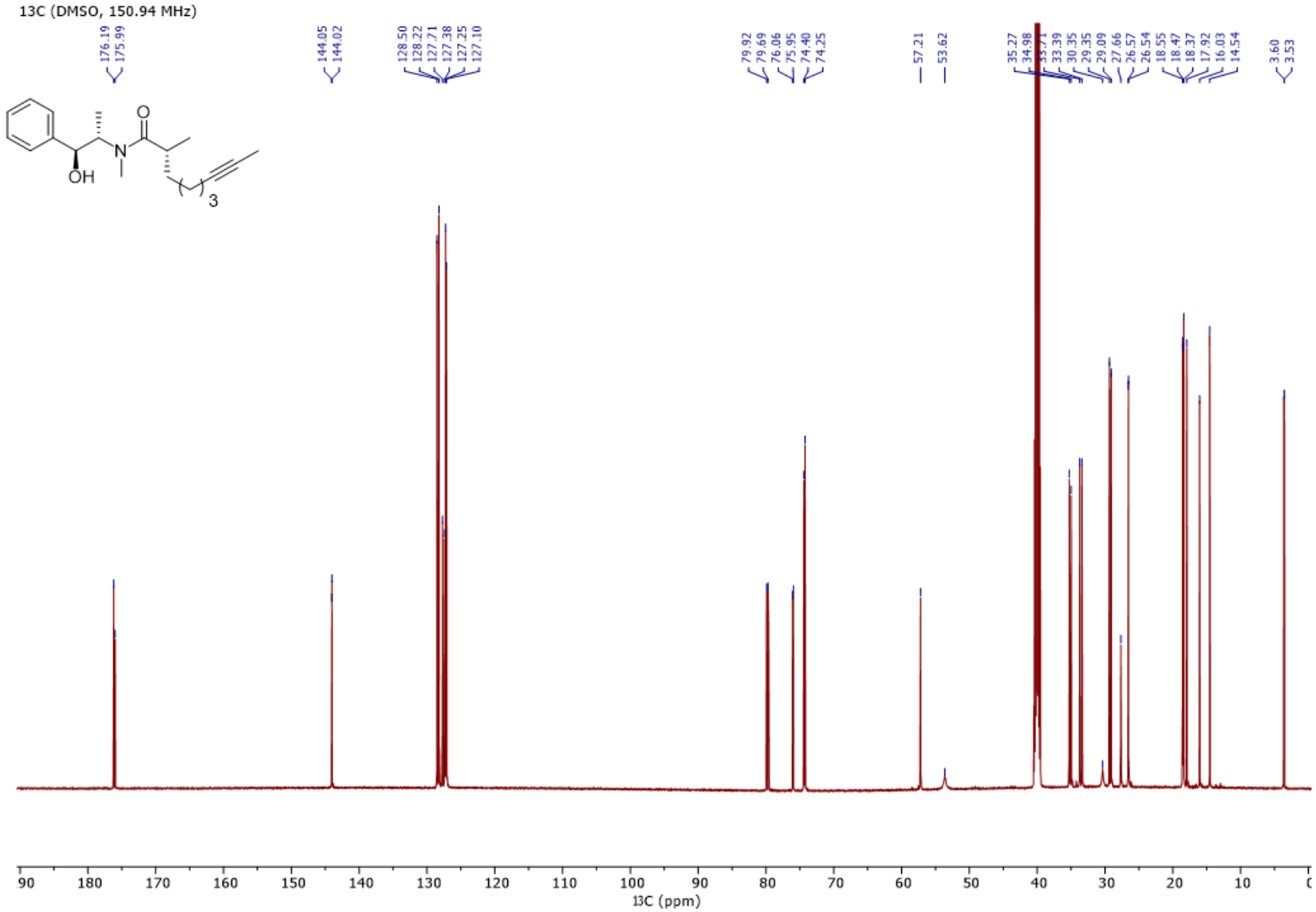
13C (DMSO, 150.94 MHz)
176.19
175.99
144.05
144.02
128.50
128.22
127.71
127.38
127.25
127.10
79.92
79.69
76.06
75.95
74.40
74.25
57.21
53.62
35.27
34.98
33.71
33.39
30.35
29.35
29.09
27.66
26.57
26.54
18.55
18.47
18.37
17.92
16.03
14.54
3.60
3.53
OH
N
O
3
90
180
170
160
150
140
130
120
110
100
90
80
70
60
50
40
30
20
10
13C (ppm)

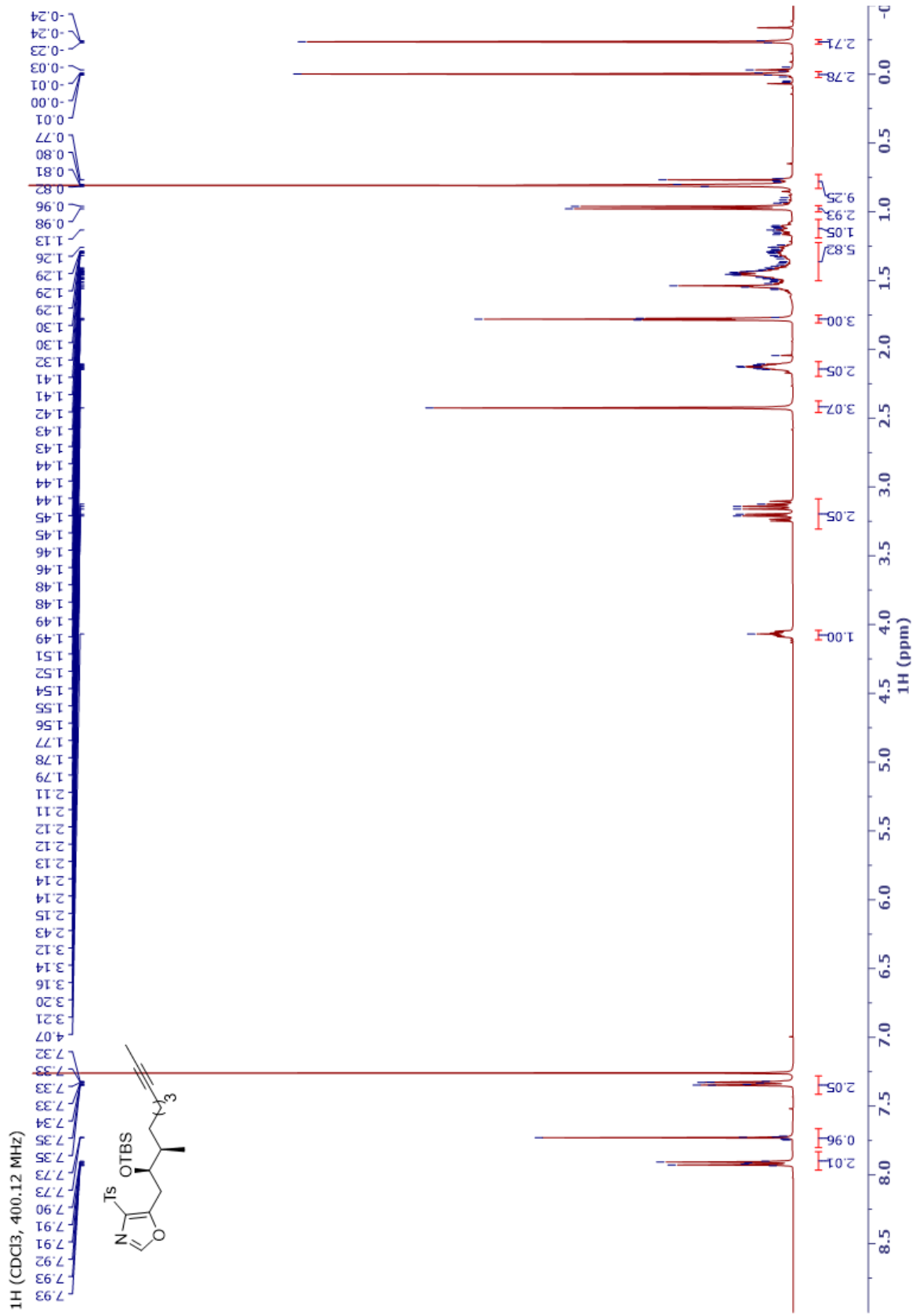
1H (CDCl3, 400.12 MHz)
1H (ppm)
OTBS
Ts
N
O

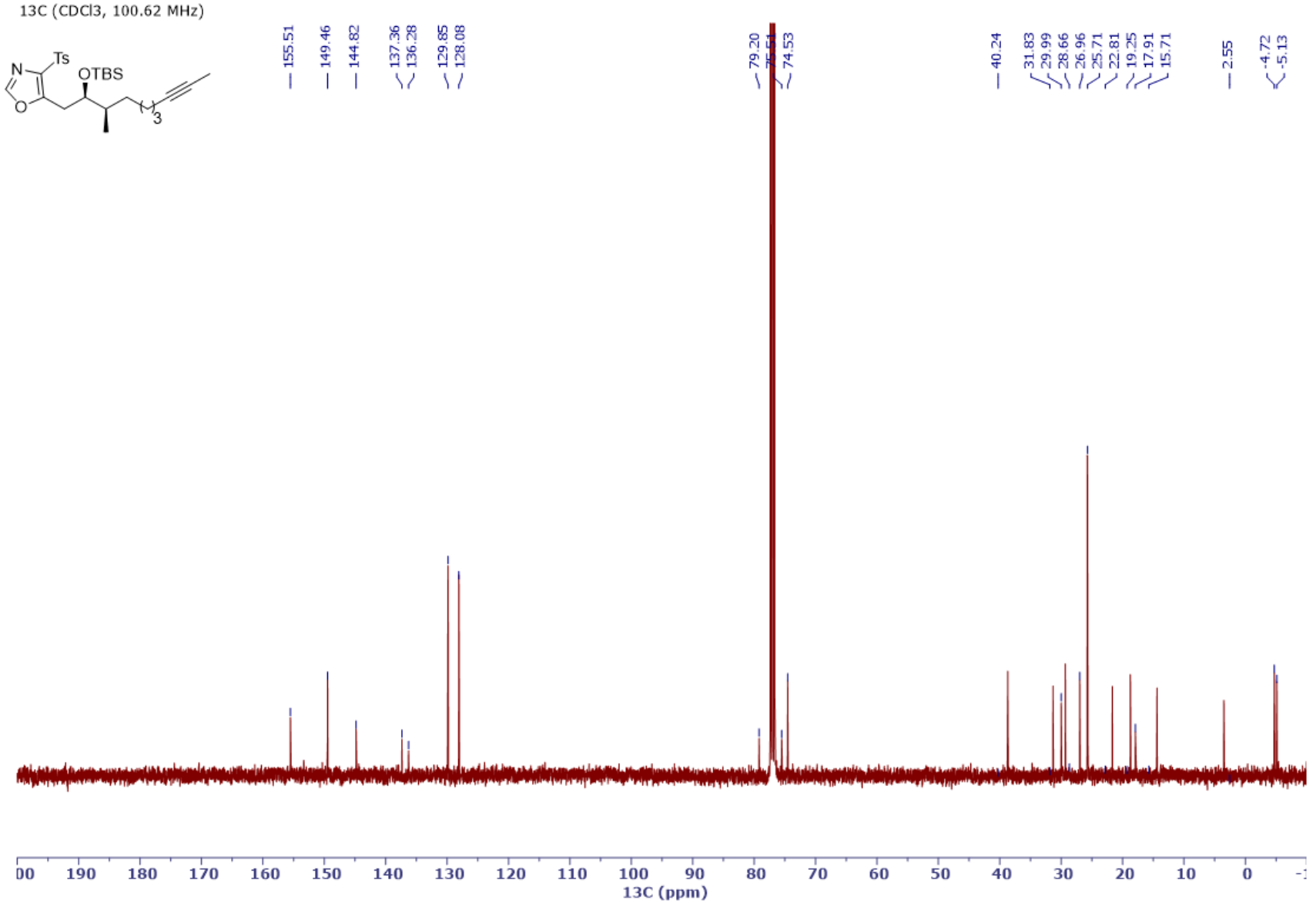
13C (CDCl3, 100.62 MHz)
Ts
N
O
OTBS
3
155.51
149.46
144.82
137.36
136.28
129.85
128.08
79.20
75.51
74.53
40.24
31.83
29.99
28.66
26.96
25.71
22.81
19.25
17.91
15.71
2.55
-4.72
-5.13
190
180
170
160
150
140
130
120
110
100
90
80
70
60
50
40
30
20
10
0
13C (ppm)

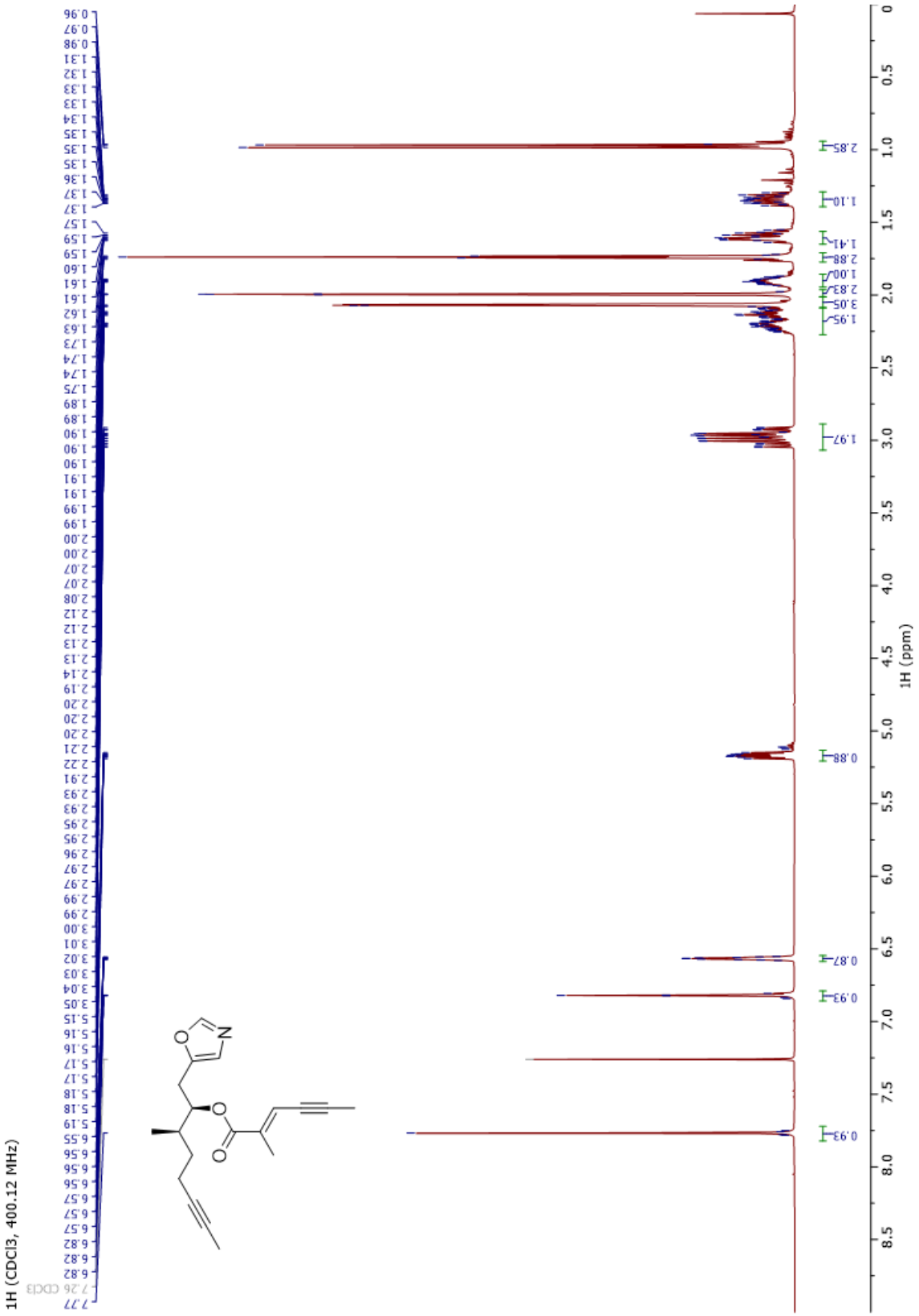
1H (CDCl3, 400.12 MHz)
1H (ppm)

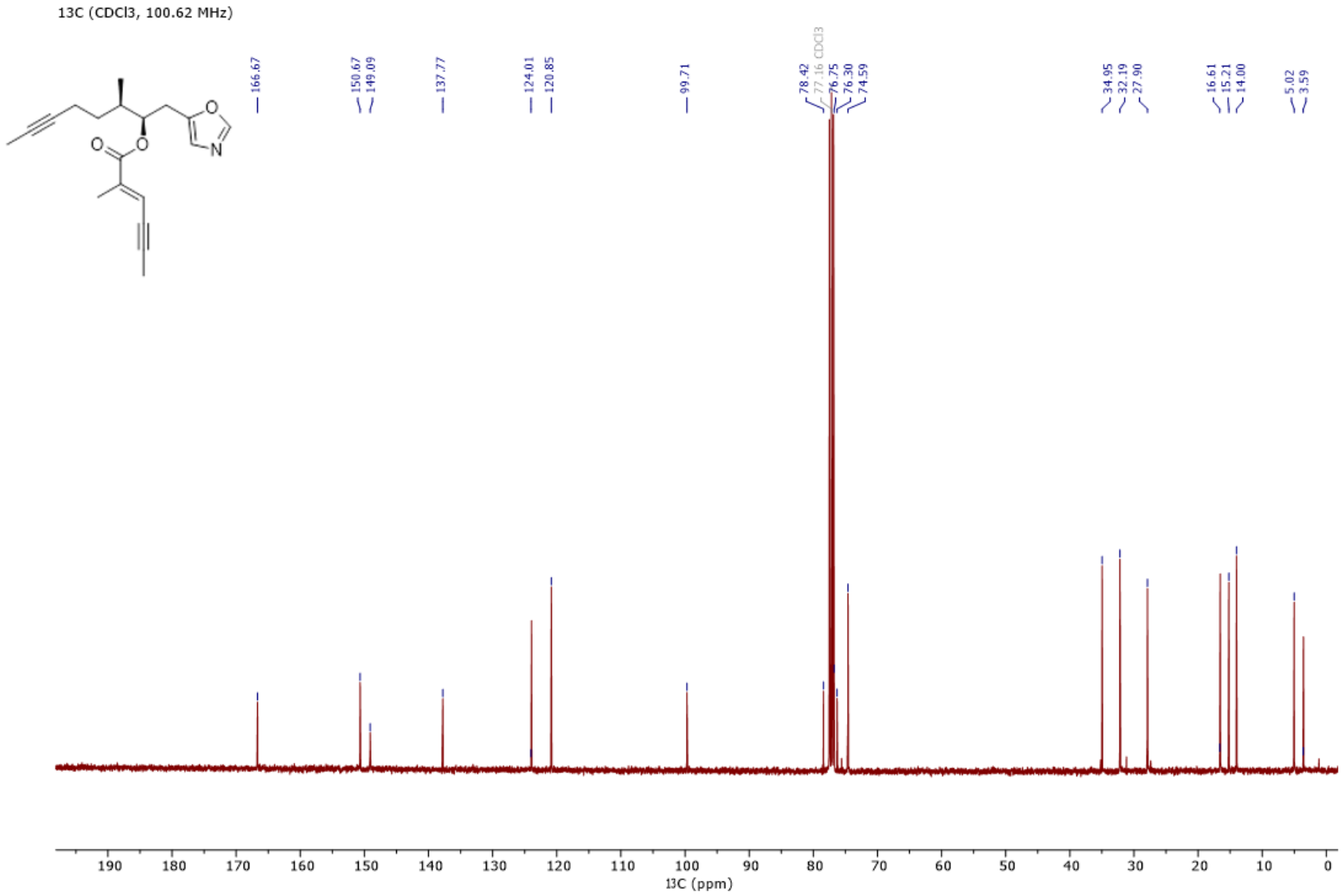
13C (CDCl3, 100.62 MHz)
166.67
150.67
149.09
137.77
124.01
120.85
99.71
78.42
77.16 CDCl3
76.75
76.30
74.59
34.95
32.19
27.90
16.61
15.21
14.00
5.02
3.59
O
O
O
N
190
180
170
160
150
140
130
120
110
100
90
80
70
60
50
40
30
20
10
0
13C (ppm)

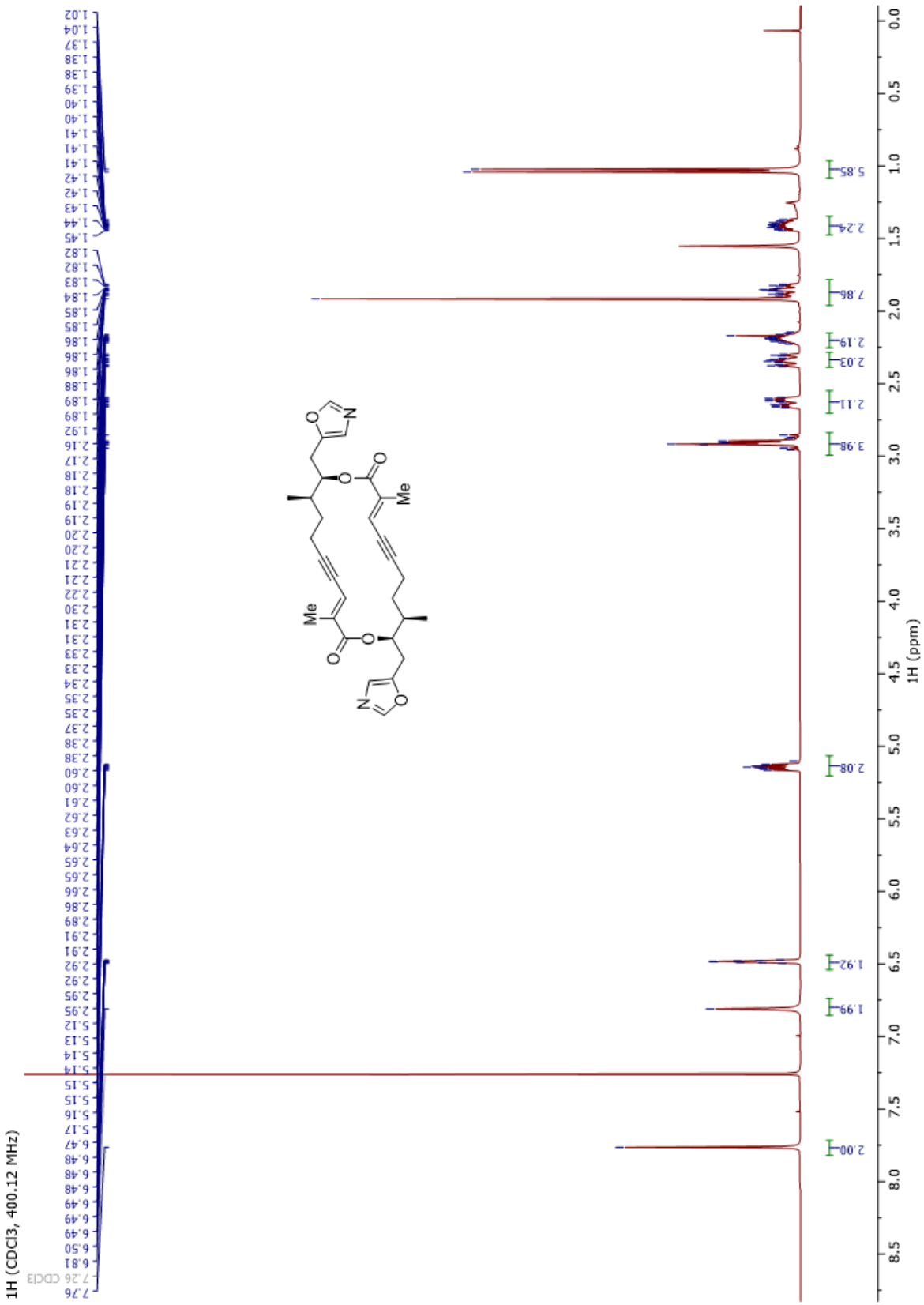
1H (CDCl3, 400.12 MHz)
1H (ppm)
Me
Me
O
N
O
O
O
O
N
O
5.85
2.24
7.86
2.19
2.03
2.11
3.98
2.08
1.92
1.99
2.00

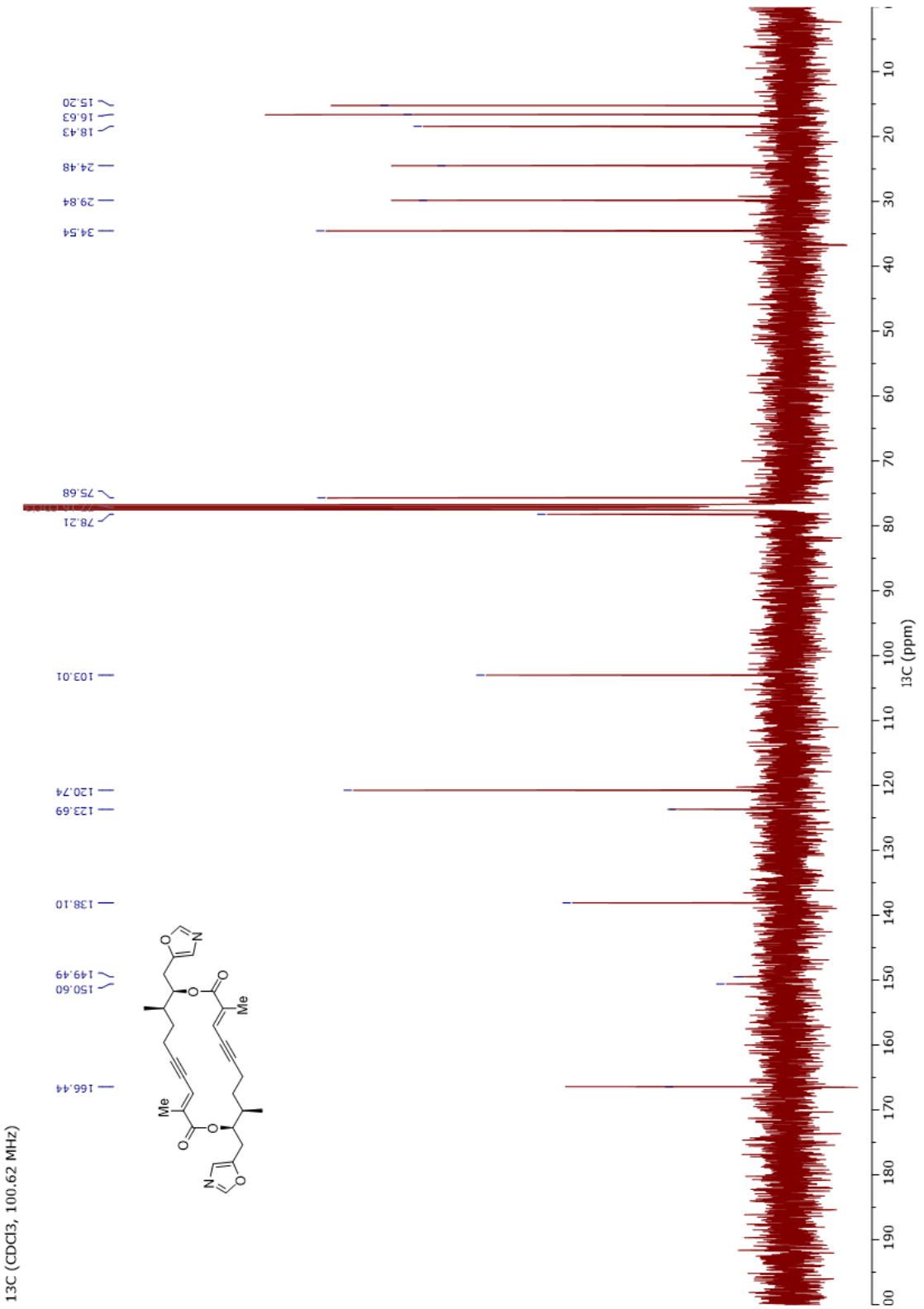
13C (CDCl3, 100.62 MHz)
15.20
16.63
18.43
24.48
29.84
34.54
75.68
78.21
103.01
120.74
123.69
138.10
149.49
150.60
166.44
Me
Me
13C (ppm)

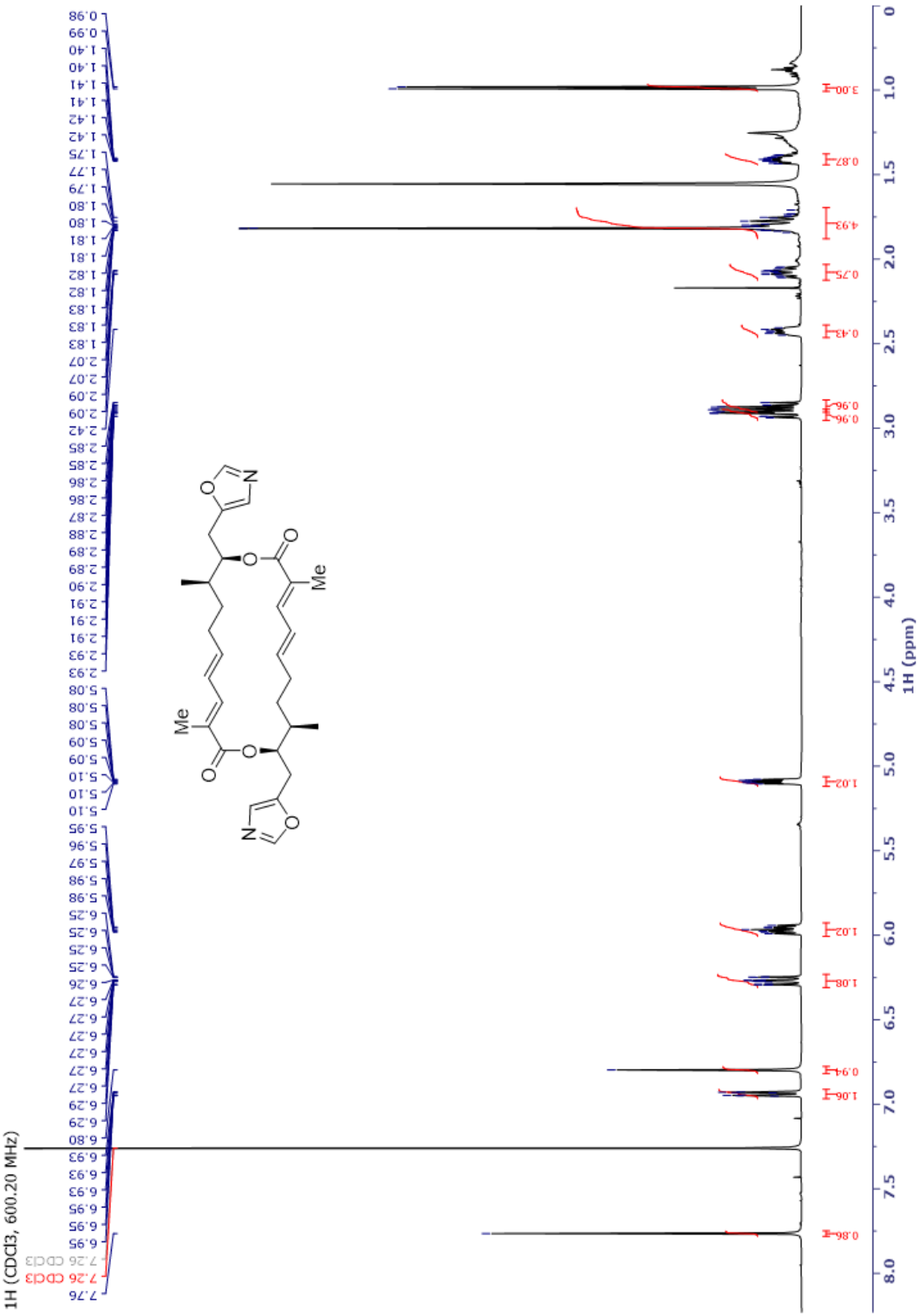
1H (CDCl3, 600.20 MHz)
7.26 CDCl3
Me
Me
1H (ppm)

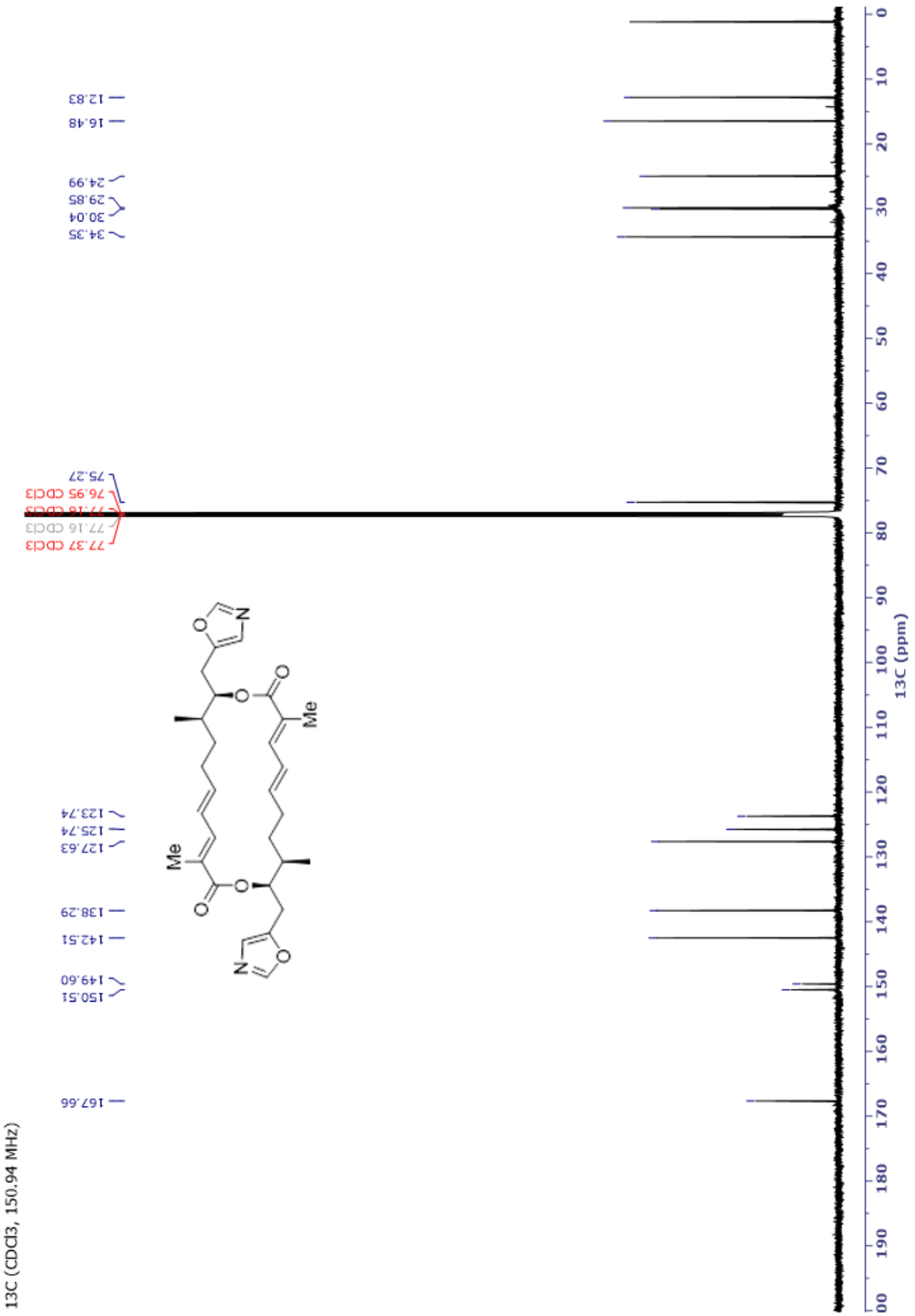
13C (CDCl3, 150.94 MHz)
13C (ppm)
12.83
16.48
24.99
29.85
30.04
34.35
75.27
76.95 CDCl3
77.16 CDCl3
77.37 CDCl3
123.74
125.74
127.63
138.29
142.51
149.60
150.51
167.66
Me
Me
O
N

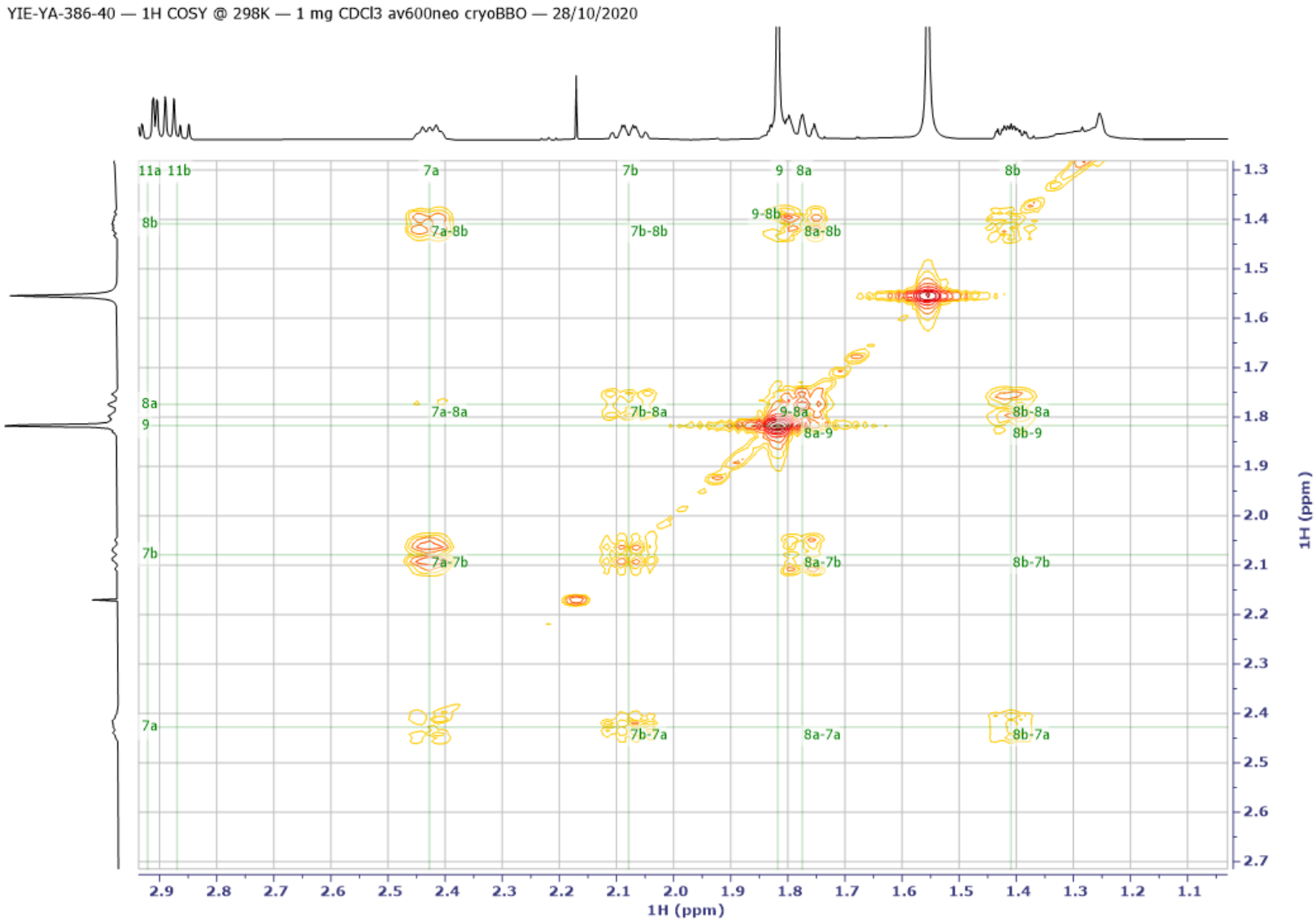
YIE-YA-386-40 — 1H COSY @ 298K — 1 mg CDCl3 av600neo cryoBBO — 28/10/2020
11a 11b
7a
7b
9
8a
8b
9-8b
7a-8b
7b-8b
8a-8b
8a
9
7a-8a
7b-8a
9-8a
8a-9
8b-8a
8b-9
7b
7a-7b
8a-7b
8b-7b
7a
7b-7a
8a-7a
8b-7a
1H (ppm)
1H (ppm)

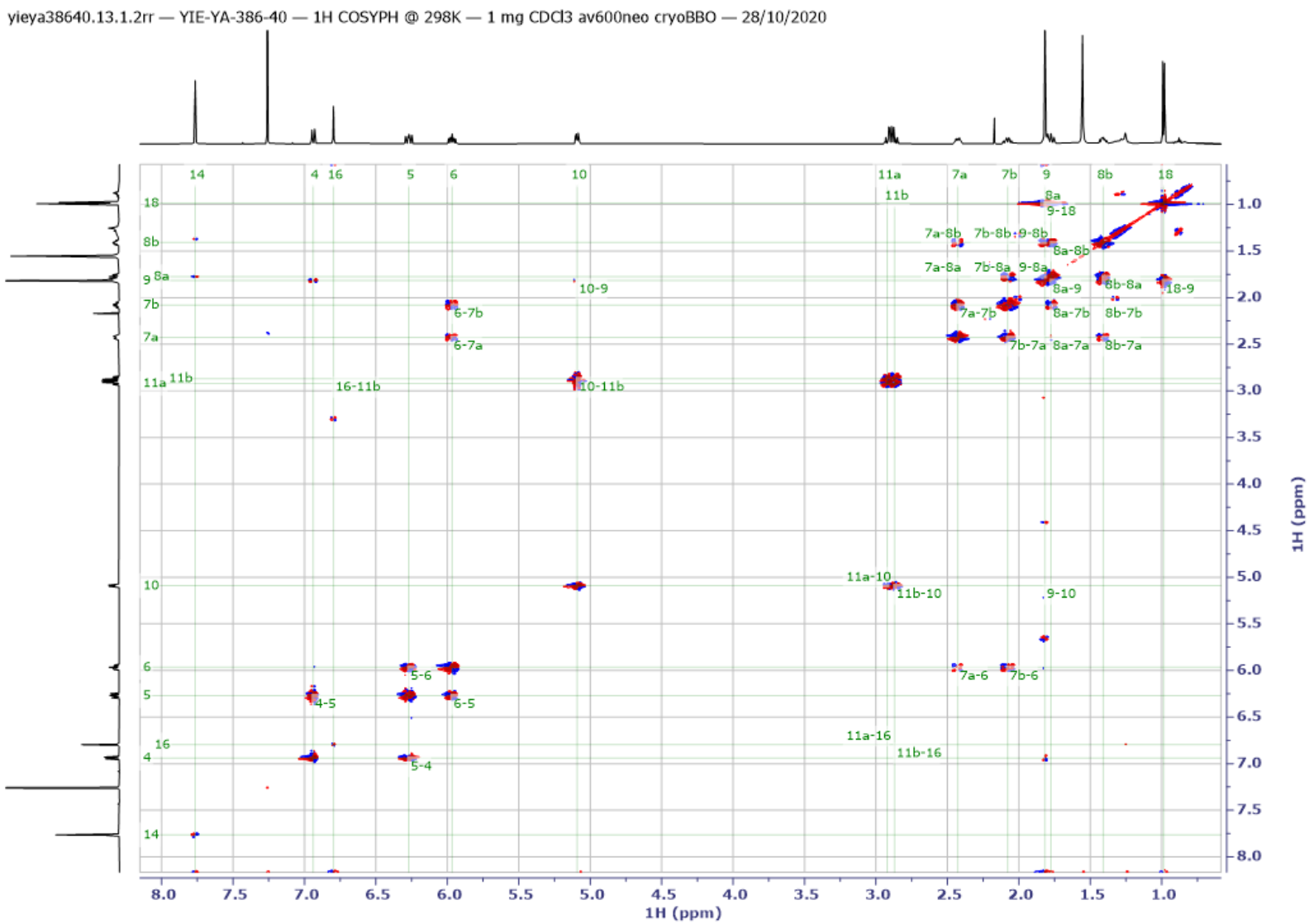
yieya38640.13.1.2rr — YIE-YA-386-40 — 1H COSYPH @ 298K — 1 mg CDCl3 av600neo cryoBBO — 28/10/2020
1H (ppm)
1H (ppm)
16-11b
10-11b
10-9
6-7b
6-7a
5-6
4-5
6-5
5-4
11a-10
11b-10
9-10
7a-6
7b-6
11a-16
11b-16
9-18
7a-8b
7b-8b
9-8b
8a-8b
7a-8a
7b-8a
9-8a
8a-9
6b-8a
18-9
7a-7b
8a-7b
8b-7b
7b-7a
8a-7a
8b-7a

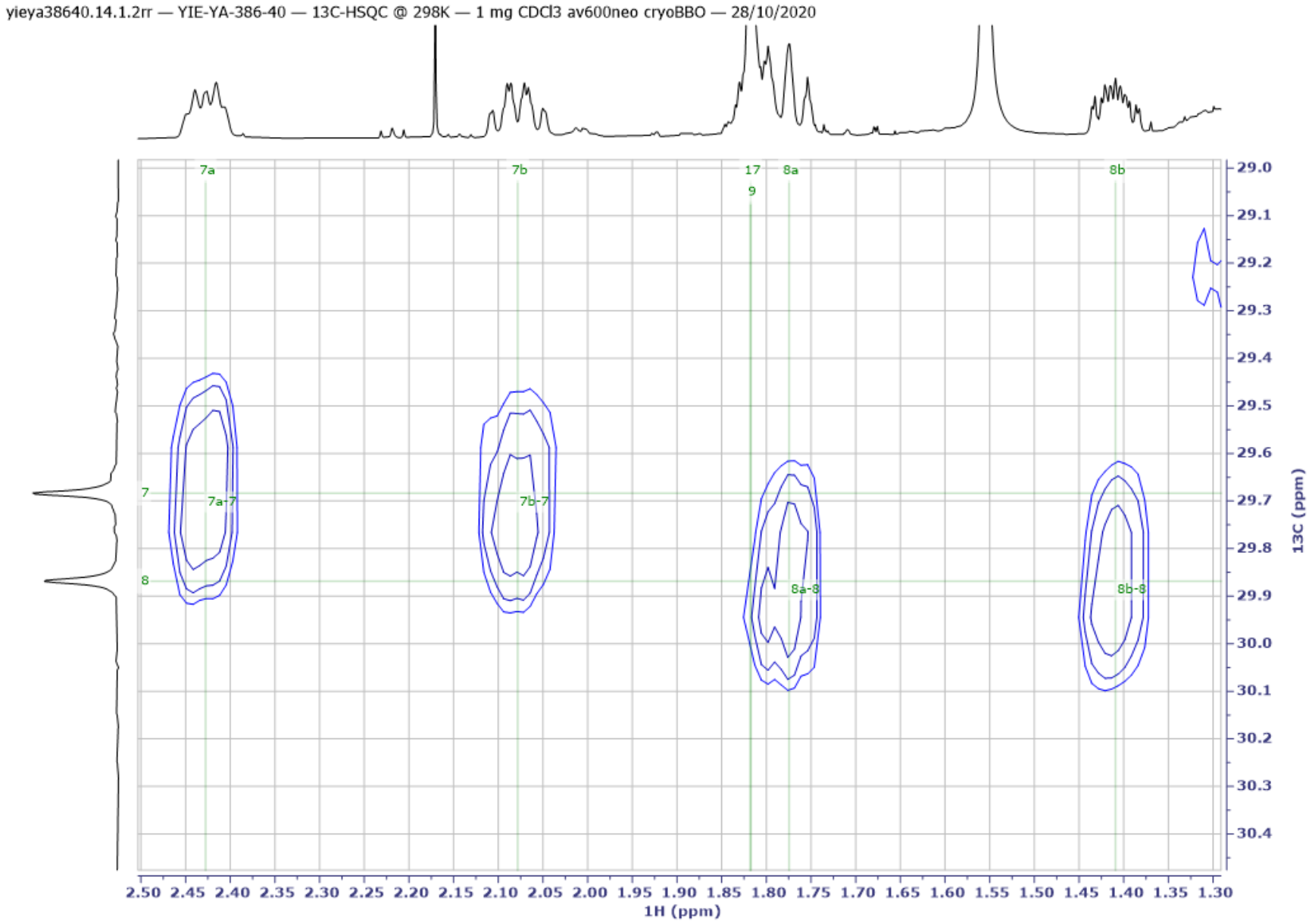
yieya38640.14.1.2rr — YIE-YA-386-40 — 13C-HSQC @ 298K — 1 mg CDCl3 av600neo cryoBBO — 28/10/2020
7a
7b
17
9
8a
8b
7
8
7a-7
7b-7
8a-8
8b-8
29.0
29.1
29.2
29.3
29.4
29.5
29.6
29.7
29.8
29.9
30.0
30.1
30.2
30.3
30.4
13C (ppm)
2.50 2.45 2.40 2.35 2.30 2.25 2.20 2.15 2.10 2.05 2.00 1.95 1.90 1.85 1.80 1.75 1.70 1.65 1.60 1.55 1.50 1.45 1.40 1.35 1.30
1H (ppm)

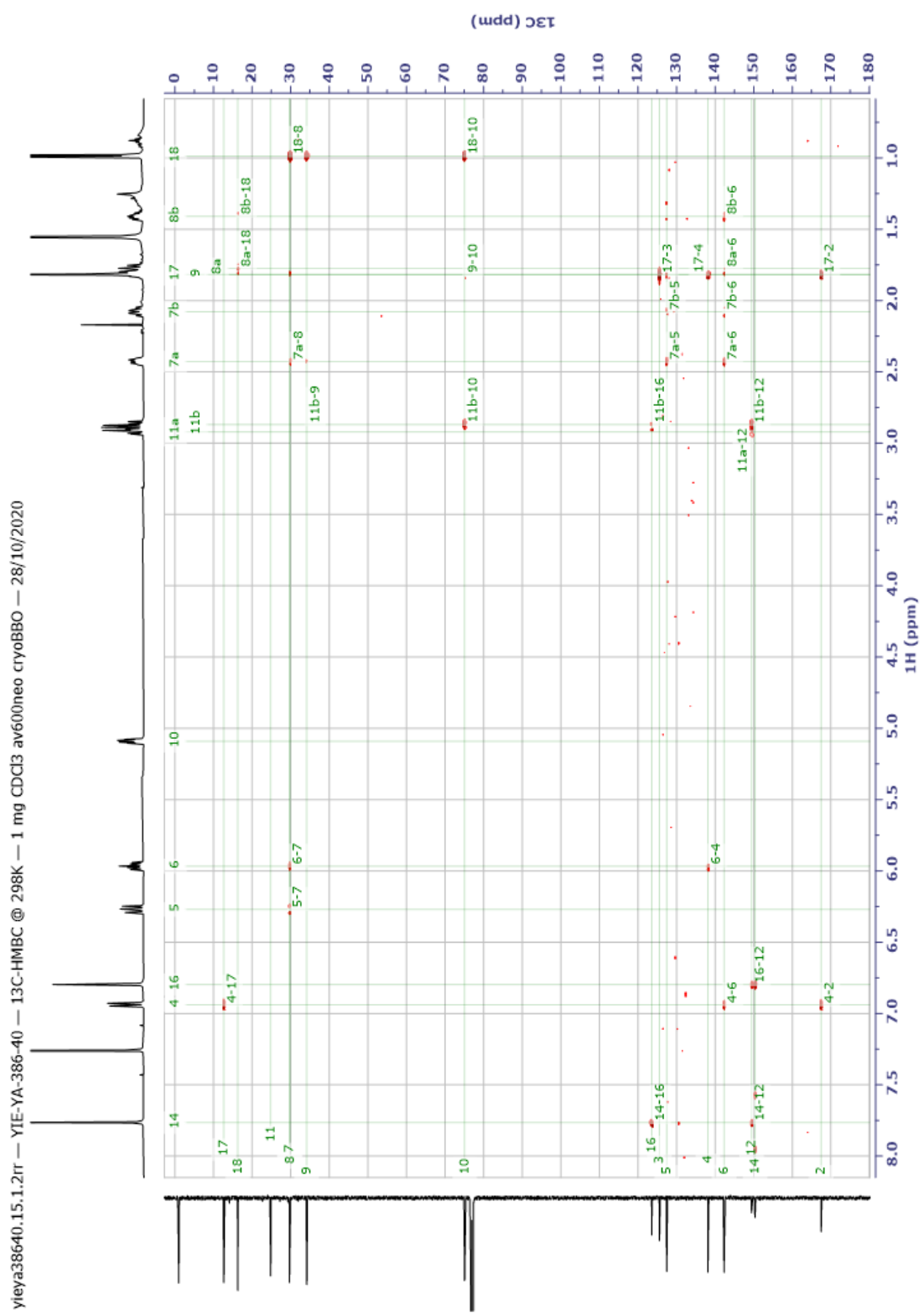
yieya38640.15.1.2rr — YIE-YA-386-40 — 13C-HMBC @ 298K — 1 mg CDCl3 av600neo cryoBBO — 28/10/2020
13C (ppm)
1H (ppm)

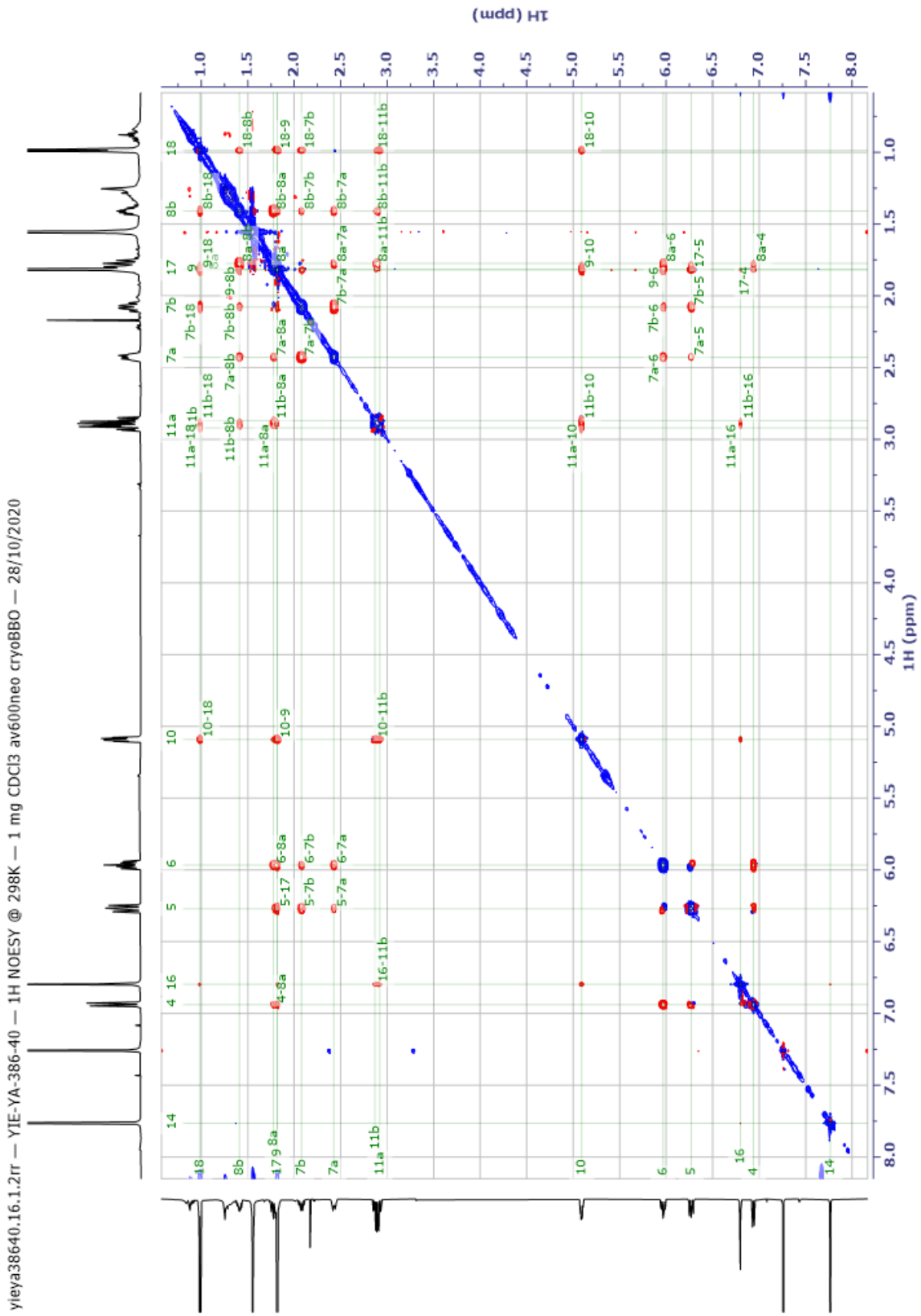
yieya38640.16.1.2rr — YIE-YA-386-40 — 1H NOESY @ 298K — 1 mg CDCl3 av600neo cryoBBO — 28/10/2020
1H (ppm)
1H (ppm)

Appendix 5: Chiral Scouting (2*R*,3*R*)-3-Methyl-1-(4-tosyloxazol-5-yl)oct-6-yn-2-ol (7a)

- HPLC Methods 8a-f: System 1; Solvent – MeOH/H_2O; Flow rate – 1.0 mL min^{-1} at ambient temperature.

Time (min)	A% MeOH	B% H_2O
0	70	30
5	90	10
10	90	10

Method	Column
8a	Chiralpak® IB N-3, 150 mm, 3 µm, ∅ 4.6 mm
8b	Chiralpak® IA-3, 150 mm, 3 µm, ∅ 4.6 mm
8c	Chiralpak® IC-3, 150 mm, 3 µm, ∅ 4.6 mm
8d	YMC Chiral Art® Cellulose-SJ, 150 mm, 5 µm, ∅ 4.6 mm
8e	Chiralpak® AS-3R, 150 mm, 3 µm, ∅ 4.6 mm
8f	Chiracel® OZ-3R, 150 mm, 3 µm, ∅ 4.6 mm

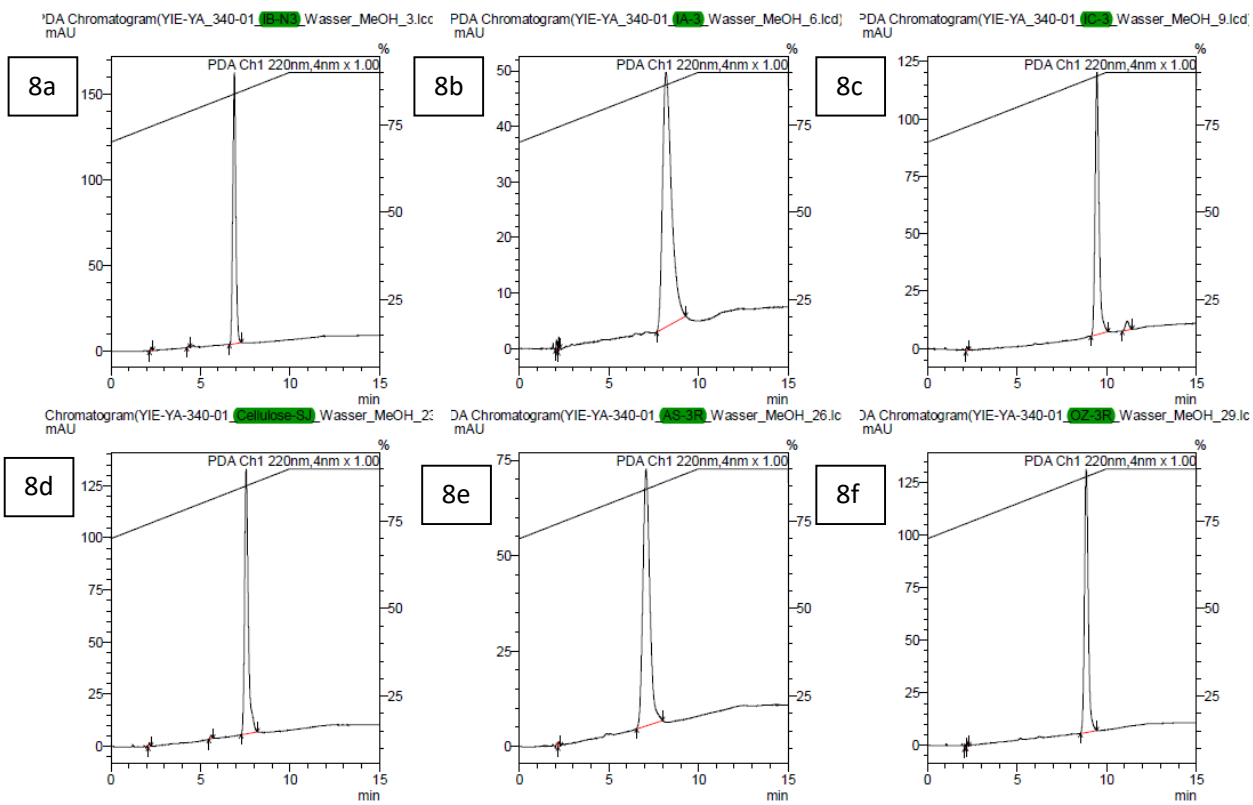

- HPLC Methods 9a-f: System 1; Solvent – MeCN/H_2O; Flow rate – 1.0 mL min^{-1} at ambient temperature.

Time (min)	A% MeCN	B% H_2O
0	70	30
5	90	10
10	90	10

Method	Column
9a	Chiralpak® IB N-3, 150 mm, 3 µm, ∅ 4.6 mm
9b	Chiralpak® IA-3, 150 mm, 3 µm, ∅ 4.6 mm
9c	Chiralpak® IC-3, 150 mm, 3 µm, ∅ 4.6 mm
9d	YMC Chiral Art® Cellulose-SJ, 150 mm, 5 µm, ∅ 4.6 mm
9e	Chiralpak® AS-3R, 150 mm, 3 µm, ∅ 4.6 mm
9f	Chiracel® OZ-3R, 150 mm, 3 µm, ∅ 4.6 mm

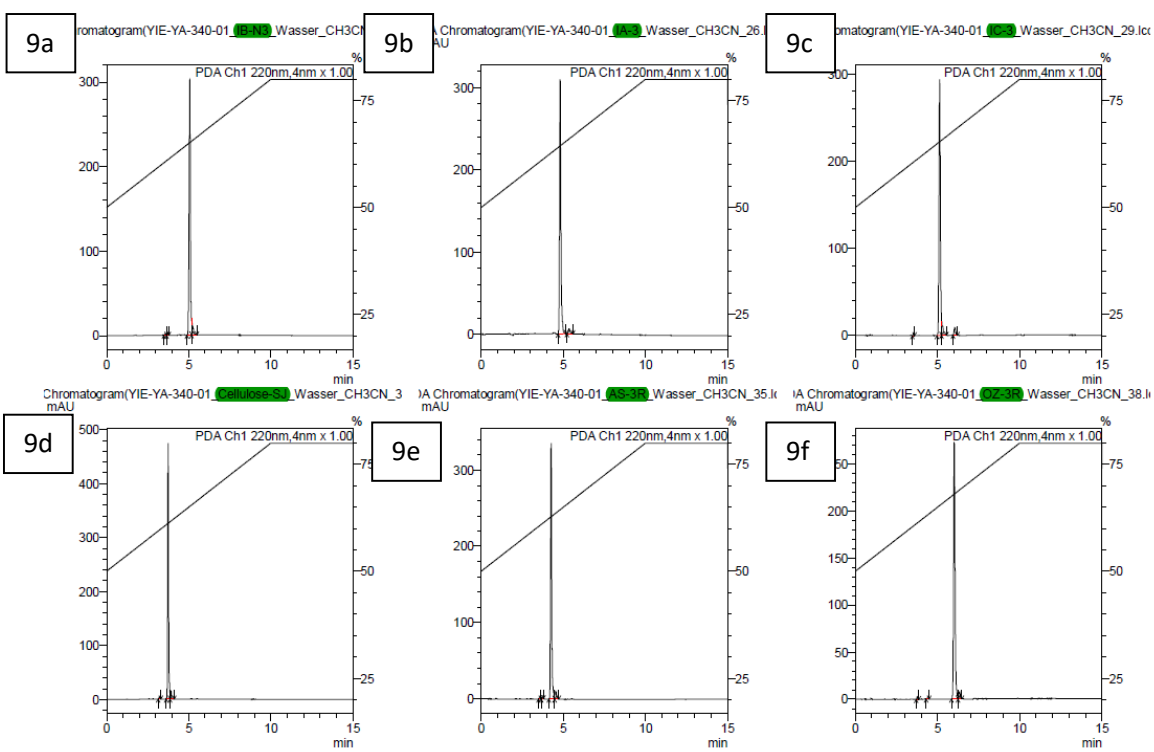

Appendix 6: Chiral Scouting (2*R*,3*R*)-3-Methyl-1-(4-tosyloxazol-5-yl)dec-8-yn-2-ol (7b)

- HPLC Methods 8a-f: System 1; Solvent – MeOH/H_2O; Flow rate – 1.0 mL min^{-1} at ambient temperature.

Time (min)	A% MeOH	B% H_2O
0	70	30
5	90	10
10	90	10

Method	Column
8a	Chiralpak® IB N-3, 150 mm, 3 µm, ∅ 4.6 mm
8b	Chiralpak® IA-3, 150 mm, 3 µm, ∅ 4.6 mm
8c	Chiralpak® IC-3, 150 mm, 3 µm, ∅ 4.6 mm
8d	YMC Chiral Art® Cellulose-SJ, 150 mm, 5 µm, ∅ 4.6 mm
8e	Chiralpak® AS-3R, 150 mm, 3 µm, ∅ 4.6 mm
8f	Chiracel® OZ-3R, 150 mm, 3 µm, ∅ 4.6 mm

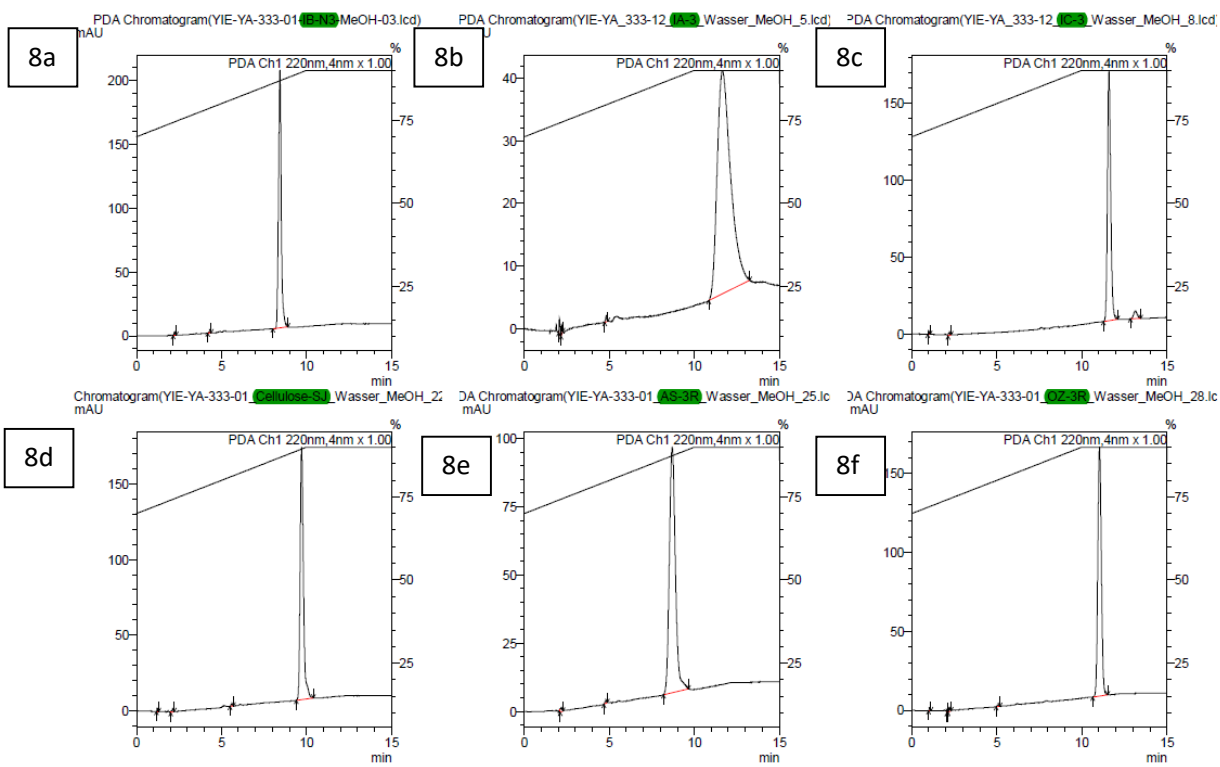

- HPLC Methods 9a-f: System 1; Solvent – MeCN/H_2O; Flow rate – 1.0 mL min^{-1} at ambient temperature.

Time (min)	A% MeCN	B% H_2O
0	70	30
5	90	10
10	90	10

Method	Column
9a	Chiralpak® IB N-3, 150 mm, 3 µm, ∅ 4.6 mm
9b	Chiralpak® IA-3, 150 mm, 3 µm, ∅ 4.6 mm
9c	Chiralpak® IC-3, 150 mm, 3 µm, ∅ 4.6 mm
9d	YMC Chiral Art® Cellulose-SJ, 150 mm, 5 µm, ∅ 4.6 mm
9e	Chiralpak® AS-3R, 150 mm, 3 µm, ∅ 4.6 mm
9f	Chiracel® OZ-3R, 150 mm, 3 µm, ∅ 4.6 mm

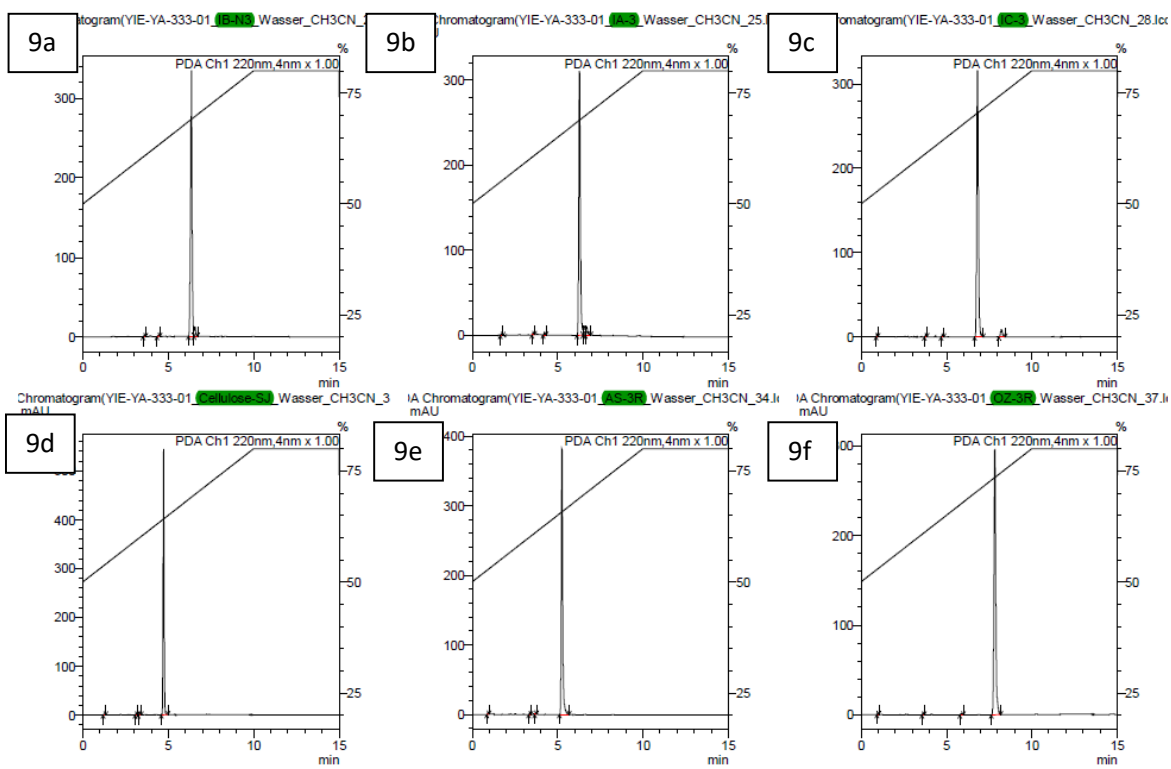

WG: Thesis/dissertation

Rights DE <RIGHTS-and-LICENCES@wiley-vch.de>

Tue 03/08/2021 09:58

To: YIANNAKAS Hector <s1215085@sms.ed.ac.uk>

Dear Ektoras Yiannakas,

The requested material is from an Open Access article, please see copyright holder below. Please follow the terms of the license;

How to cite:

Yiannakas, E., Grimes, M.I., Whitelegge, J.T., Fürstner, A. and Hulme, A.N. (2021), An Alkyne-Metathesis-Based Approach to the Synthesis of the Anti-Malarial Macrodiolide Samroiyotmycin A. Angew. Chem. Int. Ed.. https://doi.org/10.1002/anie.202105732

Kind regards

Bettina Loycke
Senior Rights Manager
Rights & Licenses

Wiley-VCH GmbH
Boschstraße 12
69469 Weinheim
Germany
www.wiley-vch.de

T +(49) 6201 606-280
F +(49) 6201 606-332
rightsDE@wiley.com

WILEY

Celebrate ***100 Years of Growing Knowledge*** with us:
2021 marks our anniversary year: VCH was founded in 1921, Wiley-VCH in 1996. Please join us in celebrating this success and have a look at our anniversary website.

Von: Wiley Global Permissions <permissions@wiley.com>
Gesendet: Dienstag, 3. August 2021 10:53
An: Rights DE <RIGHTS-and-LICENCES@wiley-vch.de>
Betreff: FW: Thesis/dissertation

From: Form Submittal Notification <formsubmittal@eloqua.com>
Sent: 02 August 2021 16:05
To: Wiley Global Permissions <permissions@wiley.com>
Subject: Thesis/dissertation

ORACLE Eloqua

Eloqua Notification System

Your personal notification of activity on your website. Target prospects, identify visitors, and develop sales relationships with your online visitors.

First Name
Ektoras

Last Name
Yiannakas

Email Address
s1215085@sms.ed.ac.uk

Company
University of Edinburgh

Pages Viewed
2

Submit Time
8/2/2021 11:05:00 AM

Form Name
form1salesW26MT

URL Of Form
https://secure.wiley.com/

Data Provided in Form

Email address
s1215085@sms.ed.ac.uk

First name
Ektoras

Last name
Yiannakas

Country
United Kingdom

State or Province

Company name
University of Edinburgh

Contact phone number
+447761062033

I am, or I am working on behalf of one of the following:
the author of this work

I want to re-use:
Journal Content

book title

isbn

bookcomments

Text permissions: number of words

Image permissions: name or number of figure

journal title

issn

doi#
10.1002/anie.202105732

journal Comments:

Please provide information on the product(s) for which you are seeking permission.

Usage type
Thesis/dissertation

Title of new work/Study number

Publisher

Publication Date

Existing reuse license number

Describe modifications

Hidden - Eloqua Campaign ID

,

Hidden - Last SFDC Campaign ID

Hidden - Source

Hidden - Campaign Code

?

View This Contact's Activity

Regarding Incident 4401841 Reuse article content permission request for thesis (https://doi.org/10.1021/jacs.0c04742)

support@services.acs.org <support@services.acs.org>
Mon 07/06/2021 17:35
To: YIANNAKAS Hector <s1215085@sms.ed.ac.uk>

ACS Chemistry for Life®

Dear Dr. Yiannakas,

Thank you for contacting ACS Publications Support.

Your permission requested is granted and there is no fee for this reuse. In your planned reuse, you must cite the ACS article as the source, add this direct link <https://pubs.acs.org/doi/10.1021/jacs.0c04742>, and include a notice to readers that further permissions related to the material excerpted should be directed to the ACS.

Sincerely,

Budimir Jelic
ACS Publications
Customer Services & Information
Website: https://help.acs.org

Incident Information:

Incident #: 4401841
Date Created: 2021-06-07T13:57:32
Priority: 3
Customer: Hector Yiannakas
Title: Reuse article content permission request for thesis (https://doi.org/10.1021/jacs.0c04742)
Description: Dear Sir/ Madam,

I am currently a final year Chemistry PhD student at the University of Edinburgh under the supervision of Prof. Alison N. Hulme. I am writing to request permission to reuse content from the following ACS article, where I am also a co-author: https://doi.org/10.1021/jacs.0c04742. I am intending to reuse the entire article for one of my thesis chapters.

Yours sincerely,

Ektoras Yiannakas

{CMI: MCID1231248}

ELSEVIER LICENSE
TERMS AND CONDITIONS

Aug 29, 2021

This Agreement between University of Edinburgh -- Ektoras Yiannakas ("You") and Elsevier ("Elsevier") consists of your license details and the terms and conditions provided by Elsevier and Copyright Clearance Center.

License Number	5138241457974
License date	Aug 29, 2021
Licensed Content Publisher	Elsevier
Licensed Content Publication	Tetrahedron
Licensed Content Title	Antimalarial 20-membered macrolides from Streptomyces sp. BCC33756
Licensed Content Author	Aibrohim Dramae,Sutichai Nithithanasilp,Wilunda Choowong,Pranee Rachtawee,Samran Prabpai,Palangpon Kongsaeree,Pattama Pittayakhajonwut
Licensed Content Date	Sep 23, 2013
Licensed Content Volume	69
Licensed Content Issue	38
Licensed Content Pages	4
Start Page	8205
End Page	8208
Type of Use	reuse in a thesis/dissertation

Portion	figures/tables/illustrations
Number of figures/tables/illustrations	1
Format	both print and electronic
Are you the author of this Elsevier article?	No
Will you be translating?	No
Title	Alkyne Metathesis: A new tool for the self-assembly of complex molecular
Institution name	University of Edinburgh
Expected presentation date	Oct 2021
Portions	Supporting information: Figure S1, page 4
Requestor Location	University of Edinburgh Office 54 Joseph Black Building David Brewster Road Edinburgh, EH9 3FJ United Kingdom Attn: University of Edinburgh
Publisher Tax ID	GB 494 6272 12
Total	0.00 USD
Terms and Conditions	

INTRODUCTION

1. The publisher for this copyrighted material is Elsevier. By clicking "accept" in connection with completing this licensing transaction, you agree that the following terms and conditions apply to this transaction (along with the Billing and Payment terms and conditions established by Copyright Clearance Center, Inc. ("CCC"), at the time that you opened your Rightslink account and that are available at any time at http://myaccount.copyright.com).

GENERAL TERMS

2. Elsevier hereby grants you permission to reproduce the aforementioned material subject to the terms and conditions indicated.

3. Acknowledgement: If any part of the material to be used (for example, figures) has appeared in our publication with credit or acknowledgement to another source, permission must also be sought from that source. If such permission is not obtained then that material may not be included in your publication/copies. Suitable acknowledgement to the source must be made, either as a footnote or in a reference list at the end of your publication, as follows:

"Reprinted from Publication title, Vol /edition number, Author(s), Title of article / title of chapter, Pages No., Copyright (Year), with permission from Elsevier [OR APPLICABLE SOCIETY COPYRIGHT OWNER]." Also Lancet special credit - "Reprinted from The Lancet, Vol. number, Author(s), Title of article, Pages No., Copyright (Year), with permission from Elsevier."

4. Reproduction of this material is confined to the purpose and/or media for which permission is hereby given.

5. Altering/Modifying Material: Not Permitted. However figures and illustrations may be altered/adapted minimally to serve your work. Any other abbreviations, additions, deletions and/or any other alterations shall be made only with prior written authorization of Elsevier Ltd. (Please contact Elsevier's permissions helpdesk here). No modifications can be made to any Lancet figures/tables and they must be reproduced in full.

6. If the permission fee for the requested use of our material is waived in this instance, please be advised that your future requests for Elsevier materials may attract a fee.

7. Reservation of Rights: Publisher reserves all rights not specifically granted in the combination of (i) the license details provided by you and accepted in the course of this licensing transaction, (ii) these terms and conditions and (iii) CCC's Billing and Payment terms and conditions.

8. License Contingent Upon Payment: While you may exercise the rights licensed immediately upon issuance of the license at the end of the licensing process for the transaction, provided that you have disclosed complete and accurate details of your proposed use, no license is finally effective unless and until full payment is received from you (either by publisher or by CCC) as provided in CCC's Billing and Payment terms and conditions. If full payment is not received on a timely basis, then any license preliminarily granted shall be deemed automatically revoked and shall be void as if never granted. Further, in the event that you breach any of these terms and conditions or any of CCC's Billing and Payment terms and conditions, the license is automatically revoked and shall be void as if never granted. Use of materials as described in a revoked license, as well as any use of the materials beyond the scope of an unrevoked license, may constitute copyright infringement and publisher reserves the right to take any and all action to protect its copyright in the materials.

9. Warranties: Publisher makes no representations or warranties with respect to the licensed material.

10. Indemnity: You hereby indemnify and agree to hold harmless publisher and CCC, and their respective officers, directors, employees and agents, from and against any and all claims arising out of your use of the licensed material other than as specifically authorized pursuant to this license.

11. No Transfer of License: This license is personal to you and may not be sublicensed, assigned, or transferred by you to any other person without publisher's written permission.

12. No Amendment Except in Writing: This license may not be amended except in a writing signed by both parties (or, in the case of publisher, by CCC on publisher's behalf).

13. Objection to Contrary Terms: Publisher hereby objects to any terms contained in any purchase order, acknowledgment, check endorsement or other writing prepared by you, which terms are inconsistent with these terms and conditions or CCC's Billing and Payment terms and conditions. These terms and conditions, together with CCC's Billing and Payment terms and conditions (which are incorporated herein), comprise the entire agreement between you and publisher (and CCC) concerning this licensing transaction. In the event of any conflict between your obligations established by these terms and conditions and those established by CCC's Billing and Payment terms and conditions, these terms and conditions shall control.

14. Revocation: Elsevier or Copyright Clearance Center may deny the permissions described in this License at their sole discretion, for any reason or no reason, with a full refund payable to you. Notice of such denial will be made using the contact information provided by you. Failure to receive such notice will not alter or invalidate the denial. In no event will Elsevier or Copyright Clearance Center be responsible or liable for any costs, expenses or damage incurred by you as a result of a denial of your permission request, other than a refund of the amount(s) paid by you to Elsevier and/or Copyright Clearance Center for denied permissions.

LIMITED LICENSE

The following terms and conditions apply only to specific license types:

15. **Translation**: This permission is granted for non-exclusive world **English** rights only unless your license was granted for translation rights. If you licensed translation rights you may only translate this content into the languages you requested. A professional translator must perform all translations and reproduce the content word for word preserving the integrity of the article.

16. **Posting licensed content on any Website**: The following terms and conditions apply as follows: Licensing material from an Elsevier journal: All content posted to the web site must maintain the copyright information line on the bottom of each image; A hyper-text must be included to the Homepage of the journal from which you are licensing at http://www.sciencedirect.com/science/journal/xxxxx or the Elsevier homepage for books at http://www.elsevier.com; Central Storage: This license does not include permission for a scanned version of the material to be stored in a central repository such as that provided by Heron/XanEdu.

Licensing material from an Elsevier book: A hyper-text link must be included to the Elsevier homepage at http://www.elsevier.com . All content posted to the web site must maintain the copyright information line on the bottom of each image.

Posting licensed content on Electronic reserve: In addition to the above the following clauses are applicable: The web site must be password-protected and made available only to bona fide students registered on a relevant course. This permission is granted for 1 year only. You may obtain a new license for future website posting.

17. **For journal authors:** the following clauses are applicable in addition to the above:

Preprints:

A preprint is an author's own write-up of research results and analysis, it has not been peer-reviewed, nor has it had any other value added to it by a publisher (such as formatting, copyright, technical enhancement etc.).

Authors can share their preprints anywhere at any time. Preprints should not be added to or enhanced in any way in order to appear more like, or to substitute for, the final versions of articles however authors can update their preprints on arXiv or RePEc with their Accepted Author Manuscript (see below).

If accepted for publication, we encourage authors to link from the preprint to their formal publication via its DOI. Millions of researchers have access to the formal publications on ScienceDirect, and so links will help users to find, access, cite and use the best available version. Please note that Cell Press, The Lancet and some society-owned have different preprint policies. Information on these policies is available on the journal homepage.

Accepted Author Manuscripts: An accepted author manuscript is the manuscript of an article that has been accepted for publication and which typically includes author-incorporated changes suggested during submission, peer review and editor-author communications.

Authors can share their accepted author manuscript:

- immediately
    - via their non-commercial person homepage or blog
    - by updating a preprint in arXiv or RePEc with the accepted manuscript
    - via their research institute or institutional repository for internal institutional uses or as part of an invitation-only research collaboration work-group
    - directly by providing copies to their students or to research collaborators for their personal use
    - for private scholarly sharing as part of an invitation-only work group on commercial sites with which Elsevier has an agreement
- After the embargo period
    - via non-commercial hosting platforms such as their institutional repository
    - via commercial sites with which Elsevier has an agreement

In all cases accepted manuscripts should:

- link to the formal publication via its DOI
- bear a CC-BY-NC-ND license - this is easy to do
- if aggregated with other manuscripts, for example in a repository or other site, be shared in alignment with our hosting policy not be added to or enhanced in any way to appear more like, or to substitute for, the published journal article.

Published journal article (JPA): A published journal article (PJA) is the definitive final record of published research that appears or will appear in the journal and embodies all value-adding publishing activities including peer review co-ordination, copy-editing, formatting, (if relevant) pagination and online enrichment.

Policies for sharing publishing journal articles differ for subscription and gold open access articles:

Subscription Articles: If you are an author, please share a link to your article rather than the full-text. Millions of researchers have access to the formal publications on ScienceDirect, and so links will help your users to find, access, cite, and use the best available version.

Theses and dissertations which contain embedded PJAs as part of the formal submission can be posted publicly by the awarding institution with DOI links back to the formal publications on ScienceDirect.

If you are affiliated with a library that subscribes to ScienceDirect you have additional private sharing rights for others' research accessed under that agreement. This includes use for classroom teaching and internal training at the institution (including use in course packs and courseware programs), and inclusion of the article for grant funding purposes.

Gold Open Access Articles: May be shared according to the author-selected end-user license and should contain a CrossMark logo, the end user license, and a DOI link to the formal publication on ScienceDirect.

Please refer to Elsevier's posting policy for further information.

18. **For book authors** the following clauses are applicable in addition to the above: Authors are permitted to place a brief summary of their work online only. You are not allowed to download and post the published electronic version of your chapter, nor may you scan the printed edition to create an electronic version. **Posting to a repository:** Authors are permitted to post a summary of their chapter only in their institution's repository.

19. **Thesis/Dissertation**: If your license is for use in a thesis/dissertation your thesis may be submitted to your institution in either print or electronic form. Should your thesis be published commercially, please reapply for permission. These requirements include permission for the Library and Archives of Canada to supply single copies, on demand, of the complete thesis and include permission for Proquest/UMI to supply single copies, on demand, of the complete thesis. Should your thesis be published commercially, please reapply for permission. Theses and dissertations which contain embedded PJAs as part of the formal submission can be posted publicly by the awarding institution with DOI links back to the formal publications on ScienceDirect.

Elsevier Open Access Terms and Conditions

You can publish open access with Elsevier in hundreds of open access journals or in nearly 2000 established subscription journals that support open access publishing. Permitted third party re-use of these open access articles is defined by the author's choice of Creative Commons user license. See our open access license policy for more information.

Terms & Conditions applicable to all Open Access articles published with Elsevier:

Any reuse of the article must not represent the author as endorsing the adaptation of the article nor should the article be modified in such a way as to damage the author's honour or reputation. If any changes have been made, such changes must be clearly indicated.

The author(s) must be appropriately credited and we ask that you include the end user license and a DOI link to the formal publication on ScienceDirect.

If any part of the material to be used (for example, figures) has appeared in our publication with credit or acknowledgement to another source it is the responsibility of the user to ensure their reuse complies with the terms and conditions determined by the rights holder.

Additional Terms & Conditions applicable to each Creative Commons user license:

CC BY: The CC-BY license allows users to copy, to create extracts, abstracts and new works from the Article, to alter and revise the Article and to make commercial use of the Article (including reuse and/or resale of the Article by commercial entities), provided the user gives appropriate credit (with a link to the formal publication through the relevant DOI), provides a link to the license, indicates if changes were made and the licensor is not represented as endorsing the use made of the work. The full details of the license are available at http://creativecommons.org/licenses/by/4.0.

CC BY NC SA: The CC BY-NC-SA license allows users to copy, to create extracts, abstracts and new works from the Article, to alter and revise the Article, provided this is not done for commercial purposes, and that the user gives appropriate credit (with a link to the formal publication through the relevant DOI), provides a link to the license, indicates if changes were made and the licensor is not represented as endorsing the use made of the

work. Further, any new works must be made available on the same conditions. The full details of the license are available at http://creativecommons.org/licenses/by-nc-sa/4.0.

CC BY NC ND: The CC BY-NC-ND license allows users to copy and distribute the Article, provided this is not done for commercial purposes and further does not permit distribution of the Article if it is changed or edited in any way, and provided the user gives appropriate credit (with a link to the formal publication through the relevant DOI), provides a link to the license, and that the licensor is not represented as endorsing the use made of the work. The full details of the license are available at http://creativecommons.org/licenses/by-nc-nd/4.0. Any commercial reuse of Open Access articles published with a CC BY NC SA or CC BY NC ND license requires permission from Elsevier and will be subject to a fee.

Commercial reuse includes:

- Associating advertising with the full text of the Article
- Charging fees for document delivery or access
- Article aggregation
- Systematic distribution via e-mail lists or share buttons

Posting or linking by commercial companies for use by customers of those companies.

20. **Other Conditions**:

v1.10

Questions? customercare@copyright.com or +1-855-239-3415 (toll free in the US) or +1-978-646-2777.

Ruthenium-Catalyzed Alkyne trans-Hydrometalation: Mechanistic Insights and Preparative Implications

Author: Dragoş-Adrian Roşca, Karin Radkowski, Larry M. Wolf, et al

Publication: Journal of the American Chemical Society

Publisher: American Chemical Society

Date: Feb 1, 2017

PERMISSION/LICENSE IS GRANTED FOR YOUR ORDER AT NO CHARGE

This type of permission/license, instead of the standard Terms and Conditions, is sent to you because no fee is being charged for your order. Please note the following:

- Permission is granted for your request in both print and electronic formats, and translations.
- If figures and/or tables were requested, they may be adapted or used in part.
- Please print this page for your records and send a copy of it to your publisher/graduate school.
- Appropriate credit for the requested material should be given as follows: "Reprinted (adapted) with permission from {COMPLETE REFERENCE CITATION}. Copyright {YEAR} American Chemical Society." Insert appropriate information in place of the capitalized words.
- One-time permission is granted only for the use specified in your RightsLink request. No additional uses are granted (such as derivative works or other editions). For any uses, please submit a new request.

If credit is given to another source for the material you requested from RightsLink, permission must be obtained from that source.

BACK CLOSE WINDOW

Expanded Helicenes as Synthons for Chiral Macrocyclic Nanocarbons

Author: Gavin R. Kiel, Katherine L. Bay, Adrian E. Samkian, et al

Publication: Journal of the American Chemical Society

Publisher: American Chemical Society

Date: Jun 1, 2020

PERMISSION/LICENSE IS GRANTED FOR YOUR ORDER AT NO CHARGE

This type of permission/license, instead of the standard Terms and Conditions, is sent to you because no fee is being charged for your order. Please note the following:

- Permission is granted for your request in both print and electronic formats, and translations.
- If figures and/or tables were requested, they may be adapted or used in part.
- Please print this page for your records and send a copy of it to your publisher/graduate school.
- Appropriate credit for the requested material should be given as follows: "Reprinted (adapted) with permission from {COMPLETE REFERENCE CITATION}. Copyright {YEAR} American Chemical Society." Insert appropriate information in place of the capitalized words.
- One-time permission is granted only for the use specified in your RightsLink request. No additional uses are granted (such as derivative works or other editions). For any uses, please submit a new request.

If credit is given to another source for the material you requested from RightsLink, permission must be obtained from that source.

BACK CLOSE WINDOW

ACS Publications
Most Trusted. Most Cited. Most Read.

Kinetic Control in the Synthesis of a Möbius Tris((ethynyl)[5]helicene) Macrocycle Using Alkyne Metathesis

Author: Xing Jiang, Joshua D. Laffoon, Dandan Chen, et al
Publication: Journal of the American Chemical Society
Publisher: American Chemical Society
Date: Apr 1, 2020

PERMISSION/LICENSE IS GRANTED FOR YOUR ORDER AT NO CHARGE

This type of permission/license, instead of the standard Terms and Conditions, is sent to you because no fee is being charged for your order. Please note the following:

- Permission is granted for your request in both print and electronic formats, and translations.
- If figures and/or tables were requested, they may be adapted or used in part.
- Please print this page for your records and send a copy of it to your publisher/graduate school.
- Appropriate credit for the requested material should be given as follows: "Reprinted (adapted) with permission from {COMPLETE REFERENCE CITATION}. Copyright {YEAR} American Chemical Society." Insert appropriate information in place of the capitalized words.
- One-time permission is granted only for the use specified in your RightsLink request. No additional uses are granted (such as derivative works or other editions). For any uses, please submit a new request.

If credit is given to another source for the material you requested from RightsLink, permission must be obtained from that source.

BACK CLOSE WINDOW